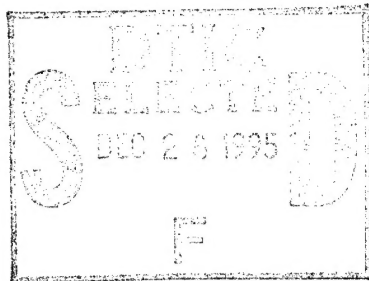
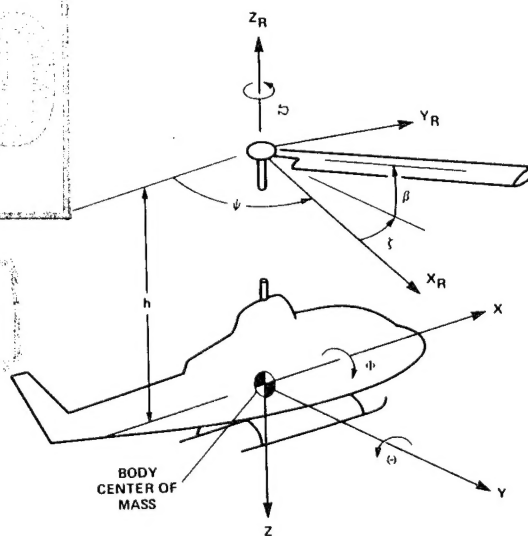


NASA/Army Rotorcraft Technology

*Volume III—Systems Integration,
Research Aircraft, and Industry*



DISSEMINATION STATEMENT II
Approved for public release
Distribution Unlimited



19951218 018

*Proceedings of a conference held at
Ames Research Center
Moffett Field, California
March 17-19, 1987*

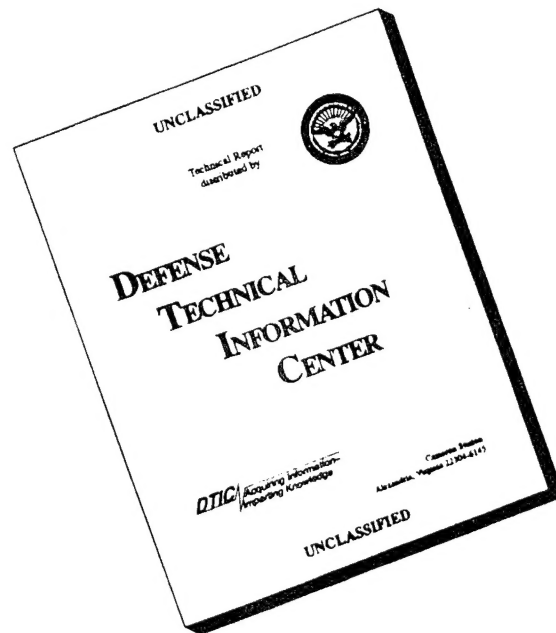
DTIC QUALITY INSPECTED 1



PLASTIC

5177004
5177004

DISCLAIMER NOTICE



**THIS DOCUMENT IS BEST
QUALITY AVAILABLE. THE
COPY FURNISHED TO DTIC
CONTAINED A SIGNIFICANT
NUMBER OF PAGES WHICH DO
NOT REPRODUCE LEGIBLY.**

NASA Conference Publication 2495

NASA/Army Rotorcraft Technology

Volume III—Systems Integration, Research Aircraft, and Industry

Proceedings of a conference sponsored by
the Department of the Army and the National
Aeronautics and Space Administration and held at
Ames Research Center
Moffett Field, California
March 17-19, 1987

Accession For	
NTIS	CRA&I <input checked="" type="checkbox"/>
DTIC	TAB <input type="checkbox"/>
Unannounced <input type="checkbox"/>	
Justification	
By	
Distribution /	
Availability Codes	
Dist	Avail and/or Special
A-1	



National Aeronautics
and Space Administration

Scientific and Technical
Information Division

1988

CONTENTS

Volume I

Introduction.....	1
Aerodynamics	
Summary.....	5
Accomplishments at NASA Langley Research Center in Rotorcraft Aerodynamics Technology.....	7
John C. Wilson	
The Developmeny of CFD Methods for Rotor Applications.....	34
F.X. Caradonna and W.J. McCroskey	
Dynamics and Aeroelasticity	
Summary.....	69
A Summary of Recent NASA/Army Contributions to Rotorcraft Vibrations and Structural Dynamics Technology.....	71
Raymond G. Kvaternik, Felton D. Bartlett, Jr. and John H. Cline	
A Review of Research in Rotor Loads.....	180
William G. Bousman and Wayne R. Mantay	
Comprehensive Rotorcraft Analysis Methods.....	312
Wendell B. Stephens and Edward E. Austin	
Rotorcraft Aeroelastic Stability.....	353
Robert A. Ormiston, William G. Warmbrodt, Dewey H. Hodges, and David A. Peters	

Volume II

Materials and Structures

Summary.....	533
Review of Fatigue and Fracture Research at NASA Langley Research Center.....	535
R.A. Everett, Jr.	
Delamination Durability of Composite Materials for Rotorcraft....	573
T. Kevin O'Brien	
Helicopter Crashworthiness Research Program.....	606
Gary L. Farley, Richard L. Boitnott, and Huey D. Carden	

Contents (continued)

Materials and Structures (continued)

Advanced Composite Airframe Program - Today's Technology.....	656
Danny E. Good and L. Thomas Mazza	

Propulsion and Drive Systems

Summary.....	681
Technology Developments for a Compound Cycle Engine.....	683
G.A. Bobula, W.T. Wintucky, and J.G. Castor	
Small Gas Turbine Engine Technology.....	698
Richard W. Niedzwiecki and Peter L. Meitner	
The Convertible Engine: A Dual-Mode Propulsion System for Advanced Rotorcraft.....	737
Jack G. McArdle	
Results of NASA/Army Transmission Research.....	769
John J. Coy, Dennis P. Townsend, and Harold H. Coe	
NASA's Rotorcraft Icing Research Program.....	802
Robert J. Shaw, John J. Reinmann, and Thomas L. Miller	

Flight Dynamics and Control

Summary.....	835
Helicopter Mathematical Models and Control Law Development for Handling Qualities Research.....	837
Robert T.N. Chen, J. Victor Lebacqz, Edwin W. Aiken, and Mark B. Tischler	
Rotorcraft Flight-Propulsion Control Integration.....	900
James R. Mihalow, Mark G. Ballin, and D.G.C. Rutledge	
Helicopter Human Factors Research.....	929
David C. Nagel and Sandra G. Hart	
Rotorcraft Handling-Qualities Design Criteria Development.....	948
Edwin W. Aiken, J. Victor Lebacqz, Robert T.N. Chen, and David L. Key	

Acoustics

Summary.....	1001
Recent Langley Helicopter Acoustics Contributions.....	1003
H.G. Morgan, S.P. Pao, and C.A. Powell	

Contents (continued)

Acoustics (continued)

Identification and Proposed Control of Helicopter Transmission Noise at the Source.....	1045
John J. Coy, Robert F. Handschuh, David G. Lewicki, Ronald G. Huff, Eugene A Krejsa, and Allan M. Karchmer	
A Decade of Aeroacoustic Research at NASA Ames Research Center...	1066
F.H. Schmitz, M. Mosher, C. Kitaplioglu, J. Cross, and I. Chang	
Aeroacoustic Research Programs at the Army Aviation Research and Technology Activity.....	1091
Yung H. Yu, Fredric H. Schmitz, and H. Andrew Morse	

Volume III

Systems Integration

Summary.....	1117
Status of NASA/Army Rotorcraft Research and Development Piloted Flight Simulation.....	1119
Gregory W. Condon and Terrence D. Gossett	
System Analysis in Rotorcraft Design - The Past Decade.....	1154
Thomas L. Galloway	
An Integrated Approach to Rotorcraft Human Factors Research.....	1167
Sandra G. Hart, E. James Hartzell, James W. Voorhees, Nancy M. Bucher, and R. Jay Shively	
Avionics Systems Integration Technology.....	1189
George Stech and James R. Williams	
Integrated Diagnostics.....	1211
Roger J. Hunthausen	

Research Aircraft


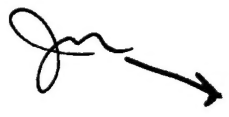
Summary.....	1233
Rotorcraft Flight Research with Emphasis on Rotor Systems.....	1234
W.J. Snyder	

Industry

Summary.....	1277
--------------	------

Contents (continued)

Industry (continued)

	An Overview of Key Technology Thrusts at Bell Helicopter Textron.....	051771	1279
	Jim Harse, Jing G. Yen, and Rod Taylor		
	Rotorcraft Technology at Boeing Vertol: Recent Advances.....		1341
	John Shaw, Leo Dadone, and Robert Wiesner		
	Recent Sikorsky R&D Progress.....		1395
	Sikorsky Aircraft Division, United Technologies Corporation		
	McDonnell Douglas Helicopter Company Independent Research and Development - Preparing for the Future.....	051772	1450
	A.C. Haggerty		
	List of Conference Attendees.....		1485

SYSTEMS INTEGRATION

Session Cochairmen:

Robert J. Huston, NASA

Thomas L. House, Department of the Army

SYSTEMS INTEGRATION SESSION

SUMMARY

Five presentations were given in the Systems Integration Session covering a broad range of technology topics and accomplishments. The first paper, "NASA/Army Rotorcraft Piloted Simulation - Current and Future Capabilities," by Gregory W. Condon and Terrence D. Gossett, addressed the quantum leap forward in capability now being achieved in rotorcraft piloted flight simulation technology. This progress is being driven by the increasingly demanding mission requirements that are driving military helicopter designs to extensively integrated systems that closely couple flying and mission management tasks, resulting in the need to simulate such systems in piloted ground-based facilities.

The second paper reviewed recent advances in system analysis techniques in rotorcraft design made possible by the rapid advances in the technology of electronic digital computers and integrated synthesis techniques. The paper "System Analysis in Rotorcraft Design - The Past Decade" by Thomas L. Galloway, summarized techniques currently in use by NASA and Army organizations in developing research programs and vehicle specifications for rotorcraft. These procedures span simple graphical approaches to comprehensive analysis on large mainframe computers.

Sandra G. Hart presented the third paper "An Integrated Approach to Rotorcraft Human Factors Research" authored by herself with her coauthors: E. James Hartzell, James W. Voorhees, Nancy M. Bucher and R. Jay Shively. The paper addressed the urgent need for information about human pilot behavior in increasingly demanding helicopter mission environments. Several active programs of human factors research were described that are underway at Ames Research Center, conducted jointly by Army and NASA scientists. These research activities range from laboratory experiments to computational modeling, simulation evaluation and inflight testing. The paper described the advantages and disadvantages of each type of research, provided examples of experimental results, and described the facilities available at Ames Research Center to conduct such research.

The fourth paper, "Avionics Systems Integration Technology" by George Stech and James R. Williams presented a summary of key avionics integration technology base efforts such as the Integrated Avionics Control System, Army Digital Avionics System, and the Digital Map Generator Programs. In addition the paper described the new Avionics Integration Research Laboratory (AIRLAB) that NASA has established at Langley Research Center for research on the integration and validation of avionics systems and the evaluation of advanced technology in a total systems context.

The fifth and last paper in the session, "Integrated Diagnostics" by Roger J. Hunthausen, summarized recently completed projects in which advanced diagnostic concepts have been explored and/or demonstrated. The projects began with the design of integrated diagnostics for the Army's new gas turbine engines, and included the application of integrated diagnostics to other aircraft subsystems. The paper also summarized a recent project which tied subsystem fault monitoring and diagnostics with a more complete definition of the total flight domain.

STATUS OF NASA/ARMY ROTORCRAFT RESEARCH AND DEVELOPMENT PILOTED FLIGHT SIMULATION

Gregory W. Condon
National Aeronautics and Space Administration
Ames Research Center

Terrence D. Gossett
US Army Aviation Research and Technology Activity
Aeroflightdynamics Directorate

INTRODUCTION

Rotorcraft research and development (R&D) piloted flight simulation is currently experiencing a quantum leap forward in capability, both for the major airframe companies and for the NASA/Army facilities. The need for sophisticated simulation capabilities is being driven by the Army's advanced mission requirements, as exemplified by the new light helicopter (LHX) series of aircraft, and by the high cost of flight development. The advanced mission requirements are moving Army helicopters toward extensively integrated systems that closely couple flying and mission management tasks, resulting in the need to simulate such systems in piloted ground-based facilities. The concomitant revolution in electronics technology has enabled these simulation needs to be met, although not at an insignificant price, both by the rotorcraft airframe companies and by the Army and NASA. Clearly the companies are achieving, for the first time, major in-house simulation capabilities. The NASA/Army capabilities are also undergoing major steps forward in their continuing role of providing more advanced R&D capabilities than are affordable by the individual companies.

The purpose of this paper is to review the status of the major NASA/Army capabilities in piloted rotorcraft flight simulation. This paper will address the requirements for R&D piloted simulation, as well as the capabilities and technologies that are currently available or are being developed by NASA and the Army at Ames Research Center to meet these needs. The application of revolutionary advances--in visual scene, electronic cockpits, motion, and modelling of interactive mission environments/vehicle systems--to the NASA/Army facilities will be addressed. Particular attention will be devoted to the major advances made in integrating these individual capabilities into fully integrated simulation environments that have been or are being applied to new rotorcraft mission requirements. The specific simulators to be discussed are the Vertical Motion Simulator (VMS) and the Crew Station Research and Development Facility (CSRDF).

THE ADVANCE OF FLIGHT SIMULATION TECHNOLOGY

The requirements for piloted R&D flight simulation emanate directly from the advanced mission capabilities that are needed by the Department of Defense, and the resultant advanced vehicle/systems that are required to meet these needs. The government facilities are being pushed towards the leading edge to address the most advanced of these mission applications and future vehicle/system concepts.

Advanced Mission Requirements

Advanced mission requirements are pushing simulation technology in two related but different directions: towards the modelling and perception of the complete external environment, and towards the modelling and representation of the on-board mission systems.

The LHX, particularly in its scout/attack (SCAT) mission in the context of a single-pilot battle captain, exemplifies this simulation challenge. This simulation requires very comprehensive modelling problems to be solved in real-time and very sophisticated cockpit and perception capabilities to be represented. The environment and mission equipment package include the role of battle captain for 11 other friendly aircraft; a threat environment with tanks, SAMs, DZUs, air-to-air Hinds, etc.; intensive communications environment with ground and air forces to include data link; extensive automatic survival equipment (ASE) and countermeasures to include RF/IR/EO/laser receivers and jammers and chaff/flares; and an extensive weapons suite to include guns, air-to-air missiles and air-to-surface missiles. The cockpit and perception capabilities include: a voice recognition and synthesis system; touch screen CRTs; programmable push buttons; data entry keyboards; and wide field-of-view helmet-mounted display with forward-looking infrared radar (FLIR) and superimposed symbology for flightpath control and targeting.

Advanced missions are requiring a much closer coupling and automation of the flight control and mission management systems with higher-level decision-making incorporated in the systems. This coupling is requiring a significant increase in the fidelity of the simulation of the mission environment and equipment, and the integration with the flight control system, the cockpit visual system and the piloting tasks. The real-time computation implications and the requirements for visual fidelity are significant.

Advanced Vehicle Configurations

Advanced vehicle configurations are pushing the requirements for simulation in two directions: representation of the basic air vehicle, and representation of the advanced systems necessary to control the air vehicle. The X-wing concept exemplifies this simulation challenge, requiring very difficult modelling problems to be solved in real time. The basic vehicle concept covers a speed range from hover to 400 knots; includes fixed, rotating and conversion operation of the rotor system;

and uses leading and trailing-edge blowing for control. The modelling of the systems required to fly the air vehicle poses even more difficult real-time modelling challenges. The fly-by-wire flight control system includes pneumo-dynamic control of rotor blowing through 20 valves; higher harmonic and rotor moment control for conversion; and transition of integrated flight/propulsion control from rotary-wing hover through conversion to fixed-wing high-speed forward flight.

Advanced vehicle systems are requiring a much closer coupling between the flight control system and the basic vehicle. This coupling is requiring a close integration in modelling the aerodynamic, structural, propulsion, and control characteristics of the vehicle with much higher-order dynamics than in the past. The real-time implications are very difficult.

GOVERNMENT SIMULATION OVERVIEW

Figure 1 summarizes the characteristics of the VMS and CSRDF in relation to advanced rotorcraft vehicle configurations and mission requirements. The government facilities at the Ames Research Center have been developed to address both of these needs, particularly through advocacy and funding by the Army.

The VMS was designed to study the flying qualities of advanced rotorcraft and VTOL aircraft. Through the years it has been enhanced to examine state-of-the-art vehicle configurations such as the tilt-rotor and the X-wing. The VMS has also been enhanced to examine more advanced mission requirements, such as air-to-air combat and single-pilot SCAT operations, with the focus on flying qualities rather than mission management. It is currently undergoing an Army-funded upgrade, called the Rotorcraft Systems Integration Simulator (RSIS), to expand its ability to support rotorcraft flying qualities simulation, particularly in the context of advanced nap-of-the-Earth (NOE) missions.

To address the combat-oriented full mission, the Army is also funding the development of the CSRDF, to be located at Ames. The simulator is being designed to study the issues of mission management for advanced missions of the future with the near-term emphasis on the battle captain for the LHX SCAT. The simulator will also include representation of advanced vehicle configurations and control-systems automation to provide proper flying-qualities consideration, but in a fixed-base mode.

The separation between flight and mission management is disappearing in advanced vehicles. The pilot and the aircraft systems must do both tasks in an integrated manner. This integration is being forged into the VMS/RSIS and CSRDF simulation capability at Ames and will provide the Government with a powerful capability to conduct rotorcraft research and development programs in a most effective and efficient manner.

VERTICAL MOTION SIMULATOR (VMS)

The VMS consists of a large motion base, interchangeable cab/cockpits, a computer-generated imagery system, and a CDC-7600 computer.

The VMS Motion Base

Description/Capabilities- The VMS motion base (fig. 2) is built around a horizontal beam which rests on two vertical pistons. The pistons are pneumatically pressurized to bring the beam to neutral buoyancy and are each driven by four 150 HP dc motors to provide the large (60 ft) vertical motion capability. A hydraulic hexapod motion system, manufactured by CAE Industries, is mounted to a lateral carriage on the beam. The lateral carriage is driven by four 40 HP dc motors to provide the second degree of large (40 ft) linear motion. The CAE motion base provides the three rotational degrees of freedom.

As part of the RSIS upgrade to the VMS (fig. 3) the CAE motion base is being replaced with the Rotorcraft Simulator Motion Generator (RSMG), a high performance, custom-designed motion base. The objective is to increase the angular rate and acceleration capabilities to those required for simulation of state-of-the-art rotorcraft in aggressive NOE flight. The third linear degree-of-freedom is also being provided. While the motion capabilities are driven by rotorcraft requirements, the resultant VMS will have enhanced capabilities for all vehicle classes. Table 1 shows the motion capabilities of the VMS, both in its current configuration and after the RSIS upgrade has been accomplished.

Motion Fidelity Effects- Two recent experiments on the VMS investigated the effects of motion cueing on rotorcraft control. The first experiment (ref. 1) investigated a helicopter autorotative landing task. Variations were made in the motion constraint logic ranging from full VMS motion through intermediate motion values typical of a large-travel hexapod and a small-travel "nudge" base down to no motion in fixed base. As shown in figure 4, landing performance degraded with restrictions in motion cueing. In addition, figure 5 shows that pilot control technique degraded with reduction in motion cueing as exhibited by collective control technique during the flare and touchdown. The second experiment (ref. 2) investigated the effect of motion variation on height control and target tracking with a simple hovering math model. The bandwidth and phase margin of the pilot-vehicle system were used to quantify the effects (fig. 6) of motion variation on the fidelity of the simulation. In holding position in the presence of vertical disturbances, pilot control gain and resultant open-loop crossover frequency were significantly depressed as the fidelity of vertical motion was reduced. In height tracking of a moving reference, gain and crossover were not greatly affected, but phase margin and tracking performance improved with increased motion fidelity. Also, figure 7 shows pilot opinion ratings of varied vehicle vertical-response characteristics were degraded with reduction in motion-cue fidelity.

The VMS Cab/Cockpit

The VMS cockpits are enclosed in cabs that are quickly interchangeable on the motion base. The basic concept is to have a pipeline of interchangeable cabs (ICabs) where one is being used for the current simulation, another is undergoing fixed-base checkout for the next simulation, and the third and fourth are being built-up for subsequent simulations. This approach significantly improves efficiency since the down-time of the motion base for cab reconfiguration is only about 4 hr. To minimize cab modifications, four ICabs have been built with their configurations optimized for specific vehicle configurations. The key consideration in cab layout (fig. 8) is the location of the CRT monitors that are used to present the outside scene to the pilot(s). The cab configurations are a single-seat rotorcraft cab, the right seat of a side-by-side dual-seat rotorcraft cab, a side-by-side dual-seat transport/Space Shuttle cab, and a single-seat fighter cab.

The RSIS upgrade to the VMS will include a new cab concept called the advanced cab and visual system (ACAVS) (fig. 9) in which a dome projection system is used to present the outside scene to the pilot(s). The cab will be compatible with the interchangeable cab interface of the motion system so that it or ICabs can be used (fig. 10). Cockpit reconfiguration will be achieved through interchangeable cockpit modules in the cab. Several modules, tailored to particular configurations such as single pilot and side-by-side dual pilot, will be developed.

The requirements to simulate cockpit systems such as heads-up displays and digital maps on the VMS continue to escalate. The specific capabilities developed to date will be covered in the section on Sample Advanced Simulations.

The VMS Visual Imagery Generation

Description/Capabilities- The VMS uses two computer-generated imagery (CGI) systems to provide out-the-window display. Both systems provide full-color, wide field-of-view scenes that accurately depict scene movement based on pilot input and aircraft response. The first CGI system acquired was a Singer Link DIG-1. It provides four channels displayed on collimated, vertical raster, 1000-line CRT monitors mounted in the cockpit with partial coverage of a field-of-view of 30° vertical by 144° horizontal. The system can display 6,000 edges at a 30 Hz frame rate.

The recently acquired Evans & Sutherland CT-5A system provides three channels projected adjacently on a dome via General Electric light valves. The field-of-view completely encompasses 60° vertical and 138° horizontal. The system can display 12,000 edges at a 25 Hz frame rate.

Fidelity Understanding/Improvements- While the Singer DIG-1 CGI, as delivered, greatly expanded the peripheral vision through the four-window cab as compared to a single CRT camera model-board system, it provided a very low level of near-field detail. It became quickly obvious, through pilot commentary, that it was crucial to be able to tailor the database to provide the cues necessary for the pilot to fly

the specific task being studied. The capability to build new CGI databases and to rapidly modify the CGI databases supplied with the DIG has been developed and used.

Both the DIG-1 and the CT-5A systems allow real-time modification of many display parameters. These include environmental effects (time of day, clouds, rain, sun angle), lighting effects (airports, cities), and weapons effects (smoke, explosions, tracers, missile trail). Each system can display a variety of moving models within the display including airborne, ground and waterborne craft.

Ames currently has the capability to develop databases for both systems to display virtually any real or imaginary scenes. Currently the databases must be created on separate development systems using various types of source data including maps, photographs, and scaled drawings. A database development system resident on a graphics workstation is currently being implemented that will allow modification and creation of databases for both systems and conversion of either type of database to the other.

The knowledge about visual-cue requirements for simulation of rotorcraft is extremely limited. Information from the VMS has been acquired mainly through experience with on-going simulations and several limited experiments to specifically study the subject. This knowledge is based mainly on pilot commentary and observations with little quantitative data. As reported in references 1 and 2, window placement is extremely important so that consistent and easily recognized position, attitude and speed cues can be obtained from the scene.

A key issue in the use of CGI systems for flight simulation has been the effect of transport delay. The issue becomes crucial for tasks that require high bandwidth control, in the range of 10 rad/sec. To mitigate the impact of transport delay in CGI scene presentations, a discrete prediction algorithm has been developed at Ames (ref. 3) for application to both rotational and translational drive signals. The "McFarland algorithm," as it is called, capitalizes on the low-pass nature of these signals and its use requires the selection of a cutoff bandwidth that is small with respect to the simulation bandwidth, but larger than the pilot's operational bandwidth. Scene dynamics then exhibit significantly improved fidelity in the frequency range up to the cutoff bandwidth.

Figure 11 shows the phase and magnitude deterioration that occurs versus frequency when the simple technique of linear projection is applied to the problem of predicting signals 66.7 msec in the future (a typical CGI transport delay). Pilots invariably object to the performance obtained with this technique. Figure 12 presents similar data using the McFarland algorithm for the same prediction interval (66.7 msec). The compensation algorithm is a function of both the selected bandwidth, 2.5 Hz in this example, and the mainframe computer cycle time, a parameter shown in the figure. For the worst case shown, the selected bandwidth, 2.5 Hz, is 20% of the simulation bandwidth, 12.5 Hz (40 msec produces a Nyquist frequency of 12.5 Hz). Computer-generated image signals within the cutoff frequency of 2.5 Hz have negligible errors; that is, CGI presentation does not manifest any transport delay.

The amplification beyond the cutoff bandwidth has not appeared to influence rotorcraft simulations, even those with high N/rev frequency content. A special processing technique to handle turbulence modelling (a broad-band phenomenon) had to be developed.

The VMS Computer System

The primary simulation computer for the VMS is the CDC 7600, a 1970s vintage high-performance computer designed for batch operation. Ames has developed a real-time operating system to support simulation on the VMS. While the resultant computation capability of the CDC 7600 is fairly fast, on the order of 10 MIPS in closed-loop real-time operation, it suffers from a severe memory limitation that requires the heavy use of overlays in all simulations.

Even with this significant level of computational performance, the CDC 7600 does not satisfy several existing requirements and many upcoming needs. The computational shortcomings result from the modelling requirements of advanced vehicle/rotor configurations and advanced rotorcraft on-board systems. Specific vehicle modelling needs include blade flexibility, in-flow dynamics, engine dynamics, rotor/fuselage interactions, and unique concepts such as circulation control rotors. Specific vehicle systems modelling needs include extensive on-board digital computation for integrated controls at very high frequencies such as integrated flight/propulsion control or higher harmonic control. These requirements affect the needed computational speed in two ways: 1) more equations of increased complexity must be solved, and 2) the equations must be solved at much higher computational frequencies to assure numerical stability at the higher frequency contents. Ames is currently in the process of upgrading its simulation capability by replacing all of its simulation computers through competitive procurement (ref. 4). The requirements are based upon analysis of the previously described needs for the next 10 yr. Two classes of computer performance are being sought with the replacement for the CDC 7600 being targeted for nominally greater than 20 MIPS in real-time operation. The speed requirements are stated in terms of benchmark programs that must meet specific time requirements.

Sample Advanced Configuration/Mission Simulations

The capabilities and the technology limitations of the VMS are best understood in the context of the leading edge simulations that have been conducted with the VMS. The following simulation programs resulted in the state of the art of VMS being expanded in many different directions.

RSRA X-Wing Vehicle Development Simulation- The RSRA X-wing research aircraft has undergone three piloted simulation investigations on the VMS: no-rotor, stopped-rotor, and rotating-rotor configurations. The computational requirements to simulate the X-wing far outdistance the capabilities of the CDC 7600 computer. The computational requirements are essentially driven by three unique aspects of the X-wing rotor system: 1) the circulation-control airfoil used in the rotor system;

2) the pneumodynamics of the circulation control system; and 3) the conversion from rotating rotor to fixed rotor and back.

The circulation-control rotor, using trailing-edge blowing over a Coanda surface, complicates the aerodynamics of the airfoil. Lift and drag coefficients over the angle-of-attack range of interest are typically stored in tables for maximum speed in real-time operations. These tables must also include variations of blowing coefficients at each of the previous data points. Since blowing effects vary with Mach number, the aerodynamic inputs to the simulation are no longer linearly normalizable by dynamic pressure.

Circulation control is used not only for performance benefits through increased lift, but also to control the lift distribution over the rotor plane. Air from a gear-box-driven compressor is provided to the slots on the aerodynamic surfaces. The flow is varied to increase lift on the retreating blade side (in rotary wing mode) and to provide maneuver control of the vehicle. Since the valves controlling the internal airflow are located in the hub, the pneumodynamics of the flow inside the blades (including compressibility of the air) must be included in the simulated control-system model.

In the past, structural dynamics did not significantly affect handling qualities. The X-wing, with forward swept wings (blades) in the stopped mode and a rigid rotor system in the rotary-wing mode, introduces structural dynamics effects into the handling qualities. Even though the X-wing blades (wings) are necessarily very stiff, they do flex under load thereby altering the load distribution and moments generated by the X-wing. In addition, the rigid rotor (no flapping or lagging hinges) transmits vibrations to the body that are not present in conventional helicopters. The X-wing design includes higher harmonic control in the pneumatics of the flight control system to counter these effects, thereby further complicating the simulation.

Helicopter Air-To-Air Combat Simulation- The air-combat role for Army helicopters has rapidly become a critical issue for research and development activities within the government and industry. Since Army aircraft frequently operate at NOE altitudes, encounters with threat aircraft are likely to occur at this low level. Fixed-wing manned simulators in government and industry have not been easily adapted to helicopter engagements because of aircraft modelling complexities and the lack of high-fidelity, low-level visual scene-generating systems. It was desired, therefore, to design a simulation system which would allow the effects of terrain to be included in an investigation of helicopter air-combat maneuvering. The helicopter modelling capability, the wide field-of-view CGI display, and the large motion travel of the NASA Ames Research Center VMS were well suited for this task, although new system capabilities were required.

These new capabilities included a dual eyepoint CGI real-time software program which allowed for two independently maneuverable views of a common visual data base. The data base was specially designed for this project as was a system of head-up and panel-mounted information displays. The enemy aircraft pilot station and equations of motion were added along with a weapons model and scoring algorithms.

Two helicopter air-combat simulation experiments have been conducted on the VMS air combat system to date (ref. 9). Numerous other studies have utilized the capability for a sub-task portion of a particular handling qualities or flight controls experiment. Example study topics have included maneuver envelope requirements, roll-control performance, tilt-rotor and longitudinal-force control comparisons, and command-augmentation system studies. Planned improvements to the system would expand the pilots' field of view, a critical factor for air combat, and allow for encounters involving multiple opponents. Nevertheless, pilot comments rate the encounters flown on the current system as very representative of flight test engagements and have praised the usefulness of the simulator tool for this task.

Side-Arm Controller and Helmet-Mounted Display Simulation- A recent requirement for the replacement of conventional cockpit controls with smaller, integrated, multi-axis controllers led to a series of VMS investigations of the effects of side-stick controller characteristics on rotorcraft handling qualities for terrain flight (refs. 5 and 6). Because of the need to evaluate a wide variety of controllers, an extremely adaptable mounting technique was devised which allowed not only the easy installation of the various controllers but also the adjustment of the position and orientation of each controller with respect to the pilot (fig. 13). This adjustment was found to be critical in determining the acceptability of any particular controller configuration. Careful calibration of the force-displacement characteristics of each controller was required to ensure the validity of the experimental results.

For these investigations, visual flight tasks were flown over a specially designed CGI database presented on the four-window display in the VMS (fig. 14). Careful design of this visual scene, especially terrain texture and obstacle placement, was required to provide compelling visual cues of the pilot's position and orientation with respect to the terrain and other obstacles (ref. 7).

To assess the effects of reduced visibility conditions on the experimental results (ref. 8), the Army's Integrated Helmet and Display Sight System (IHADSS) was installed into the simulation (fig. 15). The IHADSS is a visually coupled, helmet-mounted display of infrared (IR) imagery from a nose-mounted sensor and superimposed symbology currently operational in the AH-64 Apache helicopter. To achieve a simulation of the operational system, the simulated IR sensor image was produced by a camera-and-terrain-board visual system which responded to both aircraft and pilot head motions. The simulation software which drove the camera was run at a cycle time half that of the aircraft model to ensure a smooth response to anticipated pilot head motions. Some difficulty was encountered in mixing the stroke-written symbols with the raster IR simulation, and the resulting superimposed symbols were not as clear as in the actual system. However, the IHADSS simulation was judged to be very representative of the actual system by an experimental test pilot experienced in its use.

CREW STATION RESEARCH AND DEVELOPMENT FACILITY (CSRDF)

Introduction

The capabilities of the CSRDF are driven by emerging Army rotorcraft requirements while its architecture capitalizes on the burgeoning developments in simulation technology. The Army urgently needs a full-combat mission simulator to conduct advanced rotorcraft R&D with evolving materiel and doctrinal concepts in a realistic scenario. The requirements for the CSRDF were developed to meet both the near-term critical needs of the LHX development program and the far-term R&D needs of future Army development programs.

Overview

CSRDF has been designed to permit evaluation of either a single or a two-crew aircraft when operating as part of a full SCAT team in a scenario that exercises friendly and enemy systems of operational significance to the crew.

The scenario participants include: 1) the crew station battle captain; 2) up to three SCAT teams of four aircraft each; 3) a utility helicopter; (4) other friendly units such as AWACS aircraft, Ranger teams, and Battalion commanders; 5) up to three enemy helicopters; and 6) up to 110 ground-based threats and targets. The participants are fully active with 1) the SCAT, threat and utility aircraft under real-time control and interaction by human experimenters; 2) the friendly forces in real-time communication and interaction by human experimenters; and 3) the ground-based threats in real-time interaction by computer control.

Simulation of aircraft systems includes cockpit systems, aircraft survivability equipment, mission equipment packages, navigation, communications, and battle resource management. Each of the systems in these six categories has been simulated in consonance with modern SCAT rotorcraft technologies. The effects of variations in these systems will be assessed in the context of a full-combat situation.

A multiple deployment scenario, divided into three successive 45 min engagements, has been developed. As the mission progresses through the three engagements, the loading from threats, communications and fatigue will increase. The composite mission scenario has been designed to provide a realistic workload for the battle captain so that the mission effectiveness and associated workload can be assessed.

Facility Elements

The tandem crew station, shown in figure 16, has been designed around a fiber-optic helmet-mounted display (FOHMD) that is worn by the pilot in one of the two crew station positions. The FOHMD (fig. 17) presents a panoramic view of either the out-the-window scene or the image from a head-tracked sensor. The field-of-view of

the display (fig. 18) includes a high-resolution binocular insert where computer-generated symbology is mixed with the scene.

Figure 19 shows the components of the FOHMD system. The orientation of the helmet is tracked by an IR tracking system with acceleration compensation to minimize latencies. The orientation commands, in consonance with the aircraft motions, are used to drive the computer-image generator which calculates the proper scenes for each channel in the image presentation. The image generator drives light valves through an optical combiner to produce the picture for each eye. These pictures are transmitted by fiber-optic bundles to the helmet. The head-tracker capability results in a very large field-of-regard.

The layouts of the two crew stations are shown in figures 20 and 21. The flight controls in each crew station consist of two four-axis, limited-displacement controllers plus rudder pedals. The longitudinal, lateral, directional, and collective controls may be dynamically assigned to any combination of hand controllers and pedals in a given crew station. Systems management displays permit control of aircraft systems via various tactile entry devices such as touchpads and touchscreens. Monitoring of the combat situation is achieved through the tactical situation display (TSD) by means of a scaleable plan view of the gaming area with overlays for threat and friendly units. These may be modified using the touchscreen, as may the navigation and tactical overlays.

The simulation does not provide motion or vibration cues; however, great attention has been given to the sound and noise environment. A six-channel sound system provides directional sound cues for such items as rotor and transmission noise, weapon firing effects, dispensing of chaff and flares--all with noise levels comparable to that experienced in flight.

Blue/Red Team Stations (fig. 22) are used to control the interaction of the SCAT team members, the enemy aircraft and the utility helicopter with the crew station within the tactical gaming area. Plan-view and stylized forward-view displays (fig. 23) are the chief references for flight control. Control of the team station aircraft is through a simple joy stick. Selection of weapons, control of flight modes, and receipt and transmission of data link messages are all achieved through soft key selections on the touchscreen.

The White Team Station (fig. 24) provides the simulation of the communication intensive interactions with all elements external to the SCAT team. Ten channels of communication, with provisions for voice alteration, background chatter, and frequencies assigned under experimenter control, add realism and completeness to the simulation.

The control and coordination of the experiment is achieved through the experimenter/operator console (EOC) (fig. 25), where a team of Army experimenters and NASA personnel will control and monitor the mission scenario.

The computer architecture for CSRDF is shown in figure 26. The simulation is run under the control of a VAX 8650 host computer, iterating at the basic rate of

60 Hz. It is coupled with an array processor, running a blade-element rotor model at a 120 Hz rate. Four Microvax II microcomputers and 12 Silicon Graphics IRIS graphics workstations are connected to the host by Ethernet serial data buses. The Digital Imagery Generator (DIG) from Singer Link utilizes a Perkin Elmer PE 3250. Real-time software in the host consists of two basic parts: 1) simulation of the air vehicle, the crew environment and the system software furnished by CAE, and 2) simulation of the threat environment and crew station tactical systems provided by Flight Systems, Inc. (FSI). CAE is primarily responsible for cockpit systems, navigation, communication, and battle resources management and overall systems integration; FSI is primarily responsible for threat models and tactics, aircraft survivability equipment, target acquisition, and weapons modelling. In addition, the full visual scene, covering a 32 by 40 km database with appropriate threat systems, is provided through the Singer Link DIG.

Any simulator designed for research and development applications must be quickly and easily reconfigurable. With the CSRDF architecture of programmable displays and software modules, interactive graphics editors are provided to allow displays to be built and changed. Similarly, a syntax editor allows the voice input and output systems to be modified to suit the particular goals of each experiment. Database processors can extract macro-terrain information from the DIG to build forward-view displays and tactical-situation contour displays. Utilities allow the threat positioning and characteristics to be modified.

CONCLUDING REMARKS

Clearly the separation between flightpath management and mission management is disappearing in advanced vehicles. The pilot and the on-board systems must do both tasks in an integrated manner. This integration is being forged into the VMS/RSIS and CSRDF simulation capability at Ames. The focus of the VMS is on flying qualities/control investigations in the context of representative mission environments. On the other hand, the focus of the CSRDF is on mission-management investigations in the context of representative vehicle/control characteristics. The combined facility base provides the United States with a powerful capability to conduct leading-edge rotorcraft research and development programs in a most effective and efficient manner.

REFERENCES

1. Decker, W. A.; Adam, C. F.; and Gerdes, R. M.: Pilot Use of Simulator Cues for Autorotation Landings. 42nd Annual Forum and Technology Display of the AHS, Washington, DC, June 1986.
2. Bray, R. S.: Visual and Motion Cueing in Helicopter Simulation. NASA TM 86818, 1985.
3. McFarland, R. E.: CGI Delay Compensation. NASA TM 86703, 1986.
4. Simulation Computer Systems. Solicitation Number RF2-32863 (RHD), NASA Ames Research Center, Code: 241-1, Moffett Field, CA 94035, November 13, 1986.
5. Landis, K. H.; and Glusman, S. I.: Development of ADOCS Controllers and Control Laws. NASA CR 177339 (USAAVSCOM TR 84-A07), 1985.
6. Aiken, E. W.: A Review of the Effects of Side-Stick Controllers on Rotorcraft Handling Qualities. J. AHS, vol. 31, no. 3, July 1986, pp. 27-34.
7. Landis, K. H.; Dunford, P. J.; Aiken, E. W.; and Hilbert, K. B.: Simulator Investigations of Side-Stick Controller/Stability and Control Augmentation Systems for Helicopter Visual Flight. J. AHS, vol. 30, no. 2, Apr. 1985, pp. 3-13.
8. Aiken, E. W.; Hilbert, K. B.; Landis, K. H.; and Glusman, S. I.: An Investigation of Side-Stick Controller/Stability and Control Augmentation System Requirements for Helicopter Terrain Flight Under Reduced Visibility Conditions. AIAA Paper No. 84-0235, Reno, NV, Jan. 1984.
9. Lewis, M. S.: A Piloted Simulation of One-on-One Helicopter Air Combat in Low-Level Flight. J. AHS, Apr. 1986.

TABLE 1.- VERTICAL MOTION SIMULATOR MOTION SYSTEM PERFORMANCE LIMITS

	Displacement ft deg		Velocity ft/sec deg/sec		Acceleration ft/sec ² deg/sec ²	
	Original	RSMG	Original	RSMG	Original	RSMG
Vertical	±25	±25	±16	±16	±24	±24
Lateral	±17	±17	±8	±8	±15	±15
Longitudinal	±0	±4	±0	±4	±0	±10
Roll	±19.5	±18	±19.5	±40	±57.3	±115
Pitch	+20 -24.5	±18	±19.5	±40	±57.3	±115
Yaw	±34	±24	±19.5	±40	±57.3	±115

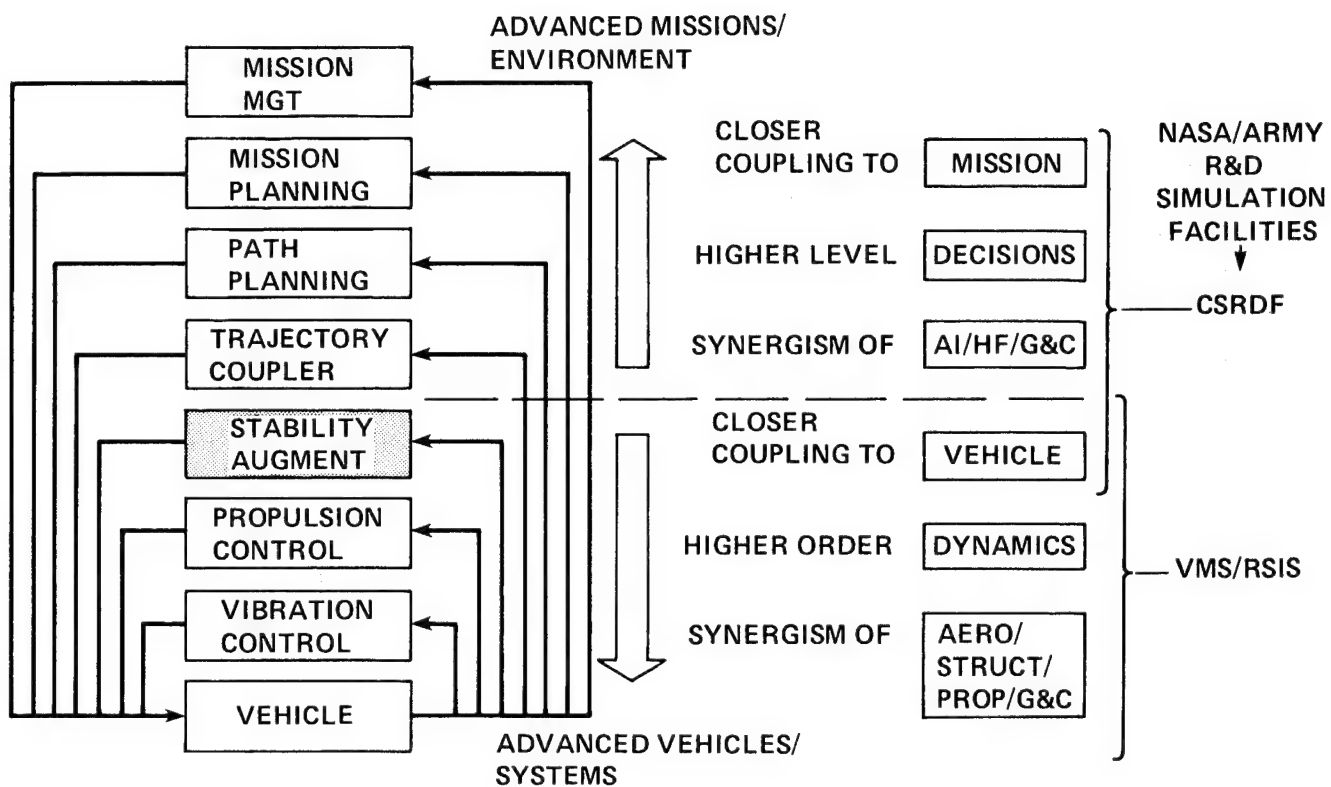


Figure 1.- Direction of rotorcraft/simulation technology.

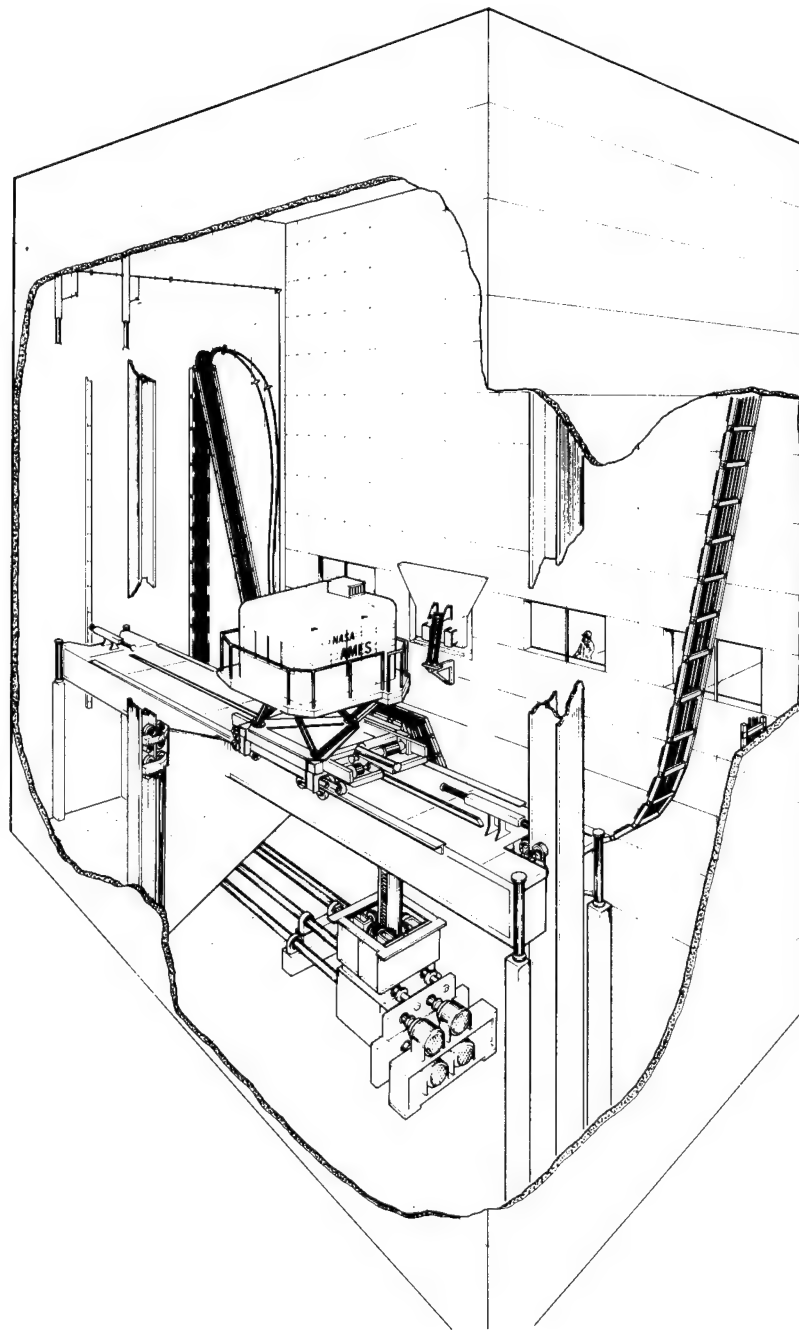


Figure 2.- Vertical Motion Simulator.

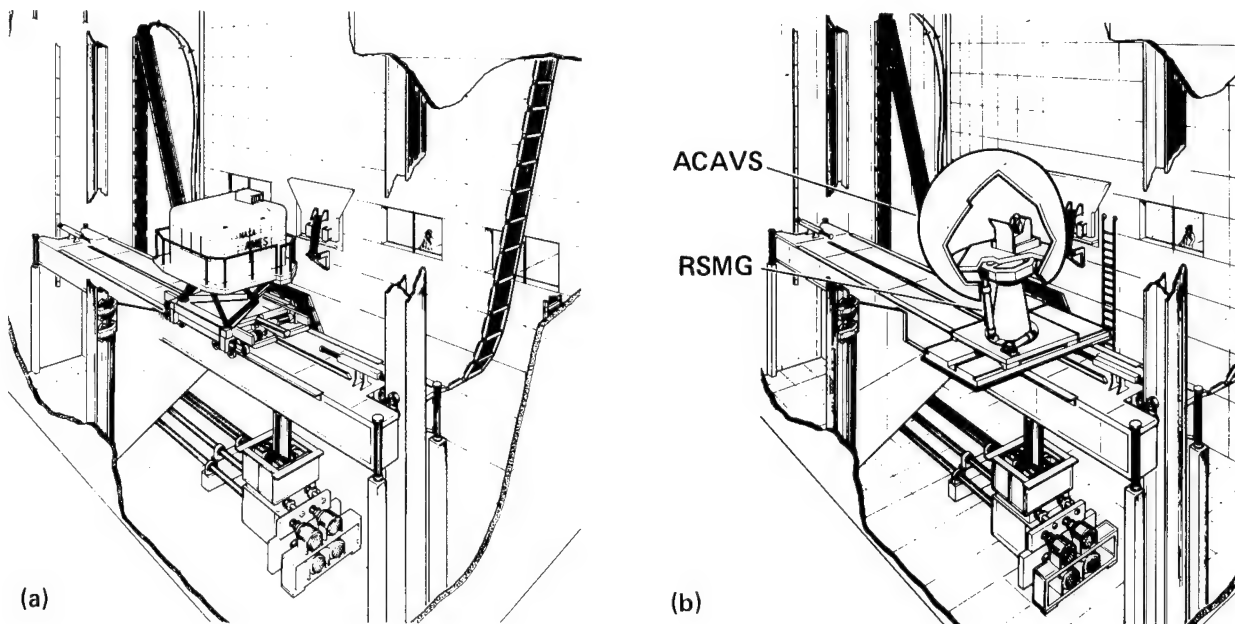


Figure 3.- Vertical Motion Simulator. (a) Existing VMS; (b) future VMS.

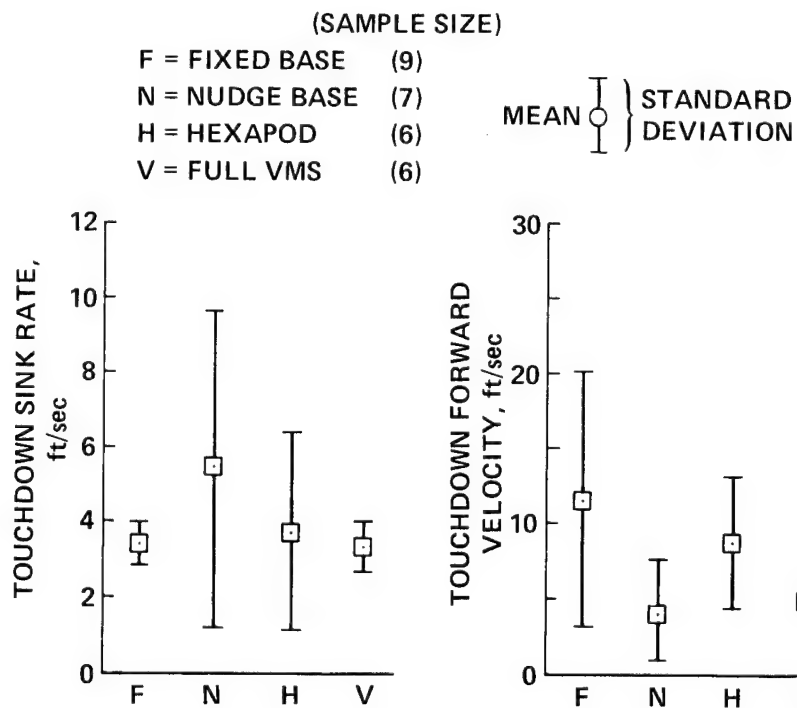


Figure 4.- Motion restriction effects on autorotation landing performance.

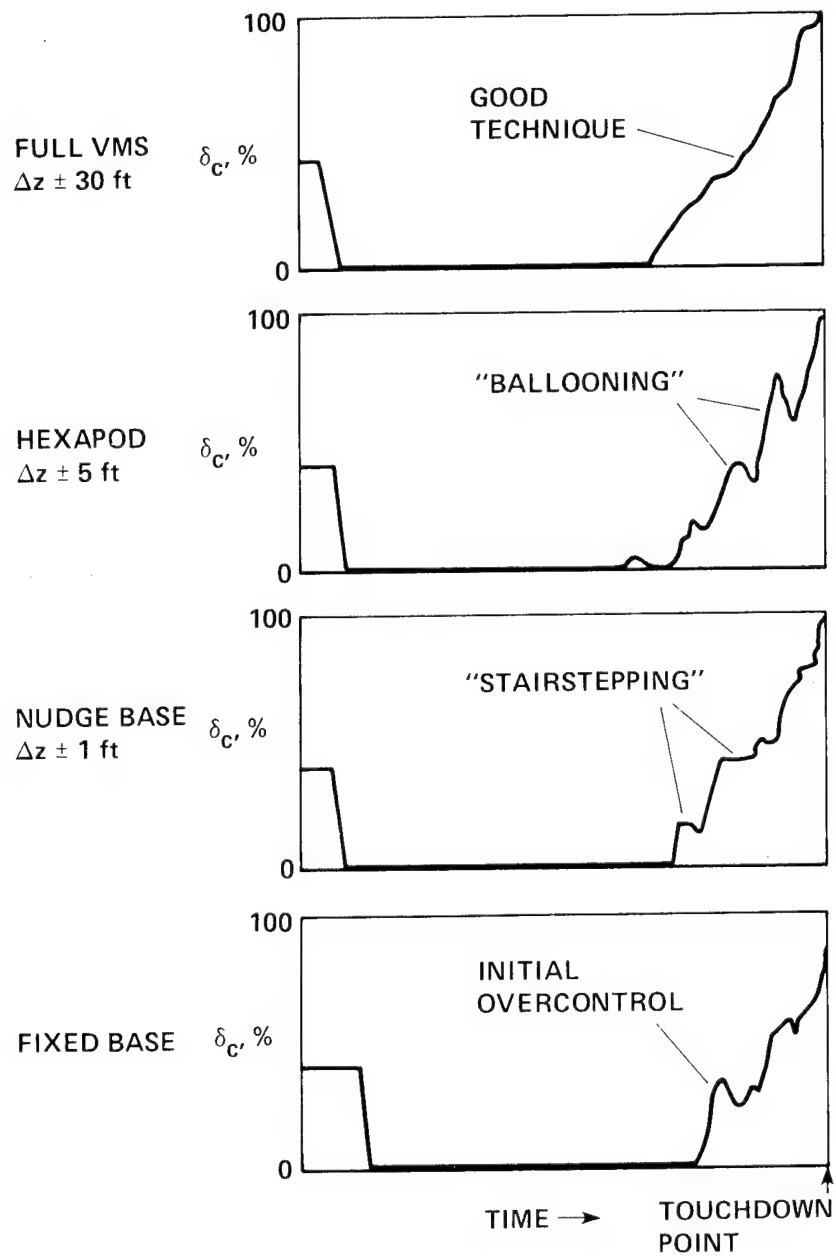


Figure 5.- Motion restriction effects on autorotation control technique.

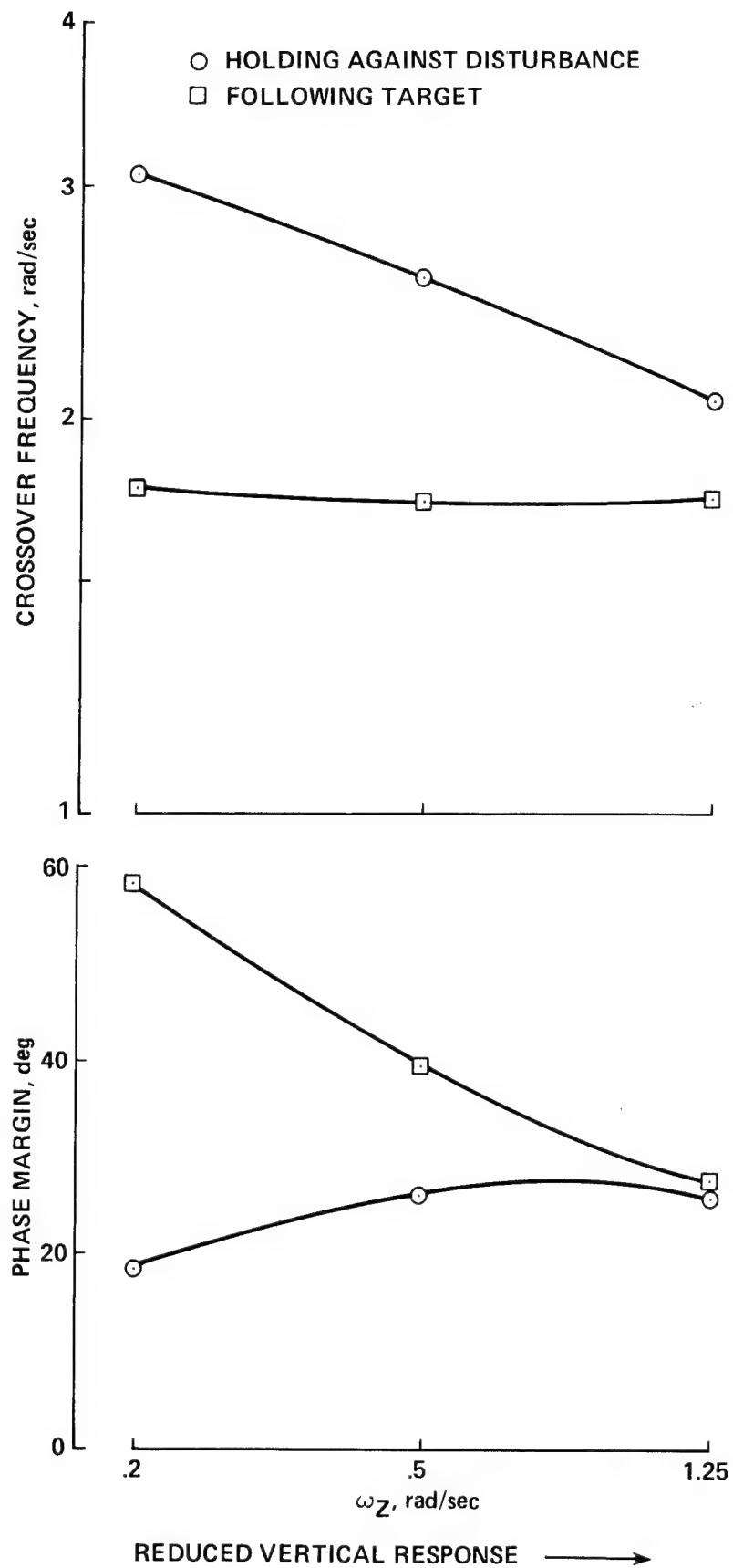


Figure 6.- Motion restriction effects on pilot/vehicle simulation fidelity.

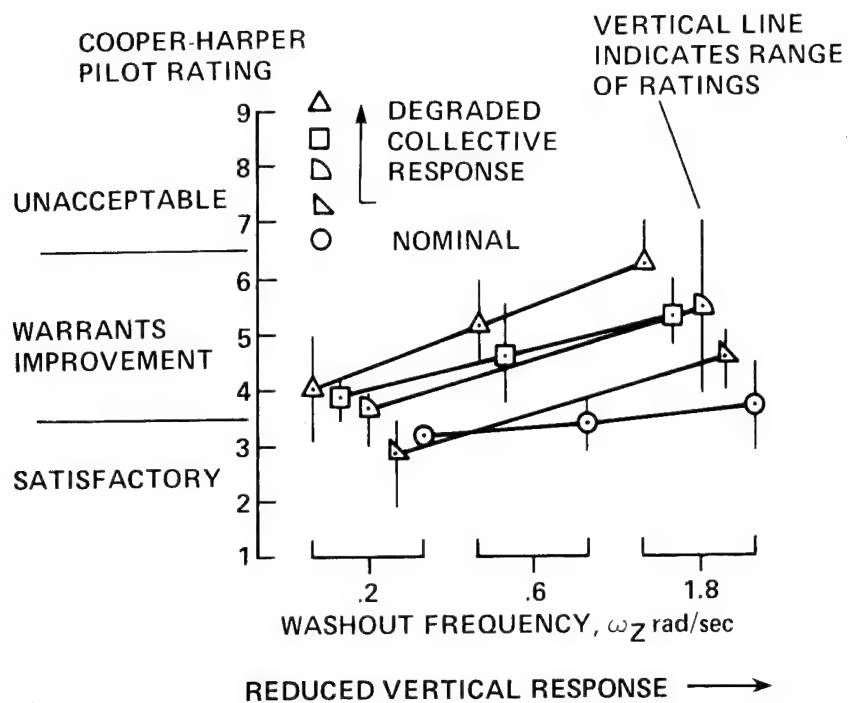


Figure 7.- Motion restriction effects on simulation fidelity for various vehicle characteristics.

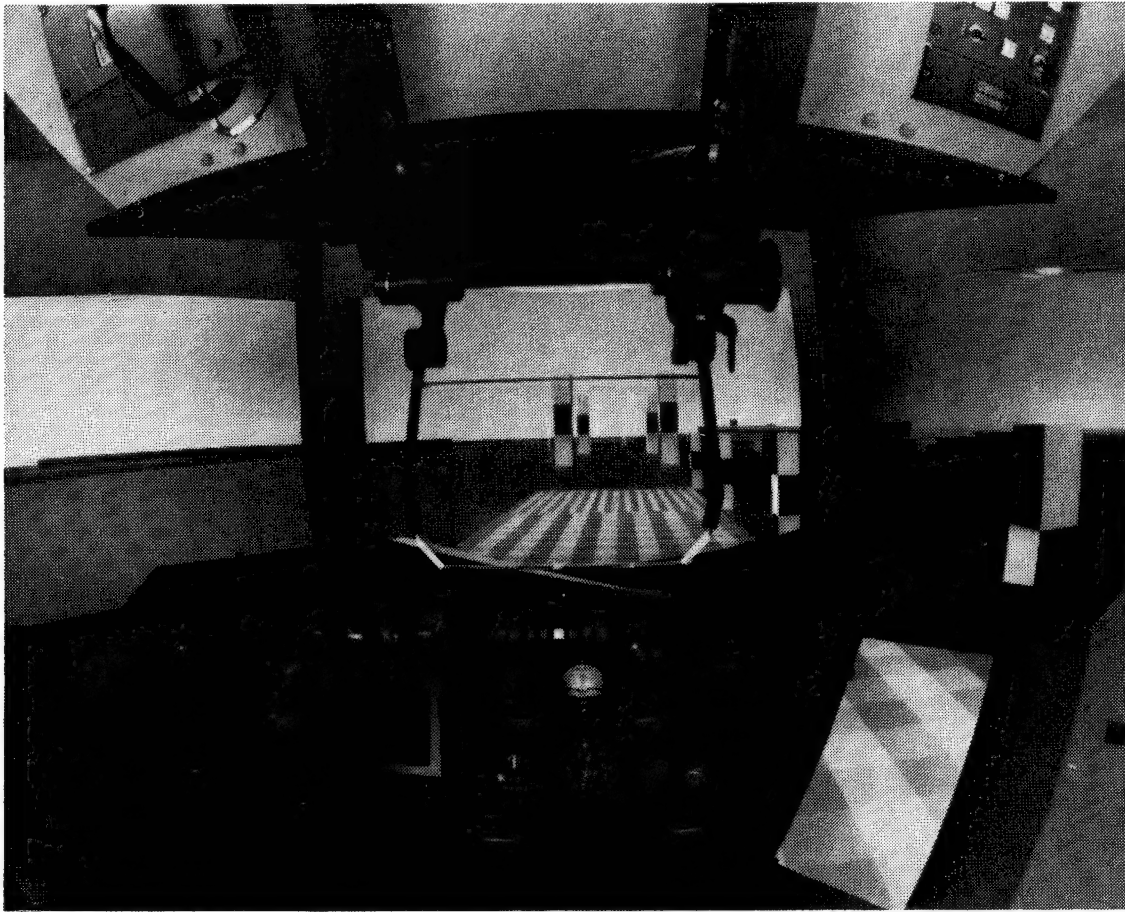


Figure 8.- Typical interchangeable cab layout.

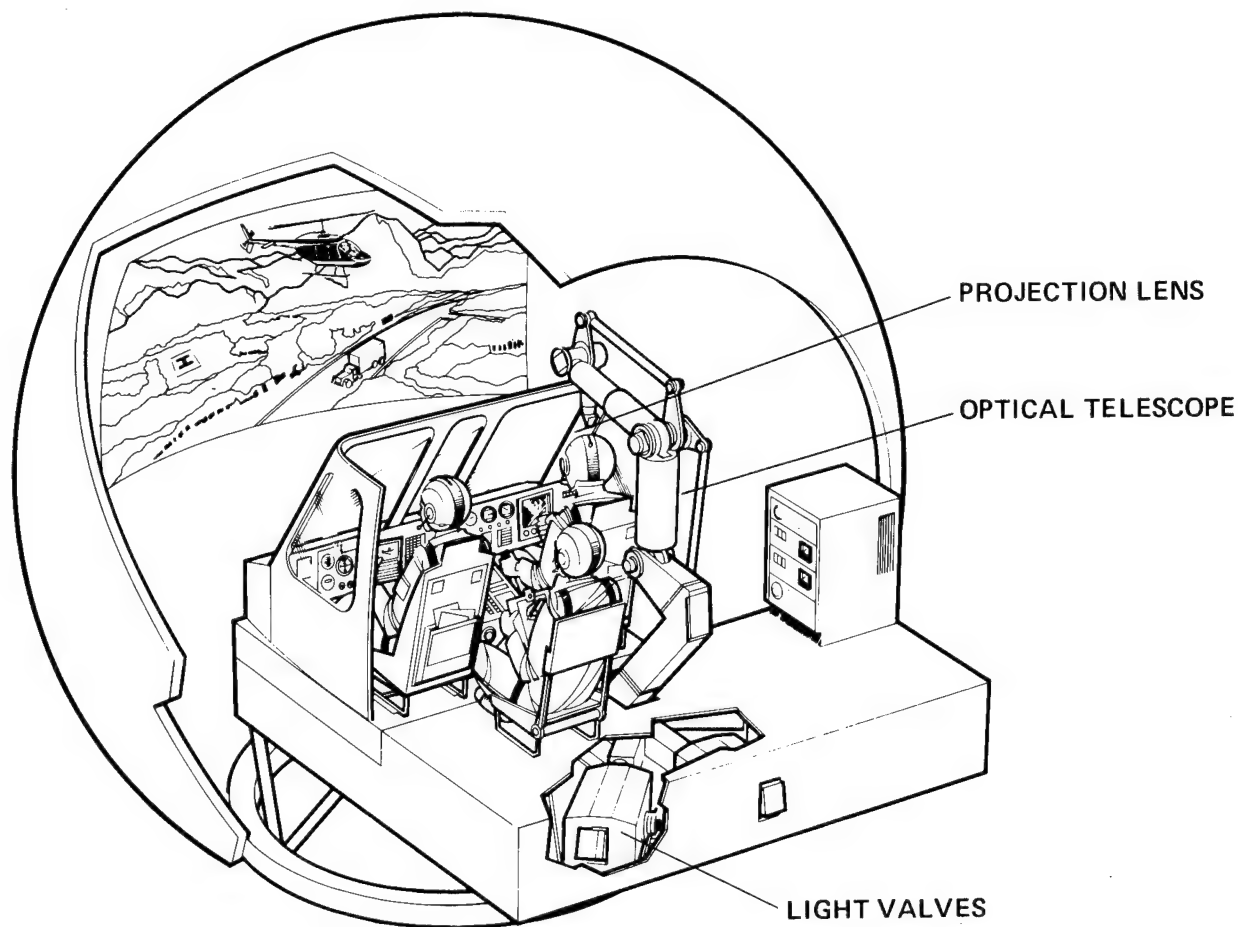


Figure 9.- Advanced cab and visual system (ACAVS).

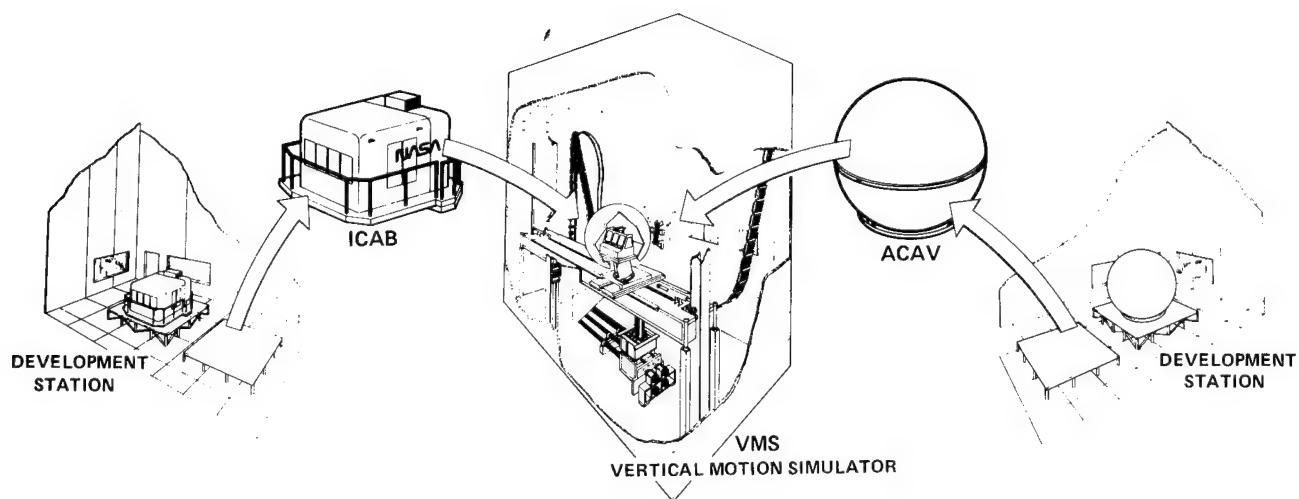


Figure 10.- VMS cockpit systems.

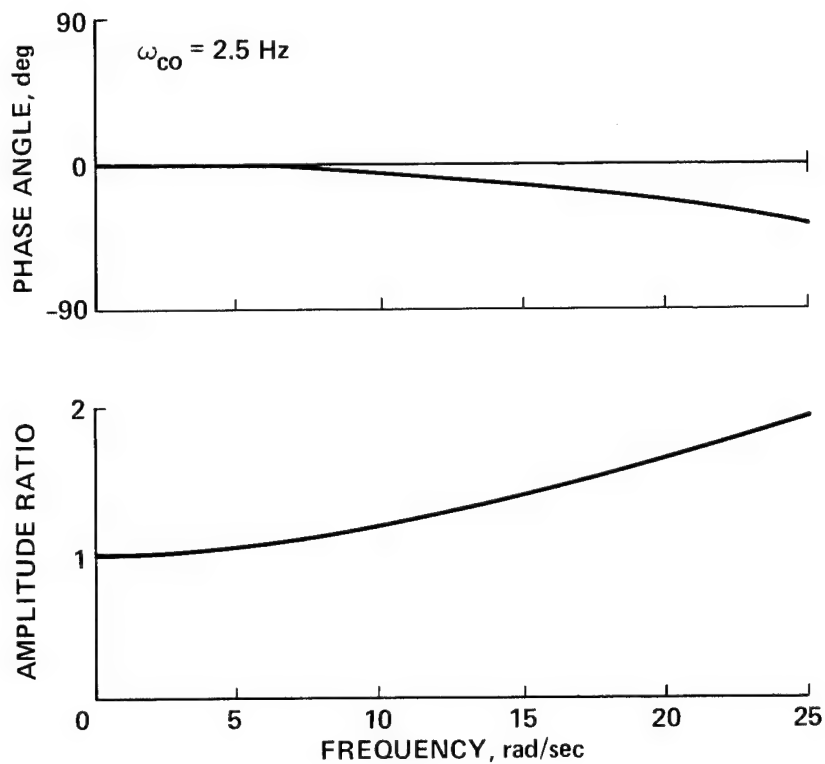


Figure 11.- CGI delay compensation with linear projection.

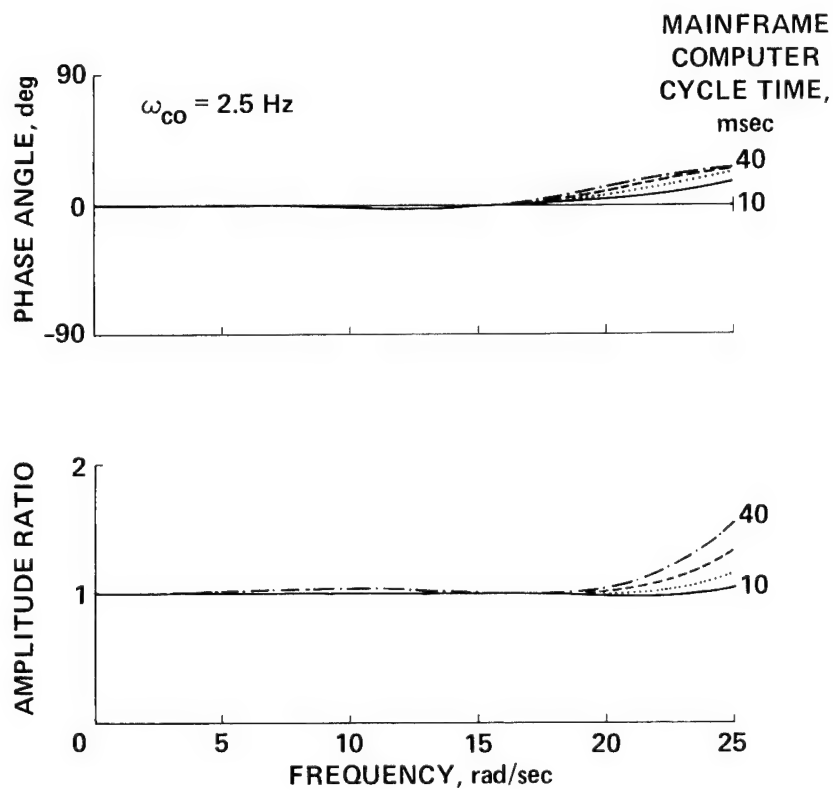


Figure 12.- CGI delay compensation with McFarland algorithm.

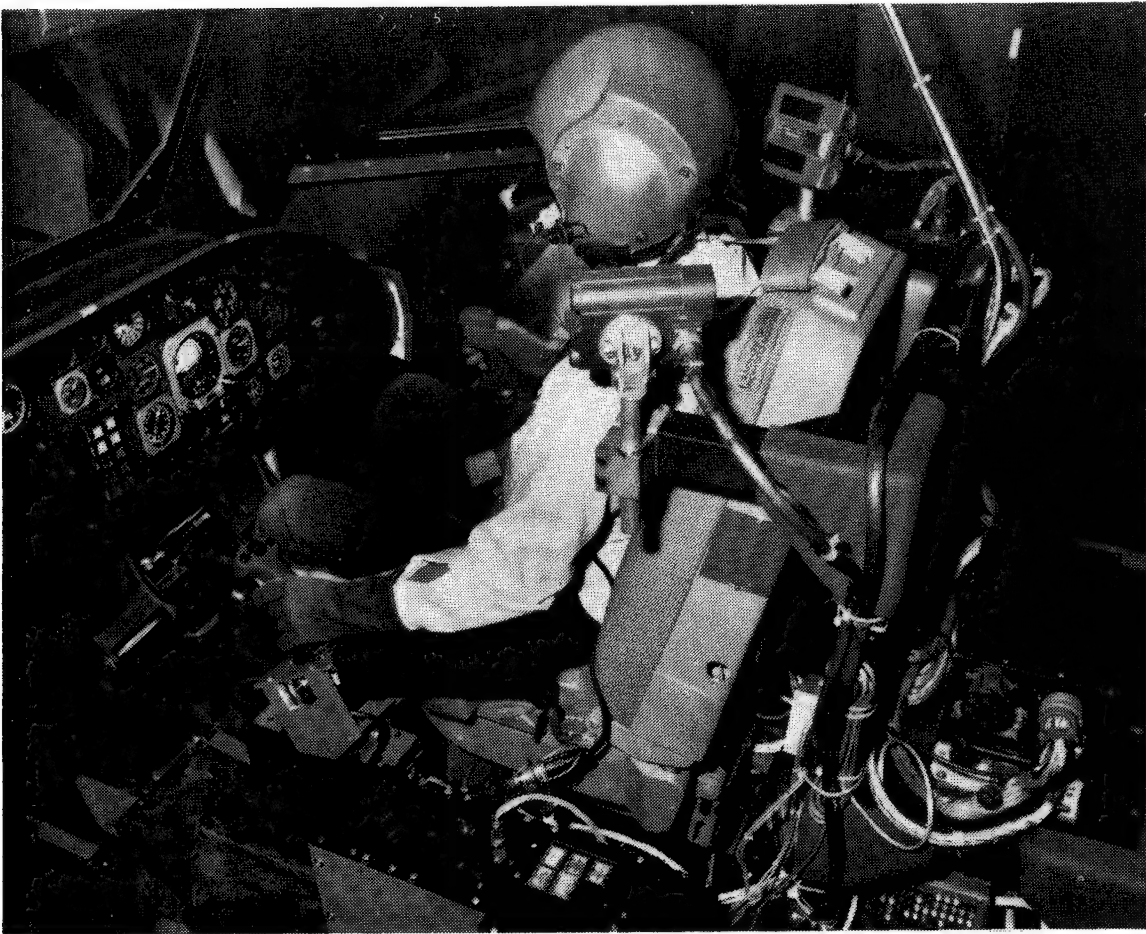


Figure 13.- Side-stick controller installation.

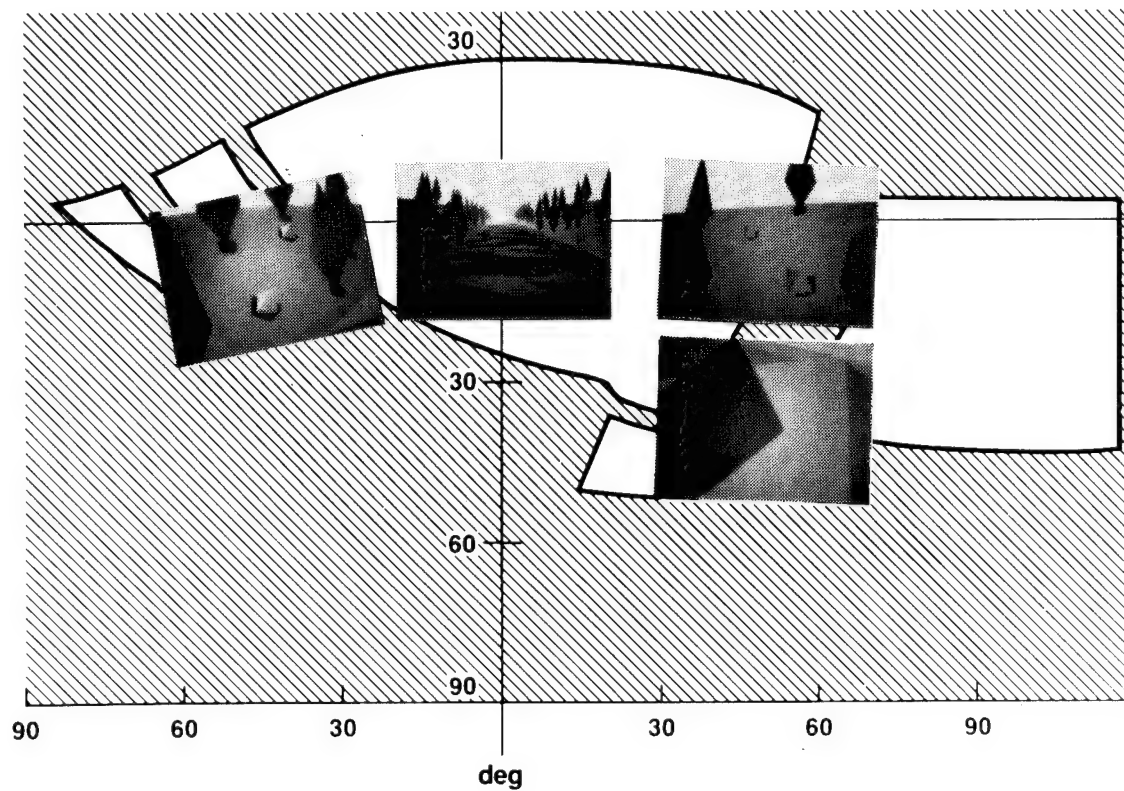


Figure 14.- Four-window computer-generated display of terrain scene.



Figure 15.- Integrated Helmet and Display Sight System (IHADS).

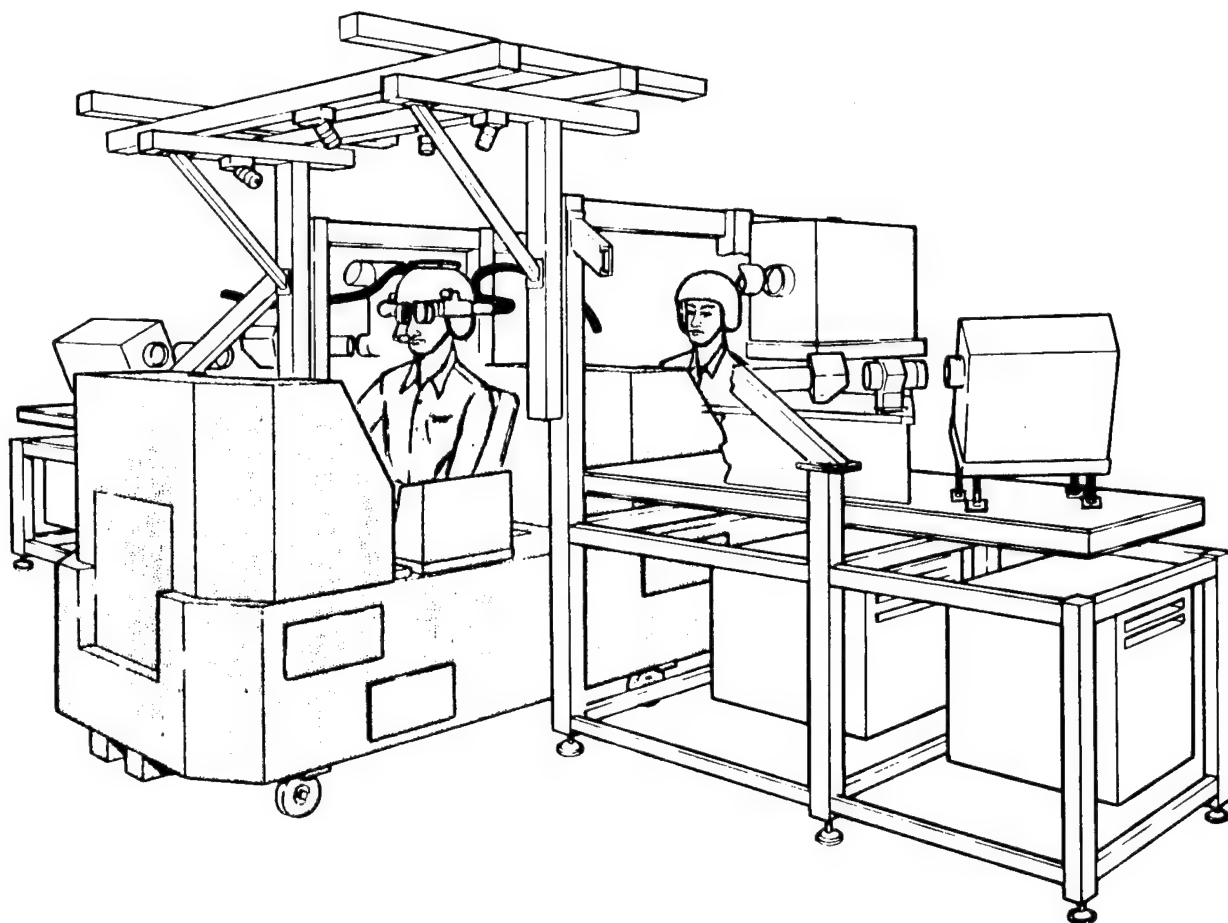


Figure 16.- Crew station structure.

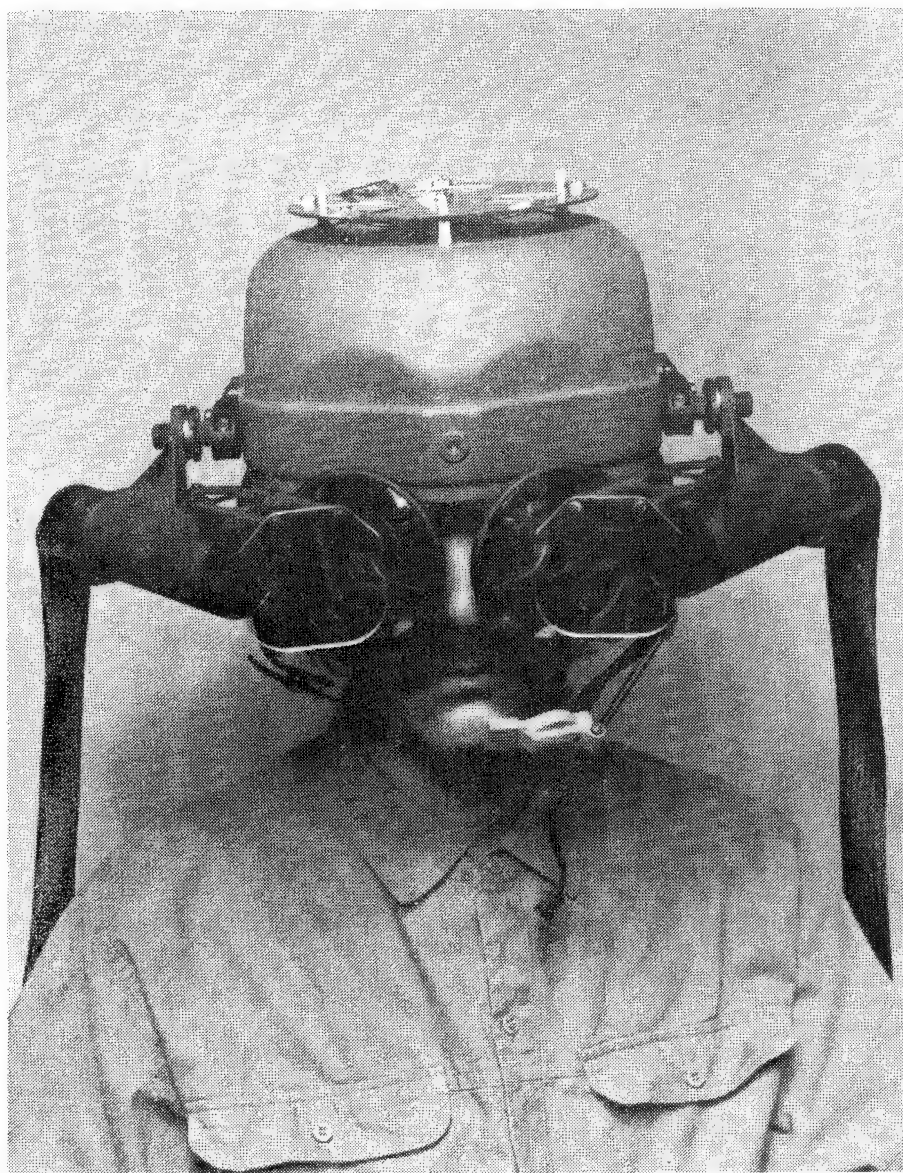


Figure 17.- Fiber-optic helmet-mounted display (FOHMD).

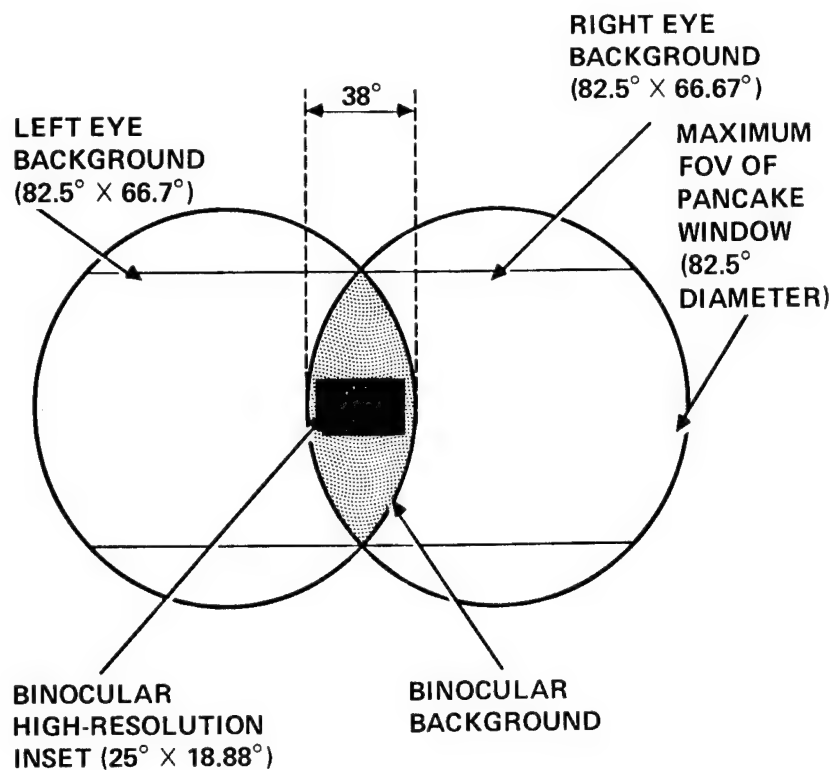


Figure 18.- FOHMD fields of view.

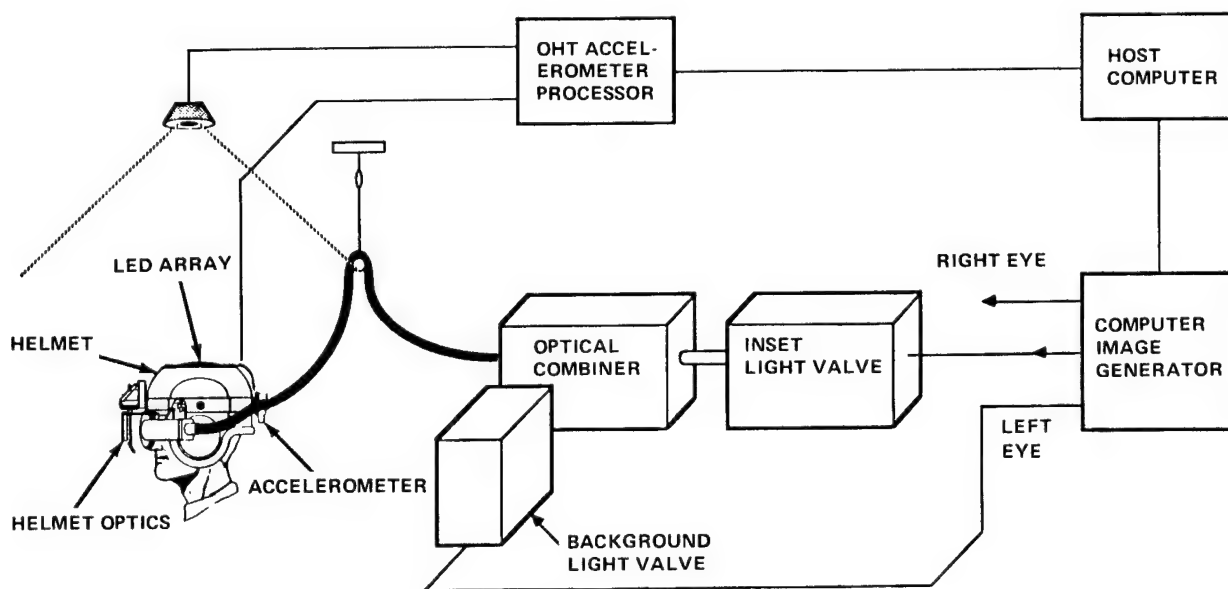


Figure 19.- FOHMD system components.

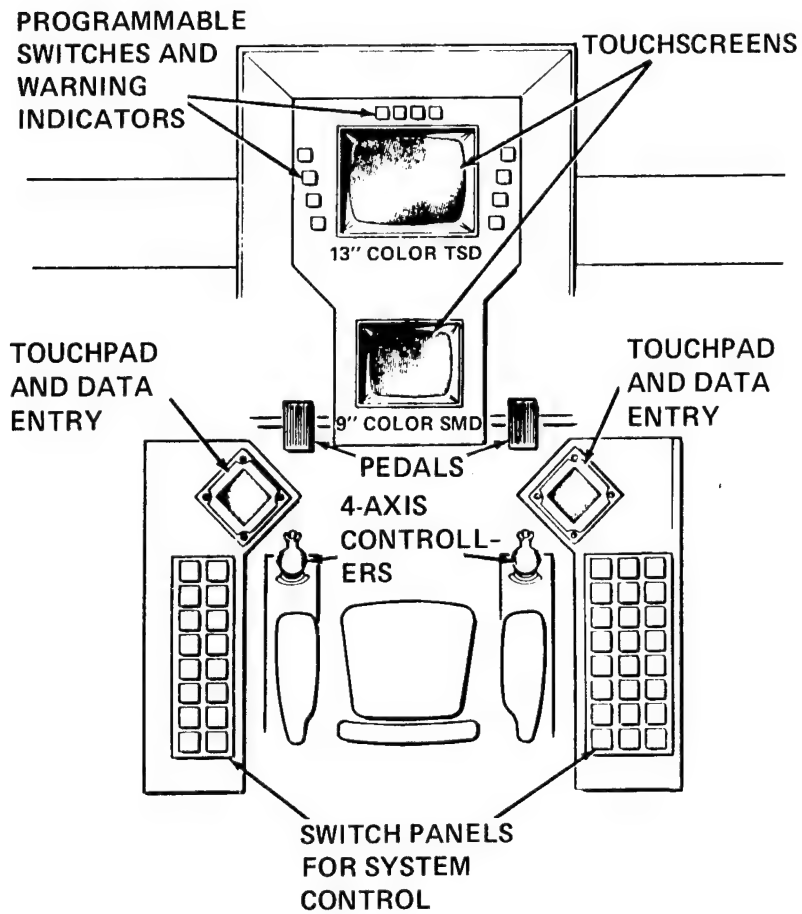


Figure 20.- Front crew station.

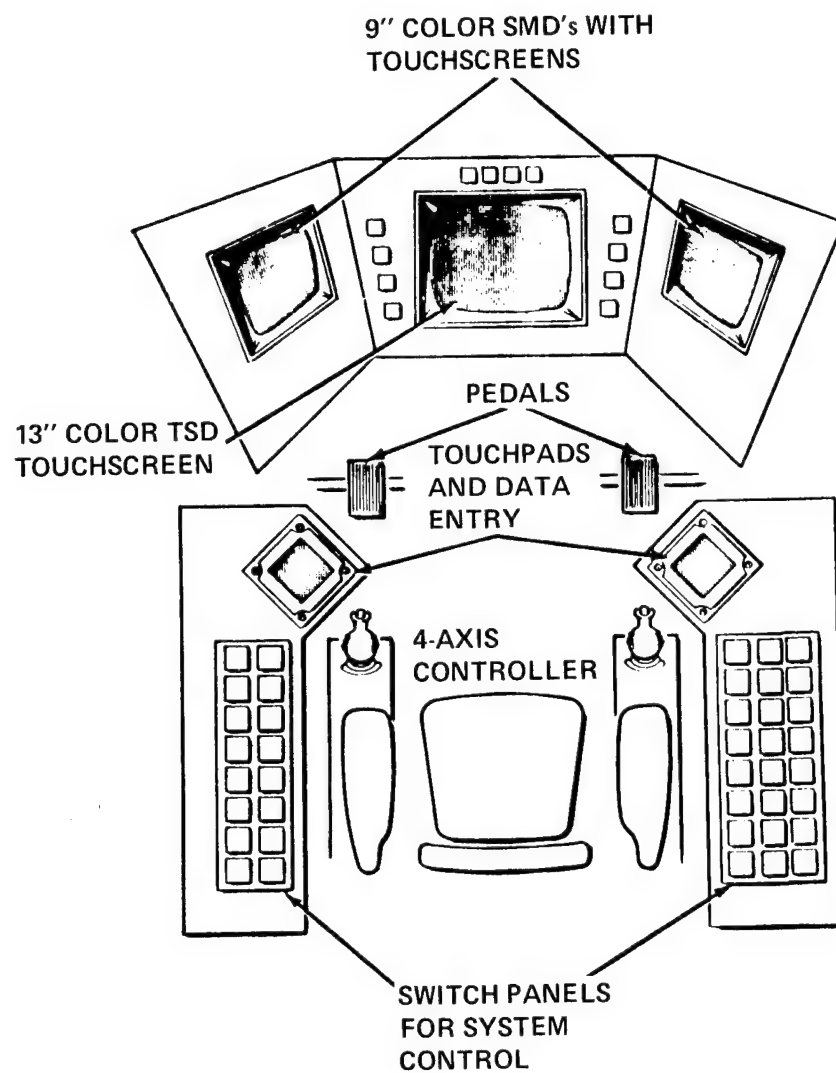


Figure 21.- Rear crew station.

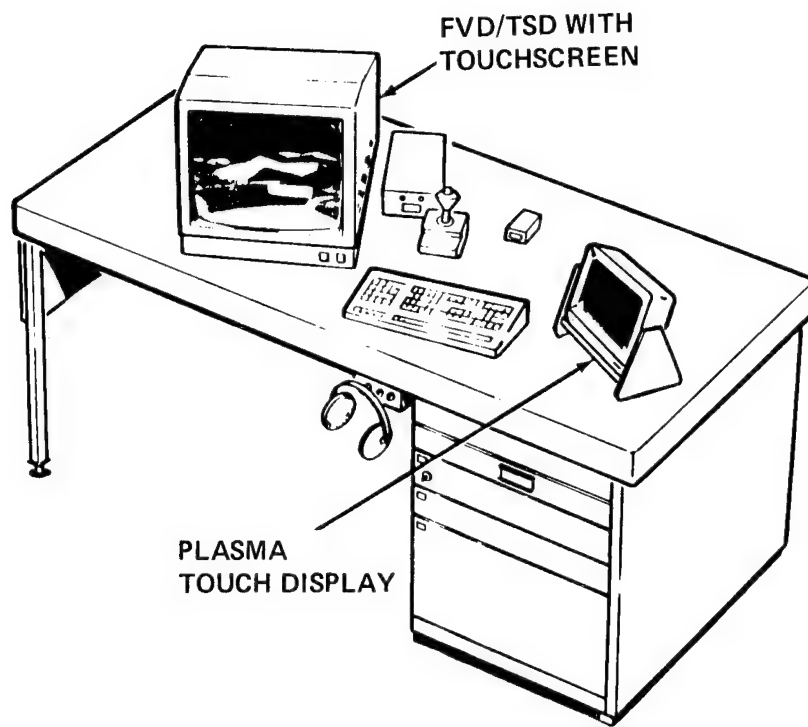


Figure 22.- Blue/Red Team station.

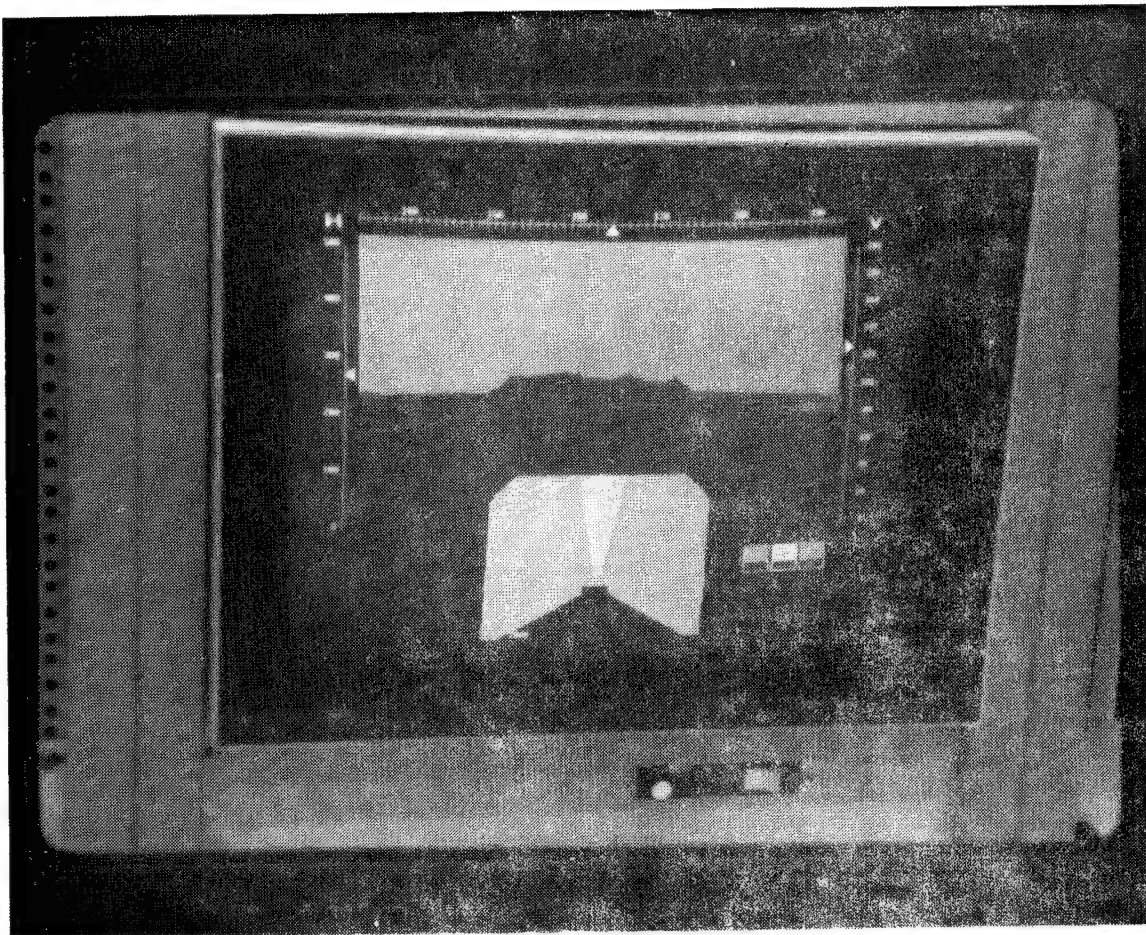


Figure 23.- Blue/Red Team forward-view display.

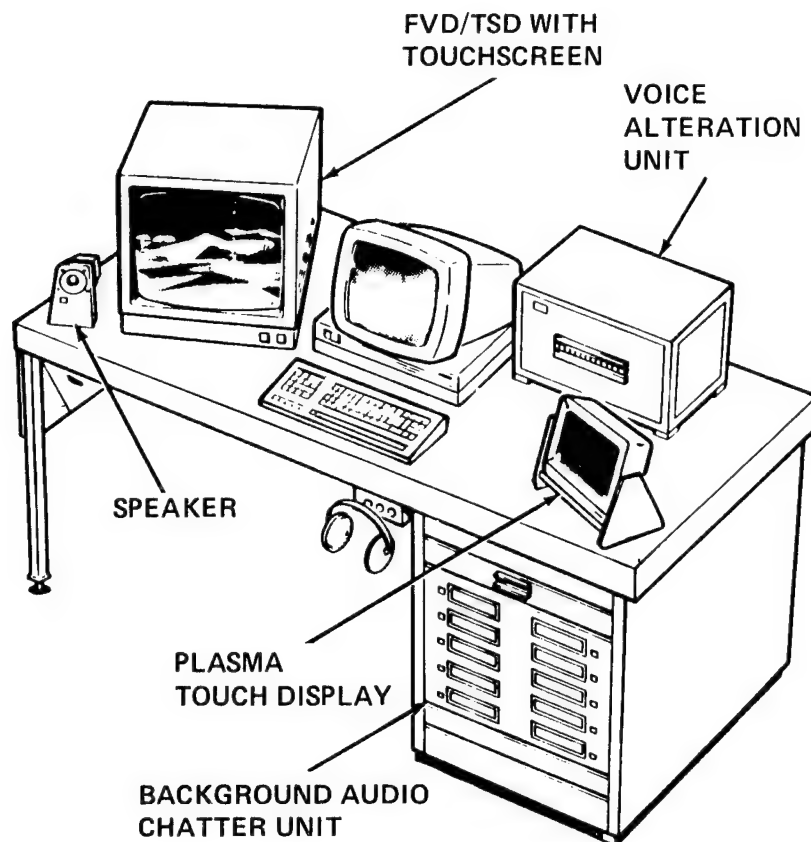


Figure 24.- White Team station.

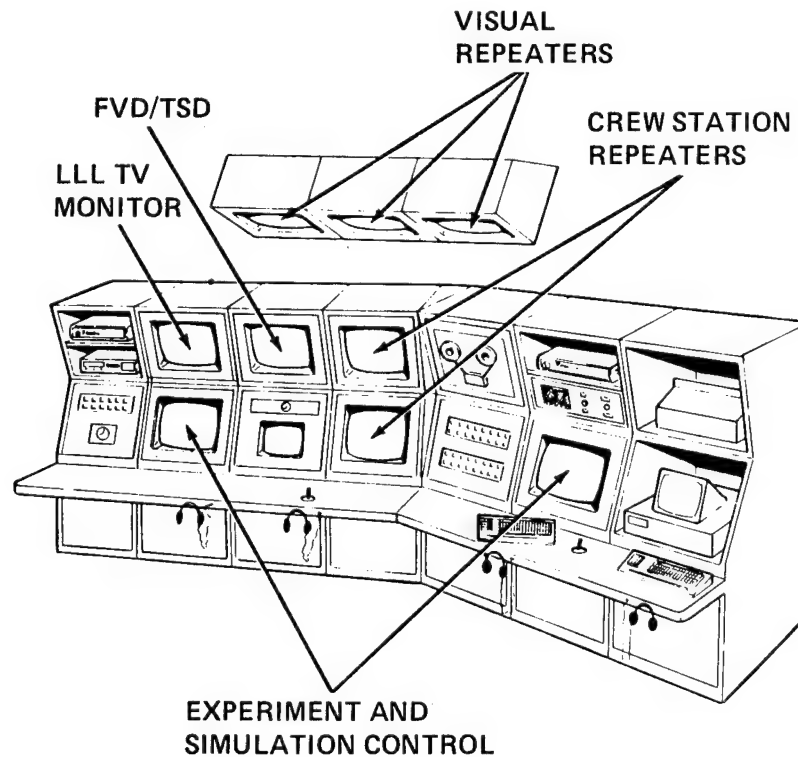


Figure 25.- Experimenter/operator console.

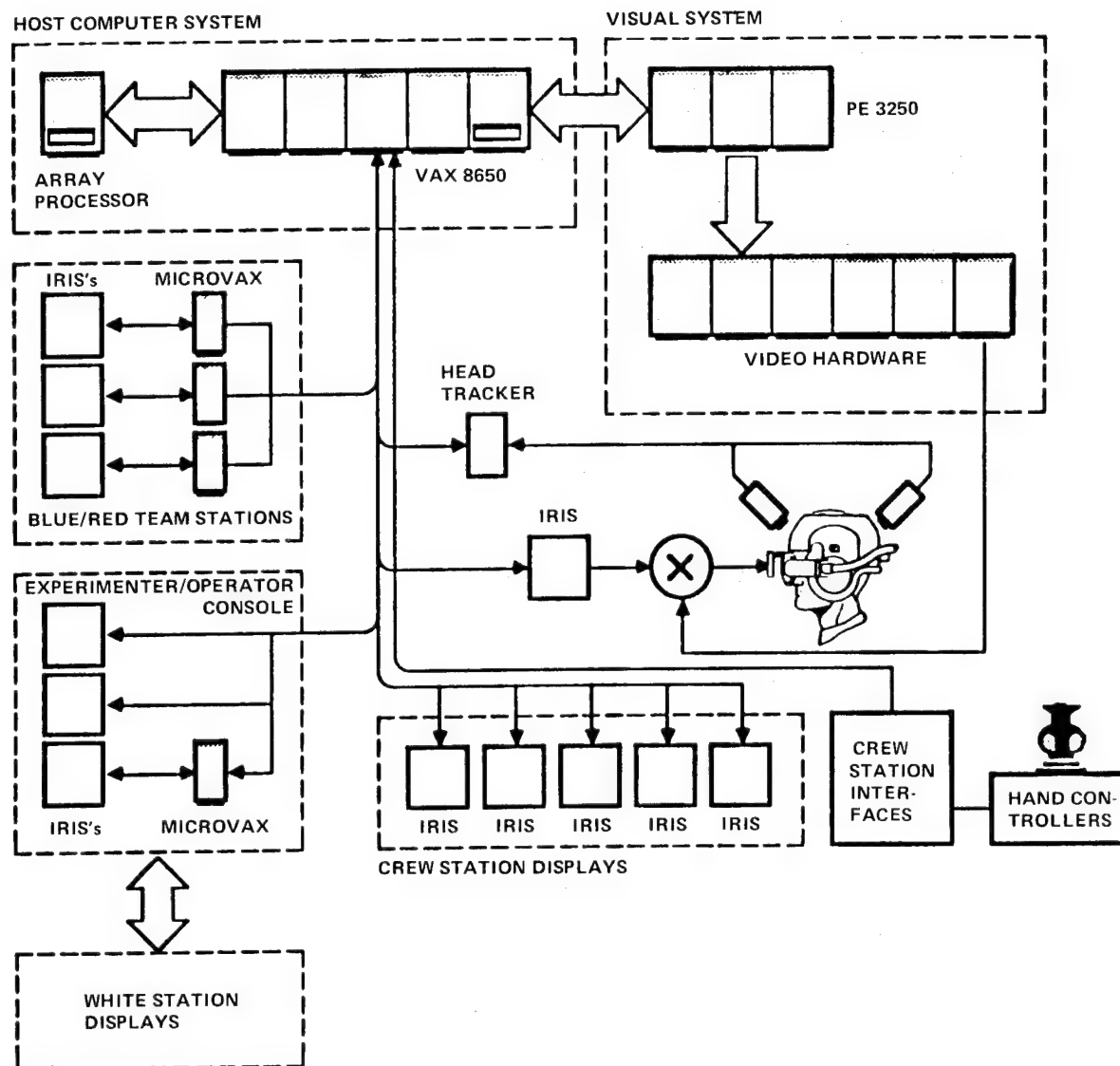


Figure 26.- CSRDF computer architecture.

SYSTEM ANALYSIS IN ROTORCRAFT DESIGN THE PAST DECADE

Thomas L. Galloway

National Aeronautics and Space Administration
Ames Research Center

Abstract

Rapid advances in the technology of electronic digital computers and the need for an integrated synthesis approach in developing future rotorcraft programs has led to increased emphasis on system analysis techniques in rotorcraft design. System analysis may be described as "putting it all together." The task in systems analysis is to deal with complex, interdependent, and conflicting requirements in a structured manner so rational and objective decisions can be made. Whether the results are wisdom or rubbish depends upon the validity and sometimes more importantly, the consistency of the inputs, the correctness of the analysis, and a sensible choice of measures of effectiveness to draw conclusions. In rotorcraft design this means combining design requirements, technology assessment, sensitivity analysis and performance benefits to evaluate system effectiveness. This paper reviews techniques currently in use by NASA and Army organizations in developing research programs and vehicle specifications for rotorcraft. These procedures span simple graphical approaches to comprehensive analysis on large mainframe computers. Examples of recent applications to military and civil missions are highlighted.

Introduction

System analysis is not an invention of the past decade, but it is receiving more widespread use in all types of design problems due to the increased availability of new desktop computing power. Reference 1 is an early example of the system analysis technique applied to VTOL missions which dates back to the 1950's. The task of system analysis is still the same. That is dealing with complex and interdependent problems in such a manner so that decisions may be made rationally and objectively. Early definitions of system analysis emphasized mathematical means and efficiency. This was largely descriptive of the methodologies that were introduced into the U.S. Department of Defense decision making by the RAND Corporation in the early 1960's. Today, the field has developed to encompass non-mathematical means of analysis and a greater concern with effectiveness, rather than mere efficiency. The systems approach is a process which involves: (a) a systematic examination and comparison of those alternative actions which are related to the accomplishment of desired objectives; (b) comparison of alternatives on the basis of the costs and benefits associated with each alternative; and (c)

explicit consideration of risk.

The rapid advances in desktop computing power during the past decade has provided the tools necessary to encourage widespread use of the system analysis approach. Figure 1 illustrates the change in computer availability and processing capability over the past decade. Ten years ago, when the 8-bit personal computer was introduced in quantity, it provided access to a more user friendly tool than the mainframes but with limited computing power. Advances in operating systems and semi-conductor technology narrowed the gap in the user-friendly concepts of the mini-computer and the power of the mainframe. The continuing advances in 32-bit chip technology has created the current era of the modern graphics workstation with highly useful desktop computing power. Continued cost reductions in these workstations has also led to their increased utilization. Moreover, advancements in networking and database management provide the capability for multiple users to share information on complex projects as well as have access to powerful super-computers. In the future, the application of artificial intelligence technology through expert systems will continue to enhance the application of the system analysis process in aerospace design problems.

System Elements

All systems begin as a gleam in the eye of someone and undergo many different phases of analysis, testing, and development before being deployed, made operational, or marketed. This is true for weapon systems, transportation systems, or new products. The role of system analysis is to develop a systematic procedure for evaluating design options against measures of effectiveness to achieve the objectives. The three basic elements of system analysis have not changed over the years. They are: (a) establishing the objectives; (b) selecting the measures of effectiveness; and (c) developing a model to use in the analysis. These elements can be considered to form a pyramid as shown in Figure 2 with the foundation being the model of the system.

In recent years there have been several software programs developed for desktop personal computers that can provide assistance in developing project outlines and plans which can contribute to establishing objectives and measures of effectiveness. This paper will not address those tools. The focus of this paper is on the modeling concepts that are used in developing rotorcraft concepts and evaluating technological advances. With the increase in desktop computing power, the engineer can now explore many design options early in the design process. This does not mean that the engineer is being replaced by the computer but that his capability is being enhanced through more powerful tools which frees him to be more creative. Although the subject here is rotorcraft, the techniques are applied throughout the aerospace industry.

System Models

For purpose of discussion the models used in the design analysis process will be divided into two major categories. One will deal with models used in the integrated analysis of a design. The other, addresses models used by specialists for analysis of a specific technical area. The models in both categories play key roles in analyzing the design options and evaluating the selected measures of effectiveness. Various levels of sophistication can be incorporated into the models that are part of the system or design analysis process. Many of the models originated 15 - 20 years ago but their utility has been enhanced with pre- and post- processors that take advantage of the more user-friendly computing environment of today. Some models are computerized versions of simple graphical approaches while others represent capability that resulted directly from the development of the modern graphical workstation.

The initial discussion will deal with models that are in the category of integration. These models are constructed so that the various technical disciplines are analyzed in such a manner so the interaction among disciplines results in a more balanced design. Figure 3 depicts the flow of information through a typical integration or synthesis model. The synthesis code estimates the vehicle performance based on input mission requirements and constraints for a given level of technology assumptions. Vehicle weight, power, and geometric characteristics are computed along with mission performance parameters. These analytical models and associated input data are generally calibrated using either experimental test results or predicted results from a more specialized analysis.

These models are useful for performing tradeoff studies, sensitivity analysis, concept comparisons and technology evaluations. They are used through out the rotorcraft and fixed wing industry. Some examples of those used by the government are listed in figure 3. References 2 and 3 describe the HESCOMP and VASCOMP models in more detail. These two models, a jointly developed Army and NASA tilt rotor model, and a Army helicopter model provided the tools necessary to perform the JVX Joint Technology Assessment study of 1982. In the initial two months of study 12,000 evaluations were performed in assessing two helicopter concepts, a tilt rotor, and a lift-fan operating over 19 different missions. In the final three months of study, 5000 evaluations were performed on the tilt rotor investigating alternate engines, rotors, wings and mission capability. These type of models coupled with the advances in computer utility are the only way the 100-125 evaluations per day could be achieved for the JVX study in that short amount of time. Being able to perform such a detailed assessment in only five months, meant a timely program, with definitive specifications, was developed to meet the services window of opportunity.

Most of these models can be run efficiently on the modern 32-bit workstations. On the other hand, using the powerful spreadsheets that have appeared on the market in recent years also provides an effective means to use simplified versions of synthesis models in the early stages of concept evaluation.

The models under the category of specialization are broken into two areas. One is classified here as configuration development, the other as specialized analysis. Figure 4 gives some examples of models in each area. The models listed under configuration development are mainly commercially available products that allow drafting type of functions to be accomplished in a very efficient and rapid manner. The modern graphics workstation is very effective in providing a user-friendly environment for these configuration development models.

The specialized analysis area refers to models that have been developed to perform detailed technical analysis of a specific discipline. As listed in figure 4 these cover the disciplines of structure and loads, aeromechanics, rotor design, and flow-field analysis. The computing power that is now available in workstations allow many of these models to be used interactively early in the design process.

There are some very natural links that can be made between the models described in the previous paragraphs. Some of these links can be automated while others still require the engineer in the loop. Figure 5 depicts the possible links. Under the specialization category there is a natural link for flow of geometric information from the configuration development model to the specialized models. The configuration tools can generate finite element grid type of input definition which is required by specialized models such as NASTRAN and VSAERO. There can be a two way flow of information between the synthesis model and the models in the specialization category. The synthesis model may contain a post-processor that can create a paneling of the resulting geometry to pass to both the configuration development area and the specialized analysis area. This eliminates considerable time in preparing the details usually required for the more complex models. Refined geometric dimensions will flow to the synthesis model from the configuration development model after the volume requirements for the various components have been packaged and the resulting vehicle envelope determined. As mentioned previously, information from the specialized analysis area can be used to calibrate the simplified techniques used in the synthesis model and also provide guidance in establishing the achievable technology levels.

Reference 4 presents the results of a study which utilized this multiple model approach to investigate the feasibility of high-speed tilting-prop-rotor aircraft. The aeromechanics calculations were performed using the Comprehensive Analytical

Model of Rotorcraft Aerodynamics and Dynamics (CAMRAD) of reference 5, a new wing airfoil was designed by a two-dimensional transonic, viscous-flow model (reference 6), the configuration definition utilized the ANVIL 4000 drafting package, and the vehicle synthesis was performed by the Army/NASA tilt rotor code. Figure 6 and 7 show three-view general arrangements of the resulting high-speed, civil transport and the high-speed, air-combat fighter designs. The civil design carries 46 passengers 600 nautical miles at 375 knots. The air-combat fighter is a single pilot design having a 200 nautical mile mission radius and a 400 knot speed capability.

Expert Systems

Although great strides have been made in the productivity and quality of the design process using the system analysis approach there still exists techniques to enhance the process in the future. Knowledge-based expert systems are being considered by many researchers in the aerospace industry to assist in the design procedure. Reference 7 provides some excellent background on how these systems can be used in aircraft conceptual design. Reference 8 describes a second generation expert system, that is currently under development, which will be used in the design of hypervelocity vehicles. The current development is structured around modules that reasons how to solve a design and analysis problem from the knowledge it has on relevant computerized models. It then manages the sequence it has drawn up to execute the models and controls the data input-output flow until the problem is solved. This "Expert Assistant" offers the potential for aiding the design process in a way that is similar to that of numerical optimization, except that it would address discrete, discontinuous, abstract, or any other non optimized aspect of vehicle design and integration. Other unique capabilities such as automatic discovery and learning in design may also be achievable. This could be developed into a tool that would allow the training of people in the system analysis process and also provide expanded analysis capability for junior-level engineers.

Concluding Remarks

The system analysis process has been significantly enhanced in the past decade because of the rapid advances in computer technology. The performance and relatively low cost of the modern workstation let small companies, small groups within an organization, and individual designers have computing power they can control right in their offices. The development of user-friendly interfaces allows existing models to be networked in an efficient manner. Engineering tasks that would take months to perform in the past can be accomplished in weeks. This increase in productivity can also allow the performance of broader trade studies to enhance the quality of the output. In the future the incorporation of expert systems will provide a "designer

assistant" that will increase the usefulness of junior engineers, make analysts of designers and vice versa, and offer the potential for further reductions in product development time and cost while increasing product quality.

References

1. Schnebly, F. David, "The Systems Approach to the Selection of VTOL Aircraft Design Specifications," Presented at the National Naval Aviation Meeting, August 5-10, 1957, San Diego, CA.
2. Davis, S.J., Rosenstein, H., Stanzione, K.A. and Wisniewski, J.S., "User's Manual for HESCOMP The Helicopter Sizing and Performance Computer Program," Boeing Vertol Company, Second Revision October 1979.
3. Schoen, A.H., Rosenstein, H., Stanzione, K.A. and Wisniewski, J.S., "User's Manual for VASCOMP II The V/STOL Aircraft Sizing and Performance Computer Program," Boeing Vertol Company, Third Revision, May 1980.
4. Johnson, Wayne, Benton, Lau H. and Bowles, Jeffery V., "Calculated Performance, Stability, and Maneuverability of High-Speed Tilting-Prop-Rotor Aircraft," Presented at the Twelfth European Rotorcraft Forum, September 22-25, 1986, Garmisch-Partenkirchen.
5. Johnson, Wayne, "A Comprehensive Analytical Model of Rotorcraft Aerodynamics and Dynamics," NASA TM 81182, 81183, and 81184, 1980.
6. Hicks, Raymond M., "An Assessment of a Modified Potential Flow Code for Calculating the Effect of Small Geometric Change on the Pressure and Forces of Supercritical Airfoils," NASA TM 84227, 1982.
7. Kidwell, George and Eskey, Megan, "Expert Systems and Their Use in Augmenting Design Optimization," AIAA Paper 85-3095, Colorado Springs, CO., October 1985.
8. Mitchell, Alan R., "Market Supremacy Through Engineering Automation," Aerospace America, Vol. 25, No. 1, January 1987.

COMPUTER TECHNOLOGY

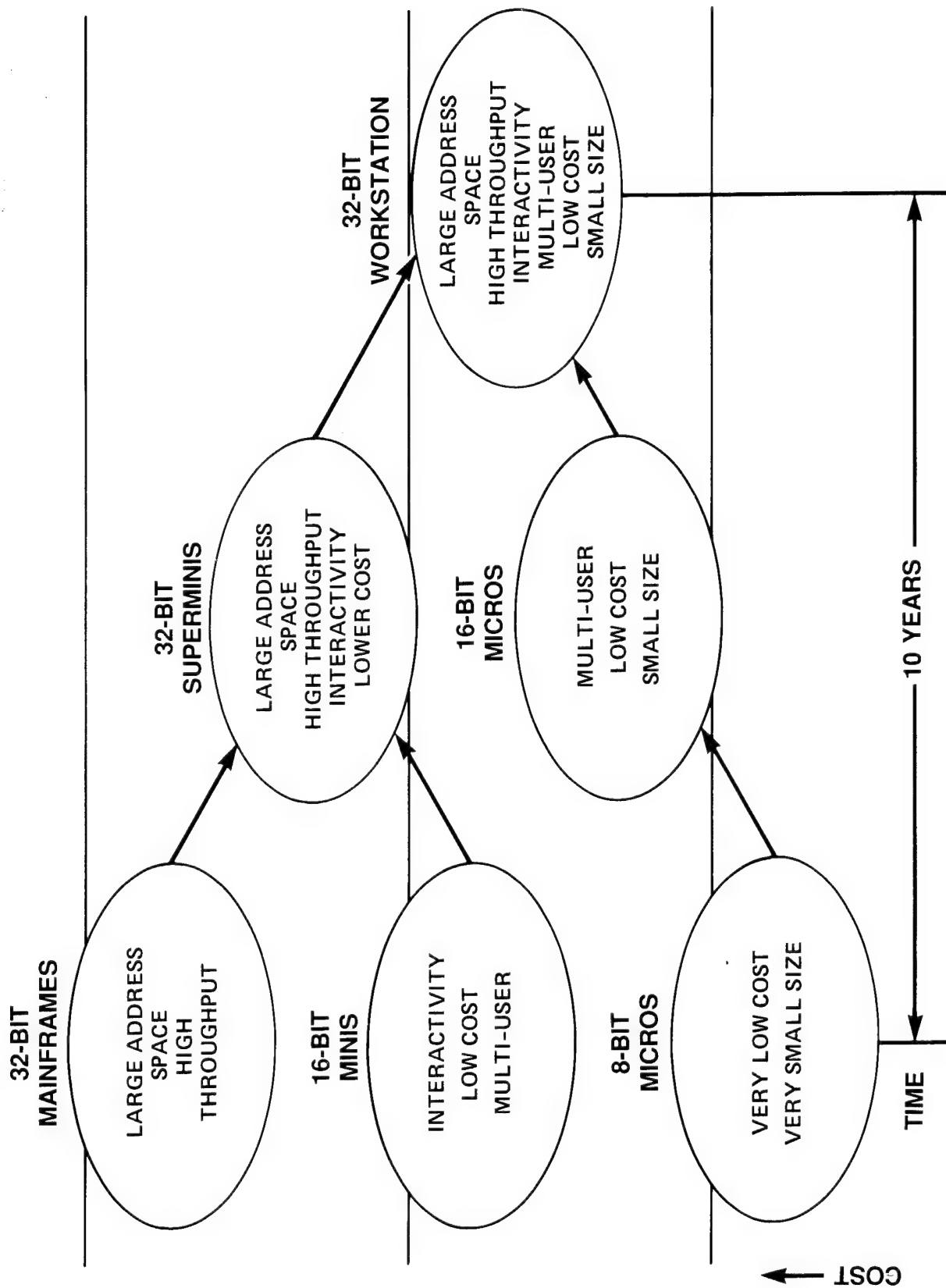


Figure 1.

MAJOR ELEMENTS OF SYSTEMS ANALYSIS

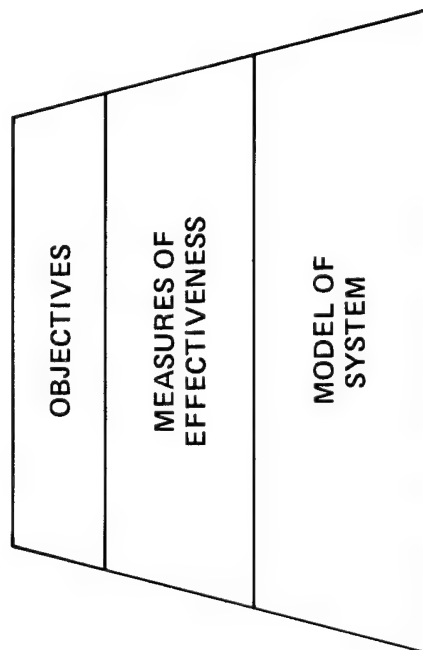


Figure 2.

INTEGRATION MODELS

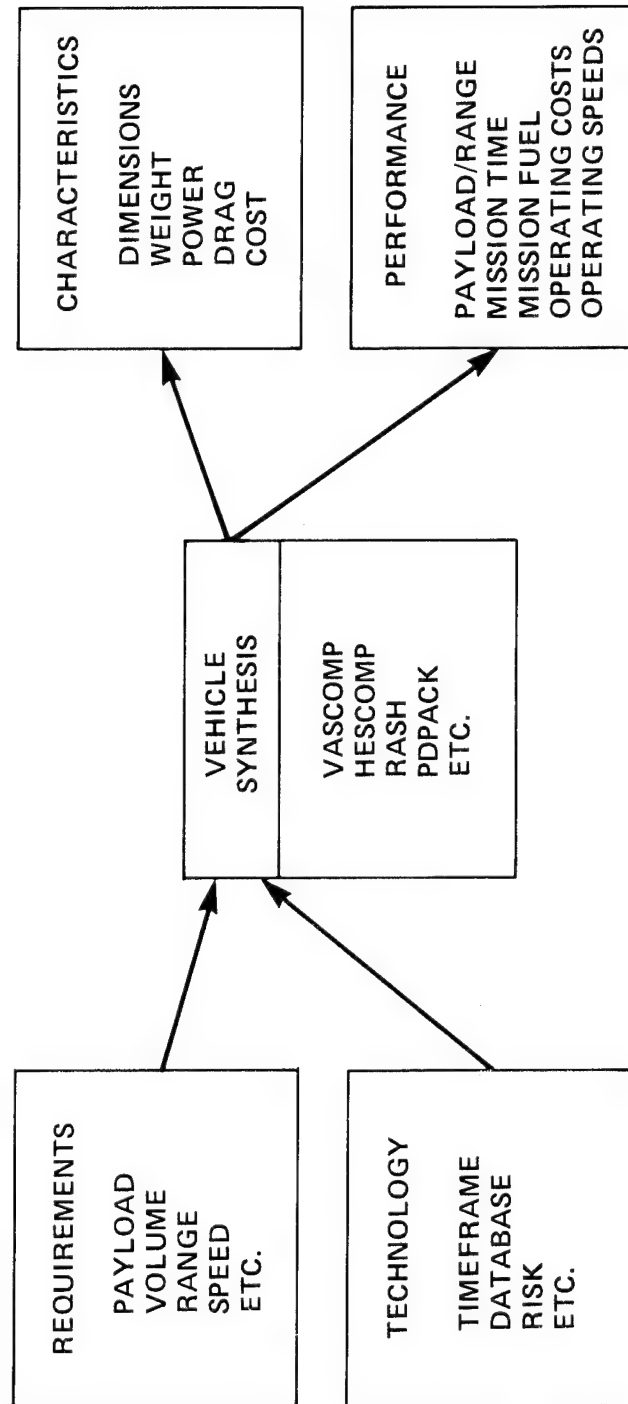


Figure 3.

SPECIALIZATION MODELS

CONFIGURATION DEVELOPMENT	SPECIALIZED ANALYSIS
CADAM CATIA ANVIL CDS ETC.	NASTRAN CAMRAD ROT22 VSAERO ETC.

Figure 4.

ROTORCRAFT SYSTEM ANALYSIS

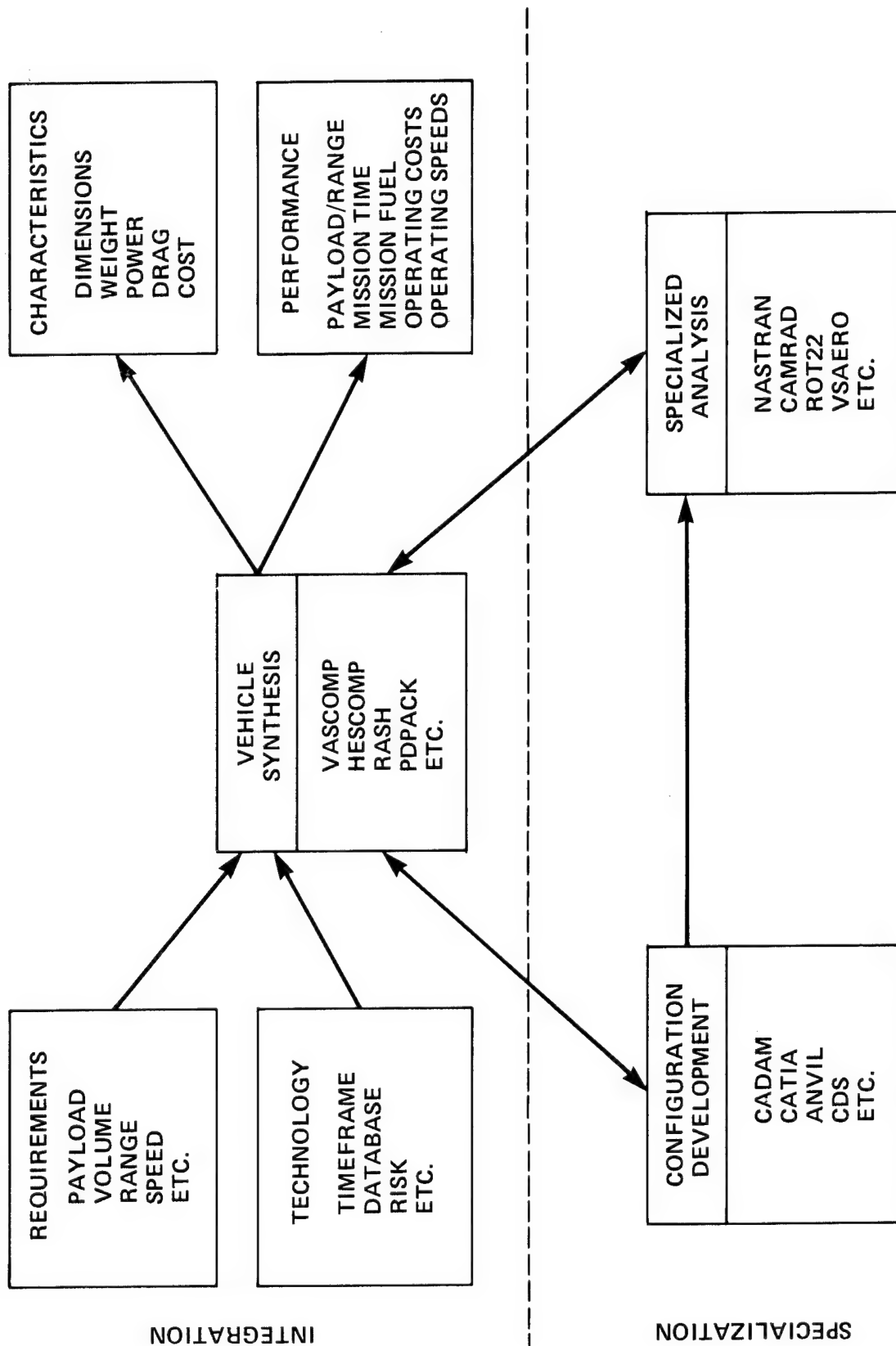


Figure 5.

HIGH SPEED CIVIL TRANSPORT DESIGN

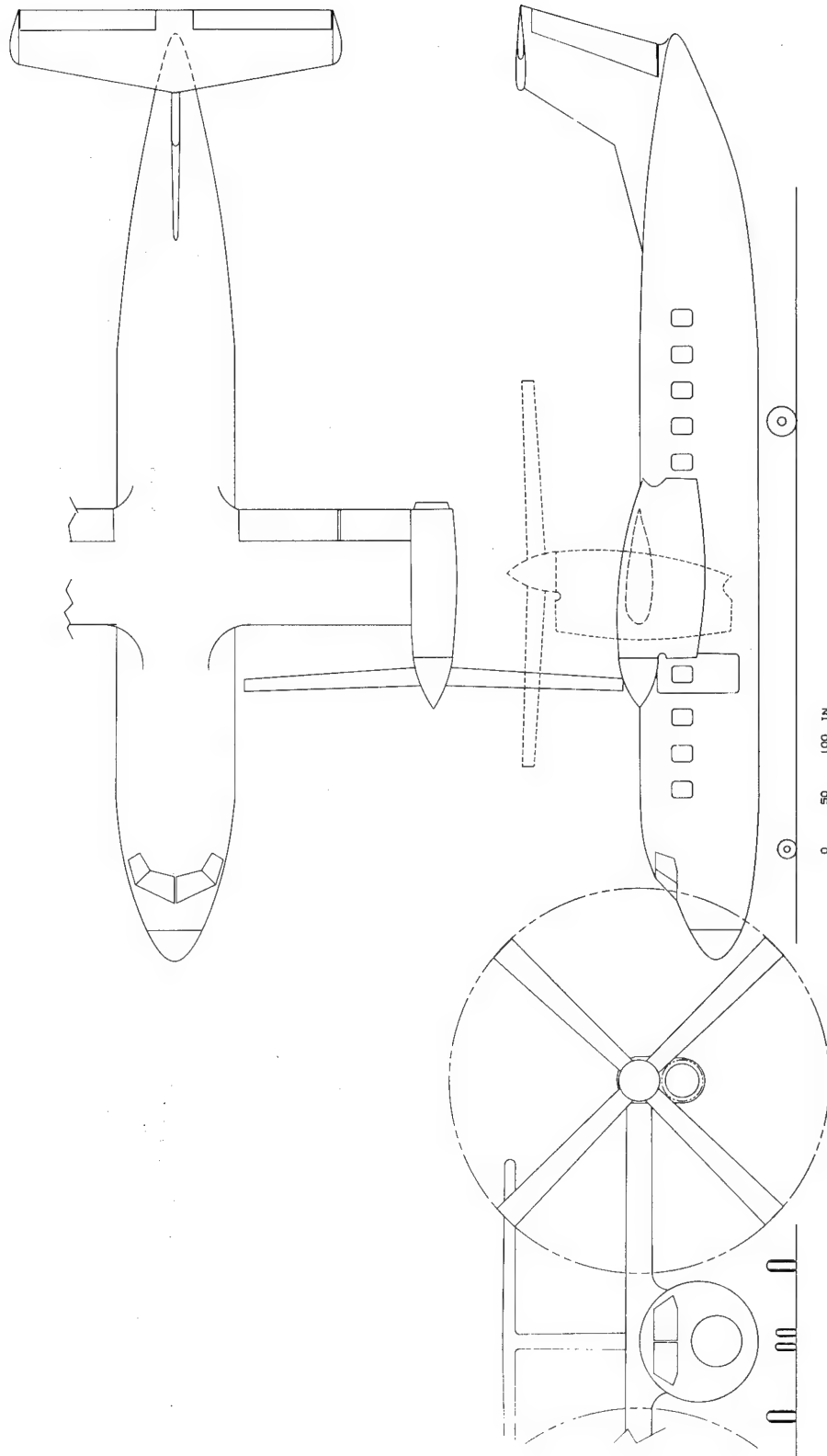


Figure 6.

HIGH SPEED AIR-COMBAT FIGHTER DESIGN

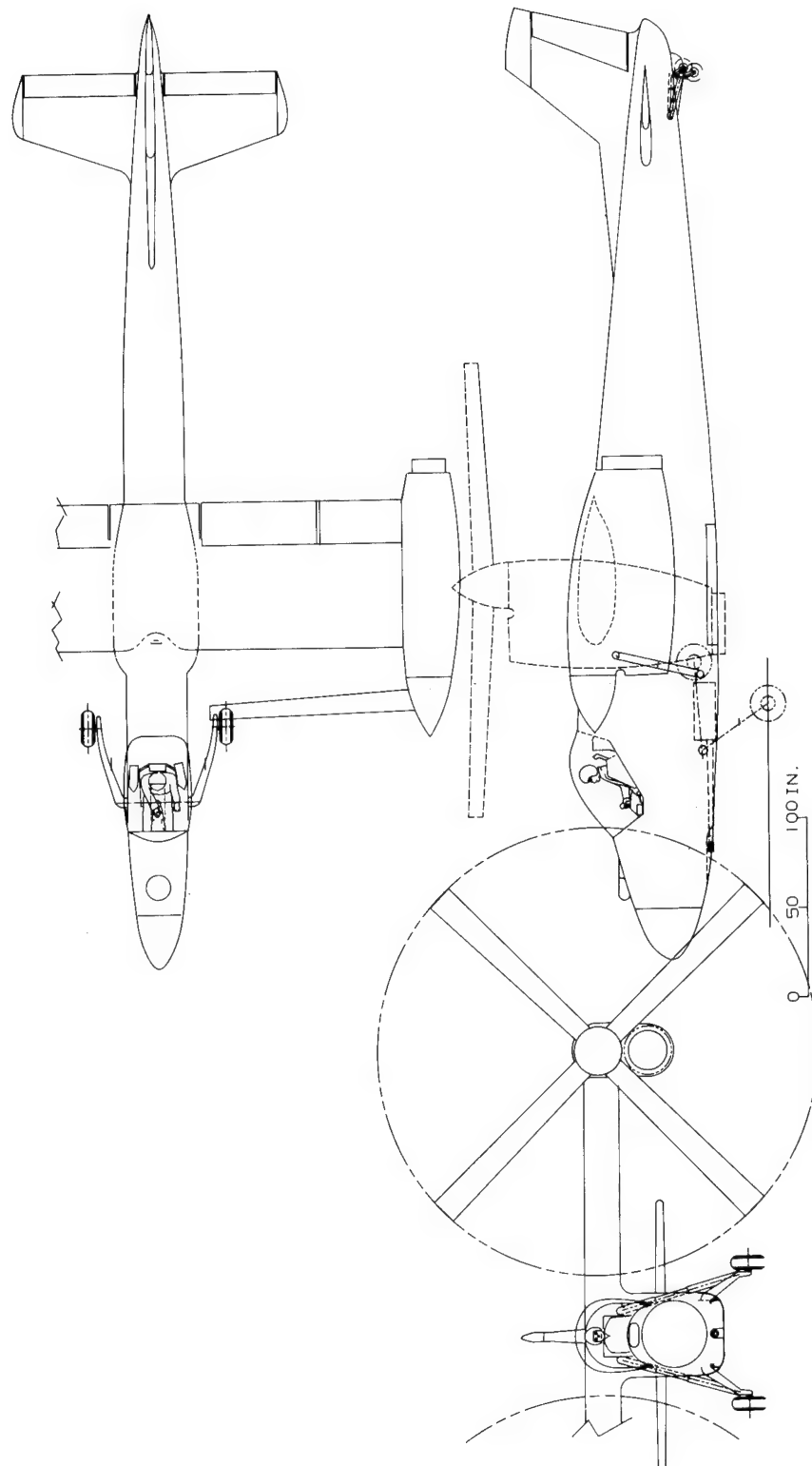


Figure 7.

AN INTEGRATED APPROACH TO ROTORCRAFT HUMAN FACTORS RESEARCH

Sandra G. Hart,
NASA - Ames Research Center
Moffett Field, CA

E. James Hartzell James W. Voorhees Nancy M. Bucher R. Jay Shively
U.S. Army Aeroflightdynamics Directorate
Moffett Field, CA

ABSTRACT

As the potential of civil and military helicopters has increased, more complex and demanding missions in increasingly hostile environments have been required. Although new subsystems are being designed to meet these requirements, mission demands may have increased to the point that pilots will be overloaded during critical flight phases. Consequently, users, designers, and manufacturers have an urgent need for information about human behavior and function to create systems that take advantage of human capabilities, without overloading them. Because there is a large gap between what is known about human behavior and the information needed to predict pilot workload and performance in the complex missions projected for pilots of advanced helicopters, Army and NASA scientists are actively engaged in Human Factors Research at Ames. The research ranges from laboratory experiments to computational modeling, simulation evaluation, and inflight testing. Information obtained in highly controlled but simpler environments generates predictions which can be tested in more realistic situations. These results are used, in turn, to refine theoretical models, provide the focus for subsequent research, and ensure operational relevance, while maintaining the predictive advantages of a theoretical foundation. The goal of this paper is to describe the advantages and disadvantages of each type of research, provide examples of experimental results, and describe the Ames facilities with which such research is performed.

INTRODUCTION

In the four decades since World War II, military and civil helicopter uses have expanded greatly. And, as an appreciation for the potential of helicopters developed, new dimensions in mission requirements evolved. As helicopters have acquired new missions, new tactics and performance requirements evolved that require the effective use of many subsystems and sensors in increasingly hostile environments. Traditionally, pilots have adapted to and integrated such increasingly complex displays and controls. However, the performance and attention demands of high technology vehicles are increasing so dramatically, that there is a growing concern that pilots will be unable to perform their missions safely and effectively. For example, the difficulty of nap-of-the-earth (NOE) missions and the complexity of systems that must be operated or managed at the same time, often imposes intolerable demands. It is becoming evident that the point has been reached where pilots are overloaded during critical phases of some missions, contributing to mission failures and the loss of life and costly equipment. Plans to reduce flight crew size (most notably to a single-member crew) will only exacerbate this growing problem. Although both cockpit and training system designers have tried to keep pace, it appears that advanced technology systems may not be making the most effective use of pilots' capabilities. Furthermore, even the most complex and expensive training systems may not prepare pilots to perform required functions effectively and safely.

There is a large gap between the information available from laboratory research about human behavior and the information required to predict pilot performance and workload in advanced helicopters flying the complex, difficult, and hazardous missions that are proposed. This deficiency may manifest itself in cockpit designs and unrealistic mission requirements that challenge human adaptability and excessive training system costs.

To provide the information that is needed, human factors researchers evaluate basic perceptual, cognitive, and manual control abilities and measure and model the relationships among such abilities, advanced design concepts, and different flight environments. They perform research in laboratories, computer simulations, aircraft simulators, and in flight. Each level of research has advantages and disadvantages and provides different types of information. The data obtained in the controlled environment of the laboratory generates detailed information about specific points and predictions about human behavior which can be tested in more realistic (but less well-controlled) situations. These results, in turn, provide a focus for subsequent research and contribute to the theoretical models. By taking advantage of a range of research facilities, the requirements of theoretical development can be balanced against those of the "real world" and operational relevance is ensured at the same time that the predictive advantages of a theoretical foundation are maintained.

This report will review the advantages and disadvantages of the different types of research. In addition, it will provide examples of the research results that have been generated by NASA and Army researchers in

collaboration with industry and academia that might be relevant to the design of advanced helicopters. Finally, the facilities available for human factors research at Ames Research Center will be described, very briefly.

LABORATORY RESEARCH

Description

Research conducted in a laboratory environment is generally simple, highly focused, and characterized by considerable experimental control. Laboratory facilities include an isolation booth (where the subject is protected from unwanted and irrelevant interruptions), microprocessors, visual and auditory displays, and discrete, vocal, and analog control devices. Experiments are designed so that the input (visual and auditory stimuli) and the output (verbal and manual responses) can be quantified accurately and directly. The intervening cognitive processes are predicted from psychological models and inferred from variations in the speed and accuracy of performance, physiological responses, and subjective ratings.

Advantages and Disadvantages

The experimental tasks used at Ames, as elsewhere, are designed to develop and test theories of human performance, memory and attention or to resolve specific applied problems in a controlled environment. Their focus is narrow, the range of factors manipulated limited, and they provide highly simplified representations of "real-world" task components without the realism of interactions among multiple subtasks. Thus, their external validity (e.g., their immediate and obvious relevance to the complexities of NOE flight in advanced-technology helicopters) is not always apparent.

However, laboratory research *can* and does provide answers to fundamental questions about human behavior, because it is possible to eliminate or control irrelevant variables and manipulate relevant variables precisely. If the theories developed are sound, their predictions can then be generalized to other situations, beyond the original vehicle-specific focus that prompted the research. Because laboratory research costs very little, and can be accomplished quickly, solutions can be provided efficiently.

Unfortunately, many useful ideas and information developed in the laboratory are not brought to the attention of designers because the researchers often do not verbalize, or test, the applicability and validity of their results to operationally-relevant tasks and environments. In addition, the results of individual, microscopic, laboratory experiments are often organized by the theories they were designed to test. However, these theories and their data bases are rarely integrated into a cohesive body of useful knowledge. Thus, the results of many laboratory experiments are not available for and do not contribute to the design process.

Examples of Research Results

Evaluation of Auditory and Visual Displays

With the advent of increasingly sophisticated helicopters, such as the UH-60 Blackhawk and the AH-64 Apache, Army helicopters are increasingly able to penetrate the Forward Line of Contact. Along with this improved mission capability has come the increased likelihood of exposure to enemy-radar-controlled air-defense systems. The current Radar Threat Warning Indicator (APR-39-V1) depicts the presence of a radar emitter by a narrow strobe line displayed on a three-inch CRT (Figure 1a). A Proportional Rate Frequency audio signal accompanies the visual display to inform pilots about the type and status of a radar emitter.

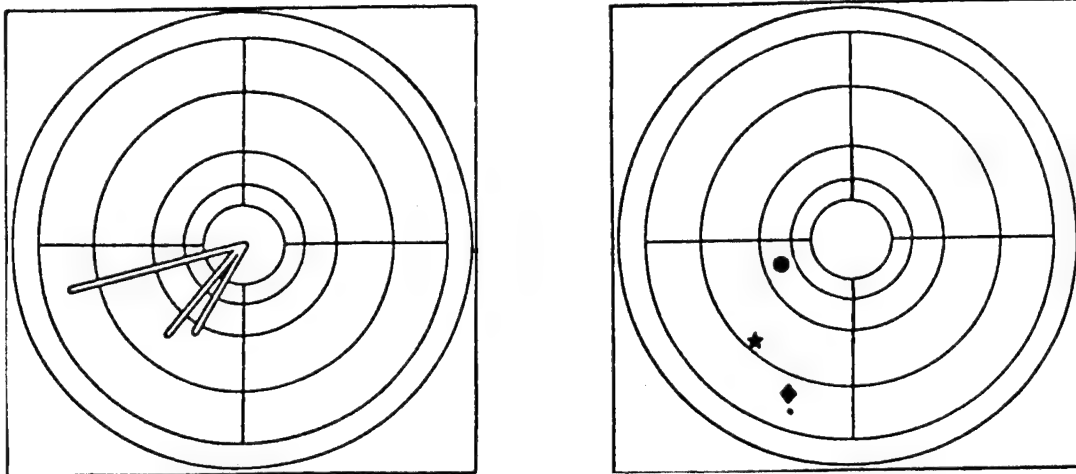


Figure 1: Current (a) and experimental (b) Radar Threat Warning Indicators

The current version has been improved with the development of a prototype APR-39 (XE-1). This display uses symbols presented on the CRT to indicate type of threat, position and status (Figure 1b), accompanied by a speech warning system to provide an optional machine-generated speech display to alert pilots to the presence or change in status of a radar emitter. Laboratory research, conducted by researchers in the NASA Helicopter Human Factors Office (Voorhees, Bucher, Remington & Williams, 1986) investigated many important attributes of the display (e.g., the symbols to be used, symbol placement and screen configuration, speech message vocabulary and construction, message display logic, and voice type). Laboratory experiments

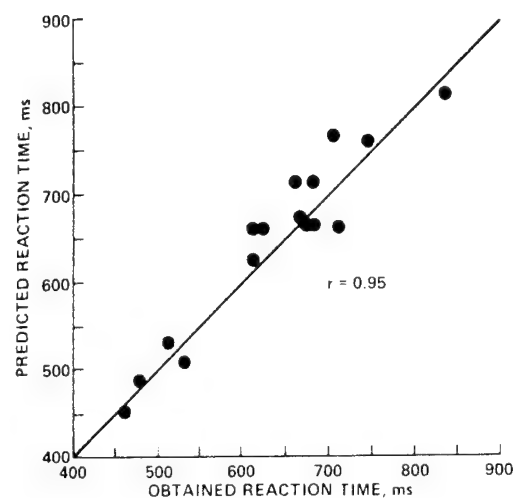


Figure 2: Obtained vs predicted reaction times for different symbols and symbol set sizes.

were conducted to determine the time required to identify visually displayed symbols and the effect of symbol set size. Figure 2 depicts the high correlation between the predicted and obtained reaction times when the predictions were calculated as a joint function of symbol design and symbol set size. As expected, reaction times increased as symbol set size was increased. Additional experiments were conducted to develop the speech warning system with a task that represented functional elements of NOE flight. Operational pilots' satisfaction ratings (given on a scale from 1 to 7) were considerably higher for the proposed system (6.5) than for the existing system (2.1). The results of these experiments led to a final set of visual symbols and auditory messages that will be used by the Army on the new generation Radar Threat Warning Indicator (APR-39-XE1).

Workload Measurement

Since 1982, researchers in NASA's Workload Program have evaluated the factors that contribute to the physical and mental workload of pilots and established measures and predictors of pilot workload that are appropriate for use under operational conditions (Hart, 1986; Hart, in press). To do so, theoretical information about workload from academia was related to the practical requirements of industrial and government organizations. The first phase of the program has been completed. The factors that contribute to pilot workload have been identified and a set of valid and practical measures have been developed: (1) the NASA Task Load Index (TLX) rating scale (Hart & Staveland, in press), (2) physiological measures (e.g., evoked cortical potentials, Kramer, Sirevaag & Braune, in press, and heart rate, Hart & Hauser, in press), (3) primary task measures (e.g., communications, Hart & Hauser, in press), and (4) secondary task measures (e.g., time production and choice reaction time, Bortolussi, Kantowitz, & Hart, 1986).

Such issues as the relationship between workload and training, the relative demands imposed by vocal or manual inputs and visual or auditory displays, the association between imposed demand levels, achieved performance, and different measures of workload were resolved. In addition, the information provided by different types of measures, and when each can (and cannot) be used, were determined. Laboratory research provided answers to specific questions in a well-controlled environment, while later simulation and inflight research verified that the results were meaningful in the "real world". The results of this fundamental research effort are now being applied to a variety of vehicle-specific problems.

However, selecting an appropriate and practical measure of workload is still difficult, due to the multi-dimensional nature of workload and the fact that different measures are selectively appropriate for different questions, tasks and test environments. Although hundreds of articles have been written describing the results obtained with one or two techniques and a specific task, it is difficult for individuals who are not intimately familiar with the literature to know what measures are available, how well they have been tested, and when they can be used. For this reason, a micro-

processor-based expert system (WC FIELDDE) was developed at Ames to aid in the selection and application of workload assessment techniques (Casper, Shively and Hart, 1986).

The system suggests measures, in descending order of utility, based on a users' answers to questions about his goals, research environment, and available facilities. It draws from a data base of widely used measures and "rules-of-thumb" provided by experts in the field to propose alternatives. In addition, it provides sufficient information for the user to make an informed choice among the suggested alternatives and to implement the techniques included in the data base. Each measure is described and evaluated, studies in which it has been used are reviewed, and references are provided to allow the user to obtain additional information.

COMPUTER SIMULATION

Description

Until recently, complex systems have been evaluated by studying how well they actually perform. The time-honored method is to design the system, construct a prototype, and then measure its performance. If performance is not acceptable, the design and prototype steps are repeated, an expensive and time-consuming process. Since hardware changes are costly, there is a reluctance to correct design mistakes and it is difficult to make meaningful empirical comparisons among alternatives. Thus, the process quickly reduces to an evaluation of a single prototype design. These limitations exhibit themselves early in the design process. All modern vehicle designs begin with mission, function, and task analyses. They represent a minutely detailed enumeration of tasks and functions that will be performed by the pilots that generate the concepts and constraints from which the final designs are derived and against which performance is judged. Due to the huge expenditure in manpower they require, they too become fixed early in the design process. Since task and time-line analyses are vehicle-specific, atheoretical, linear, and non-interactive, they represent a fixed, descriptive, sequence of events. Computer simulations, on the other hand, may be based on general theories of human behavior. Thus, they may be applied to many vehicles, allow examination (in software) of alternative designs, and provide powerful tools to answer specific questions.

They can integrate models of human performance, attention, perception, manual control, and anthropometrics with vehicle models to create an environment where control laws, design concepts, and automation options can be evaluated in software. The models and algorithms may be based on theory, empirical data, "rules-of-thumb", or expert opinion. Their value depends on the completeness of their data bases and whether or not their predictions have been verified empirically. Their focus, as defined by the vehicles to which they may be applied and the aspects of human behavior they include, may be either extremely narrow or quite broad. Computer simulations are computation-intensive, and thus require considerable speed and memory, and

may require symbolic processors and object-oriented software. Advances in computer technology have increased their power and speed to the extent that they can now adequately represent the functional tasks inherent in the tactical world of Army aviators. Static or dynamic computer simulation results are presented either graphically or numerically, providing either summary or detailed information.

"Virtual" display environments can be used to present the results of computer simulations to experimental subjects and designers for evaluation. They provide a computer-generated version of proposed features or alternative cockpit designs projected onto the visor of a helmet. A user can interact with these alternatives to examine the effects of different control laws, vehicle configurations, and interactions among display elements based on software models (Fisher, 1986).

Advantages and Disadvantages

Computer simulations allow designers to ask "what if..." questions very early in the conceptual stage of design so they can consider many alternatives in a cost effective way. This affords them the opportunity to adopt the best alternatives in the final design. In comparison to physical simulations, computer simulations are flexible and allow designers to consider design elements that do not yet exist. They can provide an excellent representation of flight-task interactions and the range of behaviors of potential human operators, depending on the quality of their data bases and algorithms. The level of control over "irrelevant" variables is excellent and replications may be obtained readily. Their external validity is not as good as piloted simulation and inflight research, however, and environmental realism is, obviously, low because the evaluations are performed in software without human operators or a physical representation of the vehicle. Nevertheless, their output may be generalized to more realistic situations if their predictions have been subjected to empirical evaluation.

Examples of Research Results

Expert System for Symbology Evaluation

Although candidate symbolologies are usually evaluated empirically, it is more cost-effective to evaluate them in software. For this reason, an expert system was developed by the Perception and Cognition Group at Ames to automate the evaluation of helicopter display symbolologies. The Ames Vision Model can be used to compute the perceptual distances among alternative symbols and fonts to provide objective criteria for selecting perceptually distinct symbols (Watson & Fitzhugh, 1986). This allows a designer to compare many alternatives to select the optimal set.

Computational Model of Visual Flow Fields

Much of the information required for flight path control at very low altitudes is obtained by monitoring the environment, with only occasional references to flight instruments. For example, height above the terrain is estimated visually, rather than by reference to an altitude indicator, and rate of movement is estimated by motion cues available from the visual scene. Software tools developed at Ames can represent the visual information reaching the pilot's eyes, model how this information is used, and generate velocity flow fields. This information can be used to: (1) analyze the visual scene requirements for various phases of flight (based on rate of movement, height above the ground, field of view, and terrain features), (2) determine the resolution and field of view requirements of helmet-mounted displays and obstacle-avoidance systems, (3) develop guidelines for the placement and properties of sensors to provide optimal information for human users, (4) provide guidance and control algorithms, and (5) specify the visual information requirements for NOE flight in low visibility. In addition, display formats are being developed to provide pilots with additional information when available visual cues are inadequate (e.g., hovering with a narrow-field-of-view, monocular display, Watson & Ahumada, 1985).

Figure 3 depicts one way that such velocity flow fields have been used to evaluate the perceptual problems that are encountered during a hover using direct visual cues. The cross represents the direction of gaze. The length of the lines represents the direction and amount of apparent movement detected by the pilot's eyes viewing the terrain. As you can see, the flow fields generated by a pitch down maneuver (Figure 3a) and by a loss of altitude (Figure 3b) are virtually identical. Such flow field representations can be used to quantify and predict the perceptual confusions encountered under different flight conditions with direct vision and to estimate the additional perceptual problems that are encountered by a narrowed field of view (such as provided by most night vision systems).

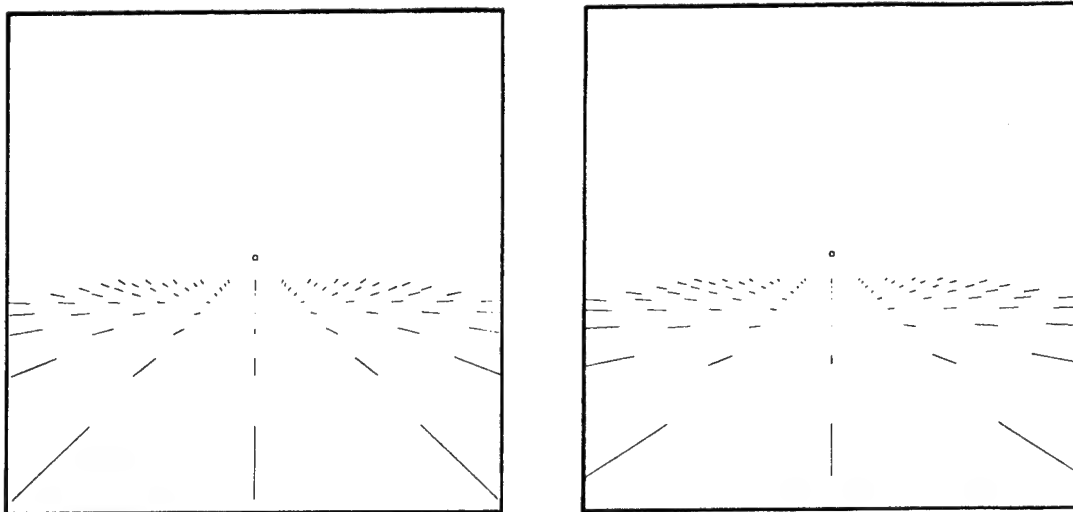


Figure 3: Flow field representations of terrain features during a pitch down (a) or loss of altitude (b) with a forward speed of 40 kts.

Model of Helicopter Vibration

The detrimental effects of vibration on visual acuity have been well documented for direct vision. They are even more severe with helmet-mounted displays where decrements are caused by relative motion between a displayed image (due to involuntary, vibration-induced head motions) and the eye. The normal vestibular-ocular reflex induces eye movements that oppose those of the head to maintain a stationary point of regard. While appropriate for viewing panel-mounted displays, it is not appropriate for helmet-mounted displays; relative motion is *produced* between the image on the head-coupled display and the eye, resulting in retinal blurring, increased errors and longer responses. Based on a computer simulation of the vibration frequencies of helicopters, an adaptive noise-canceling technique has been developed at Ames that minimizes the relative motion between viewed images and the eye by shifting displayed images in the same direction and magnitude as the induced reflexive eye movement (Velger, Grunwald, & Merhav, 1986). This filter stabilizes the images in space while still allowing the low-frequency voluntary head motions that are required for aiming accuracy.

Army-NASA Aircrew/Aircraft Integration Program

The technology gap between hardware complexity and interface design capability all too often results in systems which only work in the most benign environments. The adverse effect of this technology gap on new system capabilities motivated the Army-NASA Aircrew/Aircraft Integration (A³I) Program to provide a capability that would prevent future designs which are marginally capable or unnecessarily expensive because of inappropriate provisions for the human crewmembers.

The A³I program is a joint Army/NASA effort to produce a Human Factors Computer-Aided Engineering (HF/CAE) system. Conceptually, the system is a model and principle-based computer-graphic simulation of a manned simulation wherein models and heuristics of human performance and behavior replace the pilot. The program is focused on the concept formulation phase of future rotorcraft development. It is in this phase leading up to the final detailed design of any system that 70 to 80 percent of the life-cycle cost is determined. The objective is to provide designers with an opportunity to "see it before they build it", to ask "what if" questions, and be told "why" ideas will or will not work in the concept formulation phase. The goal is to make mistakes in software... not hardware.

Figures 4 and 5 compare the current system design process with a computer-aided design approach. Note that the current approach begins with the development of the conceptual issues leading to a design. Human engineering data and specifications are not applied until the final designs are established. From this stage on, the design process is accomplished in hardware, as indicated by the dashed-line box. The nearly insurmountable difficulty of making changes once hardware development has begun, precludes doing meaningful comparisons among alternatives and it is only after a

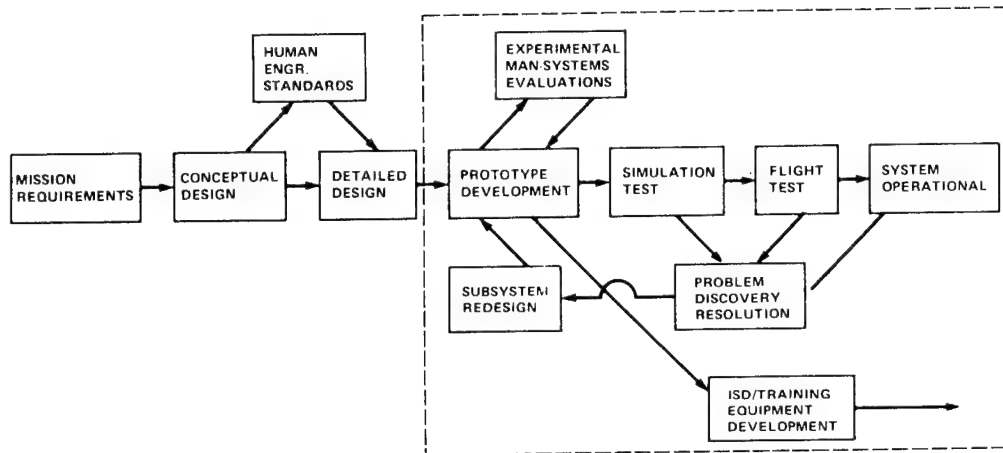


Figure 4: A schematic representation of the current development process.

physical prototype is built that training specialists can begin to estimate the cost of training systems. Thus, a design process quickly reduces to an examination of the only affordable prototype.

Figure 5 depicts the methodology under development for the A³I HF/CAE system. The elements in the dashed-line box represent utilities integrated into the A³I HF/CAE system which will be available for use early in a design process. Since people are used to obtaining information about the world visually and in three dimensions, the system provides graphic representations to give the user insight into the progress of a simulation and a global understanding of complex and interrelated man-machine factors. Traditionally, designers of helicopters have had to execute two-dimensional designs with two-dimensional tools that must serve the needs of pilots operating in a three-dimensional world. For this reason, the designer will be allowed to visualize the consequences of design alternatives in color graphics before committing to final design and hardware development.

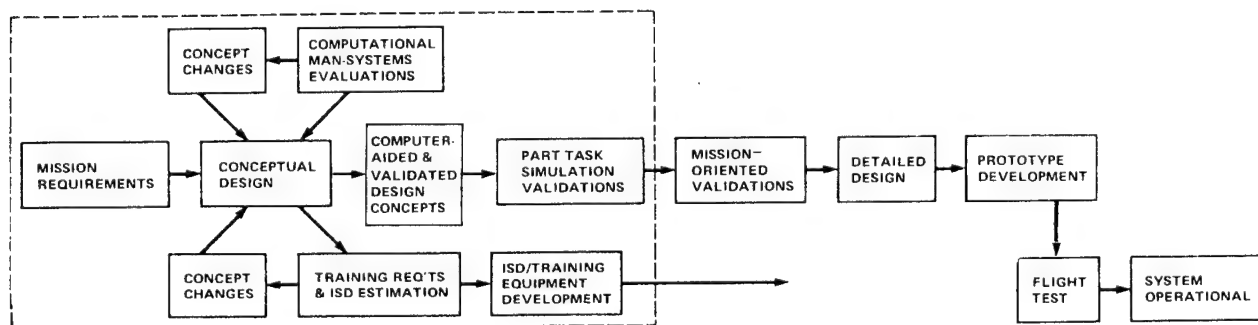


Figure 5: A schematic representation of a computer-aided development process

The use of graphic and iconic representations also facilitates communication between designers from different technical disciplines by substituting commonly understood pictures for words which may have different meanings to each. This new design methodology concept also permits training systems designers to become early participants in the design process. Further, mission specialists will be able to visualize missions and the pilot's tasks and activities before committing to final mission/task documents. Figure 6 depicts some of the initial display options available to the designer in the system.

The products associated with the A³I program that will be contained in the HF/CAE system are: (1) an automated mission editor, (2) a designer's simulation workbench which incorporates aircraft simulation models, human behavior/performance models, system function models, and workload assessment and prediction models, (3) an expert system model of training requirements, (4) CAD utilities to render cockpit layout, instruments and concepts, (5) a state variable/data information and analysis center, and (6) a simulation and integrating executive control system. The focus is on providing designers with interactive graphic tools which permit integration of sound human engineering principles early in the development process for future advanced-technology rotorcraft.

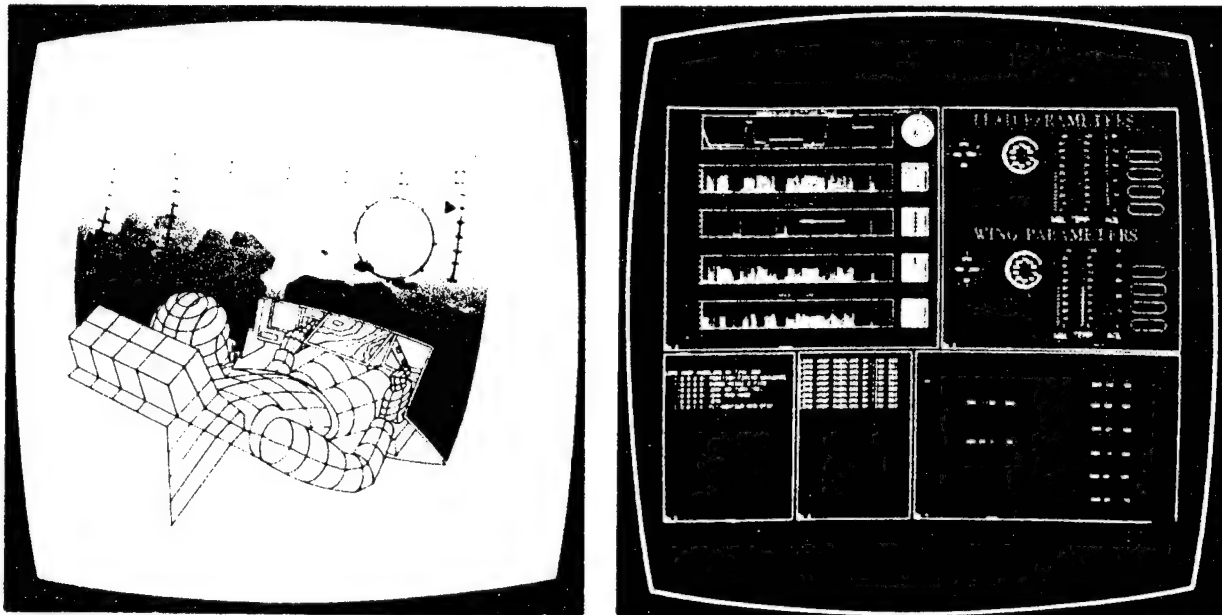


Figure 6: Graphic representation of what the pilot is seeing (a) and a dynamic, moment-by-moment representation of pilot workload, vehicle state, and the flight task components being accomplished (b).

PILOTED SIMULATION

Description

Piloted simulations attempt to reproduce the controls and displays, aircraft and control dynamics, and visual flight environment of a specific vehicle or a "generic" representation of a class of vehicles to enable pilot-in-the-loop research. Most simulators replicate the physical cockpit. However, the fidelity of simulators vary widely in other respects. For example, simulator motion capabilities at Ames range from fixed base (the Crew Station Research and Development Facility) to high-fidelity, six-degree-of-freedom versions (e.g., the Ames Vertical Motion Simulator and the Man-Vehicle Systems Research Facility).

In addition, the visual systems range from no visual scene representation (simulating instrument flight in zero-zero conditions) to monochromatic dusk/night scenes (e.g., Man-Vehicle Systems Research Facility) and complex and expensive full color, computer-generated visual scenes (e.g., the Rotorcraft Systems Integration Simulator and the Crew Station Research and Development Facility). The resolution, detail, and field of view, required depends on the tasks that will be performed in the simulator. For example, a helicopter NOE simulation demands a high-fidelity visual environment to allow pilots to fly in and around the data base at very low altitudes, whereas a procedures trainer may require no visual scene at all. Simulators also differ in the fidelity of vehicle and control dynamics - - some represent a specific vehicle, whereas others use "generic" models - - and their representation of vehicle noise and perturbations due to simulated environmental or battlefield conditions, speed, or configuration. Again, the objectives of the work that will be performed in the simulator dictates the required level of fidelity. Finally, the data available about pilot and vehicle performance varies, although most facilities err on the side of too much rather than too little; even the simplest simulation generates hundreds of pages of data so that data reduction is always a major undertaking.

Simulators are used to evaluate or compare hardware options: instruments, panel and helmet-mounted displays, control configurations, automation options, and voice I/O systems. In some cases, innovative "glass cockpit" designs and integrated side-stick controllers that do not yet exist in operational vehicles may be evaluated. Simulators are used to evaluate different vehicle dynamics and stabilization systems and to determine the effects of environmental conditions, maneuvers, crew complements, and procedures on workload and performance. Finally, they may be used for initial, recurrent, and transition training. In some cases, simulators provide a realistic environment in which specific questions can be addressed. In others, they are used to evaluate the complex interactions among flight-deck hardware and software with a pilot closing the loop between system outputs and control inputs.

Advantages and Disadvantages

The generalizability and external validity of simulation research is usually very good, depending, of course, on simulator fidelity. Although piloted simulators are not as flexible and efficient as laboratory facilities and computer simulations, they often do provide alternative vehicle models, controllers and control dynamics, display options, and simulated environments. Their representation of complex flight-task interactions is excellent. Because experienced pilots are used to fly the simulator, the representation of the human operator is realistic. However, this necessitates the use of a limited and costly resource - - operational and experimental test pilots. The environment they provide can be very realistic, although it is likely that pilots do not behave exactly as they would in the air. Even with highly realistic simulators, it is impossible to generate the stresses of actual flight and combat or to represent the complexities and unexpected situations that arise. On the positive side, because they are not the "real thing", they allow pilots to perform maneuvers that could not be performed (safely) in flight.

The primary drawback of simulation research is that simulators often cost more to develop than the vehicle simulated, and operating costs are high. However, once the initial expenditure is made, they provide a more cost-effective way to evaluate design alternatives than implementing them in a prototype vehicle. Furthermore, experimental control is often low and the number of different pilots and experimental flights that are included in individual studies is limited by the cost and availability of the simulator. Given the limitations of simulation research, no system can ever be fully examined until it is put into flight and tested in the operational environment. However, the use of full mission simulation is a critical link between laboratory research, computer simulation, and flight-test evaluation.

Examples of Research Results and Facilities

The Effects of Automated Systems on Training

The introduction of automation changes the nature of the tasks performed by pilots, the types of workload they experience, and training requirements. Thus, a series of simulation experiments are being performed by the Helicopter Human Factors Program at Ames to investigate how automation should be introduced, so as to allow pilots to develop accurate mental models of the automated system(s), and to determine how task demands should be distributed among human operator(s) and automated subsystems in advanced helicopter designs (Tsang & Johnson, in press). The experimental task involves three-dimensional flight-path control, discrete target acquisitions, monitoring and supervisory control, and decision-making. Each axis of the tracking task can be performed manually or automatically, and failures may be introduced. Pilots are trained initially with either the manual or automatic control modes, and then transitioned to the fully automated flight mode. Their performance and workload during and after

training, their responses to system failures, and the accuracy of their internal model of the automated system are assessed.

Single-Pilot Advanced Cockpit Engineering Simulation

Workload research has focused on a range of human functions from simple physical exertion to complex cognitive processing, with measures that range from subjective ratings to physiological and performance indices. After measures have demonstrated sensitivity to different types of imposed demands in the laboratory, they are evaluated in the context of more complex activities, such as simulated military helicopter operations. Here, multiple, overlapping sources of task demands and response requirements are imposed and their effects on one-and two-pilot crews evaluated.

The Single-Pilot Advanced Cockpit Engineering Simulation that was conducted in the Ames Vertical Motion Simulator is one example of such study. Several stability and control augmentation systems, coupled with different levels of automation provided alone or in combination were evaluated to compare single and dual-pilot performance and workload during low-level military operations in the NOE environment (Haworth, Bivens, & Shively, 1986). Two forms of subjective workload ratings, Cooper-Harper Handling Quality ratings, and heart rate measures, were obtained, to evaluate the effects of the experimental manipulations on the pilots. All of the measures provided converging evidence that single-pilot workload levels are high, unless significant levels of automation are provided. Due to the practical constraints typical of complex simulations, the number of pilots in the study was limited, scheduling constraints affected the experimental

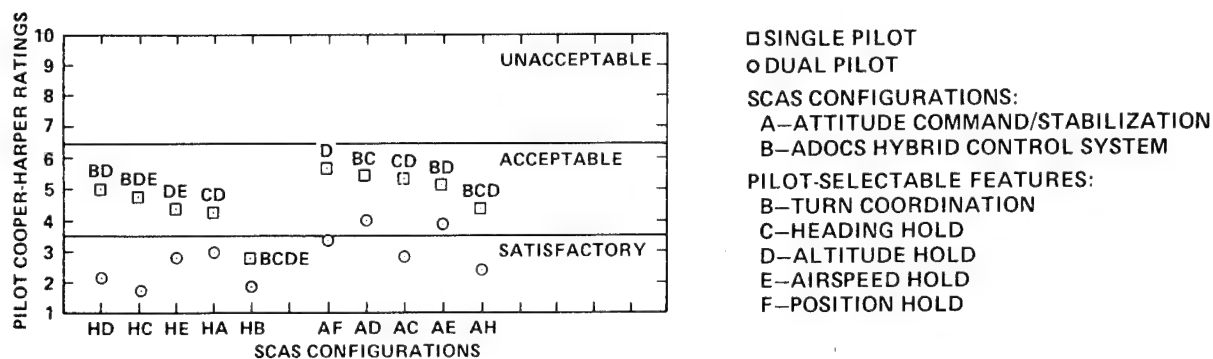


Figure 7: Cooper-Harper Handling Quality Ratings for Single- and Dual-Pilot configurations for the NOE segment.

design, and analysis of objective measures of performance proved to be an overwhelming task, due to the magnitude of the data collected. A clear difference in pilot ratings was evident between the one and two pilot crew complements, however. Figure 7 shows that only one configuration of the twenty tested was judged as satisfactory for flying NOE with a single pilot.

Both measures of workload (on-line SWAT ratings and post-flight NASA TLX ratings) were significantly correlated with each other ($r = 0.76$) and with handling quality ratings (Figure 8). However, the correlation between handling quality and workload ratings was higher for mission segments where physical control demands were the primary source of workload. The correlation was lower for segments where mental activities contributed significantly to the pilot's workload.

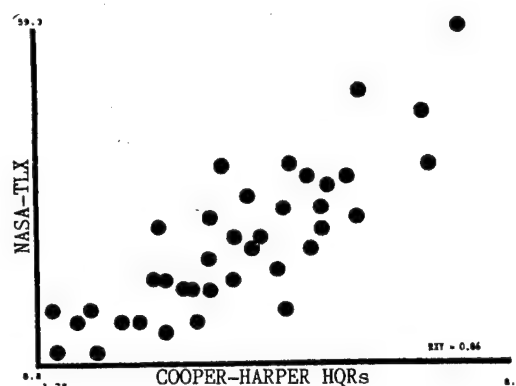


Figure 8: Relationship between Cooper-Harper Handling Quality and NASA-TLX workload ratings.

Voice-Activated Control Simulation

NASA researchers will conduct a simulation in the spring of 1987 to test the efficacy of some of the features that have been proposed to reduce the workload of a single pilot for the next-generation of Army scout/attack helicopters (such as the LHX). In particular, the effects of automation and voice-interactive versus manual input for mission-related tasks will be examined in a simulated military NOE environment (Vidulich, in press). The results of extensive theoretical and laboratory research will be used to predict the possible benefits (and drawbacks) of using the two entry systems for weapon selection, data burst transmission, and counter-measure activation under each of three levels of automation (e.g., (1) none; (2) automated turn coordination and altitude hold; and (3) automated turn coordination, and altitude and position hold). It is expected that hover and combat tasks performed with no automation will be sufficiently demanding to overload the pilot's capacity for manual-control tasks. In this case, an advantage for voice-interactive input is expected. However, this advantage should be attenuated in less demanding portions of the scenario and eliminated as increasing levels of automation reduce the need for continuous manual control activities.

Off-Axis Tracking Simulation

Even with direct visual contact with the outside scene, a large percentage of military and civilian helicopter accidents have been attributed to spatial disorientation. The problems are exaggerated with the use of narrow field of view, helmet-mounted displays and are expected to be particularly severe when a single pilot must track air and ground targets "off-axis" from the direction the vehicle is moving. Although this problem has been recognized, very limited information is available about differences in optic flow generated by out-the-window and sensor-based visual displays and about the limitations of pilots performing head-tracking tasks.

Recently, the components of visual flow that determine the direction of movement and the influence of visual flow on off-axis tracking of moving aim points were investigated in the laboratory. Here, specific target parameters (e.g., range elevation, azimuth, speed and transformation) were established and iso-velocity curves for each aircraft speed were computed and mapped against the local flow patterns viewed by pilots. This pilot study provided predictions that will be tested in simulated flight in the spring of 1987 (Bennett, Haworth, Perrone, & Shively, in press). Pilots will be required to track air and ground targets with a Honeywell head-tracker/helmet-mounted display system that presents a video image simulating the output of a remote sensor positioned on the nose of an attack helicopter. Some of the pilots will be required to detect, acquire, and track targets while flying a specified reconnaissance route, while others will perform the tracking task in a dual-pilot configuration where another simulated pilot is responsible for primary flight-path control. Vehicle speed, target range, azimuth, and elevation will be varied systematically. Detection times, acquisition times, and tracking error will be plotted as a function of local optical flow patterns projected to the pilot by the remote sensor.

Crew Station Research and Development Facility

In cooperation with the Aeroflightdynamics Directorate, NASA is constructing a realistic full-mission simulator, the Crew Station Research and Development Facility, to support Army and NASA research. The pivotal element of the facility is a two-seat tandem helicopter cockpit where the performance of operational pilots can be evaluated. Three Blue/Red team stations augment its realism by simulating other aircraft while a Mission Management Communications Station simulates supporting forces with which the crew interacts during an engagement. Experimental coordination is accomplished from the Experimenter/Operator Console, where a team of experimenters and simulation engineers control and monitor the scenario.

A composite mission scenario has been developed to produce realistic workload levels. By configuring the crew station to run with either one or two crew members, the effectiveness with which the missions are accomplished can be compared and the ability of a battle captain to control the resources of the Scout/Attack team, as well as those of his own aircraft, can be investigated under various circumstances.

A wide field of view Fiber Optic Helmet-Mounted Display which presents a panoramic view of the world coupled with sensor outputs and symbology for pilotage, threat alerts, and weapon release is the primary flight display for the pilot. Programmable display push buttons allow rapid input to critical aircraft systems such as weapons, countermeasures, and system malfunctions. Control of aircraft systems is effected using "glass cockpit" Systems Management Displays via tactile data entry devices (e.g., touchpads, touchscreens) or an interactive computerized Voice Input/Output system. The Tactical Situation Display, which displays a scalable plan view map of the

gaming area along with several overlays showing the status of threats and friendlies, is used to monitor the tactical situation. These may be modified using the touchscreen, as may the navigation and tactics overlays. Flight controls in each crew station consist of two, four-axis, limited-displacement controllers plus foot pedals (allowing full control in each crew position). The longitudinal, lateral, directional and collective controls may be assigned to any combination of the hand controllers and pedals in a given crew position. This flexibility enables the impact of various control configurations on crew member efficiency to be investigated. Further, a key consideration in the study of pilots' performance is the level of noise to which they are subjected. Thus, the crew station is surrounded by a six channel sound system that provides directional sound cues for rotor and transmission noise, weapon firing effects, dispensing of chaff and flare, and other noises that occur during a tactical mission scenario.

The changing nature of mission requirements dictates that the facility must be easily reconfigurable to support future experiments. To that end, interactive editors have been developed to modify all of the pilot interfaces and to integrate these modifications into the simulation with a user-friendly system. Data-base processors automatically extract terrain information from the visual data base to build forward view displays and Tactical Situation Display contour maps. Utilities allow the threat laydown and characteristics to be modified between experiments. Using these software tools, the facility may be radically reconfigured in a very short period of time to accommodate experimental investigations of virtually any pilot/cockpit integration issue.

INFLIGHT RESEARCH

Description

Inflight research provides the ultimate validation of the utility of new systems, designs, processes or modifications. Thus, it generally takes place after preliminary testing in the laboratory, computer-based and piloted simulation. The aircraft available at Ames for research fall along a continuum that extends from production models to highly instrumented experimental aircraft.

For example, an AH-1 Cobra helicopter is being used to investigate training and performance with a FLIR/PNVS system and voice input/output system. An experiment investigating pilot workload employed an SH-3G helicopter equipped with data collection and telemetry instrumentation. This experiment was able to take advantage of the laser tracking facilities located at Crow's Landing NALF, which provided detailed x,y and z coordinates for the aircraft during maneuvers in that area. The CH-47 Chinook helicopter represents even further modification of an aircraft for research purposes. The right seat is essentially a "flying simulator" with a reconfigurable cockpit and onboard computers that can change the dynamics of the flight controls to simulate handling qualities of different aircraft.

Advantages and Disadvantages

There are many advantages to performing research in flight. The fact that it is performed in the target environment establishes excellent external validity and generalizability, due to the realistic representation of flight task interactions and environment. While many questions can be answered in laboratories and simulators about the feasibility of new systems or designs, there is no substitute for an actual pilot flying an actual aircraft. While these represent major advantages of inflight research, there are drawbacks. Inflight research is, by its nature, focused on a specific vehicle type. Experimental control is difficult to achieve, due to various factors such as weather, traffic, aircraft downtime, etc. Unless special instrumentation is available, little or no performance data can be recorded. Further, the cost of inflight research is very high. Initial aircraft cost, maintenance, and pilots all contribute to this high cost.

In considering the advantages and disadvantages of inflight research, one of its greatest benefits is that it allows research to come full circle. That is, a project does not stop after flight test. Most experiments generate more questions than they answer, and this is certainly true of inflight research. Questions arise in operational research that might otherwise be overlooked, providing an opportunity to test techniques and designs and identify problems. Then, it is possible to complete the circle by taking these problems and questions back into the laboratory and simulators for further research. Thus, flight test is a major and necessary element of the human factors research process.

Examples of Research Results

Inflight Voice Recognition System Evaluation

Computer-recognized voiced commands and computer-generated speech messages have been proposed as methods by which pilots could interact with cockpit displays. Since visual and manual-control demands are generally high in helicopters, auditory displays and spoken commands might be less disruptive to manual flight-path control than additional visual displays or keyboard entries. In flight, recognition accuracies of 95% or better were obtained for mission segments selected to be particularly troublesome for a voice recognition system. For example, one speech recognition system was tested in a Bell Jet Ranger helicopter in level cruise, sustained turn (that created blade slap noise), approach to VNE (that created additional vibration), and hover in ground effect (that created high pilot workload). Each pilot trained the system individually to his voice for the 20-word vocabulary. Recognition accuracy was not affected by cockpit noise or vibration as much as expected. However, increased pilot workload did degrade recognition accuracy. In the NASA SH-3G helicopter, equally good recognition accuracies were found with cockpit noise levels ranging from 102 to 106 dBA, although recognition accuracy decreased from 100% to 93% as the vocabulary was increased from 10 to 36 commands. It was suggested that using a command

syntax to divide the vocabulary into subsets could have achieved a consistently high level of recognition accuracy (Coler, 1984).

Inflight Workload Research

The study of mental workload is one endeavor that has benefited from flight test validation. The Helicopter Human Factors Program recently completed an experiment in NASA's SH-3G helicopter to provide the final validation of workload measures developed in the laboratory and tested in simulated flight and to develop a database for workload prediction (Shively, Battiste, Matsumoto, Pepitone, Bortolussi and Hart, in press).

Subjective, objective, and physiological measures were employed. Four NASA test pilots flew each of two scenarios. Each flight began and ended at Moffett Field NAS. On the way to and from Crows Landing NALF, a variety of tasks were imposed: visual, TACAN, and ILS approaches, in- and out-of-ground-effect hovers, contour flight, a search task, and visual and instrument navigation (depicted by the line graphs in Figure 9). The bar graphs in Figure 9 represent the workload ratings obtained for each flight segment. Relatively high workload levels were reported by the pilots for the search task and in the hovers, as expected. The workload of instrument approaches and landings was predictably greater than for visual. Other flight segments such as flying contour with or without performance constraints, fell into functionally related groups. Measures of performance provided additional insight into pilot workload levels. Heart rate measures are currently under analysis. The data obtained from this experiment will form the foundation of a helicopter-specific computer model for workload prediction that will be incorporated into the A³I computer simulation.

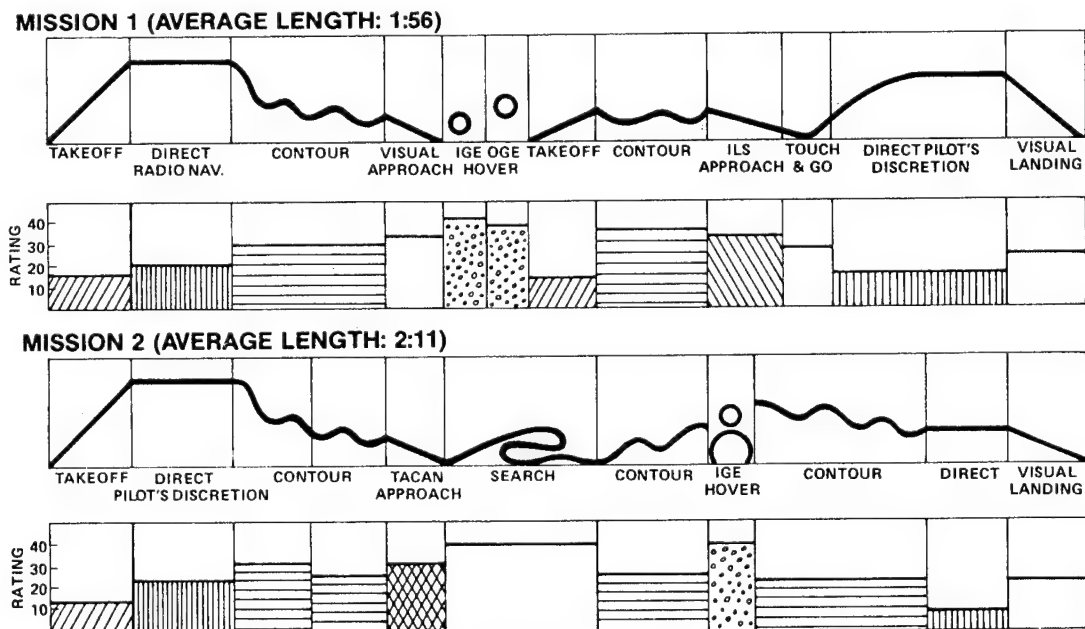


Figure 9: Stylized representation of flight segments and average workload ratings given by four pilots for two missions flown in the NASA SH-3G.

SUMMARY

At each stage in the research process, information obtained in more realistic situations can be used to refine theoretical models and provide the focus for well-controlled laboratory studies to address specific issues. The relative advantages and disadvantages of laboratory, computer simulation, piloted simulation and inflight research are summarized in Table 1.

Each level of research can contribute to developing an understanding of the capabilities and limitations of the human element in advanced-technology systems. By moving back and forth among these research environments, the requirements of theoretical development can be balanced against the requirements of the "real world". Furthermore, operational relevance can be insured at the same time that the predictive advantages of a theoretical foundation can be maintained. Finally, each environment can be used for those aspects of research for which it is uniquely suited, resulting in a cost-effective and efficient use of available resources.

Scientists must become familiar with applied problems (through participation in simulation and inflight research) and designers, engineers, and operational test and evaluation personnel must be exposed to the advantages of experimental control, a theoretical foundation, and the use of validated measures, in order to capitalize upon the advances in each others' fields. This is the unique role that a government research laboratory, such as Ames

Table 1: Summary of the Advantages and Disadvantages of
Different Research Environments.

	LABORATORY	COMPUTER SIM.	SIMULATOR	INFLIGHT
COST	LOW	MODERATE	VERY HIGH	VERY HIGH
EXPERIMENTAL CONTROL	EXCELLENT	EXCELLENT	GOOD	POOR
GENERALIZABILITY OF RESULTS	GOOD	GOOD	VERY GOOD	EXCELLENT
EXTERNAL VALIDITY	POOR	GOOD	VERY GOOD	EXCELLENT
REPRESENTATION OF FLIGHT-TASK INTERACTIONS	POOR	CAN BE EXCELLENT	EXCELLENT	EXCELLENT
REALISM OF ENVIRONMENT	POOR	POOR	GOOD	EXCELLENT
FLEXIBILITY AND EFFICIENCY	EXCELLENT	EXCELLENT	GOOD	POOR
EASE OF REPLICATION	EASY	TRIVIAL	MODERATE	DIFFICULT
QUALIFICATIONS OF EXPERIMENTAL SUBJECTS	NONE	MODELS REPLACE HUMAN SUBJECTS	MUST BE TRAINED PILOTS	MUST BE TRAINED PILOTS

Research Center, can play. Here, scientists, engineers, and pilots work in close proximity to each other and conduct collaborative research in which each take advantage of the other's knowledge and tools to provide a strong research foundation that can be transferred to industry. If nothing else, this environment creates a unique opportunity for each group to learn the other's language. This provides a vehicle for translating the considerable data base available in academia and the pragmatic experiences of designers, engineers, and pilots into a useful body of knowledge.

REFERENCES

Bennett, C. T., Haworth, L. A., Perrone, J. A., & Shively, R.J. (in press) Pilot night vision sensor tracking performance: Comparison of dual vs. single pilot configurations. *Proceedings of the AGARD Symposium on the Man-Machine Concept in Tactical Aircraft Design and Combat Automation*.

Bortolussi, M. R., Kantowitz, B. H., & Hart, S. G. (1986) Measuring pilot workload in a motion base trainer. *Applied Ergonomics*, 17(4), 278-283.

Casper, P. Shively, R. J. & Hart, S. G. (1986) Workload Consultant: A Microprocessor-based System for Selecting Workload Assessment Procedures, *Proceedings of the 1986 IEEE International Conference on Systems, Man, and Cybernetics*, 1054-1059.

Coler, C. R. (1984) Helicopter Speech-Communications Systems: Recent Noise Tests are Encouraging. *Speech Technology*, Sept/Oct, 76-81.

Fisher, S. S. (in press) Virtual Interface Environment. *Proceedings of the NASA Space Station Review*. Moffett Field, CA: NASA-Ames Research Center.

Hart, S. G. (1986) Theory and Measurement of Human Workload. In J. Zeidner (Ed.) *Human Productivity and Enhancement: Training and Human Factors in Systems Design, Volume I*. New York: Praeger, 396-456.

Hart, S. G. (in press) Measurement of pilot workload. In A. Roscoe (Ed.) *AGARDograph on Pilot Workload Assessment*, Neuville Sur Seine, France.

Hart, S. G. & Hauser, J. R. (in press) Inflight application of three pilot workload measurement techniques. Accepted for publication in *Aviation, Space, and Environmental Medicine*.

Hart, S. G. & Staveland, L. E. (in press) Development of a multi-dimensional workload rating scale: Results of empirical and theoretical research. In P. A. Hancock & N. Meshkati (Eds.), *Human Mental Workload*. Amsterdam: Elsevier.

Hartzell, E. J. (1986) *Army-NASA Aircrew-Aircraft Integration Program, Executive Summary*. Moffett Field, CA: NASA-Ames Research Center.

Haworth, L., Bivens, C. & Shively, R. J. (1986) An investigation of single-piloted advanced cockpit and control configurations for nap-of-the-earth helicopter combat mission tasks. *Proceedings of the 1986 Forum of the American Helicopter Society*, Washington, D.C.: American Helicopter Society, 657-672.

Kramer, A. F., Sirevaag, E. J., & Braune, R. (in press) A psychophysiological assessment of operator workload during simulated flight missions. Submitted to *Human Factors*.

Remington, R. & Williams, D. (1986) On the selection and evaluation of visual display symbology: Factors influencing search and identification times. *Human Factors*, 28(4), 407-420.

Shively, R.J., Battiste, V., Matsumoto, J., Bortolussi, M.R. & Hart, S.G. (in press), Inflight evaluation of pilot workload measures for rotorcraft research. *Proceedings of the Fourth Symposium on Aviation Psychology*. Columbus, OH: Ohio State University.

Tsang, P. S. & Johnson, W. W. (in press) The effects of automated systems on training and workload distribution. *Proceedings of Human Factors Society 31st Annual Meeting*. Santa Monica, CA: Human Factors Society.

Velger, M., Grunwald, A., & Merhav, S. (1986) *Adaptive Filtering of Biodynamic Stick Feedthrough in Manipulation Tasks Onboard Moving Platforms*. Technical Paper, AIAA Conference.

Vidulich, M A. (in press) The cognitive psychology of subjective mental workload. In P. A. Hancock and N. Meshkati (Eds.) *Human Mental Workload*. Amsterdam, The Netherlands: Elsevier.

Voorhees, J. W., Bucher, N. M., Huff, E. M., Simpson, C. A. & Williams D. H. (1983), Voice Interactive Electronic Warning System (VIEWS). *Proceedings of the IEEE/AIAA 5th Digital Avionics Systems Conference*, 3.5.1-3.5.8.

Watson, A. B., & Ahumada, A. J. (1985) Model of human visual motion sensing. *Journal of the Optical Society of America*, 2(2), 322-342.

Watson, A. B., & Fitzhugh, A. E. (1986) A New Look at Better Recognition, *Perception*, 15(1), A31.

AVIONICS SYSTEMS INTEGRATION TECHNOLOGY

George Stech and James R. Williams
Army Avionics Research and Development Activity
Joint Research Programs Office
NASA-Langley Research Center

Introduction

A very dramatic and continuing explosion in digital electronics technology has been taking place in the last decade. The prudent and timely application of this technology will provide Army aviation the capability to prevail against a numerically superior enemy threat. The Army Avionics Research and Development Activity (AVRADA) at Fort Monmouth, and NASA at Langley Research Center have been exploiting this "high technology" explosion in the development and application of avionics systems integration technology for new and future aviation systems.

This paper will discuss a few selected AVRADA avionics integration technology base efforts and the Avionics Integration Research Laboratory (AIRLAB) that NASA has established at Langley Research Center, for research into the integration and validation of avionics systems, and evaluation of advanced technology in a total systems context.

Avionics System Integration

Over the past decade the integration of avionics systems has developed to the point where it can be considered a technology in and of itself. Data processors, data communication links, and software are the key elements of system integration technology. The manner in which these elements are partitioned and configured is referred to as system architecture. Considerable benefits in performance, cost, weight, space, power, logistics and maintenance, flexibility, and growth potential are offered by highly integrated systems. However, to achieve these benefits and obtain the required levels of system availability and reliability, fault tolerance must be an essential and critical element in system architecture design. A fault-tolerant system architecture can provide high levels of coverage of failures and the inherent capability to reconfigure the system after a failure to thereby maintain system functionality.

Thus the system can continue to function, possibly at degraded but acceptable levels of performance, for extended periods of time. As modules fail and repeated reconfigurations occur, the avionic system will degrade gracefully. However, the aircraft will be available to fly numerous missions, with acceptable levels of performance, before maintenance actions are necessary. In addition, the high level of fault isolation capability inherent in a fault-tolerant architecture will allow isolation of the fault to the module level. Thus, maintainability is enhanced because the failure is accurately diagnosed on-line to the module level, which can subsequently be replaced by a straight forward maintenance procedure.

Integrated Avionics Control System

In the Mid 1970's, in an effort to solve the acute problems of available cockpit panel space and crew workload in Army Helicopters, AVRADA initiated the development of the Integrated Avionics Control System (IACS). IACS, employing embedded microprocessors, digital multiplex data buses, and highly integrated multifunction cockpit control/display units, embodied the leading edge of the state of the art for the mid to late 1970's time frame. The IACS block diagram and controlled avionics are shown in Figures 1 and 2 respectively. The pilot can control all communications, navigation, and identification (CNI) equipment from a single control panel. Two central control units serve as bus interface units for non-bus compatible remotely located CNI equipments and all digital data between the cockpit and remote avionics bay is via MIL-STD-1553 data bus. Fault-tolerance is accomplished via redundancy and cross-strapping techniques.

IACS was very successful in meeting its program objectives of reducing cockpit panel space requirements and reducing pilot workload. A single multi-function IACS primary control panel utilizing approximately 40 square inches of cockpit panel space replaced 240 square inches of separate functionally dedicated cockpit mounted avionics controls and equipments. Regarding workload, the United States Army Aviation Test Board concluded from operational testing at Fort Rucker, AL that "The Integrated Avionics Control System provides the pilot a cockpit management system that reduces pilot workload. All avionics can now be controlled from one central location. By spending less time in the cockpit programming different radios, the pilot is able to perform the demanding tasks associated with NOE flight more safely and efficiently."³

The importance of the IACS program was that it successfully demonstrated the benefits of integrated avionics systems to the Army and provide the basis for further avionics system development efforts. IACS provided the needed impetus to develop avionics equipments capable of MIL-STD-1553 operation and provided the basic principals by which a totally digital avionics system architecture could be conceived. Derivatives of the IACS are currently used on the Coast Guard HU-25A, HC-130H, HH-65A, the Air Force A-10, KC-135, the U.S. Navy H-3, Army SEMA, and versions of the CH-47, AH-64, and UH-60.

Army Digital Avionics System

Based upon the technical success of IACS, and continued advancement in digital technology, it became apparent that integration of the total avionics system was possible. The next step was to expand the core IACS CNI control function to include additional cockpit management functions, such as flight displays, engine displays, caution/warning advisory subsystems, electrical power, aircraft secondary systems, preflight checklists and emergency procedures. In the late 1970's the Army Digital Avionics Program (ADAS) was initiated to serve as the mechanism for this expansion and to become the cornerstone of AVRADA's technology base for integrated systems architecture and cockpit integration concepts. The subsystems integrated into ADAS are shown in Table 1 below.

AC ELECTRICAL	ENGINE/XMSN CHIP DETECTOR
DC ELECTRICAL	ENGINE OVERSPEED PROTECTION
AFCS CAUTION	ENGINE SPEED TRIM
AIR DATA	ENGINE START AND IGNITION
ATTITUDE HEADING SYSTEM	FIRE DETECTION
ATTITUDE INDICATING	FUEL LO LEVEL WARNING
AUDIO WARNING	FUEL PRIME BOOST
AUXILIARY POWER UNIT	FUEL QUANTITY
COMMAND INSTRUMENT	GUST LOCK WARNING
ROTOR BLADE DE-ICING	HEATING & VENTILATING
ENGINE INSTRUMENTS	HYDRAULICS SYSTEM
ENGINE WARNING	SEARCH LIGHT
ENGINE ANTI-ICE	TAIL ROTOR WARNING
LANDING LIGHT	TAILWHEEL LOCK
ANTI-COLLISION LIGHT	TRANSMISSION INSTRUMENTS
CABIN DOME LIGHTS	TRANSMISSION OIL WARNING
COCKPIT FLOOD LIGHTS	WINDSHIELD ANTI-ICE
COCKPIT UTILITY LIGHTS	WINDSHIELD WIPER
FORMATION LIGHTS	DRAG BEAM SWITCH
POSITION LIGHTS	CYCLIC AND COLLECTIVE SWITCHES
CONSOLE LIGHTS	VHF/FM NO. 1 (IACS)
INSTRUMENT PANEL LIGHTS	VHF/FM NO. 2 (IACS)
NNAPS	UHF/AM (IACS)
PARKING BRAKE	VHF/AM (IACS)
PITOT HEATER	IFF (IACS)
RADAR ALTIMETER	DOPPLER NAVIGATION (IACS)
RATE OF TURN	VOR/ILS (IACS)
LANDING SYSTEM	LF/ADF (IACS)
PREFLIGHT CHECKLIST	EMERGENCY PROCEDURES

TABLE 1 - SUB-SYSTEMS INTEGRATED BY ADAS

ADAS was designed to integrate the total cockpit management functions of the UH-60A Black Hawk aircraft. A system block diagram of ADAS is shown in Figure 3, and the ADAS UH-60 cockpit is shown in Figure 4. It should be noted that IACS has been incorporated into ADAS as a complete CNI subsystem that operates under dynamic bus control allocation protocol. The crew interface for the non IACS functions are four multi-function displays and two keyboard terminal units. Line select keys located around the periphery of the displays allow menu and page selection by the crew. Eight remote terminal units provide the interface to hundreds of aircraft sensors, transducers, and electrical signals. Generation of alpha-numerics and vector graphics are accomplished in two programmable signal generators. The processing elements consist of two SDP-175 16 bit microprocessors. Programming is in assembly language; however, concepts of structured software with partitioned software modules have been applied. Data communication between elements is via dual redundant MIL-STD-1553 multiplex data buses.

The ADAS system has been installed on the AVRADA UH-60A System Testbed for Avionics Research (STAR) aircraft. The flexibility and growth potential provided by ADAS is well suited for use in AVRADA's flying laboratory for testing of new architectures, avionics equipments, and concepts. The STAR in its role as a research aircraft is a vital tool in the Army's pursuit of cockpit automation and advanced avionics technologies. Concepts and equipments developed in ADAS have greatly influenced the design of and are being employed in AHIP, the first fielded digitally integrated aircraft, and the OV-1B Mohawk Block Improvement Program.

Digital Map Generator

Another significant AVRADA avionics integration effort is the Night Navigation and Pilotage System (NNAPS) for which the first practical airborne digital map generator was developed. The NNAPS is a special purpose, very high speed digital processing system consisting of flight and tactical symbology generation, topographic map display generation, and an autonomous terrain-aided navigation system. A wide variety of operator-selectable symbology formats are used to display pilotage information which is superimposed on a FLIR or TV image (Figure 5), and navigational information which is superimposed on a map image (Figure 6).

The symbology was developed at AVRADA in the flight simulator and intensively flight tested in the STAR aircraft. The map image is generated from a digitized topographic data base consisting of terrain elevations and planimetric features such as vegetation, hydrography, transportation networks, structures, etc.

This same topographic data is also accessed by a terrain-aided navigation processor which uses a Kalman filter to estimate the vehicle's position errors. When these estimates are coupled with the unaided Doppler navigation system, positional accuracies of 50 to 100 meters can be achieved.

The capability to use digitized topographic data for both map generation and other functions such as terrain-aided navigation and threat management is a major advantage of a digital mapping system over alternative map display systems which are paper map based such as projected map displays, remote film strip map readers, etc.

The first flyable digital map hardware was developed at AVRADA and flight tested in the STAR in early 1983. It consisted of storing precomputed map images on magnetic tape for recall to a digital display memory and subsequent video readout to a standard television monitor located on the instrument panel. Stationary, black & white TV map images could be displayed at several fixed orientations and scale factors. For flight demonstrations conducted at Carlisle, PA, north up 6x6km and 12x12km map formats were used exclusively. Navigation symbology which included a moving aircraft symbol driven by an unaided Doppler output was generated externally for registration and video inseting on the map image. A course line was also provided by the symbol generator for inseting on the map between check points. This system achieved high acceptance by Army test pilots during many NOE flights at Carlisle.

Concurrent with AVRADA's in-house development of this rudimentary system, a contract was awarded to the Harris Corporation, Melbourne, FL, for the design and fabrication of a Digital Map Generator (DMG) whose principal function would be the real-time generation of a topographical map portraying both terrain elevation and planimetric information in a standard closed-circuit color television format. This highly interactive, moving-map system has been delivered and installed in AVRADA's flight simulator for test and evaluation. A magnetic four-track tape unit is used as the bulk storage device for the digitized topographic data base. Terrain elevation and planimetric data are stored in a compressed format on the first two serial tape tracks to cover a 100x100km geographic area. The remaining two tracks are available for field intelligence and mission-specific data which can be added during mission planning.

During operation, the desired map position and orientation angle are transmitted to the DMG, which can process these inputs at a rate of 60 Hz. The appropriate blocks of data are read from tape into an intermediate buffering memory from which special high-speed hardware reconstructs this data at the requested display scale into a buffering scene memory.

Readout to the video display at the desired map orientation angle is accomplished with special purpose hardware processors which generate the selected contour field and execute the terrain-shading algorithms. If the aircraft position is input as the commanded map position, the map will translate and rotate smoothly in an aircraft-centered, moving-map mode with no time lags or display degradation. The maps can be displayed on any standard color television monitor.

A programmable color mixing table located in the DMG output circuitry is loaded at initialization and used to assign desired

colors to specific planimetric features such as green for vegetation, blue for hydrography, etc. A programmable symbol table is also loaded at initialization and used to assign 8x8 matrix shapes to each of the 128 point features that the DMG can process. The point symbols are pinned at their specific map coordinates but always displayed in a screen up orientation for readability.

Input/Output communication with the DMG is accomplished through a 16 bit parallel interface under external computer control. At AVRADA's flight simulator, this is done via a DR-11W interface to a DEC VAX-11/780 computer. This design offers maximum flexibility in the development of map control software which can be tailored for the user's specific applications.

Operator interaction with the DMG is accomplished with a Control Display Unit (CDU) which is also interfaced with the external computer. The CDU presents the pilot with a list of control options via a computer generated menu and transmits selected options back to the external software which sends the appropriate commands to the DMG.

There are several types of DMG interface functions which permit the operator to actively configure the map video to any desired format:

For example, The DMG may be commanded to any map coordinate stored in the compressed data base on tape. This map point may be selected to coincide with either screen center or 1/4 of the way up from bottom which affords more look ahead distance if the aircraft position is used to drive the map in a moving mode.

Map orientation angle may be driven by the aircraft heading, in which case the map will rotate in a heading up mode, or by the aircraft track or some other fixed angle, such as north, resulting in map translations only.

Map display coverage per screen area may be selected by the operator as well. There are four display scales available for Army applications - 3x3km, 6x6km, 12x12km, and 24x24km. The 6km and 12km scales appear to be the most useful during actual flight, however the 3km scale may prove useful at lower velocities and the 24km scale is desirable during mission planning use (Figures 7, 8, 9,).

Two types of shading are available for operator selection - elevation shading and slope shading. In the elevation shading mode (Figure 10), the map is shaded as a function of terrain elevation bands with the darker shades normally assigned for the higher elevations. There are eight elevation bands whose relative width and absolute vertical positioning may be chosen by the operator for optimum information content. This mode can also incorporate the aircraft altitude into the shade assignment to provide the capability for terrain avoidance.

In the slope shading mode (Figure 11), the map is shaded with sixteen levels of intensity as a function of terrain slopes. The result is a more realistic visual presentation analogous to the relief shading associated with paper maps.

One of the most useful attributes of the DMG is the flexibility afforded the operator in selecting exactly what planimetric features appear on the display. Any combination of topographical and/or tactical feature subsets may be chosen and only those features which are selected will be displayed.

Another very critical function which is accomplished with the DR-11W interface is data base interrogation. The external computer may request a block of reconstructed elevation and planimetric data from the DMG. This data is then available for manipulation by external software which executes the terrain-aided navigation and threat management computations. As stated earlier, this is a major advantage of a digital mapping system and the importance of such a capability cannot be overestimated.

Digital Map Technology developed by AVRADA has been effectively demonstrated in the Army Advanced Rotorcraft Technology Integration (ARTI) and the Air Force Advanced Fighter Technology Integration Programs. Digital Map Systems will be employed in LHX and other future rotorcraft systems.

Fault Tolerant Systems Research

AVRADA recognized the need and provided for fault-tolerance in the IACS and ADAS architectures through redundancy. Future aircraft will employ digital electronic systems to perform flight critical functions which must be ultra-reliable as failure could result in the loss of the aircraft. The design and validation of ultra reliable systems present special problems not found in the design and validation of conventional systems and new techniques and methods are needed to evaluate their performance and reliability. No longer will exhaustive testing be practical because of the excessive time required and cost incurred to build confidence that the reliability requirements can be met. Therefore, attention must be given to defining techniques and methodologies for ensuring that advanced system designs meet performance and reliability requirements without having to rely on exhaustive testing. Research is being conducted at the NASA Langley Research Center to provide an effective validation methodology, techniques for conducting comparative analyses of advanced system concepts, and guidelines for designing fault-tolerant systems that will be easier to validate.

As shown in figure 12, the work at the Langley Research Center includes development of analytical models for reliability estimation, economic assessment, and software error prediction; design proof techniques; emulation capabilities; and experimental procedures leading to the definition of a generic validation methodology.

These techniques and methods are verified and refined by applying them to specimens of fault-tolerant computers and systems using the capabilities of the Avionics Integration Research Laboratory (AIRLAB) facility. Candidate tools and techniques become a part of a proposed validation methodology that is applied to advanced system concepts or proof-of-concept hardware models in AIRLAB as illustrated in figure 13. Experiments provide information on the effectiveness of the proposed methodology and the candidate tools and techniques, as well as data on the performance and reliability characteristics of the system test specimen.

AIRLAB is a national facility that provides many opportunities for cooperative activities between NASA, industry, academia, and other government agencies by researchers who are interested in the design and validation of highly reliable fault-tolerant systems. AIRLAB became operational at the Langley Research Center in 1983 to support research that will become the basis for developing design and validation methodologies. The basic attributes and capabilities of the physical laboratory continue to evolve as the requirements for research in the area of fault-tolerant systems progress.

AIRLAB is a 7600 square foot, environmentally controlled laboratory partitioned into three distinct areas as shown in figure 14. The largest area contains eight research work stations and a central-control station. The next largest area is the computer room containing nine VAX 11/750's and a VAX 11/780. Each VAX 11/750 has 2 megabytes of memory and 56 megabytes of local disk storage. The VAX 11/780 has 4 megabytes of memory and 160 megabytes of local disk storage. All 10 of the VAX minicomputers are interconnected with a 256 kilobaud serial digital communication network with DECNET communications software. The third area contains a horizontally microprogrammable Nanodata QM-1 computer that hosts a unique diagnostic emulation algorithm for use in emulating digital devices at the lowest logical level. Each research station is configured with an extensive set of peripherals as well as digital and analog input/output devices. A block diagram for a typical research station is shown in figure 15. Four of the research stations also have MEGATEK 3-D graphic systems with high resolution color monitors. AIRLAB provides a capability for conducting experiments without the necessity of each experimenter having to learn the details of the facility hardware and software. A unique software feature of AIRLAB is the Data Management System (DMS) which is the prime interface for experimenters to access information about the laboratories capabilities. A major goal of the DMS is to allow users to be as productive as possible by providing centralized, easy access to AIRLAB capabilities and research results. The DMS collects data about experiments, organizes it, provides easy access to it, and ensures its integrity. The DMS operating environment, accessible from all AIRLAB VAX computers, is largely menu-driven and offers extensive on-line help. Log-on and log-off procedures are used to track the user's activities on the system and captures as much information automatically as possible. An on-line engineering

notebook allows the user to make notes about current work whenever desirable. The user can later search the notes both chronologically and by key words to recall information about the work. Most experimental data collected will initially be kept on-line but will eventually be archived on tape. The DMS provides the capability to facilitate accessing information in archived files using an on-line catalog of all archived files coupled with the ability to browse and search the catalog simply and easily. The DMS also includes a software configuration management system that facilitates the development of user software programs, provides problem reporting and tracking mechanisms, and provides a catalog of all the available software. For those experiments that require access to the VAX operating system, the capability is provided to move easily from the DMS to the operating system and back to the DMS. Other support software currently available is listed below.

- o OPERATING SYSTEM

VAX/VMS

VAX/ELN

- o LANGUAGES

Ada

FORTRAN

VAX - 11 ASSEMBLER

PASCAL

C

BASIC

LISP

BLISS 32

- o WORD PROCESSING AND REPORTING

MASS - 11

DATATRIEVE

- o GRAPHICS

TEMPLATE

WAND (MEGATEK)

The design of AIRLAB provides the flexibility to support a variety of research configurations. Figure 16 is an illustration of AIRLAB resources configured for conducting multiple independent experiments. Station 1 is the central control station which is directly connected to the VAX 11/780 and is used for software development and data management. Station 2 is used to demonstrate the diagnostic emulator's capability to emulate an avionics microprocessor at the gate level. Stations 3, 4, 5, and 6 are configured for an experiment that is designed to validate

assumptions made in the design proof of a fault-tolerant system synchronization algorithm. Two of the stations, 7 and 8, are used in an experiment to investigate the occurrence of software errors. Stations 9 and 10 are each dedicated to supporting one of two fault-tolerant computer system test specimens that are used for developing validation experiments to characterize fault-handling responses. Figure 17 is an illustration of AIRLAB resources configured to support integrated systems experiments. The station assignments are arbitrary, and the data distribution network is experimental and defined by the experimenter. Another possible configuration of the research stations, figure 18, would allow the experimenter to investigate new fault-tolerant computer concepts where redundant elements of the system are simulated at each station.

Two fault-tolerant computer systems that are currently installed in AIRLAB are the Software Implemented Fault-Tolerance Computer (SIFT) and the Fault-Tolerant Multiprocessor (FTMP). As the name implies, the SIFT computer shown in Figure 19 isolates faults primarily with voting techniques implemented in software. Upon detection of an error using a software voter the operating system software decides which element of the system is faulty and invokes a reconfiguration task to eliminate the faulty element. The FTMP computer has a very different architecture from SIFT as seen in Figure 20. FTMP initially detects faults in a hardware voter and error detector. The FTMP operating system software also invokes a reconfiguration task to eliminate the faulty elements of the system. Both the SIFT and FTMP computers are available for developing validation experiments and analytical procedures.

Joint Army NASA Avionics Program

In 1985 the Army Aviation Systems Command, recognizing the significance of the NASA avionics program at Langley Research Center, and the potential benefits derivable from a cooperative Army NASA avionics effort, authorized the establishment of the AVRADA Joint Research Programs Office (JRPO) at Langley. In 1986, JRPO staffing began and Army research engineers are now performing joint avionics research with NASA research engineers at the Langley Research Center facilities. In AIRLAB, Army engineers are currently participating in two joint research projects in the area of fault tolerant avionics systems. One project is directed toward the development of design guidelines and performance assessment methodologies for advanced fault-tolerant system architectures and the other is investigating methods for estimating software reliability for ultra-reliable systems. In addition to the joint fault-tolerant systems programs in AIRLAB, Army research engineers are performing cooperative research with NASA in developing code for predicting antenna performance on complex rotorcraft structures and in the investigation of advanced cockpit display technology for future rotorcraft.

The results of the joint avionics research program at Langley will compliment and provide significant input to the AVRADA technology base and developmental efforts at Fort Monmouth, NJ. During the past decade AVRADA and NASA Langley have been independently exploiting the explosion in digital technology. With the recent establishment of the Army NASA avionics program at Langley it is fully expected that the next decade of the continuing digital electronics technology explosion will be harnessed even more effectively in providing "Hi-Tech" avionics for future Army rotorcraft systems.

References:

1. Dasaro, J. A., "The Impact of Future Avionics Technology on The Conduct of Air Warfare," AAAA Army Aviation Electronics Symposium, Asbury Park, NJ, May 1986.
2. Davis, B., "Army Avionics Trends - An Evolutionary Approach AIAA/IEEE Digital Avionics Systems Conference, Fort Worth, TX, October 14, 1986.
3. Allman, D. D. and Buller, B. T., "Integrated Avionics Control System (IAES) Customer Test," U.S. Army Aviation Board, Fort Rucker, AL, 22 July 1980.
4. Campagna, R. W., "The Digital Map Generator," Army Aviation, July-August 1984.
5. Holt, H. M., et al, "Flight Critical System Design Guideline and Validation Methods," AIAA/AHS/ASEE Aircraft Design Systems and Operations Meeting, San Diego, CA, October 31-November 2, 1984.

INTEGRATED AVIONICS CONTROL SYSTEM (IACS)

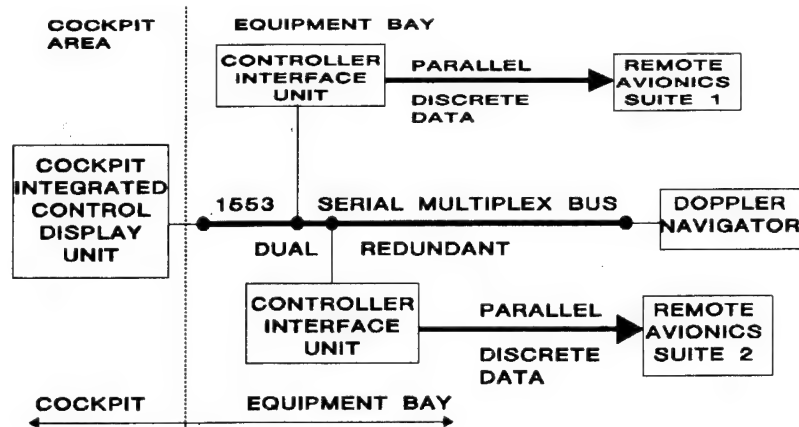


FIGURE 1

IACS CONTROLLED AVIONICS

- o VHF-FM RADIO - 2 each
- o VHF-AM RADIO
- o UHF-AM RADIO
- o VOR/ILS
- o IFF
- o ADF
- o DOPPLER NAVIGATOR
- o UHF-AM RADIO
- o SECURITY DEVICES FOR RADIOS AND IFF

FIGURE 2

ARMY DIGITAL AVIONICS SYSTEM (ADAS)

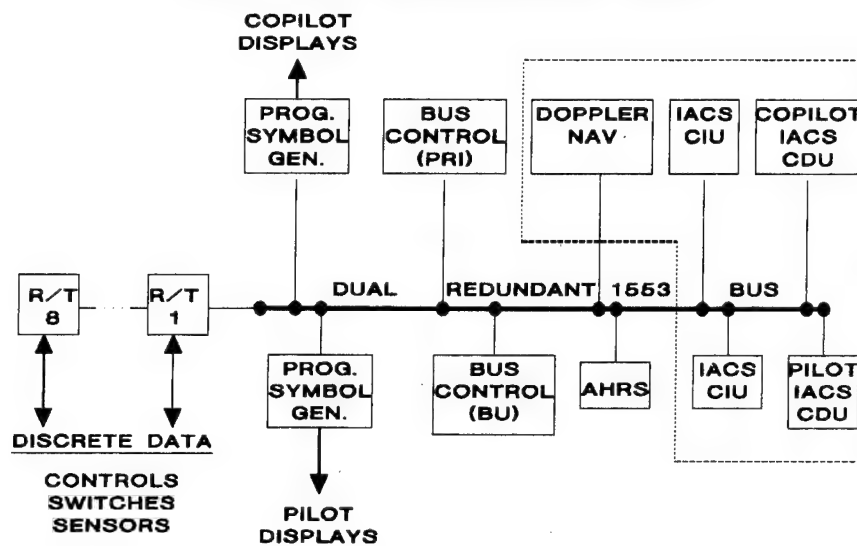


FIGURE 3

ADAS UH-60 COCKPIT

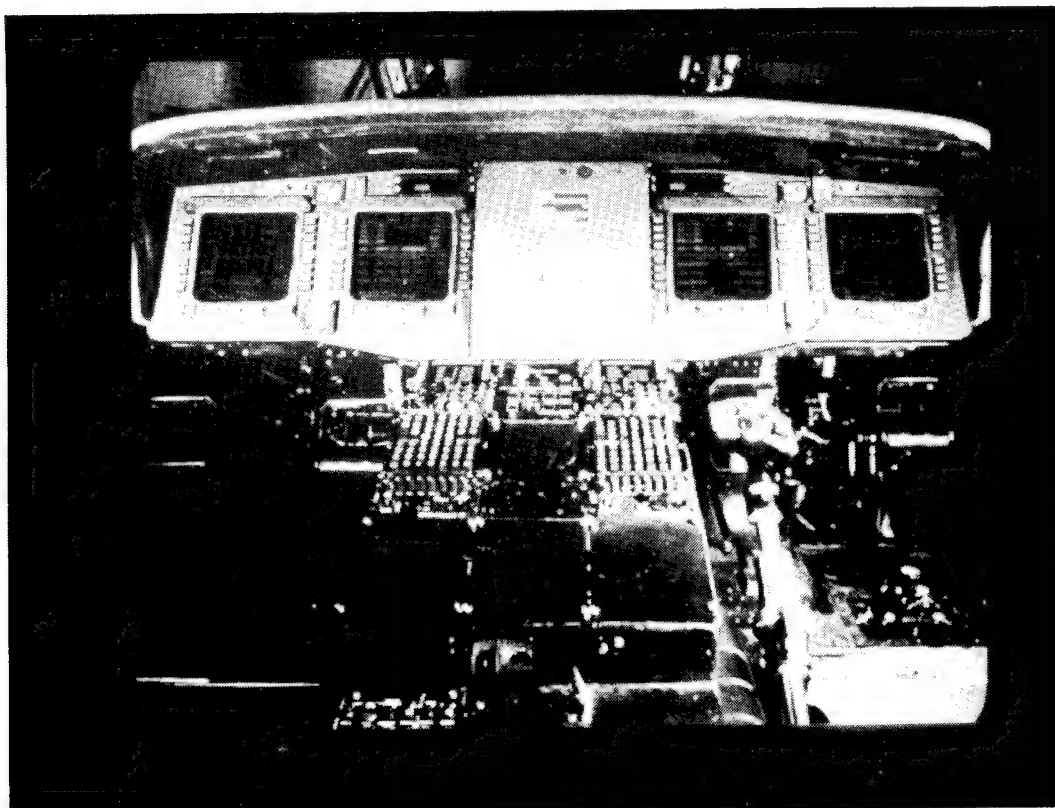


FIGURE 4

SUPERIMPOSED PILOTAGE INFORMATION

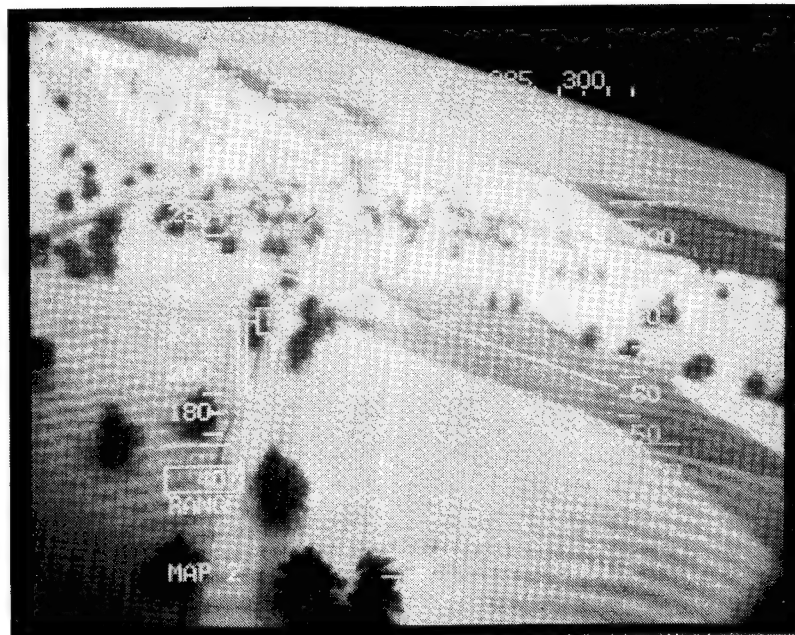


FIGURE 5

SUPERIMPOSED NAVIGATION INFORMATION

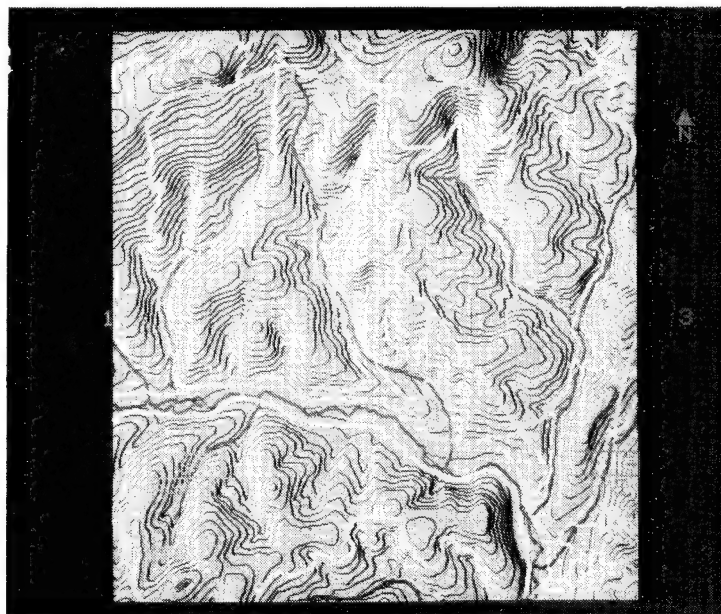


FIGURE 6

3KM X 3KM DIGITAL MAP

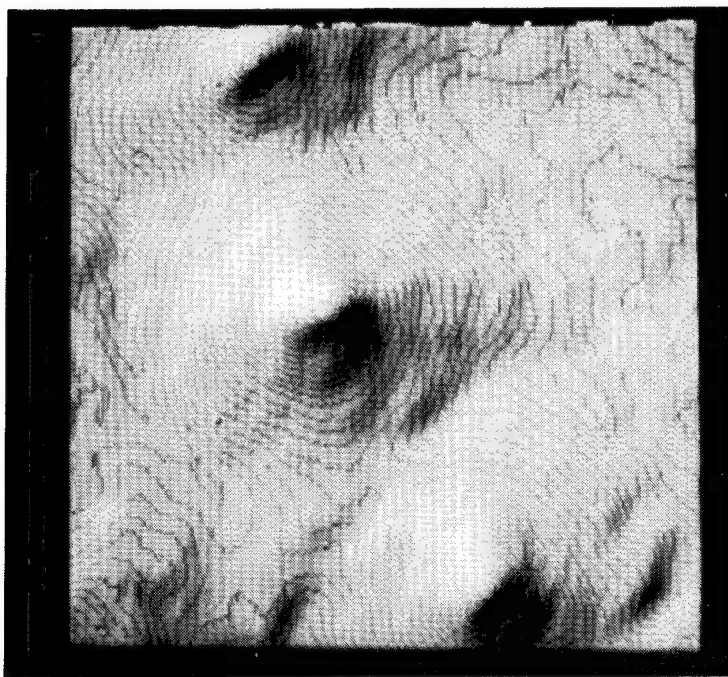


FIGURE 7

6KM X 6KM DIGITAL MAP

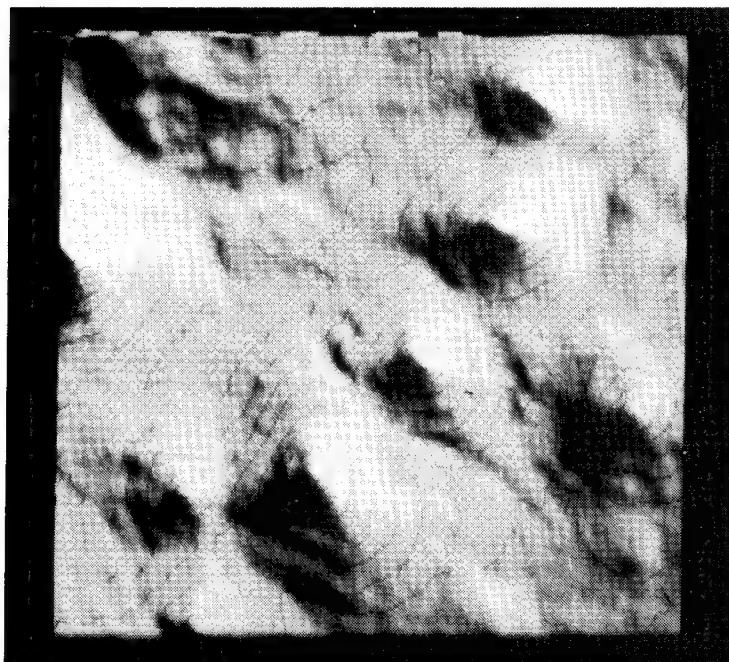


FIGURE 8

12KM X 12KM DIGITAL MAP

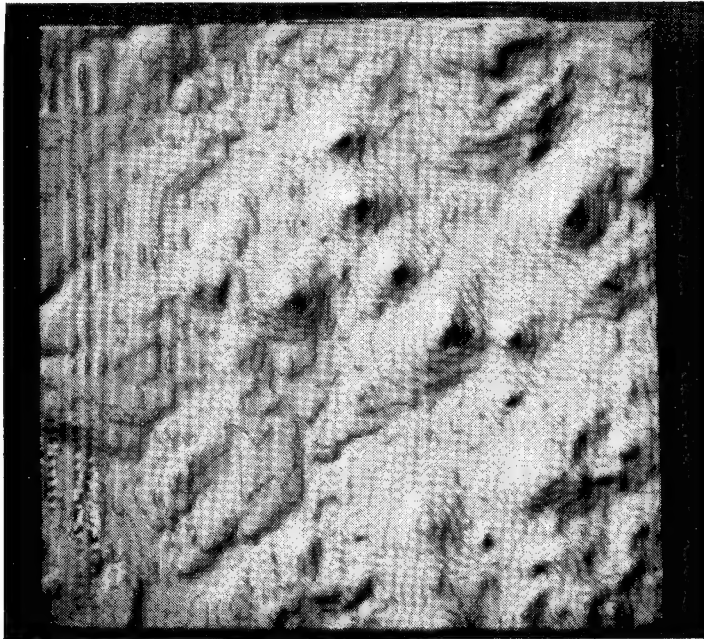


FIGURE 9

ELEVATION SHADED DIGITAL MAP

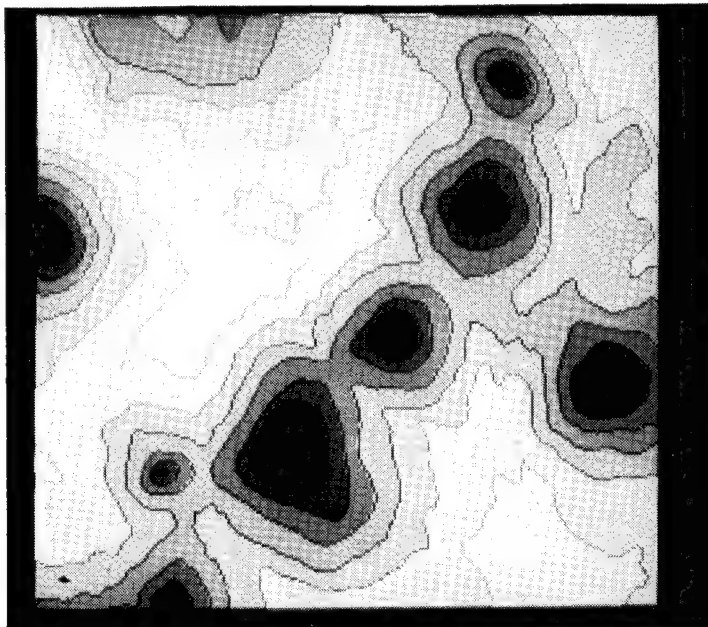


FIGURE 10

SLOPE SHADED DIGITAL MAP



FIGURE 11

FAULT-TOLERANT VALIDATION METHODOLOGY RESEARCH

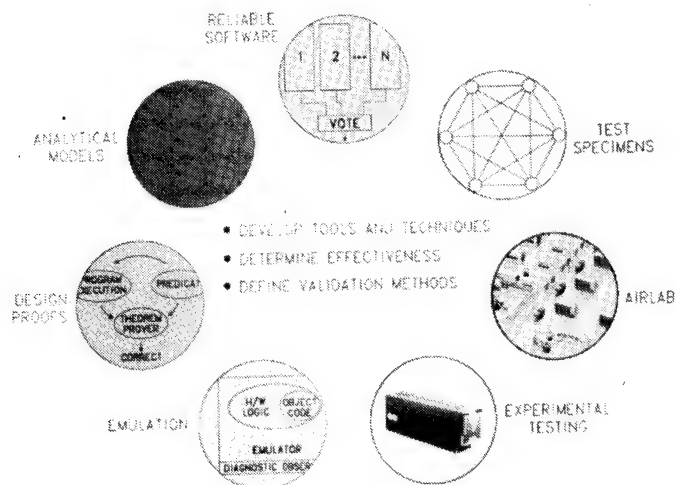


FIGURE 12

FAULT-TOLERANT SYSTEM RESEARCH

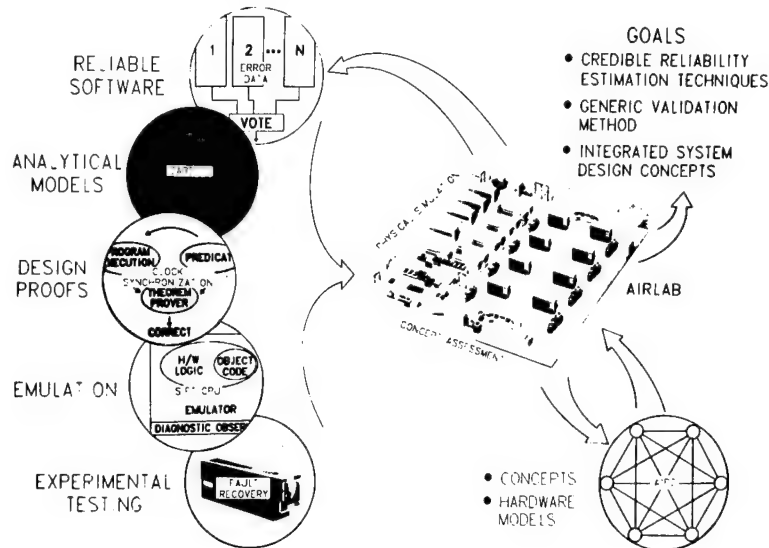


FIGURE 13

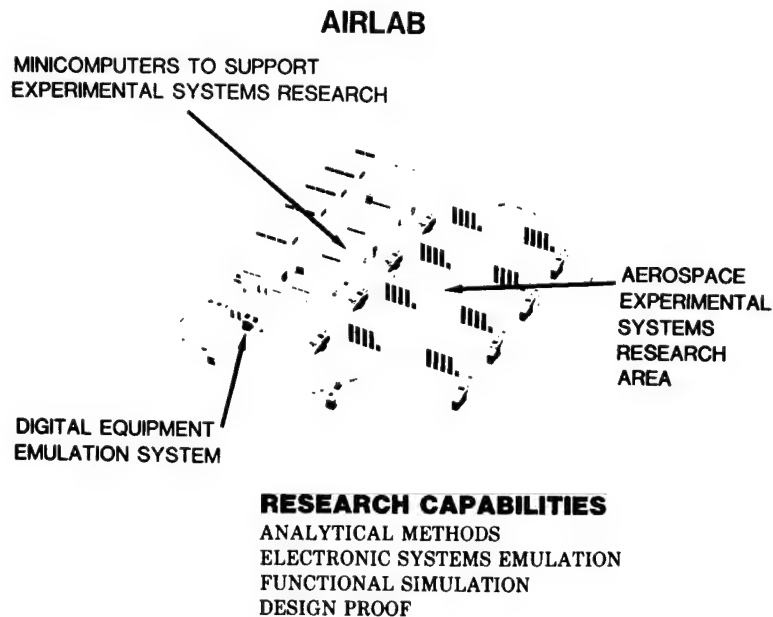


FIGURE 14

TYPICAL RESEARCH SUPPORT STATION

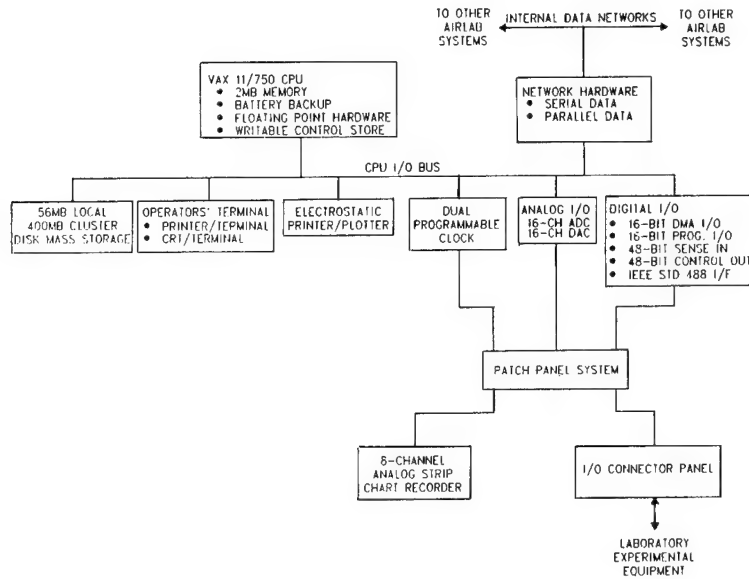


FIGURE 15

EXPERIMENTAL STATIONS MULTIPLE INDEPENDENT EXPERIMENTS

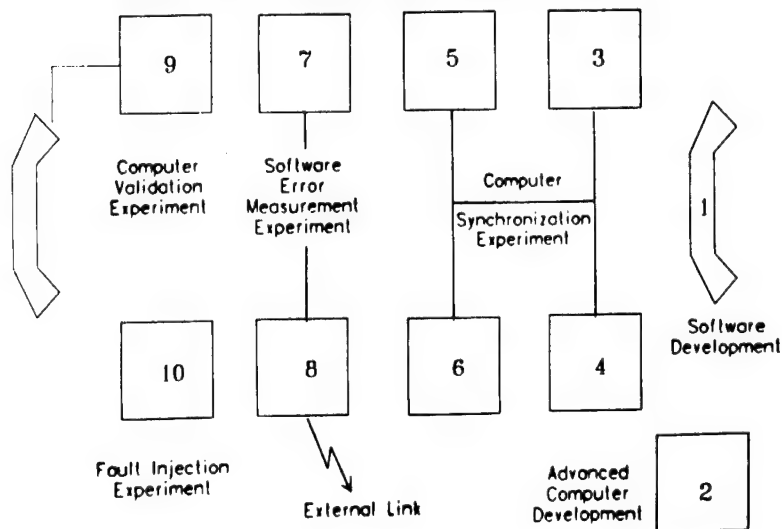


FIGURE 16

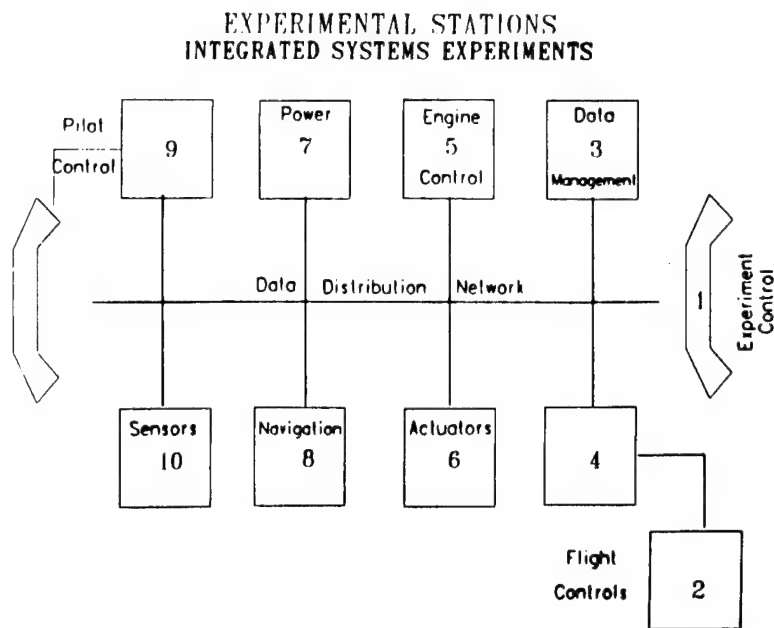


FIGURE 17

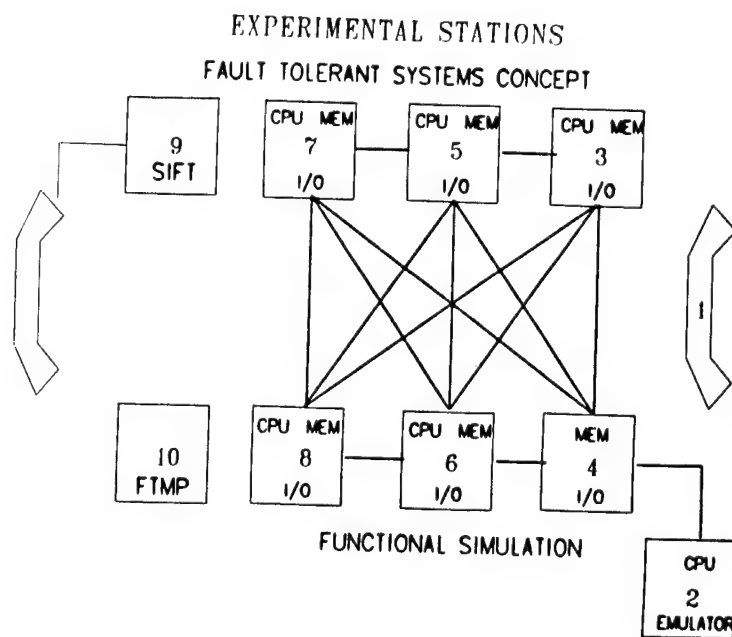


FIGURE 18

SOFTWARE IMPLEMENTED FAULT-TOLERANCE COMPUTER ENGINEERING MODEL

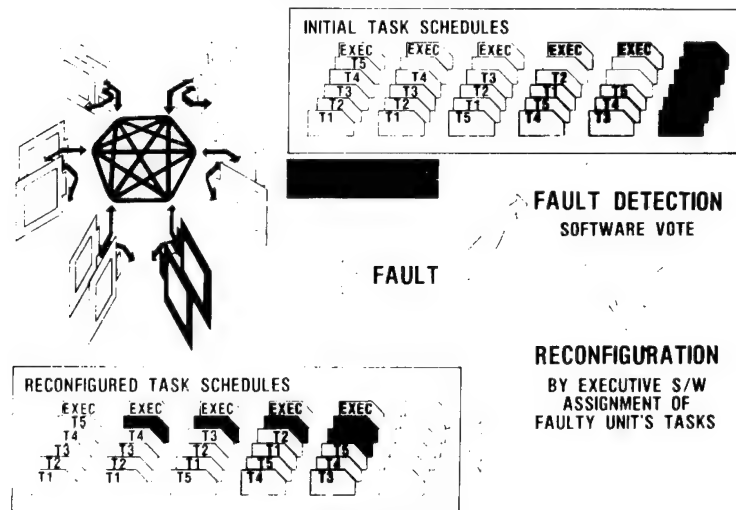


FIGURE 19

FAULT TOLERANT MULTIPROCESSOR ENGINEERING MODEL—CSDL&COLLINS

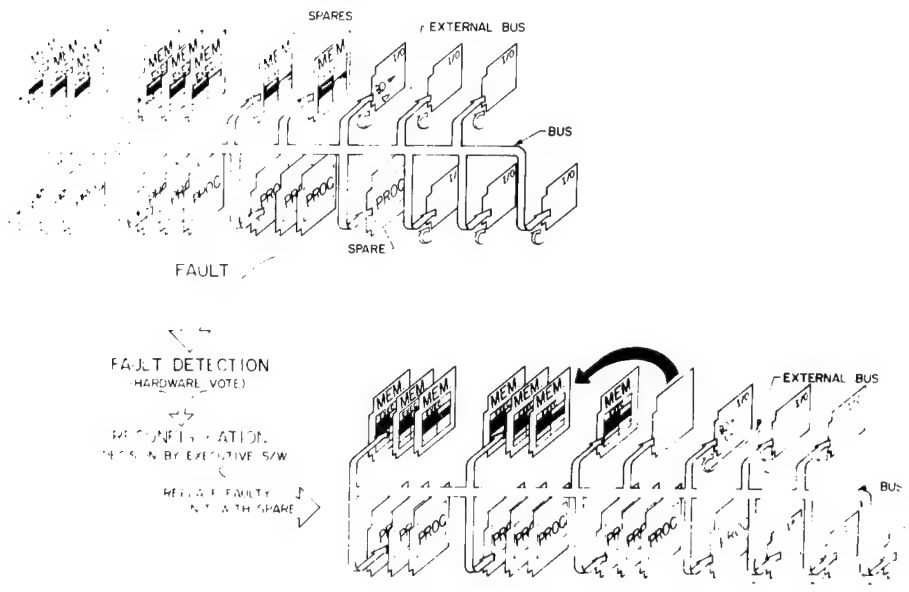


FIGURE 20

INTEGRATED DIAGNOSTICS

Roger J. Hunthausen
Aviation Applied Technology Directorate
U.S. Army Aviation Research and Technology Activity (AVSCOM)
Fort Eustis, Virginia 23604-5577

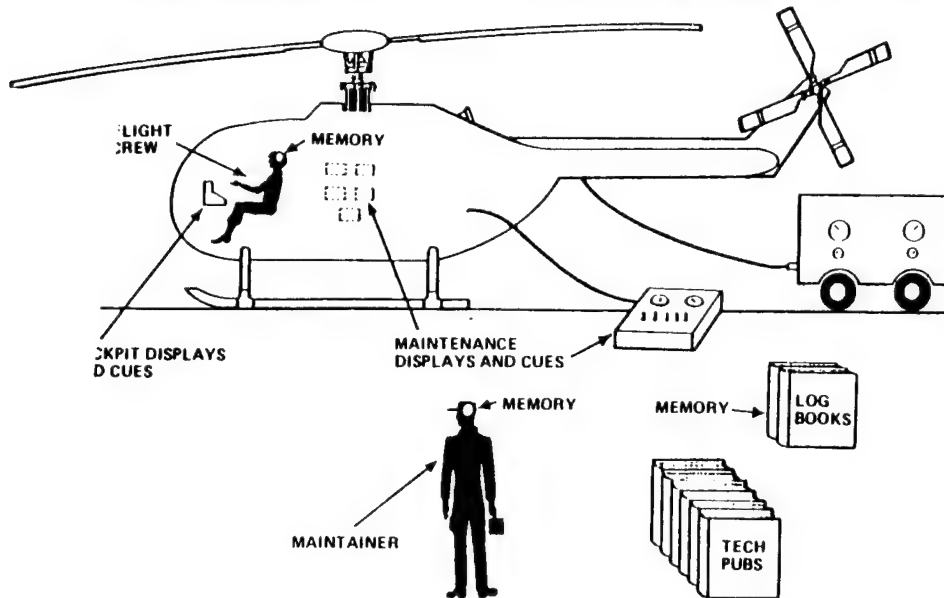
INTRODUCTION - STATEMENT OF NEED

The challenge now facing our military strategists is how to overcome the ever-increasing gap between the strength of our adversaries and that of our own existing forces. To lessen this gap, our weapon systems have become more complex and costly as a result of the increased demand for performance and in design. Both of these factors tend to exacerbate the maintenance problems. Fault location (diagnostics), in particular, is a maintenance task that is greatly affected by complexity and cost. Increased system complexity generally makes the fault location task more difficult, particularly when the basic skill level and capability of the maintenance personnel do not improve at the same rate as system performance. However, the increased cost of aviation systems and related spare parts requires that aircraft downtime be kept to an absolute minimum and that false removals of major components be reduced as much as is practical without sacrificing fault-detection capability.

Fortunately, the technological advances that lead to improved system performance can also be used to enhance system supportability. Advanced condition monitoring sensors, such as accelerometers and oil debris detectors, often permit maintenance personnel to detect and isolate a failed component soon after operation. Built-in test (BIT) and built-in test equipment (BITE) can also provide similar capabilities for electronic systems, provided the input parameters, test point location, and decision logic are correct (this will be further discussed).

The increasing sophistication of modern aircraft, the need for greater aircraft availability, and the limited pool of manpower and skills available for maintenance have placed excessive demands on current diagnostic philosophies. In actual process, no systematic approach to fault isolation is employed (Fig. 1). The test procedures in the technical manuals are often ignored, and "remove and replace" becomes the standard troubleshooting process. This may evolve into a total "shotgun approach," where all possible failed components are replaced. The complexity and unreliability of the field test equipment lead to their misuse and erroneous results. Even BIT indications are misinterpreted when fault codes must be interpreted and referenced in manuals.

Maintenance is a Problem Because . . .



. . . It is based on a loosely connected flow of inadequate measurements and information to the human intelligence of the maintainer.

Fig. 1. General condition at AVUM level maintenance.

If the elements of Fig. 1 could be tied together and offer a coherent picture of the status of the aircraft and isolate to failed components, then an integrated diagnostic system would be realized. The objective of such a system is the transformation of available data, whether from the crew, cockpit, TM's or test equipment, into useful maintenance information. The system should be able to evaluate the usefulness of the data, reject incorrect or superfluous data, and aid the personnel in the determination of the proper maintenance action. The current approach depends heavily on the experience and training of the crew and maintenance personnel to both acquire and interpret the many forms of data available. This leads to a specialization of tasks and thus the requirement for a large number of skill specialties. An integrated diagnostic approach has the potential to reduce the number of skill specialties now required and thus allow the maintenance of current capabilities even after reduction in force structure.

Another important reason for integrated diagnostics and also for condition monitoring systems was aptly detailed in a NASA study on the potential causes of pilot-error accidents. U.S. Army statistics have identified human error as the major cause in approximately 75% of all major helicopter accidents during the fiscal years 1978-1982. Table 1 is a summary of the results of a NASA study in which 110 randomly selected U.S. Army accidents were reviewed. These accidents were from the following categories: Class A accidents (those

resulting in a fatality, permanent disability, airframe loss, or costs exceeding \$500,000) and Class B accidents (hospitalization of five or more personnel, permanent partial disability, or costs between \$100,000 and \$500,000).

TABLE I

SUMMARY OF HELICOPTER PILOT ERROR ACCIDENTS⁽³⁾
AGGREGATED BY AREAS OF TECHNOLOGY NEEDS⁽²⁾

AREAS OF TECHNOLOGY NEEDS	NUMBER OF MISHAPS	NUMBER OF FATALITIES	NUMBER OF INJURIES (NONFATAL)	COST ESTIMATES	
				AMOUNT	PERCENT
NO APPARENT TECHNOLOGY IMPLICATIONS	5	0	15	\$ 5,828,440	9.3
ALTERNATIVE TO THE TAIL ROTOR	6	0	8	1,768,799	2.8
ADVANCED FLIGHT SIMULATORS	21	5	17	13,216,403	21.1
ADVANCED FLIGHT CONTROLS AND DISPLAYS	25	8	23	15,394,824	24.6
OBSTRUCTION DETECTION	20	13	42	11,962,376	19.1
AUTOMATED MONITORING & DIAGNOSTIC SYSTEMS	29	7	41	12,022,725	19.2
CONTINGENCY POWER	4	0	9	2,446,922	3.9
TOTALS FOR RECORDS REVIEWED ⁽¹⁾	110	33	155	\$62,640,494	100.0

NOTES: (1) RANDOM SELECTION FROM ARMY CLASS-A AND -B ACCIDENTS 1981-1983.

(2) NASA STUDY

(3) HUMAN ERROR IS CAUSE FACTOR IN 75% OF ALL MAJOR ARMY ACCIDENTS 1978-1982.

PUBLISHED IN RWI, APRIL 1986.

As the table indicates, 29 accidents, or 26.6%, were identified in the NASA study as preventable with new technology to assist the pilot in monitoring the performance of flight-critical systems; i.e., automated monitoring and diagnostic systems. Researchers noted that numerous accidents involved a sequence of events wherein an actual or suspected in-flight failure was misinterpreted by the pilot/crew or incorrectly diagnosed. These findings led to recommendations for advanced technology to:

1. Monitor flight-critical systems without pilot intervention.
2. Warn of adverse trends and impending system failure.
3. Correlate information or malfunctions.
4. Automatically predict and monitor performance capabilities and power demands to assist the pilot in operating within performance limitations.

This paper summarizes recently completed projects in which advanced diagnostic concepts have been explored and/or demonstrated. The projects begin with

the design of integrated diagnostics for the Army's new gas turbine engines, and advance to the application of integrated diagnostics to other aircraft subsystems. Finally, a recent project is discussed which ties together subsystem fault monitoring and diagnostics with a more complete picture of flight domain knowledge.

ENGINE DIAGNOSTICS

APPROACH

The successful fielding of the T-700 engine demonstrated the importance of incorporating maintenance and diagnostic technologies at the start of the design phase and not trading off this technology for other considerations (cost and/or weight) as the engine matured. The results of this have shown the T-700 engine to be one of the most maintainable engines within DOD inventory. This philosophy of designing in diagnostics was carried over to other engine development programs--the advanced technology demonstrator engine program (ATDE) and the modern technology demonstrator engine (MTDE). Under these efforts, the contractors were required to conduct diagnostic and condition monitoring studies to assess and identify specific diagnostic and monitoring techniques that would allow on-condition maintenance yet not sacrifice the safety of the pilot and crew. Fault isolation procedures were to be developed to identify faults to the modular or line replaceable unit (LRU) level.

From these studies, a diagnostic/condition monitoring system was defined beginning with a determination of the right mix of sensor inputs. Parameter selection was first based on the data that would normally be available from electronic fuel controls and cockpit indications since these signals were essentially free for diagnostic usages. Typical signals are listed in Table II. Additional parameters could then be selected on the basis of their usefulness/effectiveness within a given system. This is determined by system complexity, cost to monitor, and potential payback. The functions of the monitoring system can be generalized into:

1. General engine health.
2. Engine limit exceedances.
3. Engine trending analysis.
4. Fault isolation to the LRU/module level.
5. Low cycle fatigue.
6. Hot section stress.

Table III is a compilation of the various types of parameters required for the above specific areas. The final selection of parameters is obviously

dependent on system complexity. To determine which mix of parameters and techniques should be pursued, studies were conducted on system effectiveness vs. cost tradeoffs. Possible engine parameters, sensors/transducers and maintenance indicators, and ground support equipment combinations were identified and the cost and effectiveness of each were determined.

TABLE II
TYPICAL PARAMETERS

CONTROL UNIT		EMS	
T2 - COMPRESSOR INLET TEMP		PLA - POWER LEVEL ANGLE	
NG - GAS GENERATOR SPEED		KIAS - KNOTS INDICATED AIR SPEED	
NP - POWER TURBINE SPEED		PI - AMBIENT AIR PRESSURE	
Q - TORQUE		C/P - COLLECTIVE PITCH ANGLE	
PTIT - POWER TURBINE INLET TEMP		NR - ROTOR SPEED	
P3 - COMPRESSOR DISCHARGE PRESS		G - AIRFRAME G LOAD	
ΔPFF - FUEL FILTER AP SWITCH			
ECUF - ECU FAULT OUTPUTS			
COCKPIT		BLEED	
POIL - OIL PRESS		IPS - INLET PARTICLE SEPARATOR SWITCH	
TOIL - OIL TEMP		CVIB - COMPRESSOR VIBRATION	
LOIL - OIL LEVEL		TVIB - TURBINE VIBRATION	
ΔPOF - OIL FILTER AP		WOW - WT ON WHEELS SWITCH	
CHIP - CHIP DETECTORS		BLEED - CUSTOMER BLEED SWITCH	
WF - FUEL FLOW (CALCULATED)			
TFUEL - FUEL TEMP			
AICE - ANTI-ICE SWITCH			

TABLE III
PARAMETER REQUIREMENTS

	T1	P1	NG	NP	Wt	Q	MGT	TBT	COP	ECU	POIL	TOIL	LOIL	ΔPOF	ΔPFF	M PLUG	VIB 1	VIB 2	VIB 3	IGN	MAN
ENGINE GENERAL HEALTH	X	0	X	X	0	X	X	0	0		X			X	X	X	0	0	0		
OPERATING PARAMETER EXCEEDANCE			X	X		X	X														
ENGINE LRU FAULT ISOLATE																					
CONTROL SYSTEM LRU'S	X	0	X	X	0	X	X	X	X	X				X						0	0
OTHER LRU'S	X		X	X		X	X	X	X	X	X	0	0	X		X					
ENGINE TREND ANALYSIS	X	0	X	X	0	X	X		0		0	0					0	0	0		
LOW CYCLE FATIGUE			X	X																	
HOT SECTION STRESS							X	0													
OVERALL	X	0	X	X	0	X	X	X	X	X	X	0	0	X	X	X	0	0	0	0	0

MINIMUM REQUIREMENT=X

BEST CONFIDENCE=0

The various mixes of combinations are depicted in Fig. 2. Systems 1 and 2 consisted of sensors, cockpit indication, and a maintenance indicator unit for the airborne portion of the system. System 3 added a data recorder/analyzer. All systems used a portable data analyzer for ground support at the unit maintenance area with systems 2 and 3 adding a processing station at the intermediate level. System 3 was capable of interfacing with an airframe recorder if needed.

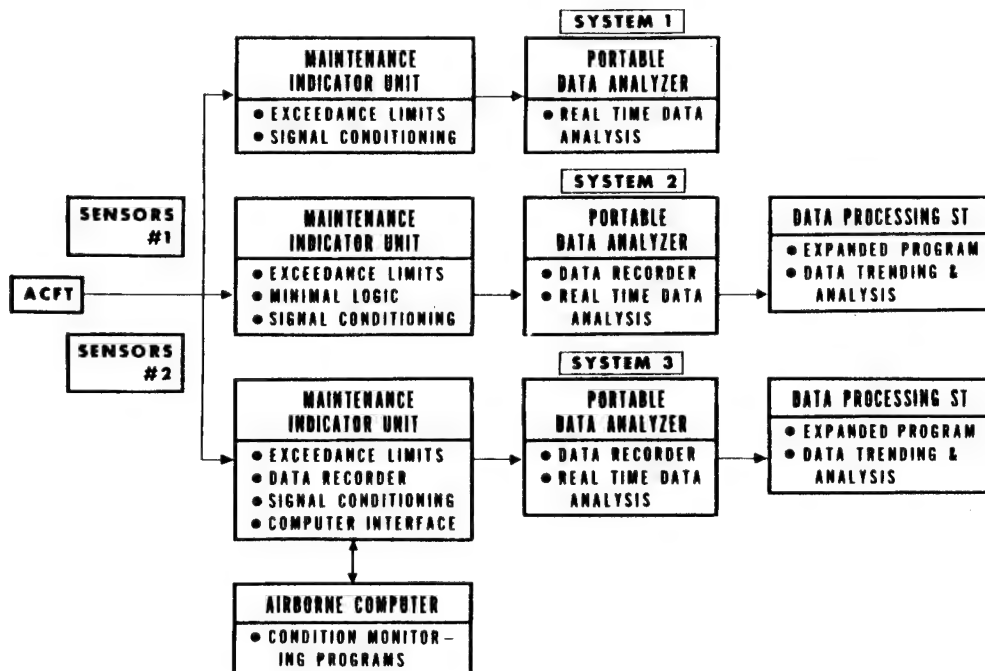


Fig. 2. Condition Monitoring Concepts

System 1 is the least complex with minimum hardware and a "no frills" approach. It requires active participation by maintenance personnel in most of the fault isolation process. All components of this system would be found at the unit maintenance level.

System 2 would have an expanded data analysis capability to reduce the human input in the fault isolation process and thereby decrease the overall possibility for erroneous maintenance decisions. This system includes a data processing station at the intermediate maintenance level to analyze the data from the ground analyzer unit. This approach offers several advantages over the system initially described. The added airborne logic capability allows this system to isolate more malfunctions to cause. Field operation of this system would not require additional ground support equipment and the need for additional dynamic testing by the portable data analyzer is reduced. Data from the portable analyzer could be further analyzed at the processing station for further fault isolation and repair.

System 3 represents a maximum capability for condition monitoring. It would virtually eliminate the need for manual malfunction troubleshooting.

An airborne recorder/analyzer would be added with this system along with an increased number of sensors. The recorder would be installed to record flight and exceedance/malfunction information. The data processing station would have data trending capability as well as fault isolation software. The maintenance philosophy for this system is a maximum analysis approach and requires the least human analysis and action of the three systems discussed. With extended in-flight condition monitoring and analysis, this system will predict many types of failures to reduce in-flight emergencies and mission aborts. Data from the cockpit display and airborne recorder would be analyzed either on board or at the data processing center, thus eliminating the need for the portable analyzer and other ground support equipment.

SYSTEM EFFECTIVENESS

The three systems were evaluated on their diagnostic effectiveness in terms of maintenance actions. The objective of the evaluation was to determine the overall probability of diagnosing known faults based on the individual system concepts and the engine parameters being monitored. In addition, costs for each system were established to give a system cost v.s. effectiveness comparison.

Fig. 3 shows the results of this evaluation and indicates that an intermediate complexity system, such as No. 2, provides the most diagnostic effectiveness at the least cost. System No. 1 requires a high degree of mechanic interaction for fault isolation without sufficient monitoring information or analysis capability. Therefore, the mechanic must rely on the diagnostic procedures in his tech manuals and on his own experience. Too often this results in erroneous decision-making and a lack of diagnostic effectiveness. The most complex system, No. 3, provides the most diagnostic effectiveness. However, there is an increase in cost of over twice that of System No. 2, primarily due to the requirements for an airborne recorder/analyzer. In addition, a drawback of System No. 3 is the extensive automatic analysis and decision-making capability of the system itself. As depicted in Fig. 4, a major driver of support costs is misidentification of good components as bad. The probability of this occurrence is very high for complex components. Fig. 5 shows a more responsive approach than a completely analytical one. Here automatic decision processes will be utilized when sufficient data on the system condition is known. Otherwise, the system must be flexible to allow the maintainer to use his judgment and experience in identifying and correcting malfunctions.

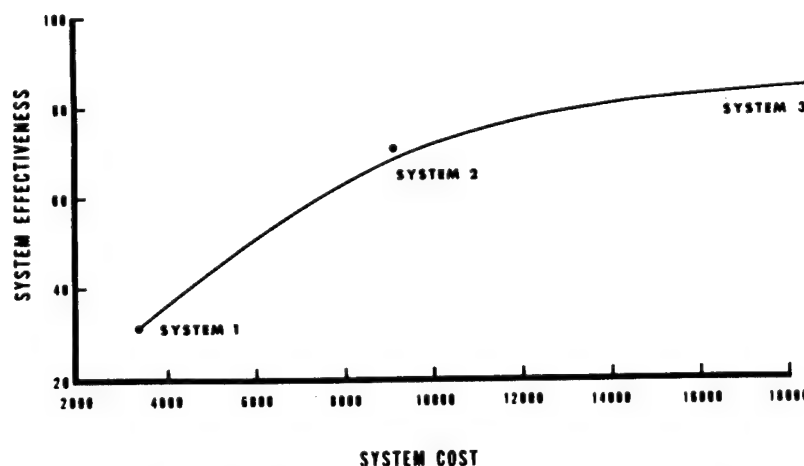


Fig. 3. Condition Monitoring Effectiveness

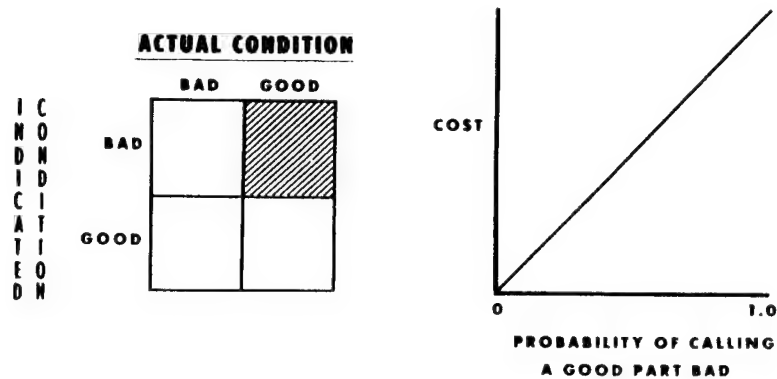


Fig. 4. The Automatic Diagnostic System Dilemma

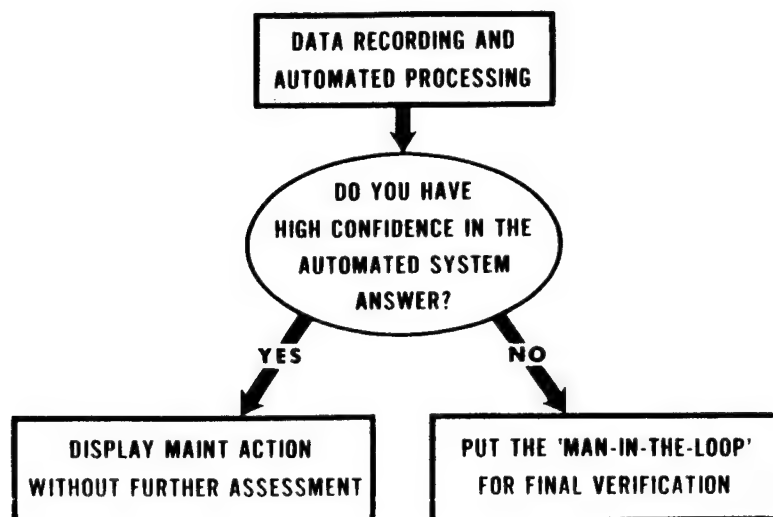


Fig. 5. Optimum Approach

ADVANCED MAINTENANCE DEMONSTRATION

DESCRIPTION

The capability of achieving a fully functional integrated diagnostic system is dependent on the incorporation of an airframe recorder/processor for real time data assessment and indication to the pilot and mechanic. However, as indicated during the engine diagnostic programs, such a system is cost prohibited if only applied to the powerplant subsystem. However, if the hardware could be used in a multifunction role, then the costs could be shared with other subsystems and the benefits increased to justify the overall procurement costs. Such a system was pursued and demonstrated under an Army program called "Advanced Maintenance Demonstration" (AMD).

The AMD was initiated in 1985 as an ambitious 4-year effort to enhance the diagnostic and condition monitoring capabilities of current and future

helicopter weapon systems. This effort is comprised of building blocks from "off-the-shelf" technology and new technology applications. These building blocks are depicted in Fig. 6 and include an airborne data recorder/processor, ground-display computer systems, and advanced diagnostic/prognostic software logic using artificial intelligence (AI) techniques. The key to achieving a successful diagnostics system is the integration of these technologies with a close regard for the human engineering disciplines; that is, how the mechanic in the field during combat can best utilize the data available to him. The system must be able to translate these vast amounts of data to useful, nonconfusing information.

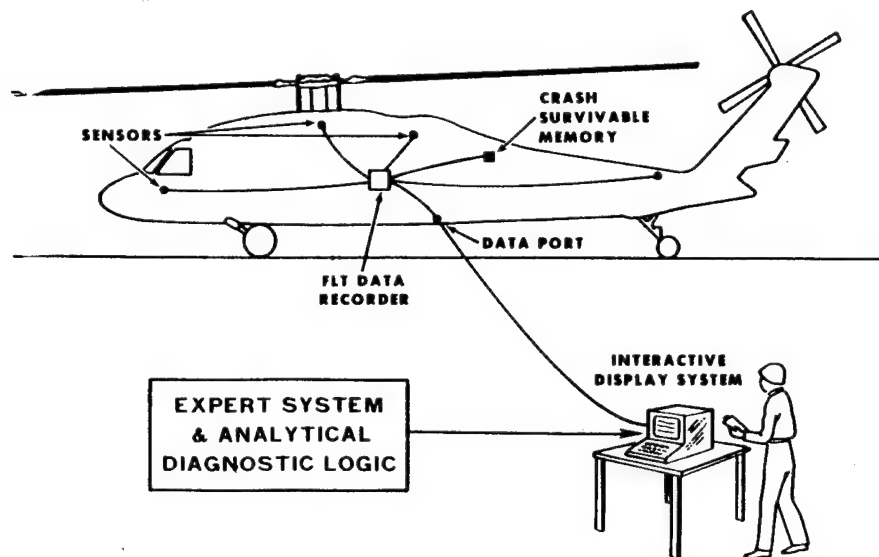


Fig. 6. AMD Approach

As previously mentioned, the key to justifying the hardware costs of such a system is by applying the equipment in a multifunctional manner. The recorder/processor is no longer monitoring just the engine, but must record and process data from the other dynamic subsystems plus the critical airframe components. Fig. 7 shows the integration of these various functions along with a crash survivable memory function and advancing technologies such as expert systems. The recorder/analyzer not only records parametric information but also provides diagnostic/prognostic analysis of equipment status and display to the cockpit and mechanic. The system also becomes a repository for the avionics built-in-test (BIT) data.

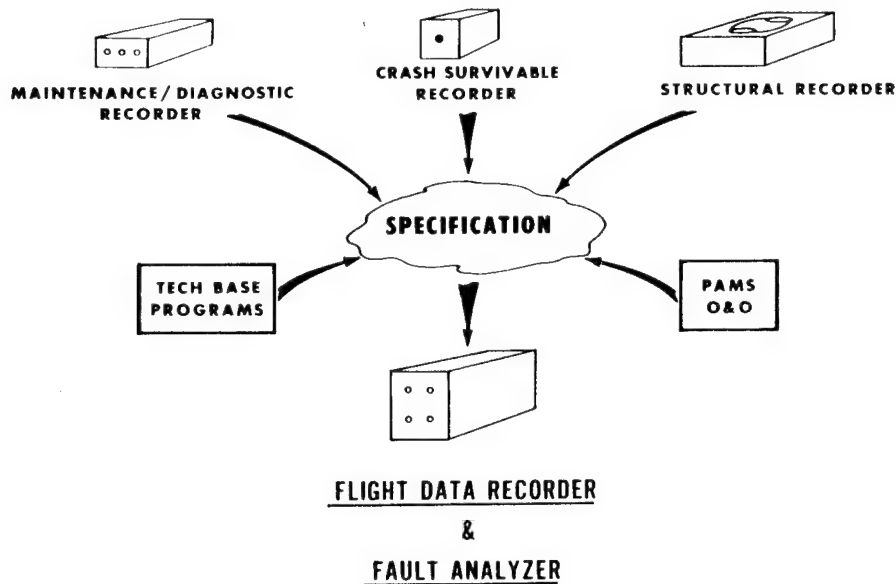


Fig. 7. Program Integration

Another essential piece of the system is an interactive maintenance aid that will guide the mechanic through sophisticated troubleshooting logic (structured around AI), as well as sort, analyze, and display data accumulated from the recorder such as exceedance or fault code data. The system must be a skill enhancement tool that can also be used for skill retention and on-the-job training, as well as interface with other computer equipment such as the automated log book (ALB) and unit level computer (ULC) systems. Figure 8 depicts the display system being used for the demo. Although this system is required to download the data from the aircraft, a production system uses a data transfer cartridge that would fly with the aircraft.

FUNCTIONS

- **GUIDES PERSONNEL THROUGH ADVANCED TROUBLESHOOTING LOGIC (INTERACTIVE)**
- **PERFORMS TRENDING ANALYSIS FOR PREDICTIVE MAINTENANCE ACTIONS**
- **ANALYZES STRUCTURAL INTEGRITY DATA FOR FLEET MANAGEMENT**
- **DOWNLOADS DATA FOR REAR LOGISTIC APPLICATIONS**



Fig. 8. Interactive Maintenance Aid

However, the most important component of any diagnostic system is the software--the decision logic which ultimately guides the mechanic to the correct maintenance action. Recorders, processors and color graphic displays can be very advanced to the point of complete automation or even voice activation. However, they become burdensome tools if the logic cannot distinguish a good versus a bad component. The software for the AMD diagnostic logic uses available techniques based on typical analytical procedures as well as AI techniques using expert systems procedures.

The AMD system was placed on AH-64 and UH-60 aircraft. The system involved the recording of selected parameters from the dynamic and structural components. To restrict excessive costs, every effort was made to utilize existing sensors. In order for this to be successful, the functions of the system had to first be defined. These included:

(1) Exceedance data from engine, rotor, drivetrain, etc. This data is to be analyzed and stored for pilot advisory as well as mechanic retrieval.

(2) Engine performance data to predict powerplant capabilities and to automatically perform "hit" checks.

(3) Engine usage and trend data.

(4) Structural usage data.

(5) Flight regime recognition data.

(6) Data for gross weight estimation.

(7) Load severity data.

(8) Life assessment data to calculate damage accrual rates.

(9) Component operating data for troubleshooting and inspection queuing.

(10) Accident and crash investigation data.

Tables IV and V list the various parameters for the UH-60 and AH-64 respectively. The AH-64 multiplex (MUX) bus traffic provided approximately 600 digital data points for diagnostic/condition monitoring purposes. This data was recorded at appropriate rates to preserve resolution and fidelity. Since recorders can only provide a finite storage capability, various compression techniques must be utilized. Data from vibration and direct strain measurements must be conditioned prior to recording due to the higher sample rates for such signals.

TABLE IV

UH-60A PARAMETERS (40 TOTAL)CONTINUOUS (24 TOTAL)

ALTITUDE (BAROMETRIC)
 ALTITUDE (RADAR)
 ALTITUDE RATE
 AIRSPEED
 #1 ENGINE TORQUE
 #2 ENGINE TORQUE
 #1 ENGINE RPM (NG)
 #2 ENGINE RPM (NG)
 #1 ENGINE RPM (NP)
 #2 ENGINE RPM (NP)
 #1 ENGINE TEMPERATURE (T5)
 #2 ENGINE TEMPERATURE (T5)
 MAIN ROTOR SPEED (NR)
 COLLECTIVE STICK POSITION
 LONG STICK POSITION
 LATERAL STICK POSITION
 LOAD FACTOR (NZ)
 PITCH ATTITUDE
 ROLL ATTITUDE
 HEADING
 OUTSIDE AIR TEMPERATURE (OAT)
 STATIONARY SWASHPLATE LOAD
 STABILATOR POSITION
 SAS/FPS COMPUTER FAULT

DISCRETE (16 TOTAL)

#1 ENGINE OIL PRESSURE
 #2 ENGINE OIL PRESSURE
 #1 ENGINE CHIP DETECTOR
 #2 ENGINE CHIP DETECTOR
 ENGINE FIRE
 APU OIL PRESSURE
 SAS WARNING
 #1 ENGINE HYDRAULIC PUMP PRESSURE
 #2 ENGINE HYDRAULIC PUMP PRESSURE
 INPUT LH CHIP
 INPUT RH CHIP
 ACCESSORY LH CHIP
 ACCESSORY RH CHIP
 INTERMEDIATE TRANSMISSION CHIP
 TAIL TRANSMISSION CHIP
 MAIN MIDDLE SUMP CHIP

TABLE V

AH-64A PARAMETERS (625+ Total)MIL-STD-1553A DATA BUS PARAMETERS
(600+ Total)

FAULT DETECTION/LOCATION SYSTEM
 TARGET ACQUISITION DESIGNATION
 SIGHT/PILOT'S NIGHT VISION SENSOR
 AIR DATA SENSOR
 30MM GUN
 HELLFIRE MISSILE SYSTEM
 2.75 IN ROCKET SYSTEM
 HEADING ATTITUDE REFERENCE SYSTEM
 INTEGRATED HELMET DISPLAY SYSTEM
 OPTICAL RELAY TUBE
 FLIGHT SYSTEM

CRASH DATA PARAMETERS NOT ON BUS
(25 Total)

#1 ENGINE FIRE
 #2 ENGINE FIRE
 AUXILIARY POWER UNIT FIRE
 #1 ENGINE RPM (NG)
 #2 ENGINE RPM (NG)
 #1 ENGINE RPM (NP)
 #2 ENGINE RPM (NP)
 #1 ENGINE TEMPERATURE (TGT)
 #2 ENGINE TEMPERATURE (TGT)
 STATIONARY TAIL ROTOR CONTROL LOAD
 STATIONARY SWASHPLATE LOAD
 MAIN ROTOR SPEED
 LATERAL STICK POSITION PILOT
 LONGITUDINAL STICK POSITION PILOT
 COLLECTIVE POSITION PILOT
 PEDAL POSITION PILOT
 STABILATOR POSITION
 PRIMARY HYDRAULIC PRESSURE
 UTILITY HYDRAULIC PRESSURE
 #1 ENGINE CHIPS
 #2 ENGINE CHIPS
 MAIN TRANSMISSION #1 CHIPS
 MAIN TRANSMISSION #2 CHIPS
 #1 NOSE GEARBOX CHIPS
 #2 NOSE GEARBOX CHIPS

A key characteristic of the on-board system is the time-tagging of fault data. This process allows analysis of a wide range of data associated with the problem to identify and isolate intermittent faults which are a significant contribution to false removals, repetitive maintenance, and extended manual troubleshooting efforts.

A typical scenario begins with a preflight inspection to ensure that the system is operating and storage space is available. (The recorder has an indication to alert the crew when 80% capacity is reached.) The pilot brings the aircraft into steady-state condition and then presses a button for the system to perform an automatic engine assessment check. The results of this check are reported to the pilot in the form of a go/no go indicator. The actual parametric data is stored for later retrieval and trending. During the mission, the pilot has the option to activate the recorder when he feels something is abnormal. Otherwise, the recorder records only faults, exceedances, and/or parameters that exceed predetermined "windowed" values. Upon return to base, the mechanic checks the recorder for any indication of a fault or exceedance. If the indicator is lit, the mechanic can then use the portable display to retrieve this data only and display it for quick assessment of the aircraft. If further troubleshooting is required, the complete data package can be retrieved from the cartridge and decompressed off-aircraft for inspection and analysis. Fault tree logic resident within the portable maintenance aid interacts with the recorded data and the mechanic to help resolve and identify the location of the problem.

If the aircraft lands and no fault or exceedance is indicated, then the mechanic can either download the data from the cartridge or bolt the covers back in (provided the recorder has not reached 80% storage capacity).

The exceedance/fault data which the mechanic can inspect alongside the aircraft can be displayed in various formats. The following figures show current examples of these formats. Fig. 9 lists a series of engine temperature recordings with the allowed time at temperature. When an exceedance has occurred requiring a maintenance action, the appropriate tech manual (TM) reference is cited. In future, more powerful systems, the complete text of the TM can be shown and thus entirely eliminate paper on the battlefield.

ENGINE STATE	(ALLOWABLE SEC)		RECORDED		TROUBLESHOOT/	
	BEFORE BEFORE		SECONDS		MAINTENANCE	
	TSHOOT	MAINT	#1ENG	#2ENG	#1ENG	#2ENG
NG>GI T4.5>850	0	12	0	0		
NG>GI T4.5>850	12	60	0	0		
NG>GI T4.5>886	0	60	0	0		
NG>GI T4.5>902	0	55	0	0		
NG>GI T4.5>906	0	50	0	0		
NG>GI T4.5>910	0	46	0	0		
NG>GI T4.5>914	0	42	0	0		
NG>GI T4.5>918	0	38	0	0		
NG>GI T4.5>922	0	34	0	0		
NG>GI T4.5>926	0	30	0	0		
NG>GI T4.5>930	0	26	0	0		
NG>GI T4.5>934	0	22	0	0		
NG>GI T4.5>938	0	18	0	0		
NG>GI T4.5>942	0	15	0	0		
NG>GI T4.5>946	0	12	0	0		
NG>GI T4.5>950	0	0	0	0		

REF: TM55-2840-248-23 PP 1-419 PARA 1-223

Fig. 9. Engine Overtemp Report

Fig. 10 shows a hard landing report based on negative feet per second. Another way of measuring this would be to place a load sensor on the landing gear. By identifying the extent of a hard landing, much confusion as to what inspection and repair tasks are required can be avoided. In addition, a history of hard landings can be trended for an aircraft, better enabling a mechanic to schedule maintenance and to predict potential problems before they occur.

LANDING VERTICAL SPEEDS						
	0-2	2-4	4-6	6-8	8-10	10
# LANDINGS	FPS	FPS	FPS	FPS	FPS	FPS
AT SPEED=	3	2	0	0*	0*	0*

TIME OF HARDEST 06:23:17.473

NO VERTICAL SPEEDS > 6 FPS RECORDED
 NO SPECIAL INSPECTIONS REQUIRED
 REF: TM55-1520-237-23-4 TASK 9 PP 9-16

Fig. 10. Hard Landing Report

Figures 11 and 12 show reports for engine and rotor overspeed, respectively. Fig. 13 is a report for discrete indicators. These discrete indicators are the various caution/advisory data that is displayed in the cockpit. Time-tagging these indicators can greatly help the mechanic in trying to resolve pesky, intermittent failures that often cannot be duplicated on the ground.

ENG SPEED	(ALLOWABLE - SEC'S)		RECORDED SECONDS		TRBLESHOOT/ MAINTENANCE	
	BEFORE TSHOOT	BEFORE MAINT	#1ENG	#2ENG	#1ENG	#2ENG
NP>110%	—	12	14.7	2.3	M	
NP>113%	0	12	0.0	1.8		T
NP>130%	—	0	0.0	0.0		

ENGINE OVERSPEED ACTION REQUIRED: (M) (T)

REF: TM55-2840-248-23 PP 1-419 PARA 1-222A

Fig. 11. Engine Overspeed Report

SIKORSKY UH60A / LSI IFIDS NVM SUMMARY
82-23709 14:30:39 1/15/87

---- NR OVERSPEED REPORT -----
 ROTOR SPEED RANGE
 102- 107- 112- 117- 122- 127- 132- 137- >
 107% 112% 117% 122% 127% 132% 137% 142% 142%
 REC'D * * *
 MIN= 0.0

NO ROTOR SPEEDS > 127% RECORDED
 NO SPECIAL INSPECTIONS REQUIRED
 REF: TM55-1520-237-23-4 TASK9 PP 9-14.1

Fig. 12. NR Overspeed Report

SIKORSKY UH60A / LSI IFIDS NVM SUMMARY
82-23709 14:30:39 1/15/87

---- DISCRETE REPORT -----
 NO.1 ENGINE OIL PRESSURE NO HITS
 NO.1 ENGINE CHIP DETECTOR NO HITS
 NO.2 ENGINE OIL PRESSURE NO HITS
 NO.2 ENGINE CHIP DETECTOR NO HITS
 ENGINE FIRE NO HITS
 APU OIL PRESSURE NO HITS
 SAS WARNING NO HITS
 NO.1 HYDRAULIC PUMP PRESSURE NO HITS
 NO.2 HYDRAULIC PUMP PRESSURE NO HITS
 INPUT MODULE LH CHIP DETECT NO HITS
 ACCESS MODULE LH CHIP DETECT NO HITS
 INPUT MODULE RH CHIP DETECT NO HITS
 ACCESS MODULE RH CHIP DETECT NO HITS
 INT TRANSMISSION CHIP DETECT NO HITS
 TAIL TRANSMISSION CHIP DETECT NO HITS
 MAIN SUMP PUMP CHIP DETECT NO HITS
 SAS/FPS COMPUTER FAULT NO HITS

Fig. 13. Discrete Report

BENEFITS

The objectives of such an integrated diagnostic approach are many: reduce repetitive and incorrect maintenance, reduce the requirement for special inspections and special purpose test and support equipment, provide adequate information to allow mechanic cross training and MOS consolidation, provide capabilities for card level fault isolation (two-level maintenance concept), provide for critical parts tracking, increase overall aircraft safety, etc. Most of these objectives are being realized through data processing and analysis off-aircraft. However, a more efficient manner of accomplishing increased aircraft safety would be through an on-board system which integrates all available flight information with the condition monitoring system. Just such a system has been defined in a recent NASA effort titled "An Artificial Intelligent Approach to On-Board Fault Monitoring and Diagnosis for Aircraft Application."

AI MONITORING SYSTEM

INTRODUCTION

The above research effort was initiated to identify guidelines for automation of on-board fault monitoring and diagnosis and associated crew interfaces. The effort began by determining the flight crew's information requirements and the various reasoning strategies they use. Based on this information, a conceptual architecture was developed that encompasses all aspects of the aircraft's operation, including navigation, guidance and control, and subsystem status. This architecture has two facets: the organization of flight domain knowledge and the problem solving process that uses this knowledge for condition monitoring and diagnosis.

ORGANIZATION OF FLIGHT DOMAIN KNOWLEDGE

Fig. 14 depicts the various categories and interconnectives for flight domain knowledge. Each level in the goal hierarchy is subservient to the one above it in the sense that it supplies the means of achieving the goals passed down to it from above. Each level provides a goal which the level beneath it must attempt to achieve. It is important to notice that there may be many different ways of achieving a particular goal; all are correct. The knowledge in each level must contain information not only on how to describe a way of achieving a particular goal but also (and perhaps more importantly) on how to determine if a particular means can or cannot satisfy a goal.

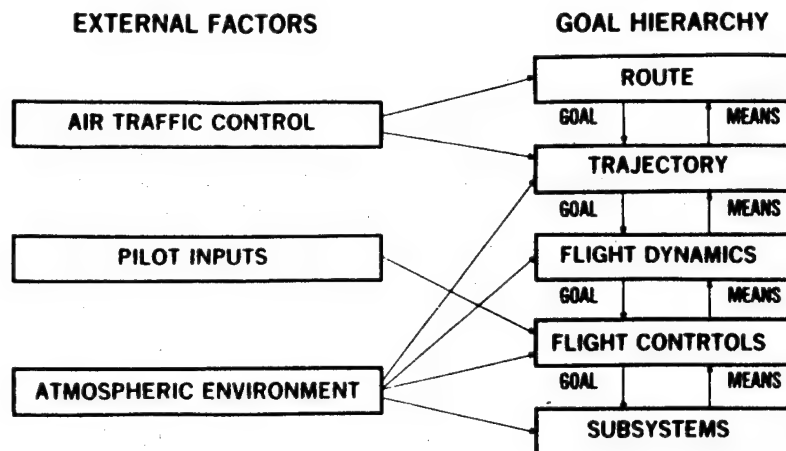


Fig. 14. Organization of Flight Domain Knowledge

There are categories of information which are not levels in the goal hierarchy but are external inputs to different levels. The atmospheric information (such as, wind, temperature, and pressure) is a set of inputs to various levels which must be taken into account when determining how to achieve a goal. Another such category is actual pilot actions for setting control inputs, switch settings, and so on. Still another category is information and instructions received from Air Traffic Control (ATC) in the form of ascent, descent, and heading commands.

This organization of flight domain information corresponds to a taxonomy of the faults in flight which might lead to accidents. The term "fault" refers to any problem which may result in some goal not being achieved if not corrected or compensated, as well as failure in a physical system. This is an important distinction in the flight domain because problems such as wind shear or the pilot giving incorrect inputs can endanger the aircraft just as much as a physical system failure.

FAULT MONITORING AND DIAGNOSTICS FRAMEWORK

A framework for the fault monitoring and diagnosis process was developed as a result of interviewing aircraft pilots and examining pilot handbooks. Although this framework is described in the context of a specific domain (i.e., engines), it is believed to be a general framework for fault monitoring and diagnosis. It was not intended to model the cognitive process that humans use for fault diagnosis but to facilitate development of representative and remaining methods for fault diagnosis and its automation.

The components of the framework are shown in Figure 15 as well as examples of the input and output for each component. As shown, the fault monitor, the fault diagnosis process, and the interface mechanism to the flight crew are all separate components. The purpose of the fault monitor is to detect when a fault occurs by examining sensor readings and generating symptoms which represent the abnormal values. These symptoms are the input to the

fault diagnosis process, whose purpose is to suggest fault hypotheses which isolate the cause of the symptoms. The diagnosis process is divided into three stages, each with a different reasoning strategy and representation. Stages are organized in order of increasing computational and representational complexity, much like humans use diagnosis strategies. Each stage is entered when prior stages are unsuccessful at diagnosing the current failure. The interface mechanism displays the diagnoses in an appropriate format to the flight crew. The interface mechanism must be sensitive to flight phase and crew workload.

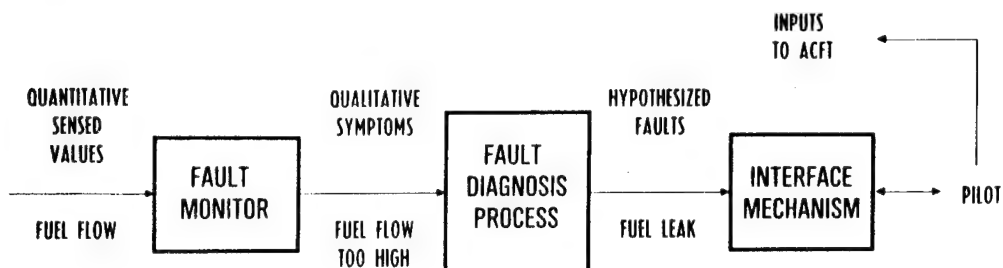


Fig. 15. Fault Monitoring and Diagnosis Process

The fault diagnosis process has several stages, as shown in Fig. 16. Each stage uses different representations and reasoning strategies. In the first stage, the symptoms are compared to fault-symptom association known a priori. These associations are a compilation of knowledge about known faults and their behavior. This stage corresponds to traditional expert systems approaches and is attempted first because it quickly identifies the most commonly occurring faults.

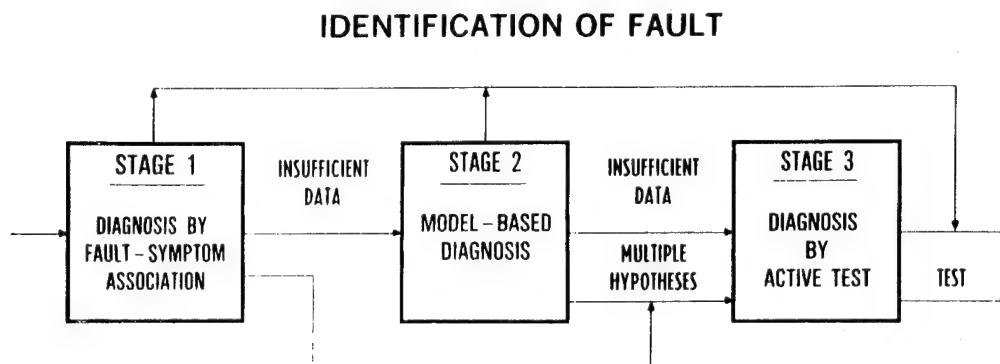


Fig. 16. Fault Diagnosis Stages

The second stage of the diagnosis process occurs when the current symptoms fail to correspond to a known fault. The purpose of the reasoning at this stage of the diagnosis process is to localize the failure and to generate as much information about the fault as possible. To generate the desired

information about the fault, the diagnostic reasoning in the second stage focuses on how the physical system works rather than on how the system fails, as was done in the first diagnosis stage. Models of functional and physical structure are used to provide the knowledge on how the system works.

Since all parameters are not observable and other factors such as system feedback are present, localization of the failure may not be possible without further information. In this situation, the third diagnosis stage is entered. Depending on the domain, performing tests to obtain further information may be done passively or actively. The third stage is responsible for proposing tests to obtain additional information, whether the tests are active or passive. In either case, the fault diagnosis system may be able to use the results to identify faults.

Implementation of this architecture is under development. A computer program called INFAMOS (Intelligent Fault Monitoring System) is being developed. The fault diagnosis system is being implemented in a computer program called DRAPHYS (Diagnostic Reasoning About Physical Systems). The first application of these models will be an aircraft turbofan engine.

FUTURE NEEDS

Most of the technology required to implement effective integrated diagnostics and other maintenance aids is available today. To be truly effective, several things must happen. First, this technology must be applied both to mission equipment and to aircraft subsystems. This requires a systems level design of the performance monitoring equipment, including subcontractor supplied BIT, in order to ensure complete coverage. Detail appropriate to the maintenance concept for the system must be available from the monitoring subsystem. An aircraft designed for three-level maintenance only requires fault isolation to the LRU level whereas, a two-level maintenance concept requires fault isolation to the module or card level. This places an increased level of complexity for the testability design of the component.

Sensor development is required to improve not only accuracy but also repeatability and reliability. An integrated diagnostic system may have the most efficient architecture possible with the most advanced and tested software logic incorporated; however, the answers will always be wrong if the inputs are not correct. In addition, development is needed in the area of load measurements where current strain gauges are high bandwidth signals which require preprocessing or data extraction prior to transmission to a data bus or flight recorder.

A final and really most important area is the development of the discrimination logic between good and bad components. In the mechanical system with its myriad of failure mode combinations and resulting symptoms, complex systems currently prohibit simple and direct techniques to determine when a component has reached its expected life. Identical components operated under similar conditions may still exhibit different symptoms for identical failure modes. Vibration analysis has been hindered by this phenomenon primarily due to the intense processing requirements and overall sophistication

of the techniques. However, as embedded processors become more powerful and memory less expensive, new analysis techniques can be implemented in attractive designs. What is still needed are the test methodologies to "nail down" the good versus bad signatures and how to use this data to alert the mechanic of impending failures prior to catastrophe but yet allow maximum usage of the component.

CONCLUSION

Application of these integrated design concepts to the next generation aircraft will provide substantial improvements in combat sustainability and in reducing logistic burdens and operating and support costs. Measured against today's systems, the next generation can be more capable, with the added complexity that capability demands, and still require less reserves both in personnel and material. All the technologies required to implement these designs are emerging and will be mature within the next few years. The challenge in achieving these gains is management of larger development or product improvement integration teams, and imposing system level design requirements up front to ensure that design goals are met.

RESEARCH AIRCRAFT

Session Cochairmen:

Wallace H. Deckert, NASA

Andrew W. Kerr, Department of the Army

RESEARCH AIRCRAFT SESSION

SUMMARY

Mr. W. J. Snyder, in his paper "Rotorcraft Flight Research with Emphasis on Rotor Systems," summarized NASA/Army rotor systems flight research over the last 50 years. His presentation included research utilizing the autogyro, R-4, H-34, H-13 Hingeless Rotor, XH-51N, AH-1G, RSRA, and UH-60. Mr. Snyder's presentation (and the written paper even more so) contained many specific examples of contributions from rotor systems flight research programs.

Mr. A. W. Kerr, session co-chairman, closed the session by stressing the importance of both rotor systems research aircraft and configurational proof-of-concept aircraft.

Rotorcraft Flight Research with Emphasis on Rotor Systems

W. J. Snyder
NASA-Ames

Abstract

NASA and NACA flight research with rotorcraft has covered a span of over fifty years; the emphasis of much of that research has been on the investigation of the rotor system. Rotor performance was the early focus of the research, but the work broadened significantly in the 50s and 60s to include dynamics and loads. In the 70s and 80s the focus has turned more toward the complex problems of noise and vibration and aeroelastics. As the problems became more and more complex, the research aircraft and instrumentation systems have become increasingly more sophisticated. The contributions of the flight research have been significant. They have included not only validation of rotor performance models but also the evaluation of advanced airfoils and the amassing of large data bases which have contributed to our understanding of vibratory airloads.

The present report discusses each of the important rotor system flight programs and the research aircraft that were utilized. The contributions of the research are highlighted, and an extensive reference list is included.

ROTORCRAFT FLIGHT RESEARCH WITH EMPHASIS ON ROTOR SYSTEMS

W. J. Snyder
NASA/Ames

Introduction

NASA and the Army have been engaged in flight research with rotorcraft for six decades beginning in the autogiro days at Langley and continuing today with both conventional helicopters and advanced concepts like X-Wing and Tilt Rotor at Ames. An important part of that research, at least over the last 25 years, has been research directed at the rotor systems. One of the first important contributions in rotor flight research was made at Langley in the late fifties and early sixties with the H-34 with pressure instrumented blades installed. The work continued through the sixties with an emphasis on hingeless rotor concepts and into the seventies with a heavy emphasis on two bladed rotors and the problems associated therewith. In the late sixties an idea was formulated for a complex, new research tool called RSRA (Rotor Systems Research Aircraft). The idea germinated and funding was provided for construction of the RSRA in the mid-seventies. The RSRA became operational after a change of primary location to Ames in the early eighties. While it has extensive capabilities, the complexities of the RSRA have resulted in a less than effective tool. As funding and manpower to support the RSRA have declined, new options to pick up the slack in research capability turned in the direction of the Army UH-60.

This paper will deal with this history of rotor systems flight research aircraft and with the contributions that they have made over the last 25 years.

Symbol List

b	number of blades
c	blade chord (inches or ft.)
C_l	blade section lift coefficient
C_{Lr}	rotor lift coefficient
$\overline{C_L}$	mean lift coefficient
C_m	blade moment coefficient
C_n	normal force coefficient
C_p	blade pressure coefficient
C_p^*	critical pressure coefficient
C_T	rotor thrust coefficient
$(D/L)_{om}$	measured profile drag/lift ratio
$(D/L)_{oT}$	theoretical profile drag/lift ratio
f_g	normal load factor (g)
g	acceleration of gravity
M_{TIP}, M	blade tip Mach Number
PSIA	absolute pressure measurement
p	aircraft rolling velocity (rad./sec.)
q	aircraft pitching velocity (rad./sec.)
r	radial location on blade (ft.)
R	rotor radius (ft.)
t	airfoil thickness (in.)
TM	Torsional Moment (lb.-in.)
V, V_r	aircraft forward velocity (ft./sec. or knots)
x	chordwise coordinate of airfoil from nose (in.)
y	normal to chord coordinate of airfoil from chordline (in.)

Symbols (cont.)

(Figure 54 abbreviations)

EB	-.....	edgewise bending gage location
NB	-.....	normal bending gage location
TB	-.....	torsional bending gage location
AE	-.....	edgewise accelerometer location
AN	-.....	normal accelerometer location

Greek

α	-.....	rotor angle of attack (degrees)
$\alpha_{(1.0)(270^\circ)}$	-.....	retreating blade angle at tip (degrees)
Γ	-.....	blade bound circulation
μ	-.....	rotor tip speed ratio
ψ	-.....	rotor azimuth (degrees or radians)
ρ/ρ_0	-.....	air density ratio
σ	-.....	rotor solidity $bc/\pi R$
Ω	-.....	rotor rotational speed (rad./sec. or RPM)

General Description of a Rotor Systems Flight Research Aircraft

Two types of flight research configurations are represented in the group of aircraft to be discussed: those that addressed specific problems such as blade vortex interactions of 2 bladed configurations, and those that served as research tools to investigate generic problems. In general the programs have been of the second type.

The general classification of those vehicles utilized to conduct rotor systems research will have, as a minimum, some rotor strain gages for the measurement of blade bending and will probably have the means to measure pitch angle and flapping plus an assortment of other aircraft parameters such as airspeed, roll and pitch rate, and cg accelerometers. These are the minimum requirements for undertaking any type of quantitative investigation. However, some qualitative information can be obtained with flow visualization methods and, of course, the conduct of rotor acoustic testing can be accomplished without any instrumentation on the aircraft if ground tracking is available.

Generally speaking, the more instrumentation available, the more that can be determined about a particular phenomenon. The number of combinations of rotor types as illustrated in the matrix in table I requires that an extensive amount of testing be accomplished to fully explore a problem area.

Phenomena of Interest in Rotor System Flight Investigations

While the number of phenomena in the rotor system that are of interest are very large, the number reduces to 5 significant types of problems as listed in Table II: vibration, noise, performance, aeroelastic stability, and gust response. Figure 1 illustrates the types of phenomena that occur in the rotor system that ultimately can result in aircraft problems. Table II also attempts to define the phenomena that are the root causes of the various problems.

The 5 problems identified in Table II provide the greatest limitation on the conventional helicopter, and any improvement in the understanding of the root causes that affect these problems will potentially be of great benefit. All of the problems and related phenomena are interrelated to the point where it is extremely difficult to design an aircraft that is free of some limitation without adversely affecting one or more of the others. The other complication, of course, is that the rotor must be designed to operate in a number of flight conditions from hover to high speed. Ultimately, the need is to be able to predict the individual phenomena and all of the interactions to the point where the design can be optimized for a given mission. The development of such prediction methods requires that the phenomena be fully explored both through small and full scale isolated rotor testing and through full-up aircraft testing in flight.

NASA(NACA)/Army Rotor Systems Flight Research Programs

Rotary wing flight research began in the 30s at Langley with early efforts with autogiros with the primary emphasis on rotor performance. Wheatley in two papers (references 1 and 2) from the early thirties describes a performance test program and theoretical prediction effort and correlation effort using the Pitcairn PC-2 autogiro. The instrumentation of that era was crude, however, the analysis of Wheatley and early researchers was the foundation for most of the prediction programs in use today. One correlation effort from Wheatley's work (reference 2) is shown in figure 2. Figure 2 shows theoretical and experimental values of rotor lift coefficient and angle of attack plotted against tip speed ratio. Even with the crude instrumentation and rather unsophisticated analysis, the correlation was very good at low tip speed ratios.

The mid-to-late forties saw the beginning of conventional helicopter flight research with the availability of the Sikorsky R-4. Gustafson in references 3, 4, and 5 reported on flight tests beginning in 1944 principally directed at performance testing. In reference 5, Gustafson and Gessow report on a flight test activity with the R-4 (figure 3) directed at blade stalling. Figure 4 from reference 5 illustrates a correlation effort between predicted and measured stall. In the figure, the ratio of drag to lift measured to predicted is plotted against retreating blade tip angle of attack. The observed divergence from a value of 1 is interpreted as the initiation of stall at the tip when the drag to lift prediction becomes very unreliable. Tuft photos taken on the blade confirmed this observation.

The fifties saw a diversification of the types of testing; the first instances of important dynamics testing began. One such flight test is discussed in reference 6 by Yeates. Yeates reports in this reference on ground and flight tests of the tandem rotor shown in figure 5. The aircraft was instrumented for vibration in both the ground (shake tests) and flight tests. The fuselage response was measured and compared for two sets of blades, one wood and one metal. Yeates in figure 6 illustrates that the fuselage response shows the effect of rotor/fuselage coupling in the flight test (2 peaks) and not in the ground test (1 peak) where the rotor was not installed.

Ludi, as reported in reference 7, moved further in the direction of full rotor system flight testing with a large single rotor helicopter test in the mid fifties. The test aircraft shown in figure 7 was flown with strain gaged blades for the measurement of flapwise, chordwise, and torsional blade moments with a particular emphasis on retreating blade stall. In figure 8 from reference 7, Ludi employs a technique similar to that employed by Gustafson. However instead of employing the ratio of measured to theoretical values of drag/lift ratio to determine the divergence due to stall, Ludi normalizes the measured blade torsional moment by dividing by the measured moment at a tip speed ratio of .24 where the rotor is not stalled. The torsional moments are observed to increase at a fairly slow rate until the tip speed ratio exceeds .24 where the moments increase much more rapidly indicating a stalled condition on the retreating side.

As illustrated in the preceding paragraphs there was considerable flight research relative to the rotor system in NACA prior to 1960, however much of the focus was on aircraft performance and the instrumentation was relatively limited. That changed around 1960 with the H-34 program. Rotor system flight research has been ongoing in NASA/NACA for over fifty years; this paper will deal principally with those experiments that have taken place in the second half of that time frame, beginning with the H-34.

The research vehicles that will be dealt with are illustrated in figure 9. This figure shows the vehicles of interest against a chronological axis with a qualitative evaluation of the research capability of each aircraft. The discussion begins with the H-34 and will end with the most current program, the UH-60. In the discussion, an attempt will be made to illustrate the highlights of the research and the contributions that were made.

H-34

The H-34 program was the most extensive rotorcraft flight test effort ever attempted when it was undertaken in the early sixties. The aircraft shown in figure 10 was extensively instrumented with, not only conventional instrumentation such as accelerometers, strain gages, airspeed, etc., but also one blade incorporated differential pressure transducers for the measurement of section pressure distributions. Early wind tunnel tests (Reference 8) had employed blade mounted pressure transducers, but this was the first flight test blade. The complete list of aircraft instrumentation can be found in reference 9. The aircraft was a conventional single rotor helicopter with a four bladed rotor. The complete description of the aircraft can be found in reference 9.

The flight test program was conducted at NASA Langley with one of the primary purposes being to develop data with which 2D airfoil pressure distributions could be compared. As reported in reference 10 by Schieman and Kelley, this was successfully undertaken. Reference 10 reports on the discrepancies uncovered on the retreating blade where section normal force coefficients exceeded the 2D stall lift conditions.

The tabulated results from the flight test are contained in reference 9. These results and the results of the companion wind tunnel test of the H-34 rotor in the 40 x 80 Wind Tunnel have become a benchmark data set for use in the validation of airloads prediction methods. Several investigators have utilized these results in their validation efforts. Included in the investigations utilizing the H-34 data is the work of Sadler (Reference 11) in comparing airloads predictions in steady maneuvers utilizing a free wake analysis with the flight test results. One such comparison is illustrated in figure 11 (Reference 11). Ward in reference 12 examined 6 cases of level and maneuvering flight data from the H-34. In figure 12 (Ref. 12), Ward shows a comparison of torsional moments, and section loading and moment coefficients for level flight and a 1.5 g pull-up maneuver which illustrates significant oscillations in the fourth quadrant for the maneuver case. In figure 13 (Ref. 12) Ward relates this behavior to vortex intersections in the fourth quadrant. More recent efforts by Hooper (Reference 13) and Esculier and Bousman (Reference 14) make extensive use of the flight and wind tunnel results in the analysis of vibratory airloads and the estimation of blade structural loads.

Despite a number of drawbacks to the data set including the frequency response of the pressure data, the accuracies of the data, the limited airspeed, and the differential transducers, the data set has been shown to be extremely valuable.

XH-13

The early sixties also saw the kindling of significant interest in the hingeless "rigid" rotor system. Very stiff non-articulated rotors with all of their inherent problems had been by-passed with the advent of the articulated rotor for autogiros. However, the development of flexible metal blades, that were far from rigid, emerged in the early sixties and permitted the further investigation of rotors which took advantage of the increased control available with a hingeless rotor.

One of the first test vehicles to employ a hingeless rotor was the modified H-13 shown in figure 14 (Reference 15). A close up of the hingeless rotor hub and slipring assembly is shown in figure 15 (Ref. 16). The aircraft was flight tested at Langley in the early sixties and the results are reported by Ward and Huston in several publications (Ref. 15-18).

As described in reference 15, the aircraft was instrumented principally for structural loads on the blade, hub, shaft, and control links; however, normal aircraft state instrumentation was also employed. A complete list of instrumentation can be found in reference 18. In reference 18, Ward focuses on the chordwise blade loads which are shown to be critical in maneuvers as illustrated in figure 16 (Ref. 18). In the figure the time histories of several parameters are plotted for a rolling maneuver from flight data. Included is the chordwise blade bending at the blade root. It is immediately obvious that the build-up in oscillatory chordwise blade bending has exceeded the endurance limit for the blade. Ward also develops in the Appendix to reference 18 a methodology for calculating the chordwise bending moments based on an equivalent hinge offset.

The tests with the rudimentary hingeless rotor H-13 led directly to the acquisition by NASA of one of three XH-51 hingeless rotor helicopters to be described in the following section.

XH-51N

The XH-51 was an advanced hingeless rotor helicopter developed for military evaluation of the hingeless rotor concept. In early 1965 NASA acquired the 3rd XH-51 produced, and the aircraft was flight tested at Langley and at the RAE in England through 1970. The XH-51N is shown in figure 17. In reference 19, Snyder describes the extensive rotor and airframe instrumentation utilized in the testing and provides a complete description of the aircraft. The aircraft was instrumented for flapwise and chordwise bending, and the mast and pitch links were also strain gaged. Likewise, the tail rotor was strain gaged for flapwise and chordwise bending. Several components of the control system were instrumented for loads and position. Accelerometers, rate gyros and vibration pickups were also utilized. Unlike the other 4 aircraft produced, the XH-51N maintained the original 3-bladed configuration, while the others were built or modified for 4 blades, including the XH-51A Compound Helicopter tested under an Army program.

The aircraft had a number of unique features including the hingeless rotor. The aircraft employed a mechanical gyro in the control system such that the pilot did not control the rotor directly, but provided force inputs to the gyro shown in figure 18; the gyro then provided control inputs to the rotor based on inputs from the pilot or from rotor feedback provided by the forward sweep of the blades. This control system was the fore runner of the control system utilized on the AH-56 Cheyenne that resulted in severely limiting problems for that aircraft. Kelley in reference 20 describes some of the control problems experienced with the XH-51N during maneuvering flight.

Another unique feature of the XH-51N was the cabin isolation system illustrated in figure 19 (Ref. 21) which was utilized to control cabin vibration. Another vibration control device employed after the fact on the XH-51N were the blade mounted masses as illustrated in figure 20 which were utilized to detune the 2nd flap bending frequency of the rotor. During the research flying with the XH-51N, the aircraft was flown both with and without the cabin isolation system and the blade masses.

Both the rotor loads and the flight dynamics of hingeless rotor configurations in maneuvering flight were investigated during the flight investigations with the aircraft. Snyder in reference 19 reported on the rotor loads encountered with the aircraft in Nap of the Earth maneuvers. Figure 21 from reference 19 illustrates that the XH-51N had even more severe chordwise and flapwise rotor bending problems than the H-13 hingeless rotor helicopter. Both the flapwise and chordwise bending moments consistently exceeded the endurance limit for the measured hub plate during maneuvers, and loads were always monitored in real time utilizing telemetry.

Ward and Snyder (Ref. 22) and Ward (Ref. 23) analytically investigated hingeless rotor blade response for an excitation caused by a concentrated force (simulated vortex) moving from blade tip to root. This work was stimulated by the high vibratory loadings experienced with the XH-51N.

One of the last experiments to be run on the XH-51N was the investigation of an active cabin isolation system to replace the passive spring utilized to isolate the cabin as was previously illustrated in figure 19. Hanks and Snyder report on the baseline aircraft tests with and without isolation and on the ground tests of the active isolation system in reference 21. Figure 22 (Ref. 21) illustrates the excessive cabin vibration levels experienced with the isolation system locked out and the blade mass removed. In the figure, cabin vibration amplitude is plotted against airspeed, and it can be seen that levels in excess of 1 g at 18 Hz are experienced in transition. This is typical of hingeless rotor helicopters with high effective hinge offset and one of the problems still to be faced with the newer bearingless rotor systems. Reduction of the effective hinge offset, as has been achieved with some of the newer designs, can help alleviate the vibration problem.

Another idea that was stimulated by the work on the XH-51N and its high vibratory loads was the concept of reducing the strength of the tip vortex through the use of the "ogee" tip. The "ogee" tip was conceived by John Ward and initial tests of the tip along with conventional tips were conducted in a small scale smoke tunnel. These preliminary tests (documented in an unpublished report by Snyder and Pegg) indicated a reduction in vorticity of as much as 40% over a conventional square tip and were encouraging enough to initiate work on a full scale evaluation utilizing a UH-1H which is discussed in the following section.

UH-1H

The UH-1H helicopter was acquired at Langley in the early 70s as a test bed for the "ogee" tip rotor. The aircraft was instrumented and baseline flight testing was initiated. The aircraft and instrumentation system are described by Mantay in reference 24. Rotor structural parameters and aircraft state parameters were measured. In addition, an in-flight acoustics measurement system (fig. 23) was mounted on the aircraft. For the "ogee" tip flights only, tip pressures were measured. A ground acoustic array was also employed.

The full scale "ogee" tip was fabricated in-house at Langley and tested both in-flight and on the Langley rotor whirl tower. Figures 23 and 24 (Ref. 24) show the test aircraft and the two test rotor configurations, respectively. Figure 25 (Ref. 24) illustrates the improvement provided by the "ogee" tip over the conventional tip for vibratory pitch link loads at low thrust coefficient values. The improvement was considerably reduced at higher rotor thrust coefficients. A similar trend was indicated with both the noise and power measurements. The results of these tests led to a follow-on investigation by the Army on an advanced rotor for the AH-1S.

In the same time frame as the "ogee" tip flight testing, a second program utilizing an AH-1G was undertaken at Langley to investigate advanced rotor airfoils. The AH-1G program is discussed in the following section.

AH-1G (Langley)

The AH-1G "Cobra" (figure 26) was acquired at Langley in the early seventies and was to become the most extensively tested vehicle since the H-34. The primary purpose for the acquisition was to undertake a series of advanced airfoil flight evaluations. As described by Morris in Reference 25, the acquired Cobra was instrumented with an onboard instrumentation system and a baseline flight test program was conducted. In this initial report (Reference 25) Morris reports on the investigation of the baseline performance characteristics of the Cobra. In following investigations, Morris conducted investigations with 3 different advanced airfoils. Special Cobra blades were fabricated to conform to the desired airfoil coordinates. The procedure is illustrated in figure 27 from reference 25. In this figure the basic spar is illustrated in the upper part of the figure. The lower part of the figure illustrates the glove build-up to the desired coordinates and also illustrates the installation of transducers. This particular section is the first airfoil tested with the Cobra—the NLR-1T. Reference 26 also describes the SRBI (Special Rotor Blade Instrumentation System) which was utilized for the testing. The SRBI (figure 28) is a rotor head mounted instrumentation package that provides the data processing for those sensors in the rotating system. The system was intended to provide the capability for telemetering data into the fuselage without the need for sliprings. However, this aspect of the system had to be abandoned and sliprings were utilized to transmit the multiplexed data into the fuselage for recording.

Figure 29 from reference 26 illustrates the installation of pressure transducers at one radial station ($r/R = .9$) on the blade. Each of the three rotors tested with advanced airfoils utilized this installation. The primary data for the investigation of blade section aerodynamics was provided by the pressure instrumentation. The results of the investigation of blade section aerodynamics of the NLR-1T are reported in reference 27 by Morris, Stevens, and Tomaine. The geometric characteristics of the NLR-1T are shown in figure 30 (Reference 27). The report covers a substantial number of comparisons and results relative to the section aerodynamics including normal force coefficients at different tip speed ratios, investigations of shock locations, and comparisons with theory. An illustration of a comparison with theory is shown in figure 31 from the report. The figure shows a comparison of measured and calculated chordwise pressure coefficient distributions for 4 different tip speed ratios— $\mu = .24$ to $.33$ at the 70 degree azimuth location. As shown, the correlation is fairly good, but worsens with higher tip speed ratios.

Figure 32 and 33 illustrate the geometric characteristics of the other two airfoils tested— the 10-64C and RC-SC2 respectively. The performance and loads results for these two airfoils are reported in references 28 and 29, respectively. The blade section aerodynamics results for these two airfoils are reported by Morris, et al, in references 30 and 31.

The seven reports, references 25 through 31, represent a significant contribution and contain a broad range of data on these three advanced airfoils. This effort was only the beginning for what became known as the "White Cobra". In 1978, the aircraft was transferred to Ames Research Center from Langley, and plans were formulated for the second major rotor pressure data acquisition program undertaken by NASA. This program is discussed in the following section.

AH-1G (Ames)

In the mid-seventies, the Army, through Bell Helicopter, undertook a monumental data acquisition effort with an AH-1G Cobra which was called the Operational Loads Survey (OLS), reference 32. Along with extensive fuselage instrumentation, two rotor blades were instrumented with strain gages, accelerometers, hot wire probes, and pressure transducers. There were more transducers involved in this test than in any previous test anywhere. When the "White Cobra" arrived at Ames in 1978 plans were formulated to acquire the rotor from the OLS for additional testing. Since the emphasis of the NASA program was on the tip aerodynamics, several more radial stations in the tip area were instrumented with chordwise pressure arrays.(fig. 34.) The instrumentation installed on the "White Cobra" for the NASA/Army Tip Aero Acoustic Test (TAAT) is described in detail in reference 33. In reference 33, Cross and Watts present a significant sampling of the data acquired during the TAAT flight program along with a complete description of the test and with an analysis of several key phenomena. A multitude of problems were encountered during this investigation that hampered the data reduction effort. The time available to conduct the test was limited by the availability of data processing equipment and, consequently, the test was conducted under less than ideal conditions, and the capability to repeat conditions and to identify

problems with data were restricted. One of the problems related to calibration changes on the pressure transducers between the OLS test and the TAAT, and the way that the problem was addressed is discussed by Watts in reference 34.

The data analysis effort for both the OLS and TAAT programs utilized DATAMAP, reference 35, as a primary tool and all data from these programs is available through DATAMAP. A sample of analyzed pressure data from the TAAT program utilizing DATAMAP taken from reference 33 is shown in figure 35. In the figure, blade pressure coefficients are plotted against rotor azimuth for each position on the chordwise array at radial station 99% for the test point at 159 knots. The influence of the shock on the blade is obvious from the figure.

In addition to performance and aerodynamic data acquired during the program, a major effort was expended on acoustic testing with the YO-3A, airborne acoustic platform. The YO-3A (fig. 36) is described by Cross and Watts in reference 36.

Utilizing the capability to access the TAAT and OLS data via a VAX computer and DATAMAP at Ames, several researchers have conducted investigations and analytical correlation efforts with the blade pressure data. Two of these activities are reported in references 37 and 38. In reference 37, Schillings of Texas A&M makes comparisons of predictions from a 2D transonic code, TRANDES, with the TAAT data. Figure 37 from reference 37, illustrates two extremes in the correlation effort. Figure 37 shows a comparison at the 75% radius position of predicted versus measured chordwise distribution of pressure coefficients. At this radial position, where the flow is reasonably 2 dimensional, the correlation is fairly good. However, at the 99% radial station, also shown in figure 37, the correlation is poor because of the 3 dimensional effects. In reference 38, Shenoy, et al, report on a correlation effort utilizing a NASA Ames developed transonic code, ROT 22. The report also documents the methods for integrating ROT 22 output with DATAMAP such that DATAMAP can be utilized as the tool for making the comparisons.

In addition to providing a massive amount of valuable data on two bladed configurations, the TAAT and OLS were a learning experience relative to future programs involving extensive instrumentation.

Much of the flight test work done during the 70's involved flight research with two bladed rotors as has been discussed in earlier sections; however, the limitation of the use of the readily available two bladed rotor helicopters from Army inventory was recognized in the late sixties, and the development of a generic research aircraft was initiated. The product of this initiation, the **RSRA** or **Rotor Systems Research Aircraft**, is discussed in the following section.

RSRA

The idea for a generic research aircraft bore fruit in the early seventies when the NASA and the Army combined to fund the development of the Rotor Systems Research Aircraft (RSRA). After the conduct of a series of pre-design studies, the full scale development of the RSRA began in 1973. The first flights of the completed aircraft occurred in 1977 at NASA's Wallops Station prior to delivery of the aircraft to NASA Ames. These first flights were conducted by the contractor.

The RSRA is one of the most complex aircraft ever constructed. A complete description of the systems and capabilities of the aircraft can be found in references 39 to 44. The aircraft can operate in three different modes, helicopter, compound helicopter (compounded either with engines alone or with engines and wing), and as a fixed wing. These three primary configurations are illustrated in figures 38, 39, and 40. The basic dynamic systems of the aircraft have been adapted from the existing S-61 helicopter, but these systems were packaged in an all new airframe with many unique capabilities. Each of the unique capabilities of the RSRA required the development of unique systems that had to be integrated into the aircraft. This uniqueness was the heart of the RSRA and became the source of many of its problems.

Detailed descriptions of the systems and the requirements for the RSRA are provided in the references so only a cursory discussion is included here. The main capability that sets the RSRA apart from all other aircraft is the rotor system balance system which is described in references 44 and 45. The capability is provided in the RSRA to measure all of the forces and moments transmitted from the rotor to the fuselage. For steady forces and moments this capability works very well and provides the capability to compare predicted rotor performance with measured performance, as well as rotor control capability and force and moment derivatives. The balance system, illustrated in figure 41, does not provide its unique capability without major effort. Not only do the individual load cells of the system require calibration, but the entire system requires calibration. The performance of this calibration has required the development and

continued upgrading of a major calibration facility. A photograph of the facility located at NASA Ames is shown in figure 42; a schematic of the facility is shown in figure 43. The facility is described completely in reference 46. As described in the earlier references, there are two different balance systems available for the RSRA. Each of the two systems are installed in one of the two aircraft. The system installed in the compound aircraft, Ames A/C #740, is a conventional balance employing load cells (fig. 41). The RSRA helicopter, Ames A/C #741, uses a unique balance system with vibration isolation capability. Both aircraft have been calibrated in the Ames facility. Acree presents the results of these calibrations in references 45 and 47. Hysteresis was a major problem with the balance system as discussed by Acree in reference 48. Figure 44 presents a calibration curve from reference 48 which illustrates this hysteresis effect. The hysteresis effect is one problem that requires further development. A more serious limitation was discovered when a preliminary attempt was made to investigate dynamic calibration of the aircraft.

Dynamic calibration is key to the measurement of vibratory forces and moments. The aircraft was shake tested as shown in figure 45 in order to develop transfer functions for dynamic loads. The aircraft proved to be too non-linear for this methodology to be effective. This non-linearity is illustrated in figure 46 where the transfer function is plotted against applied force and excitation frequency. The transfer function varied both as a function of applied force and frequency thus making it almost an impossibility to develop a calibration matrix that would allow the estimation of vibratory forces and moments in flight. This limitation cuts deeply into the capability of the RSRA to be utilized for vibration research. Alternatives to direct dynamic calibration have been investigated, but to date a fully reliable alternative approach has not been identified that would be worth the considerable investment required. In reference 49 one such alternative is described. In theory, the approach appears feasible, however, the requirement that accelerations of the transmission must be very accurately measured and the transmission system must be accurately modeled may limit its usefulness in the practical world.

Even without dynamic calibration and with hysteresis effects, the RSRA balance system has permitted the acquisition of two unique sets of data. One data set was the acquisition of fuselage download measurements in hover and low speed flight as reported by Flemming and Erickson in reference 51.

Figure 47 from reference 52, illustrates the first ever measurement of rotor hub drag in flight. In the figure, raw hub drag taken on the RSRA in flight in the fixed wing (no rotor) configuration is plotted against airspeed. Acree in reference 52 also makes comparisons with wind tunnel and model scale data.

Like the rotor balance system of the aircraft, the variable incidence wing on the RSRA also provides a unique capability. The wing provides the capability to fly in the fixed wing mode and to fly with rotors that are not capable of carrying the full weight of the aircraft. However, it also provides the capability to vary the amount of load that the rotor carries from a completely unloaded rotor to loaded well beyond the weight of the aircraft by providing negative lift on the wing. These capabilities are extremely valuable in the investigation of rotor performance over a broad range of rotor operating conditions. The wing, like the rotor balance system, falls short of fully acceptable operation. The wing balance system which employs load cells as illustrated in figure 48 has been shown to have redundant load paths. While attempts have been made to rectify the problem, they have not been demonstrated in a calibration. The hydraulic actuation system for the wing has also been a source of problems and requires an expensive modification to rectify the problems.

A third unique system of the RSRA is the emergency escape system which provides both escape capability and the capability to jettison an unstable rotor and fly home as a fixed wing. The installation of the blade severance devices is shown in figure 49. While fortunately never employed in flight, the system has worked well in ground tests. Before the aircraft could be flown in the fixed wing mode, however, a new set of ejection seats had to be installed. In the event of the installation of a new rotor on the RSRA, as is the case for the X-Wing rotor which is discussed in reference 53, a major development effort would be required to develop the pyrotechnic blade severance system.

The control system, while not unique among the many variable stability helicopters, is incredibly complex due to the fact that it has: 1) both fly-by-wire and mechanical controls which are implemented through many actuators in each axis; and 2) a requirement to change the coupling and phasing of both full rotary wing controls and full fixed wing controls. The full capability of the RSRA control system has never been fully exploited due to the limitations of the existing flight computer. Further development is also required in the controls area to make the system fully acceptable. However, the combination of the control system and the rotor balance system makes the RSRA an ideal vehicle for exploring rotor/airframe flight dynamics through the use of parameter identification. Considerable work has been done in the parameter identification and math modeling area by DuVal, Wang, Demiroz, and Talbot using the RSRA as a baseline

vehicle. These investigations are reported in references 54 through 59. Figure 50 from reference 59 illustrates the comparison of flight data for the RSRA fixed wing configuration with predicted pitch rate response from the math model derived by parameter identification methods. This work was very valuable in the development of models for the RSRA X-Wing configuration.

The RSRA, in 6 years of operation, has proven to have unique capabilities and has provided some unique flight data. The results of these flight operations with the three RSRA configurations, helicopter, compound and fixed wing are reported in two major flight test reports by Erickson, et al (References 60 and 61). In many areas, however, it has fallen short of expectations. It has been plagued by a multitude of development and design problems and is particularly susceptible to mechanical problems. These problems have resulted in a lack of productivity by the aircraft. There has also been a continuing decline in resources and experience to operate and conduct research with the RSRA. These factors combined with the requirement to conduct rotor research on modern 4-bladed rotors, which can not be performed on the RSRA without major modifications, have resulted in a recent decision to indefinitely suspend operations with the aircraft.

The requirement to conduct experiments that will provide extensive data on rotor and airframe dynamics, aerodynamics, and aeroacoustics on a modern rotor system was initially directed at the use of the RSRA. The prohibitive expenditure of resources required to adapt a new rotor to the RSRA and the existing deficiencies of the aircraft resulted in a decision not to pursue that direction. It was determined that the UH-60 was the best alternative to the RSRA for the conduct of a broad range of rotor experiments. The next section discusses the status and plans for rotor testing with the UH-60.

UH-60

The UH-60, shown in figure 51, is a modern Army helicopter with a rotor design considerably more modern than those that have previously been utilized for extensive aerodynamic testing. The planned NASA/Army program with the UH-60 will utilize a flight test aircraft located at the Army Engineering Flight Activity at Edwards AFB. The flight research will be conducted over a multi-year period as a combined effort of NASA and the Army. As described in reference 62, the program will involve several phases including both flight and wind tunnel testing of the extensively instrumented rotor system. Research directed at rotor/airframe dynamics, at rotor vibratory airloads, and at rotor airloads and acoustics will be conducted as illustrated in figure 52. Figures 53 and 54 illustrate the two highly instrumented blades under development for the program. The instrumentation includes strain gages, accelerometers, and pressure transducers on the blades. The fuselage instrumentation includes standard aircraft state instrumentation plus extensive airframe and rotor hub vibration measurements. In a certain sense, the UH-60 program will provide a modern extension of the work done of the H-34 in the early sixties; however, the objectives go far beyond those envisioned for the H-34.

A major concern in the planning for the UH-60 problem is the massive amount of data that will be required. One estimate indicates that 1/6 of a second will provide more data than is included in all the tables of the data report on the H-34 (ref. 9). No one was prepared to deal with the data acquired with the highly instrumented blades of the "White Cobra"; therefore, considerable effort is being put forth to prepare for the UH-60 testing, which will begin in 1988, to ensure that the computer tools and techniques are available. A prime objective is to have the capability to get data in the hands of all potential users in a minimum amount of time. One effort receiving considerable support is the implementation of TRENDS, reference 63, for use in the UH-60 program. Advanced versions of DATAMAP are also in the works along with supporting computer hardware.

Extreme care must be exercised to ensure that this program provides the data required for the validation of a number of advanced computer codes and comprehensive analysis programs, and for the development of several new rotor systems for military applications (LHX, ACA, and the advanced Black Hawk rotor).

Other

There are many additional important flight research programs that have not been discussed in this paper since they were outside the scope of the primary subject. Notably among these programs are the many important contributions made in the flight dynamics and guidance and control areas both at Langley and Ames. Equally important is the rotor flight research with the XV-15 tilt rotor which is discussed in a separate paper by Schroers. Finally an important new program that will complement the UH-60 research involves a high speed rotor flight research program with the Army and Boeing on the 360 aircraft.

Summary

Over fifty years of contributions by NASA and the Army through rotor systems flight research have been examined with an emphasis on the last twenty five years. During this time, the helicopter has gone from an abnormality that did a few useful things to a vehicle that is a necessity to life in this country and a major part of all military forces in the world.

Major data acquisition programs like the H-34 and "White Cobra" have been undertaken that have increased our understanding of the aerodynamic behavior of the rotor system. Specialized programs like the Ogee tip on the UH-1 and the flight tests of the hingeless rotor helicopters, the XH-13 and XH-51N, contributed greatly to our understanding of these technologies. The extensive airfoil test program also undertaken on the "White Cobra" provided valuable data on advanced airfoil configurations. Finally the RSRA, while limited by reliability and resource problems, provided unique data and served as a tool to advance the state of the art in parameter identification. As will be described in a separate paper, a major contribution of the RSRA may be through a demonstration of the X-Wing concept.

The highly instrumented UH-60 along with companion programs (High Speed 360, XV-15 ATB, and model scale tests of 360, UH-60, and ATB) will provide the opportunity to explore, over the next several years, a full range of rotor operation and to obtain the data necessary to fully validate the advanced methodologies being developed.

References

1. Wheatley, John B., "Lift and Drag Characteristics and Gliding Performance of an Autogiro as Determined in Flight"; Report 434, NACA, 1932.
2. Wheatley, John B., "An Aerodynamic Analysis of the Autogiro Rotor with a Comparison between Calculated and Experimental Results", Report #487, NACA, 1934.
3. Gustafson, F. B.; "Flight Tests of the Sikorsky HNS-1 (Army YR-4B) Helicopter. I - Experimental Data on Level-Flight Performance with Original Rotor Blades", NACA MR No. L5C10, 1945.
4. Gustafson, F. B., and Gessow, Alfred; "Flight Tests of the Sikorsky HNS-1 (Army YR-4B) Helicopter, II - Hovering and Vertical-Flight Performance with the Original and an Alternate Set of Main-Rotor Blades, Including a Comparison with Hovering Performance Theory", NACA MR No. L 5D09a, 1945.
5. Gustafson, F.B., and Gessow, Alfred, "Effect of Blade Stalling on the Efficiency of a Helicopter Rotor as Measured in Flight", Technical Note 1250, NACA, Langley Memorial Laboratory, Langley Field, Va. APRIL 1947.
6. Yeates, John E, Jr. "Flight Measurement of the Vibrations Encountered by a Tandem Helicopter and a Method for Measuring the coupled Response in Flight", NACA TN 3852, Langley Aeronautical Laboratory, Langley Field, Va. December 1956.
7. Ludi, LeRoy H., "Flight Investigation of Effects of Retreating-Blade Stall on Bending and Torsional Moments Encountered by a Helicopter Rotor Blade", Technical Note 4254, NACA, Langley Aeronautical Laboratory, Langley Field, Va. May 1958.
8. Churchill, Gary B. and Rabbot, "Experimental Investigation of the Aerodynamic Loading on a Helicopter Rotor Blade in Forward Flight", RM L56107, NACA, Washington, OCTOBER 25, 1956.
9. Scheiman, James; "A Tabulation of Helicopter Rotor-Blade Differential Pressures, Stresses, and Motions as Measured in flight"; NASA TMX-952, Langley Research Center, Langley Station, Hampton, Virginia., March 1964.

10. Scheiman, James and Kelley Henry L., "Comparison of Flight Measured Helicopter Rotor Blade Chordwise Pressure Distributions and Two-Dimensional Airfoil Characteristics"; CAL-TRECOM Symposium on Dynamic Loads Problems Associated with Helicopters and V/STOL Aircraft, Buffalo, New York, June 26-27, 1963.
11. Sadler, S. Gene, "Main Rotor Free Wake Geometry Effects on Blade Air Loads and Response for Helicopters in Steady Maneuvers", Vol.1 Theoretical Formulation and Analysis of Results"; NASA CR-2110, September 1972.
12. Ward, John F., " Helicopter Rotor Periodic Differential Pressures and Structural Response Measured in Transient and Steady State Maneuvers", Journal of the American Helicopter Society, Presented at the 26th Annual Forum of the American Helicopter Society, June 16-18, 1970.
13. Hooper, W. E., "The Vibratory Airloading of Helicopter Rotors", Associazione Industrie Aerospaziali, Boeing Vertol Company, Ninth-European Rotorcraft Forum, Paper #46, Stresa, Italy, September 13-15, 1983.
14. Esculier, Jacques and Bousman, William G., "Calculated and Measured Blade Structural Response on a Full-Scale Rotor", Proceedings of 42nd American Helicopter Society Annual Forum, Washington, June 1986.
15. Huston, Robert J., "An Exploratory Investigation of Factors Affecting the Handling Qualities of a Rudimentary Hingeless Rotor Helicopter ", NASA TN D-3418, Langley Research Center, Langley Station, Hampton, Va., May 1966.
16. Ward, John F., "A Summary of Hingeless-Rotor Structural Loads and Dynamics Research", Presented at the Symposium on Noise and Loading Actions on Helicopter V/STOL Aircraft and Ground Effect Machines, University of Southampton, Southampton, England, Aug. 30- Sept. 3, 1965.
17. Ward, John F. and Huston, Robert J., " A Summary of Hingeless-Rotor Research at NASA/Langley", Presented at the Twentieth Annual National Forum of the American Helicopter Society, Wash. D.C., May 13-15, 1964.
18. Ward, John F., "Exploratory Flight Investigation and Analysis of Structural Loads Encountered by a Helicopter Hingless Rotor System", Langley Research Center, Langley Station, Hampton, Va. NASA TN D-3676. November 1966.
19. Snyder, William J., "A Summary of Rotor-Hub Bending Moments Encountered by a High-Performance Hingeless-Rotor Helicopter During Nap-of-the-Earth Maneuvers", NASA TN D-4574. Langley Research Center, Langley Station, Hampton Va. May 1968.
20. Kelley, Henry, Pegg, Robert J. and Champine Robert A. "Flying Quality Factors Currently Limiting Helicopter Nap-Of-The-Earth Maneuverability as Identified by Flight Investigation" NASA TN D-4931, Langley Research Center, Langley Station Hampton, Va. December 1968.
21. Snyder, William J. and Hanks, Brantley R., "Ground Test of an Active Vibration Isolation System for a Full Scale Helicopter", Presented at the 43rd Shock and Vibration Symposium, Pacific Grove, Ca. December 5-7, 1972.
22. Ward, John F. and Snyder, William J. "The Dynamic Response of a Flexible Rotor Blade to a Tip-Vortex Induced Moving Force", AIAA Paper No. 69-203, AIAA/AHS VTOL RESEARCH, DESIGN, AND OPERATIONS MEETING, Georgia Institute of Technology, Atlanta, Georgia, February 17-19-1969.
23. Ward, John F., "The Dynamic Response of a Flexible Rotor Blade to a Concentrated Force Moving From Tip to Root", Langley Research Center, Hampton, VA, NASA TN D-5410, September 1969.

24. Mantay, Wayne R., Campbell, Richard L. and Shidler, Phillip A., "Full Scale Testing of an Ogee Tip Rotor", Structures Laboratory, U S Army R & T Laboratories (AVRADCOM) and NASA Langley Research Center.
25. Morris, Charles E. K. "A Flight Investigation of Basic Performance Characteristics of a Teetering-Rotor Attack Helicopter," NASA TM 80112, June 1979.
26. Morris, Charles E. K., Tomaine, Robert L., and Stevens, Dariene D. "A Flight Investigation of Performance and Loads for a Helicopter with NLR-1T Main-Rotor Blade Sections" NASA TM 80165, October 1979.
27. Morris, Charles E. K., Stevens, Dariene D., and Tomaine, Robert L.; "A Flight Investigation of Blade-Section Aerodynamics for a Helicopter Rotor having NLR-1T Airfoil Sections", NASA TM 80166, AVRADCOM TR80-B-2, January 1980.
28. Morris, Charles E.K., Tomaine, Robert L., and Stevens, Dariene D., "A Flight Investigation of Performance and Loads for a Helicopter with 10-64C Main-Rotor Blade Sections", NASA TM 81871, AVRADCOM TR 80-B-2, October 1980.
29. Morris, Charles E.K., Tomaine, Robert L. and Stevens, Dariene D., "A Flight Investigation of Performance and Loads for a Helicopter with RC-SC2 Main-Rotor Blade Sections", NASA TM 81898, AVRADCOM TM 81-B-1, December 1980.
30. Morris, Charles E. K., "A Flight Investigation of Blade Section Aerodynamics for a Helicopter Main Rotor Having 10-64C Airfoil Sections", NASA TM 83226, December 1981.
31. Morris, Charles E.K., "A Flight Investigation of Blade-Section Aerodynamics for a Helicopter Main Rotor Having RC-SC2 Airfoil Sections"; NASA TM 83298, March 1982.
32. Shockey, G.A., Williamson, J.W. and Cox, C.R., "AH-1G Helicopter Aerodynamic and Structural Loads Survey", USAAMRD-TR-7639, Bell Helicopter Textron, Feb. 1977.
33. Cross, Jeffrey L., and Watts, Michael, E. "Tip Aerodynamics and Acoustics Test-A Report and Data Survey", Draft NASA RP, January 7, 1987.
34. Watts, Michael E., "Supplementary Calibration Test of the Tip-Aerodynamics-and-Acoustics-Test Pressure Transducers", NASA TM 88312, JULY 1986.
35. Philbrick, R.B., "The Data from Aeromechanics Test and Analytic-Management and Analysis Package (DATAMAP)-Vol. One-Users Manual" USAAVRADCOM TR-80-D-30A, Bell Helicopter Textron, Dec. 1980.
36. Cross, J.L., and Watts, M.E., "In-flight Acoustic Testing Techniques Using the YO-3A Acoustic Research Aircraft", AIAA-83-2754, AIAA'83, AIAA/AHS/IES/SETP/SFTE/DGLR 2ND FLIGHT TESTING CONFERENCE, Las Vegas, Nevada, November 16-18, 1983.
37. Schillings, J.J., "Mach Number Correlation for a Two Dimensional Helicopter Rotor Blade Analysis in the Tip Region," NASA CR 177430, CONTRACT NCA2-OR773-101, October 1986.
38. Shenoy, K.R., Waak, T. and Brieger, J. T., "Development of a ROT22-DATAMAP Interface", NASA CONTRACTOR REPORT 177403, CONTRACT NAS2-10331, April 1986.

39. Condon, Gregory W. , "Rotor Systems Research Aircraft (RSRA) Requirements for , and Contributions to, Rotorcraft State Estimation and Parameter Identification. Presented at the AGARD Flight Mechanics Panel Specialists Meeting on "Methods for Aircraft State and Parameter Identification," Hampton, Virginia, November 5-8, 1974.
40. Letchworth, Robert and Condon, Gregory W., "Rotor Systems Research Aircraft (RSRA)", Presented at the AGARD Flight Mechanics Panel Symposium, Vallorie, France June 9-12, 1975.
41. Moore, Frederick L, and Occhiato, John J., "The Basic Flying Characteristics of the Rotor Systems Research Aircraft," Presented at the 33rd Annual National Forum of the American Helicopter Society, Washington, D C, May 1977.
42. Huston, Robert J. et al: "The Rotor Systems Research Aircraft-A New Step in the Technology and Rotor System Verification Cycle. Presented at the AGARD Flight Mechanics Panel Symposium on "Rotorcraft Design", Ames Research Center, Moffett Field, Ca. May 16-19, 1977.
43. White, Samuel, Jr. and Condon, Gregory W., "Flight Research Capabilities of The NASA/Army Rotor Systems Research Aircraft", Paper No. 72, Presented at the Fourth European Rotorcraft and Powered Lift Aircraft Forum, Stresa, Italy, September 13-15, 1978.
44. Burks, J. S., "Rotor Systems Research Aircraft (RSRA)-Rotor Force and Moment Measurement System, AIAA/SETP/SFTEE/SAE/ITEA/IEEE 1St Flight Testing Conference, Las Vegas, Nevada, November 11-13, 1981.
45. Acree, C. W. Jr., "Results of the First Complete Static Calibration of the RSRA Rotor-Load-Measurement System." NASA TM 2327, August, 1984.
46. Acree, C.W., Baker, F.A., Wellman, J. B., Smith, M.O., Domonoske, D.J., Mathias, J. R., and Burdick, S.C., "RSRA Calibration Facility Operations Manual", NASA TM 84389, August 1983.
47. Acree, C. W. Jr., "Preliminary Results of the First Static Calibration of the RSRA Helicopter Active-Isolator Rotor Balance System", NASA TM84395, November 1983.
48. Acree, C.W., "Performance of the Rotor System Research Aircraft Calibrated Rotor Loads Measurement System" Presented at the 38th Annual Forum of the American Helicopter Society, Anaheim, CA., May 1982.
49. Du Val, Ronald W.; Bahrami, Moshen; and Acree, C.W.; "The Use of Parameter Identification for Dynamic Calibration of the Rotor Systems Research Aircraft", AIAA ATMOSPHERIC FLIGHT MECHANICS CONVENTION, Seattle, Washington, Aug. 1984.
50. Du Val, R. W., and Bahrami, M. "Estimation of Dynamic Rotor Loads for the Rotor Systems Research Aircraft: Methodology Development and Validation" NASA Contractor Report 177362, Contract # NAS2-11688, May 1985.
51. Flemming, Robert J., and Erickson, Reuben E. "An Evaluation of Vertical Drag and Ground Effect Using the RSRA Rotor Balance System", 38th Annual Forum of the American Helicopter Society, Anaheim, CA. May 1982.
52. Acree, C.W., "Preliminary Report on In-Flight Measurement of Rotor Hub Drag and Lift Using the RSRA" NASA TM 86764, October 1985.
53. Linden, A. W., and Biggers, J. C.; "X-Wing Potential for Navy Applications"; Proceedings of the 41st Annual Forum of the American Helicopter Society, Ft. Worth, 1985.

54. Du Val, R. W.; "Inertial Dynamics of a General Purpose Rotor Model"; NASA TM 78557; Ames Research Center; March 1979.
55. DuVal, R. W.; "The Use of Frequency Methods in Rotorcraft System Identification"; First AIAA Flight Test Conference; AIAA Paper 81-2386; Las Vegas, 1981.
56. Wang, J. C., Demiroz, M. Y., and Lym, K.; "Rotorcraft System Identification: Flight Test Planning, Model Structure Determination"; San Jose State University, NASA Final Report, 1984.
57. Wang, J.C., DuVal, R. W., and Demiroz, M. Y.; "A Practical Approach to Rotorcraft Systems Identification"; Proceedings of 39th American Helicopter Society Forum, 1983.
58. Wang, J. C., Demiroz, M. Y., and Talbot, P. D.; "Flight Test Planning and Parameter Extraction for Rotorcraft System Identification"; Proceedings of International Flight Test Conference, Las Vegas, 1986.
59. DeMiroz, Mustafa, Y. "Identification Of Rotor Systems Research Aircraft (RSRA) Rigid Body Dynamics in Time and Frequency Domains" The Department of Aeronautics and Astronautics and the Committee on Graduate Studies of Stanford University in Partial Fulfillment of the Requirements for the Degree of Engineer, June 1986
60. Erickson, R.E, Kufeld, R.M., Cross, J.L., Hodge, R.W., Ericson, W.F., and Carter, R.D.G., "NASA Rotor System Research Aircraft FLight-Test Data Report: Helicopter and Compound Configuration, NASA TM 85843, August 1984.
61. Erickson, R.E., Cross, J.L., Kufeld, R.M., Acree, C.W. Nguyen, D. and Hodge, R.W. "NASA Rotor Systems Research Aircraft: Fixed-Wing Configuration Flight-Test Results", NASA TM 96789, February 1986.
62. Watts, M. E., and Cross, J. L.; "The NASA Modern Technology Rotors Program"; Presented at the AIAA/AHS/CASI/DGLR/IES/ISA/ITEA/SETP/SFTE 3rd Flight Testing Conference; Las Vegas, April 1986.
63. Bondi, M. J.; "Trends"; Prepared Comments-Proceedings of the 2nd Decennial Specialists on Rotorcraft Dynamics; NASA-Ames/American Helicopter Society; NASA CP2400; Nov. 85.

TABLE I. REPRESENTATIVE ROTOR TYPES

NUMBER OF BLADES	TEETERING/ GIMBALED	FULLY- ARTICULATED	HINGELESS (PITCH BEARINGS)	BEARINGLESS
2	S	-	-	-
3	S	S,T	S	-
4	S	S,T	S	S
5	-	S	-	-
6	-	S	-	-
7	-	S	-	-
S = SINGLE ROTOR T = TANDEM ROTOR				

TABLE II. HELICOPTER PROBLEMS AND RELATED ROTOR PHENOMENA

<div>PHENOMENON</div> <div>PROBLEM AREA</div>	TRANSONIC FLOW	DYNAMIC STALL	DYNAMIC BLADE LOADS	BLADE VORTEX INTERACTION	MAIN ROTOR/TAIL ROTOR INTERACTION	ROTOR INFLOW	ROTOR WAKE	GUSTS
VIBRATION	X	X	X	X	X		X	X
NOISE	X			X	X	X	X	X
PERFORMANCE	X	X			X	X	X	
AEROELASTIC STABILITY		X	X			X		
GUST RESPONSE								X

AERODYNAMICALLY
GENERATED NOISE

- IMPULSIVE
- THICKNESS
- BLADE-VORTEX
INTERACTION
- BROAD BAND

ROTOR

- INFLOW
- WAKE

TRANSONIC
FLOW

SHOCKS

TIP VORTEX
TRAJECTORY

DYNAMIC STABILITY

- TORSION
- FLAP
- LEAD-LAG

DYNAMIC
STALL

DYNAMIC
BLADE LOADS

DYNAMIC HUB LOADS

- VIBRATION
ISOLATION

FIGURE 1. Illustration of aerodynamic and dynamic environment of the helicopter rotor.

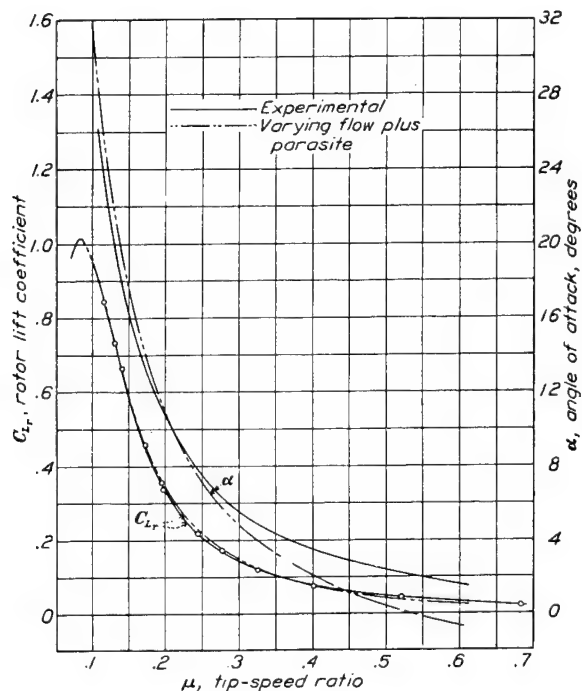


FIGURE 2. Experimental and calculated lift coefficient and angle of attack of PCA-2 autogiro rotor.



FIGURE 3. R-4 test helicopter at Langley Field.

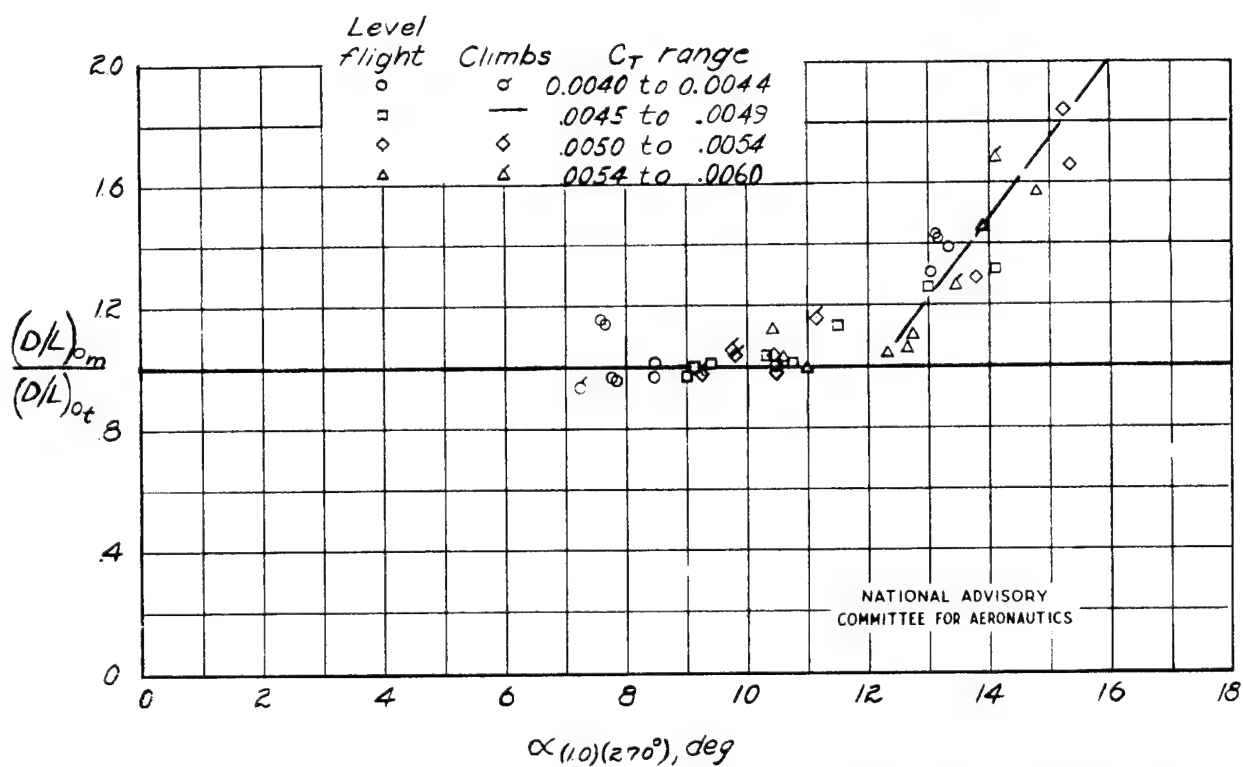


FIGURE 4. Variation of the ratio of measured values of rotor-profile drag-lift ratio to theoretical value with the calculated angle of attack of the retreating blade tip.

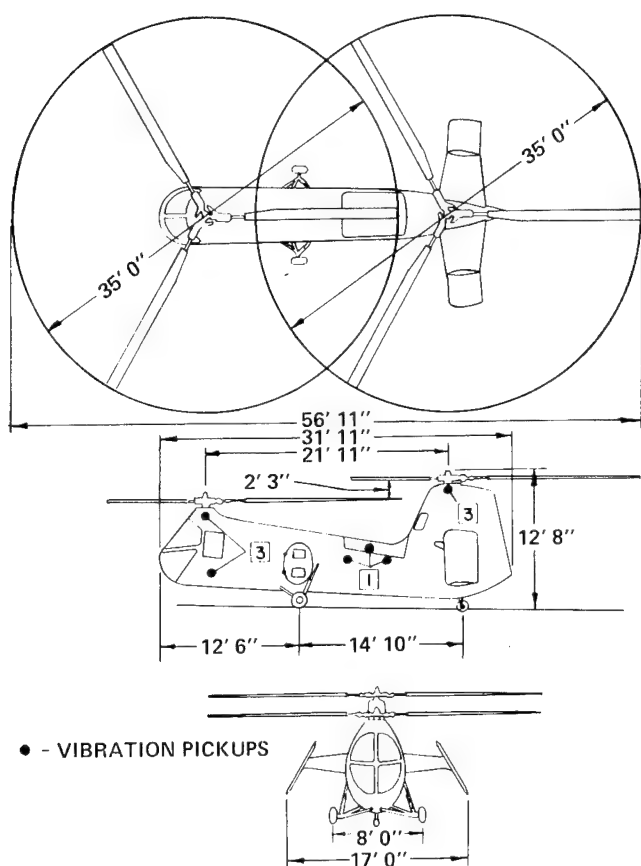


FIGURE 5. Test helicopter showing location of vibration pickups and number of components measured.



FIGURE 7. H-19 test helicopter at Langley Field.

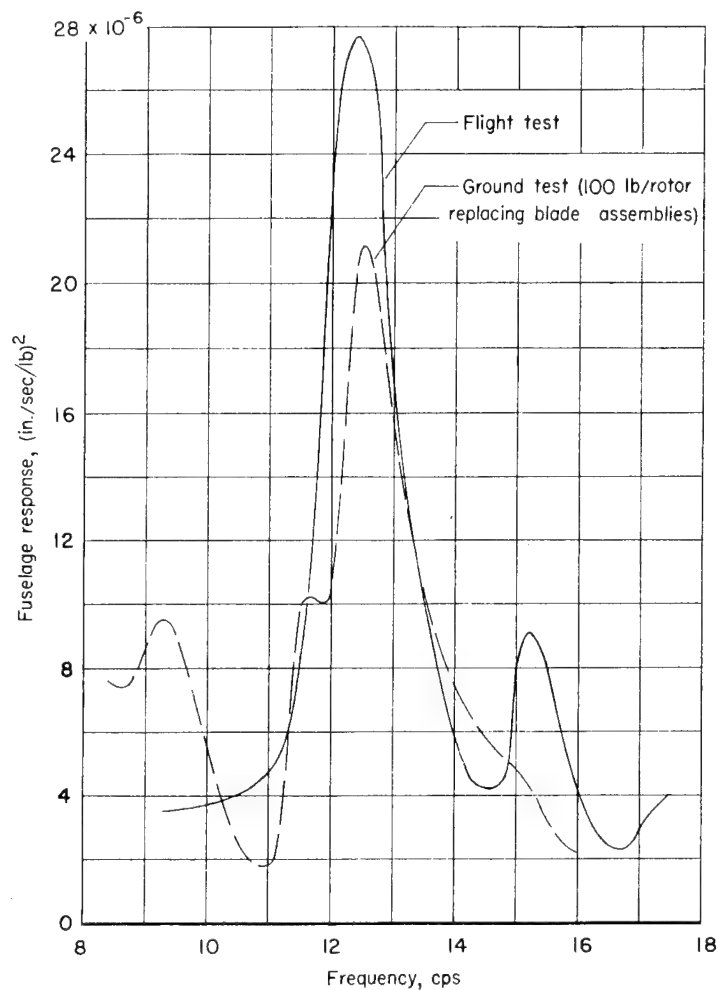


FIGURE 6. Coupled response of helicopter structure measured at the front rotor for wood blade configuration (rotor speed = 273 rpm; forward speed = 55 knots) compared with ground-measured response.

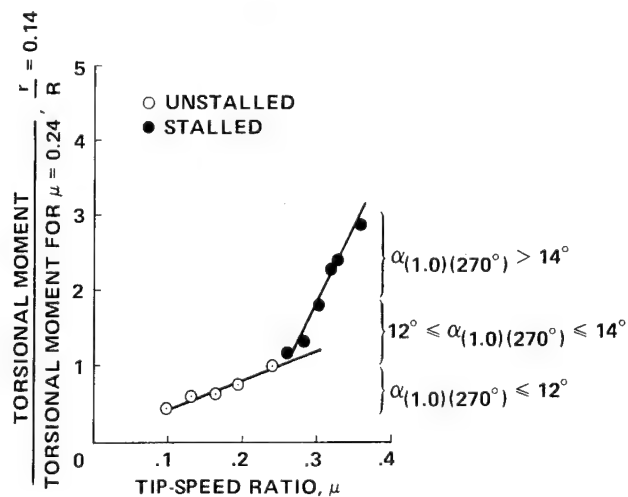


FIGURE 8. Vibratory torsional moments as a function of tip-speed ratio for unstalled and stalled steady forward flight.

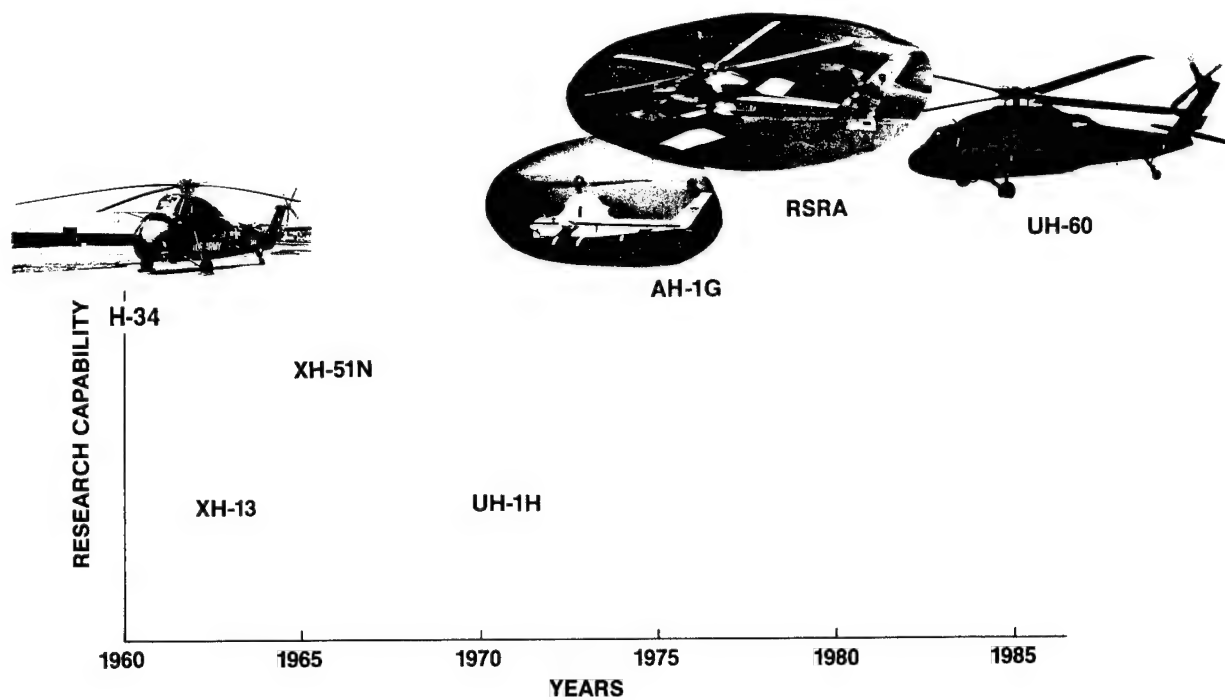


FIGURE 9. Twenty-five years of NASA/Army rotor flight research aircraft.



FIGURE 10. H-34 test helicopter at Langley Research Center.

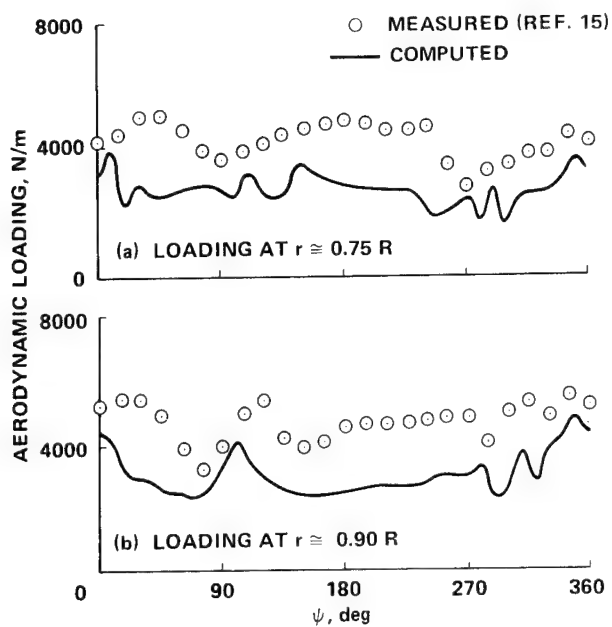


FIGURE 11. Section aerodynamic loading for H-34 in right turn, $\mu=0.224$, $f_g=1.5$.

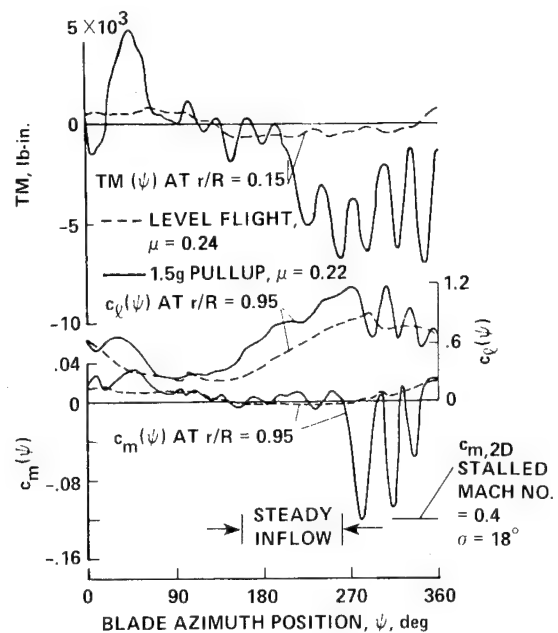


FIGURE 12. Comparison of level flight and 1.5 g pullup time histories of section loading and moment coefficients and blade torsional response.

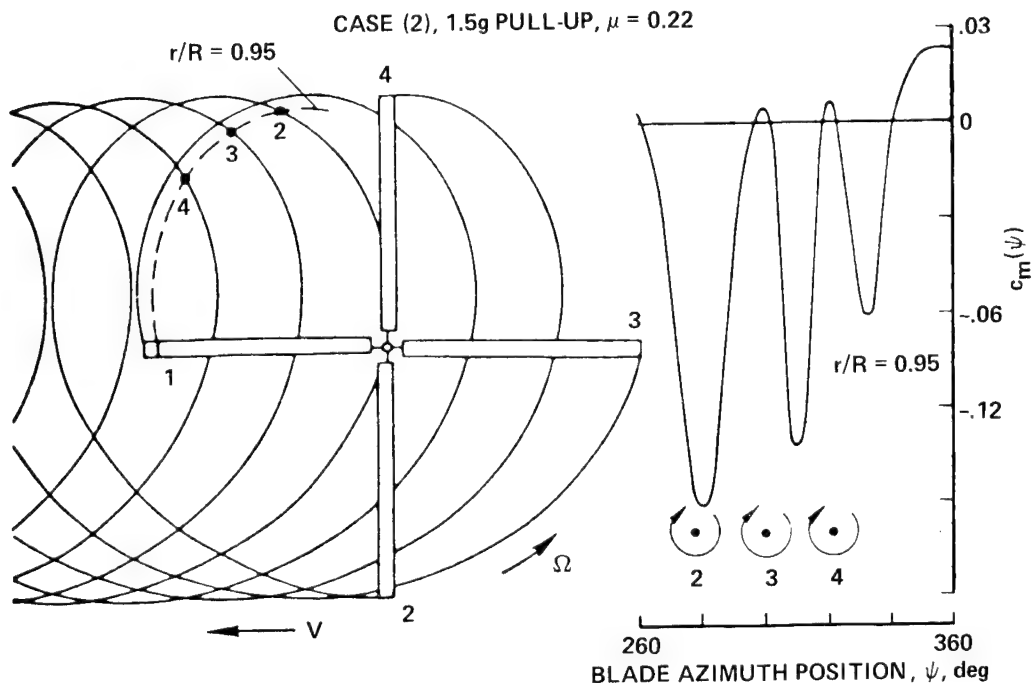


FIGURE 13. Wake helical pattern and correlation of vortex crossings with aerodynamic pitching moment fluctuations for H-34; $\mu=0.22$, 1.5 g maneuver.



FIGURE 14. H-13G hingeless rotor test helicopter at Langley Research Center.

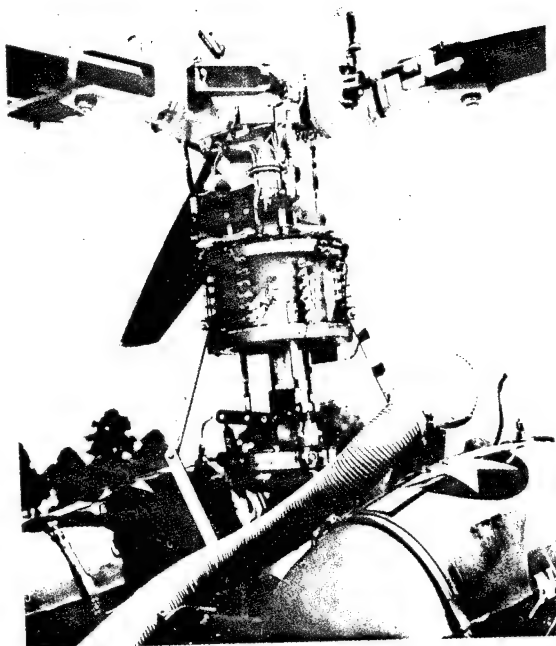


FIGURE 15. H-13G hingeless rotor hub and slipring assembly.

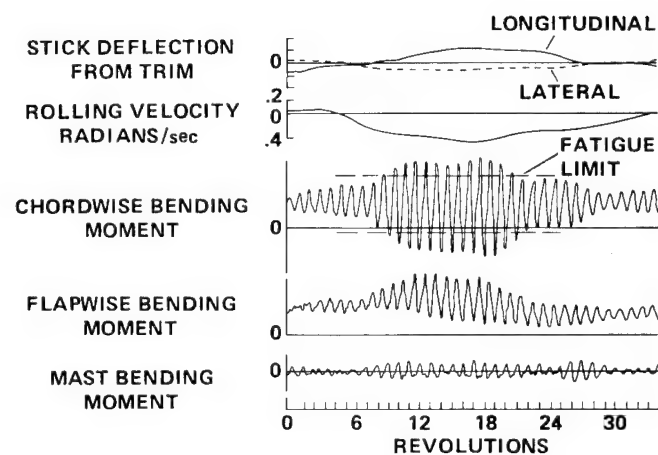


FIGURE 16. Structural loads time history during lateral maneuver with hingeless rotor helicopter in level flight at a forward speed of 80 mph.



FIGURE 17. XH-51N hingeless rotor research helicopter at Langley Research Center.

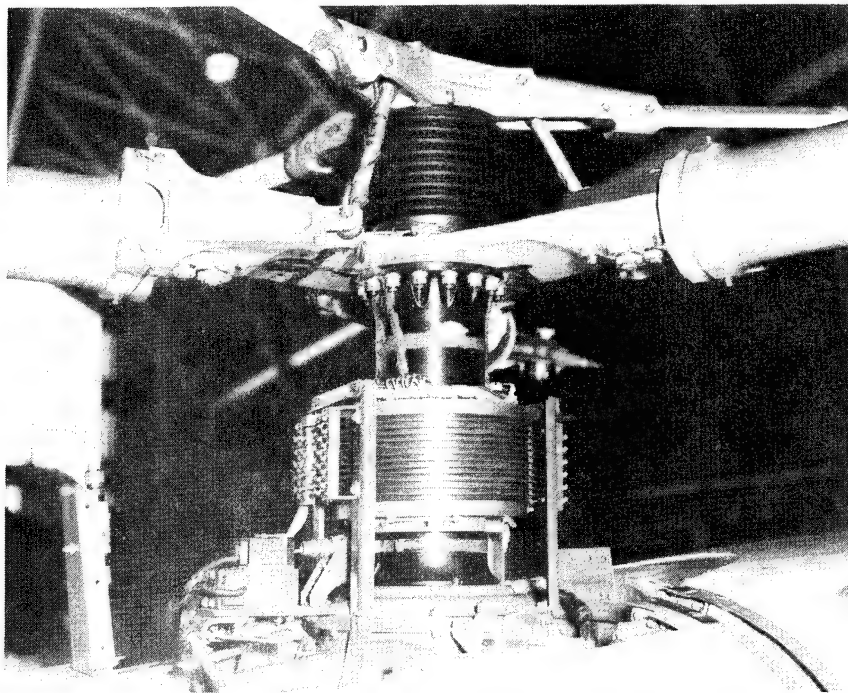


FIGURE 18. XH-51N rotor hub and control gyro.

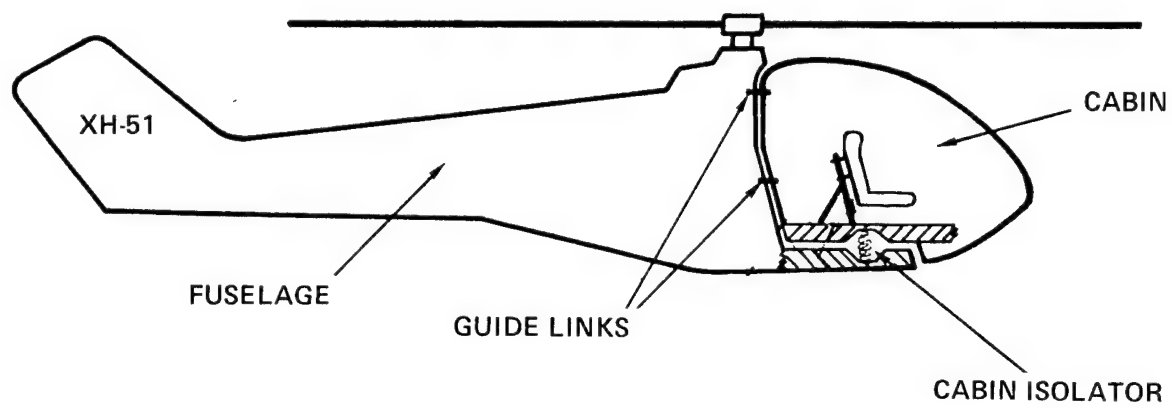


FIGURE 19. Passive cabin isolation system installation on XH-51N helicopter.

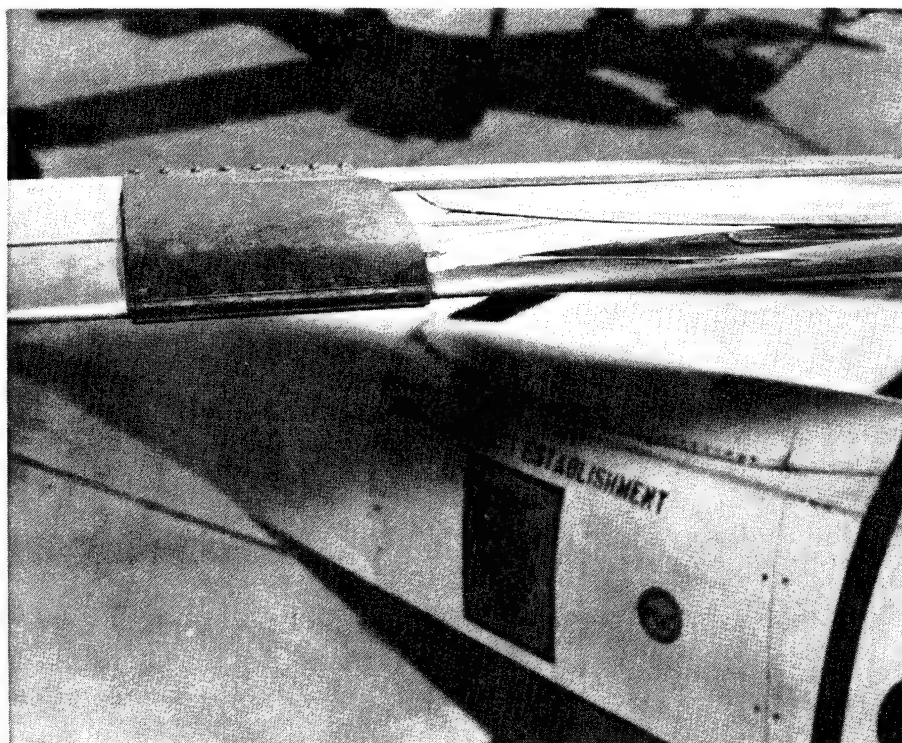


FIGURE 20. Blade tuning mass installed on XH-51N rotor blade.

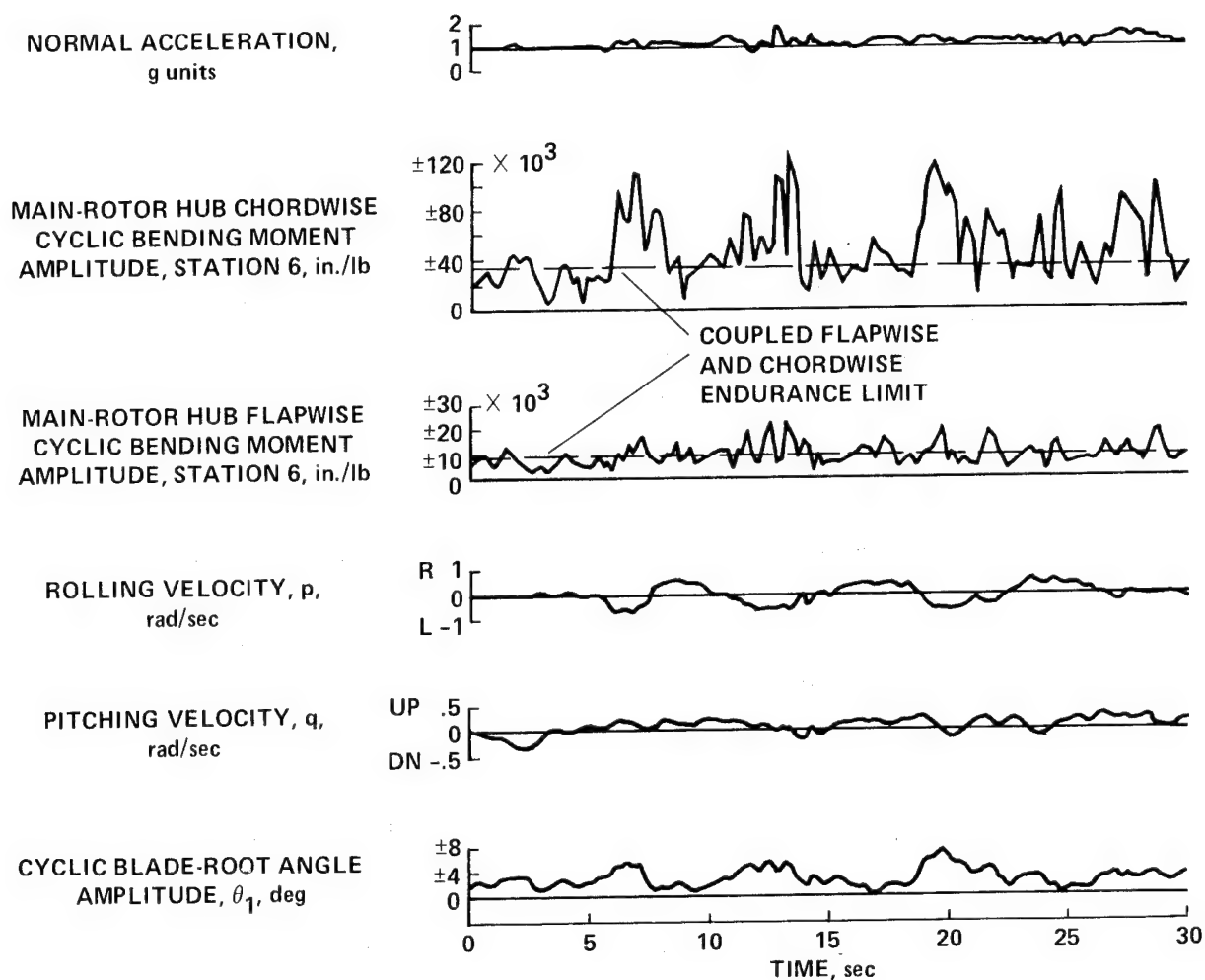


FIGURE 21. Slalom-course maneuver performed at 45 to 50 knots through 200 ft. spaced markers with the XH-51N.

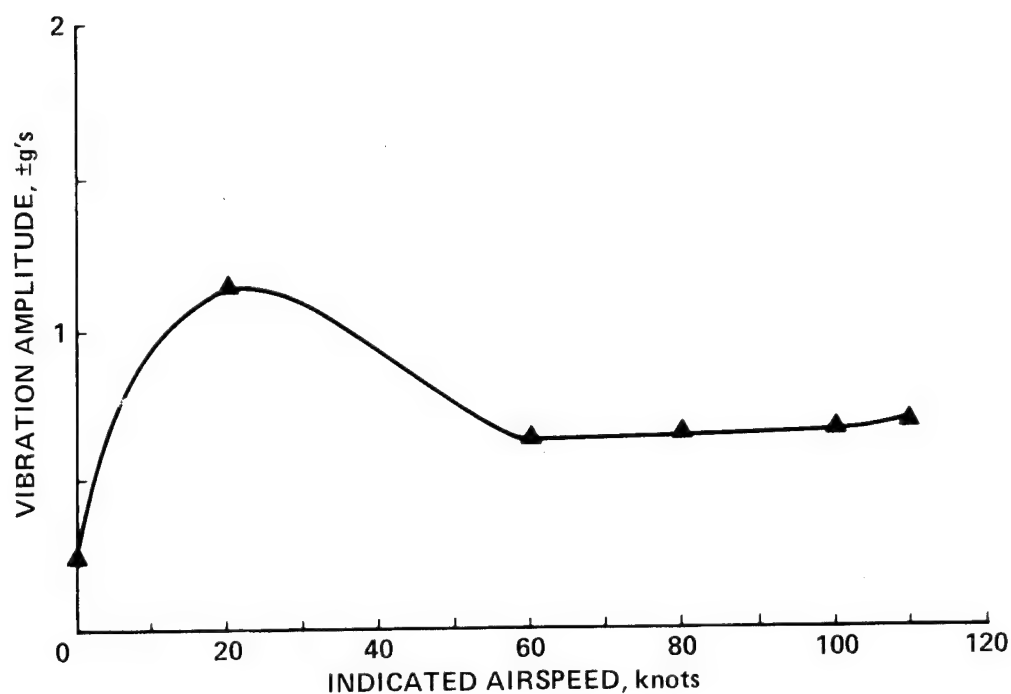


FIGURE 22. XH-51N 18 Hz. vertical vibration at pilot's station in flight with non-isolated cabin.

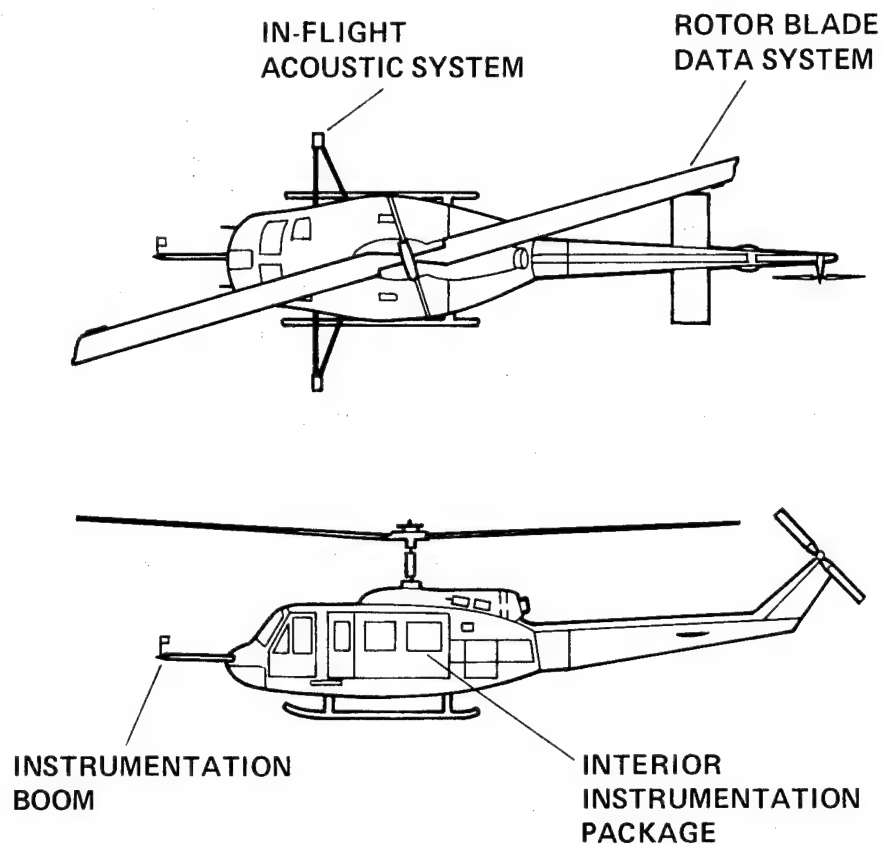


FIGURE 23. UH-1H test helicopter for "ogee" tip test program.

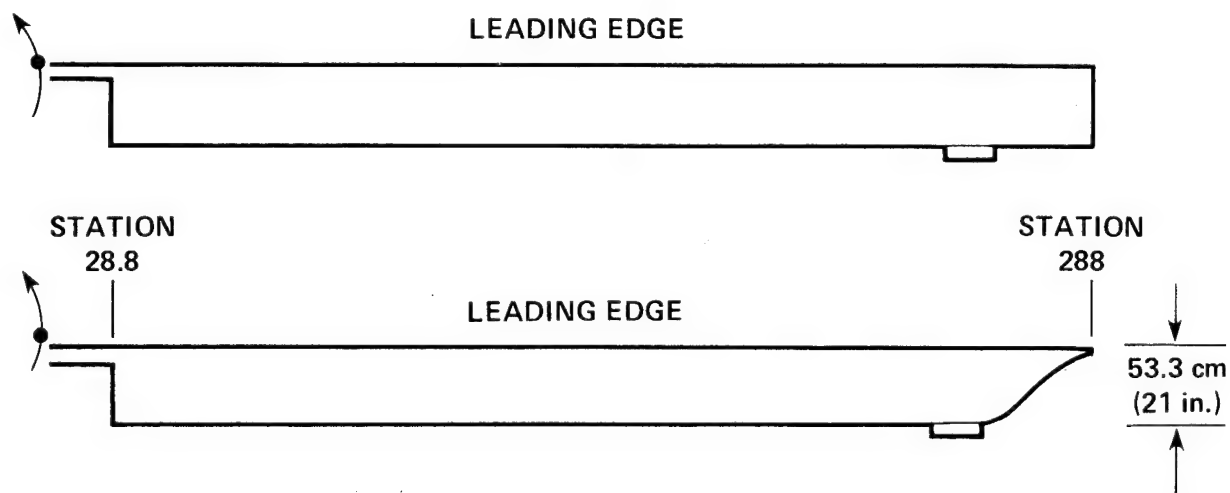


FIGURE 24. "Ogee" and standard test rotor planforms.

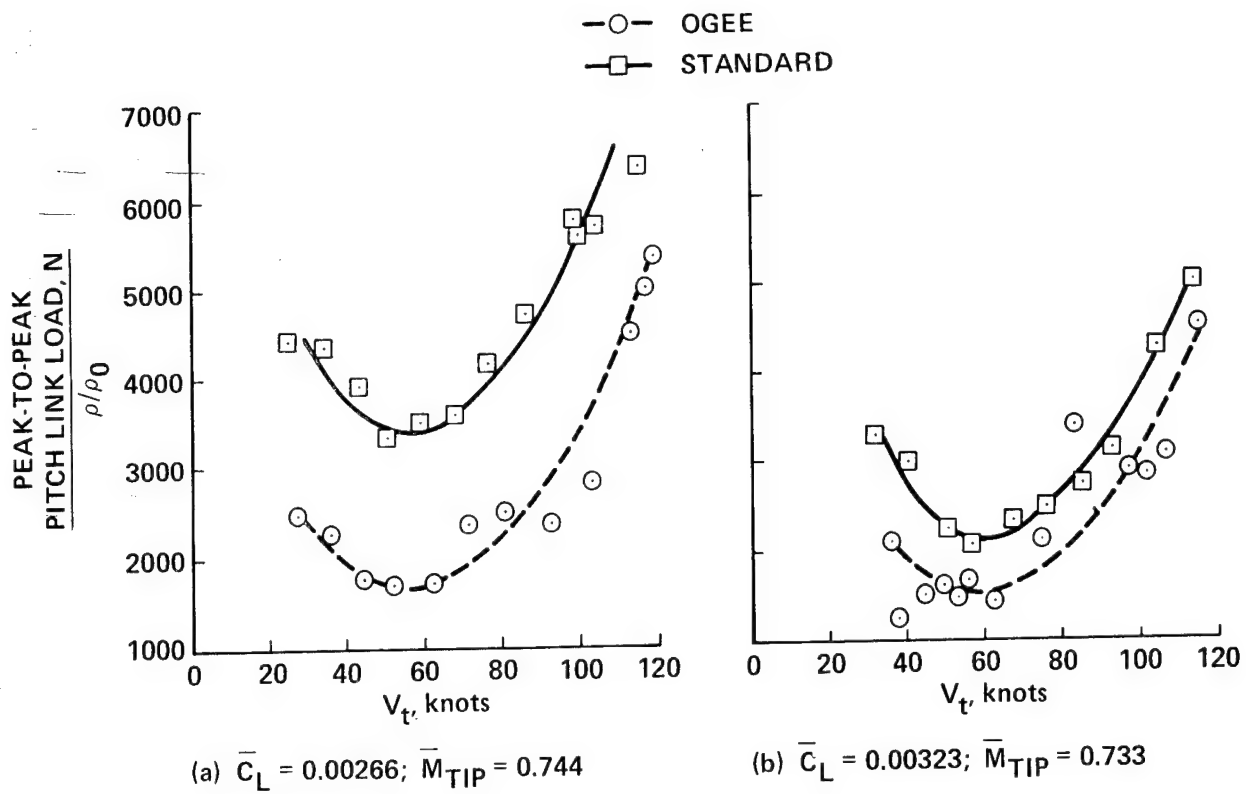


FIGURE 25. UH-1H oscillatory pitch link loads in level flight for standard and "ogee" tip rotors.



FIGURE 26. AH-1G "White Cobra" test helicopter at Langley and Ames.

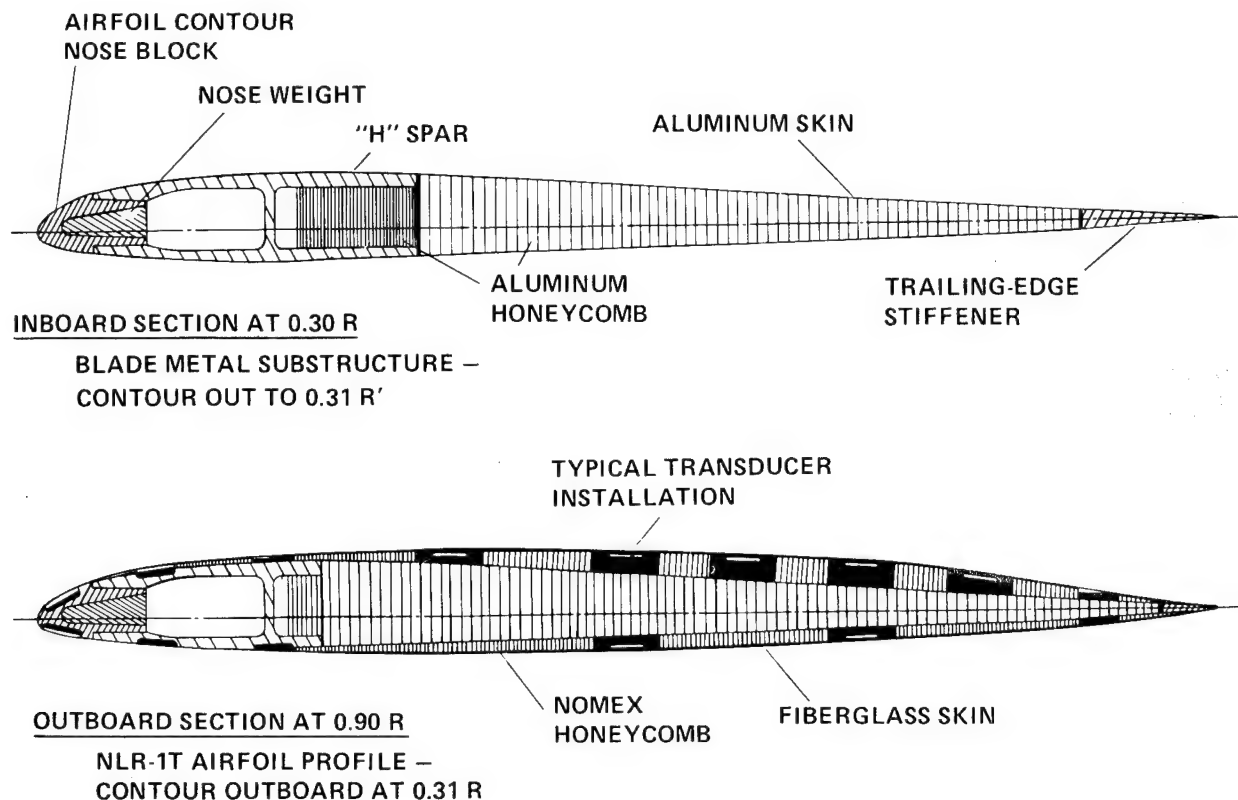


FIGURE 27. Cross section of AH-1G blades modified with NLR-1T airfoil.

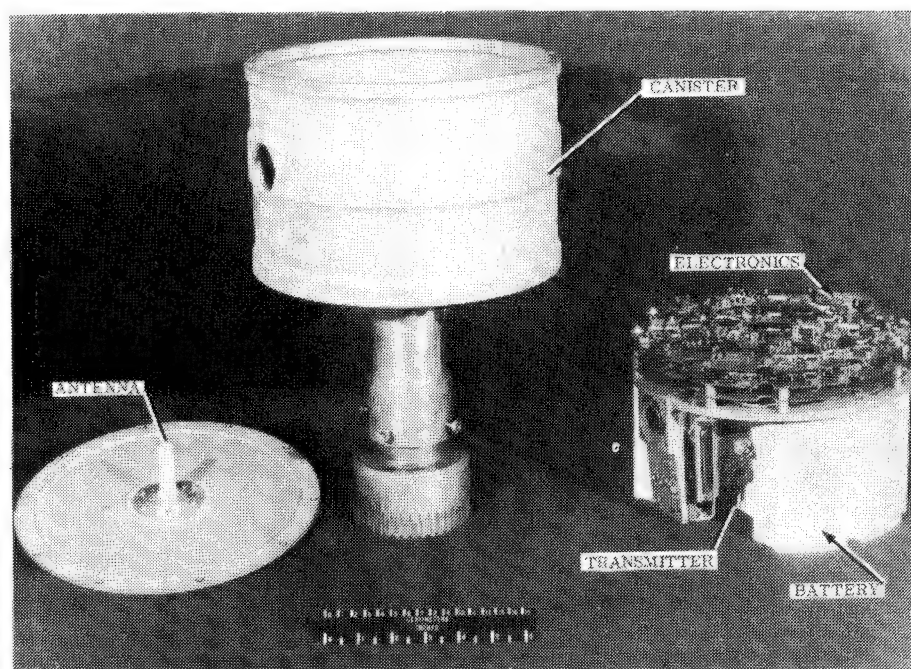


FIGURE 28. Special Rotor Blade Instrumentation system (SRBI) cannister and system for AH-1G airfoil program.

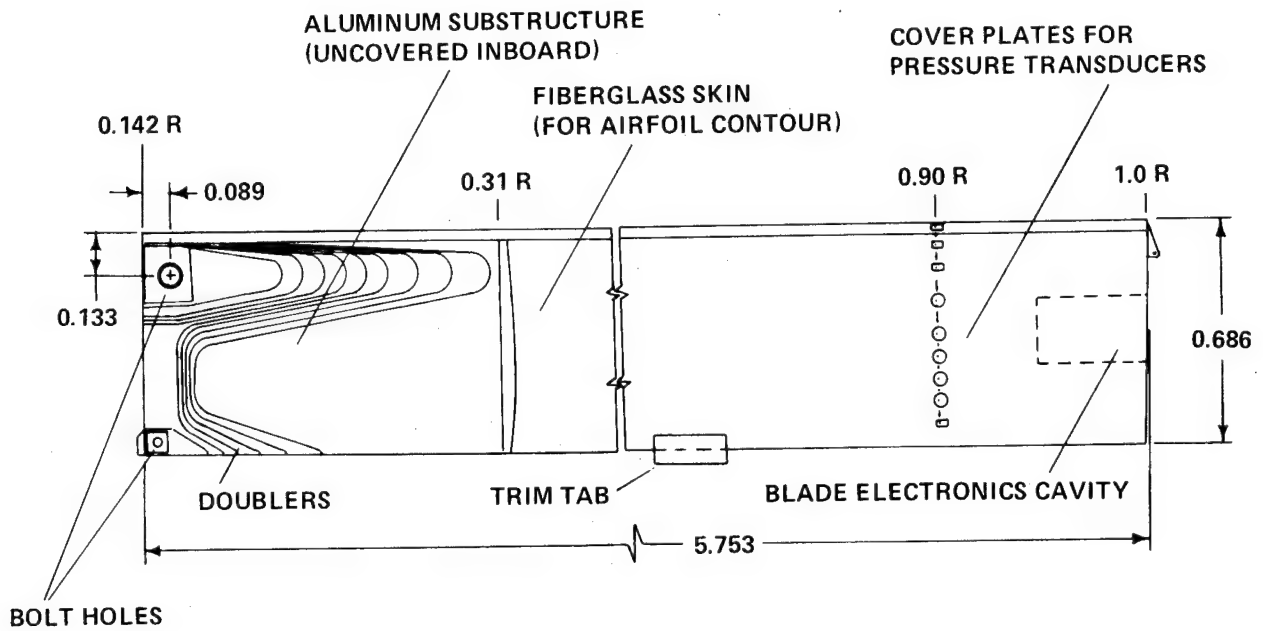


FIGURE 29. Planform of AH-1G main-rotor blade showing pressure transducer locations for airfoil tests. Dimensions in meters.

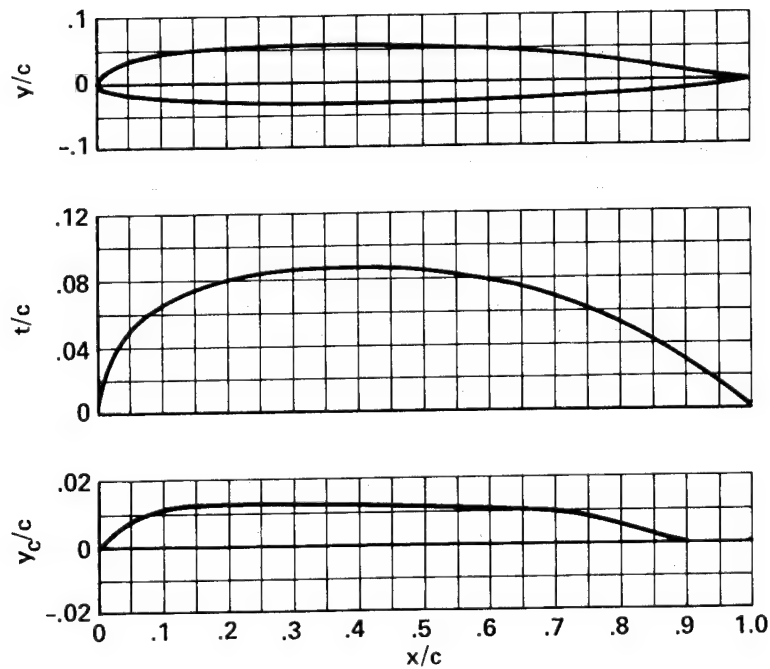


FIGURE 30. Geometric characteristics of NLR-1T airfoil.

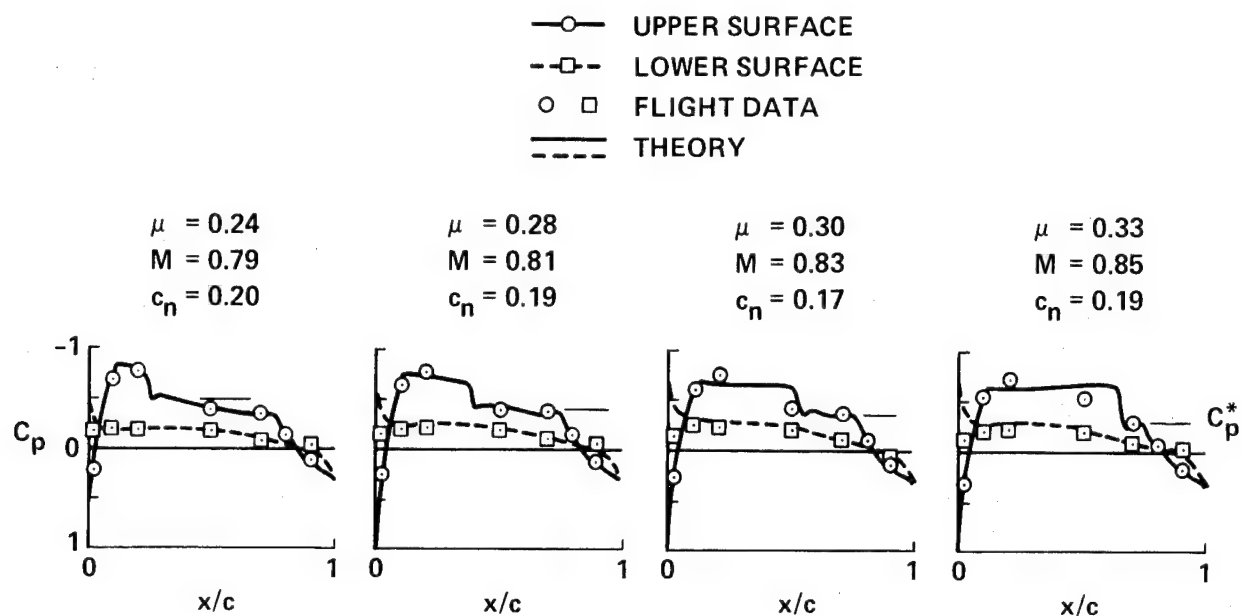


FIGURE 31. Comparison of flight data and theoretical blade-section pressure distribution for an azimuth of 70° ; $r/R=0.9$.

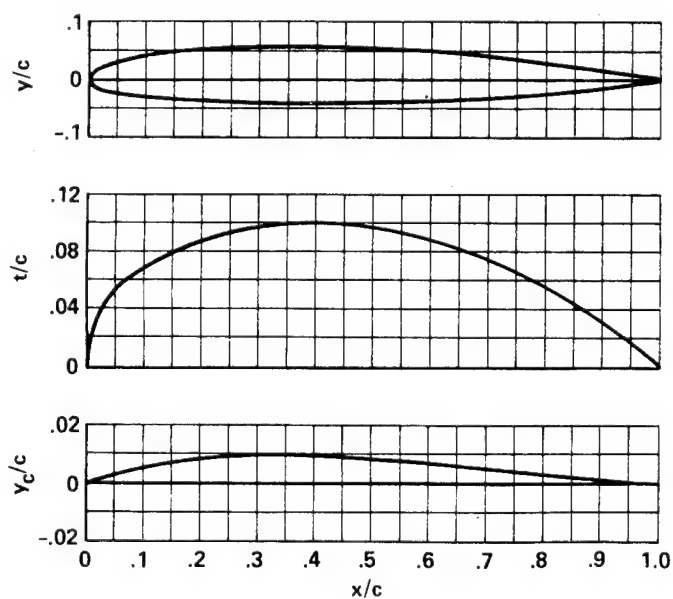


FIGURE 32. Geometric characteristics of 10-64C airfoil.

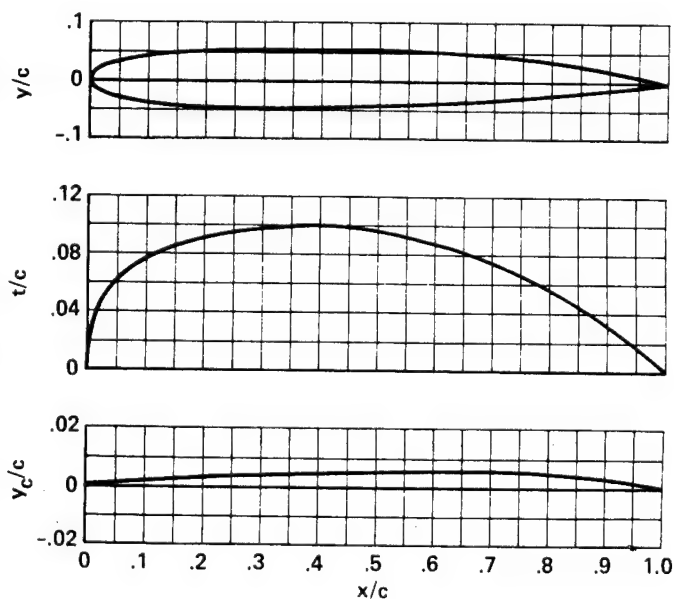


FIGURE 33. Geometric characteristics of RC-SC2 airfoil.

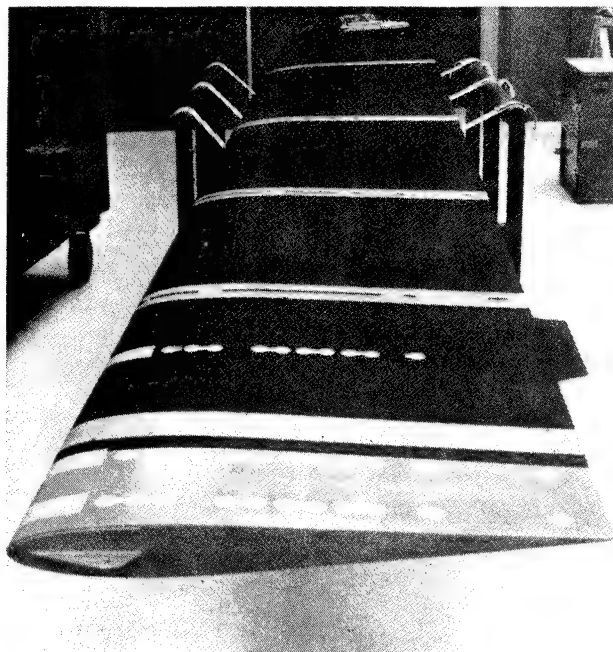


FIGURE 34. Instrumented blade for AH-1G Tip Aero Acoustic Test (TAAT) program.

GROSS WT = 8016 lb, SHIP MODEL AH-1G, $r/\text{RADIUS} = 0.99$
 CYCLE AVERAGE: TAAT DATA, ALL SENSORS EXCEPT BAD ONES

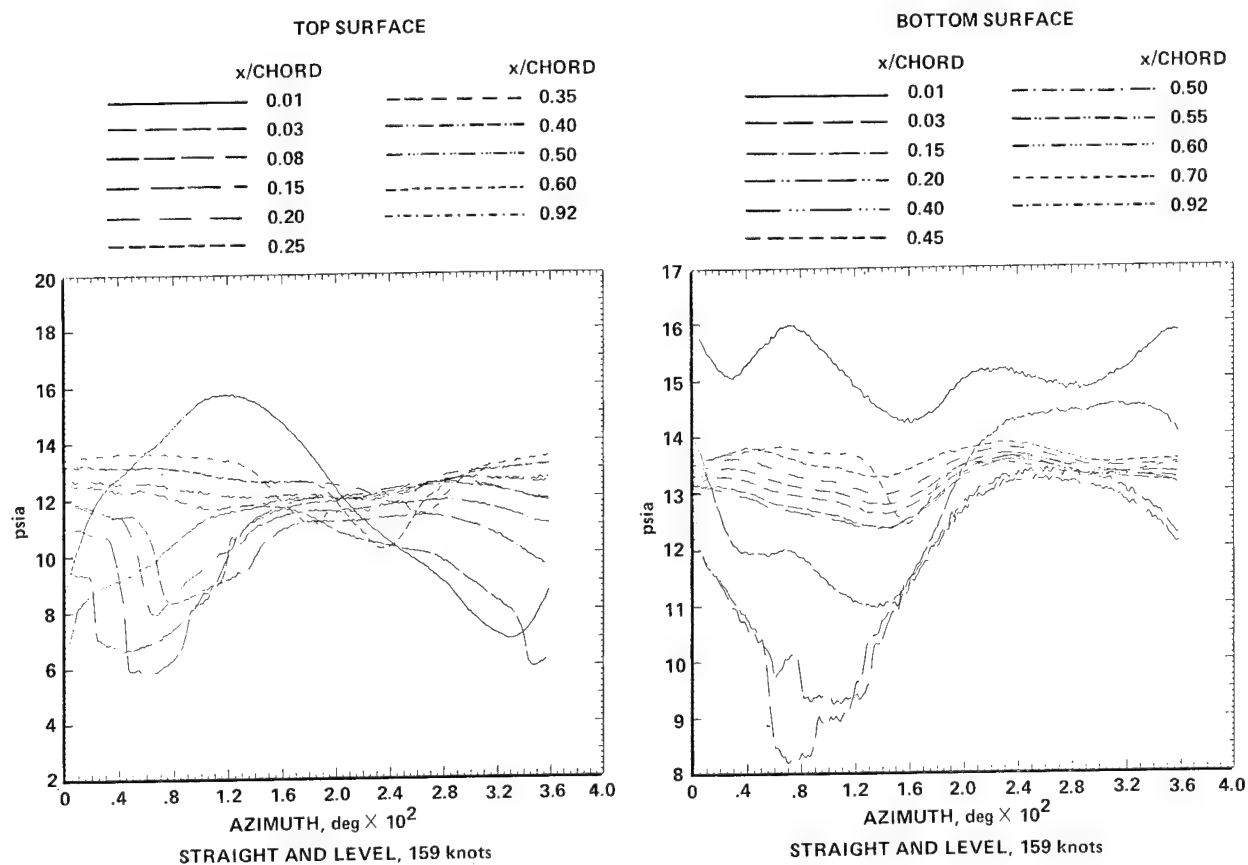


FIGURE 35. Blade pressure measurements (AH-1G) at 99% radius and 159 knots.

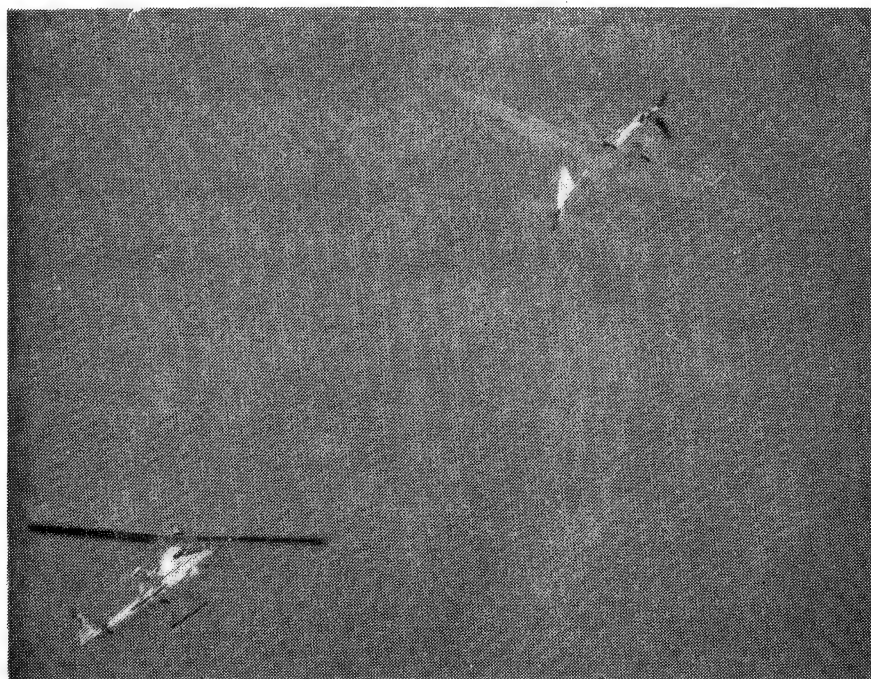


FIGURE 36. YO-3A airborne acoustic platform aircraft in test formation with AH-1G "White Cobra" during TAAT program.

LEVEL FLIGHT AT 158 knots
 $C_{T/O} = 0.069$, GROSS WT = 8016 lb, MODEL AH-1G
 MACH NO. = 0.701

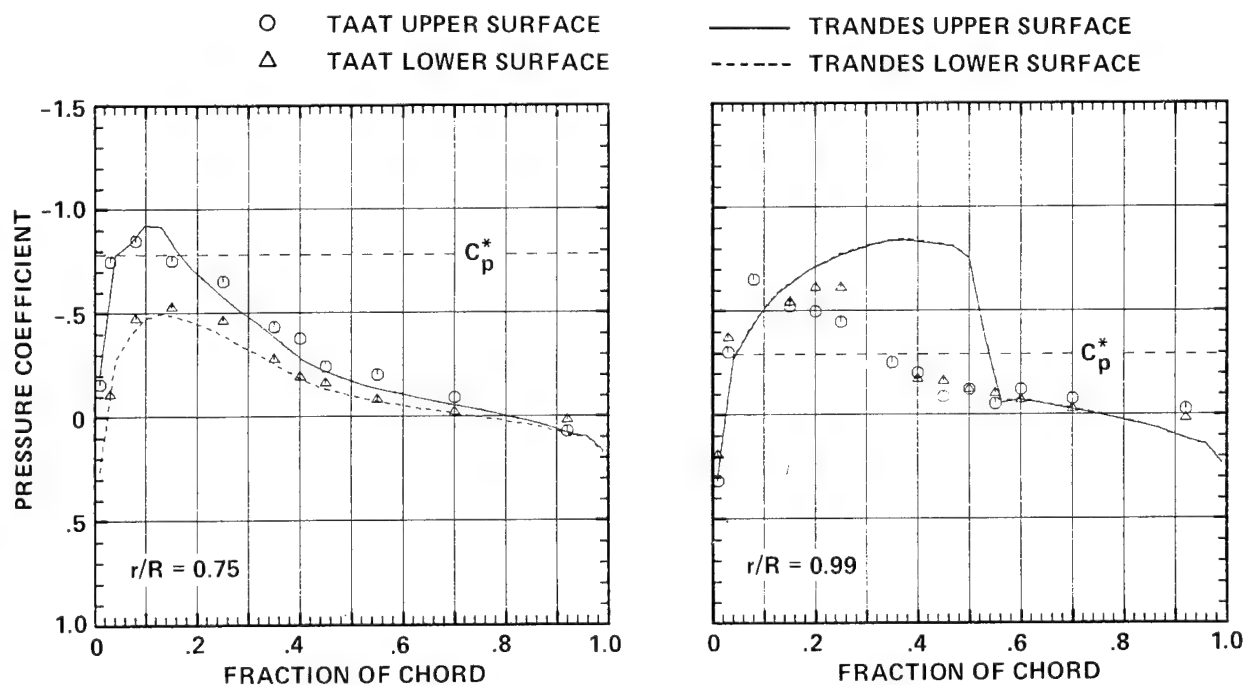


FIGURE 37. Comparison of chordwise pressure distributions for an azimuth angle of 120° and radii of 75% and 99% for AH-1G TAAT program.



FIGURE 38. RSRA helicopter configuration at Ames Moffett.



FIGURE 39. RSRA compound helicopter configuration at Ames-Moffett.

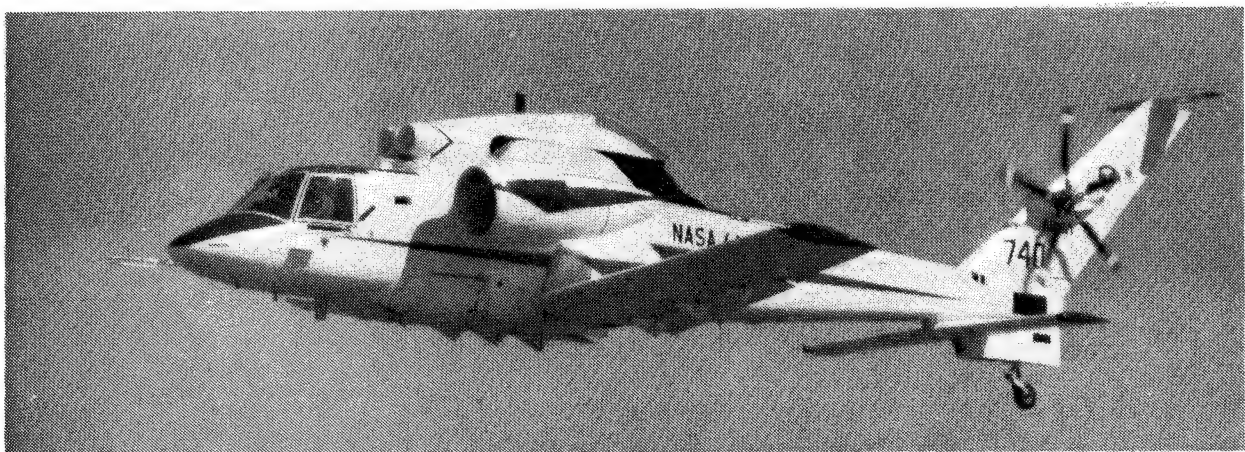


FIGURE 40. RSRA fixed wing configuration at Ames-Dryden.

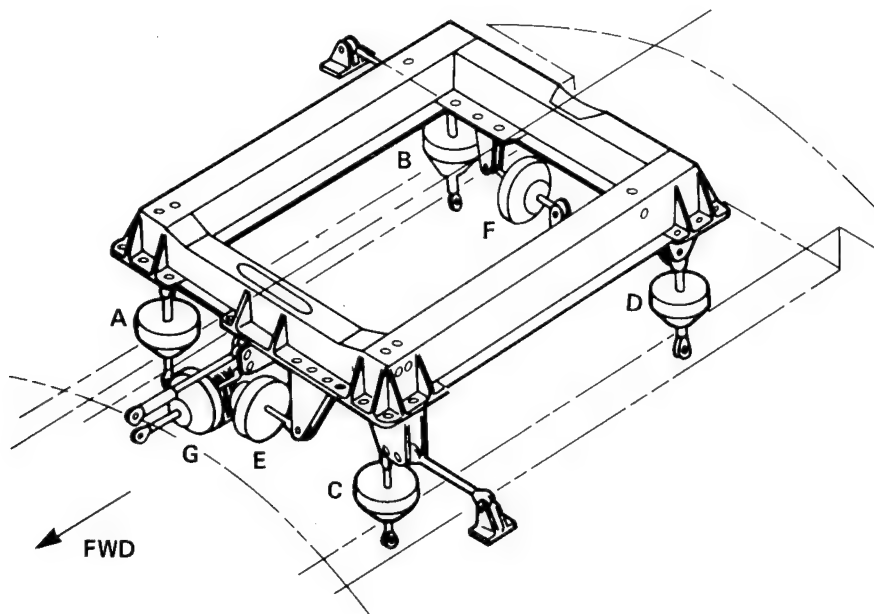


FIGURE 41. RSRA main rotor load measurement system configuration.

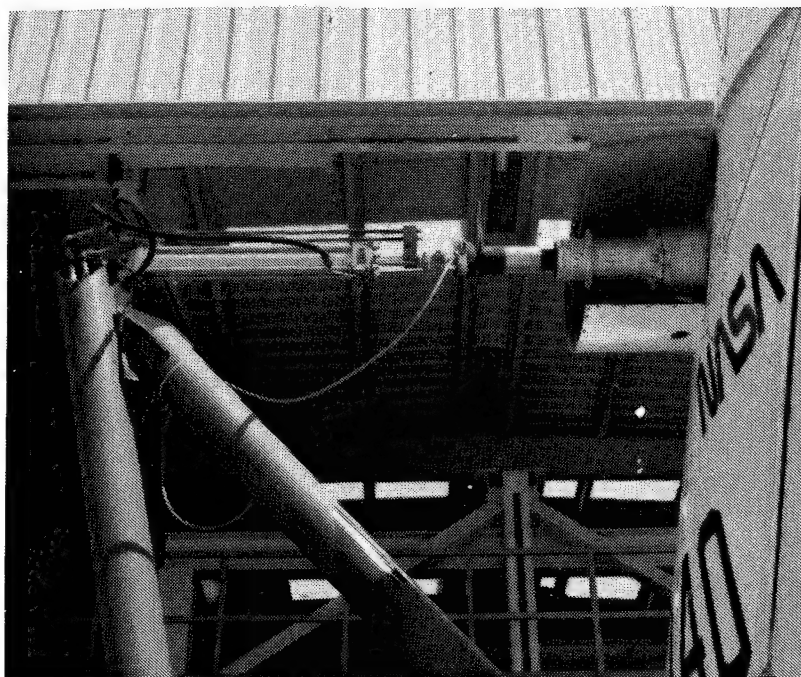


FIGURE 42. RSRA load measurement system calibration facility.

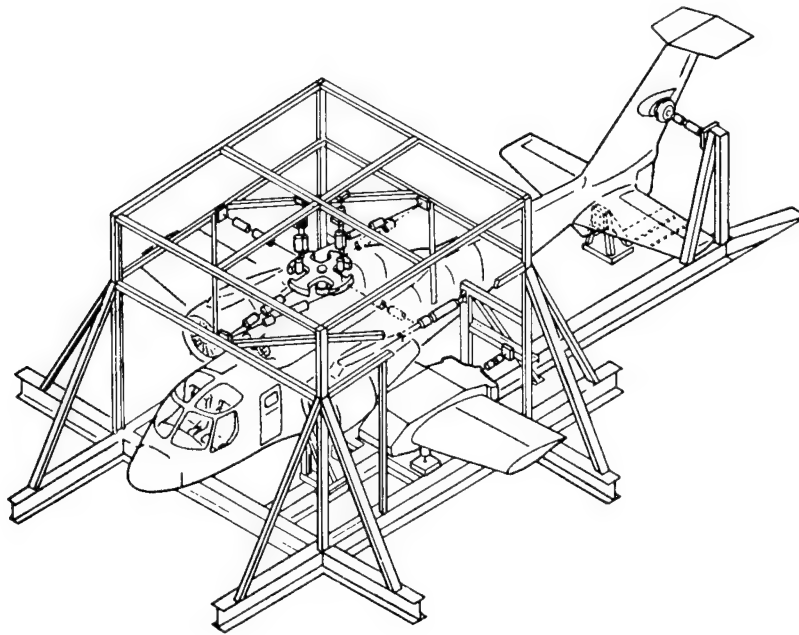


FIGURE 43. Sketch of RSRA load measurement system calibration fixture.

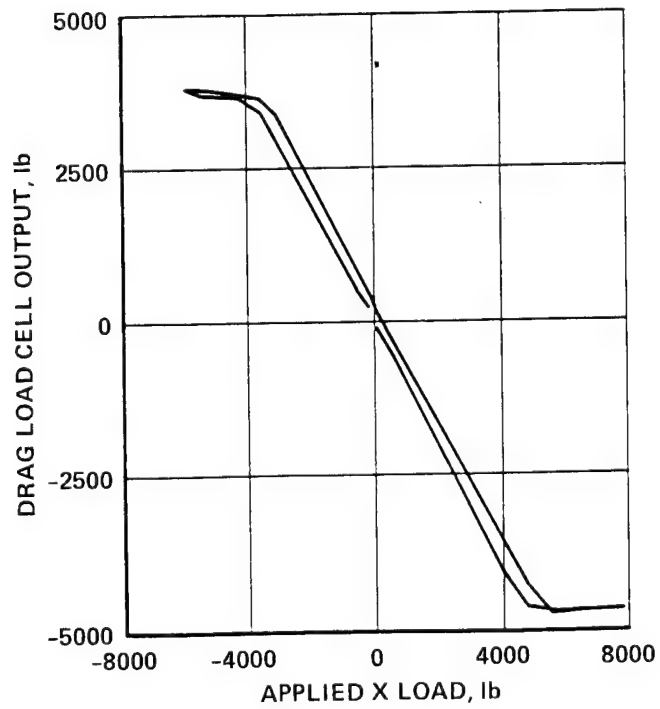


FIGURE 44. RSRA drag load cell output vs. applied longitudinal calibration load illustrating hysteresis.

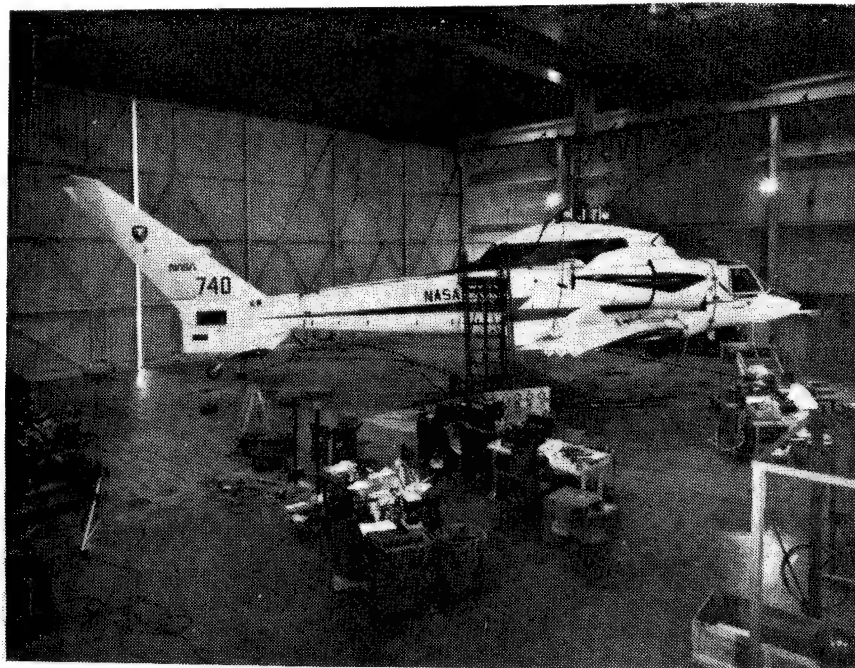


FIGURE 45. RSRA shake test setup.

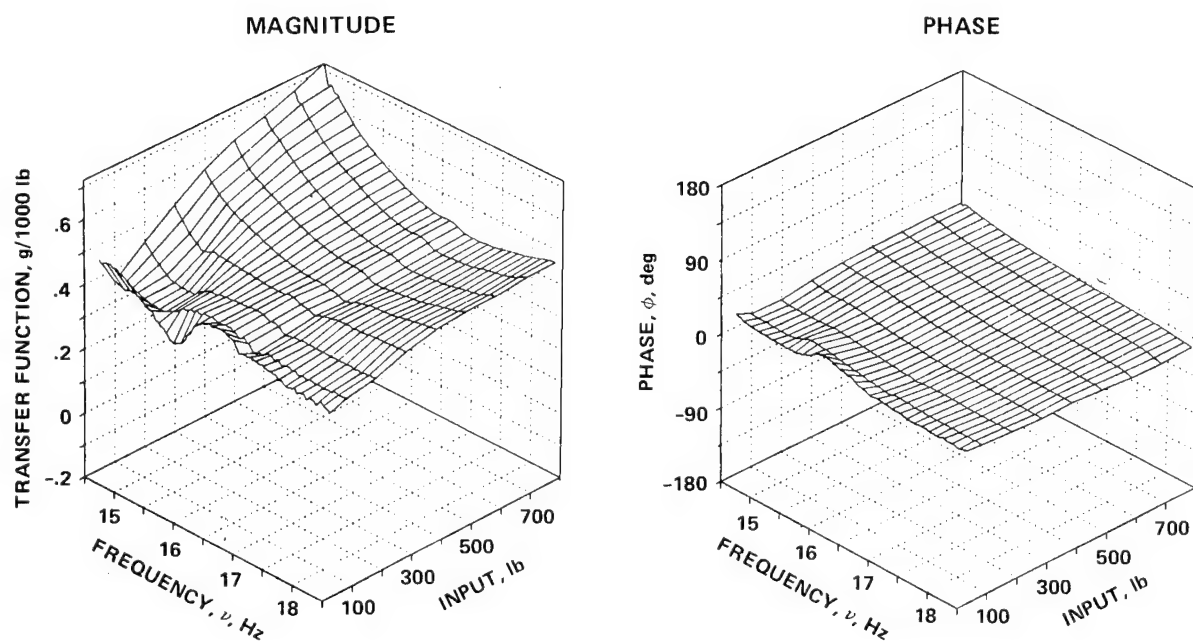


FIGURE 46. Calculated transfer functions for RSRA shake test illustrating non-linearity with force and frequency.

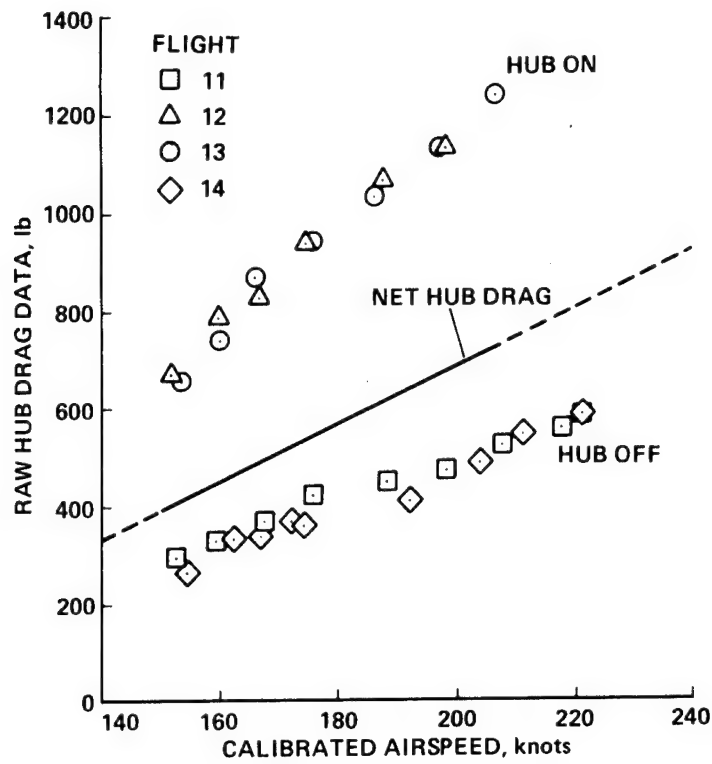


FIGURE 47. Inflight measured hub drag of RSRA versus airspeed.

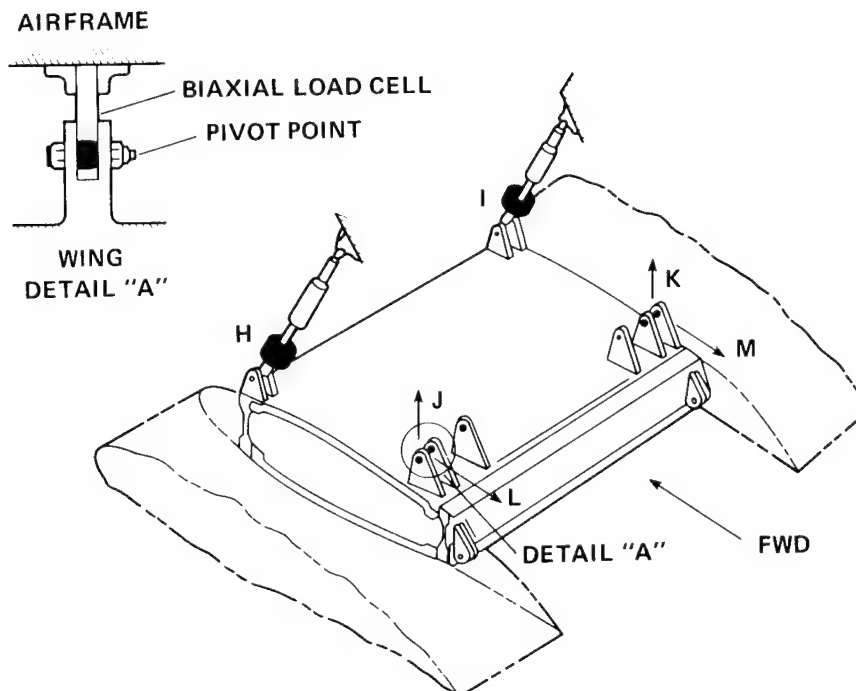


FIGURE 48. RSRA wing flight load measurement system configuration.

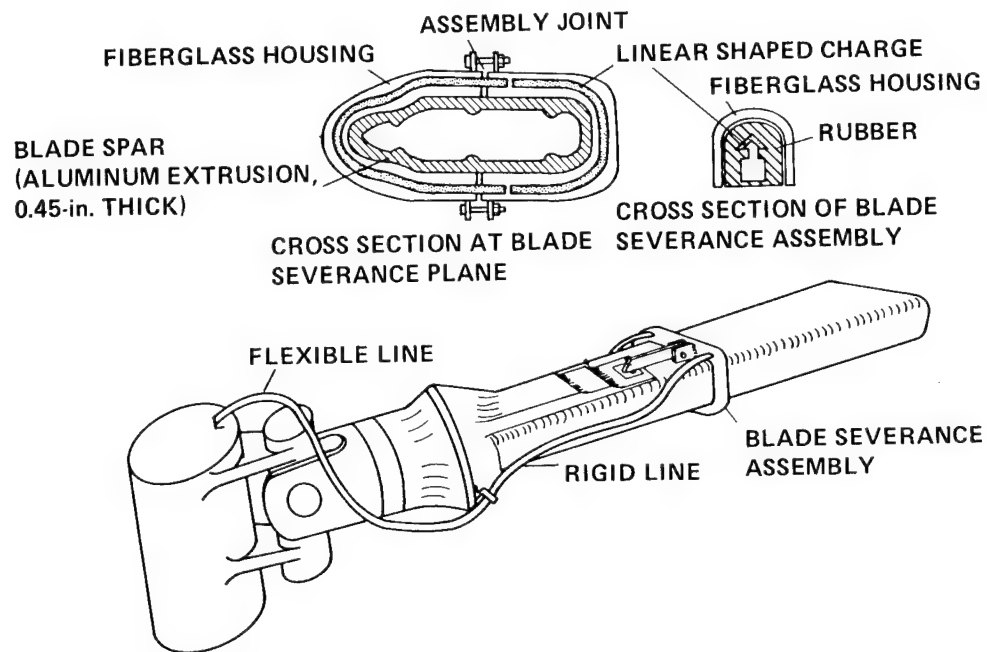


FIGURE 49. RSRA blade severance assembly.

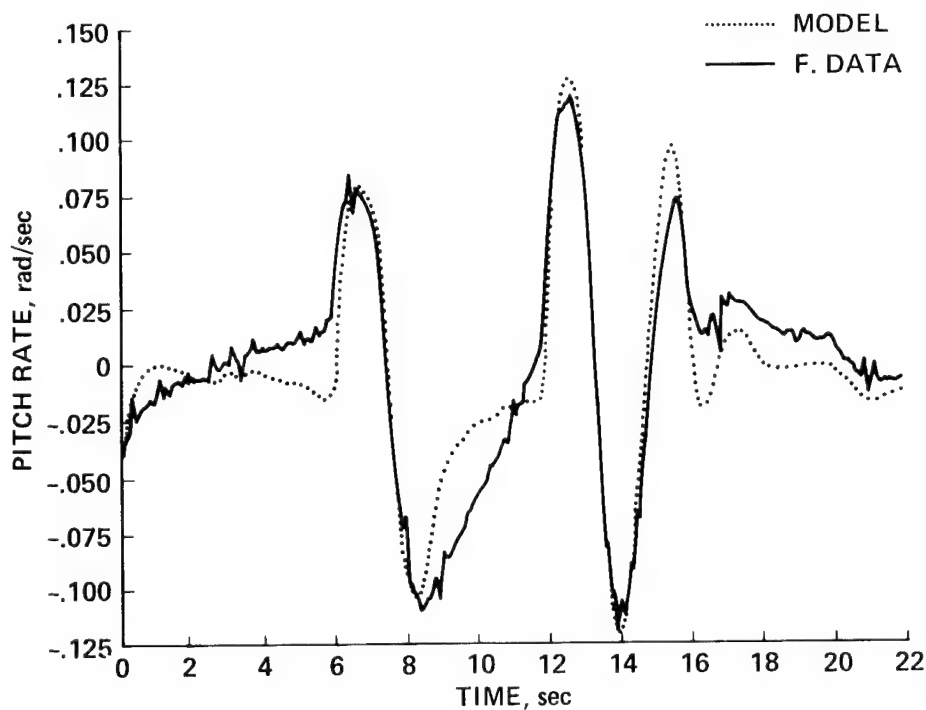


FIGURE 50. RSRA fixed wing flight data versus linear model (obtained from flight data) response for pitch rate.



FIGURE 51. UH-60, modern Army helicopter, at AEFA for NASA/Army comprehensive flight research.

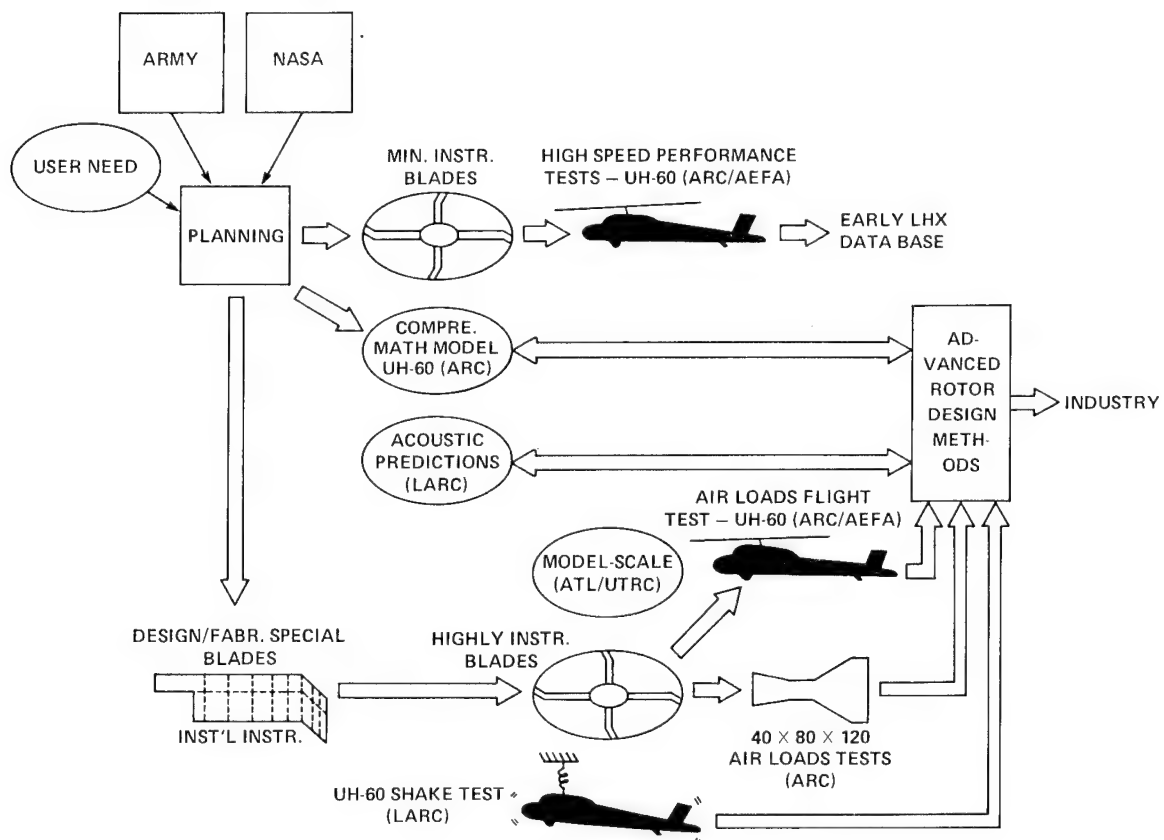


FIGURE 52. NASA/Army UH-60 comprehensive research program.

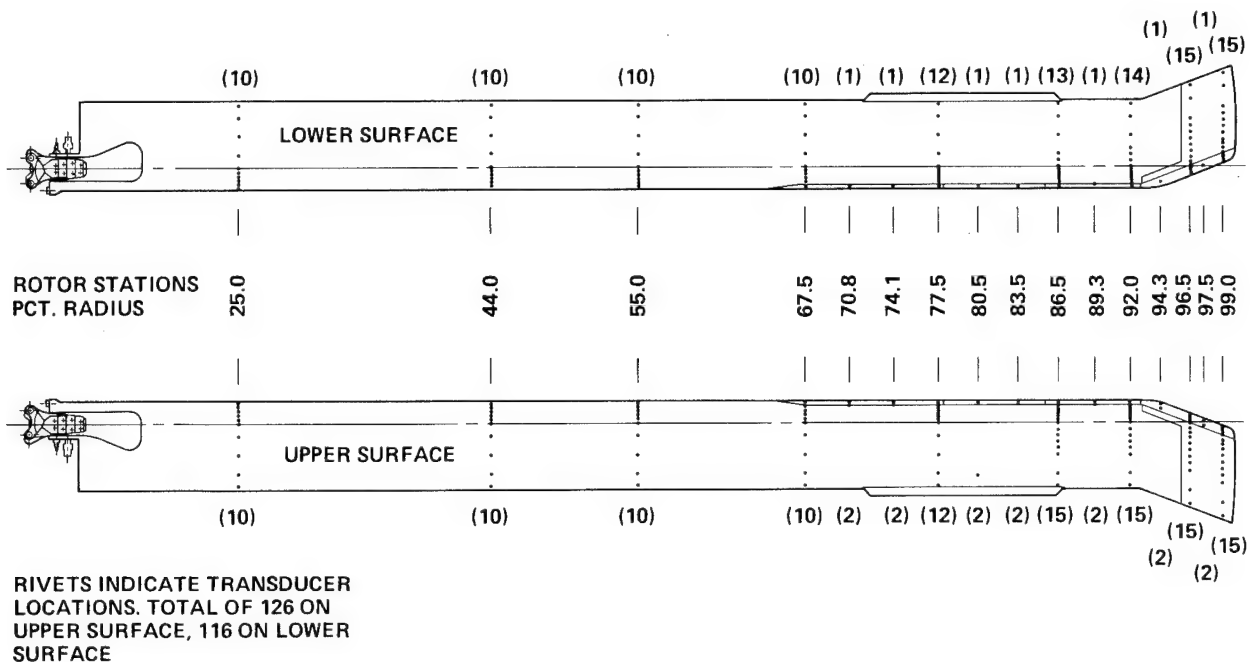


FIGURE 53. Pressure instrumented blade layout for UH-60 rotor research program.

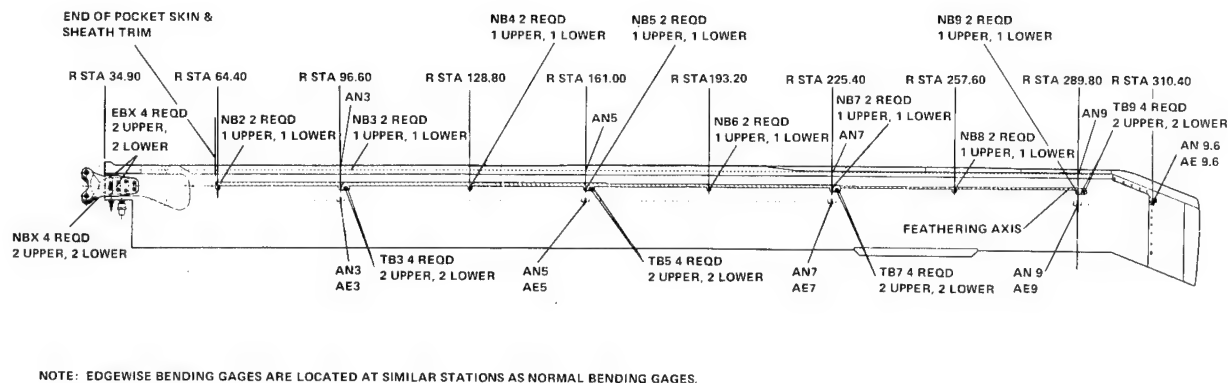


FIGURE 54. Strain gage and accelerometer instrumented blade for UH-60 program.

INDUSTRY

Session Chairman:

David S. Jenney, AHS

INDUSTRY SESSION

SUMMARY

This session included presentations by Bell Helicopter, Boeing Vertol, Sikorsky Aircraft and McDonnell Douglas Helicopter Company of research and development conducted under their IR&D programs. Each company selected its own topics for emphasis. While there are many other companies in the industry doing rotorcraft-related IR&D, the limited time of this one session permitted only highlights from the four largest U.S. manufacturers.

For Bell, Jim Harse summarized their advanced rotor program leading to the successful bearingless Model 680 experimental rotor system. A 680-type rotor is now planned for the Marine AH-1W. Jing Yen presented Bell's methodology development including a new family of airfoils and correlation of several aerodynamic and dynamic methods. Then Rod Taylor showed advanced concepts of tilt rotors and tilt-fold rotors. He showed that Bell and Boeing Vertol are building a 525 lb tilt rotor RPV which is expected to fly this fall.

For Boeing Vertol, John Shaw led off with a survey of R&D progress in several areas. These include Model 360 scale model rotor testing in the DNW (Dutch) wind tunnel, successful 3D panel code predictions of fuselage pressure distributions, wind tunnel tests of closed-loop HHC on a CH-47D model rotor and the use of an Expert System to assist in rotor track and balance flights as implemented on the CH-47D. Leo Dadone then followed with a review of ten years of high speed rotor research. A key milestone in that development was definition of the Model 360 rotor (airfoil, tip taper, etc.) in 1982. A model of that rotor was tested at BV in 1985 and at DNW in 1986. Meanwhile, studies of H-34 blade loads data led to a better understanding of the source of rotor vibrations and of the importance of the near wake. These fundamentals are being incorporated in new low-vibration rotor designs. Finally, Bob Weisner presented the status of the Model 360 aircraft program. Many of the composite parts that have been built were shown including rotor head, shafting, fuselage and cockpit components. Whirl test of the rotor was recently completed.

The Sikorsky program was presented in two parts. Bill McClure presented two major avionics integration efforts, the SHADOW advanced cockpit test program and the RSRA/X-Wing Vehicle Management System. The SHADOW has flown a variety of single pilot controller configurations with a variety of vehicle control laws. At present the 4-axis right hand controller looks very feasible for normal flight, with the ability to take over collective control with the other hand in high workload situations. The RSRA/X-Wing controls, through the quad-redundant flight control computers, not only the rotor but also airplane surfaces, the compressor, rotor braking and locking and higher harmonic inputs for vibration control. The system architecture and verification process were described. Jim Satterwhite presented air vehicle R&D on HHC and on advanced rotors. The S-76 was flown to 150 Kn with open-loop HHC to obtain extensive, good quality design data. Rotor improvements through anhedral blade tips and through a new family airfoils was shown. Compared to the current production UH-60A rotor, both better hover and better high speed performance can now be expected with these developments. Al Haggerty presented a wide spectrum of McDonnell Douglas Helicopter IR&D programs. These included the NOTAR and the HHC experiments on the OH-6, and both model and flight test work on the bearingless "HARP" rotor. The HARP has now flown virtually the complete Model 500E flight envelope. In analytical work, coupled rotor/fuselage analyses are showing improved agreement with the AH1G data base. Optimization schemes are being applied to rotor design to produce a balance among conflicting requirements. Advanced cockpit work includes both single-pilot experiments in a modified Apache and the definition of an improved AH-64"B" crew station. The Apache will be tested in air-to-air experiments at Patuxent. In preparation, evasive maneuvers have been flown and an air-to-air mission analysis including an "intelligent adversary" was developed. Finally the new experimental facilities at MDHC were shown briefly.

Although three hours is not a lot of time for presentation of several hundred million dollars worth of IR&D, a great deal was presented in this session and it hopefully stimulates the audience to read the full written papers.

1279-1340

AN OVERVIEW OF KEY TECHNOLOGY THRUSTS AT BELL HELICOPTER TEXTRON

Jim Harse, Jing G. Yen, Rod Taylor

Bell Helicopter Textron Inc.
Fort Worth, Texas

This paper will provide insight into several key technologies at Bell. Specific topics include the results of on-going Independent Research and Development (IR&D) in advanced rotors, methodology development, and new configurations. Each subject area highlights some of the research activity now in progress, its supporting technology development, and the results to date.

The discussion on advanced rotors, in Part I, highlights developments on the composite, bearingless rotor, including the development and testing of full-scale flight hardware as well as some of the design support analyses and verification testing.

The discussion on methodology development, in Part II, concentrates on analytical development in aeromechanics, including correlation studies and design application. Specific emphasis is given to aerodynamic, dynamic, and handling qualities methodologies as they relate to advanced design requirements.

The final topic, new configurations, in Part III, presents the results of some advanced configuration studies, including a report on hardware development in progress.

PART I. ADVANCED ROTORS

The continuing IR&D efforts at Bell cover the entire spectrum of technologies applicable to rotary wing aircraft. From survivability to flight simulation, from advanced material applications to tailored airfoils, achievements in IR&D have made it possible to incorporate enhanced safety, performance, and mission capabilities into future designs, along with lower cost of ownership. This has put Bell in a good position to meet the challenges of the LHX and V-22 programs and remain competitive in the helicopter marketplace. Many contracted R&D programs have been initiated to further explore and refine technologies that have come from Bell IR&D programs.

Since the late 1970's, Bell has concentrated on the use of composite materials in the development of advanced rotor hubs and blades. The evolution of rotor blades from metal to composite materials was straightforward and preceded the development of composite hubs. Composite materials not only made rotor blades corrosion resistant, but the unidirectional properties of these composites resulted in fail-safe structures with unlimited life.

The use of composite materials in rotor blades also provided greater opportunities for performance and vibration optimization through aerodynamic and dynamic tailoring. Bell's contributions to the development of composite rotor blades include the following:

- (1) First FAA certification in 1978
- (2) Three designs currently in production (all IR&D)
- (3) Four prototype designs currently undergoing extensive flight testing (3 IR&D)
- (4) Two designs under development and now in the fabrication phase (1 IR&D)

ROTOR HUBS

The application of composite materials to hubs was a much more challenging task because of the design requirements for functionality as well as structural design soundness. The thrust of Bell's efforts was to replace the flap, lag, pitch-change, and blade retention mechanisms with composite structures. The key was to fully exploit the anisotropic properties of composite materials in unique designs, not merely replace the metallic structural hub components that have isotropic loading and support the usual bearings and hinges of conventional hub designs.

The first step was to develop a single structure made of fiberglass/epoxy that could carry all of the flight loads and support the blade retention/pitch change bearings. This structure is referred to as the "yoke" at Bell. In this concept, the yoke also forms a flapping flexure that eliminates the flapping degree-of-freedom from the pitch change bearings, thus making the bearings, bearing support structure of the yoke, and the lead-lag damping mechanism more compact. The resulting hub design is fail-safe because of the composite materials out of which it is made, and maintenance free because of the elastomeric materials in the pitch change bearings and lead-lag dampers.

A composite yoke designed to replace the titanium yoke on the Bell Model 412 rotor hub is now undergoing qualification testing (fig. 1-1). It will be the first hub component to receive on-condition FAA certification. The rotor hubs for the Bell Model OH-58D Army Helicopter Improvement Program (AHIP), which is in production, and the Bell Canada Model 400 also have composite yokes (fig. 1-2). For rotors with pitch change bearings, these designs are structurally efficient because the primary loads are carried by the unidirectional fibers, as in the composite blade designs.

BEARINGLESS HUBS

The next step in rotor hub development at Bell was to eliminate the blade retention/pitch change bearings. The simplicity and weight savings of such a design would be significant because the bulky and heavy bearing housings would be gone and the bearing support structure (with its isotropic loading) would be replaced with an alternate yoke geometry loaded in a more efficient manner. To evaluate the benefits and assess the risks of a bearingless main rotor, Bell initiated the Model 680 program.

After a series of model tests, design layout studies, and dynamic analyses, Bell designed the rotor system shown in figure 1-3. It consists of a one-piece yoke with four arms extending radially from the center area to the blade roots. The shear-restraint pivots are mounted at the inboard end of the yoke and damper sets connect the shear restraints to pitch change cuffs. The outboard end of the cuff connects to the yoke and the blade root. The blades are modified Model 412 blades with nearly 5 feet removed from the inboard end and metallic plates bonded to the upper and lower surfaces to provide the hub attachment. These blade modifications resulted in a bulky and aerodynamically "dirty" yoke/cuff/blade attachment area, but it served the purpose for the hub concept evaluation.

The component of interest is the yoke. Each arm is able to accommodate a pitch change in excess of 35° in each direction. At the same time, the yoke carries the blade centrifugal and lifting forces, transmits engine torque, and allows flapping and lead-lag motions. These functions of the yoke are obtained by discrete tailoring of the dynamic and structural cross-section properties. This is realized by a series of filament-wound fiberglass/epoxy belts, shown in figure 1-4. These belts are interleaved in a closed-cavity tool, shown in figure 1-5, that molds the yokes. Additional off-axis plies of fiberglass/epoxy tape are added in the mast attachment area and taper out as necessary to support the shear-restraint pivot and shape the flapping portion of the yoke.

YOKE STRUCTURAL TECHNOLOGY

Full-scale fatigue tests of complete rotor hub assemblies were conducted to evaluate the structural integrity of the design and to support the experimental flight tests. A hub assembly was subjected to about 275 percent of the maximum level flight oscillatory loads. Delaminations beginning at the corners of adjacent arms of the yoke were induced early during the testing, but the test was continued at that load level for a sufficient number of cycles to demonstrate the fail-safe features of the design. At the conclusion of the test, no significant loss in stiffness could be detected. The original Model 680 yoke that was flight tested was flown throughout the entire flight envelope and at high-g maneuvers without any problems.

To better understand and improve the delamination characteristics of the yoke, an extensive analysis and a series of coupon and component tests were performed. A finite element model of the corner area was made (fig. 1-6). The analysis showed that the large corner radius, which would be beneficial in a metal structure, is actually detrimental in a composite structure. This is because of the large number of ply terminations required to form the corner. The analysis was expanded to the flapping flexure portion of the yoke to explore opportunities to improve the delamination strength in this area (fig. 1-7). The analysis also considered the consequences of manufacturing improvements such as fewer and thicker belts of the unidirectional rovings and fewer off-axis plies of tape. The results of this analytical study and design support coupon tests showed that better management of Poisson's ratio mismatch by special ply sequencing between the belts would significantly improve the interlaminar stresses and the delamination strength. It was also found that a slight resculpturing of the outer flapping flexure contour would also reduce the overall surface fiber stresses. The improvements were incorporated in a second-generation Model 680 yoke, shown in figure 1-8, that was also evaluated in the fatigue test machine. The delamination problem in the corners was eliminated and the test loads were periodically elevated until the next delamination mode was found. This occurred at an outboard location in the flapping flexure of the yoke. This new delamination mode is also fail-safe and provides approximately 70 percent of additional load ability over the original design, which is well above the maximum flight loads.

→ An analysis performed on the area of the delamination showed that it was initiated by an interlaminar stress concentration at a free edge. Bell has conducted research on this problem and has developed an innovative adhesive inner-layer concept for delamination arrestment. This concept is shown in figure 1-9. The key point is to use a high-strain ductile adhesive layer at the critical interfaces at the free edge. This changes the initial delamination mode from a brittle fracture to a more ductile fracture. Proper positioning of the adhesive layers results in a reduced interlaminar normal stress distribution through the thickness of a given laminate under a given load, as shown in figure 1-10. Numerous coupon tests have verified this approach. Figure 1-11 shows that the static delamination strength of coupon test specimens with adhesive layers is nearly double that of specimens without adhesive layers. Dynamic improvements have also been found in fatigue test coupons. An interesting aspect of this technology is that the adhesive layer acts as a buffer between critical plies. This buffer tends to delay the propagation of transverse cracks to adjacent plies, which would then develop into a delamination between those plies. This can be seen in the photomicrograph of the edge of a coupon in figure 1-12. This concept has been applied to the yoke and will be tested in the near future. The analysis shows that an additional 20 percent of load ability can be realized for this design.

MODEL 680 FLIGHT TEST RESULTS

In May 1982 the first flight of the Model 680 rotor system on a Bell Model 222 aircraft was made (fig. 1-13). Some of its accomplishments are listed below:

- (1) Nearly 600 flight-hours
- (2) Split "S" maneuvers with dives exceeding 210 knots
- (3) 2.8g to -0.1g maneuvers routinely performed
- (4) Demonstration rides for over 1000 people
- (5) No rotor limitations

In addition to successfully demonstrating the manufacturing, structural, and stability aspects, thus making it possible to realize the direct benefits of a bearingless rotor system, the Model 680 rotor system has also displayed excellent handling qualities and vibration characteristics.

The Model 680 was flown on the Model 222 helicopter without a stability augmentation system. The gust penetration and control response were excellent. There was no tendency for the nose to tuck under during a pushover or pitch up in turbulence, so there was no corrective action required by the pilot. During low-g maneuvers, there were no noticeable trim changes in lateral cyclic. Control coupling was in harmony throughout the flight regime. All of the indications are that this system could be FAA certified for single pilot IFR conditions without a stability augmentation system. These features are the result of the well-defined rotor kinematics, isolated rotor stability, and low-vibration aspects that the rotor system possesses.

The most noticeable and outstanding feature of the Model 680 rotor system is the very low vibration level throughout the cabin under all flight conditions, including extreme maneuvers. A summary of the cabin vibrations in all seats, all directions, all gross weights, all centers-of-gravity, and all altitudes of the Model 680 rotor with two LIVE units is presented in figure 1-14. The LIVE units lower the vibration levels primarily at transition where the vertical excitations are the largest. The hundreds of data points represented in this figure demonstrate the consistently good vibrations resulting from the rotor dynamics that have been experienced by hundreds of passengers.

These excellent dynamics represent the "nodalized rotor technology" at Bell. This technology concept goes beyond rotor natural frequency placement to nulling the potential hub shear and moment excitations from the rotor by tailoring the blade mode shapes. This patented concept has three key elements:

- (1) Low-mass, high-stiffness hub
- (2) Concentration of mass at an inboard blade location
(further inboard than that for conventional frequency placement)
- (3) Discrete blade stiffness

These ingredients are all found in the bearingless rotor concept and exploited in the Model 680 rotor design. A series of model tests has also verified this technology.

The outer contour of the pitch change cuffs serves as a fairing that reduces the drag coefficient for most of the hub. Even though the bearingless hub has a greater radial extent, the parasitic drag was found to be less than that of conventional rotor hubs. The radial location of the hub/blade attachment area caused a profile power loss that was observed in hover and at minimum power forward flight. Subsequent testing with temporary fairings showed that the profile power loss could be recovered. Wind tunnel hub drag tests have also shown that the parasitic drag could be further reduced with refinements in the cuff geometry.

ADVANCED LIGHT ROTOR

The use of the modified Model 412 blades meant that the aerodynamics were not optimum because of the "dirtiness" of the hub/blade attachment area and the radial distribution of airfoils that had been optimized for the Model 412 radial locations and rotational speeds. However, with the successful demonstration of all the other features of the Model 680 rotor system, the time had come to integrate advanced aerodynamic technology with new rotor blades optimized for application with the rotor hub. Bell also took this opportunity to employ an innovative plastic tooling concept to minimize the tooling costs and lead time. These new rotor blades for the Model 680 hub are called the Advanced Light Rotor (ALR).

Four unique airfoils with different thicknesses were developed for the ALR blades. These airfoils were tailored for their specific aerodynamic environments along the rotor blade span and optimized for best lift, drag, drag divergence Mach number, pitching moment, and lift-to-drag ratio where it is most advantageous. Also, the pitch change cuffs were made integral with the blades. The integral cuff design reduces the weight and size of the hub-to-blade interface and provides a smooth transition from the elliptical cross section of the inboard cuff to the first tailored airfoil. The ALR blades also incorporate the nodalized rotor technology of mass and stiffness tailoring. The tooling is shown in figure 1-15. The ALR blades with the Model 680 rotor hub installed on the test aircraft are shown in figure 1-16. At this writing, the flight testing has just begun. The aeromechanical stability has been verified and the vibrations

are as good as the original Model 680 rotor system. Envelope expansion and performance flights are underway.

ADVANCED ROTOR TECHNOLOGY IMPLEMENTATION

The next application of Bell's advanced rotor technology is a bearingless main rotor for helicopters in the 14,000- to 18,000-pound class. This larger rotor system employs the basic Model 680 concept with enhancements and considerations applicable to a rotor system of this size. The new rotor system is shown in figure 1-17. One major difference is that there are two yokes, one for each opposing pair of blades, to minimize tooling costs and size. Another major difference is that there are separate yoke-to-cuff and cuff-to-blade attachment joints to provide manual fold ability, reduce the thickness of the cuff and blade root, and simplify blade root construction. Removable fairings for this area were designed to provide a smooth surface over the cuff and blade cutouts, which are necessary for folding clearances. The advanced structural concepts, hub dynamics, tailored airfoils, and nodalized rotor technologies are all incorporated in the large bearingless rotor design. This rotor system will be first demonstrated on an AH-1W helicopter in late 1987 (fig. 1-18).

The advanced bearingless rotor will expand the mission potential of the AH-1W helicopter. Direct benefits in reliability, maintainability, vibration, and handling qualities will provide lower cost of ownership, reduced crew fatigue, and improved performance of avionics and armament systems. The composite hub and blades were designed to have greatly improved ballistic survivability. The positive and negative g maneuver envelopes will be expanded with the rigid rotor. The aerodynamic improvements will provide over 1000 pounds more payload, 20 knots more speed, greater vertical rate of climb, and increased hover altitude. All of these features will not only enable the AH-1W to better perform its current missions, they will also enable the helicopter to execute multimission roles and dedicated air-to-air combat with alternate fire control and weapons systems.

Other spinoffs from Bell's advanced rotor technology include four U.S. government contracts to further explore various aspects, the foundation for the LHX rotor system, and confidence to apply a bearingless main rotor system to the next generation of Bell's helicopter products.

PART II. METHODOLOGY DEVELOPMENT

The importance and complexity of analytical development and design application in the field of aeromechanics have been widely recognized in the rotorcraft community. New developments in the methodologies of aerodynamic performance, airloads, rotor vibratory loads, aeromechanical stability, aircraft vibration,

and handling qualities, among others, are presented each year at the AHS National Forum and specialists' meetings. The following discussion concentrates on some of the recent accomplishments at Bell in the field of aeromechanics methodology. Specific emphasis is given to analytical tool development, correlation studies, and design applications as they relate to advanced design requirements.

AERODYNAMICS

Airfoil Design

Bell uses a system called Aerodynamic Design and Analysis Methodology, or ADAM, in the design of its advanced airfoils. The ADAM system's inverse design capability is used to develop airfoils with aerodynamic properties that will satisfy particular performance requirements. The V-22 airfoils were designed using this system. Figure 2-1 shows the maximum lift coefficient at Mach 0.4 and the drag divergence Mach number at a lift coefficient of zero for several Bell airfoil sections, including those for the V-22. For comparison purposes, the NACA 64 series of airfoils used in the XV-15 rotor are also shown.

The advanced airfoils developed at Bell in recent years have met their design objectives. The V-22 tilt rotor airfoil designs are used as an example. The V-22 aerodynamic design objectives and priorities are shown in figure 2-2. In comparison with the XV-15, the following aerodynamic goals were to be achieved:

- (1) Improved maneuverability in helicopter mode at 40 knots.
- (2) The same low-drag characteristics at 300 KTAS at 20,000 feet, cruise, as in the XV-15.
- (3) No compressible divergence drag up to 350 KTAS at 20,000 feet, cruise.
- (4) High lift/drag ratio for hover efficiency.

The basic airfoil design requirements called for a set of four airfoils, one each at the 0.25, 0.5, 0.75, and 1.0 blade radial stations (r/R). Constraints on the thickness and maximum pitching moment were also imposed on the design. These are shown in figure 2-2.

As an example of the results of the ADAM system's inverse design capability, the 12-percent thick V-22 airfoil (XN12 in figure 2-1) will be evaluated here. After an extensive theoretical evaluation of the new section, wind tunnel tests of the airfoil were conducted in the Boeing Supersonic Wind Tunnel (BSWT) facility. The measured data shown in figure 2-3 were obtained from the BSWT. Also shown in the figure are the design objectives. The data indicate that all goals were met except the cruise drag coefficient C_d at $C_l = 0.2$ and $M = 0.65$.

The XN12 airfoil was also previously tested in the United Technology Research Center (UTRC) wind tunnel for Advanced Technology Blade (ATB) evaluation. Comparisons of the XN12 data from the UTRC tunnel with those from the BSWT indicate that the UTRC results are slightly lower in $C_{\ell_{\max}}$ (e.g., $\Delta C_{\ell} = 0.1$ at $M = 0.4$), C_d , C_{m_0} , and L/D . For the XN-12 at $C_{\ell} = 0.2$ and $M = 0.65$, a drag coefficient of 0.00535 was measured in the UTRC tunnel (shown in figure 2-3). Since the design goal of $C_d = 0.006$ falls between the data from the two wind tunnels, it is believed that the designed XN-12 airfoil satisfies the low-drag requirement and closely meets the other design objectives.

Transonic Blade Design

Three-dimensional transonic flow codes are being developed in the technical community that determine the potential flow pressure distribution about arbitrary blade configurations. However, in order to determine the torque difference between two different blades, an evaluation of the viscous effects must be included. An approach to this problem being pursued at Bell is to couple a boundary layer routine with the potential flow routines. This produces a drag and torque distribution over the blade due to viscous effects. In addition, the displaced blade surface can be evaluated in the potential flow code to determine those changes in the flow field solution due to boundary layer displacement. This method can be used to develop blade tip shapes that minimize the advancing blade drag and eliminate shock-induced separation.

Figure 2-4 shows, for comparison, the measured pressure distribution on the OLS blade, a theoretical two-dimensional airfoil result, a theoretical three-dimensional potential flow solution, and the theoretical three-dimensional flow results after a boundary layer was added. Data show that the two-dimensional results greatly overpredict the shock strength. The three-dimensional potential flow code calculates a much more realistic pressure distribution for this case. However, the drag calculated from this analysis is very low, since the forward displaced sonic zone produces a leading edge suction. This type of result from the potential flow codes leads to erroneous conclusions when comparing the torque calculations of different tip shapes. The pressure distribution with the displaced boundary layer surface is only slightly changed from the potential solution. However, the drag from this analysis, including the effect of additional boundary layer growth due to the forward displaced shock wave, is more useful than the pressure distribution in the evaluation of an advancing blade performance at high tip Mach numbers.

Rotor Lateral Flapping at Low Advance Ratio

The significance of fore and aft nonuniformity in rotor inflow to rotor lateral flapping at low advance ratio was identified by

Harris (ref. 1). Work presented in references 2 and 3 suggest that at low advance ratios, it is necessary to use a free wake geometry calculation to achieve a desired correlation in rotor lateral flapping. Reference 2 also states that the calculated values of the flapping motion are sensitive to details of the wake structure, especially the viscous core radius of the tip vortices.

A recent attempt in the correlation of rotor lateral flapping was conducted at Bell using a simplified nonuniform inflow representation in C81. The math model can be stated as

$$v_i = \frac{4}{3} \bar{v}_i \chi (1 + K \cos \psi) + \text{tip vortex effects}$$

where \bar{v}_i is the average value of the induced velocity across the disc as determined from momentum theory, χ is the nondimensional blade station (0 = root, 1 = tip), ψ is the blade azimuthal position (0 when blade is over the tailboom), and K is the nonuniform inflow parameter. K is a function of the advance ratio as depicted in figure 2-5.

Correlations in rotor flapping and rotor power were conducted using the data computed by the simplified C81 nonuniform inflow analytical model and those measured by Harris in reference 1. The results are shown in figures 2-6 through 2-8. Shown also are the analytical data calculated using the C81 uniform inflow model. For comparison, analytical data from CAMRAD with uniform inflow, undistorted wake, and free wake models are also presented. In these calculations, a delta drag coefficient of 0.006 was added to the baseline V23010-1.68 airfoil data table to account for the Reynolds number effect.

Figure 2-9 presents the induced velocities along the rotor's longitudinal axis, calculated with C81 and CAMRAD at an advance ratio of 0.08. It is seen that though the C81-computed induced-velocity distribution does not compare directly with that of the CAMRAD, the resultant effect on the lateral flapping is in close agreement. This is apparent when one refers to the equation (7) in reference 1.

The results in figures 2-6 through 2-8 indicate that the C81 simplified nonuniform inflow model is as good as the CAMRAD free wake model in predicting rotor lateral flapping at low advance ratios, that the rotor power predicted with the C81 uniform inflow correlates with the test data, and that the C81 nonuniform inflow model underpredicts the rotor power required by 7 percent.

Tilt Rotor Aerodynamic Performance

The primary methodologies used to analyze and predict the aerodynamic performance of tilt rotors in the hover and axial flow

states are AR7906 (hover) and its derivative AR7907 (axial flow). These computerized methodologies are based on a blade element rotor model using lifting surface theory and a circulation-coupled prescribed wake. These performance programs apply to a wide variety of rotors, ranging from the low disk loading, low-twist helicopter rotor to the high disk loading, high-twist rotor of the tilt rotor aircraft. A correlation of calculated and measured performance for the XV-15 tilt rotor is shown in figure 2-10 for hover and figure 2-11 for axial flow (i.e., propeller mode).

The performance methodology applied to the tilt rotor forward flight in conversion modes is ARAM46. ARAM46 is also based on a blade-element model that includes unsteady and three-dimensional aerodynamics. A correlation of the calculated results with test data for an isolated proprotor is shown in figure 2-12.

Panel Method Pressure Calculations and Correlations

Three-dimensional panel methods are being used at Bell to distribute the aerodynamic loads on new vehicles. This is being done in order to produce as accurate a load distribution as possible so that the minimum weight structure can be developed. At the present time these panel codes represent the most versatile and efficient approach to solve for the aerodynamic loads about complicated configurations at low Mach number.

Panel code validation. - In order to gain experience in the use of the three-dimensional panel method results, several correlations between calculated and measured airload distributions have been conducted. Some examples of these correlations are presented here.

Figure 2-13 shows the V-22 wing cross section with its flap deflected 30° . As can be seen, this is a very complicated geometry that is difficult to model because of element interference and flow separation. In figure 2-13 the calculated pressure distribution on this configuration is compared to the measured pressure distribution. The VASAERO (ref. 4) panel modeling used in this case included boundary layer calculations, the wake models for the separation location on the flap, and the wake of the main wing. To simulate a two-dimensional flow field, the main wing for the panel model had an aspect ratio of 30 whereas the aspect ratio of the actual V-22 wing is 5.5. As can be seen, the theoretical results compare with the measured values quite well for this case.

Figure 2-14 depicts the measured and calculated pressure distribution along the V-22 spinner. In this case the pressure distributions correlate very well for the clean spinner case. It should be noted that no effort has been made so far to model the blade holes, blade root end, and eyebrows using a panel method. A comparison of the VASAERO panel results and measured pressures at station 359.9 on the nacelle of the V-22 is given

in figure 2-15. It shows that the panel method results are reasonably good, even over this complicated shape.

As part of the V-22 inlet design studies, a VSAERO panel model was generated to evaluate the internal flow characteristics of candidate geometric configurations. This model was iteratively modified to eliminate external flow separation on the inlet at critical flight conditions. An essentially separation-free design was necessary to achieve the inlet head loss and distortion goals established for the V-22 inlet. A wind tunnel test program was conducted to measure the performance of the configuration selected. The model represented the right hand engine nacelle and stub wing of the V-22 at 0.4 scale. A comparison of the calculated and measured static pressure distribution in helicopter mode from this test is shown in figure 2-16. The agreement between the predicted and measured results is remarkable, considering the complexity of the configuration. Equally good agreement was obtained for the transition and cruise flight modes.

Air loads distributions. - Because of the excellent results produced in these and other VSAERO correlations, this code is being used to distribute the air loads on the V-22 airframe. Accurate air load distributions are required to minimize the structural weight of the vehicle.

The V-22 airframe model was used to determine the downwash angle and total lift of the empennage. The Generic Tilt Rotor (GTR) simulation program was used to fly maneuvers to determine the most critical total point load conditions. At these conditions the VSAERO code was used to determine the distributed air loads for input into the NASTRAN structural analysis program. A LOADS component of the ADAM system is being developed to automate this process. A preliminary beam bending moment distribution on the empennage from the VSAERO pressure distribution produced by ADAM/LOADS for this case is given in figure 2-17. It shows the kind of results that may be produced for complicated three-dimensional configurations and applied to structures design.

DYNAMICS

Nodalized Rotor

The vibration characteristics of the four-bladed hingeless rotor exhibit high 4/rev vibrations in a low-speed transition regime because of blade-vortex interaction. As airspeed increases from the transition flight, the 4/rev vibration level first decreases, then increases again as the helicopter flies faster. The primary excitation forces are the hub 4/rev vertical shear and the hub 4/rev pitching and rolling moments. The sources of the hub 4/rev vertical shear and 4/rev moments are the blade root 4/rev vertical shear and the 3 and 5/rev beamwise bending moments, respectively. Therefore, it is feasible to achieve the desired low 4/rev airframe vibration by minimizing the blade

response in the 3/rev, 4/rev, and 5/rev harmonic components. Bell's nodalized rotor technology approach is to judiciously tailor rotor structural and aerodynamics properties in such a way that inertial loads cancel out blade aerodynamic loading at rotor hub, forming a nodal point.

The methodology of the nodalized rotor leads to the following specific design features:

- (1) An extremely stiff and lightweight hub.
- (2) A large concentration of mass near the 40-percent blade radius.
- (3) A reduction in mass in the outboard 30 percent of the blade.
- (4) An increased beamwise and chordwise stiffness for the entire blade.

An analytical prediction of the benefit of the nodalized rotor over a conventional design indicated a 40- to 45-percent reduction in hub loads in the low-speed transition. (The conventional design referred to here is a rotor design achieved using the conventional frequency separation criteria.) To validate the analytical prediction, one-fifth scale aeroelastic models with an NACA 0012 airfoil and a constant chord were fabricated for both the conventional design and the nodalized rotor. The models were then tested in identical back-to-back flight conditions in the LTV low-speed wind tunnel. Comparisons of measured and predicted hub loads versus the tunnel speed (plotted in units full-scale speed) are presented in figure 2-18. The results indicate that the predicted reduction in hub loads is conservative.

To further explore the nodalized rotor concept, a model rotor was designed and fabricated with advanced airfoils and highly tapered planform blade. This effort is being conducted under a NASA-Army contract. The thrust-weighted chord of the tapered blade is equal to the constant-chord 0012 airfoil blade tested earlier. The predicted hub loads of the aerodynamically optimized nodalized rotor are also shown in figure 2-18. The weight penalty of the aero optimized nodalized rotor versus the conventional design is about 0.3 percent of the gross weight. Wind tunnel testing of the aero optimized nodalized rotor will be conducted in the NASA-Langley Transonic Dynamics Tunnel (TDT) in March 1987. The two models previously tested in the LTV low-speed wind tunnel will also be tested in the TDT for comparison purposes.

Tilt Rotor Loads

The aerodynamic interference between the wing and tilt rotor blades is the primary source of the oscillatory blade and hub

loads. For tilt rotors with three-bladed gimbaled hubs, such as the XV-15 and V-22, the aerodynamic interference between the wing and rotor is responsible for the high 2/rev and 3/rev blade beam loads, 2/rev and 4/rev blade chord loads, and the 3/rev hub in-plane shears in the airplane cruise mode. The flow field of the wing is approximated in Bell's computer program DYN5 (ref. 5) and recently in C81 by superimposing the flow field of an elliptical profile at zero angle-of-attack on that of a flat plate representing the wing angle-of-attack (figs. 2-19 and 2-20). The ellipse simulates the wing thickness while the flat plate represents the circulation. The interference is assumed to be zero on the outboard half of the rotor disk (away from the wing, i.e., $0 < \text{azimuth} < 180^\circ$).

To analyze the aerodynamic interference between the prop rotor and fuselage more sophisticatedly, the panel method, computer program VSAERO (ref. 4), was used to calculate the change in flow field around a blade element due to the presence of the wing, spinner, nacelle, or fuselage. Changes in the flow field for blade elements due to the presence of the airframe were calculated using VSAERO and the DYN5 simplified analytical model. Results are compared in figure 2-21. Good agreement is evident between the two analytical approaches near the 270° azimuthal position (when the reference blade is positioned right in front of the wing). The differences between the two analyses are due to the assumptions made in the simplified model that any aerodynamic interference on the outboard half of the rotor disk is neglected and that flow blockage, other than by the wing, is not included.

The VSAERO-calculated change in the flow field was input to the C81 computer program using a table look-up. This analytical approach (C81/VSAERO) was used to predict the V-22 rotor loads in the cruise airplane mode. Figures 2-22 and 2-23 show comparisons of computed and measured blade loads in the first four harmonic components. Without the aerodynamic interference representation (data not shown), the correlation of the 1/rev is still good, but the computed higher harmonic components are nearly zero. Using the DYN5 flow approximation method, good correlations (data not shown) are achieved in the 1/rev and 2/rev components, but not so good correlations are observed in the 3/rev and 4/rev components. A harmonic analysis of the change in the blade angle-of-attack (fig. 2-21) due to the aerodynamic interference reveals that the VSAERO data consist of 2/rev, 3/rev, and 4/rev values of 0.79° , 0.54° , and 0.36° , respectively. The corresponding results from the DYN5 data are 0.70° , 0.41° , and 0.19° , respectively. It is seen that the simplified analytical model does well for the 2/rev. It is, however, not adequate for 3/rev and 4/rev blade load predictions.

The C81/VSAERO methodology was used to predict the V-22 3/rev hub in-plane shears and the results are presented in figure 2-24. The V-22 3/rev hub in-plane shears were also inferred using

the pylon vibrations and transfer functions measured on the 0.2-scale aeroelastic model. The hub loads from the inferred method seem to agree quite well, both in trend and in magnitude, with those predicted by the theory.

Tilt Rotor Wing/Pylon Dynamics

The accuracy of a dynamic analysis of the wing, pylon, and pylon support structure is critical to not only cabin vibrations but also to oscillatory loads and prop rotor stability. MSC/NASTRAN Version 63 was used to perform the dynamic analyses. To validate the modeling methodology for the V-22, a full-scale wingtip box test was conducted (ref. 6). The test specimen consisted of an 8-foot span from the outboard end of the V-22 wing, and included a mass-simulated pylon, and an actual pylon support structure. Prior to the vibration test, stiffness tests and measurements of mass and inertia properties were conducted. The measured stiffness and inertia properties were then used in the posttest analysis. Figures 2-25 and 2-26 show, for comparison, measured frequencies along with those of pretest and posttest analyses. The results indicate that the finite element model is proper, as evidenced by the pretest analysis, and that the current structural dynamics modeling of the wing/pylon structure is adequate for the in-flight wing/pylon modes prediction.

Prop rotor Stability

Prop rotor stability has been investigated at Bell since the 1960's. Linear and nonlinear analyses (DYN4 and DYN5) have been developed and wind tunnel tests of scaled aeroelastic models have been conducted. Extensive experience in correlation has been acquired. To aid in modeling a prop rotor with a coning flexure, such as the V-22 design, an eigenvalue analysis was recently developed (ref. 7). The analysis is called ASAP (Aeroelastic Stability Analysis of Prop rotors). The ASAP analysis models a modal airframe, an elastic rotor on a gimbaled hub with flapping, coning and lead-lag motions, and a lumped parameter drive system. The airframe modal parameters are calculated using the NASTRAN finite element dynamics model. A general automatic flight control system (AFCS) is also included. The blade aerodynamics can employ either the 3/4 radius approach or two-dimensional blade element theory. The airframe aerodynamics include airframe force and moment nondimensional derivatives and control surface deflection force and moment nondimensional derivatives so that control inputs from the SCAS will generate forces and moments on the rigid body and elastic modes of the airframe.

The application of the ASAP computer codes to prop rotor stability was validated using the stability data measured on the V-22 0.2-scale semi-span aeroelastic model. Figure 2-27 shows the correlation of wing beam and wing chord damping in percent critical versus the airspeed. The degree of correlation is satisfactory.

HANDLING QUALITIES

Rotorcraft Frequency-Domain Identification

Many criteria in the recently updated helicopter handling qualities specification (ADS 33) are based on transfer function parameters derived from linear models of the aircraft. To demonstrate compliance with these criteria requires flight test generated frequency response data. This is a new requirement for the rotorcraft community. The Army (ref. 8) has demonstrated the practicality of producing the data and has developed data-reduction algorithms that not only fit the raw data but also identify the equivalent parameters of the transfer function represented by the data.

To gain experience in these techniques, some recent flight tests of the Model 222/680 helicopter were devoted to generating frequency response data. Data were taken for cyclic and pedal inputs at several forward flight speeds in the 80 to 125 KTAS range. Sinusoids at various frequencies were input through the roll, pitch, and yaw SCAS actuators, as appropriate, with the aircraft trimmed at the desired speed and without pilot control inputs. Where possible the sine wave amplitudes were adjusted until the resulting aircraft attitude oscillation was approximately $\pm 7.5^\circ$ in the driven axis. Good data were obtained in the 0.5 rad/sec to 8-10 rad/sec range. Below 0.5 rad/sec the input periods became too long and the aircraft changed trim state before an adequate data sample could be collected. Above 8-10 rad/sec aircraft response became too small to record, even with the SCAS actuator operating at full authority. For handling qualities the 8-10 rad/sec limitation may not be a problem, since most of the interesting characteristics reside at lower frequencies. The 0.5 rad/sec limitation does preclude identification of some important low-frequency characteristics such as the phugoid and spiral modes. Therein lies a topic of interest for future development of this technique at Bell.

The frequency response data were subsequently compared with equivalent C81 results for the Model 222/680. This provided a check on the accuracy of computed frequency responses based on the transfer function parameters calculated by C81. Typical results are shown in figure 2-28. The measured gains are matched quite well by the computed gain response. The same is not true for the phase response. If, however, we draw on reference 8 and related fixed-wing experience (ref. 9), which justify the inclusion of the e^{-Ts} or pure delay term in the numerator of the calculated transfer function to account for high-frequency and unmodeled or nonlinear effects, the phase responses come into better agreement. In this case it was found that an equivalent pure delay of 145 milliseconds was necessary to correlate the data. With this modification the estimated transfer function for the sample case becomes:

$$\frac{\theta}{\delta_{F/A}} = \frac{0.99 e^{-0.145s} (s + 0.07)(s + 0.82)}{\left[s^2 + 2(0.14)(0.25)s + 0.25^2 \right] \left[s^2 + 2(0.82)(1.75)s + 1.75^2 \right]}$$

where all parameters except $e^{-0.145s}$ were determined by C81.

As driven by ADS 33 and the success of this preliminary effort, Bell will continue to evolve its capability in the techniques of in-flight frequency responses and application of these data for specification compliance and math model refinement.

Tilt Rotor Airplane Mode High-g Maneuvers

The capability of C81 to predict high-g maneuvers for tilt rotors in airplane mode was recently validated. The validation was based on a correlation with measured XV-15 flight test data. The measured data were recorded during flight 290, counter 1014, of XV-15 Ship 702. The aircraft entered the maneuver at 216 KIAS by initiating a right roll with SCAS on. The bank angle change was 82° in 2.5 seconds. During the course of the roll, aft stick was applied, generating a peak pitching rate of 40 deg/sec. The control applications resulted in a 4.2g load factor at 214 KIAS. A total of 40 seconds of data was taken during the maneuver, and the 20 seconds of data where the peak load factor occurred are shown in figure 2-29.

The C81 analytical model includes aerodynamic descriptive data for the rotors, wings, fuselage, and aerodynamic surfaces. The dynamics of the rotors were modeled through a modal representation with 10 elastic modes. The analysis was performed with SCAS off. The pilot control inputs in C81 were adjusted to reflect the control surface deflections due to pilot stick inputs and the SCAS effect. Computer simulation was limited to 10 seconds near the time when the maximum load factor occurred. The analytical data are also presented in figure 2-29 for comparison.

The results indicate that the peak load factor is predicted within 0.2g and that the predicted roll rates and roll attitudes are within 4 deg/sec and 4° , respectively. Correlations in pitch rates and pitch attitudes are good. The peak transient loads of the blade and the pitch link of the right rotor (not shown in figure 2-29) are predicted with a maximum discrepancy of 10 percent.

CONCLUDING REMARKS

The thrust of the activities described in this paper is to provide adequate methodologies so that the development of advanced military rotorcraft can be undertaken with a minimum risk. As indicated, some progress has been made in achieving this goal, but the challenge has by no means been met. Bell

fully recognizes and appreciates the extent of the challenge and has committed to continue the development of the aeromechanics methodology.

REFERENCES

1. Harris, F. D.: Articulated Rotor Blade Flapping Motion at Low Advance Ratio. Journal of the American Helicopter Society, vol. 17, no. 1, Jan. 1972.
2. Johnson, W.: Comparison of Calculated and Measured Helicopter Rotor Lateral Flapping Angles. Journal of the American Helicopter Society, vol. 26, no. 2, April 1981.
3. Johnson, W.: Assessment of Aerodynamic Models in a Comprehensive Analysis for Rotorcraft. NASA TM 86835, October 1985.
4. Maskew, B.: Program VSAERO, A Computer Program for Calculating the Nonlinear Aerodynamic Characteristics of Arbitrary Configurations: User Manual. (Prepared for NASA Ames Research Center, Moffett Field, CA., under Contract NAS2-8788.) April 1982.
5. Yen, J. G.; Weber, G. E.; and Gaffey, T. M.: A Study of Folding Proprotor VTOL Aircraft Dynamics, Volume 1. AFFDL-TR-71-7, September 1971.
6. Sprangers, C.A.; and Stevenson, M. K.: Results of the V-22 Preliminary Design Wing Test Program. Paper presented at the 42nd Annual Forum of the AHS, June 1986.
7. Hsieh, P. Y; Levenson, W.; and Parham, T.: Aeroelastic Stability Analysis of Proprotors (ASAP). BHTI Report 301-909-003, July 1986.
8. Tischler, M.; Leung, J.; and Dugan, D.: Identification and Verification of Frequency Domain Models for XV-15 Tilt Rotor Aircraft Dynamics. NASA TM 86009, August 1984.
9. Hoh, R.; et al.: Proposed MIL Standard and Handbook - Flying Qualities of Air Vehicles, Volume II: Proposed MIL Handbook. AFWAL-TR-82-3081, November 1982.

PART III. ADVANCED CONFIGURATION STUDIES AND HARDWARE DEVELOPMENT

Part III presents some results of advanced tilt rotor configuration studies conducted by the Preliminary Design group at Bell. The first section discusses concept evaluation of military and commercial configurations of manned aircraft. The second section presents an idea for an unmanned tilt rotor for shipboard operation and describes a prototype development program being performed by the predesign groups of Bell and their tilt rotor partner, Boeing Vertol, to build and demonstrate a 500-pound gross weight tilt rotor unmanned aerial vehicle for use by the military forces of the U.S. and friendly allies.

MILITARY AND COMMERCIAL CONCEPTS

V-22 Derivatives

The V-22 Joint Services Vertical Lift Aircraft (fig. 3-1) is well along in its full-scale development, with first flight scheduled for mid 1988. The V-22 is an unarmed utility/transport aircraft designed as a Marine assault vehicle. It is equipped for shipboard operation and incorporates a folding wing and rotors and a fuselage with an aft loading ramp to facilitate loading and unloading. The fuselage and cockpit are unpressurized.

The first derivative application of the V-22 is for antisubmarine warfare (ASW) missions. Figure 3-2 illustrates the V-22 ASW configuration concept. Search equipment includes expendable sonobuoys, onboard processing, FLIR, radar, and ESM. A magnetic anomaly detector and dipping sonar are used for localization. The V-22 ASW has the ability to soft deploy and monitor large acoustic sensors for screening purposes, and because of its ability to hover and fly at low speeds in the helicopter mode, it can retrieve advanced sophisticated sensors for redeployment. The high cruise speed and ability to operate from a variety of decks are also a significant advantage. The aircraft carries up to four torpedoes or antisurface missiles.

Because the basic V-22 carries no weapons, an armed escort aircraft with similar flight performance is needed. Obviously a helicopter would be too slow, and typical fighters are too fast. The simplest solution is a modified V-22 with counter air weapon systems adapted as shown in figure 3-3. Since the V-22 was optimized for other applications, it does not present the best configuration for an air-to-air combat aircraft. A smaller aircraft might be more suitable for this mission. Although weight fraction trends are adverse for a smaller aircraft, its reduced target size and increased agility offset the penalty. Figures 3-4 and 3-5 show two alternative configurations for a V-22 escort. The performance of these aircraft is closely matched to the V-22.

The next V-22 derivative is a commercial version with minimum change (fig. 3-6). Obviously, some of the military requirements - such as IR suppressors, bladder tanks, and wing and rotor folding - would be eliminated to reduce cost and weight. A commercial derivative could carry up to 31 passengers and enough fuel for up to 600 miles. One of its primary uses might be as a light cargo transport for overnight package express.

Commercial Applications

Three possible tilt rotor configurations have been developed for the specific requirements of commercial operations. The driver in commercial applications is productivity, which, by definition, demands optimization of performance and cost. A cleaner shape for lower drag and the maximum payload for a given gross weight are primary factors in productivity.

Trade-off studies were conducted on the three configurations. The first configuration resembles the XV-15 in that a high wing placement is used with tilt nacelles and an "H" tail (fig. 3-7). The second configuration relocates the wing at the bottom of the fuselage (fig. 3-8). Although interference drag is slightly greater with the low wing placement, overall drag is reduced because the wing spars can now pass through the belly below the cabin floor, allowing an unrestricted cabin height and minimum fuselage profile. The low wing also allows retraction of the landing gear into the wing roots, eliminating the need for sponsons. The "T" tail configuration reduces interference drag by minimizing the number of surface intersections.

The third configuration, a somewhat more radical departure from convention, is a low-wing, fixed-engine aircraft with a canard surface forward and twin fins aft (fig. 3-9). Use of the canard to carry approximately 20 percent of the weight of the aircraft accomplishes several things. First, it reduces the wing area and, hence, the rotor download during hover. This in turn minimizes the installed power requirements, yielding a lower empty weight. The lifting canard also allows a more favorable cg placement ahead of the leading edge of the wing root. This position more closely approximates the cg position during hover, resulting in less cg shift from hover to cruise flight. Reduced cg travel minimizes hub stiffness requirements and provides indiscriminate loading. The lifting control surface reduces the total lift in cruise, minimizing the induced-drag penalty. The usual objections to a canard include the difficulty of handling during landing, but since takeoff and landing of the tilt rotor are done in the helicopter mode, the canard has no effect on that flight regime.

The three configurations were sized for a gross weight of 20,000 pounds and then evaluated parametrically for drag and empty weight. A comparison of the three aircraft reveals that the canard is the best configuration from the standpoint of both drag and weight, as shown below:

<u>Configuration</u>	<u>Empty Weight (lb)</u>	<u>Drag (ft²)</u>
High wing, H-tail	15,407	12.1
Low wing, T-tail	15,109	10.1
Low wing, canard	14,834	8.7

Additional variants of the canard configuration have also been studied. Figure 3-10 shows an interesting executive transport that uses a highly swept midwing configuration. This aircraft, having a compact pressurized fuselage like a Lear jet, accommodates the wing carry-through structure aft of the cabin, outside the pressure vessel. The increased sweep produces a longer chord length for a given wing thickness, reducing drag. The high sweep angle also improves rotor flapping clearance, allowing shorter pylons and thus minimizing cg shift. Use of the canard permits optimum cg placement.

Figure 3-11 shows a concept for an airliner, also with a canard. As illustrated in the figure, the fuselage can be configured for a load of 75 passengers or a load of typical cargo containers.

Technology issues associated with commercial tilt rotor development include stability and controllability of the canard configuration. This can be evaluated in wind tunnel tests on a typical scale model, as well as performance and loads implications resulting from the impingement of shed vortices from the canards on the rotor discs.

Low wing placement results in a reduced vertical distance from the rotor disc to the vertical cg of the aircraft, reducing control power in the longitudinal (pitch) direction. Analysis shows that small increases in hub flapping restraint will suffice to provide the necessary control moment during hover; however, increased hub stiffness may have an effect on the mechanical stability of the rotor/wing system. Again, this might possibly be investigated in a scale model or perhaps in full scale using the XV-15.

The large stiffness requirement of tilt rotor wings, as well as the cross shafting that must be carried in the wing, results in increased wing thickness. Sweeping the wings produces a greater chord length for a given thickness, but requires careful structural design to prevent instability. Wind tunnel testing of these configurations would be useful and could be done on a scale model.

Tilt-Fold Rotors

The ultimate development of the tilt rotor concept is the tilt-fold configuration. An example of a concept for a tilt-fold fighter is shown in Figure 3-12. The technology to develop this concept in full scale already exists. Bell tested a tilt-fold rotor system sized for the XV-15 in the NASA-Ames 40- by 80-foot

wind tunnel in 1972 (fig. 3-13). Recent developments in convertible engines (fig. 3-14) will make powerplants for this type of aircraft available in the necessary timeframe.

Figure 3-15 shows a possible concept for a shipboard-compatible tilt fold rotor aircraft that could be used for ASW missions among others.

REMOTELY PILOTED VEHICLES (RPVs)

Another interesting advanced configuration study of tilt rotor applications is the field of unmanned aerial vehicles (UAVs) or, as they are more commonly called, RPVs. Conventional fixed-wing RPVs require large, costly equipment for launch and recovery, reducing system mobility and flexibility. Rotary wing concepts permit vertical takeoff and landing, eliminating the launch and recovery systems, but are significantly restricted in cruise performance and efficiency. These same restrictions led to the development of the tilt rotor in the first place.

A recent Navy requirement for a midrange RPV specified high subsonic speeds, a 300-nmi radius of action, air launch capability, and the ability to be landed in the ocean for later recovery by helicopter. Figure 3-16 summarizes these requirements.

Figure 3-17 presents a typical mission profile for the midrange RPV. It will be observed that the purpose of the air launch requirement is to extend the radius of operation. Typically, the RPV would be carried aloft by an A-6 for air launch 100 nmi from the carrier. The RPV would then perform its mission by flying to its target 300 nmi away and returning to its approximate launch point, where it would be dropped in the ocean for recovery by helicopter and then air lifted back to the carrier. The total mission time would be at least 4.25 hours and could go as high as 5.5 hours, if the RPV were as slow as allowed by the specifications.

Figure 3-18 presents a concept for a tilt rotor RPV to perform the mission noted above. Figure 3-19 summarizes the weights and performance of the tilt rotor RPV. Examining this vehicle with regard to Navy requirements shows that the aircraft could take off from any vessel with a 30- by 30-foot pad and, cruising at 204 knots - although somewhat slower than desired - could fly 400 nmi in and 400 nmi back to a vertical landing in only 4 hours, eliminating the requirement for the carrier, the A-6, the helicopter, and the need to flush salt water from the systems upon return (fig. 3-20).

The advantages of a tilt rotor RPV are many. In addition to eliminating the need for launch and recovery equipment (reported to require one C-5A for transport), the aircraft's ability to hover can be used for applications such as soil sampling and operation from unprepared areas. It can be landed and taken off

at the front line by handing off control to a forward operator. This will allow courier service as well as observation. It is much more compatible with shipboard operation since net recovery on a pitching and rolling deck is nearly impossible, while a simple hauldown mechanism will allow landing the tilt rotor from a hover.

Hardware Development

The advantages of the tilt rotor concept in an RPV became obvious, along with a quick, inexpensive way to evaluate it, as engineers were performing wind tunnel model testing for the V-22 program. Figure 3-21 shows a 20-percent Froude scale model of the V-22 undergoing testing in the wind tunnel. The size and direct applicability of some of the model hardware led to an idea for an R&D concept demonstrator. Figure 3-22 shows a sketch of the aircraft. Figure 3-23 presents a schematic of the drive system concept and figure 3-24 shows the nacelle. The control mechanization is similar to that in the XV-15. Figure 3-25 shows the modular concept of the airframe, which will be fabricated from foam core, glass skin sandwich panels.

Figure 3-26 summarizes the weights and performance of a 500-pound gross weight tilt rotor aircraft for use as an RPV. Bell and its tilt rotor partner, Boeing-Vertol, are jointly engaged in the design and fabrication of hardware for the concept demonstrator aircraft. As shown by the schedule in figure 3-27, the first flight is expected in late summer, 1987, with flight demonstrations by the end of the year.

CONCLUSIONS

Part III has presented several future applications of tilt rotor aircraft for both military and commercial markets. These applications offer significant advantages to the user. Indeed, several markets have already been announced and the continued development of the tilt rotor will make it available to fill those needs.

Technology development will allow enhancement of the capabilities of the tilt rotor. Effects of hub stiffness on wing stability, controllability/stability of canard configurations, and effect of high wing sweep on drag are some of the interesting challenges that must be studied prior to full-scale development. The technology exists today to develop a tilt-fold rotor aircraft with speed capabilities in the transonic range.

Finally, hardware development in small-scale models will allow low-cost concept demonstration of a very interesting application of tilt rotor technology.

The future of the tilt rotor is exciting indeed!

MODEL 412 ROTOR SYSTEM WITH COMPOSITE YOKE

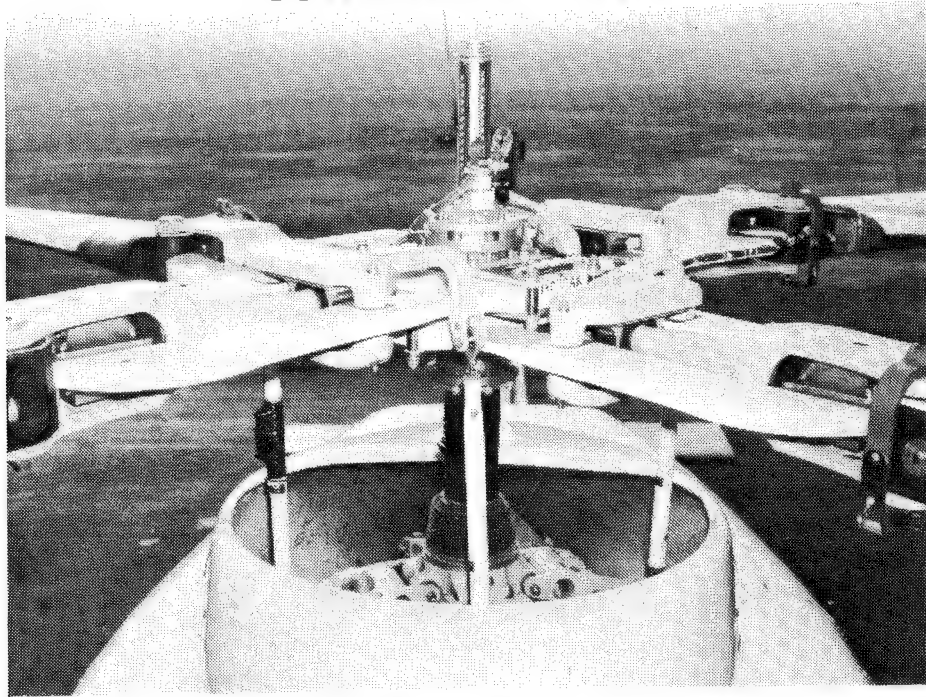


Figure 1-1

OH-58D ROTOR SYSTEM WITH COMPOSITE YOKE

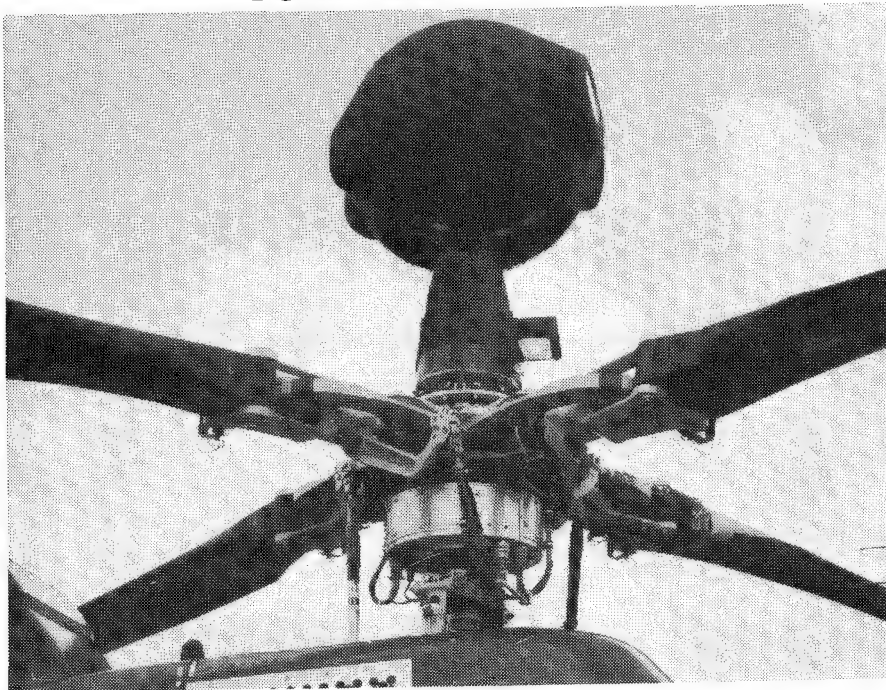


Figure 1-2

MODEL 680 ROTOR SYSTEM

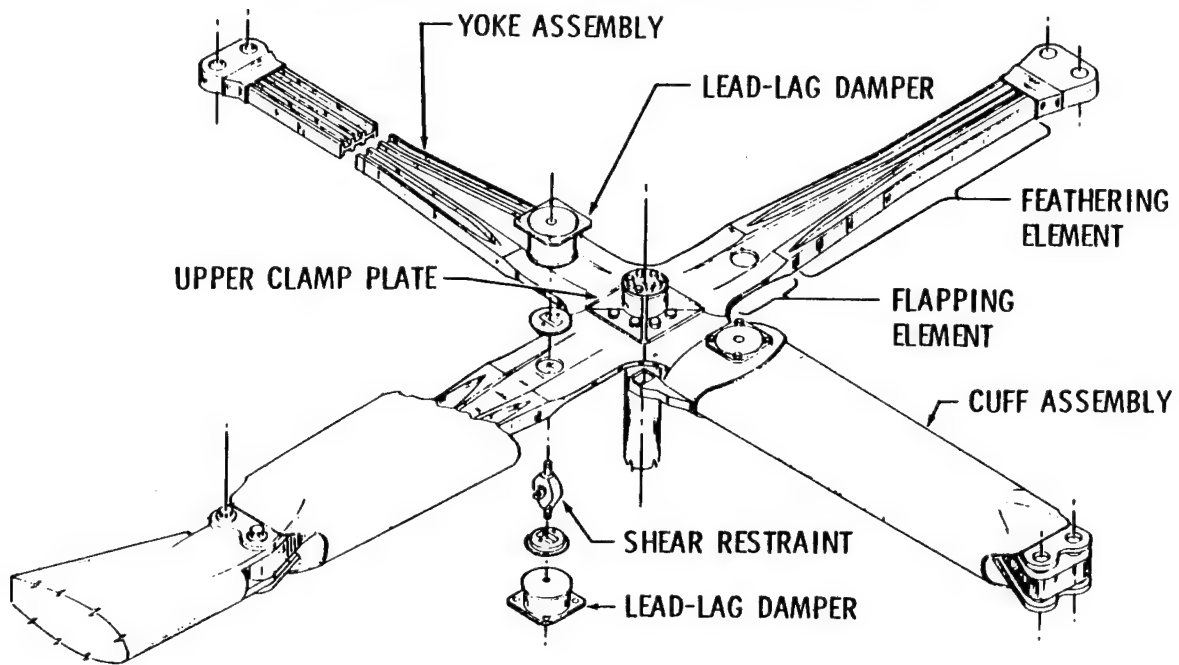


Figure 1-3

FIBERGLASS/EPOXY FILAMENT WOUND BELT FOR MODEL 680 YOKE ASSEMBLY

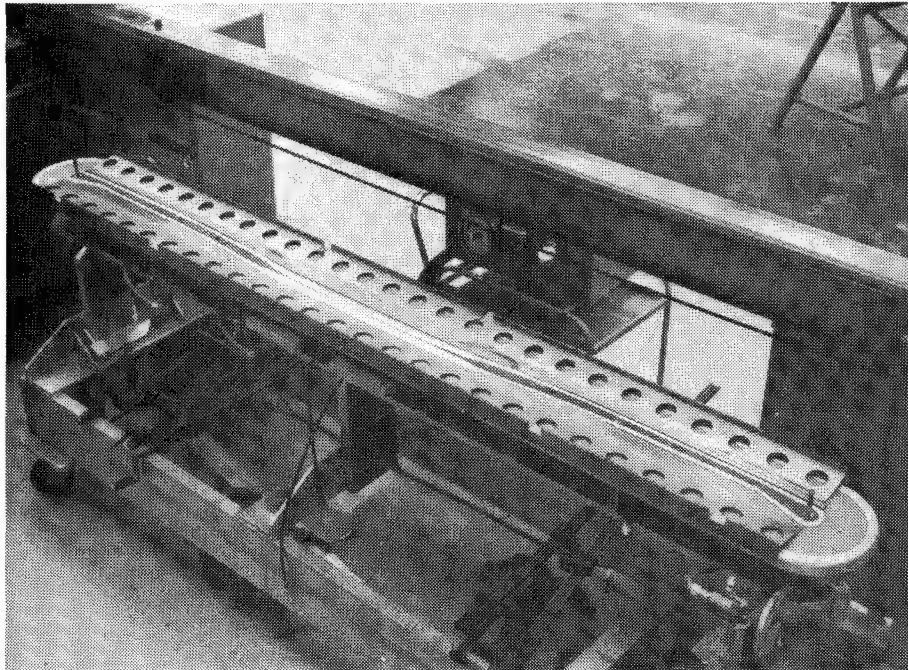


Figure 1-4

MODEL 680 CAVITY BOND TOOL

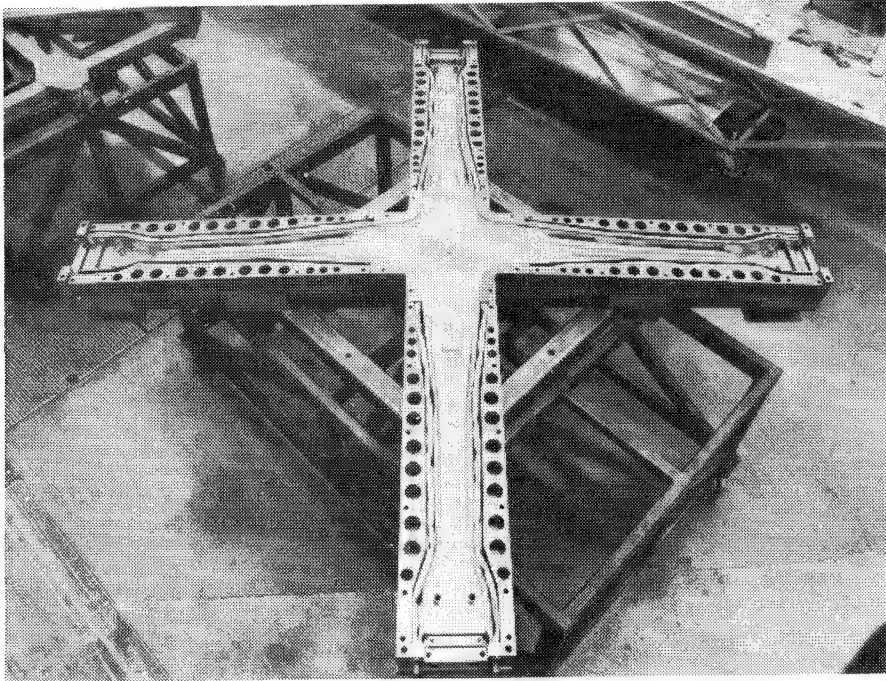


Figure 1-5

LAYERED FINITE ELEMENT MODEL OF QUARTER YOKE

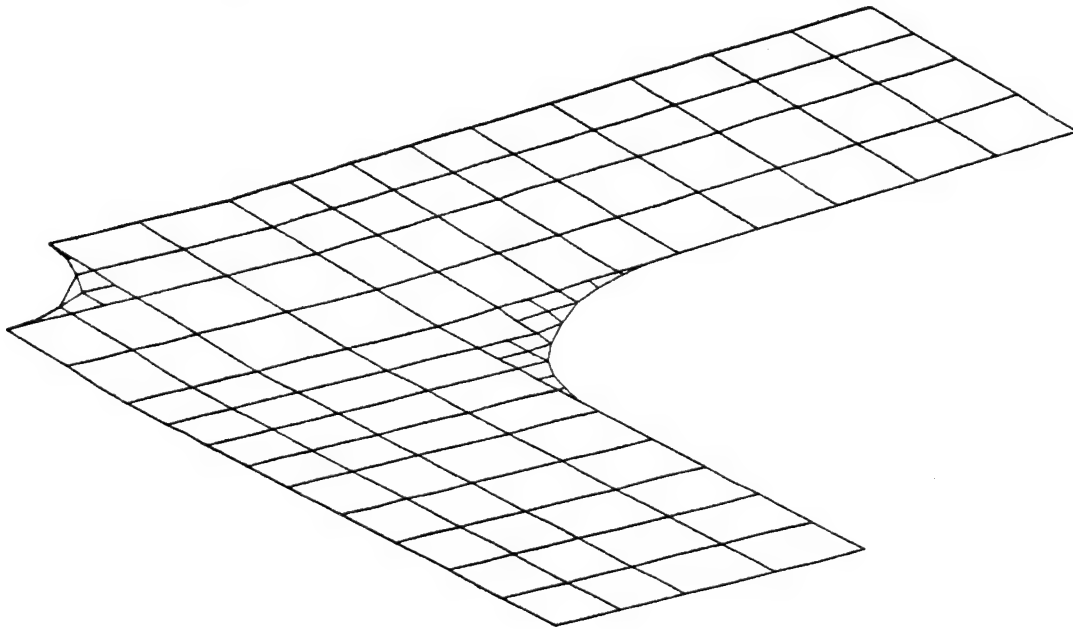


Figure 1-6

TWO - DIMENSIONAL FINITE ELEMENT MODEL OF SPANWISE SECTION OF YOKE

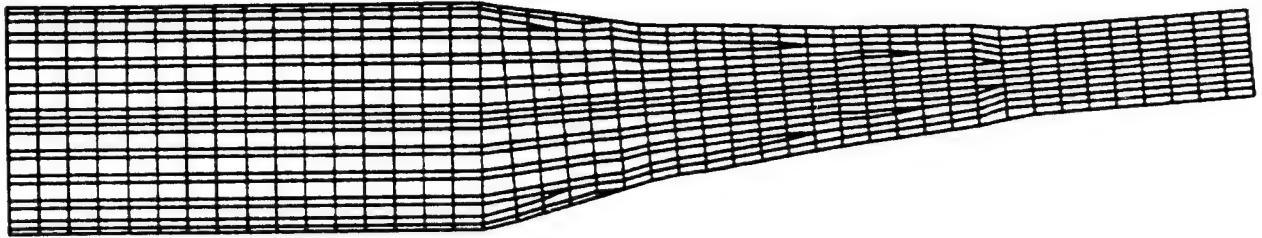


Figure 1-7

CENTER SECTION OF SECOND GENERATION MODEL 680 YOKE

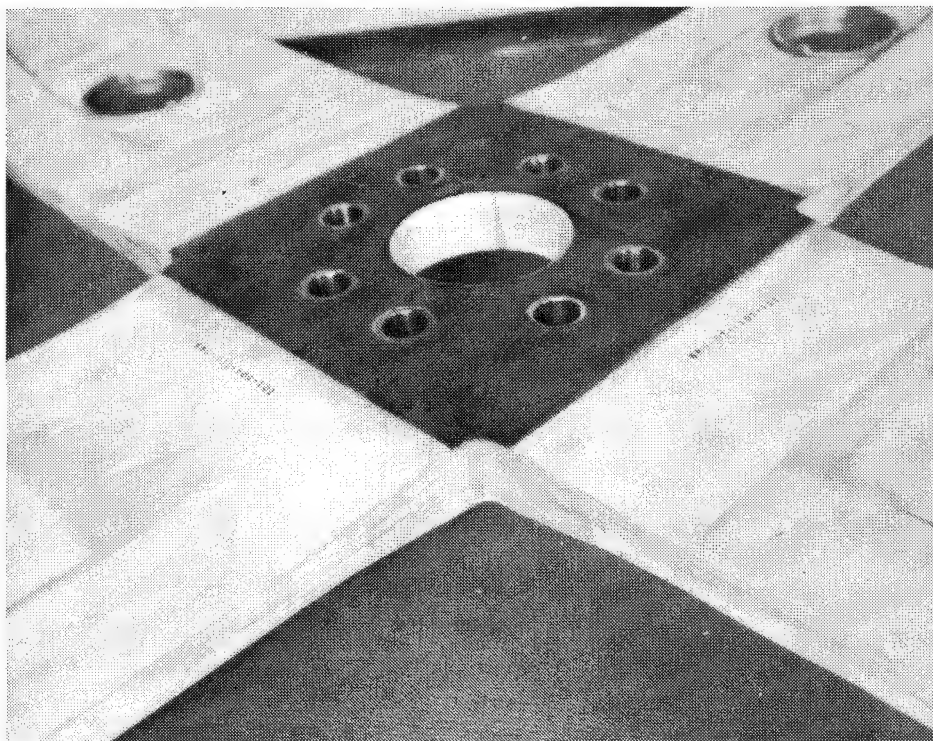


Figure 1-8

ADHESIVE INNER LAYER FOR DELAMINATION ARRESTMENT

BASIC CONCEPT

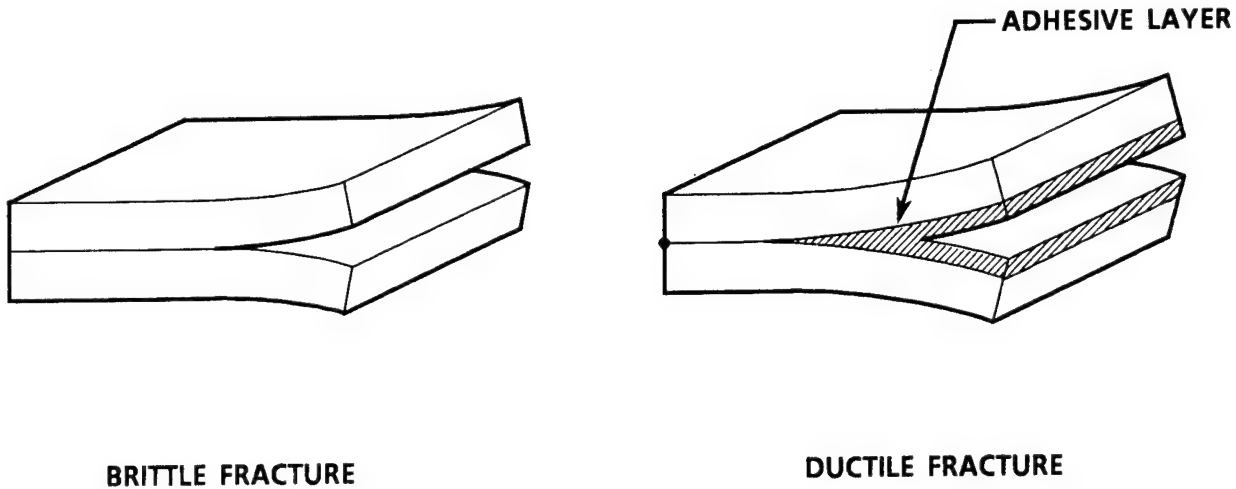


Figure 1-9

INTERLAMINAR NORMAL STRESS DISTRIBUTION THROUGH THE THICKNESS

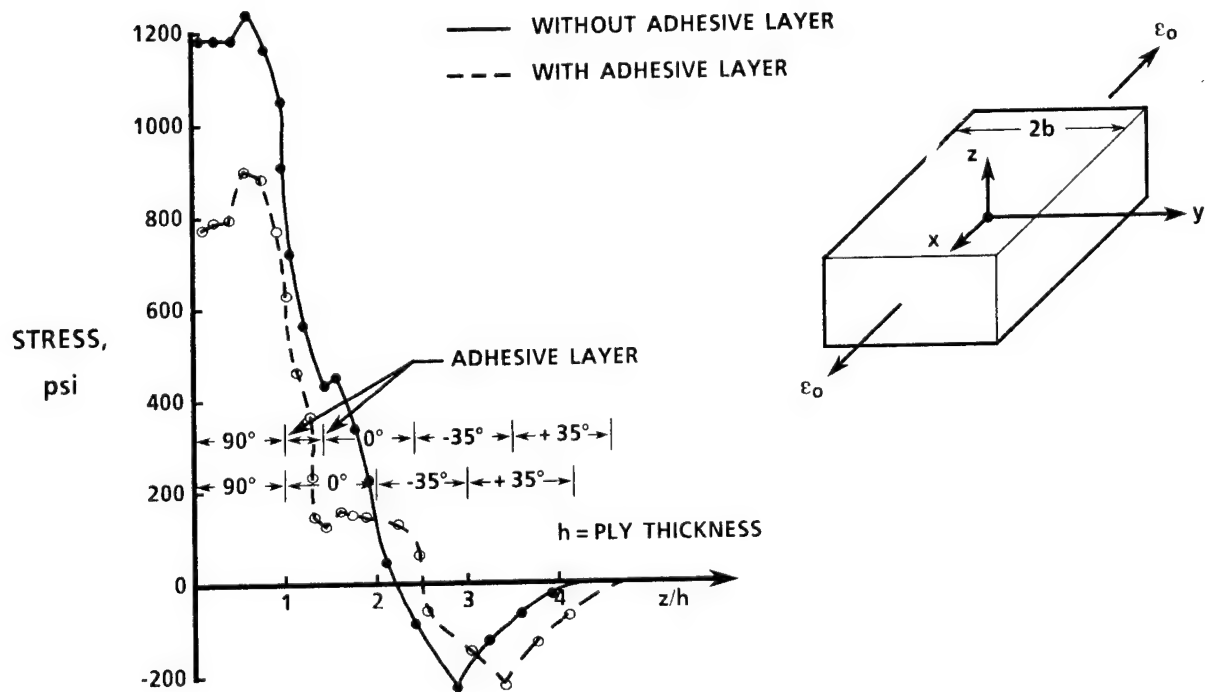


Figure 1-10

X-RAY RADIOGRAPHY OF TEST COUPONS

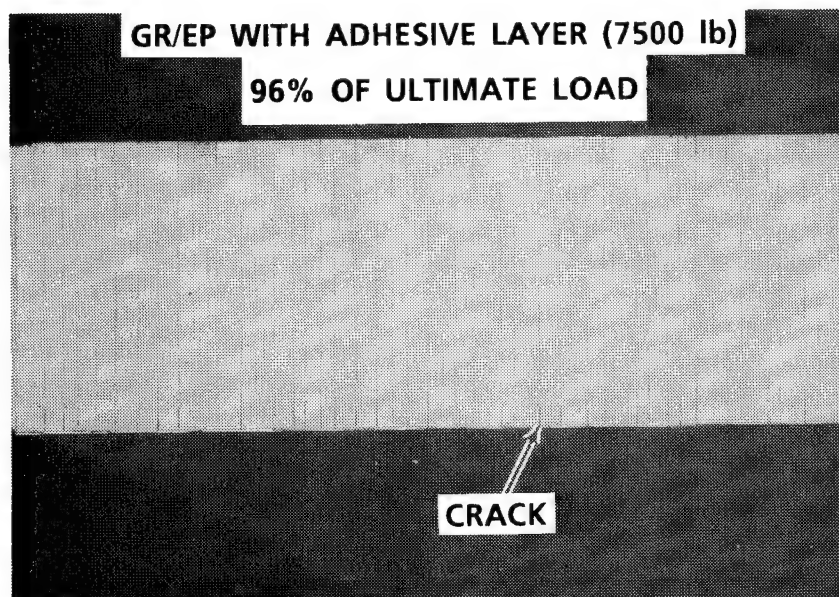
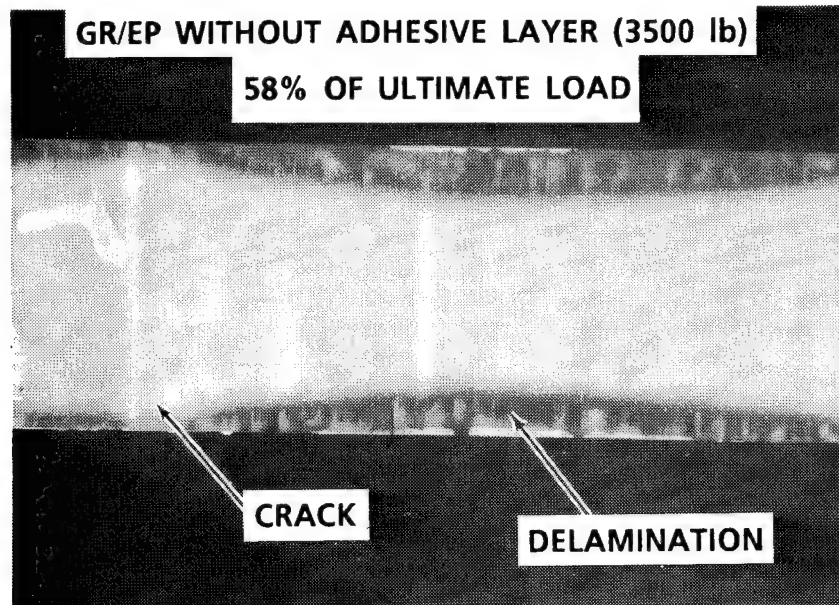


Figure 1-11

PHOTOMICROGRAPH OF TEST COUPON WITH TRANSVERSE CRACK

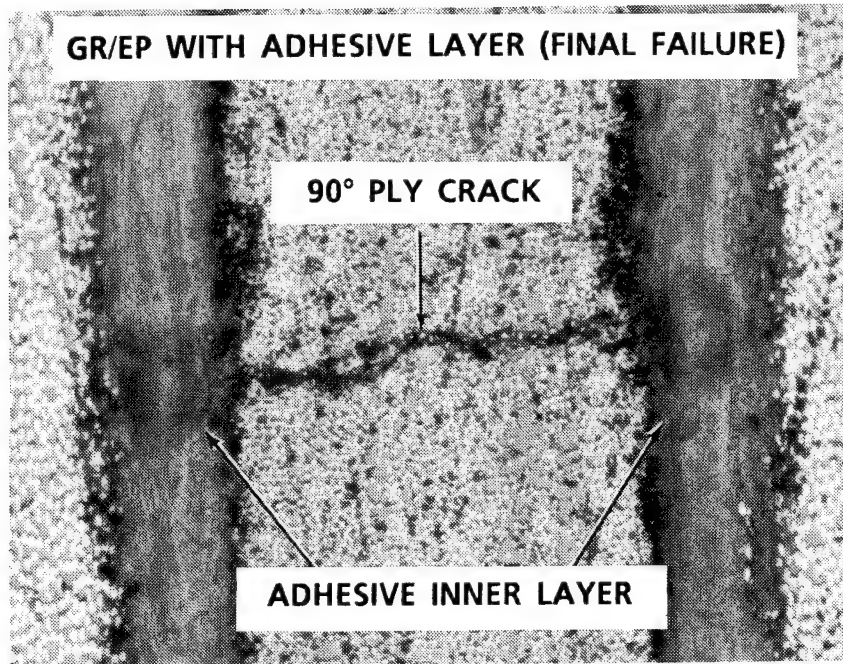


Figure 1-12

MODEL 680 ROTOR SYSTEM IN FLIGHT



Figure 1-13

MODEL 680 VIBRATION SUMMARY

222/680 LOAD LEVEL SURVEY AUGUST 1982
ALL SEATS, ALL DIRECTIONS, ALL G.W./C.G.'s

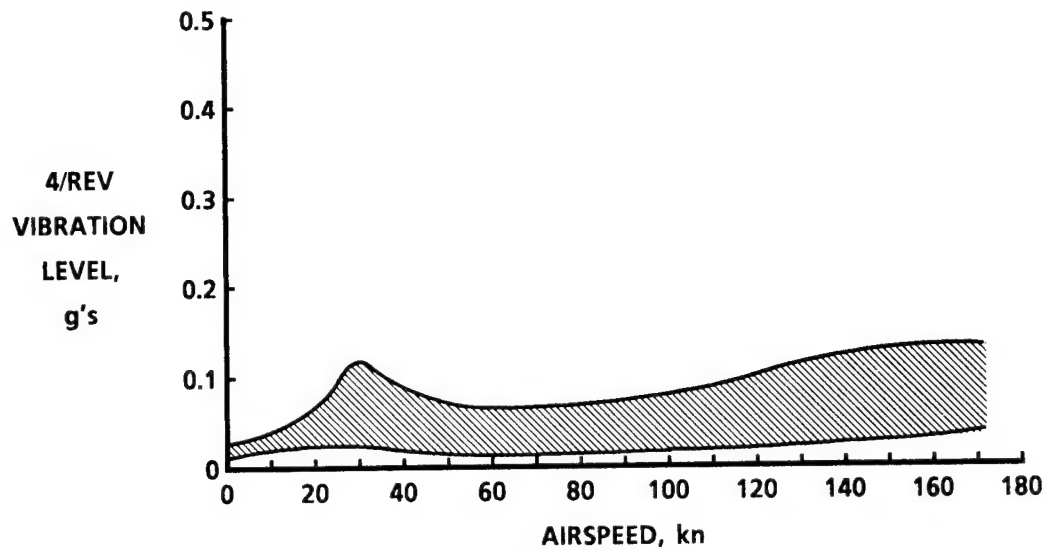


Figure 1-14

ALR BLADE TOOLING

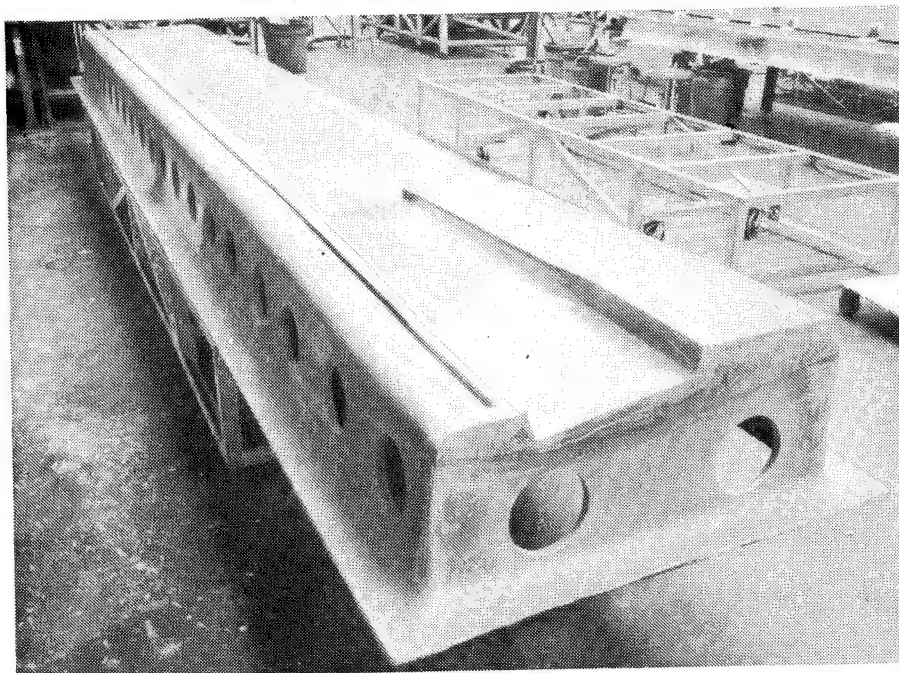


Figure 1-15

ALR BLADES WITH MODEL 680 ROTOR HUB

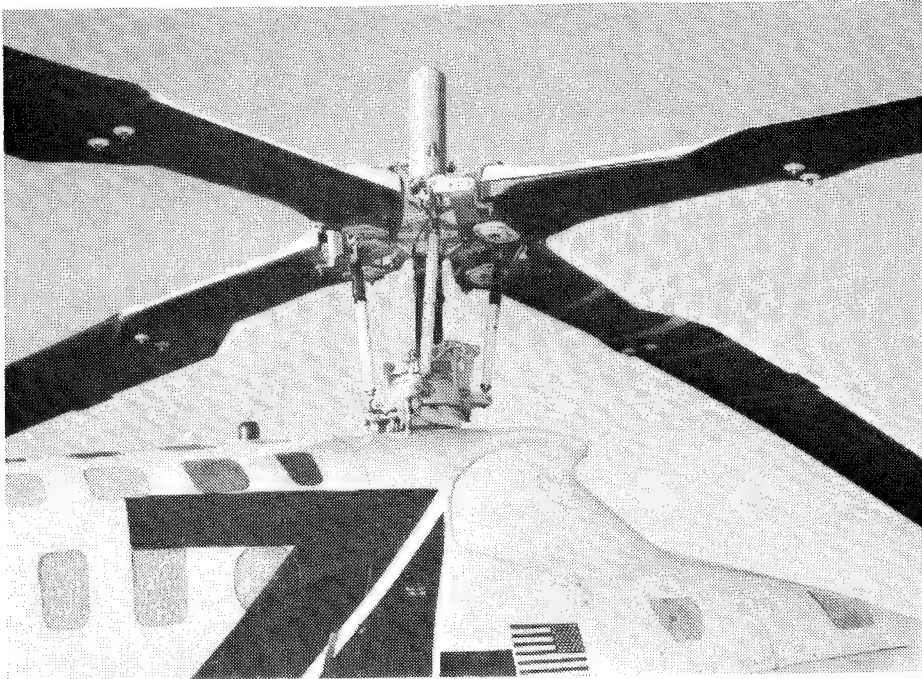


Figure 1-16

BELL ADVANCED BEARINGLESS ROTOR SYSTEM FOR 14,000 - 18,000 POUND HELICOPTERS

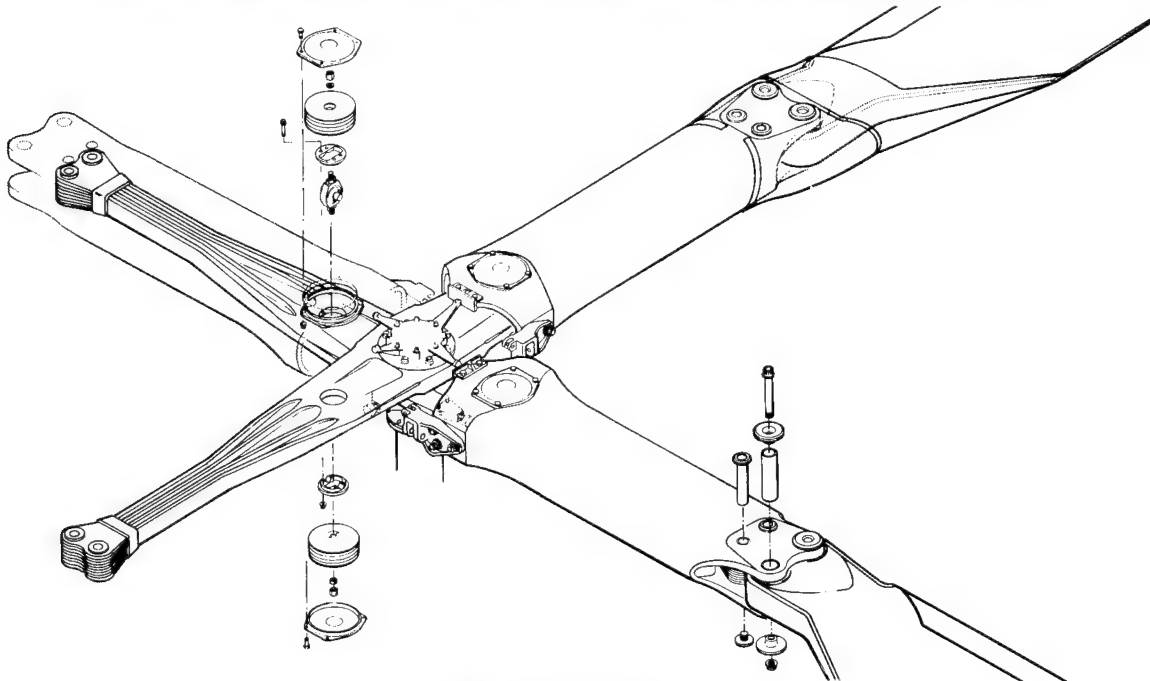


Figure 1-17

AH-1W HELICOPTER WITH ADVANCED BEARINGLESS ROTOR SYSTEM

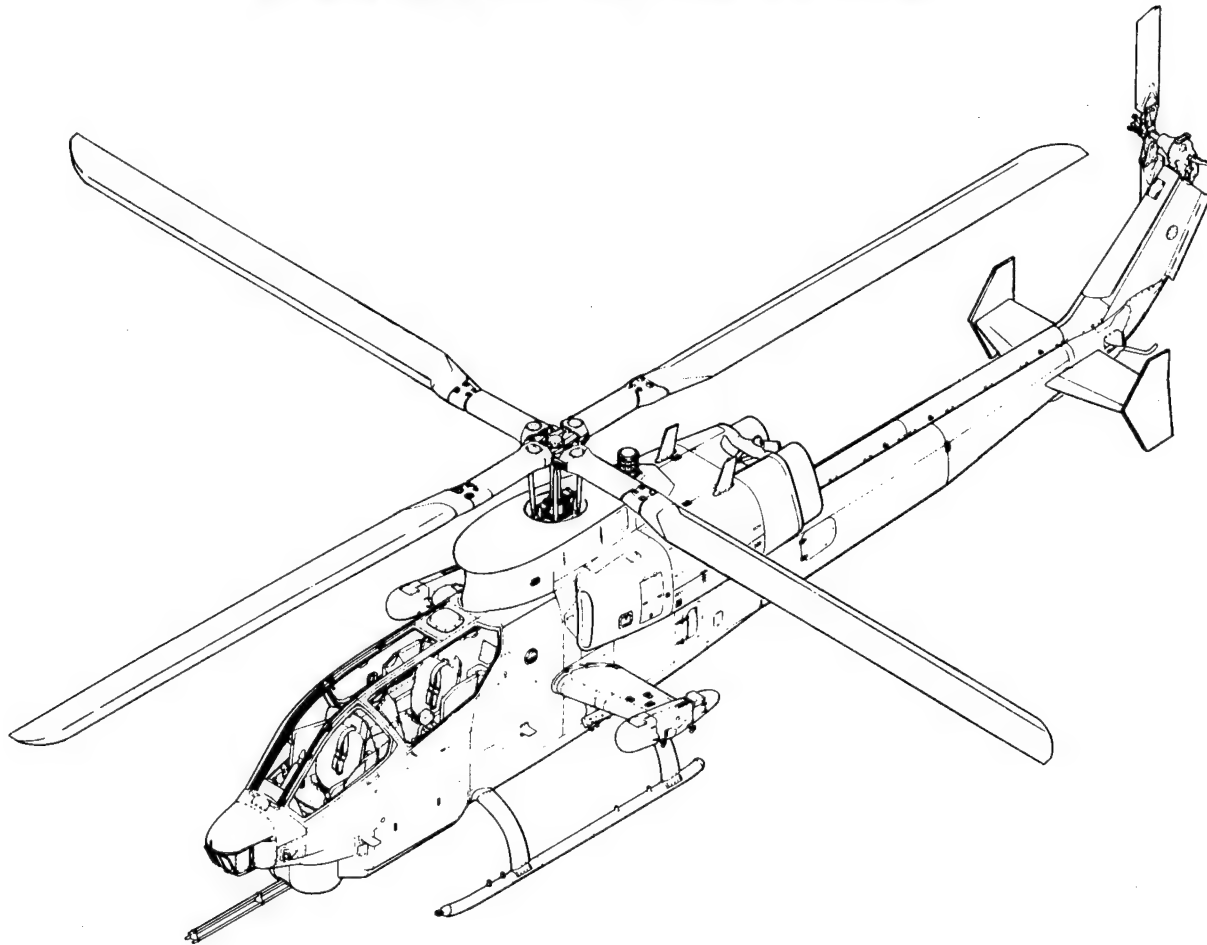


Figure 1-18

COMPARISON OF BHTI ROTOR AIRFOIL CHARACTERISTICS

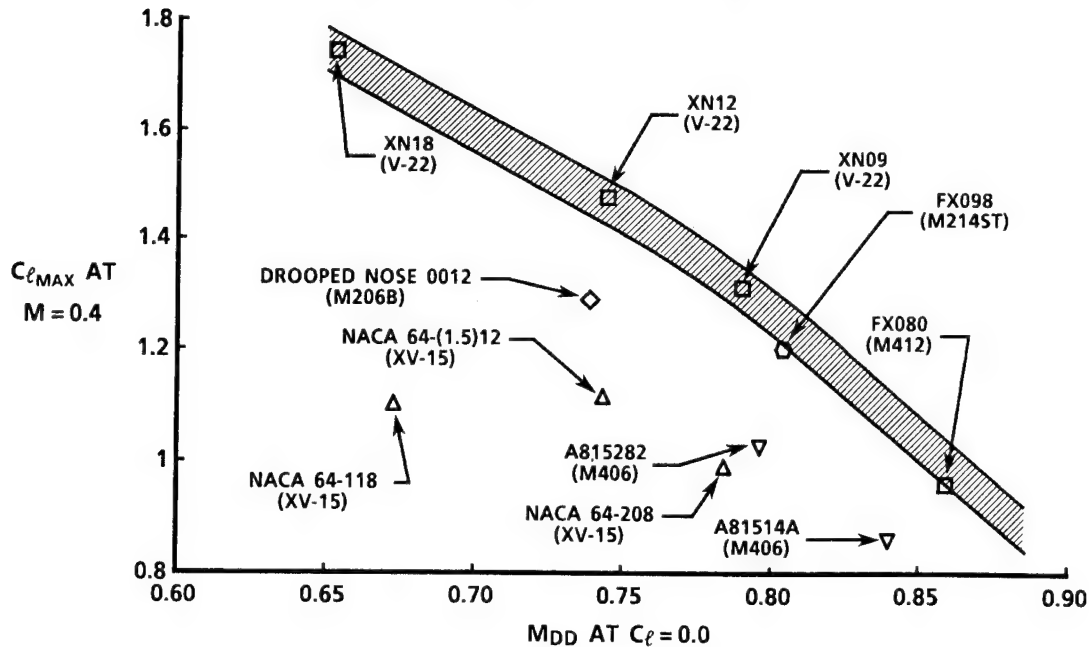


Figure 2-1

TILT ROTOR AIRFOIL DESIGN GOALS AND CONSTRAINTS

RADIAL STATION r/R	DESIGN CONSTRAINTS		AERODYNAMIC DESIGN OPTIMIZATION GOALS			
	t/c	INCOMP. C_{m_0}	MANEUVER ($C_{l_{max}}$)	CRUISE (C_d)	MAX. SPEED (M_{DD})	HOVER (L/D_{max})
1.0	0.09	-0.02	1.35 @ $M = 0.6$	0.006 @ $C_l = 0.3$ $M = 0.75$	0.81 @ $C_l = 0.3$	80.0 @ $M = 0.65$
0.75	0.12	-0.03	1.40 @ $M = 0.45$	0.006 @ $C_l = 0.2$ $M = 0.65$	0.72 @ $C_l = 0.2$	95.0 @ $M = 0.5$
0.50	0.18	-0.05	1.50 @ $M = 0.3$	0.007 @ $C_l = 0.0$ $M = 0.57$	0.64 @ $C_l = 0.0$	80.0 @ $M = 0.3$
0.25	0.28	-0.12	1.35 @ $M = 0.19$	0.018 @ $C_l = 0.0$ $M = 0.51$	0.59 @ $C_l = 0.0$	50.0 @ $M = 0.2$

Figure 2-2

COMPARISONS OF DESIGN GOAL WITH WIND TUNNEL DATA, XN-12 AIRFOIL

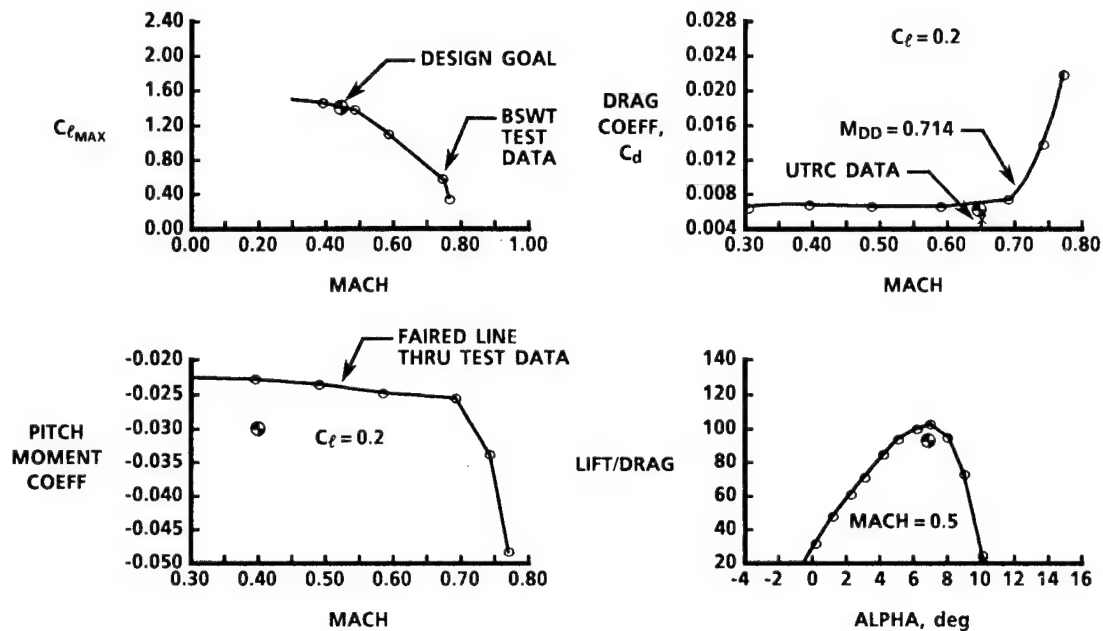


Figure 2-3

ROT22/OLS PRESSURE DISTRIBUTION CORRELATION AT 95 PERCENT RADIUS

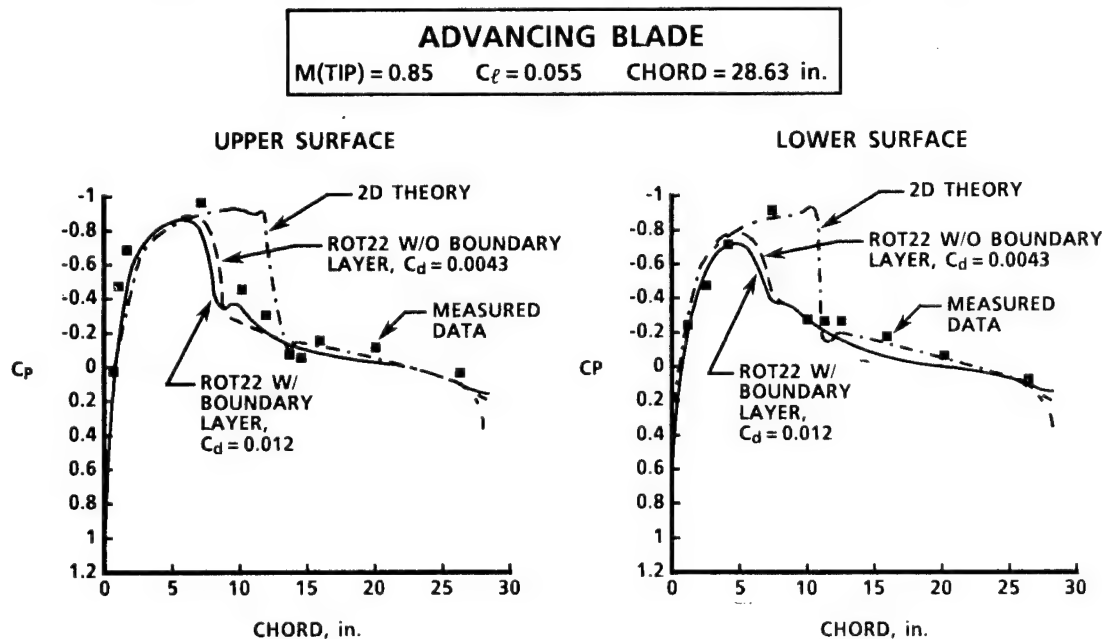


Figure 2-4

C81 NONUNIFORM INFLOW CORRECTION FACTOR

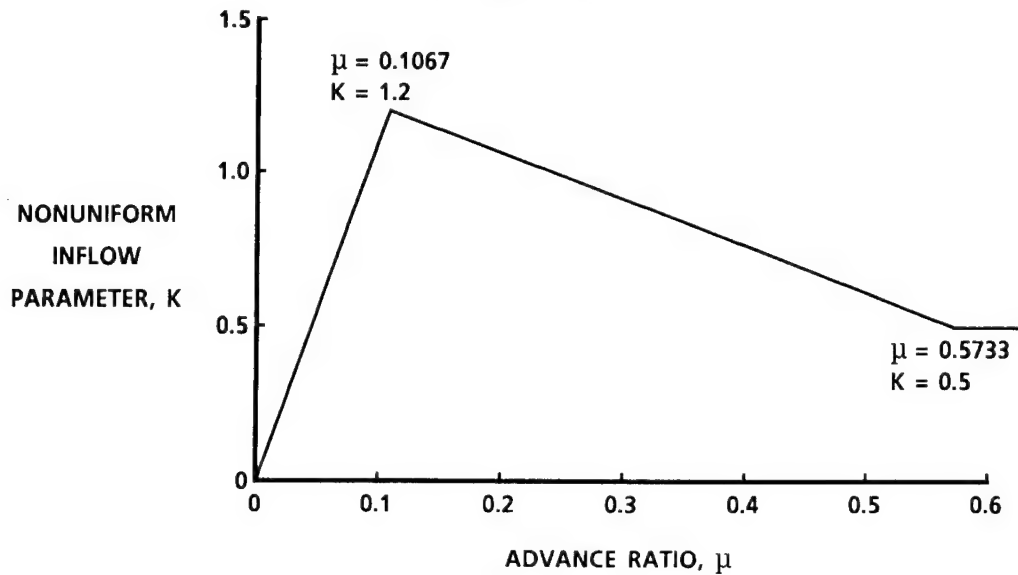


Figure 2-5

CORRELATION IN LATERAL FLAPPING

$C_{T/\sigma} = 0.08$	TIP SPEED = 450 ft/sec	SOLIDITY = 0.0892
$\alpha_{TPP} = +1^\circ$	RADIUS = 2.73 ft	CORE = 0.05

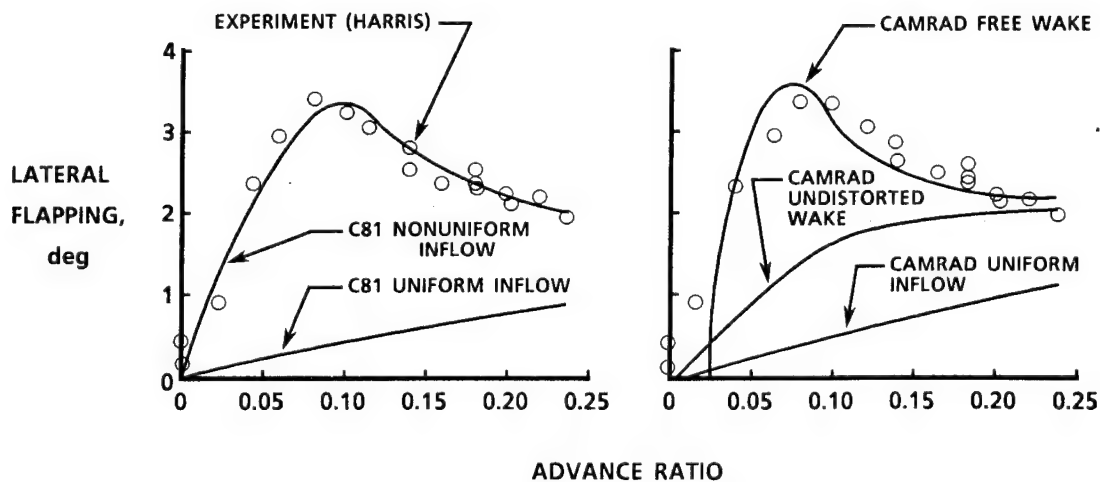


Figure 2-6

CORRELATION IN LONGITUDINAL FLAPPING

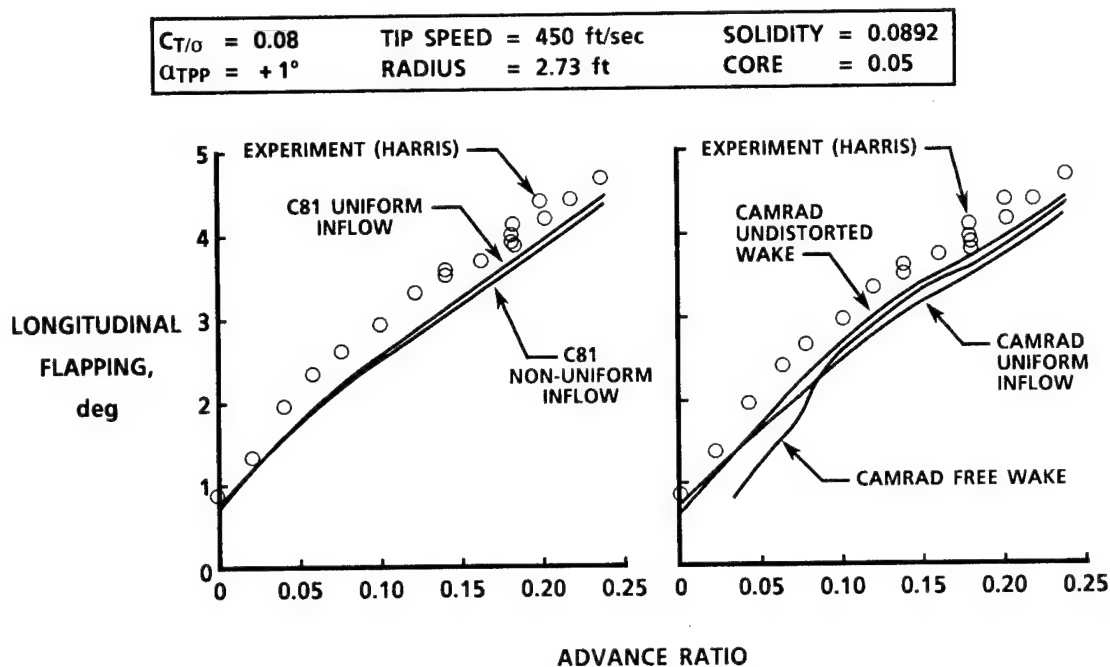


Figure 2-7

CORRELATION IN ROTOR POWER

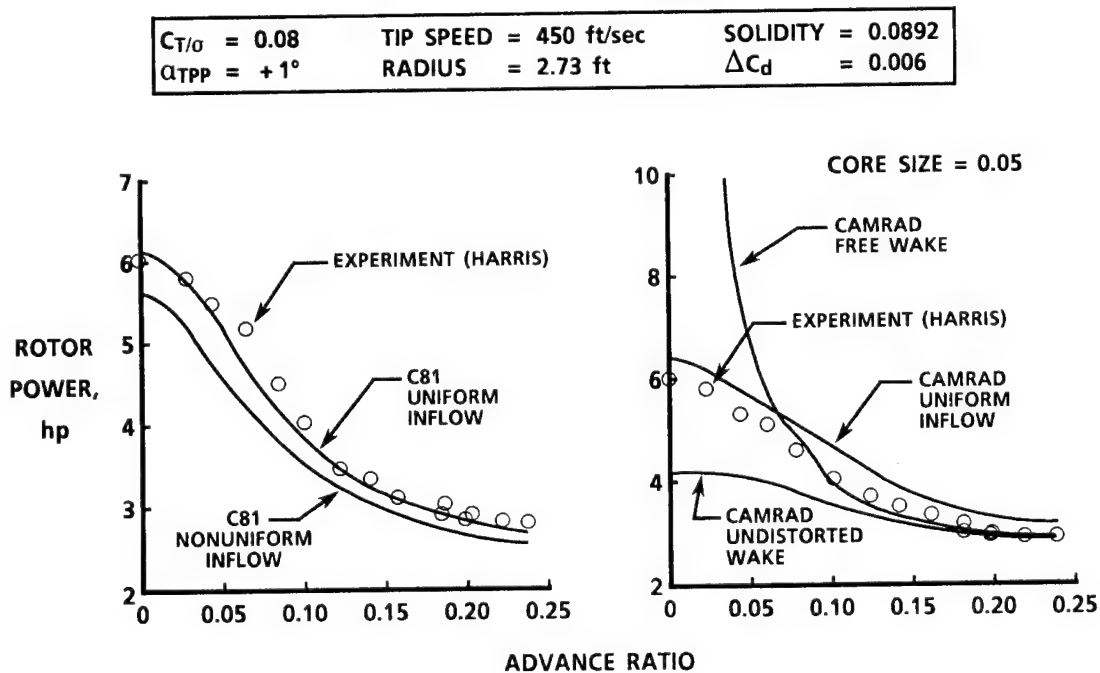


Figure 2-8

FORE AND AFT INDUCED-VELOCITY DISTRIBUTIONS

$C_{T/\sigma} = 0.08$	TIP SPEED = 450 ft/sec	SOLIDITY = 0.0892
$\alpha_{TPP} = +1^\circ$	RADIUS = 2.73 ft	ADVANCE RATIO = 0.08

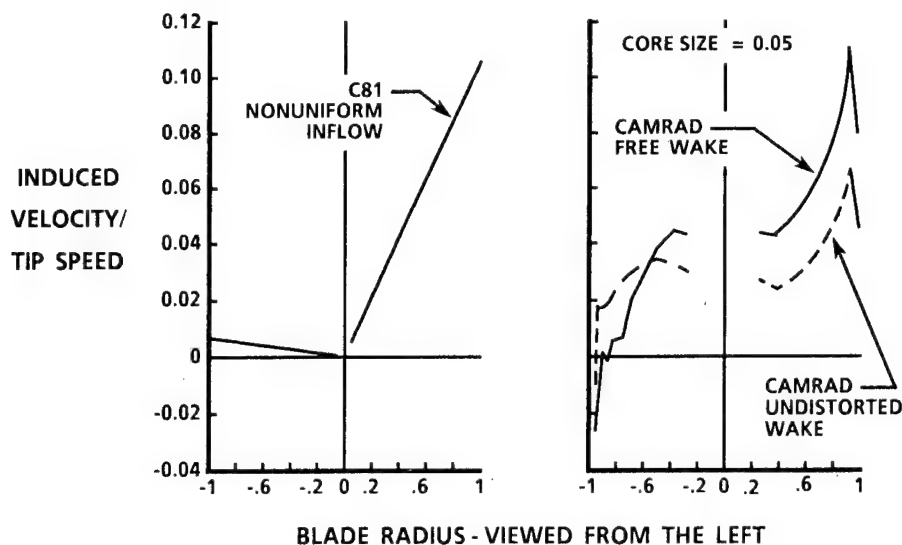


Figure 2-9

XV-15 HOVER PERFORMANCE CORRELATION

ISOLATED ROTOR

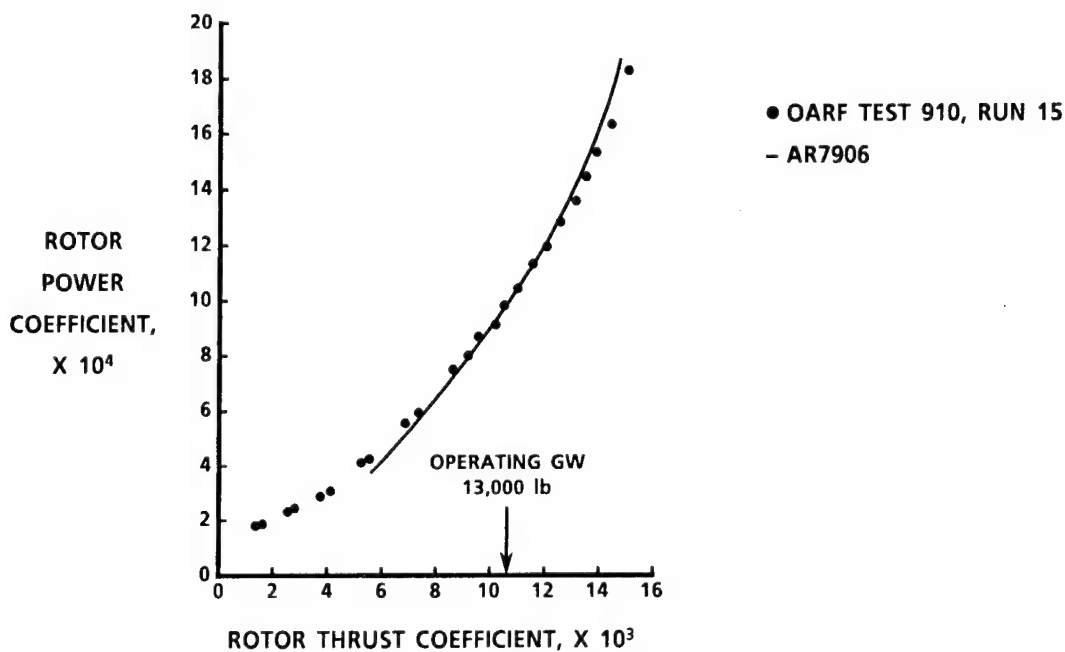


Figure 2-10

XV-15 PROPROTOR EFFICIENCIES CORRELATION

ISOLATED ROTOR

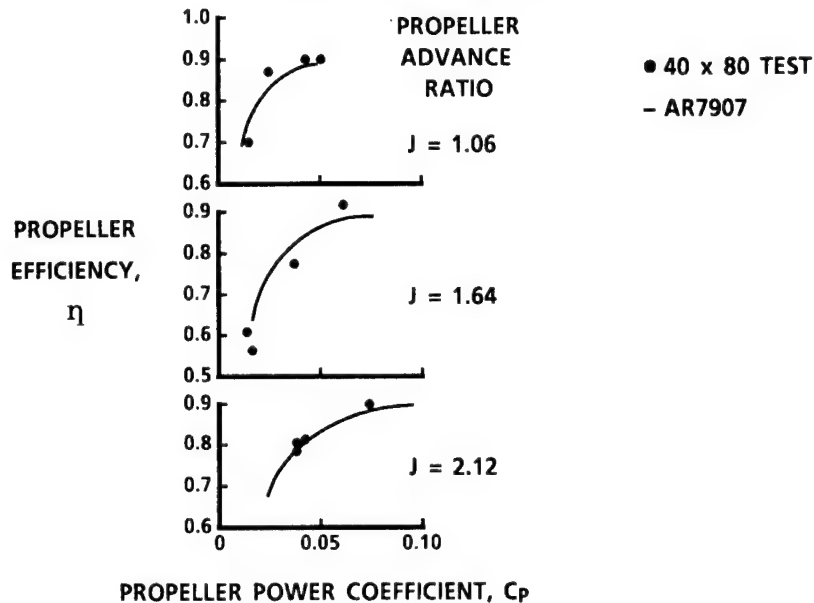


Figure 2-11

CONVERSION MODE XV-15 PROPROTOR PERFORMANCE CORRELATION WITH THEORY

ISOLATED ROTOR

40 X 80 TEST DATA PT.	○	□	◇	△	▽	▷
NACELLE ANGLE	77°	77°	60°	60°	30°	30°
ADVANCE RATIO	0.18	0.32	0.23	0.32	0.24	0.34

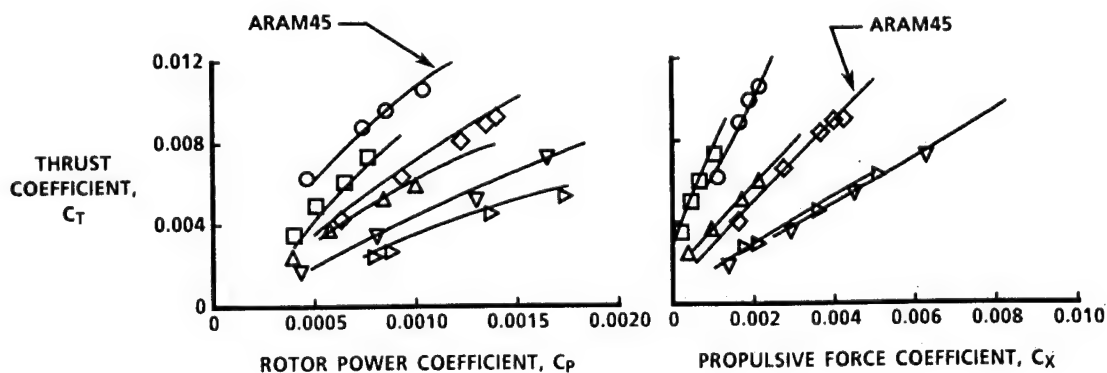


Figure 2-12

VSAERO AND TEST CORRELATION

ASPECT RATIO 30 WING PANEL MODEL

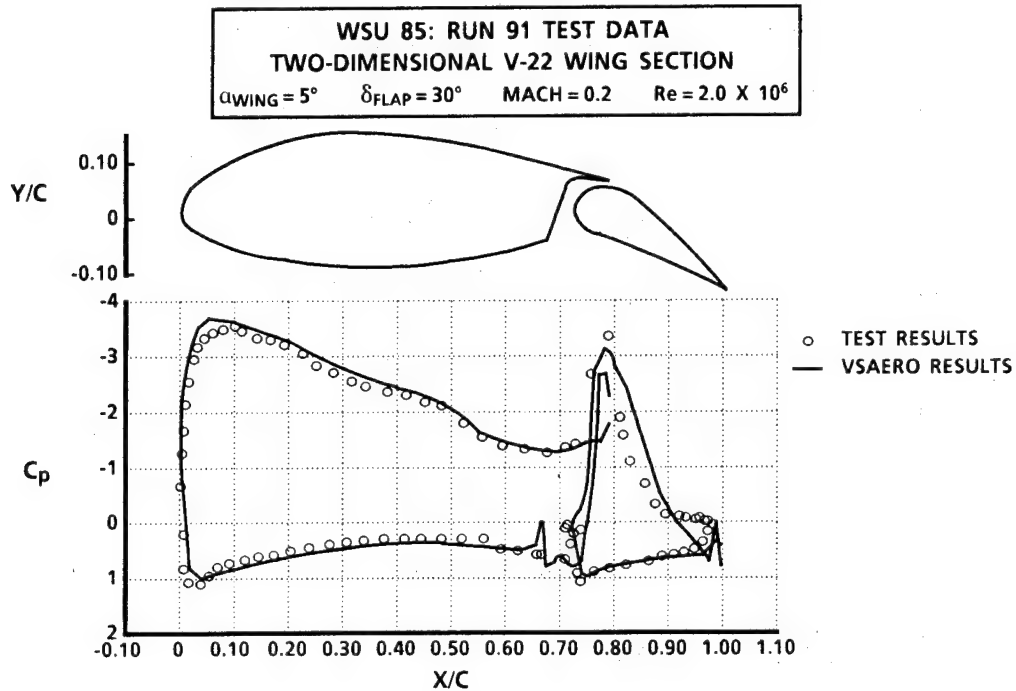


Figure 2-13

VSAERO AND TEST CORRELATION

V-22 SPINNER PANEL MODEL

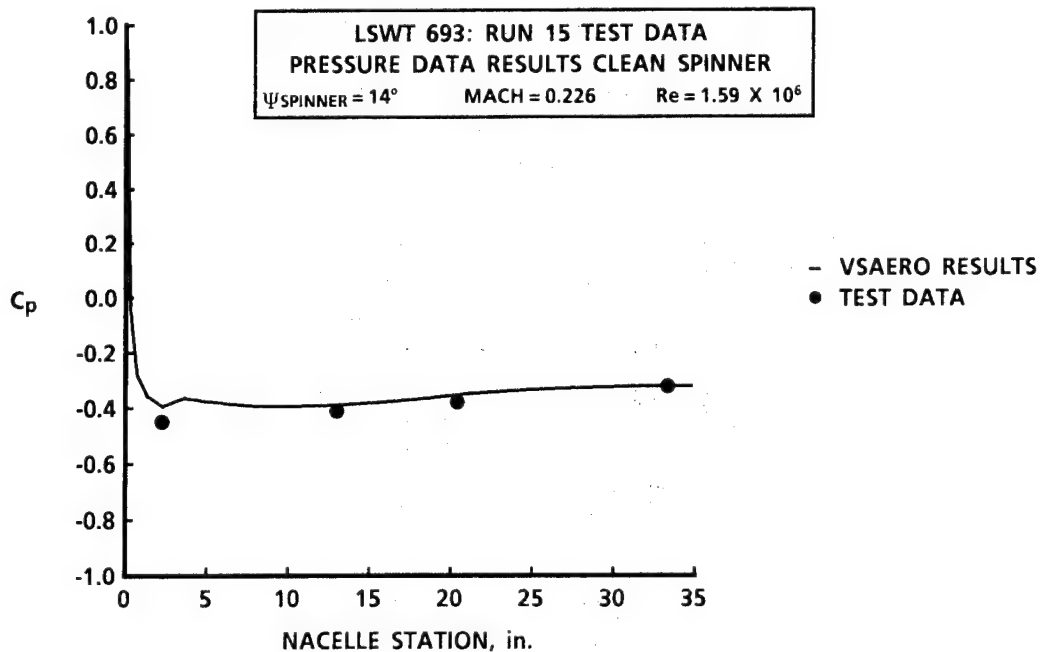


Figure 2-14

VSAERO AND TEST CORRELATION

WING/NACELLE PANEL MODEL

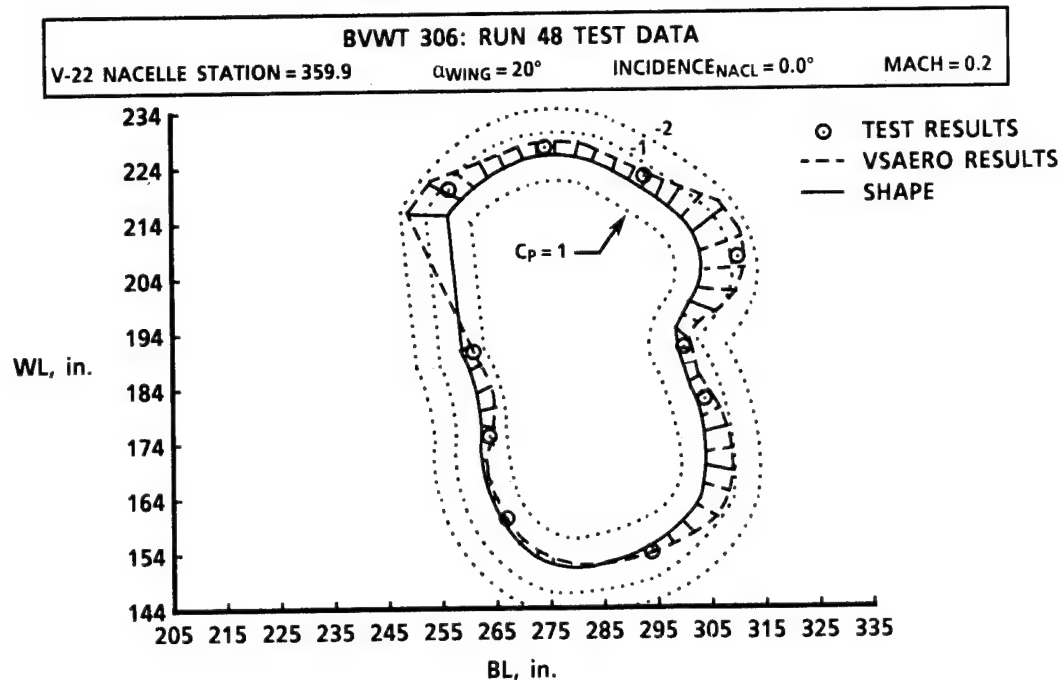


Figure 2-15

VSAERO AND TEST CORRELATION

V-22 INLET PANEL MODEL

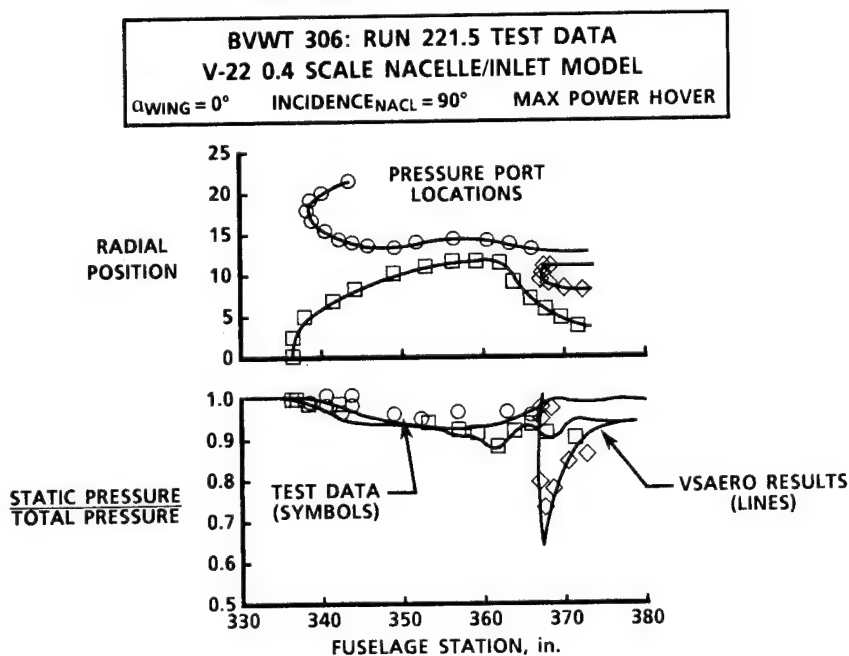


Figure 2-16

VSAERO TILT ROTOR AIRLOAD DISTRIBUTION

EMPENNAGE PANEL MODEL
SYMMETRICAL PULLOUT

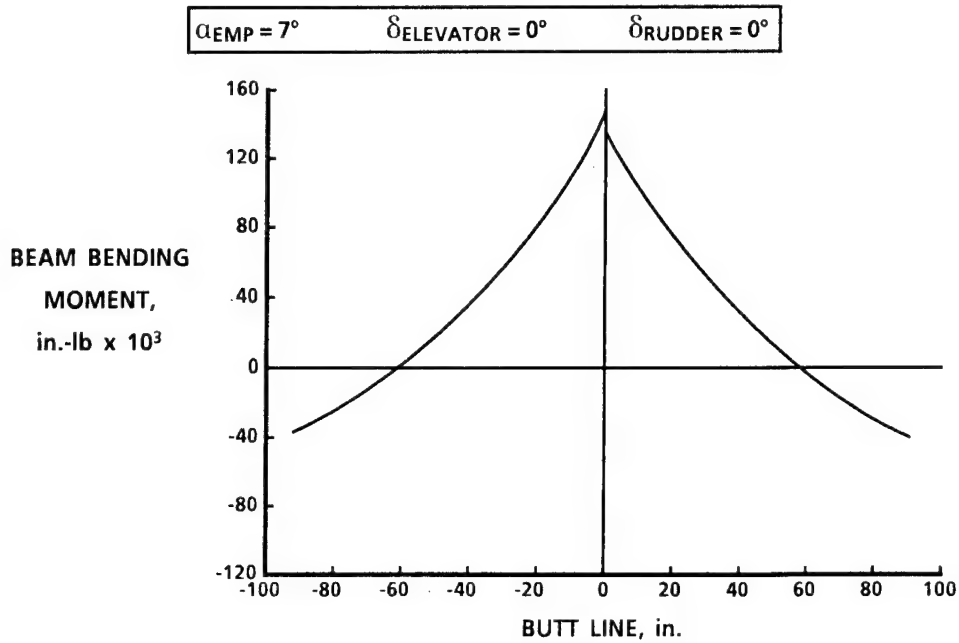


Figure 2-17

NORMALIZED 4/REV VERT. HUB SHEAR & 3/REV BLADE ROOT BEAM MOMENT VS AIRSPEED

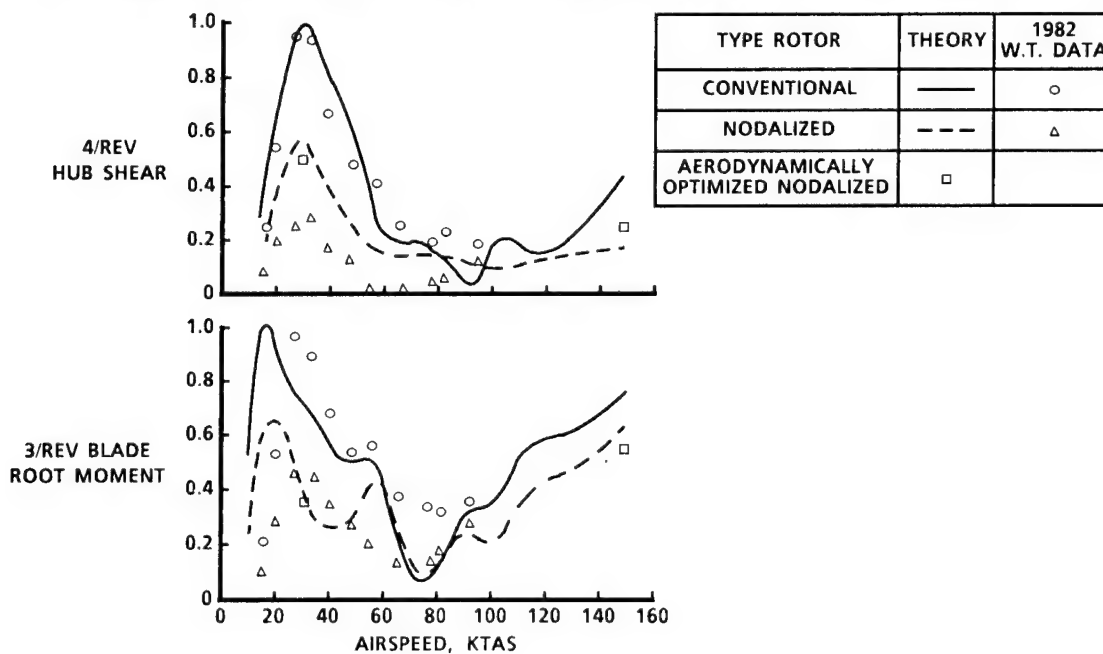


Figure 2-18

TYPICAL GEOMETRY FOR TILT ROTOR AIRCRAFT IN AIRPLANE MODE

AND THE INTERFERENCE VELOCITIES, ΔU_p & ΔU_t

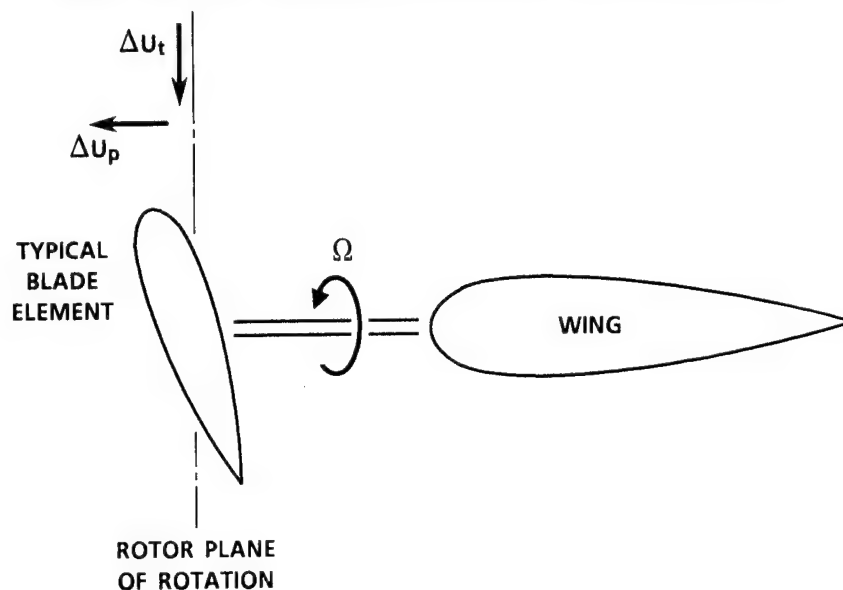


Figure 2-19

DYN5 SIMPLIFIED ANALYTICAL MODEL OF THE WING'S FLOW FIELD



Figure 2-20

CHANGE IN FLOW FIELD AT BLADE 60% RADIUS DUE TO THE PRESENCE OF AIRFRAME

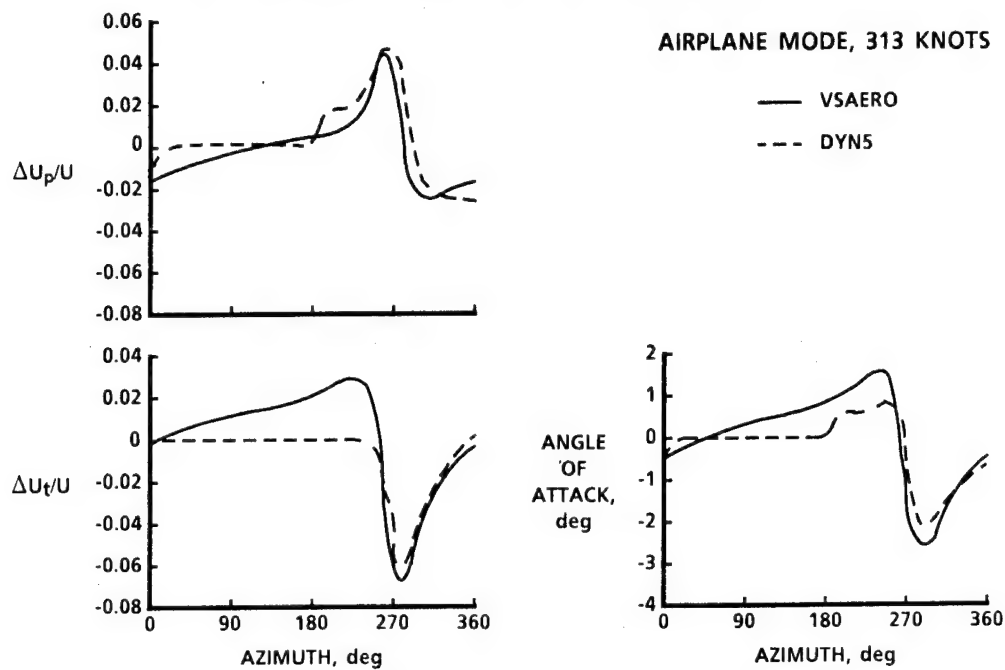


Figure 2-21

COMPARISON OF MEASURED AND CALCULATED BEAMWISE MOMENTS

V = 100 KEAS, RPM = 742, AIRPLANE MODE, WINDMILL

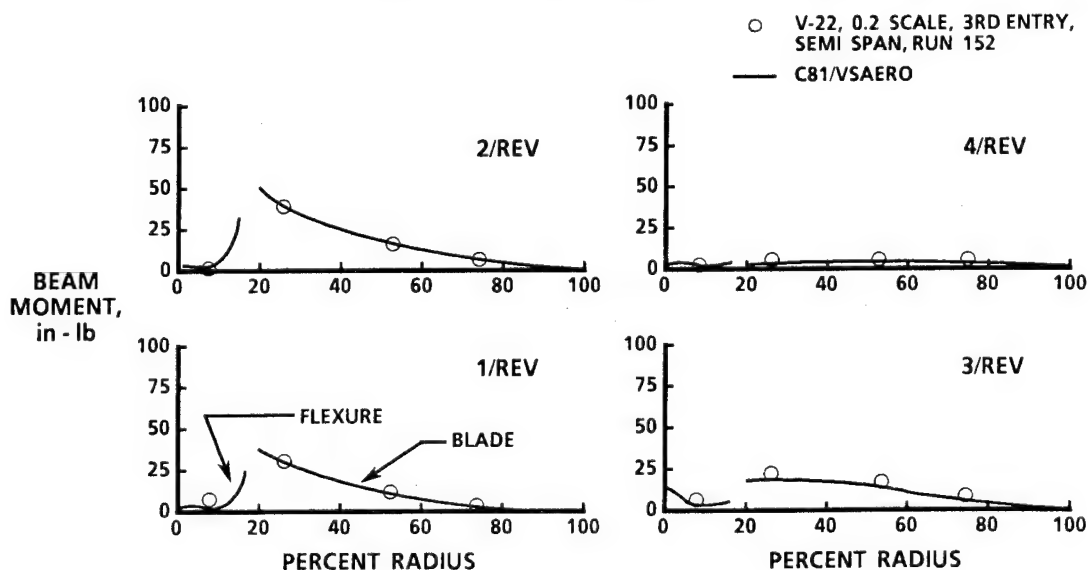


Figure 2-22

COMPARISON OF MEASURED AND CALCULATED CHORDWISE MOMENTS

V = 100 KEAS, RPM = 742, AIRPLANE MODE, WINDMILL

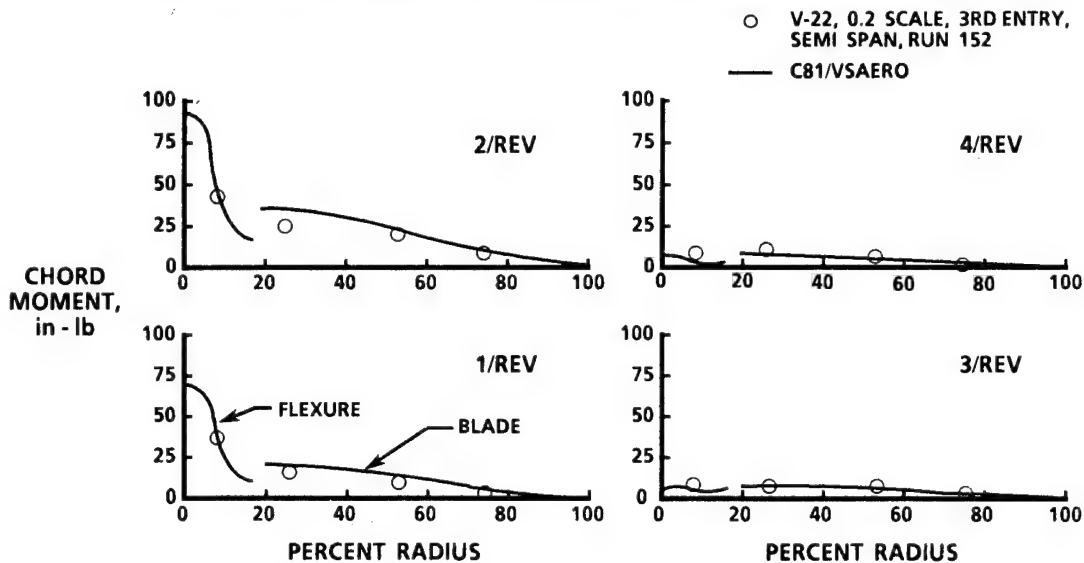


Figure 2-23

V-22 0.2-SCALE HUB SHEARS CALCULATED USING C81/VSAERO

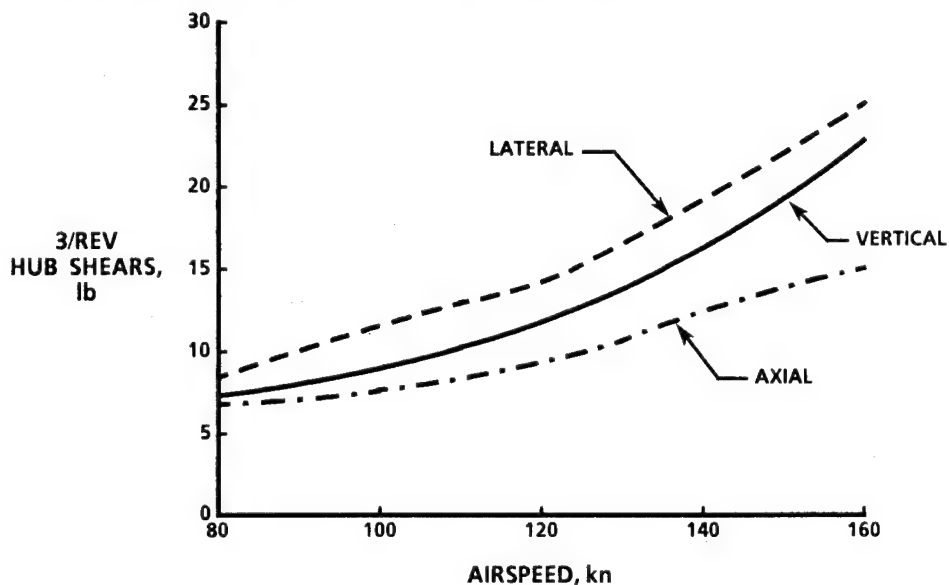


Figure 2-24

WINGTIP BOX FREQUENCY SUMMARY

PYLON AT 90° (HELICOPTER MODE)

MODE DESCRIPTION	MEASURED FREQUENCY (Hz)	ANALYSIS FREQUENCY (Hz)	
		PRETEST	POSTTEST
FIRST WING BEAMWISE BENDING	4.570	4.863	4.664
PYLON PITCH	5.202	4.514	4.89
PYLON YAW (WING AND PYLON OUT OF PHASE)	11.260	12.595	12.629
WING TORSION	27.160	24.287	28.910

Figure 2-25

WINGTIP BOX FREQUENCY SUMMARY

PYLON AT 0° (AIRPLANE MODE)

MODE DESCRIPTION	MEASURED FREQUENCY (Hz)	ANALYSIS FREQUENCY (Hz)	
		PRETEST	POSTTEST
FIRST WING BEAMWISE BENDING	5.757	5.269	4.937
FIRST WING CHORDWISE BENDING (WING AND PYLON IN PHASE)	8.026	8.919	8.313
PYLON YAW (WING AND PYLON OUT OF PHASE)	15.078	16.385	15.057
WING TORSION	24.471	25.953	25.027

Figure 2-26

CORRELATION OF PROPROPOTOR STABILITY

925 RPM (104%), PYLON OFF THE DOWNSTOP

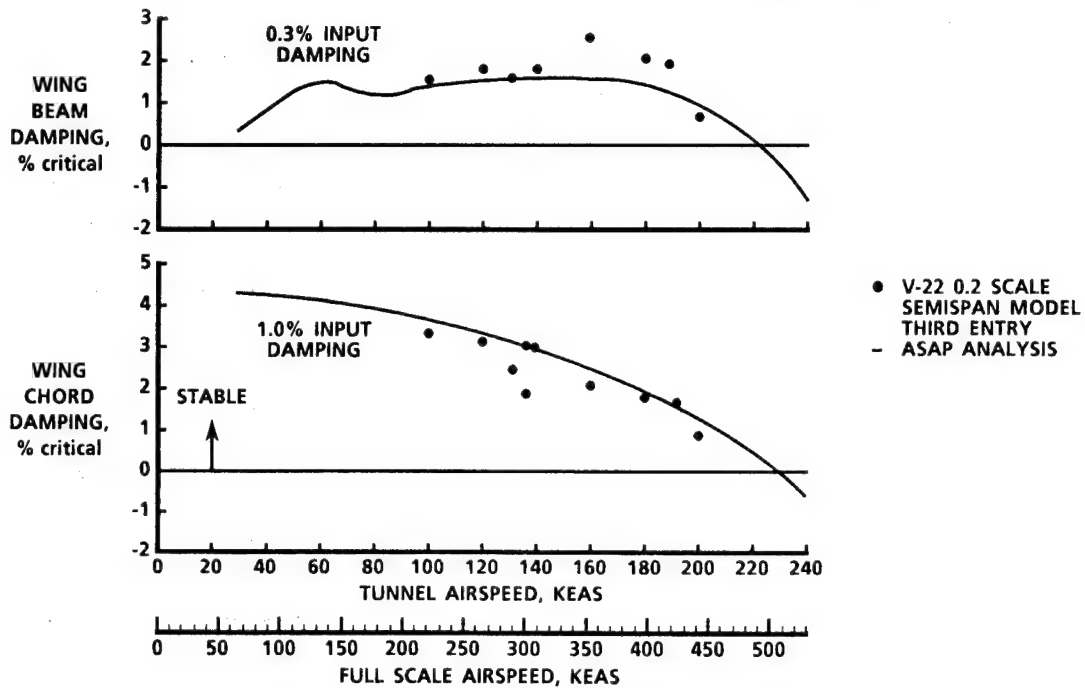


Figure 2-27

PITCH ATTITUDE RESPONSE TO LONGITUDINAL CYCLIC, 100 KIAS

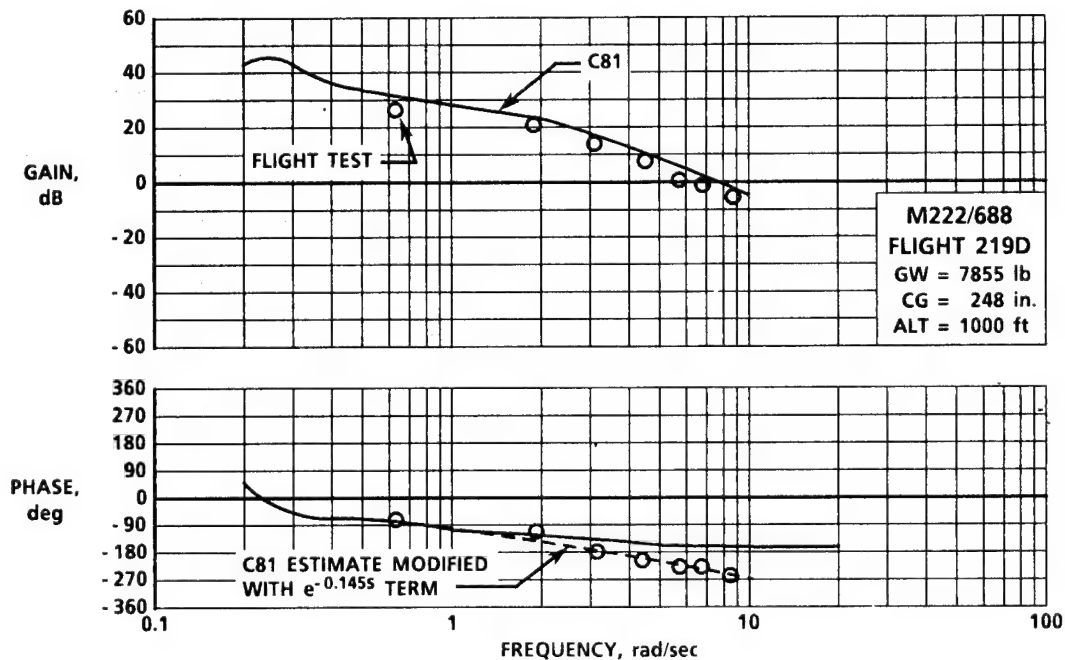


Figure 2-28

XV-15 AIRPLANE MODE, 4.2 G MANEUVER, 216 KIAS

SHIP 702 GW = 13590 lb CG = 298.5 in.

— FLIGHT 290, CTR 1014

--- C81

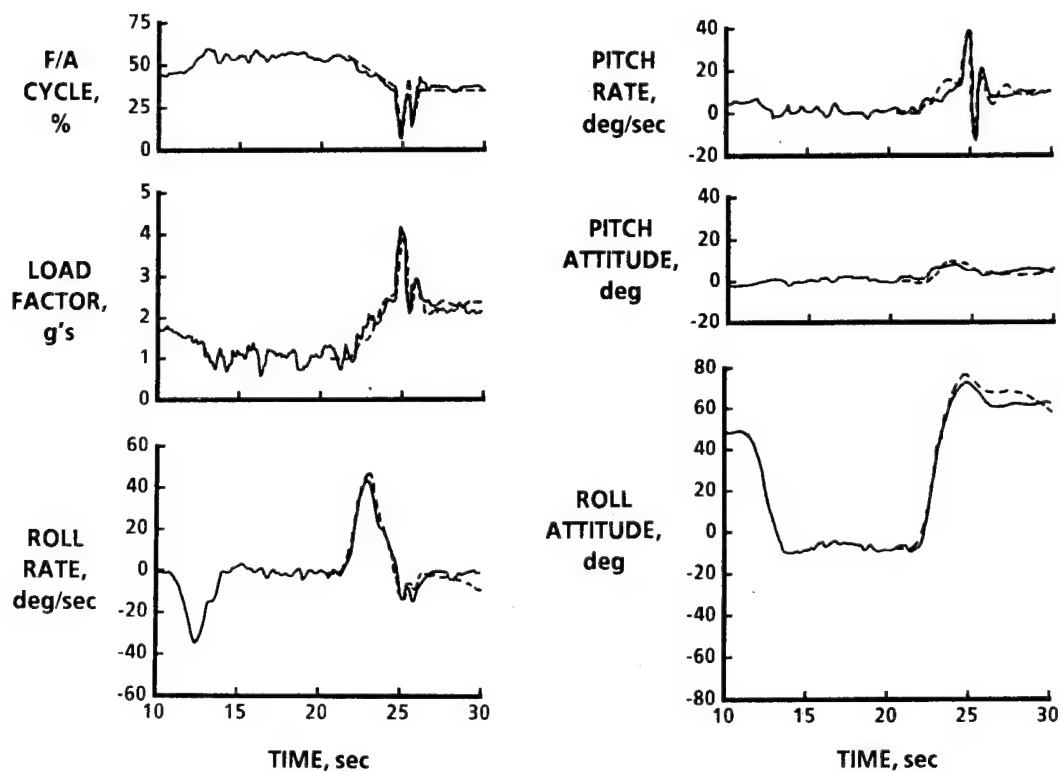


Figure 2-29

V-22 JOINT SERVICES VERTICAL LIFT TRANSPORT

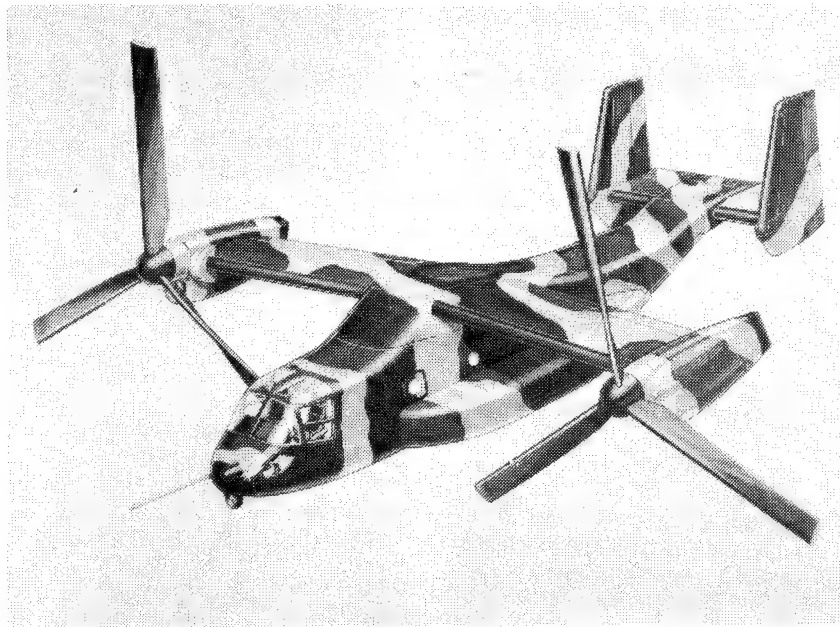


Figure 3-1

V-22 TILT ROTOR ASW AIRCRAFT

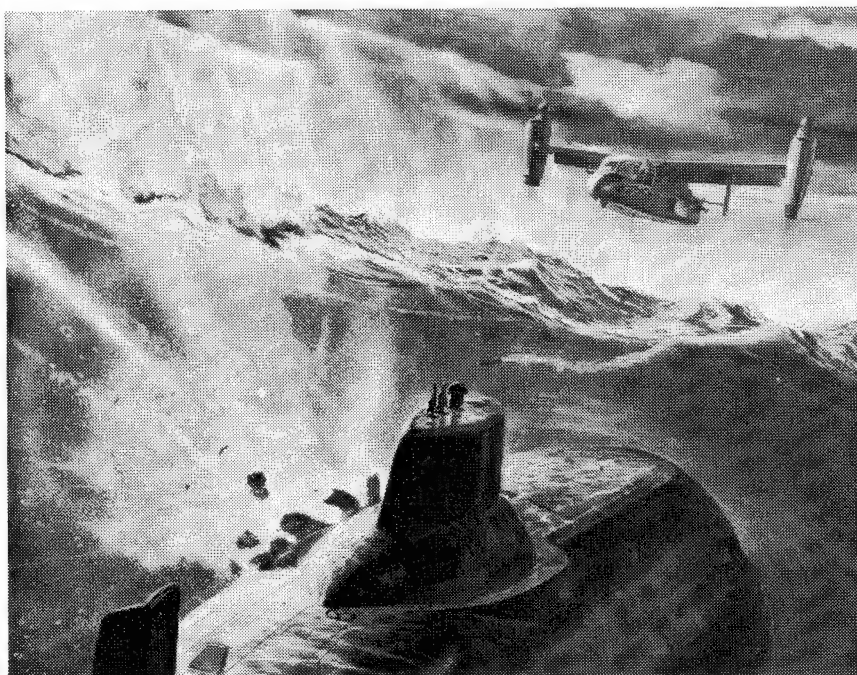


Figure 3-2

V-22 GUNSHIP

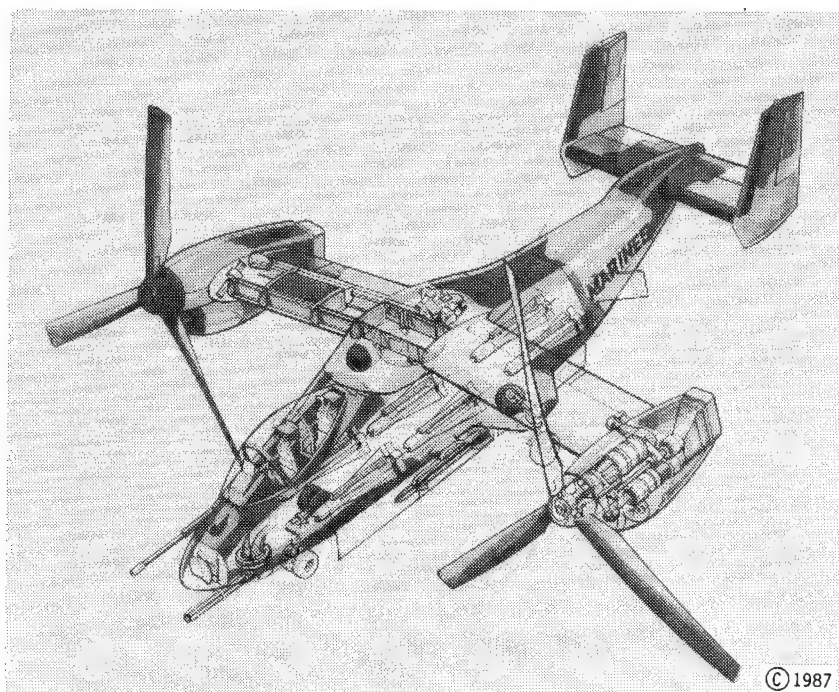


Figure 3-3

MEDIUM MIDWING GUNSHIP

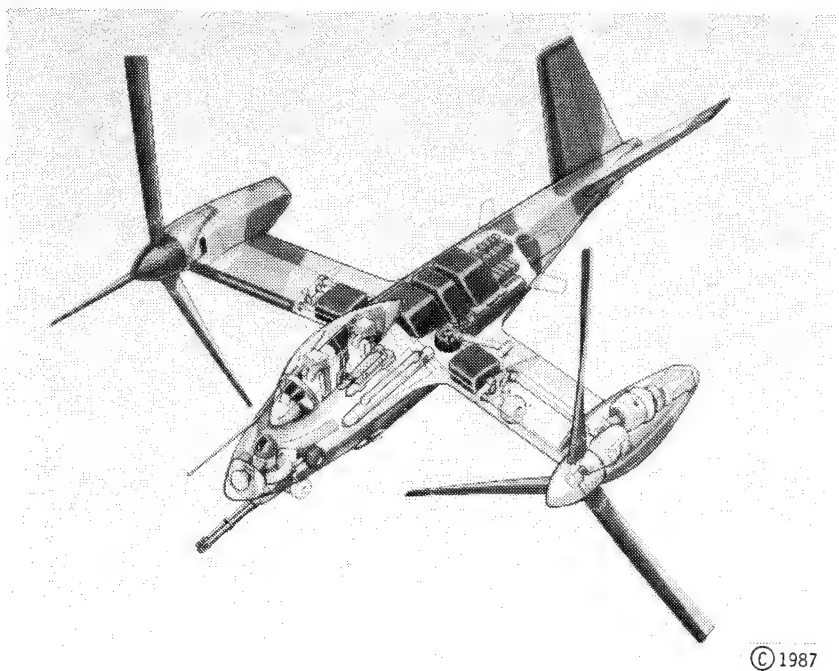


Figure 3-4

MULTIPURPOSE LIGHT TILT ROTOR GUNSHIP

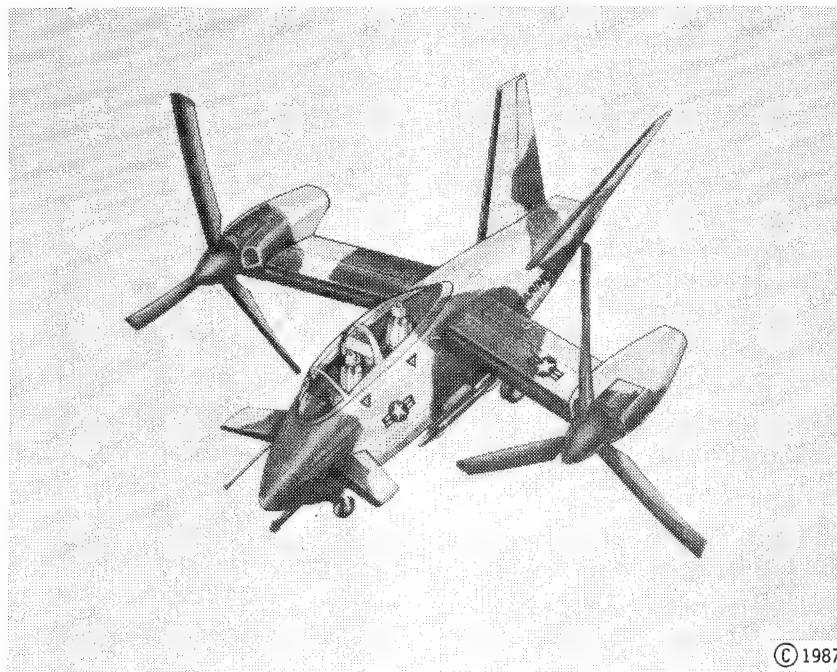


Figure 3-5

COMMERCIAL VERSION OF V-22

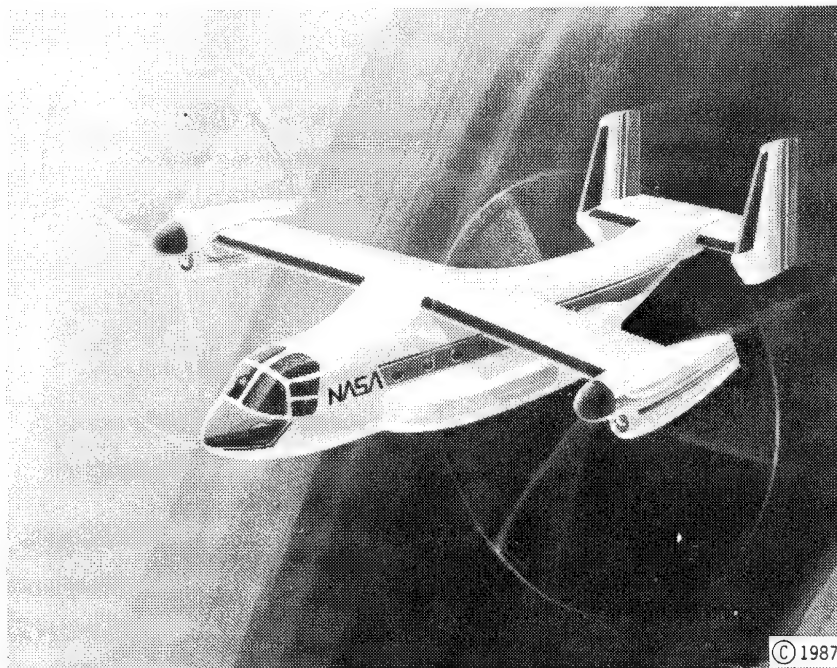


Figure 3-6

COMMERCIAL TILT ROTOR CONFIGURATION 1

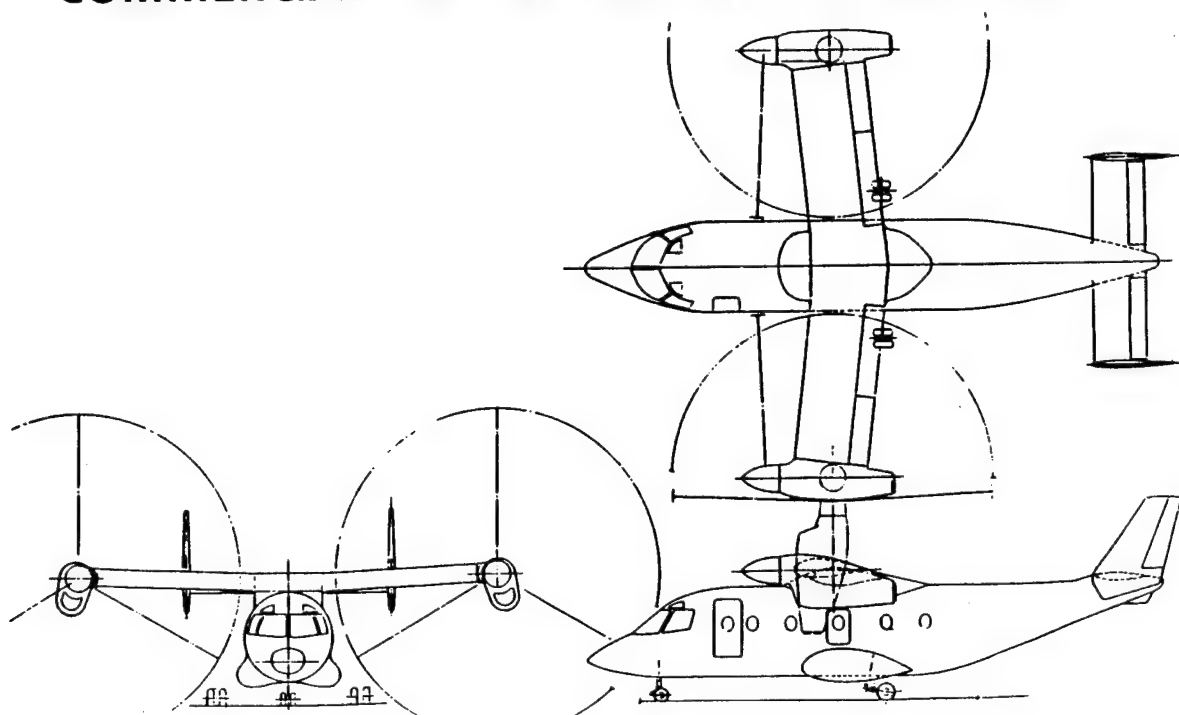


Figure 3-7

COMMERCIAL TILT ROTOR CONFIGURATION 2

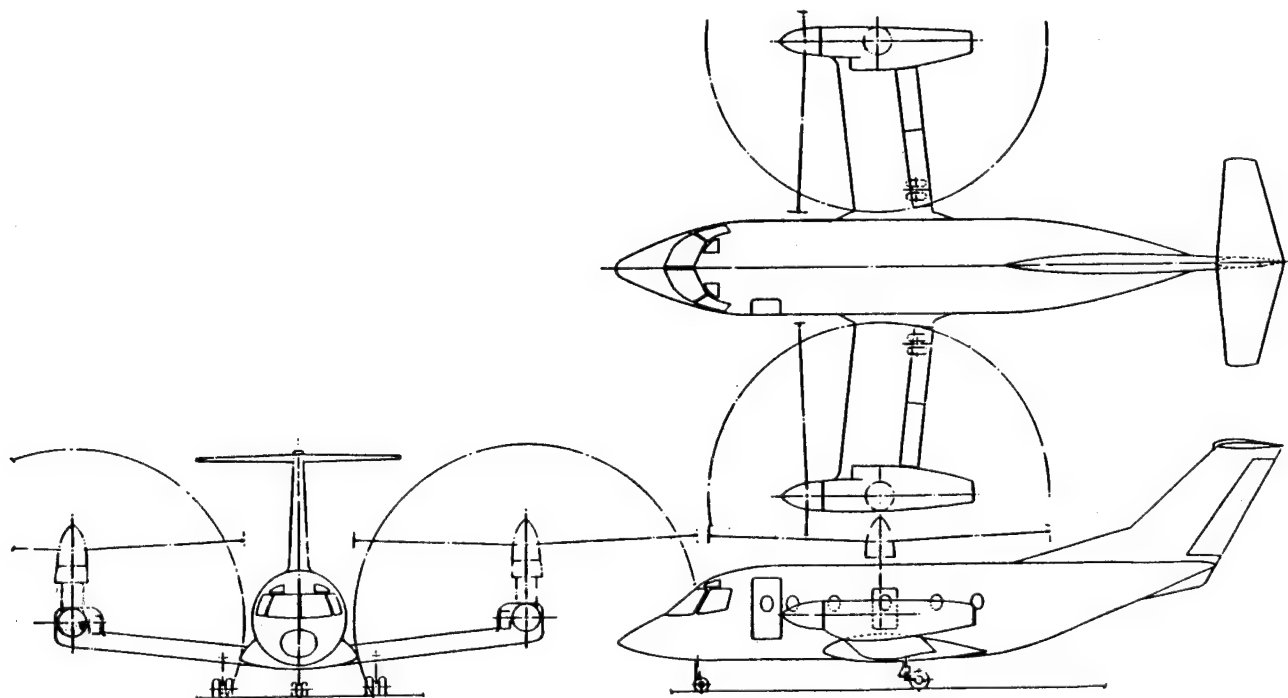


Figure 3-8

COMMERCIAL TILT ROTOR CONFIGURATION 3

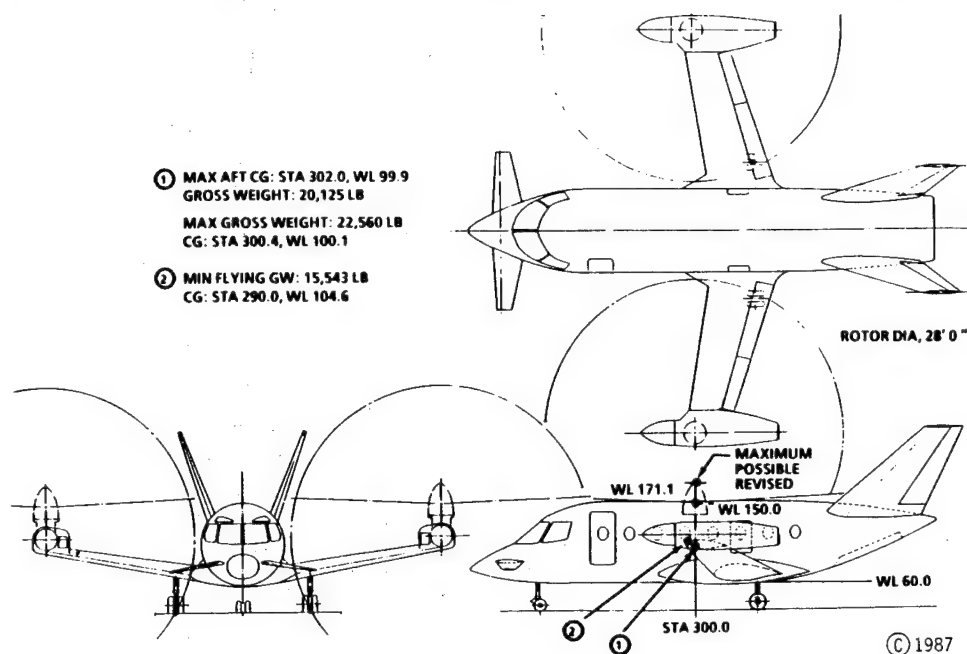


Figure 3-9

TILT ROTOR EXECUTIVE TRANSPORT

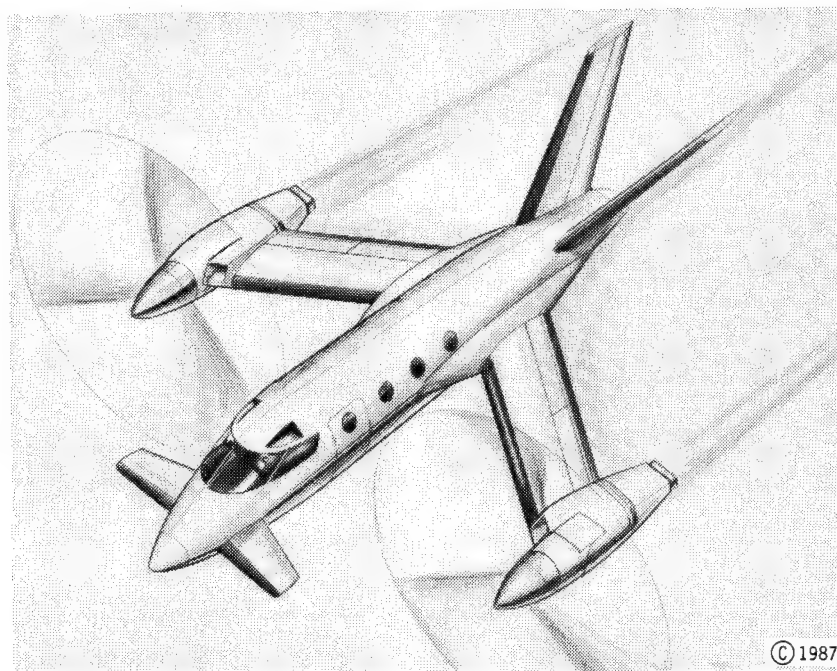


Figure 3-10

TILT ROTOR AIRLINER

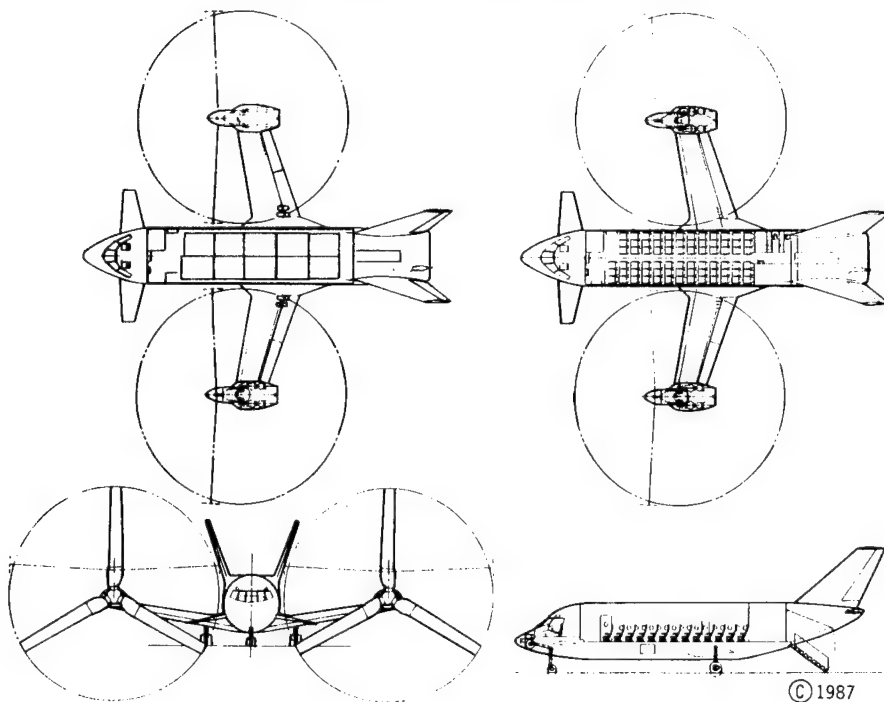


Figure 3-11

TILT-FOLD FIGHTER AIRCRAFT

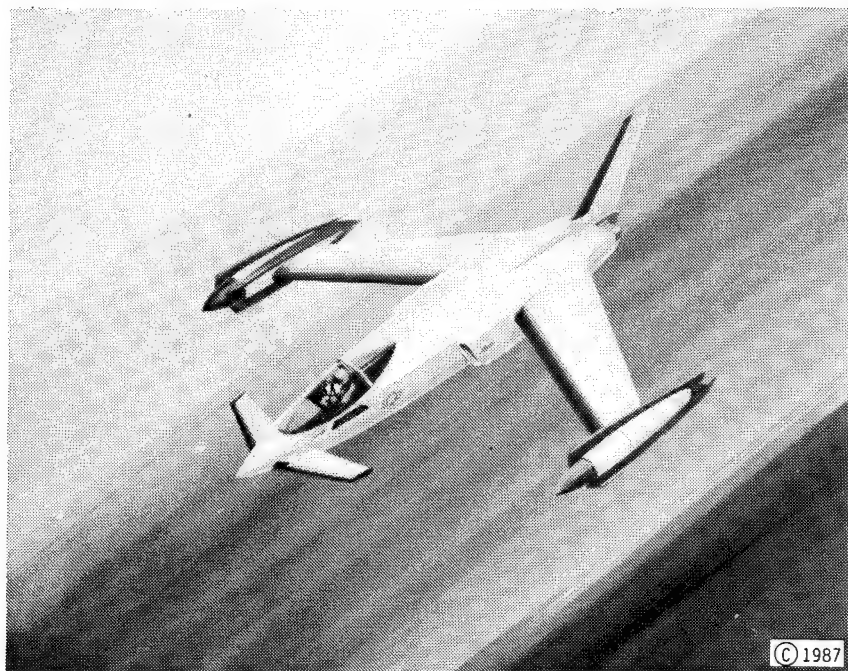


Figure 3-12

FULL-SCALE TILT-FOLD ROTOR TEST

NASA'S 40- BY 80-FOOT WIND TUNNEL

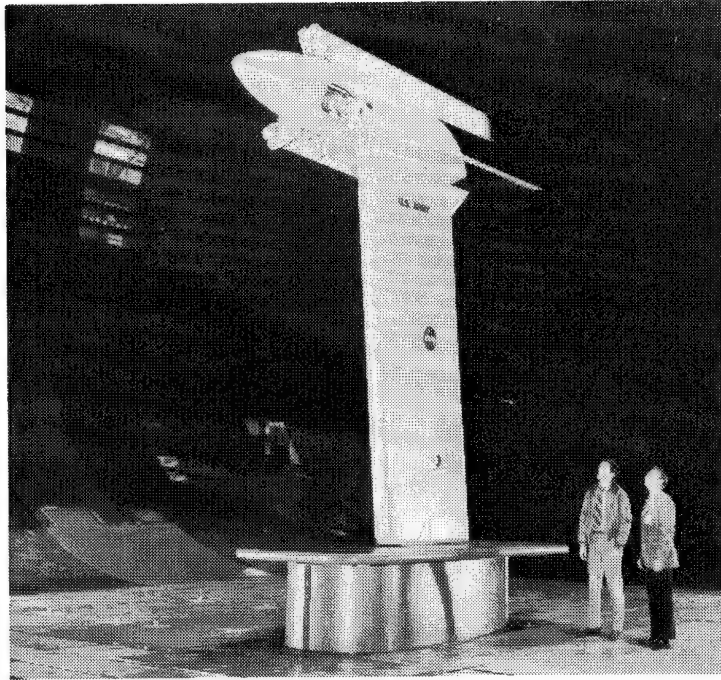


Figure 3-13

CONVERTIBLE-ENGINE CONCEPTS

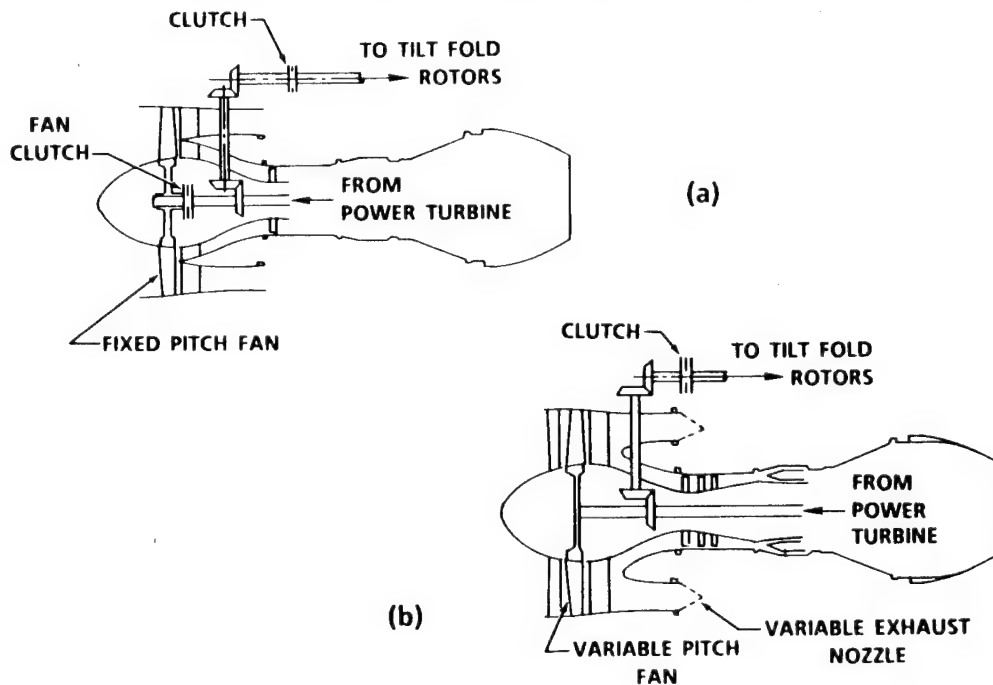


Figure 3-14

SHIPBOARD-COMPATIBLE TILT-FOLD ASW AIRCRAFT

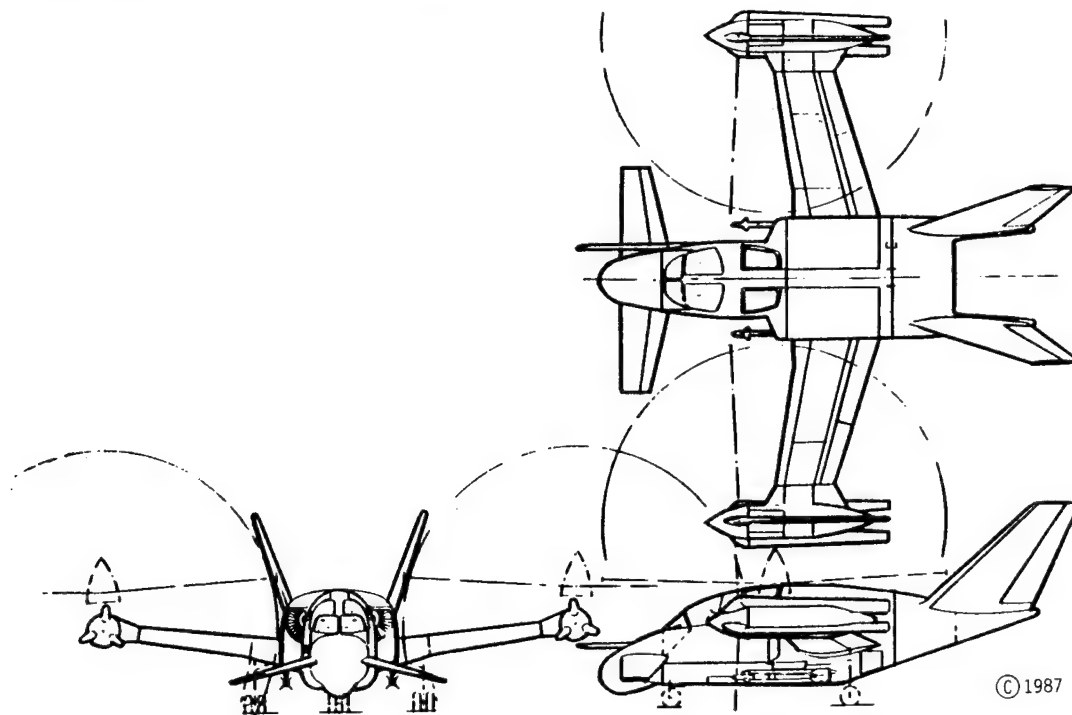


Figure 3-15

MIDRANGE RPV REQUIREMENTS

PARAMETER	REQUIREMENT
SPEED	MEDIUM TO HIGH SUBSONIC
ALTITUDE	LOW TO 30,000 FEET
MAXIMUM RANGE (RADIUS)	300 NAUTICAL MILES (EXTEND TO 400 NMI WITH AIR LAUNCH)
FLIGHT TIME	2 TO 3 HOURS
LAUNCH	GROUND, SURFACE, AIR (A-6)*

*NOT REQUIRED IF RPV HAS SUFFICIENT RANGE.

Figure 3-16

MIDRANGE RPV MISSION PROFILE

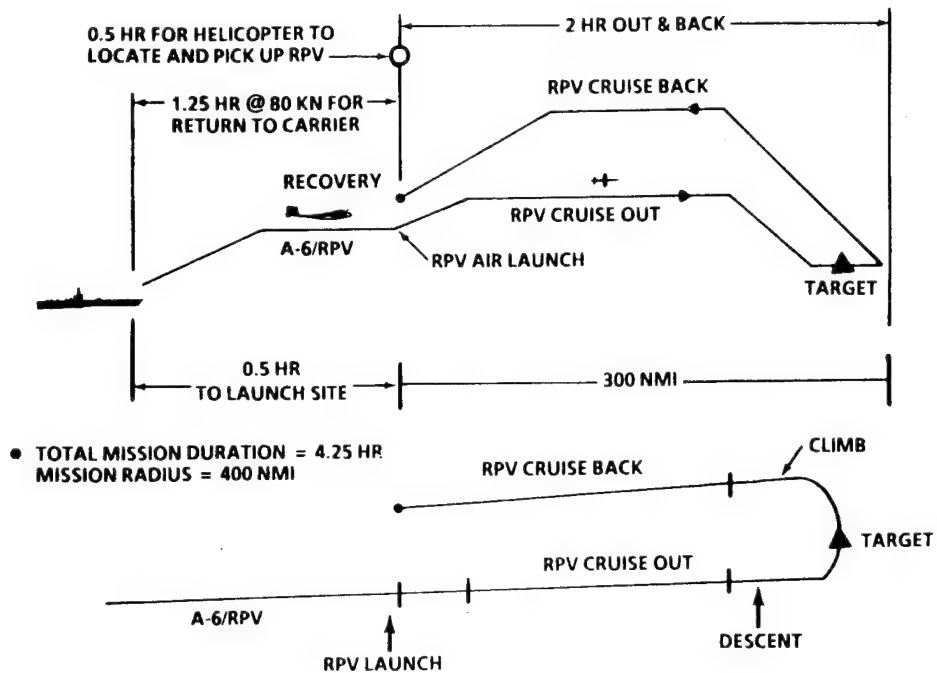


Figure 3-17

CONCEPTUAL TILT ROTOR RPV

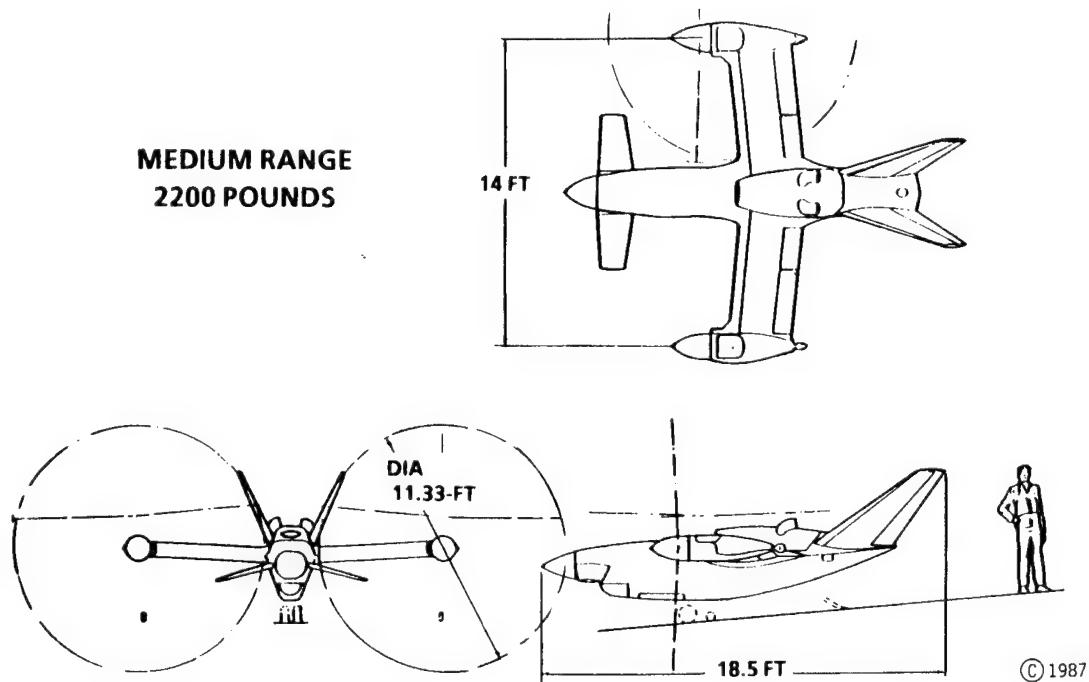


Figure 3-18

WEIGHT AND PERFORMANCE SUMMARY

2200-POUND TILT ROTOR RPV

WEIGHT

EMPTY WEIGHT	1150 LB
MAX FUEL CAPACITY	830 LB
MAX PAYLOAD ALLOWANCE	300 LB
MAX GROSS WEIGHT	2200 LB

PERFORMANCE AT 10,000 FT

MAX RANGE, 10% RESERVE	894 NMI
LONG RANGE CRUISE SPEED	204 KN
MAX SPEED	245 KN

Figure 3-19

TILT ROTOR RPV MISSION PROFILE

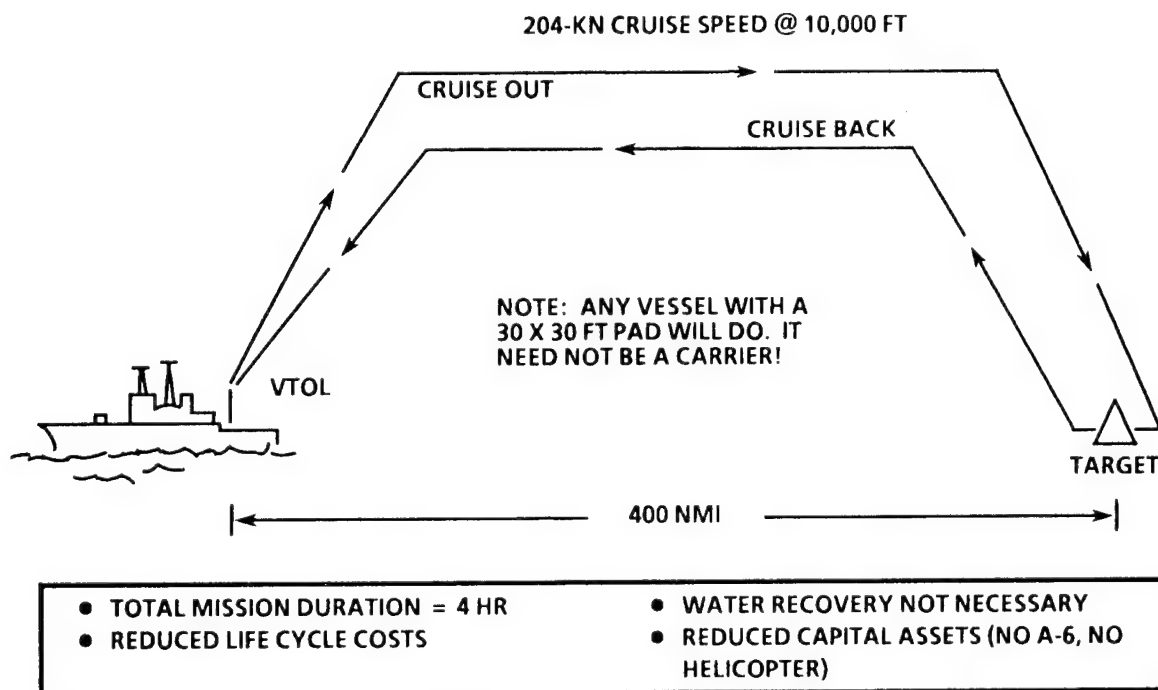


Figure 3-20

V-22 WIND TUNNEL TEST

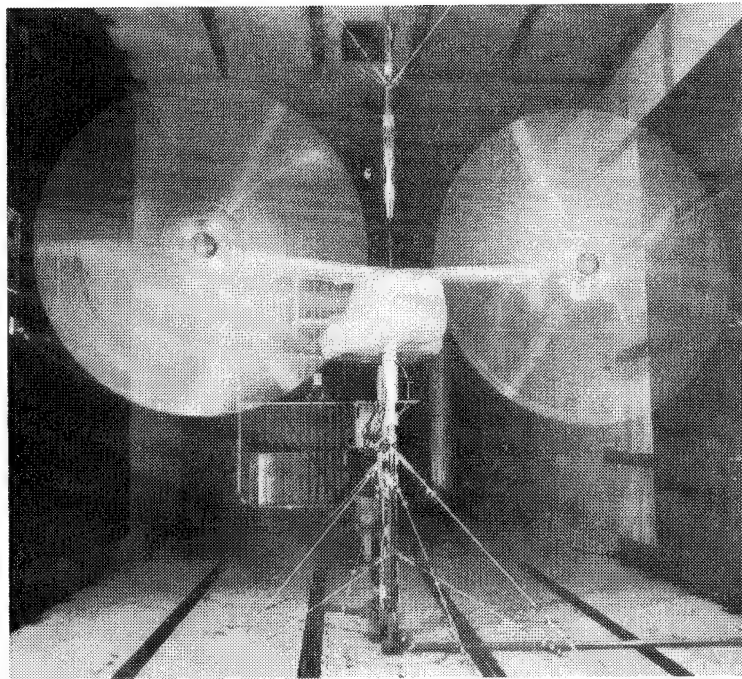


Figure 3-21

TILT ROTOR RPV DEMONSTRATOR

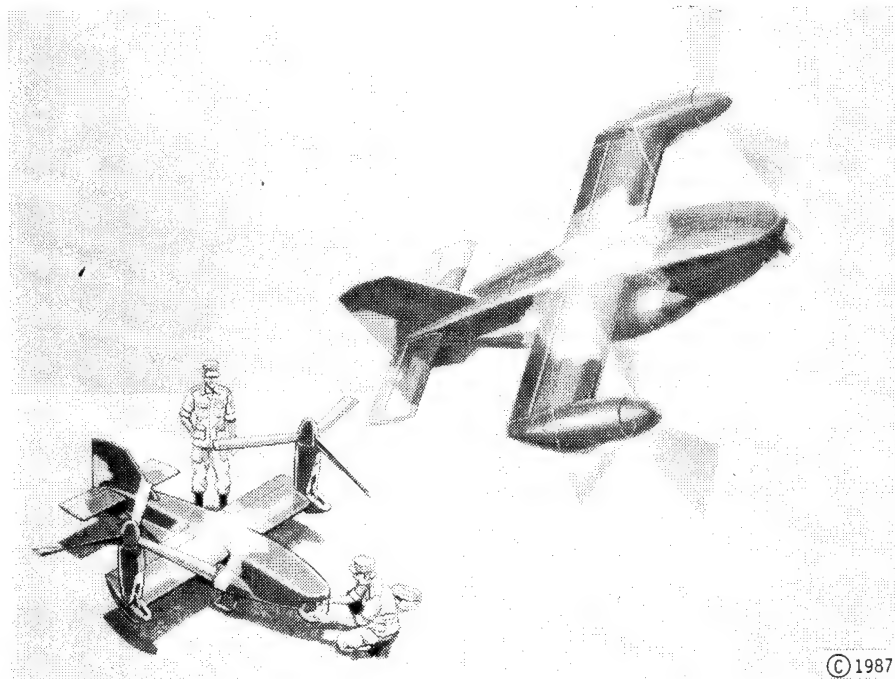


Figure 3-22

© 1987

SCHEMATIC OF RPV DRIVE SYSTEM

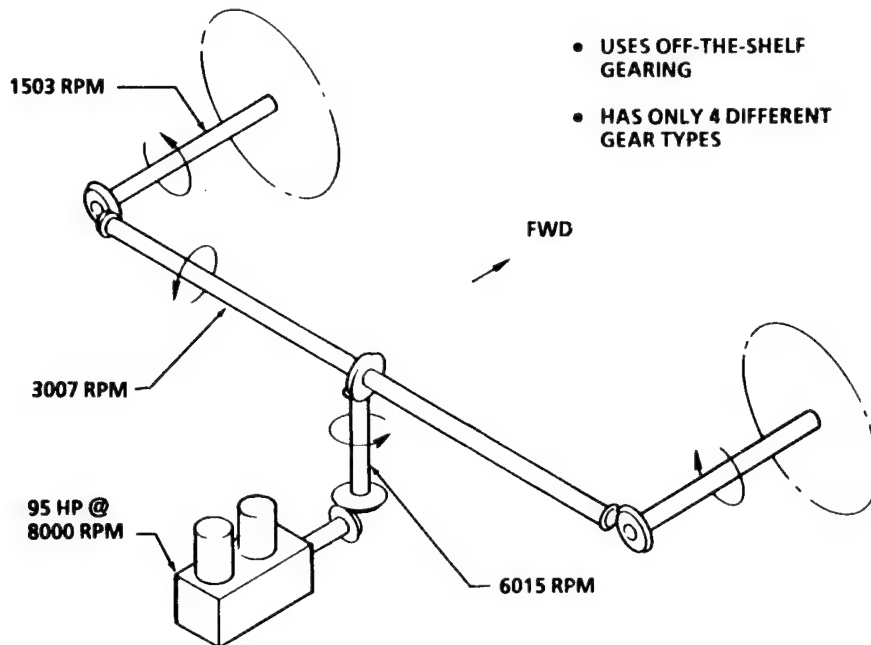


Figure 3-23

SCHEMATIC OF RPV NACELLE CONTROL MECHANISM SIMILAR TO XV-15

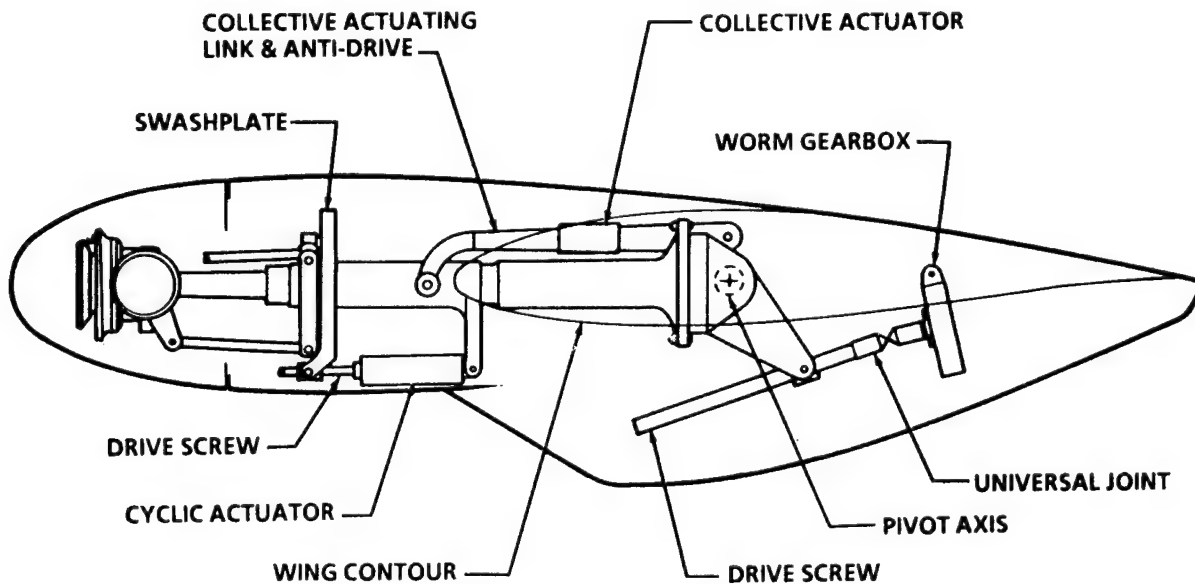


Figure 3-24

MODULAR STRUCTURE OF TILT ROTOR RPV

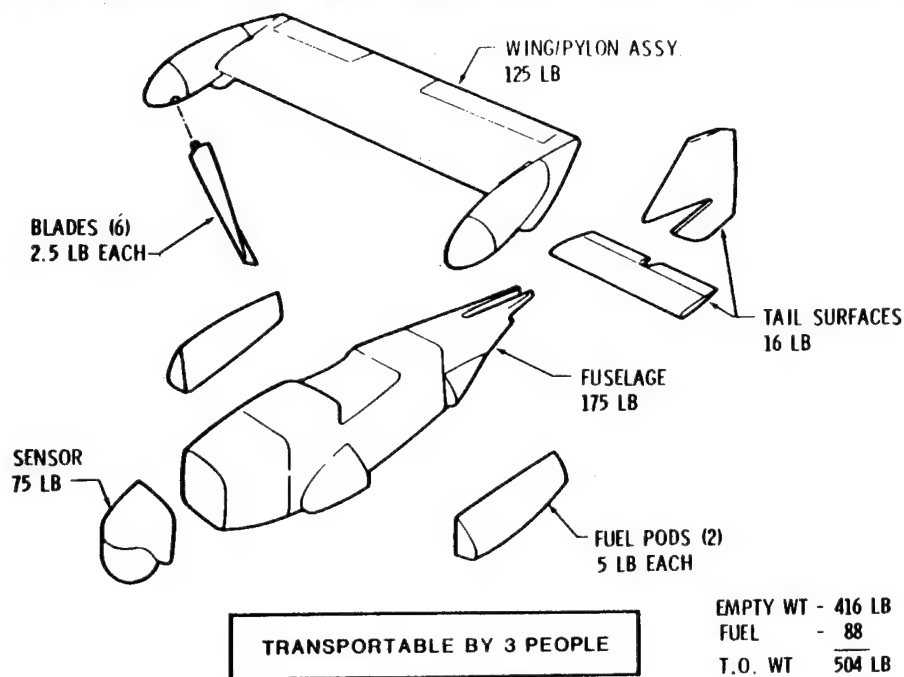


Figure 3-25

WEIGHT & PERFORMANCE SUMMARY PRODUCTION TILT ROTOR RPV

WEIGHT

EMPTY WEIGHT	350 LB
FUEL ALLOWANCE	100 LB
PAYLOAD ALLOWANCE	75 LB

PERFORMANCE

MAX SPEED	160 KN
HOVER OGE	7,500 FT
ENDURANCE	5+ HR
CEILING	25,000 FT

Figure 3-26

SCHEDULE FOR TILT ROTOR RPV DEMONSTRATOR

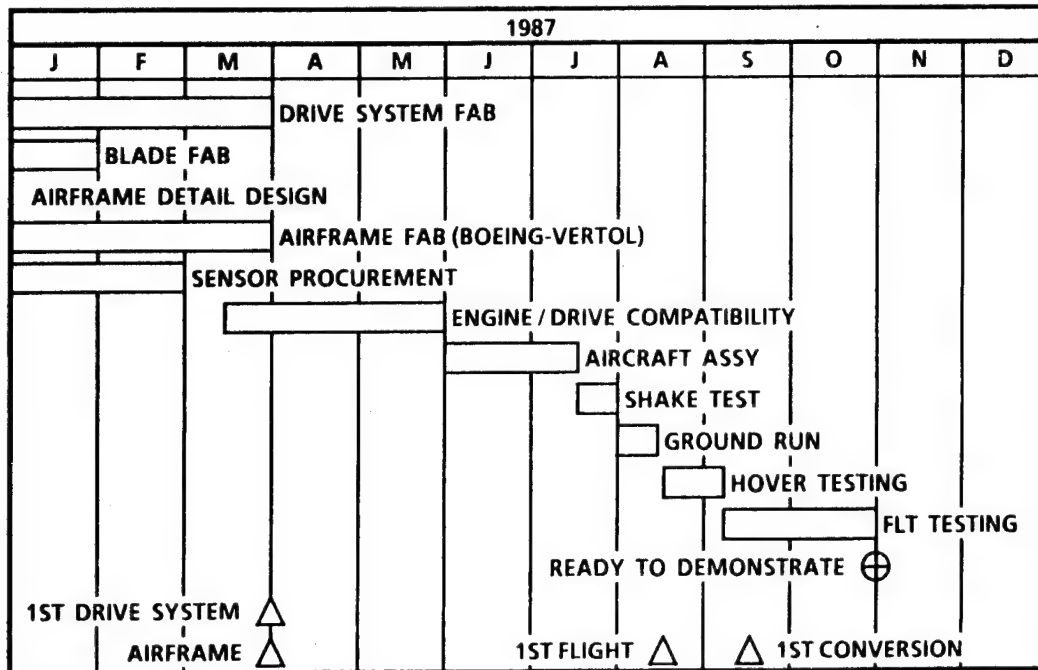


Figure 3-27

ROTORCRAFT TECHNOLOGY AT BOEING VERTOL: RECENT ADVANCES

John Shaw, Leo Dadone, and Robert Wiesner
Boeing Vertol Company

ABSTRACT

This paper presents an overview of key accomplishments in Boeing Vertol's Independent Research and Development (IR&D) program during the past several years, and a more detailed review of two IR&D projects of particular significance: high speed rotor development and the Model 360 Advanced Technology Helicopter. Areas addressed in the overview are: advanced rotors with reduced noise and vibration, 3-D aerodynamic modeling, flight control and avionics, active control, automated diagnostics and prognostics, composite structures, and drive systems.

OVERVIEW

Key rotorcraft programs currently in progress at Boeing Vertol are the V-22 Osprey tiltrotor (in full scale development), the LHX light helicopter family (in preliminary design), and the Model 360 Advanced Technology Helicopter (in final assembly prior to flight testing). These aircraft are shown in Figure 1.

To support these and other, future rotorcraft developments, Boeing Vertol is conducting an aggressive research program across the entire range of rotorcraft technology, with emphasis in seven areas:

- o Advanced rotors with reduced noise and vibration
- o 3-D aerodynamic modeling
- o Flight control and avionics
- o Active control
- o Automated diagnostics and prognostics
- o Composite structures
- o Drive systems

The first five of these areas reflect rapidly advancing computing technology which is applied both in design (math modeling, optimization, computer-aided design) and on the aircraft itself (e.g. fly-by-optics, higher harmonic control, expert systems). The last two areas reflect rapidly advancing materials technology.

The past five years have been marked by major progress in all of these areas. This paper begins with an overview of key accomplishments,

emphasizing the Independent Research and Development (IR&D) program, followed by a more detailed review of two particular IR&D highlights: high speed rotor development and the Model 360 Advanced Technology Helicopter.

ADVANCED ROTORS

Boeing Vertol IR&D on advanced rotors is focused on the development of design methodology for high speed, high performance rotors with low vibration and noise. This involves improving predictive methods for vibration and noise, evaluating low vibration and low noise design approaches, and developing optimization technology. Central to all of these activities have been major breakthroughs in the understanding and modeling of vortex wakes, complemented by comprehensive improvement of the supporting data base using an array of wind tunnel models with better aerodynamic and vibratory load instrumentation than ever before. Many of these advances are described in some detail in a later part of this paper. IR&D programs have been a vital base for current contract R&D programs to develop the airloads and induced velocity program element for the Second Generation Comprehensive Helicopter Analysis System - 2GCHAS (U. S. Army-Ames), to develop and test an advanced bearingless rotor concept in the 40- by 80-ft. wind tunnel (NASA-Ames), and to design and test an Advanced Technology Blade for the XV-15 tilt rotor aircraft (NASA-Ames).

The data base for advanced rotor acoustics was greatly increased in 1986 by testing a dynamically scaled, pressure-instrumented model of the Boeing Vertol Model 360 rotor in the German-Dutch acoustic wind tunnel (DNW). The test installation is shown in Figure 2. The Model 360 data, which shows the benefits of second-generation transonic airfoils and tapered blade tips, will be used in 1987 to validate predictive methodology for rotor noise of all types, particularly blade/vortex interaction and shock noise. (Validation is already under way using data from earlier testing of a similar model in the Boeing Vertol wind tunnel² under NASA contract, as a part of the National Rotor Noise Research (NR)² program). Recent improvements have been made in the predictive methodology, particularly in the area of thickness noise for tapered blades.

The data base for advanced rotor aerodynamics and vibratory loads was also greatly increased by the Model 360 rotor test in the DNW. This data, extending to almost 200 knots, will be used to validate recently improved high speed rotor loads methodology including new wake models, as well as transonic codes developed by NASA (Dr. I. C. Chang), the U. S. Army (Dr. F. X. Caradonna), and Dr. L. N. Sankar at Georgia Institute of Technology. This work is described in greater detail in later sections of the paper.

Development of optimization technology has focused on the reduction of vibratory hub loads by tailoring blade physical properties. Major reductions of vertical hub loads have been shown analytically; current work involves the inplane hub loads. Recent results are shown in Figure 3.

Vibratory airloads of the tilt rotor configuration were explored recently as a part of the IR&D program by testing a scaled, powered model of the V-22 Osprey in the Boeing Vertol wind tunnel. This provided a data base to validate methodology for the wing-rotor aerodynamic interaction.

3-D AERODYNAMIC MODELING

The Boeing Vertol IR&D program on 3-D aerodynamic modeling addresses the development of predictive methodology in two areas: a) airframe pressure distributions and b) rotor/airframe aerodynamic interactions.

The methodology developed to date for airframe pressure distributions involves potential flow panel methods, primarily PANAIR and VSAERO. These are being applied to cases which involve separated flow, a key element of rotorcraft aerodynamics. While the emphasis in fixed-wing aircraft design is the elimination of separated flow, separation can only be minimized, not eliminated, in V/STOL aircraft. The modeling of separated flow becomes critical in the definition of blunt fuselages and afterbodies. The VSAERO code has been formulated specifically to model separated flows and wakes. Figures 4 and 5 illustrate recent progress in applying and validating this methodology using pressure distributions measured in the wind tunnel. Figure 4 shows test/theory correlation in the prediction of tiltrotor fuselage pressure distributions. Figure 5 shows test/theory correlation in the prediction of wind tunnel mounting system interference effects.

Interactional aerodynamics concerns mutual interference effects between the airframe and the rotor(s), specifically (a) the rotor inflow changes and wake distortion induced by the airframe and (b) the steady and vibratory pressures induced by the blades and rotor wake on fuselage, wings, empennage etc. Preliminary rotor-on-fuselage and fuselage-on-rotor methodology involving non-impinging wakes was developed and validated a number of years ago. Today's V/STOL design requirements make it necessary that flow separation and fully interactive and impinging wakes be introduced in the potential flow models. Major progress has been made in this area in the past several years.

Plans for 1987 call for work with TRANAIR, a transonic panel code developed by Boeing under contract to NASA-Ames, and subsequently with Euler codes developed by NASA-Ames and the U. S. Army.

FLIGHT CONTROL AND AVIONICS

Boeing Vertol has led the industry in the development of advanced flight control systems, having flown the first two demonstration fly-by-wire systems for rotorcraft (TAGS, 1969 and HLH/Model 347, 1972), flown the first demonstration fly-by-optics system for any aircraft (ADOCS, 1985), developed the first production fly-by-wire system for rotorcraft (V-22, 1987), and developed the first all-digital AFCS for rotorcraft which incorporates Large Scale Integrated electronics (the 1750A microchip processor) and higher order language (JOVIAL-73) (Model 360, 1987). As an important part of these programs, Boeing Vertol has led in the development and integration of sidearm control. IR&D has been an important element in developing the technology base for these key advances. The critical thrust has been to simplify the system hardware to achieve high reliability. IR&D has been -- and is being -- used to develop fault-tolerant system architectures, methodology for error-free software, and sidearm controller technology. Optical-hydraulic valves, the least-developed element of fly-by-optics, are also being

evaluated in the IR&D program. Additionally, IR&D is aimed at development of computer-aided control law design methodology and improvement of simulation models, methodology for flight control/structural interaction, and analyses of rotorcraft flight dynamics.

To support the V-22 Osprey, the LHX program, and the R&D programs just described, the Boeing Vertol Flight Simulation Laboratory is being upgraded in major ways. The most important of these are an advanced Evans and Sutherland CT6 Computer Image Generation system with special features appropriate to LHX mission requirements and with capability to fly two aircraft "eyepoints" simultaneously over the same terrain (Figure 6); a dome for projection of computer-generated images over the entire 360° field-of-view; and a six degree of freedom motion base with interchangeable cab capability (initially V-22 or LHX). The expanded simulation facility occupies 25,000 square feet, and is located adjacent to an avionics integration facility. Together, the two facilities allow complete piloted checkout of flight control/avionics hardware and software functions prior to flight. This reduces flight control/avionics flight development cost and increases flight safety through pre-flight piloted simulation of difficult mission profiles and fault conditions. The integrated laboratory is a key element in validating the flight control/avionics software utilized in highly automated next-generation aircraft.

ACTIVE CONTROL

Boeing Vertol has a major IR&D program in active control which is focused primarily on higher harmonic control (HHC) applied to conventional rotor blades through the swashplate. The program has addressed the full range of HHC design issues in depth, using a combination of analysis and wind tunnel testing. This IR&D is unusually comprehensive relative to other HHC programs in the rotorcraft industry: it has addressed both three- and four-bladed rotors, articulated and hingeless rotors, single and tandem configurations, fixed-gain, scheduled-gain, and adaptive controllers, actuator mechanical and servoloop design, and performance improvement as well as vibration reduction. Wind tunnel testing of a scaled CH-47D rotor in 1984 was particularly successful, demonstrating a fully effective, fixed-gain control law over the entire test envelope up to 188 knots (Figure 7) plus precise high frequency actuator control and long-life actuator mechanical design. This testing provides an excellent data base for design of full-scale HHC systems which are both effective and efficient. The results have been utilized in contract R&D work for the U. S. Army - AATD for preliminary design of an HHC system for the UH-60A Black Hawk. Current efforts include evaluation of active control in a variety of new applications.

AUTOMATED DIAGNOSTICS AND PROGNOSTICS

Boeing Vertol's IR&D work in automated diagnostics and prognostics includes the development of several expert systems. The first of these, a system for rotor track and balance of newly built aircraft, was developed in 1986. That system will soon be greatly expanded to form an expert system which diagnoses all types of 1/rev vibration problems on fielded aircraft, under contract to U. S. Army - AATD. The benefits of these systems in reducing

the number of test flights required for track and balance are shown in Figure 8. The same AATD contract has already extended exploratory IR&D work on flight control system diagnostics to a complete expert system for this purpose. Further IR&D projects to develop prognostic systems for transmissions and flight control actuators are now under way. Also under development is an automated NOE navigator, the first element of an automated pilot's associate which will include on-line diagnostics and prognostics.

COMPOSITE STRUCTURES

Boeing Vertol IR&D on composite structures has been focused since 1981 on a major project which has advanced the state of the art in every area of structures technology: the Model 360 Advanced Technology Helicopter. The Model 360 is presently in final assembly and is scheduled to fly in early 1987. This innovative aircraft embodies two major thrusts in composite structures: a) a very significant reduction of airframe weight and cost through wide use of composite honeycomb structure, and b) major extension of the damage/defect tolerance achievable with composites to the dynamic system wherever possible. Accomplishments in these areas are discussed in some detail in a later part of this paper. IR&D has also been used to conduct a research program in conjunction with MIT's Technology Laboratory for Advanced Composites initially to evaluate damage tolerance of graphite composite shear panels and more recently to develop a theoretical model for cumulative fatigue damage in composites.

DRIVE SYSTEMS

IR&D work in drive systems has included the development of 3-D finite element modeling techniques for gears and their supporting bearing systems, evaluation of improved gear steels and advanced housing materials, and evaluation of gear surface coatings to increase transmission efficiency and reduce lubrication requirements. The work on gear modeling, illustrated in Figure 9, is unique and valuable. It has led to the development of a gear rim thickness factor which enables more efficient and reliable design and which has been added to AGMA standards. It has also led to a modification of the AGMA standard for the size factor used in spiral bevel gear design. The work on improved gear steels³ has led the industry in three areas: application of high-hot-hardness (H^3) steels which greatly increase safety under conditions of marginal lubrication; development of cleaner steels which increase safety under all conditions; and application of fracture mechanics to establish threshold stress levels for zero crack propagation as a function of material cleanliness. The evaluation of advanced housing materials led to a contract R&D program with U.S. Army - AATD for full-scale evaluation of graphite/polyimide and FP/magnesium metal matrix composite housings. Additionally, Boeing Vertol has just completed R&D under contract to U. S. Army - AATD for development of large transmission technology, through improvements to transmissions designed for the Heavy Lift Helicopter. This program achieved successful operation of the highest power level gear mesh ever built for aircraft application (over 10,000 HP). A further IR&D accomplishment in 1986 is the development of the first integrated all-composite shaft and coupling designed to tolerate high misalignment angles (Figure 10). The extremely light weight and simplicity of this shaft-coupling combination are unique advantages in providing dynamic

stability in applications with next-generation, high-speed gas turbine engines (e.g. the T800).

HIGH SPEED ROTOR DEVELOPMENT

The emphasis in today's helicopter rotor development is high speed, with low vibratory loads and low noise. To this end, Boeing Vertol is conducting a multi-disciplinary program to gather the test evidence and develop the methods necessary to design better rotors. The feasibility of improving upon the current generation of advanced rotor systems is considerably enhanced by recent advances in computational methods and testing techniques.

ADVANCED ROTOR DEVELOPMENTS PRIOR TO 1982

As summarized in Reference 1, a family of airfoils optimized for use on high speed rotors was designed and tested in 1978. These airfoils, the VR-12 to VR-15 sections, were defined for high Mach number penetration on the advancing side without compromising the high lift performance necessary to avoid dynamic stall over the retreating side. Wind tunnel tests of rotors employing the new sections started shortly after the 2-D airfoil tests.

An extensive series of advanced rotor wind tunnel tests was carried out in the Boeing Vertol Wind Tunnel (BVWT) between 1978 and 1982. These tests, summarized in Reference 2, demonstrated that conventional helicopter rotors can be flown at speeds beyond 200 knots while still producing useful lift and propulsive force. One configuration was tested up to 231 knots, the speed limit of the wind tunnel. Figure 11 shows one of the model rotors installed in the BVWT. Of all the configurations tested at that time, the one that achieved the best compromise between performance and loads employed the new family of high speed airfoils and a 3:1 chord taper over the 10 percent of span. This rotor was selected for the Model 360 helicopter.

The advanced rotor tests in the BVWT showed the straight, tapered tip configuration to be better than other configurations employing various amounts of tip sweep. That conclusion will be re-evaluated periodically, considering such recent developments as those reported in Reference 3. For the present, the Model 360 rotor system is the best of all those that Boeing Vertol has evaluated in the wind tunnel. It will be flight tested in 1987, and it is the baseline for the investigation of more advanced rotors.

During the advanced rotor wind tunnel test program, flight at very high speeds was achieved at the cost of relatively high vibratory hub loads. High speed was not limited by power, but by safety-of-flight limits on the fatigue loads experienced by the model blades and control system. Close examination of the performance and loads near the rotor limits did not yield any useful clues about the fundamental source of the vibratory loads.

NATURE OF VIBRATORY AIRLOADS

A breakthrough in identifying the causes of the vibration experienced by helicopter rotors in high speed flight came with a re-examination of existing NASA test data for the H-34 rotor. As described in Reference 4, a detailed time history of blade airloads, obtained by integration of

measured surface pressures, can be harmonically analyzed and reconstituted to identify the radial and azimuthal extent of the loads associated with different harmonic components. Figure 12 shows an example of a cartesian, isometric display of the H-34 data as measured in Reference 5. Complete airloads (harmonics 0 to 10) and vibratory airloads only (harmonics 3 to 10) are presented. Clearly, the largest vibratory airloads occur at the tip as the blade travels from the first to the second quadrant. To the extent that they are a forcing function driving the vibratory response of the entire helicopter, any reduction in these airloads should result in a reduction in the overall rotor induced vibration.

Although the design of low-vibration rotors depends on the prediction of vibratory airloads, none of the rotor analysis codes available in 1983 produced satisfactory predictions. This lack of agreement between test and theory is illustrated in Figure 13, from Reference 4.

DEFINITION OF APPROACH

Between 1983 and 1984 systematic attempts were made to quantify the mechanism behind the vibratory airloads observed in the H-34 data. The main cause of the poor predictive capability was finally determined to be the incorrect modeling of the rotor wake over the advancing side of the disc.

As illustrated in Figure 14, the tip of the advancing blade of a rotor in high speed flight experiences negative loading. This negative loading is the source of trailed vorticity of negative sign, but the wake models available at that time did not have provisions for regions of locally reversed vorticity.

The following approach was proposed to understand and reduce the wake effects contributing to vibratory airloads:

- a) Gather experimental evidence on the structure of the wake and on the magnitude and phase of the vibratory airloads.
- b) Develop more representative wake models and integrate them into rotor analysis codes which properly couple all aerodynamic and dynamic effects.
- c) Design and demonstrate by wind tunnel test low-vibration and low-noise rotors.

The low noise goals arise from the fact that the wake not only causes vibratory airloads, but is also a significant contributor to the acoustic signature of a rotor. If the interaction between rotor and wake can be changed to reduce vibration, it should be possible to change it to reduce noise.

FLOW VISUALIZATION

The first experimental objective was to confirm that negative loading on the advancing tip results in a discrete region of "negative" trailed vorticity. A towing tank test carried out at Flow Industries, in Kent, Wash., during the fall of 1984 provided this confirmation.

A typical flow visualization record, along with an interpretation of the flow picture, is shown in Figure 15. Reference 6 reports on the most significant test conditions. This was the first test in water of a helicopter rotor model equipped with cyclic controls. The model was a four-blade, 16 inch diameter, geometrically scaled H-34 rotor. The conditions examined in the towing tank test included some of the advance ratios of the original H-34 test, Reference 5.

Although the towing tank records were informative it would have been more desirable to investigate the rotor wake in air, but flow visualization (and measurement) in air for forward flight conditions at realistic tip speeds has been, so far, disappointing. There is some hope, however, because promising new techniques have been recently perfected which will make it possible to carry out instantaneous rotor wake measurements.

ADVANCED WIND TUNNEL TESTS

Between 1982 and 1985, a rotor set of dynamically scaled and pressure gage instrumented model blades was designed and built at the Boeing Vertol Wind Tunnel. This rotor, a 1/5 scale model of the Model 360 rotor, was tested in February 1985. Only a limited amount of data was acquired because of instrumentation difficulties, but the measured airload distributions were in qualitative agreement with the airloads from the H-34 test. Figure 16 shows two typical airload distributions. More details about this test are presented in Reference 7.

A new set of blades was built between 1985 and 1986. In this blade set, the reliability of the pressure transducer installation was greatly improved. The new blade set, shown in Figure 17, was successfully tested in a joint Army/NASA/Vertol aeroacoustic program at the Duits Nederlandse Windtunnel (DNW), during the summer of 1986. Digitized and finally reduced data will be available by mid-1987.

In the DNW tunnel, testing was carried out up to a speed of 199 knots. From a preliminary review of the data it appears that most of the pressure instrumentation, including the tip pressure gages, operated correctly throughout the test.

ROTOR WAKE MODEL DEVELOPMENT

Key features of the B-65 rotor performance and airloads analysis are shown in Table 1. Until recently, the wake models in B-65 and other Vertol rotor codes were "kinematic", namely their geometry was determined on the basis of blade motions, inflow velocity and averaged induced downwash without any wake distortion, or free-wake, effects.

-
- o Lifting-line model
 - o Azimuthal resolution options (increments between 5 and 15 degrees)
 - o Spanwise resolution of up to 39 stations
 - o Uniform and non-uniform downwash
 - o Betz rollup approximations
 - o Kinematic and free (CDI) wake options
 - o Delayed rollup vortex sheet (trailed and shed)
 - o Articulated and rigid rotors
 - o Two-dimensional airfoil data base
 - o Unsteady aerodynamics/Dynamic stall delay
 - o Three-dimensional tip relief effects
 - o Tip sweep model
 - o Elastic properties by modal representation
 - o Flapping and flap bending by either time or frequency domain solution
 - o Upwash/interference effects
 - o Time-averaged and instantaneous performance and airloads
 - o Provisions to interface with other codes
-

Table 1 - Key features of the B-65 forward flight rotor analysis

During 1984, systematic calculations involving the kinematic wake models were carried out to investigate how the wake roll-up assumptions influenced the prediction of vibratory airloads. The conclusion was that no roll-up is better than the wrong roll-up. The use of extended (delayed roll-up) vortex sheets yielded airloads which were low in amplitude but otherwise in excellent agreement with the measured data. This was the evidence necessary to initiate the development of wake models with more representative far-wake vorticity distributions, including the modeling of the wake trailed by negatively loaded blade tips. Two options were available:

- (1) To modify the existing kinematic wakes so that multiple (more than two) vortices could be introduced wherever necessary.
- (2) To formulate a totally new model, including free-wake effects.

The decision was made to do both. The kinematic wakes were modified in-house, while the development of the free wake was subcontracted to Continuum Dynamics, Inc., (CDI), of Princeton, N. J., and Dr. D. Bliss from Duke University.

Although much effort has been directed to the development of free wakes, free wakes are not always necessary. Kinematic wake models are useful when the wake is not too close to the rotor blades. This is generally the case when the rotor produces a significant propulsive force. It is not true at small tip path plane angles when the propulsive force is small. The changes to the kinematic wake model were conceptually simple: options were introduced for various distributions of rolled up far wake vortices, with a maximum of ten, and a substantial improvement was observed in the agreement with the H-34 data.

When the flow causes the wake to move close to the rotor blades it becomes necessary to account for local wake distortion effects. While past experience with free wakes had been disappointing because of poor convergence and high costs, the CDI model includes new features which considerably improve the efficiency and accuracy of the wake calculations, particularly in addressing vibratory airloads.

Figure 18 illustrates the key characteristics of the CDI wake. The main advantages are:

- o The use of curved vortex elements. These allow the modeling of the wake with few vortex segments where a larger number of straight segments would be needed. The use of curved elements also simplifies the calculation of self-induced wake distortion effects.
- o The modeling of the wake by a system of lines of constant vorticity, not separating trailed and shed vorticity components. In the presence of large gradients the vortex lines are closely spaced. Widely separated lines indicate regions with low gradients.

One small difficulty is that the wake does not originate at fixed collocation points along the blade and therefore a near wake has to be introduced to provide some transition between the blade and the body of the wake.

Computer assisted graphics have been used to display both the wake geometry and the associated induced velocity field. Figure 19 is an example of the CDI wake geometry as introduced into B-65. A computation grid perpendicular to the disc plane and passing through the blade shows the in-plane components of the velocities induced by the all the vorticity in the rotor flow field for that particular rotor position. Figure 20 shows the instantaneous velocities induced on a rectangular computation grid along the disc plane. These displays were developed to assist in code checkout and test/theory correlation.

TEST/THEORY CORRELATION - H-34 DATA

Because of the new kinematic and free wakes, considerable improvements have been made in the prediction of vibratory airloads. Figure 21 compares the measured and calculated vibratory airloads for the same condition shown earlier in Figure 13. The agreement between test and theory is now good. Although both the CDI and Betz wake models require further improvements to make them more generally useful, it is finally possible to examine by analysis candidate low-vibration rotor configurations.

LIMITS OF THE LIFTING LINE APPROACH - BVI MODELING

Significant efforts are under way to model helicopter blades as three-dimensional lifting surfaces, but, as promising as they are, the new Computational Fluid Dynamics (CFD) codes cannot be used without the wake and inflow information currently provided by lifting line rotor codes. Figure 22 summarizes the blade/vortex proximity effects of concern in determining the range of validity of lifting line rotor analysis methods. The only instance in which lifting line and discrete-vortex wake models are correct without any empirical adjustment is when the separation between wake and blade is at least one chord. At distances of less than one chord the lifting line modeling becomes increasingly questionable. Events leading to an actual encounter between blade and vortex cannot be modeled with any degree of accuracy, although useful trends might be produced by introducing empirical considerations.

Methods modeling the full transonic encounter between a vortex and a two dimensional airfoil have been available for some time, but to define low vibration rotors the more localized blade-vortex interaction (BVI) effects did not need to be modeled as urgently as the overall rotor wake. Of more immediate concern has been an assessment of the limits of validity of the lifting line approach. A two dimensional Joukowski transformation, described in Reference 8, was used for this purpose. Systematic calculations, as shown in Figure 23, were carried out. As mentioned earlier, a preliminary conclusion was that lifting line methods are valid for blade/vortex separation distances of at least one chord, Figure 24. This also means that a free wake model is an essential prerequisite to the correct formulation of the blade/vortex interaction problem, since the modeling of the details of blade vortex proximity effects is not useful until the position of the wake relative to a blade can be accurately estimated.

COUPLING OF B-65 WITH CFD CODES

The evaluation of the transonic flow field over the tip of rotor blades has been a research objective at NASA and Army Research Centers for years. Boeing Vertol, as the other helicopter manufacturers, has been following with great interest the CFD developments. Early versions of the CFD codes were acquired and tried as soon as they became available. These codes are:

- o ROT-22, a NASA/Ames modification of FL022, Reference 9,
- o TFAR-1 and TFAR-2, more recently developed at NASA/Ames, References 10 and 11,
- o FDR, developed at the Army's Aeroflightdynamics Directorate, Reference 12.

Euler and Navier-Stokes solvers are being currently developed and will become operational over the next few years.

What these codes have in common is that they can evaluate the flow field around a rotor blade, one azimuth position at a time, as long as boundary conditions can be defined from an external source. What these codes cannot do is to:

- o Relate the flow field to the forces a rotor has to produce to maintain a given flight condition,
- o Couple the airloads with the flapping motions and elastic deflections of the blades,
- o Evaluate the rotor wake.

Wake effects, blade motions and deflections, rotor forces and suitable boundary conditions are obtained from lifting-line rotor analysis codes. At Boeing Vertol the information necessary to carry out CFD rotor calculations has been produced by means of the B-65 rotor analysis code. Open-loop coupling only has been attempted so far, with very encouraging results.

Recent calculations carried out by means of the FDR, TFAR-1 and TFAR-2 codes to match test conditions from a pressure instrumented blade test are described in Reference 7. Figure 25 is an example of pressures calculated by means of B-65/TFAR-1 for comparison with test data from the BVWT. Plans are being made to implement soon some form of closed-loop coupling involving B-65, with the CDI free wake, and the CFD rotor codes.

INVESTIGATION OF LOW-VIBRATION ROTOR CONCEPTS

Systematic B-65 calculations have been started to investigate the feasibility of low vibratory airloads rotors. The CFD codes will be used to better understand and model the tip flow environment so that, when possible, more accurate empirical models can be defined and introduced in the lifting line codes.

An example of vibratory airloads trends obtained by means of the B-65 analysis is shown in Figure 26. A parametric study of useful low vibratory airloads trends is the first step in the definition of the next generation of advanced helicopter rotors.

MODEL 360 ADVANCED TECHNOLOGY HELICOPTER

The Boeing Model 360, shown in Figure 27, is unique by virtue of its extensive use of composites. Combinations of glass and graphite are utilized in the blades, hubs, controls, rotor shafts, airframe, and landing gear components. The application of advanced materials is coupled with a high-performance rotor and modularized assembly techniques to provide a focal point for technology development at Boeing Vertol. This section of the paper reviews components developed as part of the Model 360 Advanced Technology Helicopter Program.

ADVANCED HIGH SPEED ROTOR

The construction of the Model 360 rotor blade, shown in Figure 28, is similar to that of the CH-47 and CH-46 currently in fleet use. The basic structural element is the spar, which is composed of unidirectional fiberglass for axial stiffness and strength. To provide the torsional stiffness required for flight at high speed the blade is covered with bias-ply of fiberglass/graphite.

Developed with the support of 4,720 hours of wind tunnel testing, the blade incorporates the VR12/VR15 airfoils, the latest step in transonic airfoils, together with a tapered tip planform. Model rotor tests substantiated the significant performance improvement, shown in Figure 29, available from the rotor. As shown, the hover efficiency is improved by 6 percent and the cruise efficiency by 23 percent relative to current rotor systems. This rotor, in combination with the low drag Model 360 fuselage, will provide a cruise speed capability of 200 knots.

COMPOSITE DRY ROTOR HUB

The Model 360 hub, shown in Figure 30, has evolved from all glass to mixed modulus construction. A combination of glass and graphite was chosen to meet stiffness and fail-safety requirements.

Primary load paths are through composite structures and elastomeric bearings. Continuous wound hybrid tension loops support the elastomeric flap and lag bearings. These non-viscous bearings do not require lubrication and are expected to provide a significant reduction in mean time to removal relative to rolling element bearings.

Unique to the composite hub is the use of a single hinge for both lag motion and blade folding. This feature provides a significant parts count reduction compared to a three-bladed conventional folding hub. The CH-46 hub and fold mechanism have 1,799 parts; the new four-bladed rotor has approximately 60 percent fewer parts. Due to the reduced parts count and the

use of elastomeric bearings and corrosion-resistant composite material, a 60 percent reduction in maintenance manhours is predicted.

COMPOSITE UPPER CONTROLS

The use of composites has been extended to the upper control system. Benefits of the composites include weight savings, improved fail-safety characteristics, and a corrosion-free assembly. As shown in Figure 31, components such as the swashplate, slider/slider guide, and gimbal ring utilize composite material in their construction. The design is of mixed graphite and fiberglass to achieve approximately a two-fold stiffness increase, compared to metal controls without a weight penalty. Composite construction is coupled with the use of elastomeric rod ends and bearings to avoid spurious vibratory control inputs resulting from deflections.

Graphite content is limited in the control elements and all other mixed-modulus fatigue-critical parts to maintain the soft, safe failure modes and excellent ballistic tolerance of fiberglass construction.

DRIVE SYSTEM

The Model 360 drive system utilizes CH-47 components. Unique to the system, however, are composite forward and aft rotor shafts which are shown in Figure 32. These rotor shafts were chiefly designed to meet stiffness requirements and therefore contain a large fraction of graphite laid at an angle which is effective for both longitudinal stiffness and torsional strength. In addition, circumferential wraps increase bearing allowables at the upper and lower ends. At the upper end, the composite rotor hub is attached by longitudinal bolts connecting to barrel nuts in the wall of the shaft tube. At the lower end, a steel planet carrier is attached to the shaft tube by radial pins.

During static and fatigue tests of the aft rotor shaft, that portion of the shaft which is normally encapsulated in the transmission was heated to 215°F to properly simulate the operating environment.

As a portion of the Model 360 program, composite forward and aft structural transmission covers and sync shafts, shown in Figure 33, were fabricated and tested.

COMPOSITE AIRFRAME

The Model 360 composite airframe, shown in Figure 34, has as its target a 25% reduction in weight, an 86% reduction in parts, and a 93% reduction in fasteners compared to a conventional metal fuselage. Skin panels are composed of KEVLAR skins over a NOMEX core, while the frame and longeron sections are composed of unidirectional graphite caps, NOMEX core, and KEVLAR face sheets. Composites are utilized not only in the skins and frames but in the major support fittings such as the main and nose gear backup structure shown in Figure 35.

The all-composite fuselage was fabricated with a minimum of tools. Skin panels were fabricated in a single cure operation in low cost tools. A single assembly fixture was used to position the ring frames and the longerons. Skin panels were placed in position from the outside. This manufacturing sequence is illustrated in Figure 36.

Cost savings obtained from the use of the Model 360-type tooling/fabrication methods are contained in Figure 37. Model 360 figures are based on results achieved by Boeing during assembly of the primary structure. As compared to conventional metal structure, tooling costs were reduced by 90% and non-recurring costs by 45%.

A shake test of the primary structure including the engines, forward and aft transmission assemblies, and cabin and cockpit floor modules was conducted as part of the Composite Airframe development program. The test showed that the airframe structure meets desired stiffness requirements.

A static proof load test of the primary airframe structure substantiated the ability to meet the planned flight test envelope which includes speeds to 200 knots and maneuvers of 3g's. The composite airframe is shown suspended in the shake and static test fixtures in Figure 38.

MODULARIZED ASSEMBLY

The composite airframe consists of five major subsystem modules, as shown in Figure 39. These subsystems include the tunnel, cockpit, fuselage, nose enclosure, and cabin floor/fuel assembly. The modularization concept greatly reduces manufacturing time and expense.

A unique palletized concept is employed in the Model 360 for mounting the avionics and lower controls. The cockpit pallet, shown in Figure 40, contains avionics and electrical racks, pilots' seats, composite instrument panel, and controls. The pallet, including all the on-pallet wiring, is assembled as a unit outside the airframe.

The cabin floor/fuel system module is of composite sandwich construction using unidirectional fiberglass/epoxy faces for durability and damage resistance. The integral underfloor fuel tanks contain crashworthy fuel cells. The one-piece floor/fuel unit shown in Figure 41 is assembled outside the airframe and the fuel system is pressure checked prior to installation.

Both the cockpit and cabin module are mounted on vibration isolators as illustrated in Figure 42. The entire cockpit module is mounted on four vertical, two longitudinal, and one lateral Improved Floor Isolation System (IFIS) units. These units isolate the cockpit floor from the airframe in the six axes - lateral, vertical, longitudinal, pitch, roll, and yaw. All units are designed for dual frequency operation (isolation at both 4/rev and 8/rev).

Vibration isolation of cargo and fuel is used to prevent fuselage frequencies from passing through resonances at rotor frequencies when large variations in cargo and fuel weight occur. The system is similar to that on the commercial Chinook. It maintains a nearly constant, nonresonant fuselage natural frequency for all fuel and cargo loads while minimizing cabin vibration at the same time.

SUBSYSTEMS

To reduce program costs, proven subsystem components from the Model 234, CH-47D, and CH-46, have been used throughout the Model 360 where feasible.

Subsystems developed for the Model 360 include composite landing gear components, a digital automatic flight control system, a modularized hydraulic system, and an advanced, multiplexed avionics system (see Figure 43).

A fully retractable tricycle gear arrangement was developed as part of the Model 360 program. A unique aspect of the main gear is the use of composites in the construction of the main beams and retraction bellcranks. Constructed of graphite, the beams represent a weight saving of 88 lb compared to steel beams.

The Model 360 cockpit includes an advanced electronic installation developed by the Allied Bendix Aerospace Corporation. Interface with the aircraft and its subsystems is by way of keyboards and electronically generated multifunction displays. The many customary round dial instruments and the warning and caution panels are replaced with multifunction cathode ray tube displays.

Large Scale Integrated electronics and higher order language are used in the Honeywell all-digital automatic flight control system. The system provides tailored command responses and stability as a function of flight condition.

APPLICATION OF MODEL 360 TECHNOLOGY

The technology developed as part of the Model 360 program will result in improvements in performance, maintenance, reliability, availability, and cost. As noted in Figure 44, this technology is providing support to other major Boeing Vertol programs such as the V-22, LHX, and Growth CH-47 in terms of composite manufacturing and assembly techniques and high speed rotor development.

REFERENCES

- (1) Dadone, L.; "Rotor Airfoil Optimization: An Understanding of the Physical Limits". Presented at the 34th Annual AHS Forum, Washington, D. C., May 1978. Preprint No. 78-4.
- (2) McVeigh, M. A. and McHugh, F. J.; "Recent Advances in Rotor Technology at Boeing Vertol". Presented at the 38th Annual AHS National Forum, Anaheim, Ca., May 1982.
- (3) Hopkins, H.; "Fastest Blades in the World". Flight International, 27 December 1986, pp 24-27.
- (4) Hooper, W. E.; "The Vibratory Airloading of Helicopter Rotors". Presented at the Ninth European Rotorcraft Forum, September 13-15, 1983, Stresa, Italy. Paper No. 46.
- (5) Rabbott, J. P., Lizak, A. A. and Paglino, V. M.; "A Presentation of Measured and Calculated Full Scale Rotor Blade Aerodynamic and Structural Loads". USAAVLABS, TR 66-31, July 1966.
- (6) Jenks, M. and Bartie, K.; "Towing Tank Test of a Scale Model H-34 Rotor at Flow Industries, December 1984". Boeing Document No. D210-12356-1, October 29, 1985.
- (7) Cowan, J., Dadone, L. and Gangwani, S.; "Wind Tunnel Test of a Pressure Instrumented Model Scale Advanced Rotor". Presented at the 42nd Annual Forum and Display of the American Helicopter Society, Washington, D. C., June 1986.
- (8) Poling, D. R., Dadone, L. and Telionis, D. P.; "Blade-Vortex Interaction". Presented at the AIAA 25th Aerospace Sciences Meeting, January 12-15, 1987, Reno, Nevada. Paper No. AIAA-87-0497.
- (9) Arieli, R. and Tauber, M. E.; "Analysis of the Quasi-Steady Flow About an Isolated Lifting Helicopter Rotor Blade". Joint Institute for Aeronautics and Acoustics, JIAATR-24, August 1979.
- (10) Chang, I-Chung; "Transonic Flow Analysis for Rotors, Part I - Three Dimensional, Quasi-Steady, Full-Potential Calculation," NASA TP 2375, 1985.
- (11) Chang, I-Chung; "Transonic Flow Analysis for Rotors, Part II - Three Dimensional, Unsteady, Full Potential Calculation," NASA TP 2375, 1985.
- (12) Caradonna, F. X., Tung, C., and Desopper, A.; "Finite Difference Modeling of Rotor Flows Including Wake Effects," Journal of AHS, Volume 29, No. 2, page 26, April 1984.

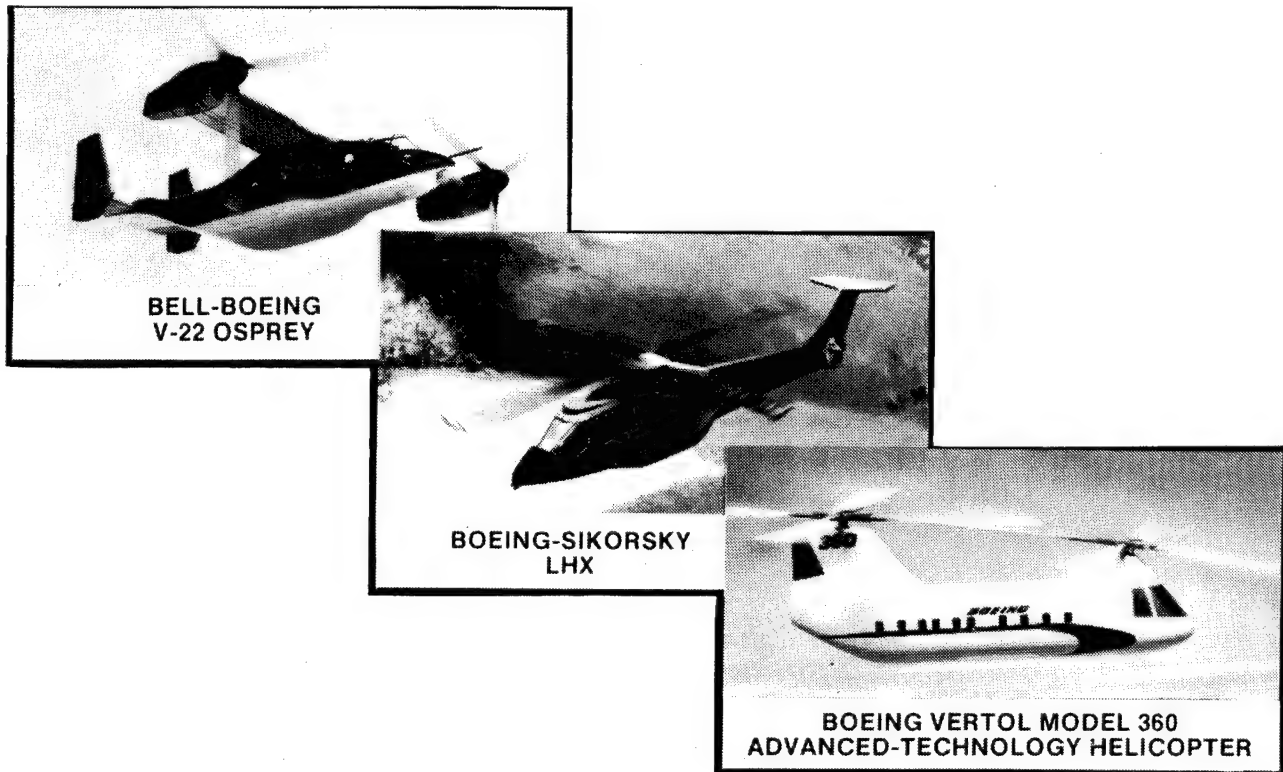


Figure 1. Current Major Programs at Boeing Vertol

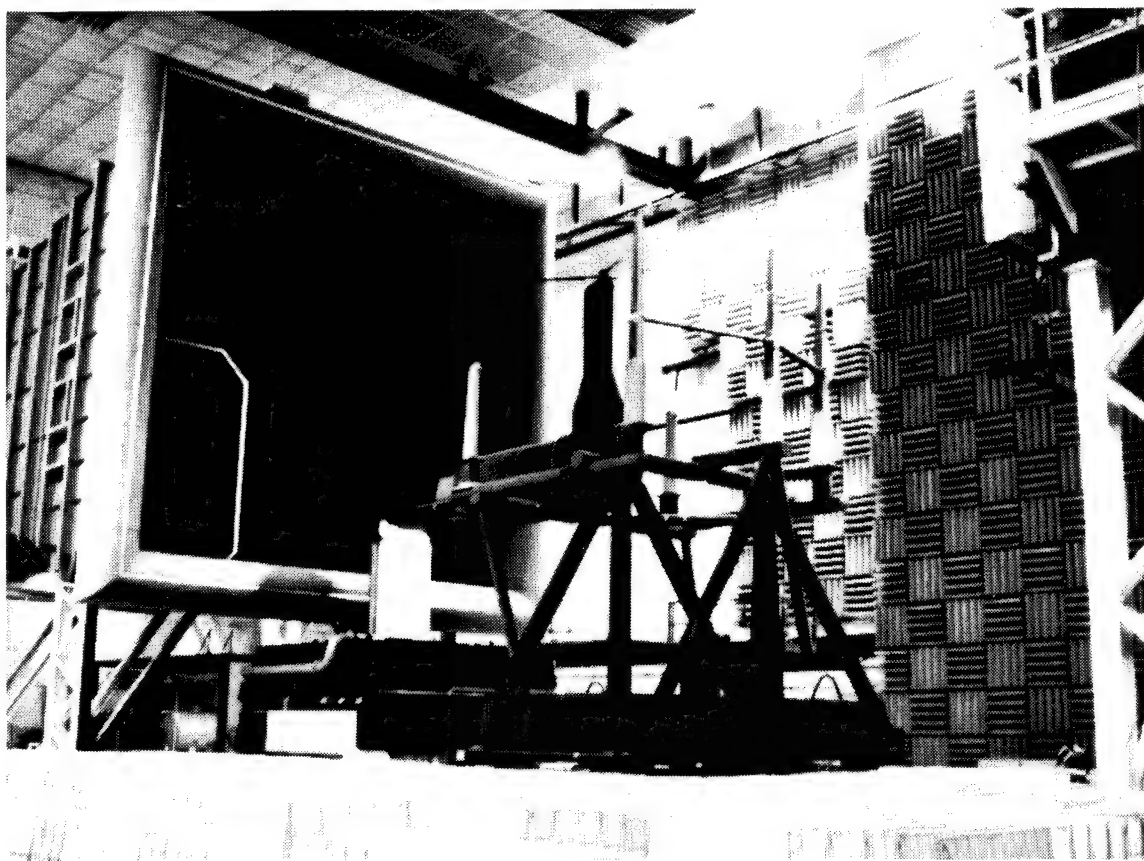


Figure 2. Dynamically Scaled, Pressure-Instrumented Model 360 Rotor Installed in the DNW Acoustic Wind Tunnel

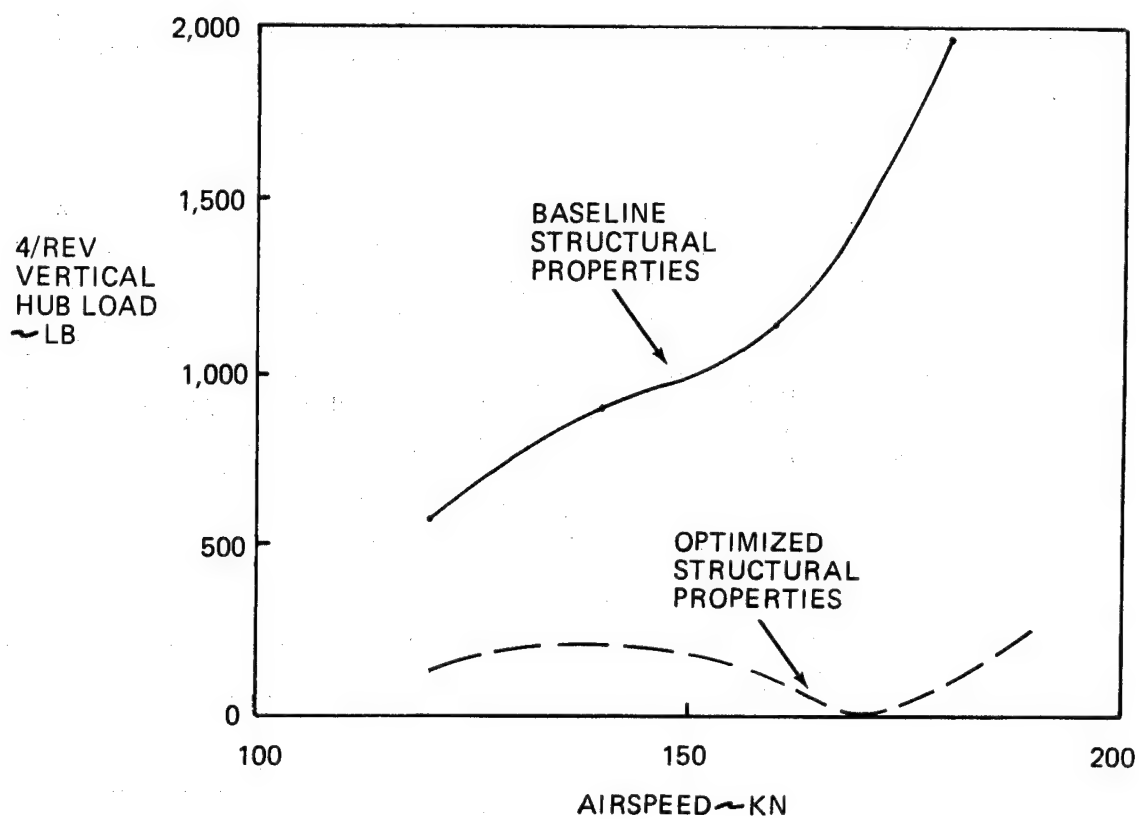


Figure 3. Predicted Vibration-Reduction Benefits of Rotor Blade Structural Optimization

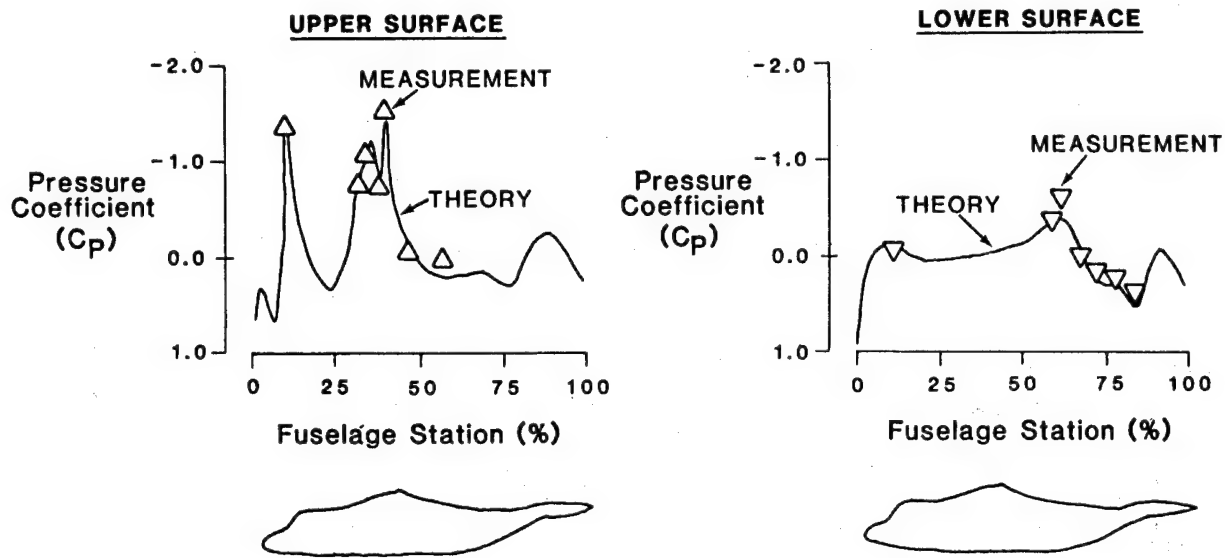


Figure 4. Correlation of Fuselage Pressure Distributions Predicted by 3-D Panel Code and Measured on Wind Tunnel Model ($\alpha = 5^\circ$, $M = 0.2$, Centerline Pressures)

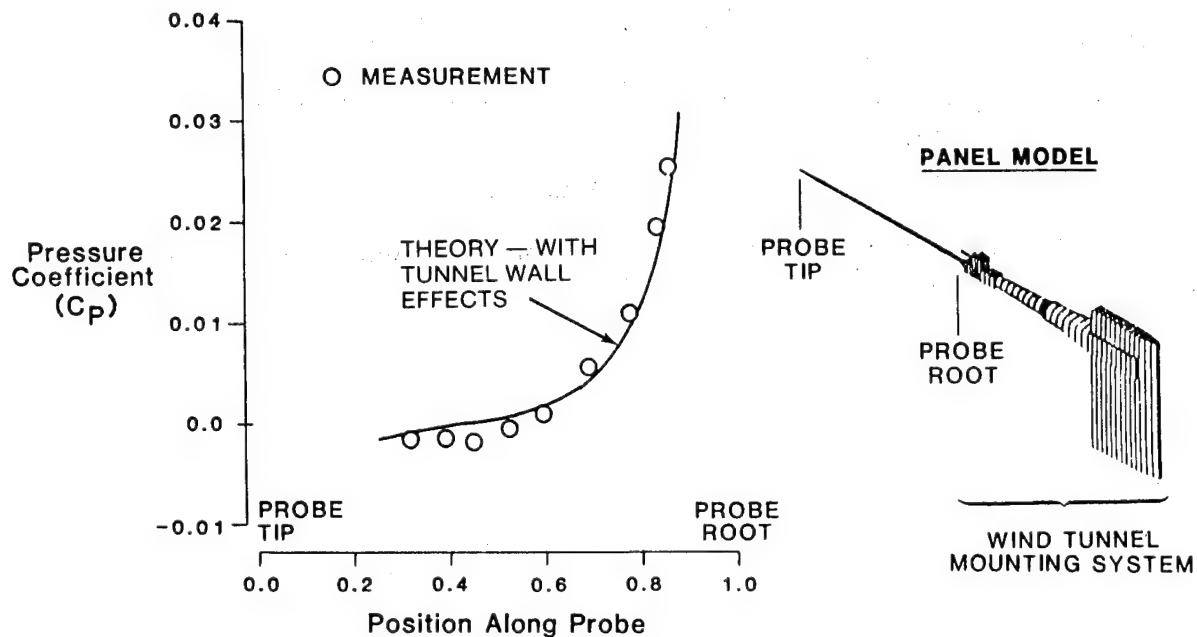


Figure 5. Wind Tunnel Pressure Distribution Caused by Mounting System: 3D Panel Code Prediction vs Measurement

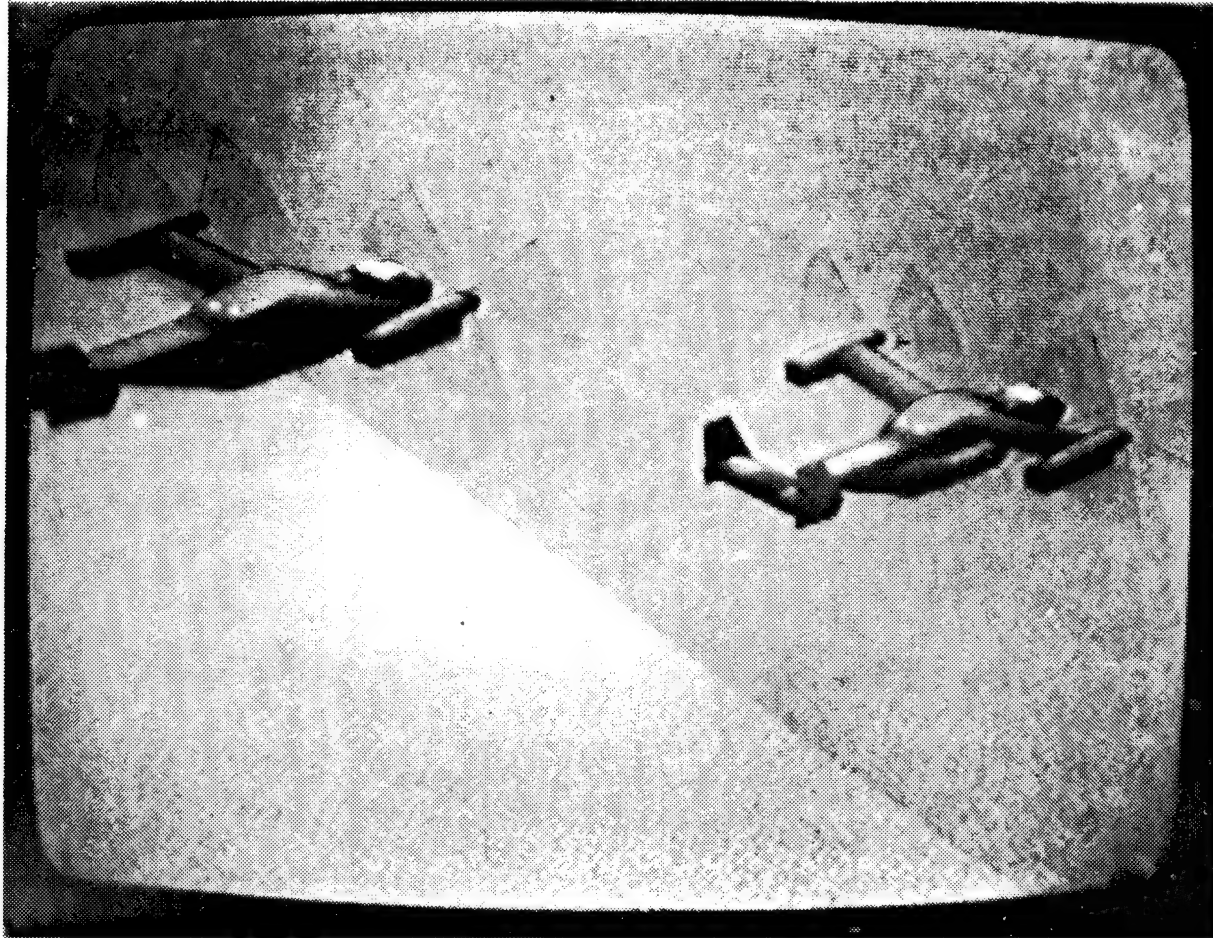


Figure 6. Computer Generated Image from Evans and Sutherland CT6 System
Recently Installed in the Boeing Vertol Flight Simulation Laboratory

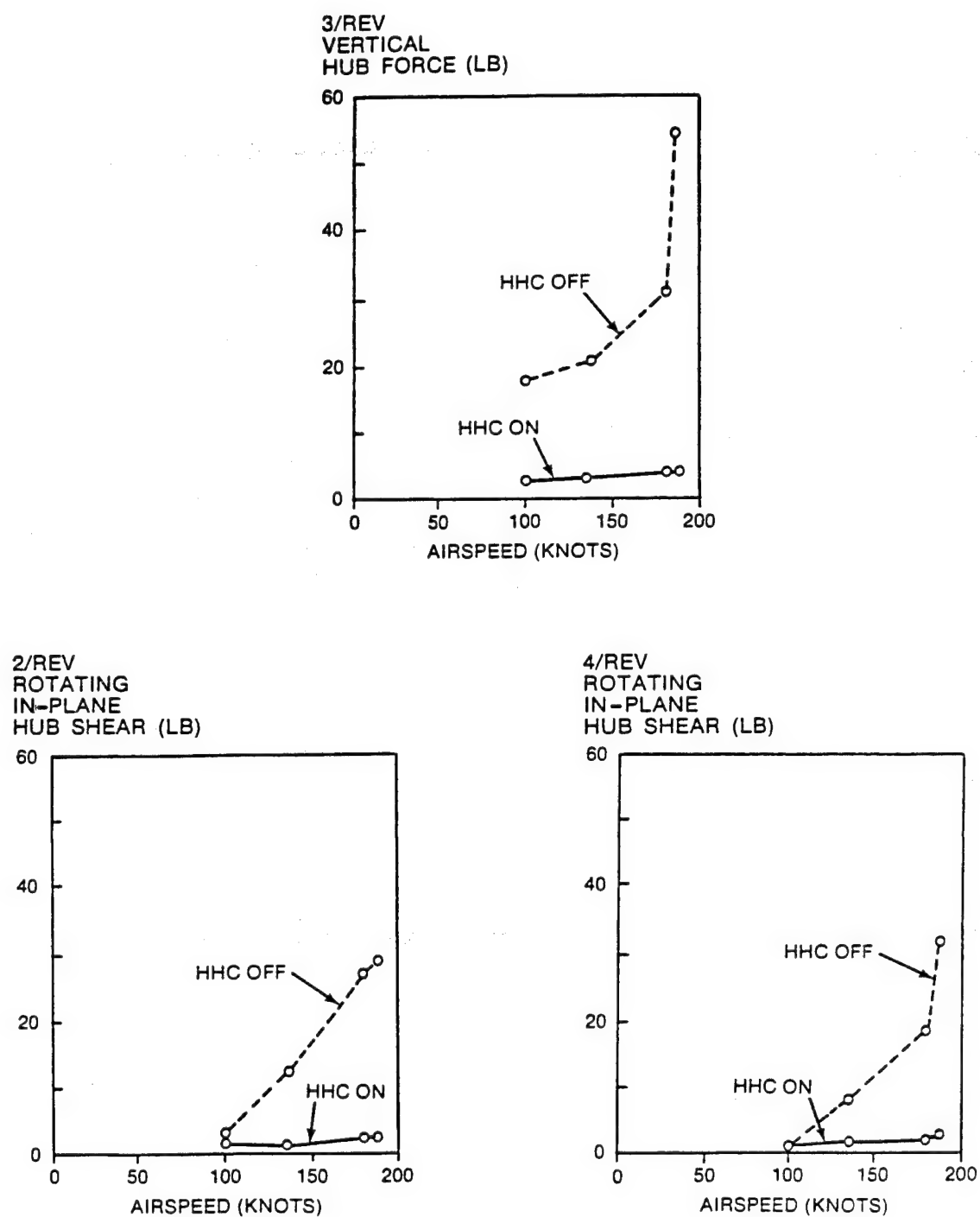


Figure 7. Major Vibratory Load Reduction Demonstrated in the Boeing Vertol Wind Tunnel Using Higher Harmonic Control

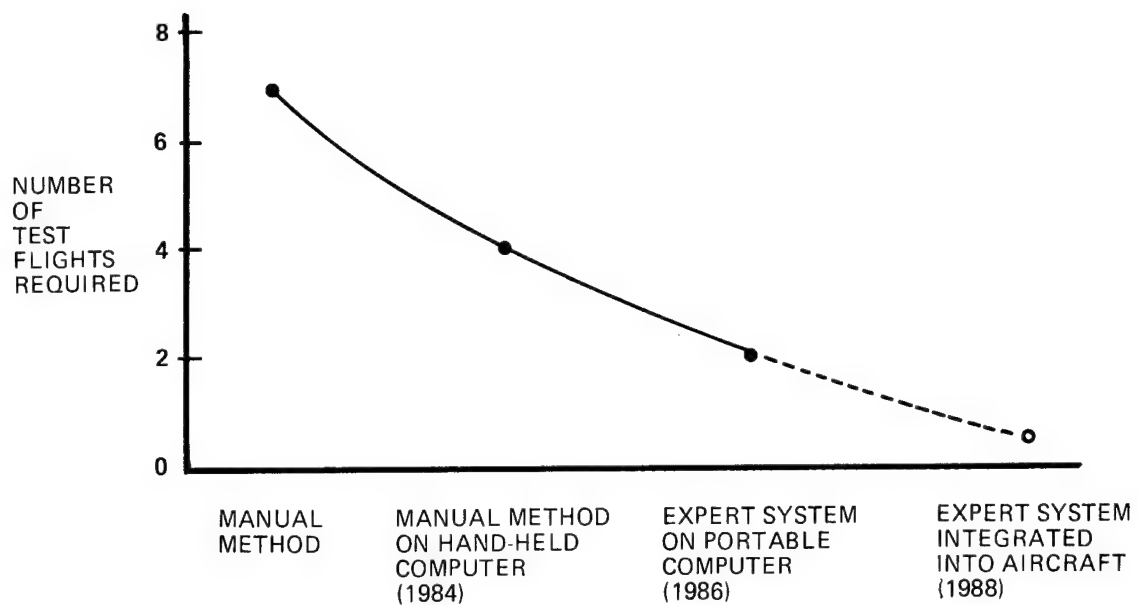


Figure 8. Reduction of Test Flights Required for CH-47D Rotor Track and Balance by Using Expert Systems

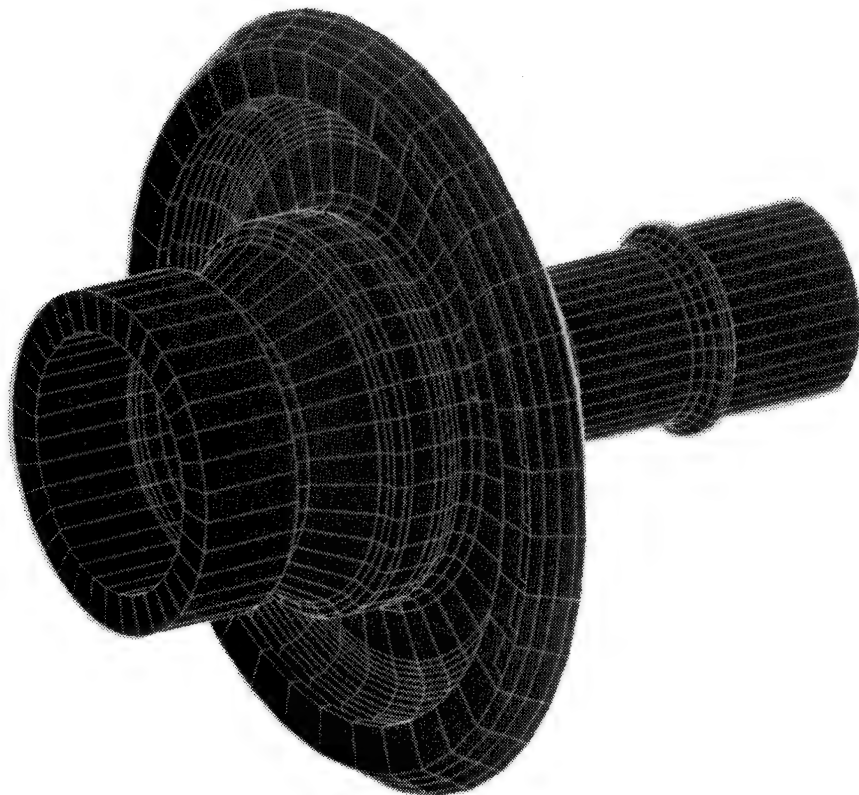
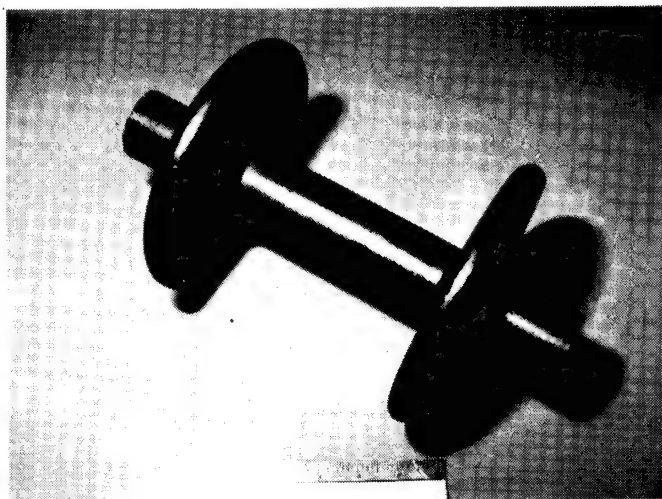
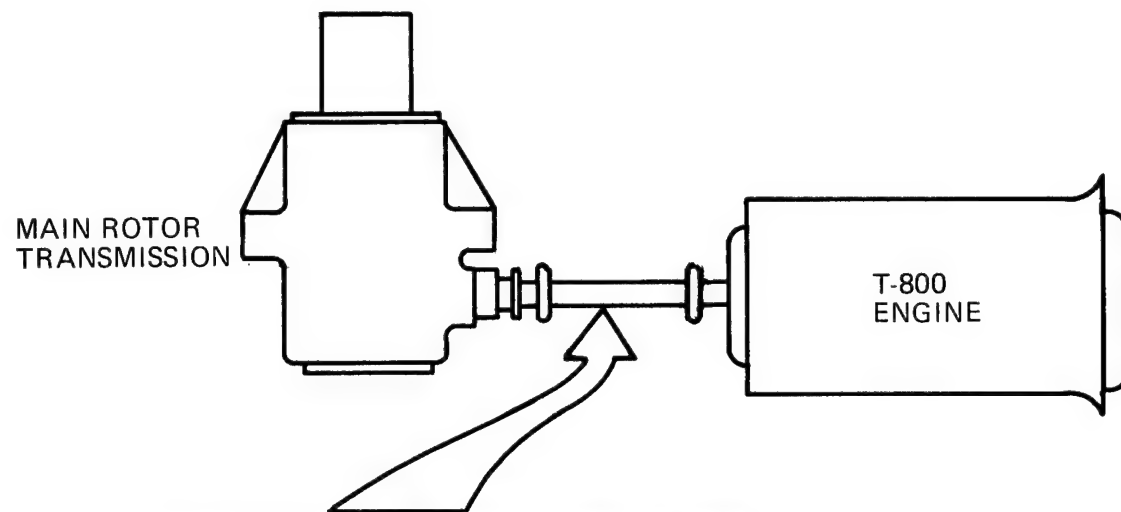


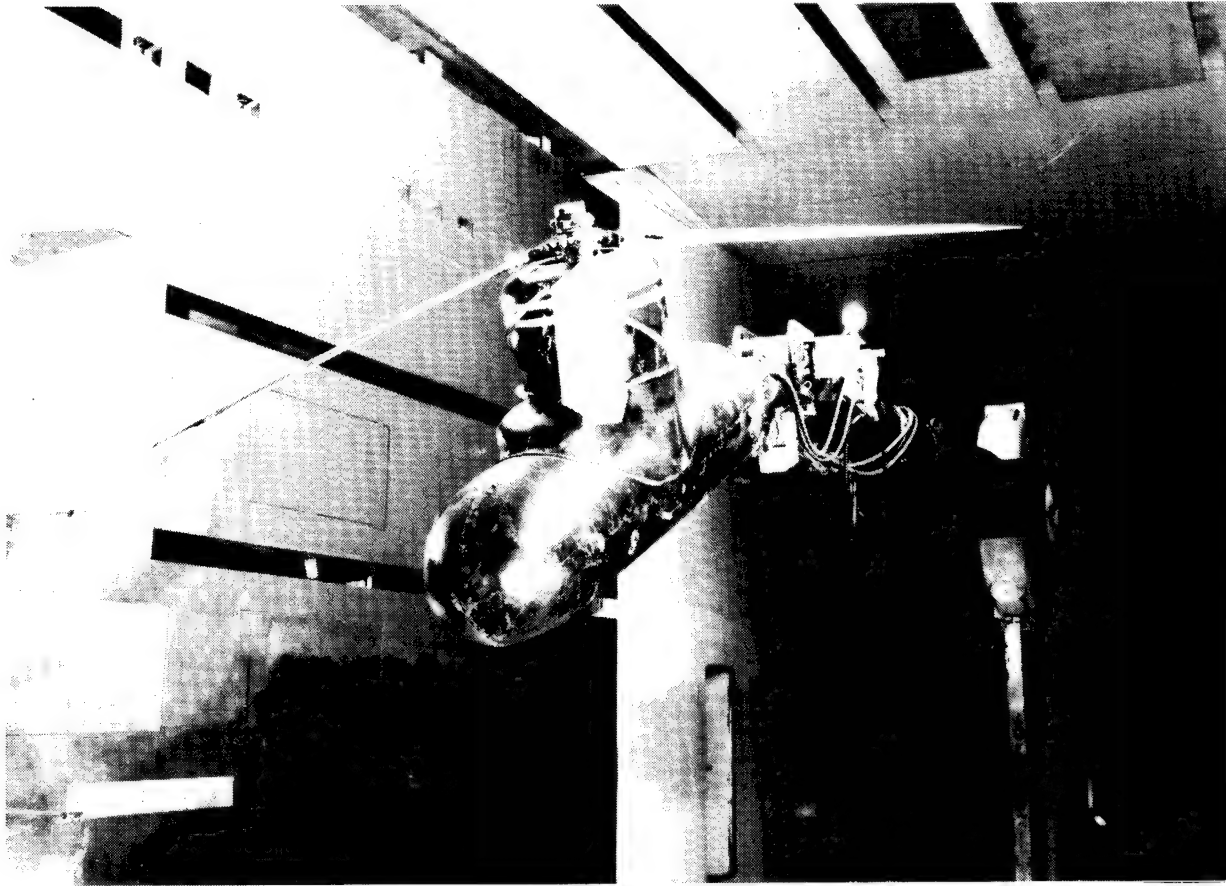
Figure 9. Three-Dimensional Finite-Element Model Used for Design of a Lightweight, Fully Integrated Shaft/Bearing Race/Spur/Spiral Bevel Gear System



23,000 RPM
1300 HP

C76914

Figure 10. Integrated All-Composite Shaft and Coupling Designed for Large Misalignment Angles



C42537

Figure 11. Single-Rotor Helicopter Model Test Stand

$$V = 150 \text{ KN} \quad \alpha_s = -5^\circ \quad \mu' = 0.39$$

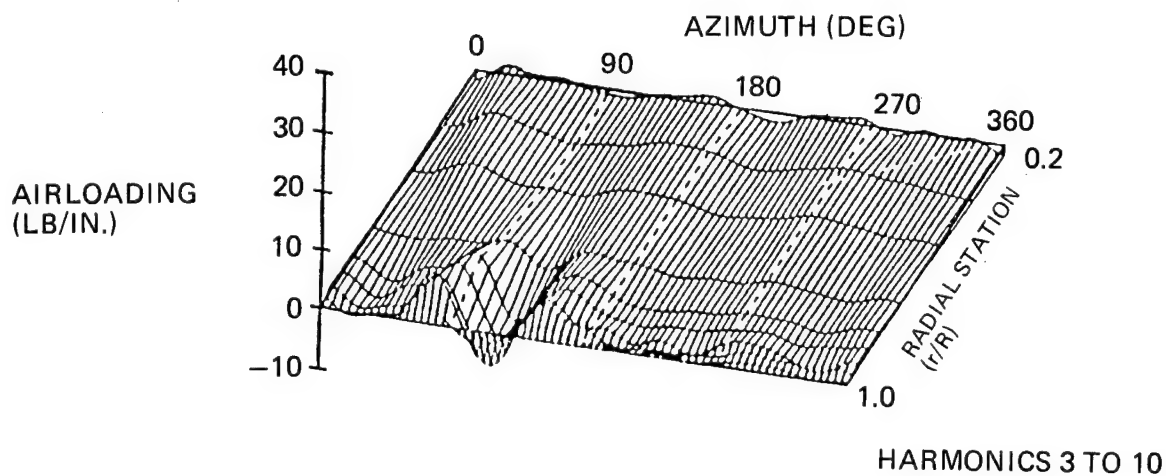
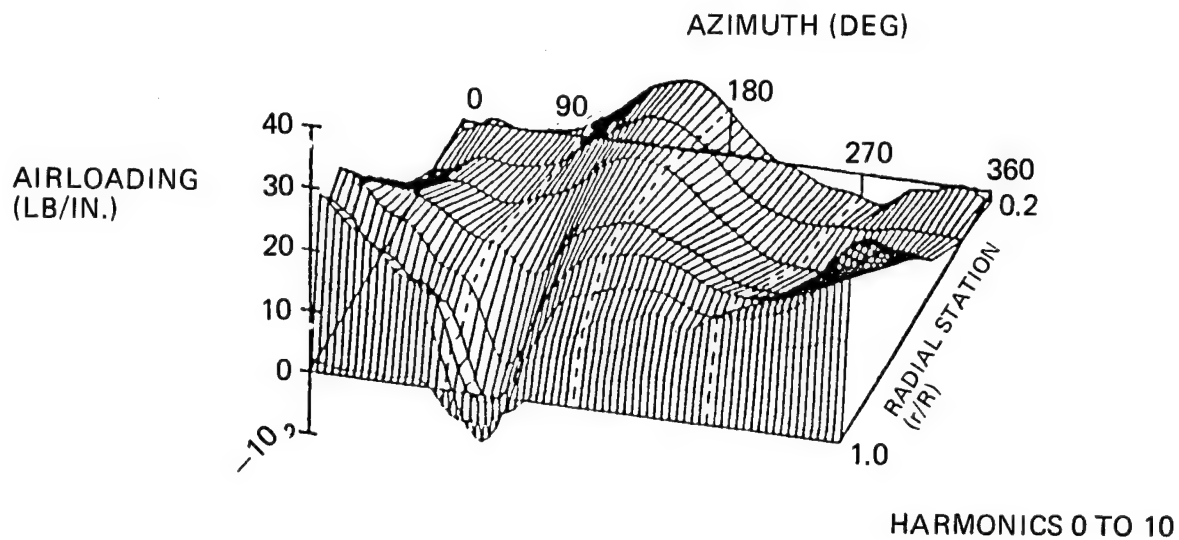


Figure 12. H-34 Data — 150 Knot Case

$V = 150 \text{ KN}$
 $\alpha_s = -5^\circ$
 HARMONICS 3 TO 10

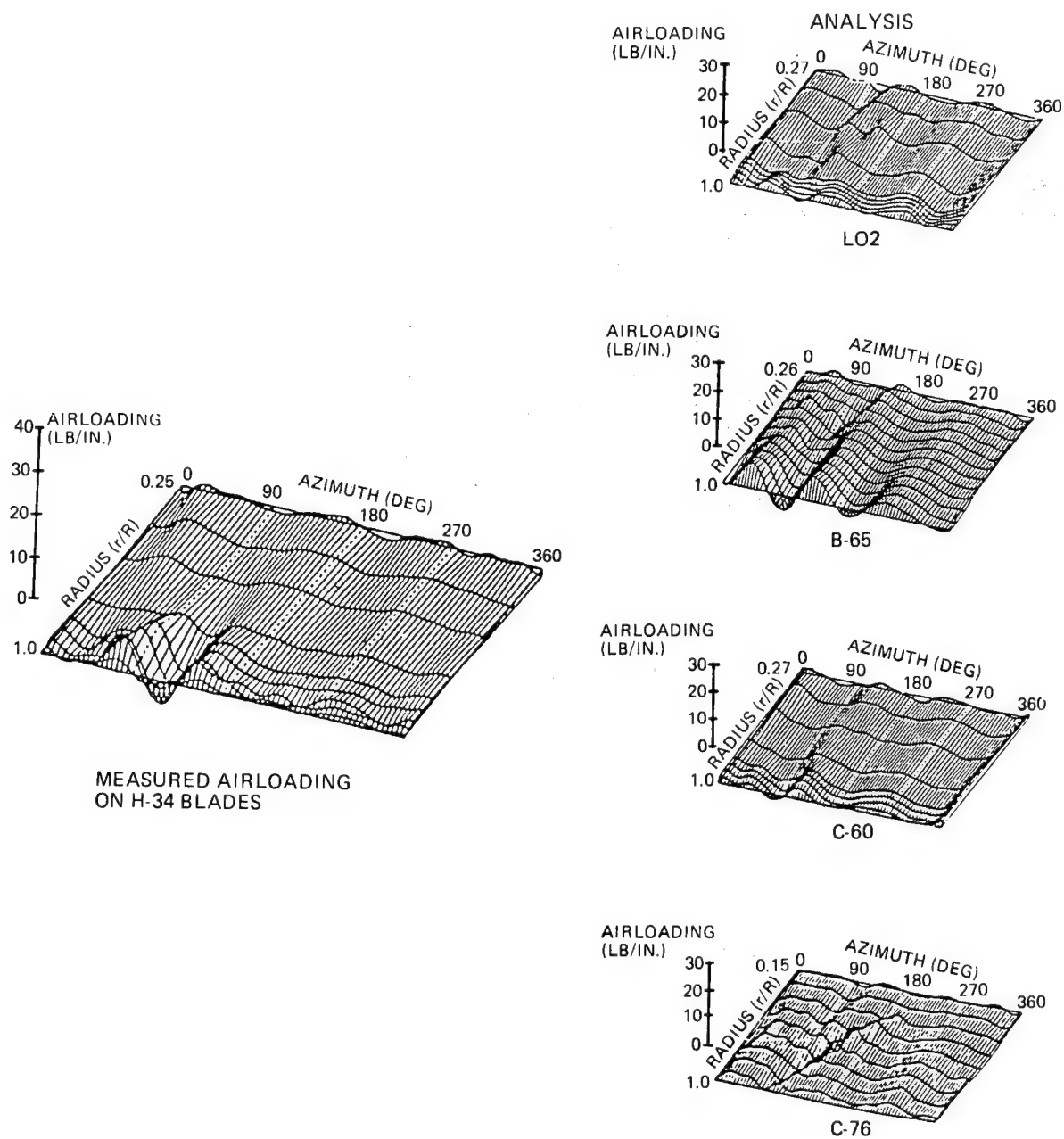


Figure 13. 1983 Test/Theory Correlation

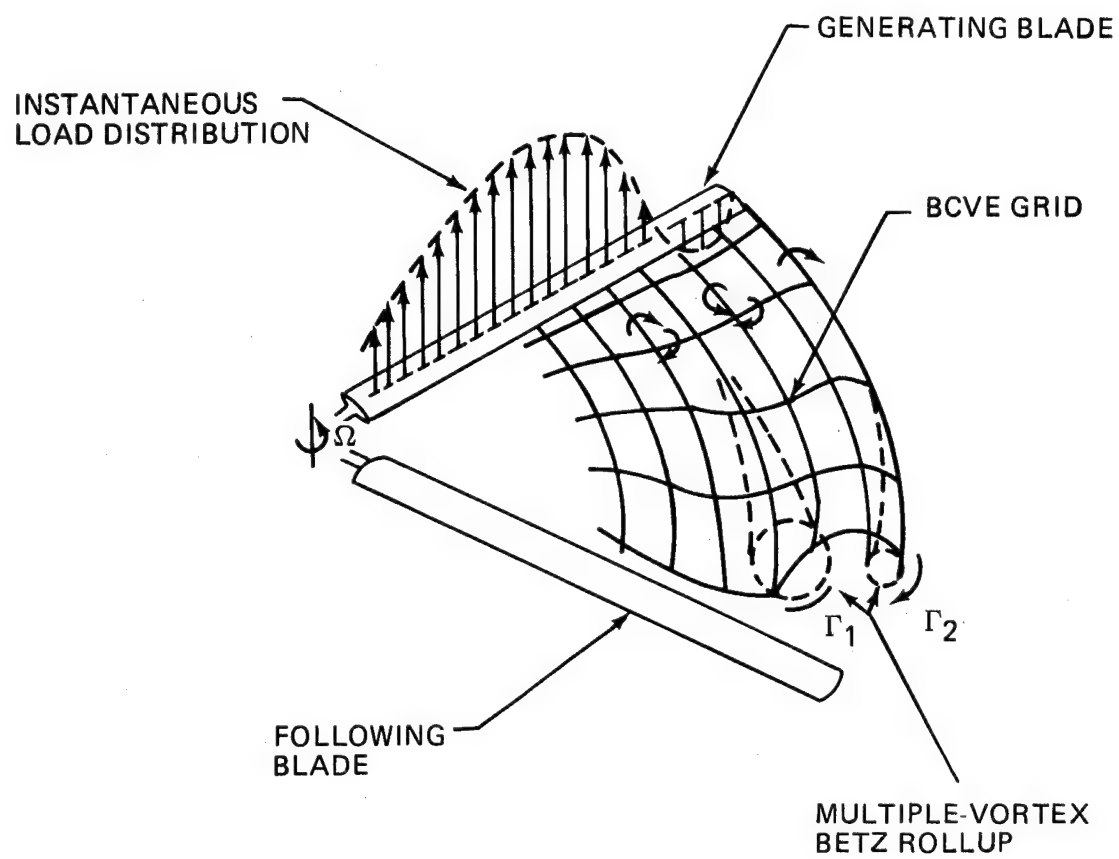


Figure 14. Illustration of Multiple Wake Rollup

KINEMATICS OF UNDEFLECTED TIP TRAILERS

$$\begin{aligned}\mu &= 0.39 \\ \alpha_S &= -15^\circ \\ \psi &= 66^\circ\end{aligned}$$

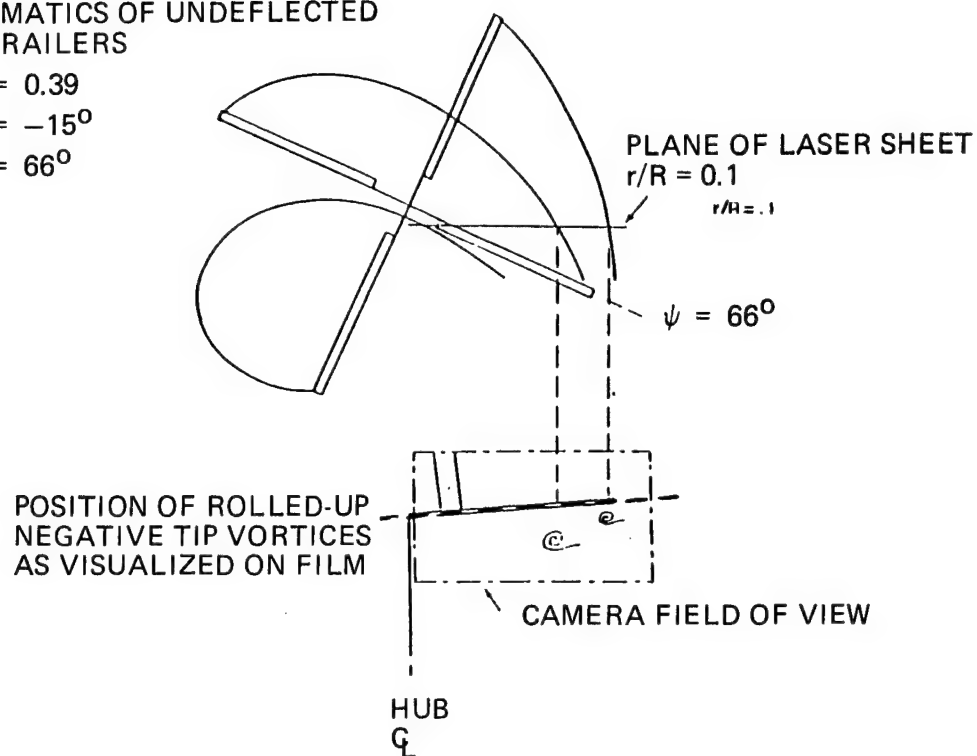
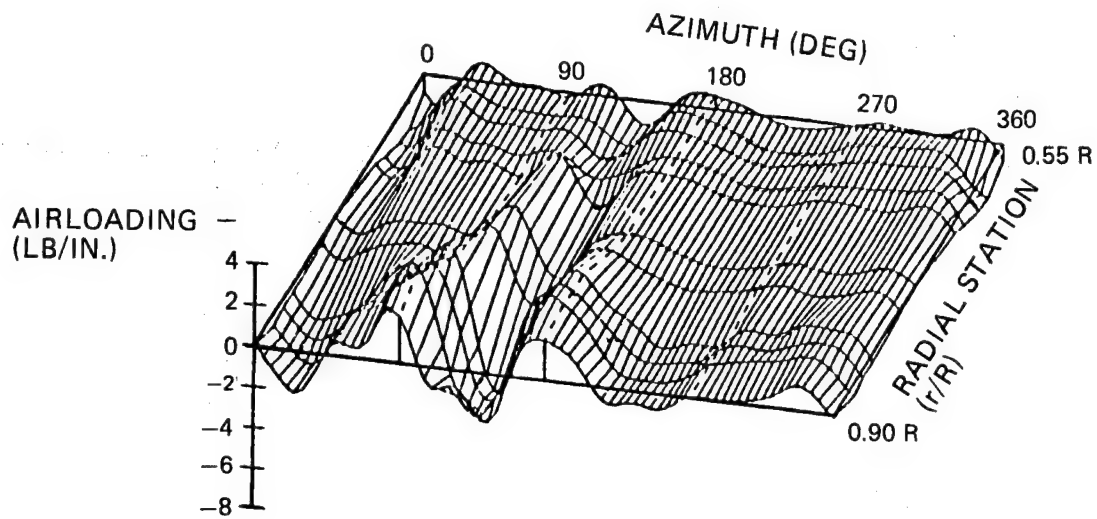


Figure 15. Towing Tank Test Results for H-34 Model Rotor. Example of Wake Kinematics

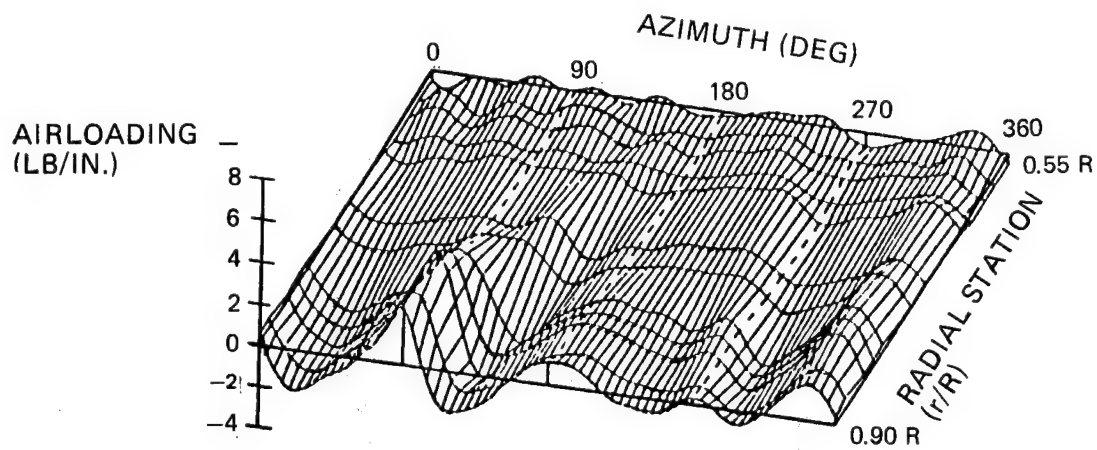
$$C'_T/\sigma_T = 0.07, \bar{X} = 0.05$$

BVWT 313 RUN 128 TP 8 $\mu' = 0.35$ $V = 146$ KN



HARMONICS 3 TO 10

BVWT 313 RUN 128 TP 6 $\mu' = 0.25$ $V = 104$ KN



HARMONICS 3 TO 10

Figure 16. Effect of Speed on LE Deduced Blade Airload Distributions

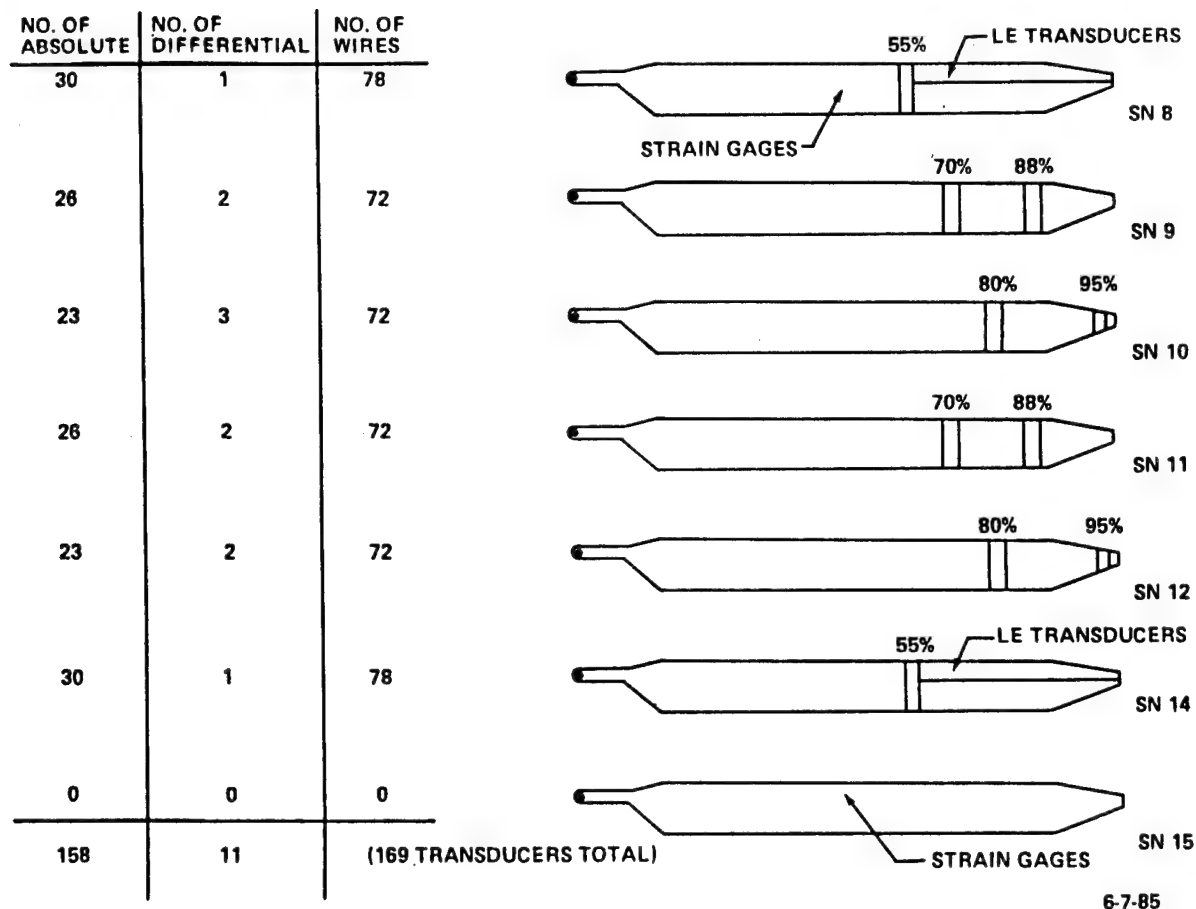


Figure 17. Pressure Blades for BVWT and DNW Tests

ROTOR WAKE MODEL DEVELOPED BY CONTINUUM DYNAMICS, INC, PRINCETON, NJ

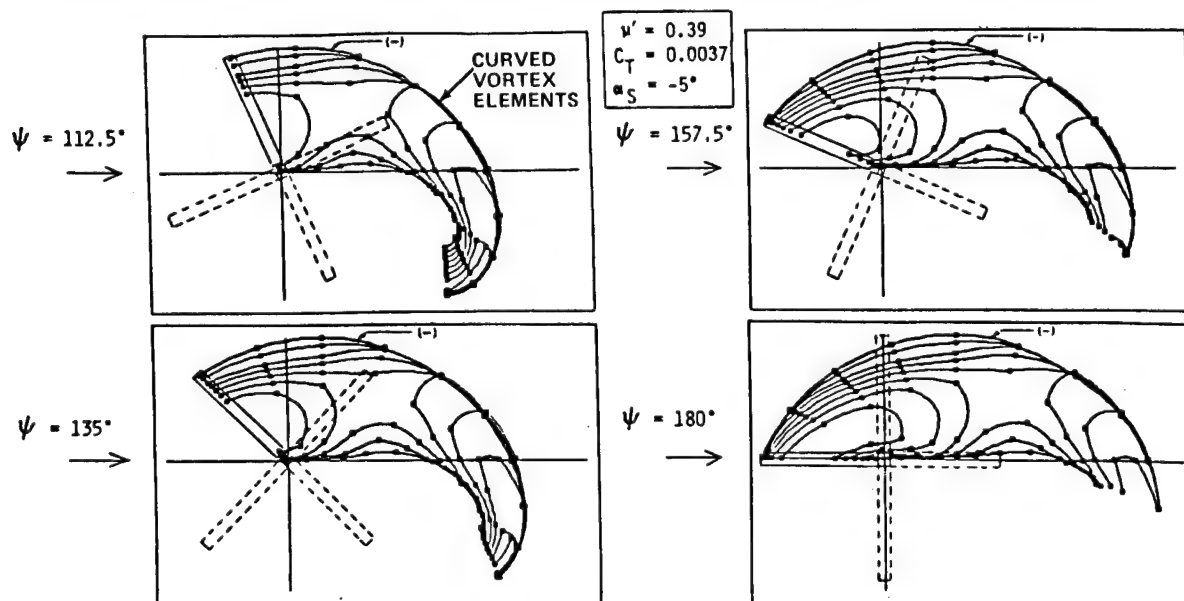


Figure 18. Top Views of Calculated Free-Wake Solutions for the H-34 Rotor (CDI)

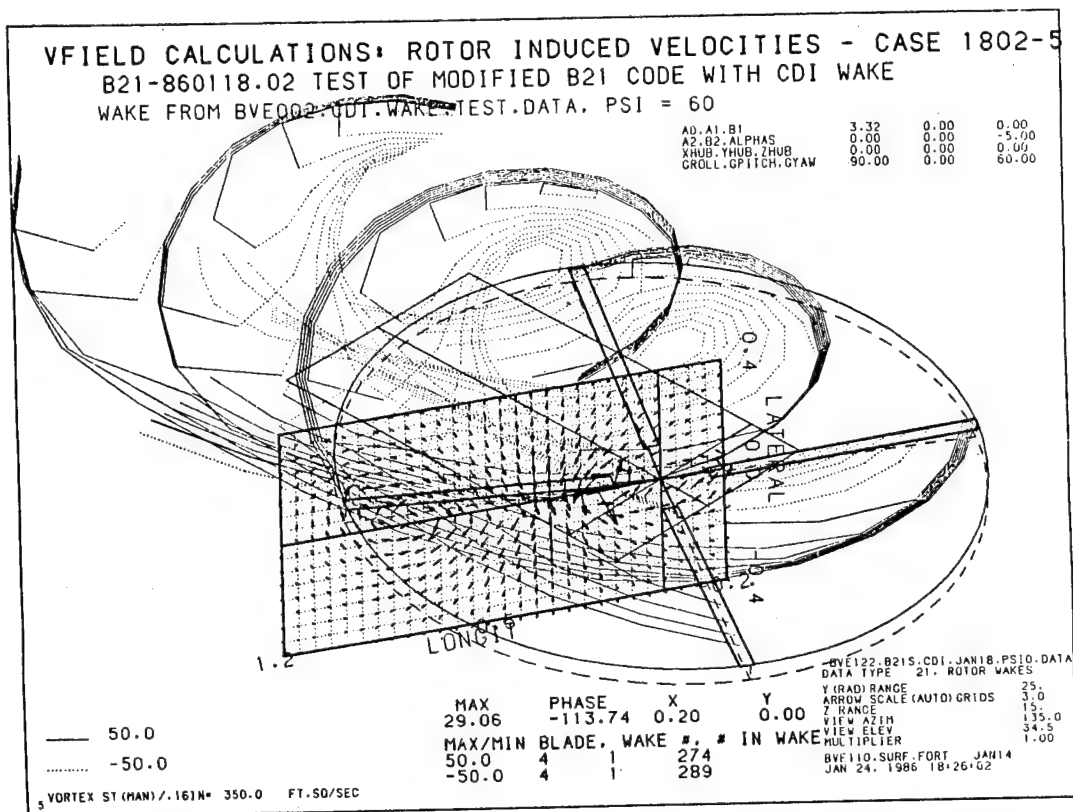


Figure 19. CDI Wake Effect on a Computation Plane Perpendicular to a Blade

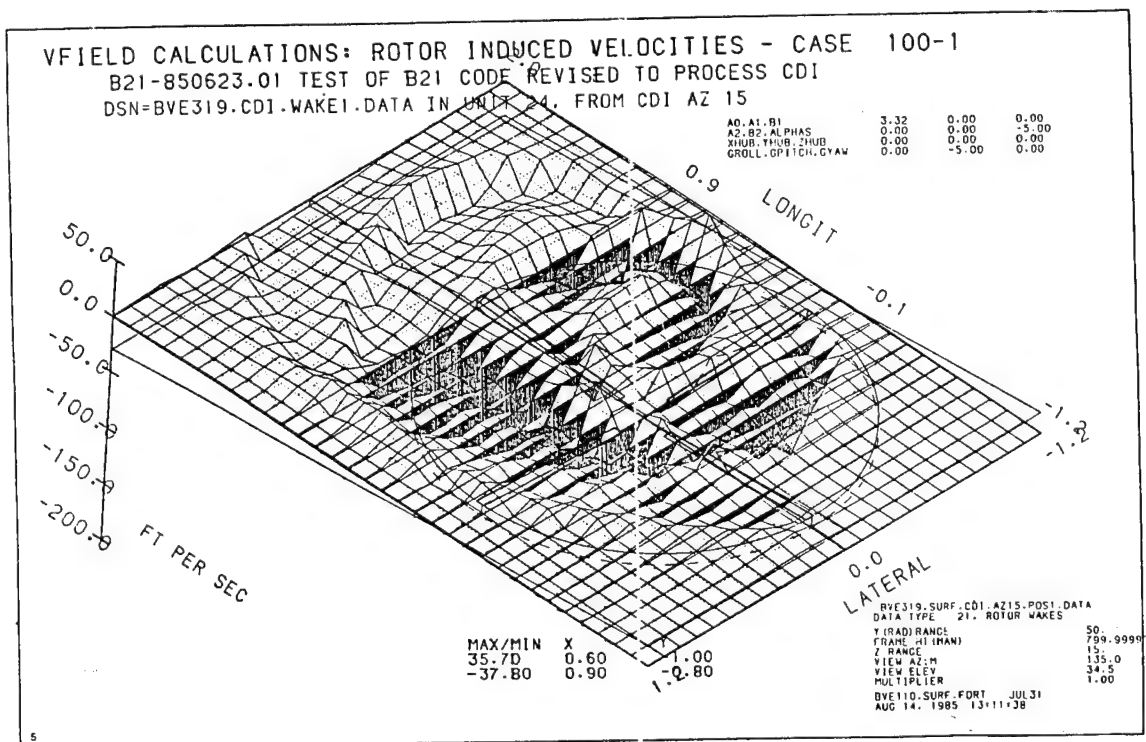


Figure 20. Velocities Induced on a Horizontal Computation Plane

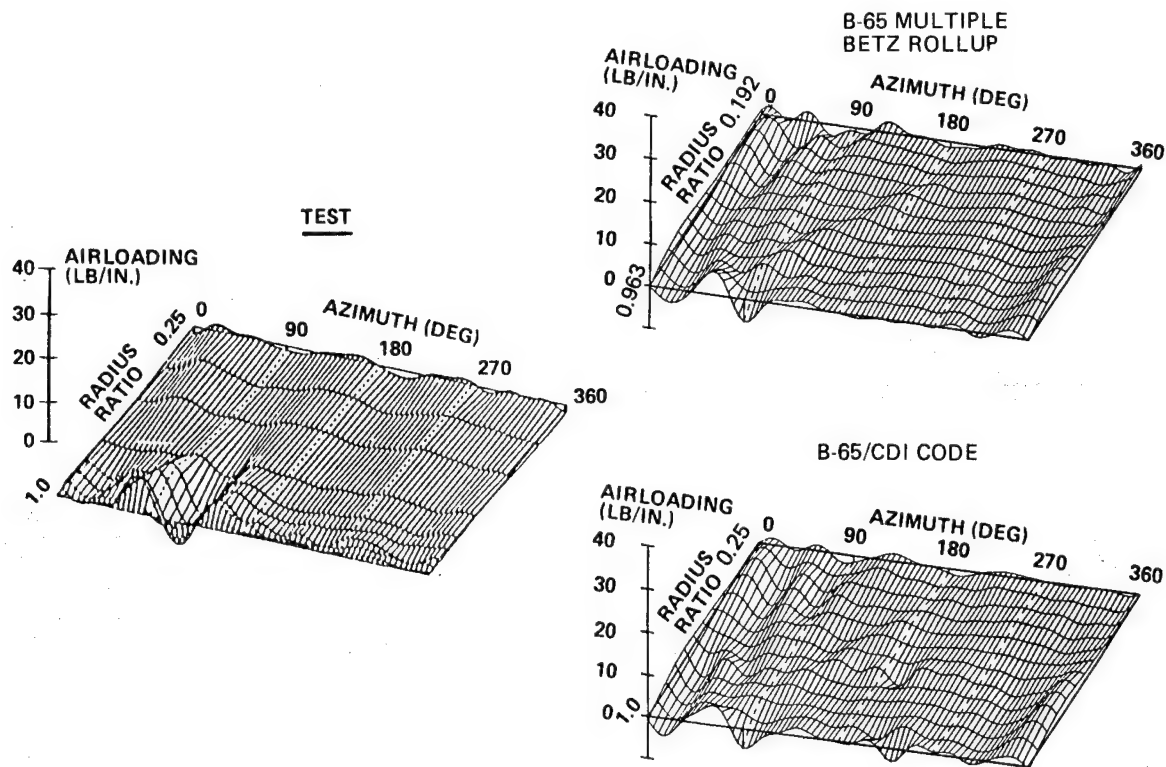
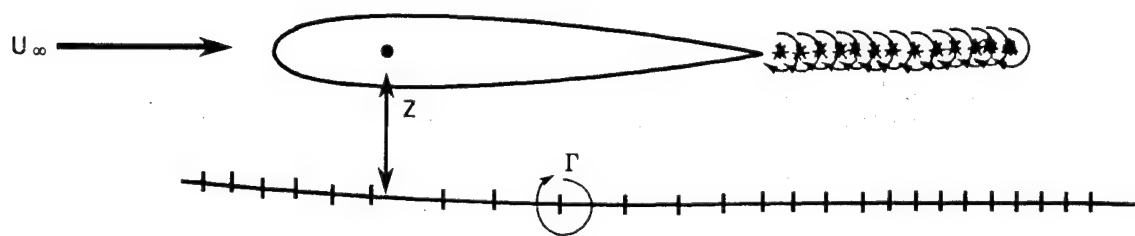


Figure 21. New Wake Models Improve Prediction of Vibratory Airloads



- | <u>$z > \text{chord}$</u> | <u>$z < \text{chord}$</u> | Blade/Vortex
Encounter
<u>$z = 0$</u> |
|--|--|---|
| <ul style="list-style-type: none"> • Lifting line valid • Kinematic wakes useful • Weak local 3D effects • Wakes must have correct vorticity distribution • Important for vibratory airloads • Transonic CFD codes | <ul style="list-style-type: none"> • Lifting line marginal • Free wakes needed • Moderate local 3D effects • Approximation of BVI possible • Important for noise and vibration • Euler codes under development | <ul style="list-style-type: none"> • Lifting line useless • Local 3D methods and free wakes • Strong local 3D effects • Accurate BVI needed • Critical to noise reduction • Viscosity effects |

Figure 22. Illustration of BVI Regimes

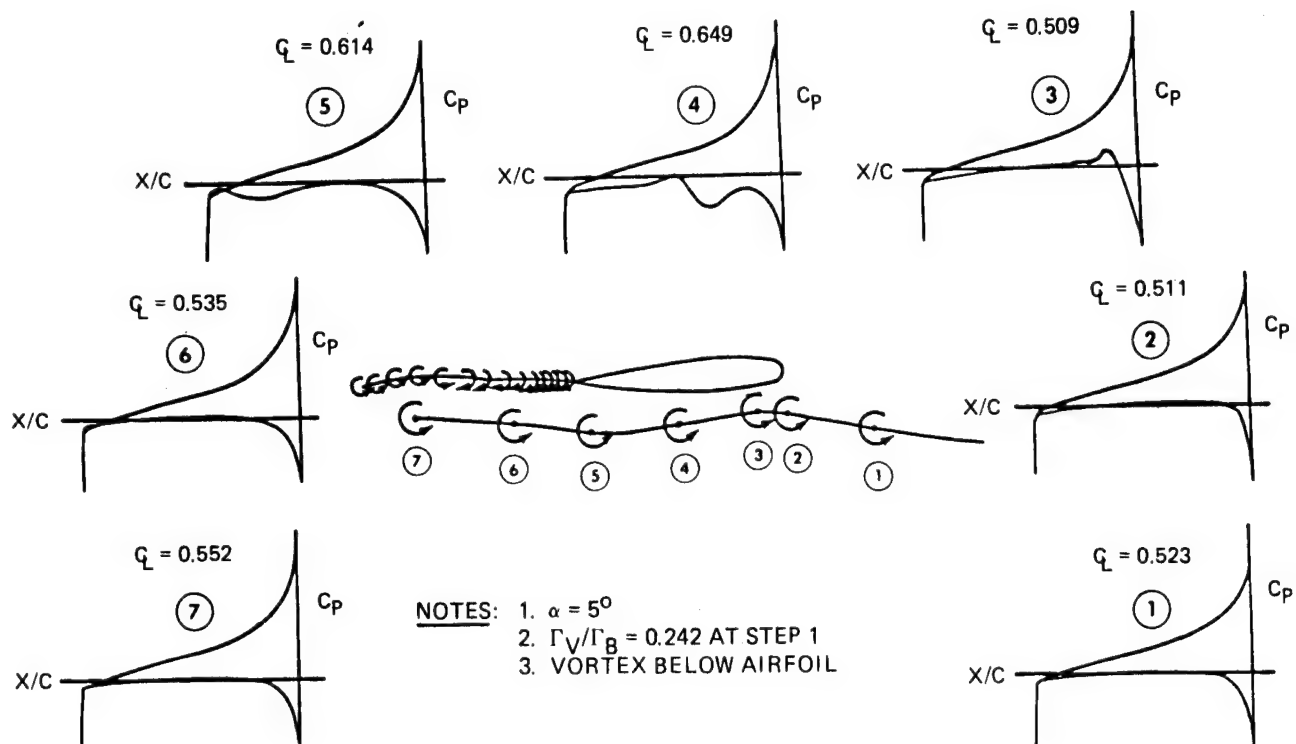


Figure 23. Effect of Blade Vortex Interaction on Instantaneous Pressure Distribution Evaluated by Joukowski Transformation Method

LIFTING LINE VERSUS EXACT SOLUTION

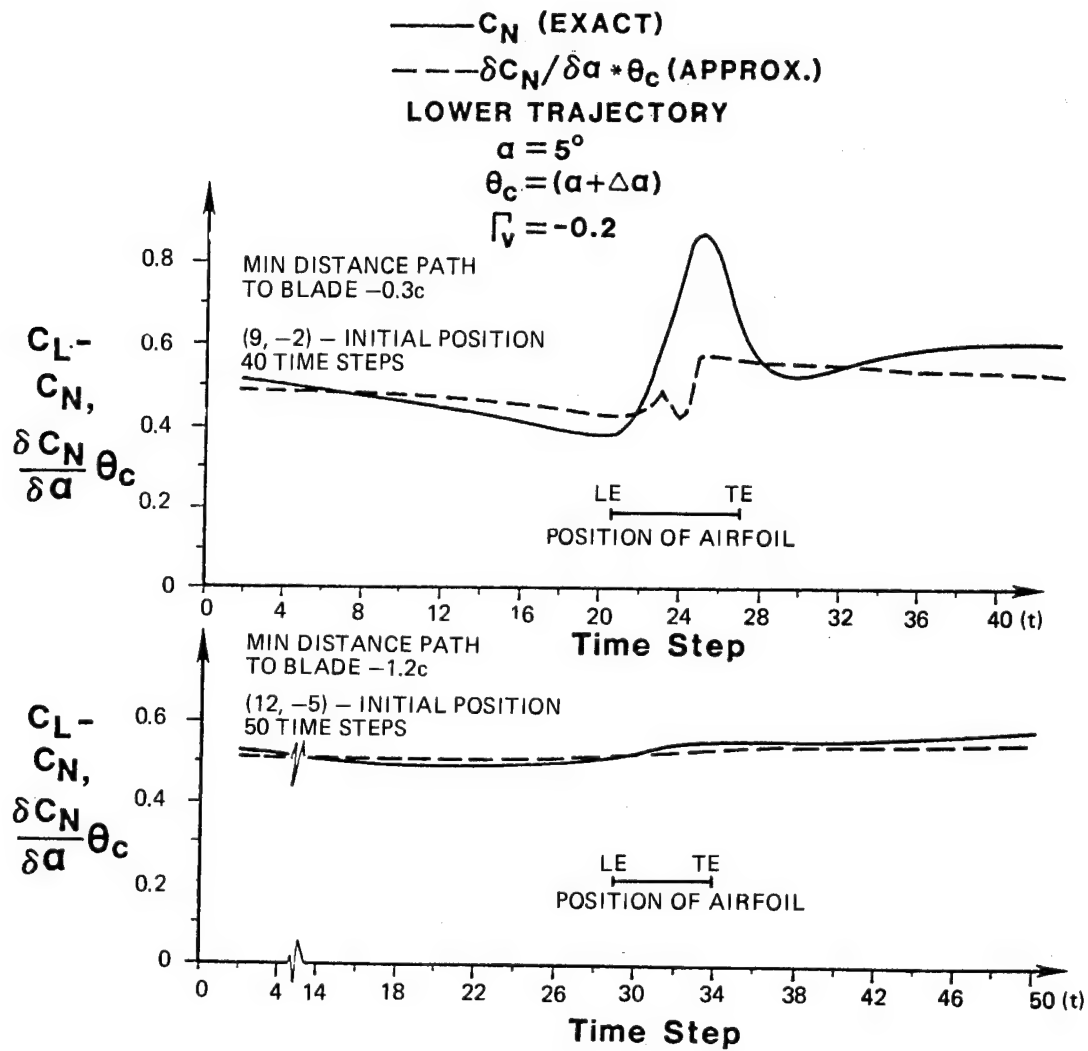


Figure 24. BVI Effects Estimated by Joukowsky Method

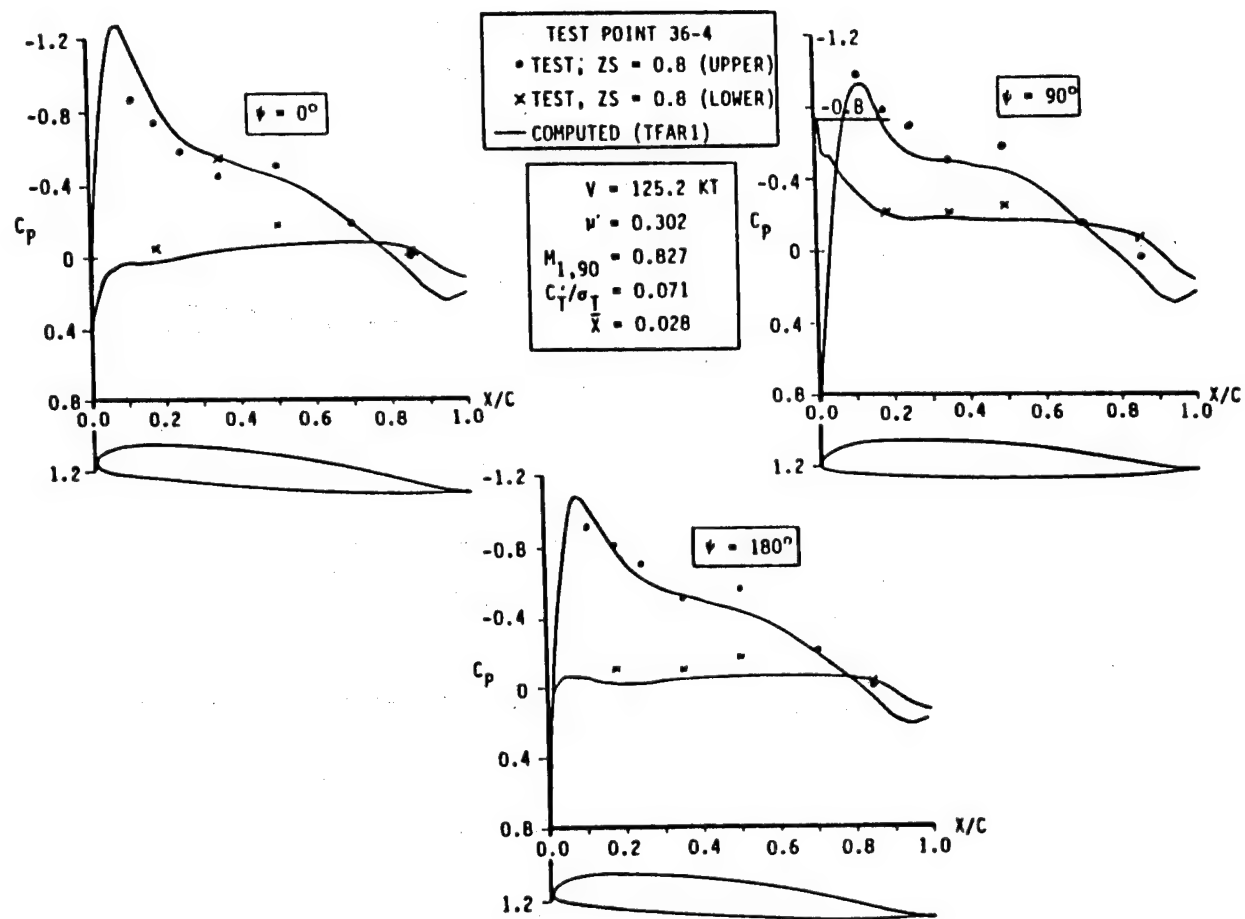


Figure 25. Test/Theory Correlation of BVWT 313 with B-65/TFAR-1

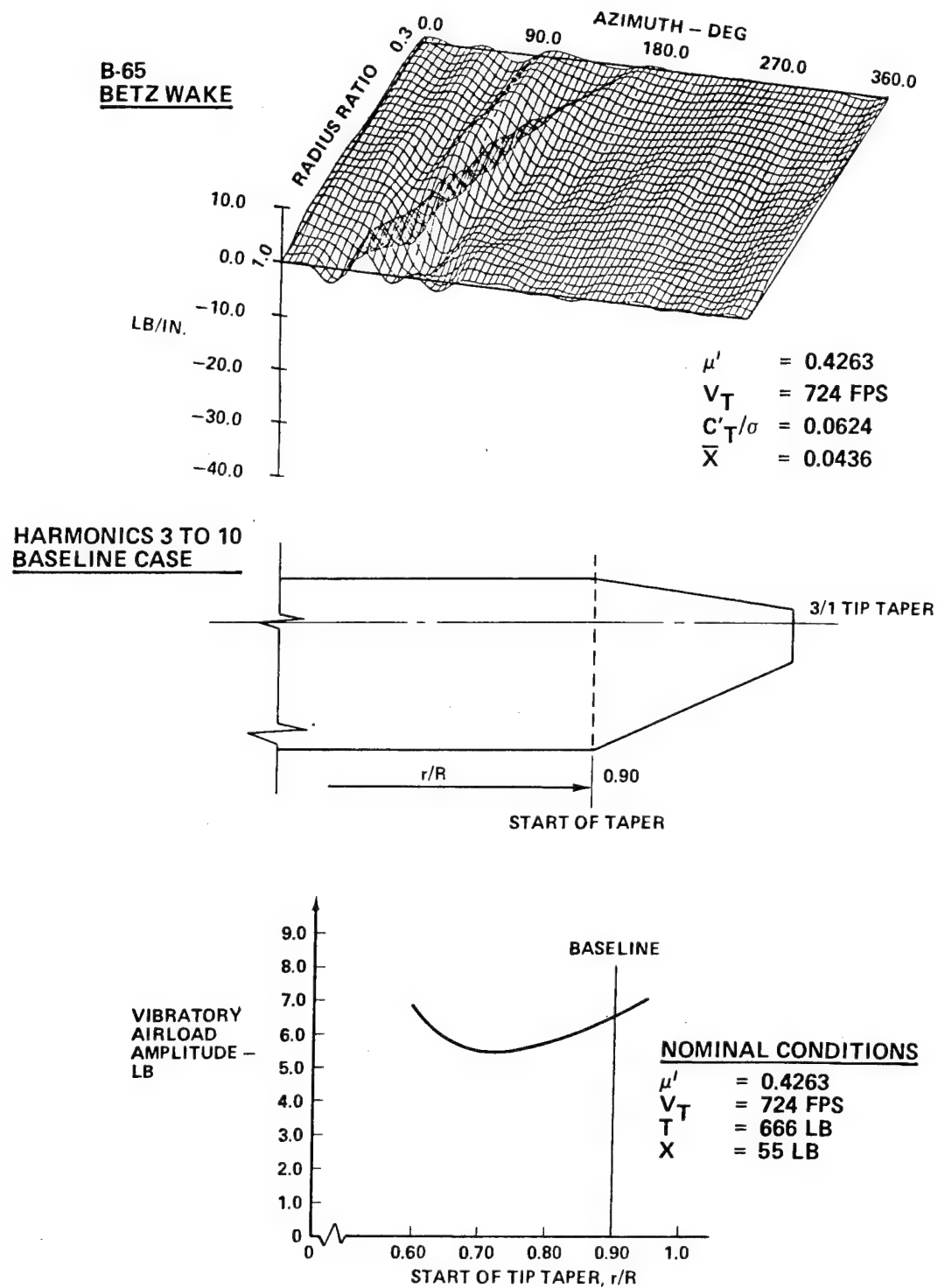


Figure 26. Vibration Reduction Trends

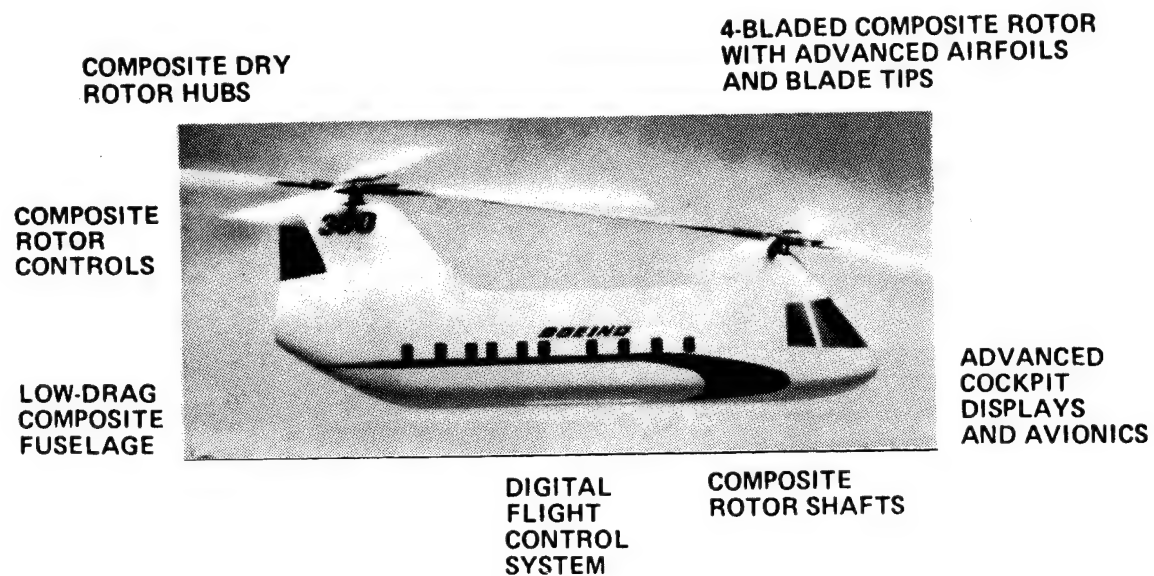


Figure 27. Model 360 Advanced Technology Helicopter

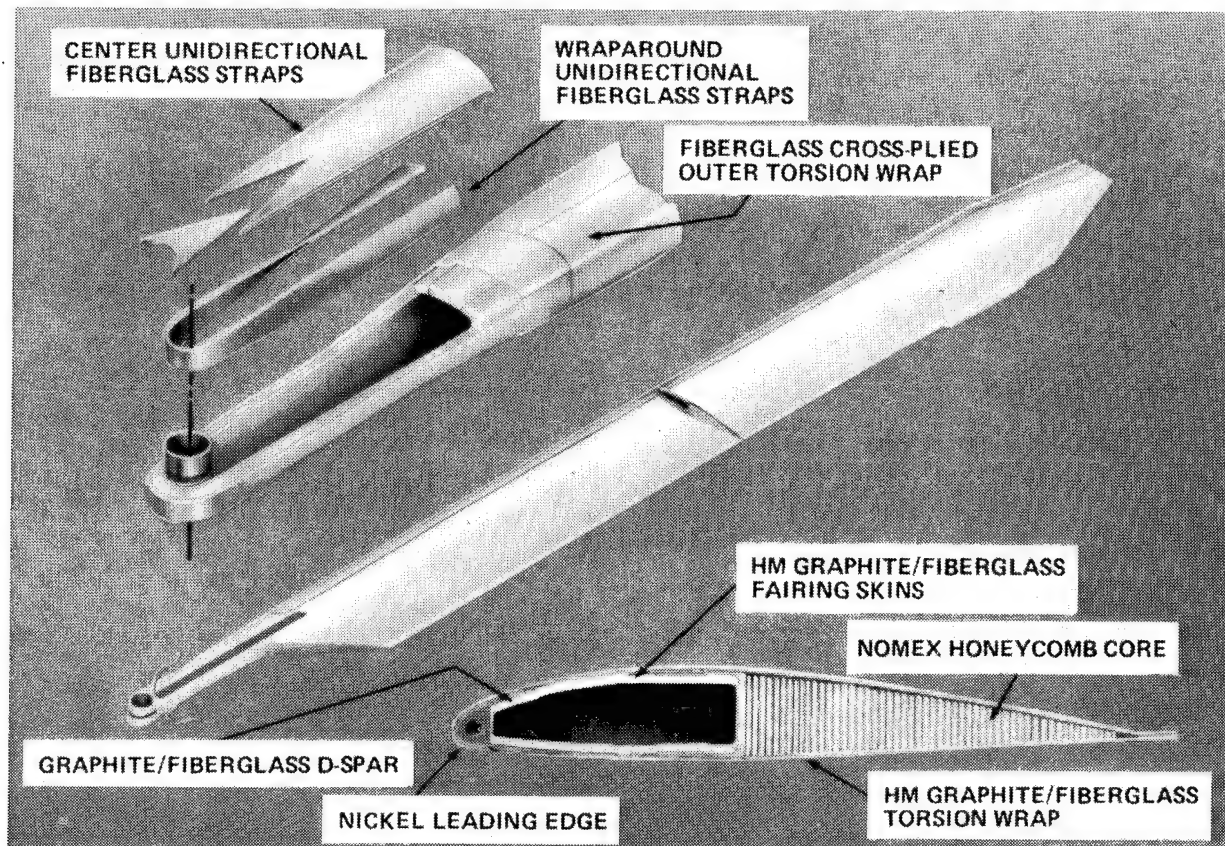


Figure 28. Model 360 High-Performance Rotor Construction (VR-12/VR-15 Airfoils)

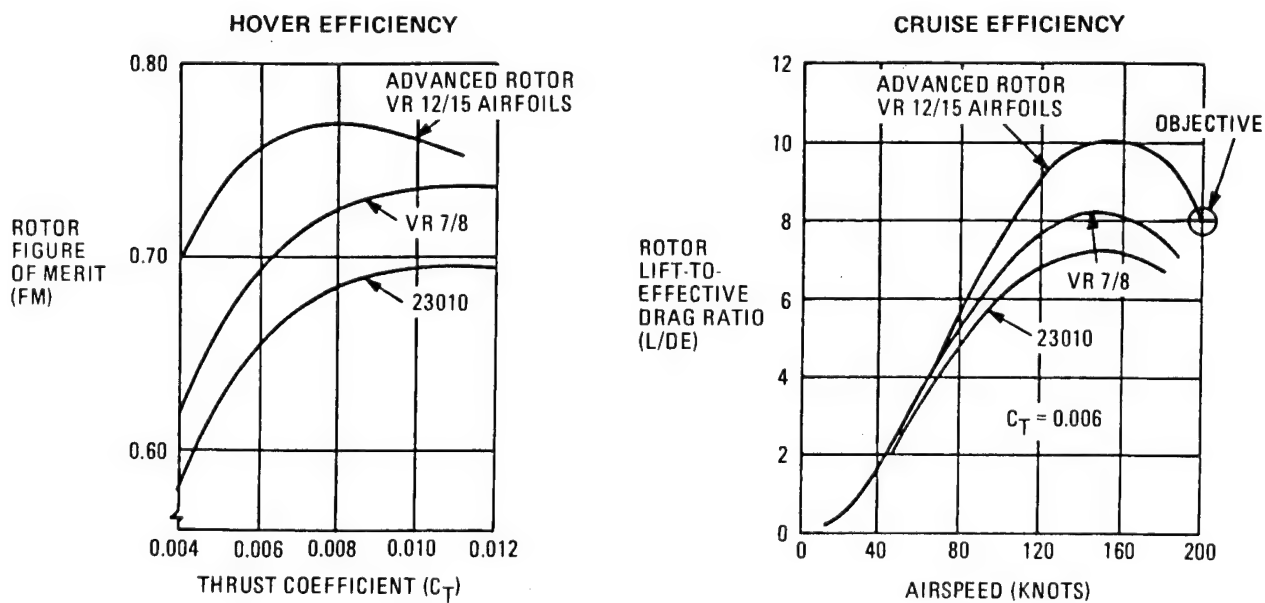


Figure 29. Model 360 High-Performance Rotor Wind Tunnel Results

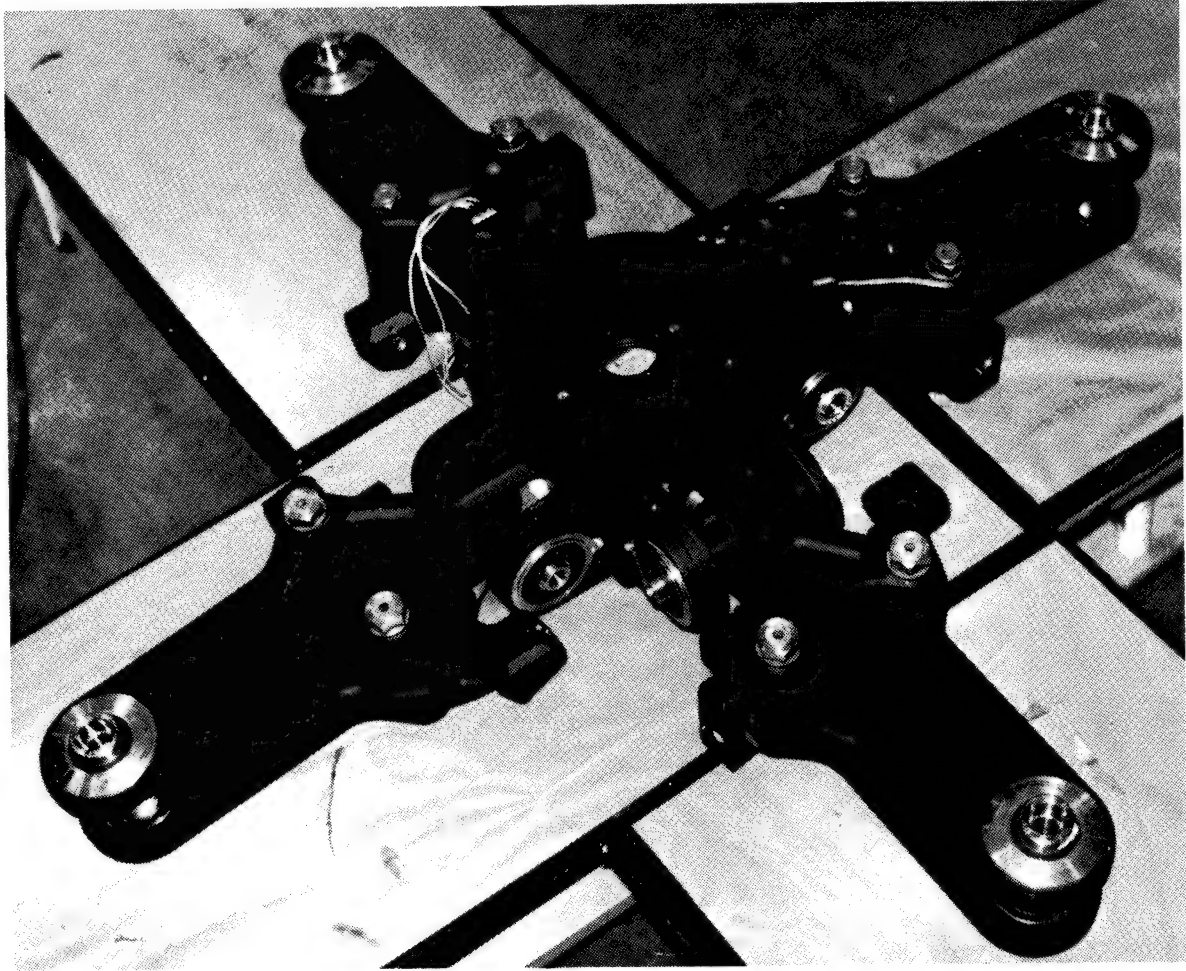
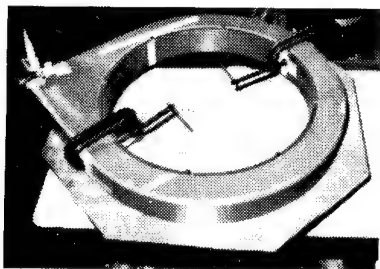
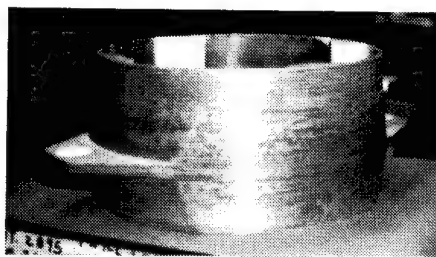


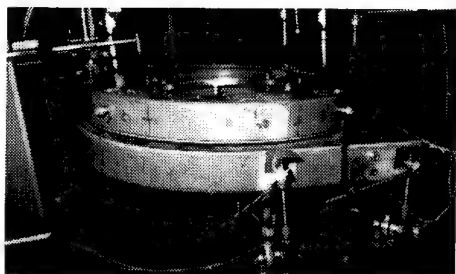
Figure 30. Model 360 Composite Dry Hub



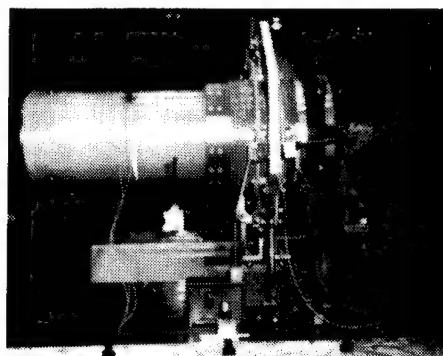
Swashplate Ring



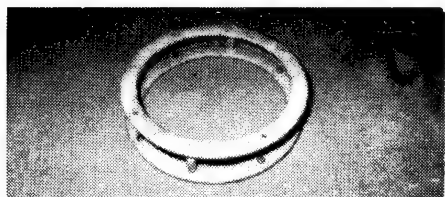
Slider



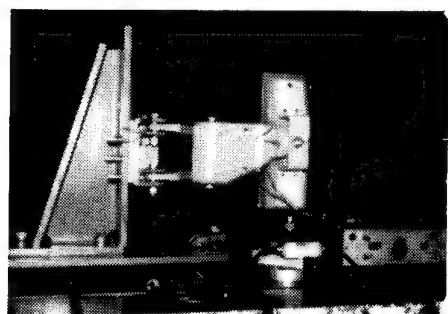
Swashplate Assembly



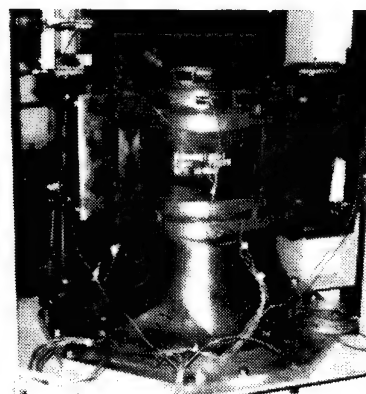
Slider Guide Assembly



Gimbal Ring

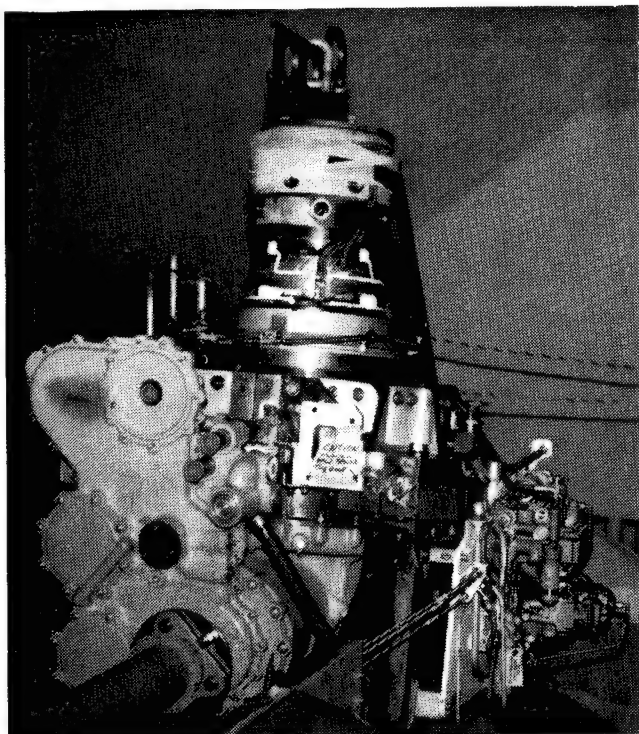


Scissors

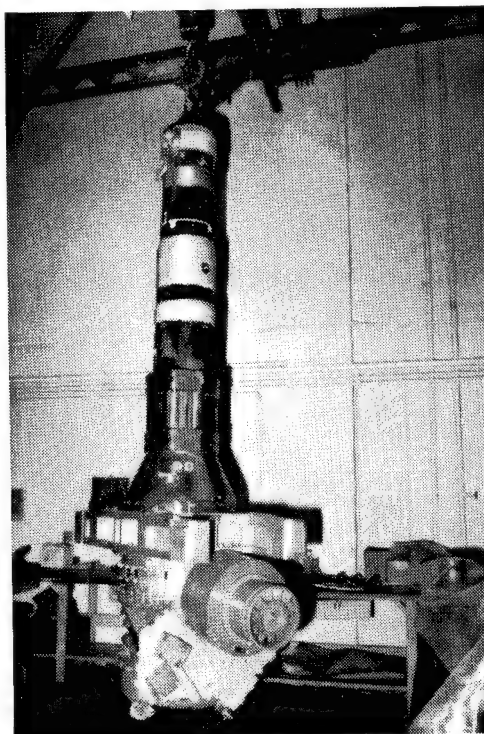


Standpipe-Actuator
Supports

Figure 31. Model 360 Composite Rotor Controls

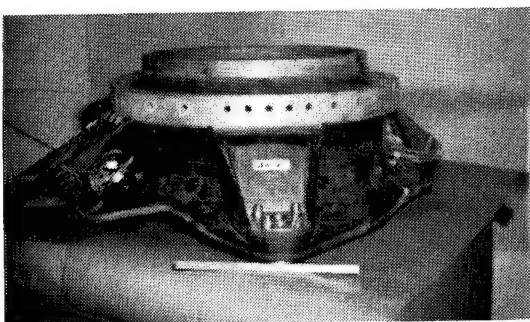


Forward Transmission

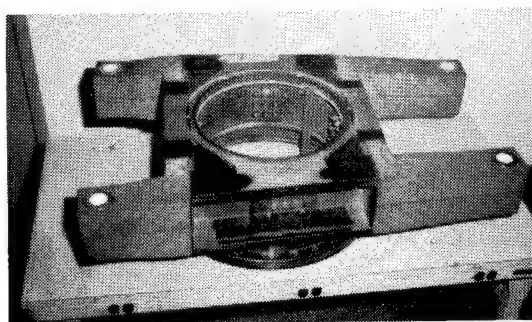


Aft Transmission

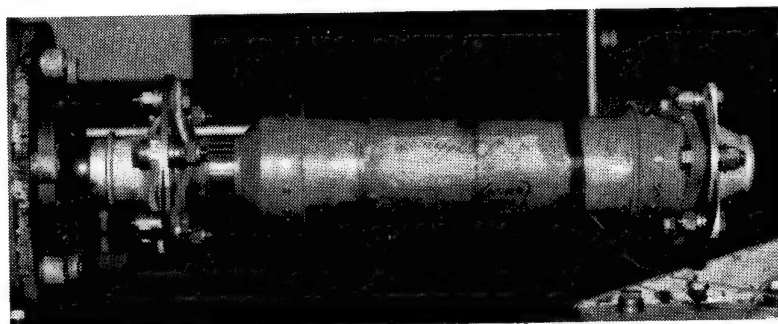
Figure 32. Model 360 Drive System: Composite Rotor Shafts



Forward Transmission Cover

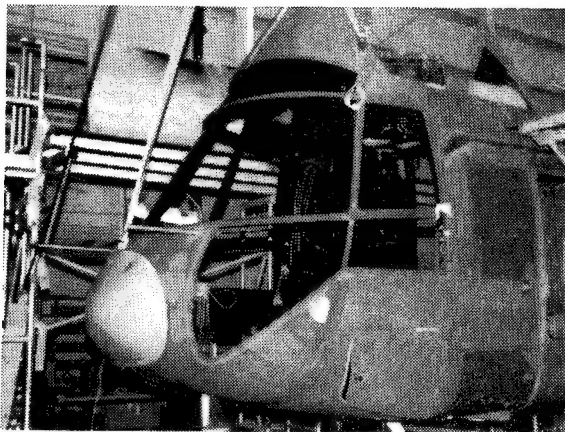


Aft Transmission Cover

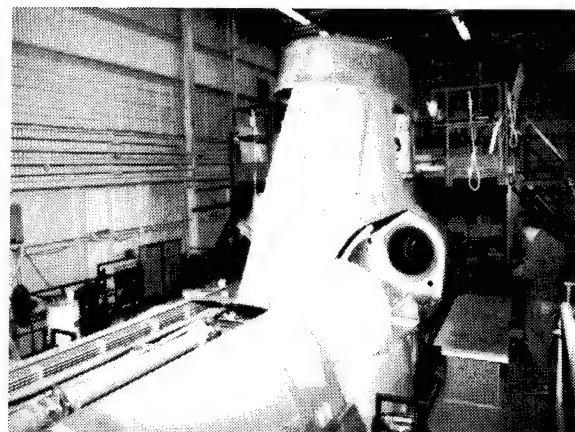


Synchronizing Shaft

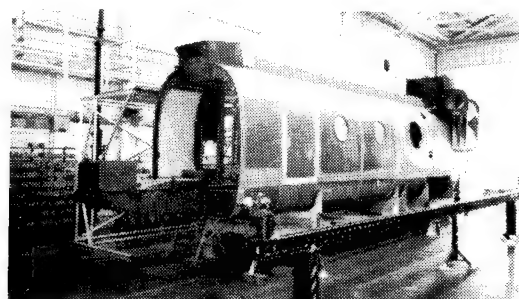
Figure 33. Model 360 Drive System: Composite Components



Nose Enclosure

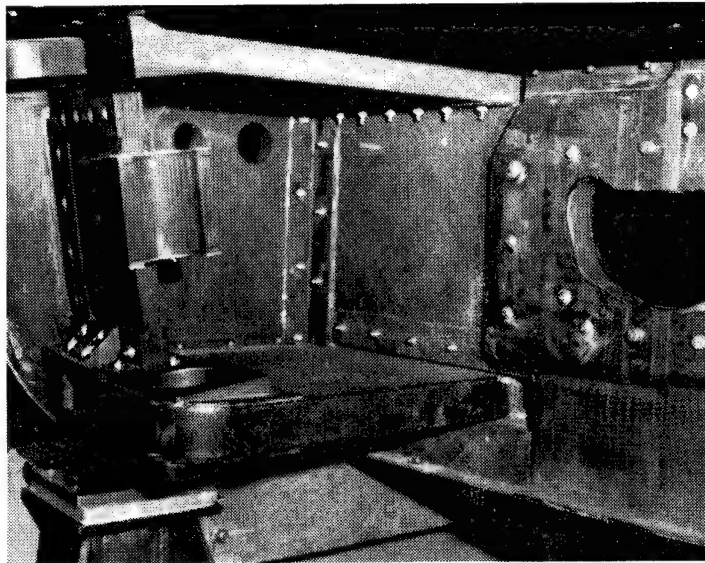


Aft Pylon Fairings

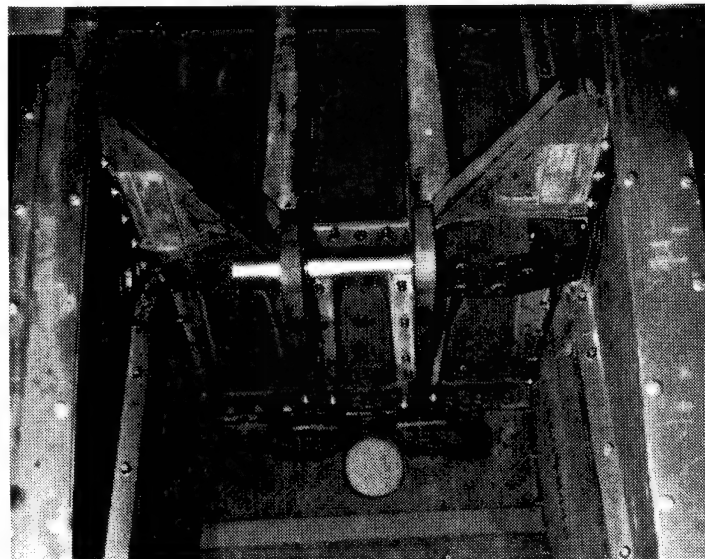


Primary Structure

Figure 34. Model 360 Composite Fuselage



Main Landing Gear



Nose Gear

Figure 35. Model 360 Fuselage Composite Backup Structure

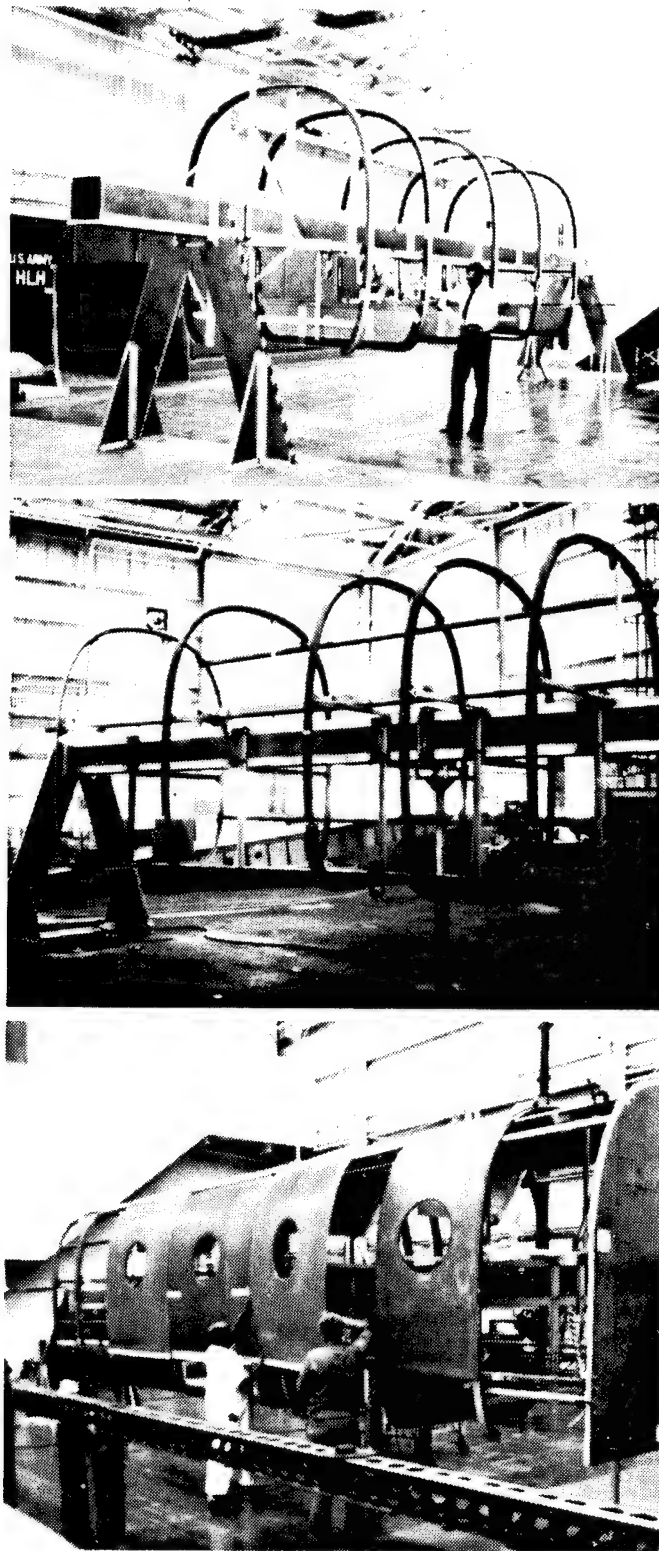


Figure 36. Model 360 Composite Fuselage Assembly

• **PROTOTYPE TOOLING COST:**

COMPOSITE AIRFRAME

\$ 1,153/FT²

SHEETMETAL

\$15,000/FT²

• **PROTOTYPE RECURRING COST:**

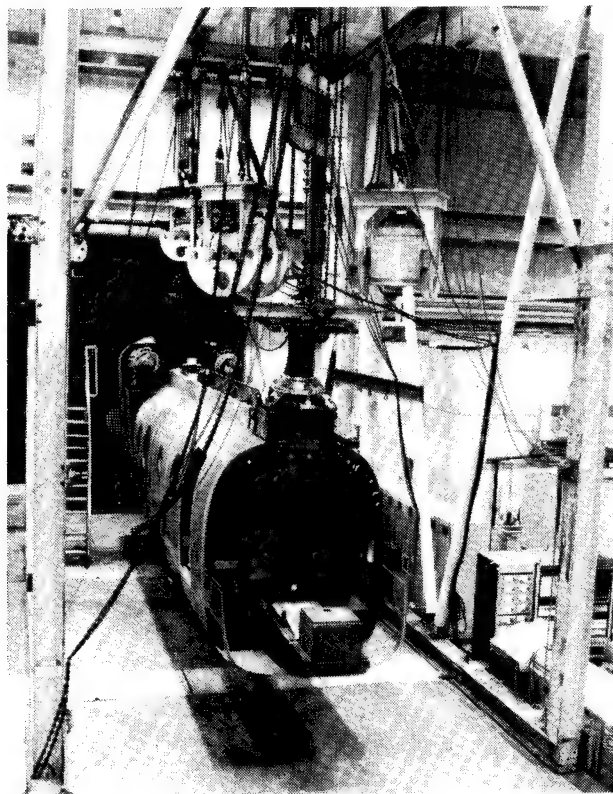
NO. 1 COMPOSITE AIRFRAME

12.5 MH/LB

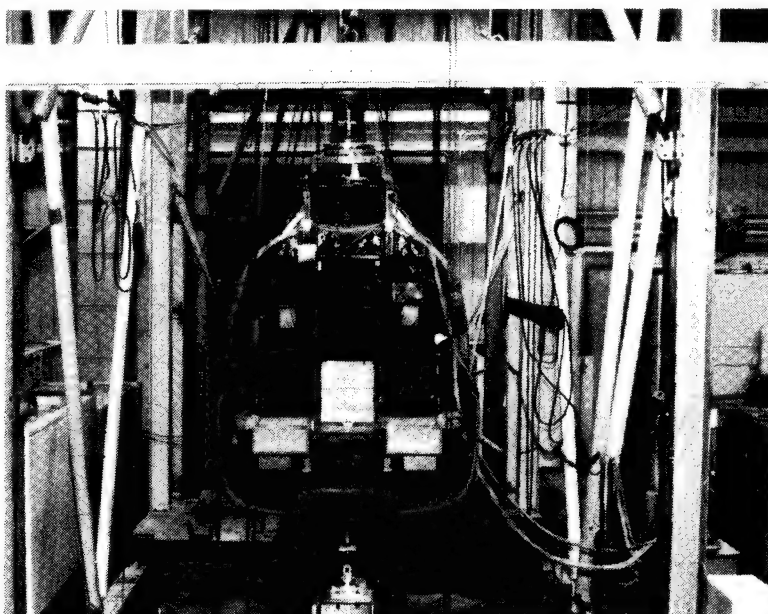
NO. 1 SHEETMETAL AIRFRAME

22.0 MH/LB

Figure 37. Cost Experience with Advanced Composite Airframe



Shake



Static Load

Figure 38. Model 360 Composite Fuselage Development Tests

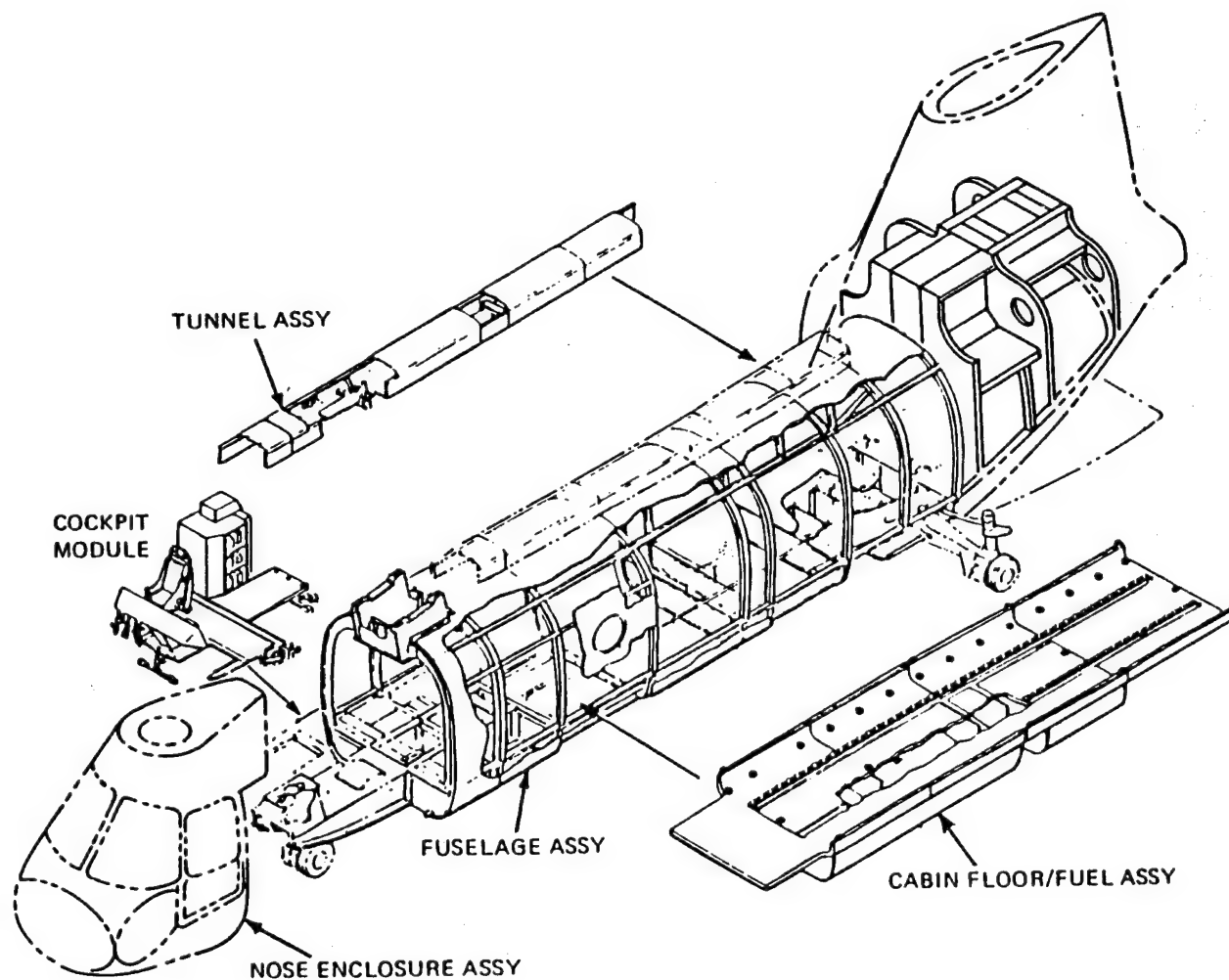


Figure 39. Model 360 Fuselage and Subsystem Modules

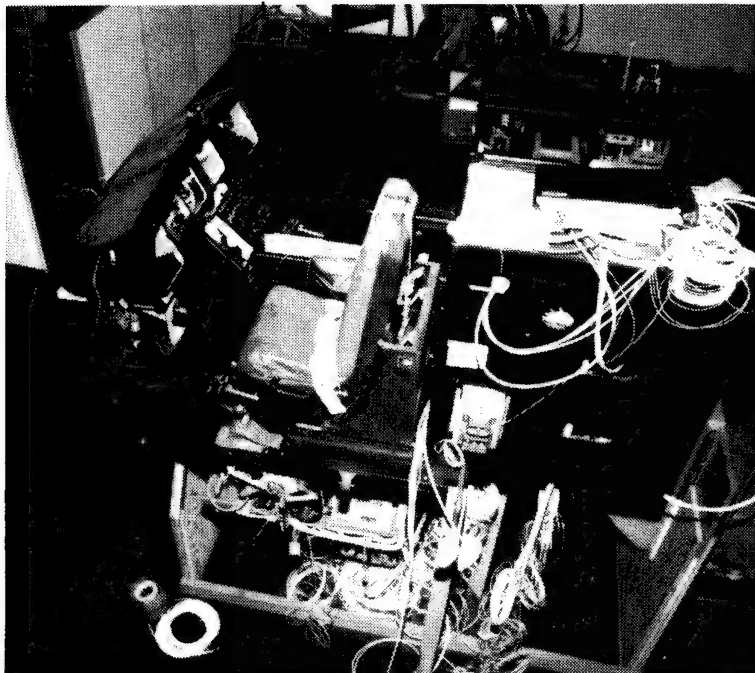
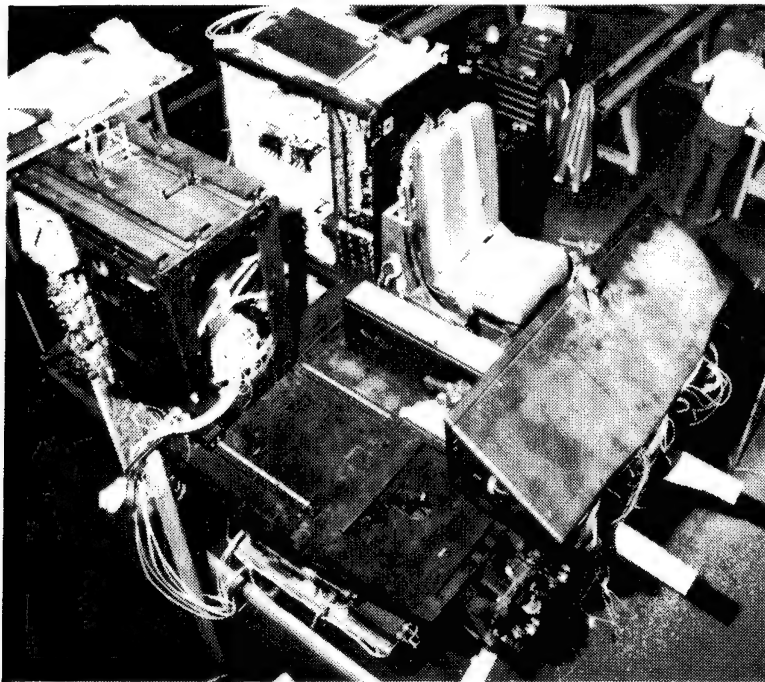


Figure 40. Model 360 Cockpit Module Assembly

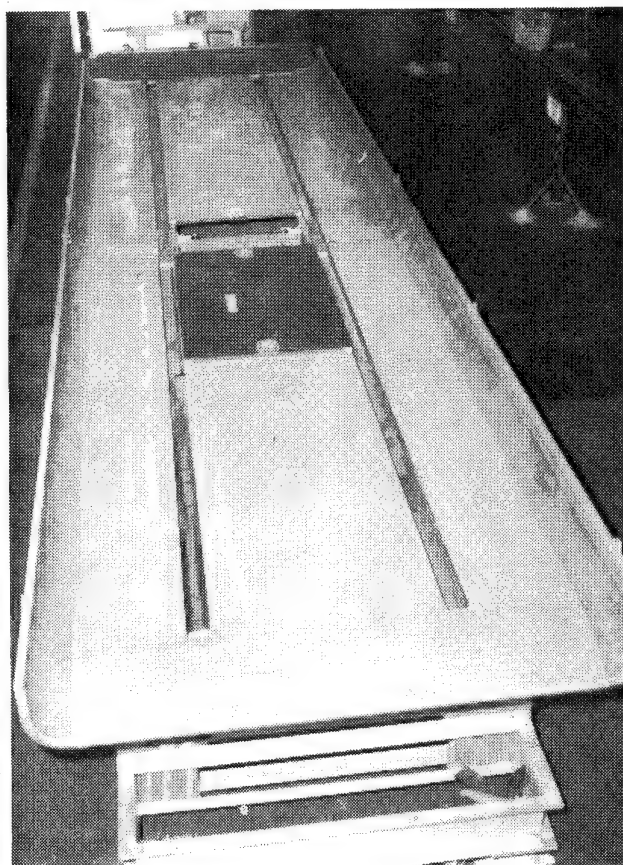
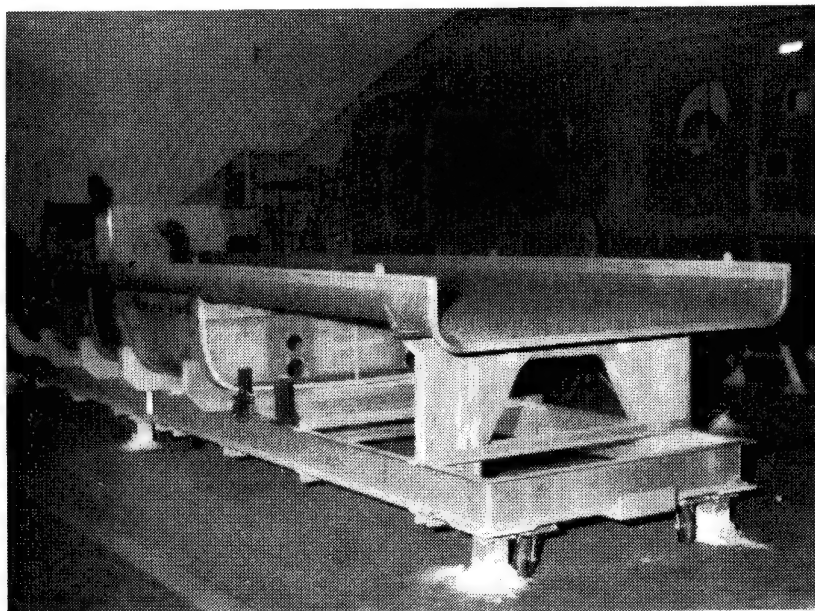


Figure 41. Model 360 Composite Floor Module

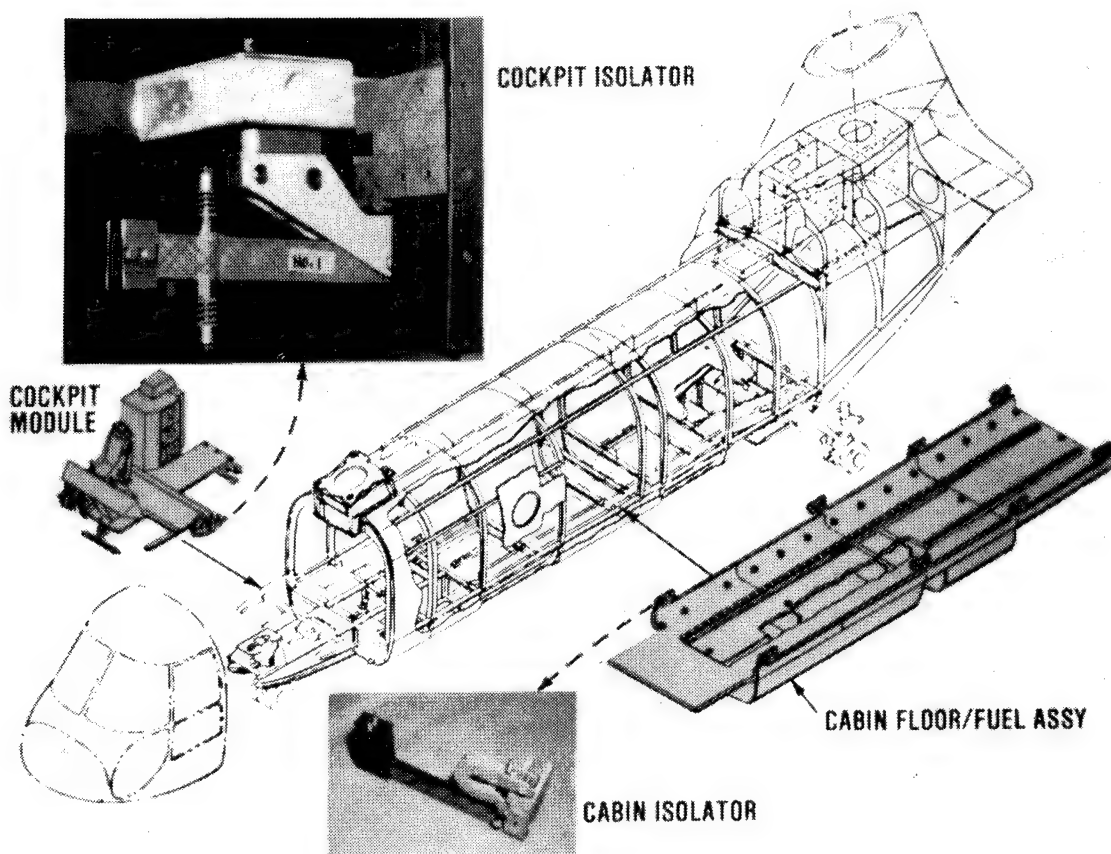
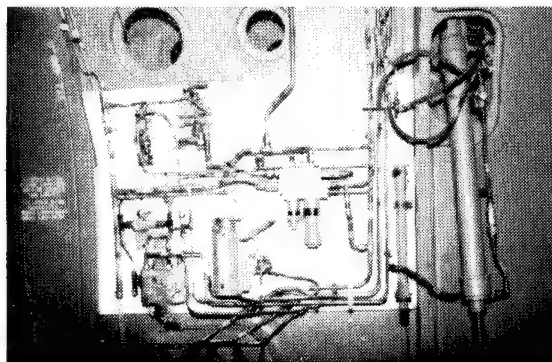
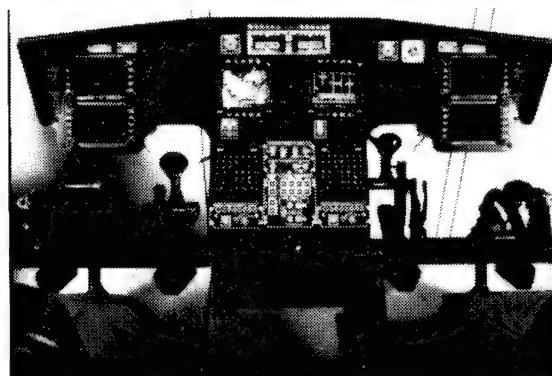


Figure 42. Model 360 Vibration-Isolated Modules

- Modularized Hydraulics



- Digital AFCS
- Integrated Avionics System



- Composite Landing Gear Components

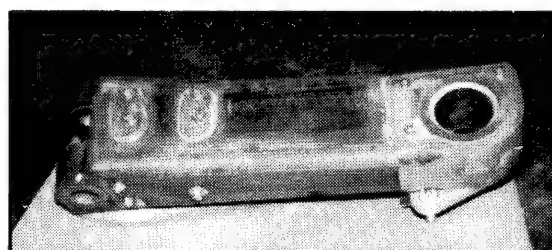


Figure 43. Model 360 Advanced Subsystems

	V-22	CH-47 GROWTH	LHX
COMPOSITE STRUCTURES			
— DEMONSTRATE TOOLING CONCEPTS	X	X	X
— DEMONSTRATE EFFICIENT DESIGNS	X	X	X
— DEVELOP DIRECTLY APPLICABLE: TOOLS		X	
FLIGHT HARDWARE		X	
— DEVELOP EFFICIENT SUBSYSTEM INTEGRATION CONCEPTS	X	X	X
ADVANCED ROTOR SYSTEM			
— HIGH-SPEED FLIGHT, 200 KNOTS		X	X

Figure 44. Model 360 Aerodynamic and Material Research Supports Boeing Programs

RECENT SIKORSKY R&D PROGRESS

Abstract

This paper summarizes the recent activities and progress in four specific areas of Sikorsky's independent research and development program. No attempt is made to cover the full spectrum of R&D activities. In fact, even some major thrusts over the past few years are not covered. Since the beginning of the S-76 design in 1974, Sikorsky has been aggressively developing the technology for using composite materials in helicopter design. This effort included ACAP, of course, but has gone beyond that now to concepts as those incorporated by Sikorsky in the Piaggio P-188.

Four specific topics are covered here: advanced cockpit/controller efforts, fly-by-wire controls on RSRA/X-Wing, vibration control via higher harmonic control, and main rotor aerodynamic improvements.

Sikorsky Helicopter Advanced Demonstration of Operational Workload (SHADOW) aircraft successfully flew structural flights in 1985. An electronic Fly-By-Wire flight control was incorporated and the evaluation pilot avionics that permit single pilot operation were installed. Single piloted flight test of the SHADOW aircraft began in 1986. This flying test bed is being used to evaluate various configuration of CRT displays, sidearm controllers and voice interactive systems as proposed candidates for the U.S. Army family light helicopters designated LHX.

Sikorsky has full authority fly-by-wire flight-critical control system in test for RSRA/X-Wing. The multi-processor quad-redundant flight control computer system has undergone successful initial testing in a laboratory installation. This computer complex is believed to be, with the exception of the space shuttle, the most sophisticated flight critical system in existence today. The software associated with this application controls essentially all aspects of the vehicle's mechanisms. This software is now undergoing extensive verification and validation. In the process of this software confirmation the complete vehicle management system is being exercised in the specially developed X-Wing Vehicle Management Systems Laboratory.

Sikorsky's full authority fly-by-wire flight control systems has been aided by the IR&D supported development of the redundancy management methodology and an automated software verification methodology. Redundancy management methodology was formulated and utilized to establish a systematic approach for the development of the X-Wing flight-critical control system design. Also evolved was a library of preferred software and hardware approaches to implement those redundancy concepts. The automated software verification has been based on obtaining identical output responses from dissimilarly programmed test software and from actual flight system software when both are subjected to a common input. As changes are made to the program, both sets of software are modified and are exercised automatically with thousands of pre-selected control input combinations through a computerized procedure resident on a host computer.

A flight test of open-loop higher harmonic control has been conducted on the S-76 aircraft. This project extended the envelope of HHC experimental flight test investigation to gross weights of approximately 10,000 lbs. and 150 knots forward speed. A 1.5-hour ground test and 23-hour flight test provided a demonstration of the effectiveness of HHC in the control of vibration, replacing the conventional rotor head and airframe absorbers.

Substantial vibration reduction was achieved by applying preset amplitudes and phases of HHC through the main flight controls servos. Test conditions showed vibration reduction through a series of maneuvers as well as in level flight. The objective of providing a body of engineering data on the effects and requirements of HHC was also met. Measurements were made of the effects of HHC on loads, stresses, aerodynamic performance and acoustics. The HHC servo motion amplitude and hydraulic flow requirements to control vibration at high speed were also determined. These data are invaluable to support extrapolation of HHC applications to new aircraft such as the LHX.

Rotor performance has been upgraded through both refined geometry and improved airfoils. To minimize the unfavorable performance and noise effects of blade tip vortices in proximity to the top of the following blade, blades were modified to incorporate anhedral (droop) on the blade tips. Model and full scale hover tests showed significant performance benefits, and analysis predicted no adverse effects in forward flight. Flight tests were then conducted which verified that and provided useful blade loads data.

A third-generation high life airfoil, the SC2110, was developed as a replacement for the SC1094R8. This airfoil section was designed to retain the high maximum lift capability of the earlier section but possess significantly reduced drag at high Mach numbers and a higher drag divergence Mach number. It is significant that the

entire design process was carried out analytically using 2-dimensional computational fluid dynamic methodology. Subsequent wind tunnel testing of the optimized design fully validated the predicted results. The new airfoil design, while retaining the excellent C_{LMAX} characteristics of the BLACK HAWK high life section, has transonic drag levels no greater than the BLACK HAWK outboard section. This represents a very large improvement in airfoil technology.

SIKORSKY HELICOPTER ADVANCED DEMONSTRATION OF OPERATIONAL WORKLOAD (SHADOW)

SHADOW is an experimental helicopter, based on an S-76A, that is exploring the functional, automation and integration requirements necessary for single pilot operation of future military rotorcraft. This paper describes the physical aircraft, its flight controls and the avionics that supported the ARTI flight test experiments including visibility tests.

Aircraft Description

The physical layout of the crew and equipment will be described starting with the forward portion of SHADOW and working aft. The host aircraft is a standard Sikorsky S-76A with the nose-located electronics bay removed and an excellent visibility, single pilot cockpit attached by the means of longerons extended from the original aircraft (Fig. 1). The Evaluation Pilot for a total crew of five (Fig. 2). In the main cabin, there is a Safety Pilot (in the conventional location) with mechanical flight controls and standard S-76A instruments, an Evaluation Copilot beside him with electronic flight controls, and two Flight Engineers in the passenger cabin area (EP) sits up in the EP cockpit has full aircraft status and control with the exception of engine and landing gear control for safety reasons.

Using "glass" instrumentation in the EP cockpit (Fig. 3) permits extensive use of both traditional symbology as well more highly integrated icons to reduce pilot workload. A Honeywell monocular (part of IHADSS) Helmet Mounted Display (HMD) is the primary display medium. A Polhemus Navigation magnetic head tracker is used to determine head angles. There are two center console mounted Rockwell-Collins full color Head Down Displays (HDD) called the Tactical Situation Display (TSD) and System Management Display (SMD). There is a bezel assembly made by Photoetch with 24 switches, 6 on a side, for each HDD. There are 5 Honeywell Programmable Display Pushbuttons (PDP's) on either side of the TSD. A Dorman-Bogdonoff touchscreen is on each of the HDD's. A Shure microphone is used for both standard ICS and the Hamilton-Standard Voice Interactive System (VIS). The VIS is actuated by a two position rocker switch located on the right-hand flight control grip. The Northrop 8-12 micron FLIR turret is mounted at the extreme forward portion of the fuselage. A standard SH-60 Seahawk seat is used. There are miscellaneous control and test panels and the ICS panel located on either side of the seat.

The FBW system uses Measurement Systems dual-redundant, strain gauge type, limited motion flight control transducers. The grips are a Sikorsky custom design made by Bendix. A Sikorsky "slide" type control can be used in place of the left side flight control. The foot pedals, for optional yaw control (2+1+1 configuration),

are either force or limited motion type. Pilot and cockpit avionic cooling is provided by a Keith air conditioning system.

Figure 4, SHADOW avionic layout, shows the placement of the various boxes. Individual box location was carefully chosen to eliminate the need for ballast to establish proper center of gravity (CG).

ARTI - Flight Test

The flight test objectives were to investigate design questions which could not be adequately dealt with in the ground-based simulator and to provide a real world anchor point for simulation results. The first step was development of a flight control system that was both safe and a reasonable approximation of LHX pilot workload. The aircraft was then utilized to investigate cockpit visibility HMD FOV and HMD symbology.

Flight Controls Tests

The purpose of the flight controls tests were to ensure the flight safety of the Sidearm Control System (SCS) and that pilot workload was sufficiently low to perform the other ARTI experiments. Tests of the SCS stability, shutdowns, overrides, stick sensitivities and SCS configurations (2+1+1, 3+1, and 4+0) were performed.

With the present Shadow-ARTI control laws, the pilots preferred to use the 3+1 configuration which included the right hand 3 axis sidearm controller for pitch, roll, and yaw control along with a left hand displacement collective stick. All the configurations shared deficiencies which were a function of using force instead of displacement controls. Increasing the compliance of the force controller as well as control law improvement may help to alleviate these problems. Inadvertent pitch and roll rates during takeoff and landing were noted. Improved logic to fade in/out stabilization during these maneuvers should help to solve this problem.

The workload of the Shadow-ARTI flight control system, although reasonable for the initial ARTI studies, was still too high to perform NOE tasks. The additions of altitude stabilization, altitude hold and heading hold should lower pilot workload enough to perform NOE tasks. These features are included in the Sikorsky

Model Following Control Laws which are in shakedown flight testing.

Cockpit Visibility Test

The exterior cockpit vision requirement is an issue with major impact on the design of the ARTI/LHX cockpit. LHX concepts have ranged from "windowless" to versions which maximize the glass area. Between these extremes are questions which relate to the size and shape of consoles and their associated glareshield, the need for chin windows and the masking of overhead windows by roof-mounted EOTADS (Electro-Optical Targeting and Designation System) units. These studies used the basic Shadow as a baseline for the evaluation of likely cockpit design features. Three experimental configurations were evaluated. The first configuration represents a two CRT design with the displays arranged vertically. The second configuration was also a two CRT design but with the displays arranged horizontally. The third was a horizontal arrangement of three CRTs. Each of these has advantages and disadvantages in terms of functionality and cockpit geometry but the purpose of this study was to look at their effect on external vision while flying a variety of tasks which sample the critical elements of the LHX mission. Each of these had no chin windows because of crew armor protection. In addition, all had no overhead windows to simulate the EOTADS position.

Three Sikorsky pilots tested all the configurations and were asked to perform the same maneuvers for each. These included hovering, hover turns, a bob-up, a figure-eight and sideward flight at low speed, cruise flight at 2000 ft., and two different landings. These maneuvers required the pilot to use several areas of external visibility: over-the-nose, forward-low, down, side and overhead. All tests were conducted with the integrated helmet and display sighting system (IHADSS) with symbology from the on-board Gaertner display generator. The Polhemus head tracker provided data to the display generator on the pilot's head position in azimuth, elevation and roll. The position data from the head tracker was recorded on a strip chart recorder in the aircraft along with aircraft attitude, altitude, and airspeed. During all maneuvers, over-the-shoulder video with a voice track was recorded. At the conclusion of the flight each pilot was given a form for comment on the configurations tested and an overall rating. The rating system was based on the traditional Cooper-Harper rating scale, with the wording modified for this investigation.

Pilots comments indicated several critical areas of visibility. In the hovering tasks, 30 to 45 degrees of azimuth on either side of the console was the primary area for forward-low reference with the chin windows giving peripheral cues to aid in position and altitude control. There was degradation in performance in hover for lateral station keeping with the loss of chin windows and

continuing loss of performance with larger consoles. The loss of visibility forward-low was also evident in increased time when executing an approach to land.

The precision of hover and hover turns is clearly affected adversely by cockpit configurations that have diminished exterior vision. Pilots compensate for the lack of vision by increasing the amplitude and frequency of their head motion. This adds to cockpit workload and is reflected in the pilot ratings of the configuration. Pilot comments point out the importance of the overhead and chin windows. The overall conclusion from this study is an understanding of how the tradeoffs between external visibility and other design parameters can significantly impact both pilot performance and workload.

HMD FOV Test

The field of view of a helmet-mounted display has been identified as a major driver of technical risk for the single pilot LHX. The purpose of this study is to assess the effects of field of view on flight performance. It is recognized that there are several HM design parameters which impact pilot performance, i.e., resolution brightness, etc, besides FOV. Due to experimental limitations, we confined our investigation to field of view alone. Three configurations were compared with a baseline which consisted of the IHADSS display unit mounted on a standard IHADSS helmet. Thus, with the baseline the symbology was presented in a 30° x 40° area, but the FOV was only restricted by the helmet itself.

To modify the helmet field of view, three masks were created which could be taped directly to the pilot's helmet. These masks restricted the field of view to 30 x 40, 40 x 80 and 60 x 120 degrees of azimuth and elevation respectively.

The procedures and format of the investigation were identical to the cockpit visibility experiment. Three Sikorsky pilots tested all the configurations and performed the same maneuvers. The tests were conducted with symbology presented on the IHADSS.

Similar to the cockpit visibility experiment, the data indicated a trend of decreasing pilot performance as the field-of-view was reduced. This could be seen in comparisons of pilot performance, the frequency of head motion in the cockpit, and the pilot comments. The accuracy of the hovering tasks were those most affected by the restricted field of view.

There is a strong overall relationship between performance precision and HMD field of view. In addition, an increase in pilot effort to compensate for FOV restriction is clearly evident in the head motion data for tasks involving anything but straight ahead vision. The results of these tests will facilitate the LHX HMD development.

HMD Symbology

The Shadow HMD symbology was virtually identical to that used in the simulation. Evaluation of this symbology, for the most part, was done in the fixed-base simulation. However, several aspects of the symbol set could only be properly evaluated in actual flight. Additionally, the flight tests validated the simulator fidelity.

In general, the concept of "contact analog" symbology, where the symbology overload and supplemented cues from the outside visual world, worked very well in flight. The cues were very natural because of the close correspondence to contact flight cues. Pilots using the cues for the first time had no difficulty interpreting the display and no control reversals were observed.

Summary

In summary, the ARTI Task VI Flight program has proven SHADOW to be a flexible, "flying" simulation. The close correspondence of its cockpit and symbology with the ground-based simulator have provided an excellent mix of capabilities. This similarity have helps to anchor the simulation results to the real world. by alternately flying SHADOW and the ground-based simulator, the program pilots are very aware of simulation strengths and weaknesses.

Several important single pilot issues have been considered. The aircraft has provided the truly unique opportunity to investigate cockpit visibility in flight at a time when the LHX design can be modified. This study has shown the sensitivity of visual workload and performance precision to cockpit configuration. The HMD field of view study clearly confirms the need for a wide field of view helmet display system.

X-WING/RSRA FLY-BY-WIRE VEHICLE CONTROL SYSTEM

The RSRA/X-Wing program mates a circulation control rotor with the NASA Rotor Systems Research Aircraft (RSRA) for the prime objective of demonstrating an inflight conversion to a stopped rotor state, a unique capability of the X-Wing rotor (Fig. 6). The control system of such a vehicle faces significant challenges. It must first be designed to accommodate the equivalent of three vehicles since the X-Wing operates in a rotary wing mode, a fixed wing mode, and in the interim conversion state. It must achieve rotor cyclic control via a pneumatic medium. It is a full authority fly-by-wire system for all functions, except the existing aileron, rudder and elevator controls which are retained from the RSRA, and provides a mechanical override capability for the safety pilot. For the evaluation on the RSRA it must provide control sharing in recognition of an 20,000+ pound rotor capability mated with a 30,000 plus pound vehicle. Furthermore the control system rapidly evolves into a Vehicle Management System (VMS) controlling many subsystems and providing functions beyond the classical flight control system-this driven both by prudent, efficient design and by redundancy requirements of allied subsystems.

A review of the X-Wing plant identifies the major functions required of the VMS (Fig. 7):

- Control of the circulation control rotor
- Main rotor blade collective pitch control
- Automatic conversion control
- Pneumatic system control
- Air data computation
- Vibration alleviation via Higher Harmonic Control (HHC)

The control approach defined to meet those challenges includes the elements of: an integrated Vehicle Management System, full redundancy treatment for the X-Wing control portions, use of the RSRA both as a safety backup and for control sharing and a digital fly-by-wire approach. A design goal was to be transferable as a stand alone system to a pure X-Wing vehicle.

Major subsystems are the pneumatic, rotor conversion, HHC and the mechanical collective. The pneumatic control includes compressor control via Inlet Guide Vane (IGV) positioning to provide required plenum pressure, modulating discharge valves to avoid compressor stall and the pneumatic control valve actuators to establish the airflow to each blade's leading and trailing edges. The conversion subsystem controls both the steady states (rotary and stopped) of the rotor via locking actuators and the conversion between those states via the clutch or the rotor brake/indexing functions for the rotary and stopped conversions respectively. Vibration alleviation is provided by the HHC system which is

implemented in two forms, a scheduled system resident in the flight critical portion of the VMS and a closed loop active HHC configured in a fail safe (dual) computer module. The mechanical collective pitch subsystem is a quad electrically controlled, dual hydraulic powered system providing a range of $\pm 10^\circ$ operating against the very formidable loads of the rigid rotor.

System redundancy is predicated upon the design goals of two-fail operational for similar failures in flight critical systems and fail-safe for "mission" critical elements. The architectural implementation is basically quadruple electrical and dual hydraulic. Elements such as the computers, sensors, and electrohydraulic servo valves are quadruple. In some areas equivalent redundancy has been achieved by structuring the system to avail the program of existing hardware or the unique features or a subsystem (Fig. 8,9). The clutch control system is an example of the former where dual Clutch Control Units (CCU) are supplemented by the quad flight control computers which provide independent monitoring, selection, and backup control. The PCV's illustrate the latter. Features such as twenty-four valves about the perimeter sampled two at a time by the blade receivers are supplemented by averaging springs to position a bypassed actuator at a position midway between its neighbors. The combination of these permit the PCV actuator to be configured with only dual electrical coil servo valves.

Software redundancy is addressed by the inclusion of Back-Up Control Software (BUCS) in recognition of the common mode software failure mode (Fig. 10). It treats the probability that error free software may not exist, in spite of extensive verification and validation, in a 120,000 line program. The BUCS design utilizes isolated, dissimilar software executed by the same quadruple computers. It is activated by either automatic transfer, when certain failure conditions are encountered, or pilot initiated transfer. Simplicity, which equates to high confidence in software quality when subjected to extensive validation, is the essence of the BUCS. Accordingly it is configured with a very simple control law adequate to affect a precautionary landing.

Major hardware elements of the system are the Flight Control Computer (FCC), the Actuator Control Module (ACM), and the Pneumatic Control Valve (PCV). The FCC is a Z8002 microprocessor - based computer with a very extensive input/output signal conditioning complement mandated by the multiplicity of system sensors and actuators. It's throughput capability exceeds two and a half million operations per second, achieved by virtue of a lattice matrix architecture which provides four microprocessors per channel in a parallel/co-processor configuration.

The complete computer ship set is comprised of four boxes (Fig. 11) all containing identical MFCS and BUCS (flight critical) functions. In addition, 2 of the boxes contain AFCS and the other two boxes contain an active HHC (Higher Harmonic Control).

The ACM is a standardized quadruple actuator interface between the FCC and the hydraulic ram which is sized for the load of the specific application. It exhibits hydologic, hydraulic shutdown interlock, and IBIT features. The PCV actuator is a hydraulic powered actuator controlled by either of two computers. Two actuators are housed in an assembly, one for the leading edge valve and one for the trailing edge valve control via concentric shafts.

The design phases are essentially complete and emphasis has shifted to development and test of the system and its target vehicle. These phases are structured to progressively evaluate the system at higher level of integration prior to committing to the ultimate objective of an inflight conversion. Addressed hereafter are the wind tunnel testing, Ames vertical Motion System evaluation, software verification, hardware airworthiness evaluation, integrated system validation, power system test bed survey, and flight demonstration (Fig. 12).

The wind tunnel testing is conducted with a one sixth aerodynamically scaled RSRA fuselage outfitted with a circulation control rotor and a pneumatic distribution system. Control of the rotor can be effected either manually from an operator's console or automatically from a SEL computer based implementation of the vehicle management system. The data generated by this testing, which explores the stopped rotor, conversion, and rotary wing envelopes, provides a data base to judge the adequacy of or update the models used to analyze the control system needs and to evaluate the efficacy of the implementation during the system validation testing.

Several entries into the Ames Vertical Motion Simulator provided an opportunity to evaluate the controllability of the air vehicle in its several modes of flight with the intended control laws modeled. The evaluation addressed the full-up control laws (MFCS), submodes of the MFCS for degraded operation (direct link and plenum dump), and the backup control software (BUCS) mode. This testing provided an early indication of the viability of these modes under various flights and landing conditions. A comparison of the simulator model when flown rotor off with the actual flight test observations on aircraft 740, formed the basis of the simulation model validation.

The software verification is conducted by Hamilton Standard (HSD) (the provider of the FCC and its software). It is a highly automated process subjecting the software to approximately 1400 test cases designed by a HSD systems engineering team (as differentiated from the software engineering team which designed the software) and monitored for total coverage of the SA requirements by SA digital system engineers (Fig. 13). The automation is provided by the HSD designed Systems Integration and Test Stand (SITS) which serves both as a software development and test facility (Fig. 14). The PDP11 based SITS includes actuator and sensor simulators, fault insertion means and brassboard (RAM) versions of the FCC. In addition an extensive library of software provides functions such as test case development, expected results comparison, and editing.

A special provision has been provided to address the flight control law (as opposed to executive, redundancy management and built-in-test) portion of the software. This area is deemed to be judged by the most subjective criteria and hence prone to the most revision and subsequent reverification. To expedite that process, an automated software verification system was developed and is in operation (Fig. 13). It is based on obtaining identical output responses from dissimilarly programmed test software and from actual flight system software when both are subjected to a common input. As changes are made to the program, both sets of software are modified (independently) and are then exercised automatically with a multiplicity of preselected control input combinations through a computerized procedure resident on a host computer.

The airworthiness evaluation of the flight control system hardware is a relatively conventional approach patterned from MIL-STD-810C. The FCC, for example, is subjected to high/low temperature operational evaluation, vibration resonance search and cycling, shock, humidity and EMI testing. All as a confirmation of design criteria and the effectiveness of features such as the heat transfer means and filter pin connectors. The flight critical nature of the components is further addressed by a broad application of "burn-in" conditioning during the fabrication/acceptance test process. For the FCC, this includes random vibration and ten thermal cycles, the last five of which must be failure free.

The most extensive and detailed testing applied to the VMS is the system integration and validation testing conducted in the Vehicle Management System Laboratory (VMSL) (Fig. 16). This is a hardware in the loop/real time simulation test of the entire control system as commanded by the software resident in the FCC's. The VMSL is a specially developed facility for the RSRA X-Wing providing for semi-automatic application of test conditions to the system under test.

Key elements of the VMSL are:

- A Sikorsky-based second SITS is the heart of the VMSL providing the semi-automated testing ability. It includes the capability to generate and store test cases and apply simulated faults via its sensor and actuator simulators.
- Dual SEL-9780's host the aerodynamic and pneumatic aircraft simulations. The simulation is a real time derivative of the master GENHEL model used for the handling qualities analysis and control system design.
- Brassboard (laboratory) FCC configured with RAM are included for early development work. Flightworthy (EPROM) units can be substituted individually, or as a set, to test flight hardware prior to usage.
- A fixed based cockpit with side by side seating representative of the RSRA is provided to permit pilot interaction evaluation for effects/response and procedures refinement. This is outfitted with a simple display to provide VFR flight tasks.
- A Ground Based Data System (GBDS) identical to those at the wind tunnel and flight test sites for data collection, storage, and processing. It includes a link between the three systems to share data bases and permits comparison between predictions and results.
- A full complement of sensors and actuators, including the 48 actuator PCV array and, with simulated loads, are included.
- Hydraulic and electrical supplies including the digital power switching units which provide the uninterrupted power for the FCC's.

The integration and validation testing is achieved by the application of an array of test cases to the system (Fig. 17). The program is structured to progressively qualify the system for PSTB, stopped rotor (SR) flight, rotary wing (RW) flight, and conversion flight. Two software programs are involved: The stopped rotor/direct link (SR/DL) package utilized for the first two phases (PSTB and SR) and the Unified Control Laws (UCL) used for the latter two phases (RW and conversion). The SR/DL is a simplified derivative of the UCL created to provide earlier availability for flight. A estimated 5000 test cases are being created for validation. The PSTB release assumes 750 successful

tests; the SR flight 2080 including the 750 for the PSTB. The testing validates such features as redundancy management including reconfiguration, dynamic response, stability, compressor control, actuator management, built in test and BUCS.

The propulsion system Test Bed (PSTB) is a power train endurance test facility typical of those applied to most new aircraft programs. For the RSRA X-Wing its role has been expanded to be a part of the control system validation process. Several entries are intended, addressing the progressively increased functions provided by the VMS. The first entry precedes the stopped rotor blowing flight phase and focuses upon the pneumatic control and distribution system. The high power demand (2000 HP) and flows (29 lbs per second) preclude the inclusion of a real compressor in the VMSL, making its validation cases dependent on computer models.

The PSTB confirms not only the ability of the VMS to control the compressor but also the operation of the PCV system in the presence of flow. Specific emphasis is upon regulation of plenum pressure, response to demands, the effect of pneumatic lags, and the stall avoidance and recovery operation. Later tests address the hub moment force (HMF) sensing system, in terms of accuracy and cross axis effects, and the conversion system operating in the presence of actual inertias and loads but with the obvious exception of forward flight effects.

The culmination of all the testing is a successful in-flight conversion. The flight program is structured as a gradual buildup to that event (Fig. 18). First emphasis is upon the rotor-less RSRA flying as a fixed wing aircraft. This starts as a replication of the qualifying work done on RSRA #740 in 1984 and incrementing the gross weight and vertical center of gravity to the X-Wing design points. The X-Wing rotor is then installed first as a two bladed "Wing" and then in the four bladed X- both without circulation control activated. The next phase introduces the circulation control blowing while flying in the stopped rotor configuration. The VMS is operational with the stopped rotor/direct link software executed by the FCC to provide pneumatic subsystem control and flight control of both the CCR rotor and the fixed wing surfaces. The conversion system is mechanically "locked" into the stopped rotor configuration. The BUCS is also installed as a necessary safety feature for any flight test. The next two flight phases require the full operational VMS as represented by the Unified Control Law (UCL) software programs for the FCC. The rotary wing phase explores the other end condition of the conversion. The VMS provides the means to turn up the rotor during the ground starting procedure and then maintains the rotor coupled to the propulsion system via the clutch. Vehicle control during flight is effected via the VMS which also commands fixed wing surfaces to effect the necessary load sharing.

Also required during the rotary and conversion flight phases is the higher harmonic control system. The mandatory bounding of vibration is provided by the scheduled (as a function of airspeed, rotor RPM and load) HHC contained in the quadruple MFCS. This is supplemented by the dual active HHC whose commands are added to those of the scheduled HHC. The active HHC is responsive to observed vibrations and particularly addresses transients such as encountered due to maneuvering flight, gusts, or resonance crossing during conversion.

The conversion phase is also approached gradually by use of the conversion abort feature. A conversion can thereby be initiated, permitted to progress to a rotor RPM difference and then returned to the initial condition. This is possible starting from either end state with software safeguards included to preclude a "turnabout" at a resonant frequency point. The flight control provided by the VMS is as its name implies, a unified control using essentially the same control law structure for rotary, stopped and conversion control. Some gains are adjusted with rotor speed and the rate crossfeeds and controls crosscoupling germane to the rotary mode are phased out.

Many features are included in the basic system to support system flight development. These include (Fig. 19):

- Ultraviolet erasable memory to permit program update without the risk of RAM
- Alternate gain selections by axis which switches in an alternate array of gains previously validated as safe thru VMSL testing.
- Test inputs to provide response measurement in all axes when the system is pertubated by pulse, sine, step or doublet inputs of selectable frequency and amplitude.
- HHC optimization panel to alter the scheduled HHC coefficients amplitude and phase a limited amount.
- Realtime and stored data acquired by the inflight data measurement system which monitors the cross channel data links and records and telemeters a predetermined complement of data.
- The program monitor and control unit (PMCU) to permit flight line interogation of the FCC for fault code readout and system diagnosis.

C. Higher Harmonic Control

In recent years requirements for reduced vibration have become stringent. Thus, it is mandatory to develop and demonstrate weight-effective, airframe vibration control. For current generation helicopters the rotor speed may be varied by large percentages, e.g., 11% on S-76, to optimize aircraft characteristics such as external acoustics and performance. This may make the use of more conventional fixed-tuned vibration control devices more challenging because of weight constraints and adverse frequency response characteristics. Analytical studies, wind tunnel tests and flight tests (References 1, 2, and 3) have demonstrated higher harmonic control (HHC) to be a viable technology for vibration control. Briefly, the concept underlying HHC is that reductions in $N\Omega$ frequency airframe vibrations can be achieved by oscillating the rotor blade in pitch at $(N-1)\Omega$, $N\Omega$, $(N+1)\Omega$ frequencies in the rotating system, where N is the number of blades and Ω the rotor speed.

The present paper describes a successful full scale open loop HHC effort on the Sikorsky S-76 at forward speeds up to 150 knots, Figure 20. This is the first demonstration of HHC on a 10,000 lb. helicopter at moderately high airspeeds compared to previous full scale testing. The flight test results demonstrate that for the 10,000 lb. S-76, HHC can substantially reduce vibration without incurring severe penalties in blade loads and rotor performance. In addition, a novel way of implementing the higher harmonic control other than through the conventional swashplate is also described.

Vibration Characteristics of the S-76

The S-76 is a modern medium size helicopter used mostly in the commercial market for VIP transport and offshore oil missions. For both these missions the ride quality in the cockpit and cabin is extremely good. This four-bladed rotor system is designed to minimize the 4P (4 per rev, 19.5 Hz at 100% NR) vibration in conjunction with rotating system 3P and 5P inplane bifilar absorbers with cycloidal tuning bushings. The ride quality in the forward cockpit is further enhanced by the use of a variable tuned fixed system vibration absorber. Reference 4 discusses details of the dynamic design. The self-tuning nature of the bifilars and the nose absorber allow for rotor speed operation over a 11 percent range to optimize performance. While this system works well, it requires 2.75% of the design gross weight. The possibility of achieving lower weights with an HHC controller makes this concept of potential interest. Additionally, while the self-tuning features of the current system allow for rotor speed variations to optimize performance, a much larger range of operating speed changes can be accommodated with HHC.

Objectives of Flight Test Program

The primary objective of the flight test program was to determine the extent of HHC open loop vibration reduction attainable in the S-76. This included simultaneous vibration reduction at several locations in the aircraft. The capability to generate vibratory blade pitch motion using the main rotor hydraulic servos, as well as the attendant change in control and rotor system loads were evaluated.

Modifications to S-76 for HHC Open Loop Flight Test

Figure 21 shows the mechanical and electrical elements of the HHC system. This figure shows the main rotor servos and the modified valves which improve the servo high frequency response. Figure 21 also shows the HHC electro-hydraulic driver actuators that were installed on the input side of the main servos. The HHC controller electronic components are shown in the top left hand side of Figure 21. Figure 22 is a schematic diagram of the modified S-76 control system. The lateral main rotor servo is not shown for clarity.

The S-76 is normally equipped with rotor head mounted 3P and 5P inplane bifilar absorbers and a nose mounted variable tuned vibration absorber. The bifilars were removed and the nose vibration absorber was turned off during the HHC flight testing. The HHC control system inputs were generated by use of the HHC control panel (Figure 21) which provides electrical signals to the HHC electro-hydraulic driver actuators.

Flight Test Data Results

Figure 23 shows the results of the HHC longitudinal cyclic mode on two vibration parameters as a function of HHC input phase angle during level flight at 80 knots. The vertical aircraft nose vibration is particularly sensitive to this HHC input and exhibits the characteristic sine wave shape that was also identified in Reference 2. This behavior may be understood by viewing the resultant vibration level as a vector sum of the baseline vibration with HHC off and the vibration induced by the HHC blade pitch oscillations. The lateral pilot overhead vibration, by comparison, is not as sensitive or as well behaved relative to the HHC longitudinal cyclic mode input.

Figure 24 illustrates the maximum cockpit vibration reduction attained with HHC. Note that the magnitude of HHC vibration reduction is essentially constant with airspeed. The vibration levels in the cockpit with HHC are generally less than .10 g's up to 100 knots, but then begin to increase rapidly with airspeed.

This behavior is due to an upper limit on the magnitude of HHC blade pitch that can be generated with the existing hydraulic pump capacity. There is little doubt that larger higher harmonic blade pitch angles would allow the vibration level to be reduced to less than .10 g's at higher airspeeds. Similarly, Figure 25 shows a comparison of vertical aircraft nose vibration during climb, partial power descent and turns. These data were obtained by using the optimum HHC setting determined for level flight and this setting was then held constant during the maneuver. Note that during the 45 degree and 60 degree angle of bank turns the vibration reduction due to HHC is essentially the same as that attained during level flight. It is expected that even greater vibration reductions could be achieved with larger HHC blade pitch motions.

Structural data from the HHC flight testing show that control system vibratory loads generally increase with HHC input. An example of this is the plot of pushrod vibratory load versus airspeed, which is shown in Figure 26. The HHC input for these data corresponds to the longitudinal mode input, utilized to minimize vertical aircraft nose vibration. It should be noted that although pushrod vibratory loads are increased by the use of HHC, they are still well below the endurance limit. The effect of HHC blade pitch oscillations on main rotor blade, flatwise vibratory bending moments is illustrated in Figure 27. Again, the loads generally increase due to HHC, but are not large enough to be limiting.

Figure 28 is a plot of main rotor torque versus airspeed, which represents the level flight performance of the aircraft with HHC on and off. The HHC input is the same longitudinal mode input described in the preceding paragraph. These data were obtained by maintaining the HHC setting constant in level flight. A data record was then taken with HHC off and then one with it on. A comparison of the main rotor torque reveals no significant performance change due to HHC in level flight over the speeds for which performance data were obtained.

Oscillating Jet Flap

One method for implementing higher harmonic control for helicopter rotors is to produce time-varying pitching moments using a pulsating jet flap. These pitching moments would induce blade torsional oscillations to control blade loading and therefore reduce airframe vibration. The advantages of this technique include having no moving parts (outside of the air supply to the jet), having low power requirements, and producing low inertial loads. In this concept the jet would exit the blade trailing edge along a section between 80 and 90% of the radius. Locating the jet exit on the lower (pressure) surface of the blade would

provide both the required unsteady torsional motion and a steady untwisting of the blade in forward flight. Use of a Coanda surface rather than a pure jet flap is recommended to increase the pitching moment response to a given jet momentum coefficient.

The aerodynamics of this technique have been studied experimentally using an SC1094-R8 airfoil that was modified to incorporate a Coanda jet at the trailing edge of the blade surface (Fig. 29). The jet exited from a 0.03-in.-high, 2-ft-wide slot located in the center of an 8-ft-wide S-76 blade section. Jet pressure and frequency were varied. Wind tunnel tests were conducted at Mach numbers of 0.4 and 0.7.

Unsteady surface pressures were measured using twenty-four miniature pressure transducers located along the airfoil centerline (Fig. 29). The normal force and pitching moment coefficients were determined by a Gaussian integration along the airfoil chord. The static pressure at the jet exit and the total pressure in the plenum inside the airfoil were used to determine the jet momentum coefficient. Figure 30 presents a representative time history of this coefficient.

One example of the results is shown in Figure 31. The mean (time-averaged) pressure distribution is characterized by a peak in $-C_p$ in the jet region on the pressure surface. The pressure amplitude at the fundamental jet frequency is also highly peaked in the jet region. The phase of the pressure on each surface increases slightly with distance from the leading edge of each surface, and maintains a 180 degree phase separation between the surfaces.

Loops showing the variation of the pitching moment about the quarter chord with jet momentum coefficient are shown in Figure 32 for jet frequencies of 5 and 25 Hz. The primary difference between the two curves is the increased hysteresis at 25 Hz for low values of momentum coefficient. Figure 33 shows the variation of the amplitude of the normal force and pitching moment coefficients at $M = 0.4$ with jet frequency, mean angle of attack, and regulator pressure. The data appear self-consistent, and, especially at the higher pressures, to vary smoothly as a function of all three independent variables.

One of the primary results of this study is shown in Figure 34. This figure shows that the pitching moment amplitude is nearly a linear function of the jet momentum coefficient amplitude. The slope does not seem to change greatly with angle of attack or reduced frequency. The predictable and generally well behaved aerodynamic response demonstrated in this experiment indicate that it would be feasible to generate rotor control moments using the

oscillating jet flap concept. The relationship between the normal force and pitching moment and the momentum coefficient for these very low flow rates are proved to agree with predicted values thus confirming that adequate higher harmonic vibratory pitch could be provided with the predicated low power levels.

Key Design Issues Associated With Implementation of HHC at Higher Airspeeds

HHC Amplitude at Higher Airspeed

During the S-76 HHC flight test it was found, as expected, that the amplitude of the higher harmonic blade pitch was limited by the hydraulic fluid flow capacity. It is expected that higher amplitudes of the blade pitch would lead to further reductions in hub loads (main rotor shaft bending moments) and consequently further reductions in airframe vibration. Blade root pitch measurements during the flight test showed that the optimum blade pitch for best vibration reduction was primarily composed of the 3P component and that the maximum amplitude of this 3P component obtained with the present hydraulic system was approximately $\pm 1^\circ$. Implementing HHC in aircraft in approximately the same weight class as the S-76 but at higher operating airspeeds would require HHC blade pitch amplitudes in excess of $\pm 1^\circ$. Both analysis and a semi-empirical method based on flight test data project that $\pm 2^\circ$ of high harmonic blade pitch amplitude would be required for an S-76 operating at an airspeed of 150 knots.

Weight Considerations

The weight of the present open loop HHC system in the S-76 is 75 lbs this figure represents the mechanical and electrical components that were installed in the S-76. The basic philosophy behind the S-76 HHC flight test was to design and test a prototype system as "proof of concept" with minimum change to the aircraft. In line with this objective, additional hydraulic hardware that would have been required to obtain higher harmonic blade pitch amplitudes larger than 1° was not installed. To increase the HHC amplitude to, say, $\pm 2^\circ$ would require a longer primary servo stroke (at 4P), thus requiring larger hydraulic fluid flow rates which in turn would require installation of larger capacity pump(s), reservoir(s), and cooling system(s). It has been estimated that such an HHC system would weigh 115 lbs.

Hydraulic Power Considerations

The hydraulic power requirement would depend upon whether the HHC system was operating in the collective or the cyclic mode. In the collective mode all three main (primary) servos would operate (at 4P) with the same displacement and phase; this mode of operation consumes the maximum hydraulic power. In the longitudinal cyclic

mode, only the fore and aft primary servos would be active (at 4P), whereas in the lateral cyclic mode only the lateral servo would be active (at 4P). Thus the lateral cyclic mode requires minimum hydraulic power. However, it was observed during the flight test that this mode by itself was not as effective in suppressing airframe vibration as the other two modes. Hence, in the following estimates only the collective and longitudinal cyclic modes are considered. The hydraulic power requirement per stage (there are two stages in the S-76 hydraulic system) is given by

$$\text{Horse Power} = NP_s (2\pi f) (X_{\text{RMS}}) (A) \left(\frac{1}{C_1}\right) \left(\frac{1}{C_2}\right)$$

where

- N = number of servos active
- P = hydraulic supply pressure, psi
- f^s = frequency of operation, (4P), Hz
- X_{RMS} = servo piston stroke, in, RMS
- A = piston area, in²
- C_1 = 1714 (gallons per minute)(psi)/(HP)
- C_2 = 3.85 (in³/sec)/(gallons per minute)

Substituting typical values for the various parameters in the power expression gives, conservatively, the total HHC hydraulic power requirement in the collective mode to be 144 horse power and in the cyclic mode to be 40 horse power. The fuel associated with this power would, of course, add to the effective weight of an HHC system.

Seal Life

Another area of concern in implementing HHC on a production aircraft is the life of the seals in the main rotor servos operating at the high frequencies associated with HHC. Two S-76 servos were set-up for testing. The test spectrum consisted of a four segment spectrum of 40 minutes duration, with 10 minute segments. The test centers around the 4P frequency with a low frequency (0.5 Hz) signal superimposed to represent AFCS (automatic flight control system) signals. The first test was terminated after 550 hours and 50 million HHC cycles. No leakage or unusual wear could be observed. The units were disassembled and the seals in both servos were found to be in very good condition. More extensive test would be needed to fully qualify the system. Jet flap could alleviate this concern, however, it would complicate the blade design.

Closed Loop HHC

Implementation of closed loop HHC in the S-76 has been considered and several key issues have been identified. Of these, the type of control law is perhaps the most important and will be discussed briefly. There are several types of control laws that can be used in a closed loop HHC system and these range from the real time self adaptive to the gain scheduling, e.g., Reference 5. The most recent closed loop investigation (Reference 6) demonstrates that a fixed-gain feedback control law can effectively suppress rotor hub loads. This is in contrast to other efforts (Reference 5, for example) where an adaptive controller was required for vibration suppression. The results of Reference 6 are encouraging because a fixed gain control law provides faster response due to less computations required to obtain an optimal HHC input compared to an adaptive control law. Also, Reference 6 notes that fixed gain control laws can be expected to be robust whereas adaptive controllers may be subject to instabilities.

Concluding Remarks

Open loop HHC has been successfully demonstrated at speeds up to 150 knots in a 10,000 lb aircraft. Substantial reductions in airframe vibration were attained; even higher reductions are possible by increasing the amplitude of the higher harmonic blade pitch which was limited by the current aircraft hydraulic system.

The test data show that HHC increases the pushrod loads and generally increases the blade loads. These increases, however, are not large enough to be limiting.

A novel idea of providing HHC to the blades has been explored through wind tunnel tests and proved to be conceptually feasible. The oscillating jet flap has been predicted to have low power consumption and likely reduction in weight.

References

1. Bell Helicopter Company. "An Experimental Investigation of a Second Harmonic Feathering Device on the UH-1A Helicopter". U.S. Army Transportation Research Command, Fort Eustis, Virginia, TR62-109, June 1963.
2. Wood, E.R., Powers, R.W., Cline, J.H., and Hammond, C.E. "On Developing and Flight Testing A Higher Harmonic Control System", Presented at the 39th Annual Forum of the American Helicopter Society, St. Louis, Missouri, May 1983. Also, Journal of the American Helicopter Society, January 1985, Volume 30, No. 1.
3. Walsh, D., "Flight Test of an Open Loop Higher Harmonic Control System on an S-76A Helicopter", Presented at the American Helicopter Society 42nd Annual Forum and Technology Display, Washington, D.C., June 1986.
4. Niebanck, C., and Girvan, W., "Sikorsky S-76 Analysis, Design and Development for Successful Dynamic Characteristics". Proceedings 34th Annual Forum of the American Helicopter Society, Washington, D.C., May 1978.
5. Molusis, J.A., Hammond, C.E. and Cline, J.H. "A Unified Approach to Optimal Design of Adaptive and Gain Scheduled Controllers to Achieve Minimum Helicopter Rotor Vibration". Proceedings of the 37th Annual Forum of the American Helicopter Society, New Orleans, La., May 1981; Journal of the American Helicopter Society, April 1983.
6. Shaw, J., Albion, N., Hanker, E.J., and Teal, R.S. "Higher Harmonic Control: Wind Tunnel Demonstration of Fully Effective Vibratory Hub Force Suppression". Proceedings of 41st Annual Forum of the American Helicopter Society, Fort Worth, Texas, May 1985.

ROTOR PERFORMANCE IMPROVEMENTS

ANHEDRAL TIP FLIGHT EVALUATION

In 1977-1980 Sikorsky Aircraft conducted an in-house program to design, fabricate, and evaluate the effect of a swept, tapered, full-scale, anhedral tip design on hover performance and noise of the UH-60A BLACK HAWK main rotor. This new tip was designed to be interchangeable with the standard tip cap with only minor modifications to the tip cap joint. The resulting advanced rotor system is shown in Figures 35 and 36 mounted on Sikorsky Aircraft's 10,000 hp whirlstand.

The results of whirlstand tests, which were conducted in the first quarter of 1980, were most encouraging. Not only was hover thrust for a constant rotor power input increased more than 1.8% over the operating envelope comparing the anhedral tip blade with the standard blade, but rotor noise was also reduced 2 PNdb.

The anhedral tip combines the feature of anhedral (droop) with planform taper and compound sweep. The remaining features of the production tip, namely spanwise twist and airfoil section are retained. The fundamental basis for "drooping" the blade tip is to alleviate the interference effects of the tip vortex by increasing its separation from the other blades in the rotor system. By drooping the blade tip, the tip vortex is shed lower into the rotor wake. As the tip vortex extends rearward toward the next following blade, it then passes farther below that blade. The resulting local flow distortions at the following blade are significantly reduced and rotor power and noise are beneficially affected. This tip concept is applicable to most helicopters.

In 1981 a full-scale flight test program to evaluate the prototype anhedral blade tips on a prototype YEH-60B aircraft was initiated. This program was jointly sponsored by the Applied Technology Laboratory, USARTL (AVRADCOM), the NAVAL air Systems Command, and Sikorsky Aircraft. The purpose of the program was to:

1. Define the structural environment of the modified tip and blade to augment future design efforts.
2. Substantiate free hover and vertical climb performance characteristics of anhedral tips, compared to the standard production configuration.
3. Evaluate effects of anhedral tips on level flight performance and power required.
4. Assess data acquired in tests 1 through 3 above for potential impact of anhedral tips on aircraft handling qualities.

5. Evaluate acoustic signature of the anhedral tips.

The results of the test confirmed the potential of the anhedral tip.

Figures 37 and 38 respectively present the rotor speed and load factor envelopes explored in the test as a function of calibrated airspeed. Vehicle gross weight was limited to one value by the program scope. As indicated, the anhedral tip main rotor flight envelope included an advancing blade Mach number of 0.919 and an advance ratio of 0.410, these were attained at 100% main rotor speed of 258 RPM. Rotor speeds from 90 to 110.7% Nr in auto-rotation and a load factor of 1.91 G's were recorded. The rotor remained stable for all flight conditions. The anhedral tip had no significant effect on the inboard portion of the main rotor blade, control loads, or cockpit vibration. However, the anhedral tip increased the blade flatwise stress in the area of the tip cap attachment. This was corrected by adding 5 simple stiffening clips to the affected area, which increased the strength of the tip rib and for the same loads reduced the stresses.

The hover and vertical climb data were analyzed as a function of the aircraft heading with respect to the residual winds (always less than 4 knots). This approach acknowledges wind influence on main rotor-tail rotor interference and is effective in reducing attendant data scatter. Figures 39 and 40 respectively indicate the benefits of the anhedral tip geometry observed in both flight regimes. For hover the average increase in lift capability was 2% gross weight based on main rotor power and 2.4% based on total power. Likewise the vertical climb data indicated power reductions of 2% and 1.6% at vertical climb rates of 500 FPM and 1000 FPM respectively.

Level flight results of the anhedral and standard tip performance tests are shown in Figure 41. Figure 41 presents nondimensional speed/power data and includes curve fits of the form $f(x) = A_0 + A_1/X + A_2x^2 + A_3X^3$ for both the anhedral and standard tip configurations. Data are corrected to standard sea level conditions and tests for both configurations were conducted at the same referred gross weight and rotor speed. The maximum speed difference is on the order of 1 knot at constant power in the cruise speed range. A statistical T-test of the data with a confidence level of 90% shows no significant difference.

Although specific handling quality flights were not addressed in the test program, data obtained during structural and performance flying was examined for handling qualities implications. This review showed no significant impact of the anhedral configuration. Some small differences were, however, noted. Since these could become more pronounced at higher loadings, a more rigorous appraisal was recommended as a follow-on test.

As previously mentioned, one objective of the flight evaluation was acquisition of forward flight acoustic data that would compliment the hover data previously acquired on the Sikorsky whirl tower. That data showed a 2dB noise reduction in hover. The forward flight acoustic data were acquired using the microphone array and instrumentation located at the Development Flight Center's Acoustic Range in West Palm Beach, Florida. Data were acquired using microphones at 1.2 meters and 0.020 meter above ground level. Level flight passes over the acoustic range at reciprocal headings were conducted at 80, 120, and 140 KIAS.

The acoustic test data, reduced into one-third octave bands in intervals of 0.5 second and PNLTm (Perceived Noise Level Tone Maximum) and EPNL (Effective Perceived Noise Level) values, show no differences between the two sets of data at the tested flight speeds.

When measured in terms of gain in mission capability, the effect of anhedral tips on the performance of the UH-60A and its derivatives is quite dramatic. This is even more impressive when one considers that the gains are achievable through changes only in the tip cap. For the UH-60A primary mission, the takeoff ceiling can be increased by over 500 feet, or the vertical climb rate can be increased by 230 fpm, or the takeoff gross weight (i.e., useful load) can be increased by 2% (320 pounds). Also, at fixed conditions the reduced main rotor power can be used to offset power consumed by other systems such as hover infrared suppressor or an air conditioning system. The useful load increase can be used to carry added mission equipment, more payload, or additional fuel, the latter increasing mission time from 2.30 to 2.56 hours, an additional 16 minutes or 11%.

The mission and performance increment trends noted above also apply to SH-60B and to other H-60 helicopter derivatives. In addition, the SH-60B is required to perform payload deployment or sonar dipping missions where takeoff gross weight is restricted due to a midpoint hover requirement. Application of the anhedral tip for these missions is even more beneficial; payload is increased by up to 420 lb.

3RD GENERATION ROTOR AIRFOIL DEVELOPMENT AT SIKORSKY AIRCRAFT

Rotor Tip Airfoils

Five full scale rotorcraft airfoils (Figure 42) were tested in March and April 1982 in the NASA Ames Eleven-Foot Transonic Wind Tunnel for full scale Reynolds numbers at Mach numbers from 0.3 to 1.07. The models, which spanned the tunnel from floor to ceiling, included two modern baseline airfoils, the SC1095 and SC1094 R8, which have been previously tested in other facilities. Three advanced transonic airfoils, designated the SSC-A09, SSC-A07, and SSC-B08, were tested to confirm predicted performance and provide confirmation of advanced airfoil design methods.

The maximum lift coefficients at a Mach number of 0.3 for the SC1095 and SC1094 R8 were 1.37 and 1.72, respectively. The transonic airfoils had maximum lift coefficients of 1.40, 1.22, and 1.15 for the SSC-A09, -B08 and -A07, respectively. Drag divergence Mach numbers at zero lift for these airfoils were .808, .780, .833, .848 and .860. Prior to stall and drag divergence the pitching moments were generally between 0.010 and -0.015.

The airfoil analysis codes agreed well with this data, with the Grumman GRUMFOIL code giving the best overall performance correlation. The NYU Transonic Airfoil code predicted airfoil pressures and drag divergence well, but errs in the calculation of pitching moment. The Texas A&M TRANDES/TRANSEP codes show good correlation over the full range of test conditions. The AMI CLMAX code predicts the relative maximum lift coefficient of the thicker airfoils well, but fails to predict the maximum lift coefficient of the SSC-A07. The maximum lift coefficients measured in the test exceed the CLMAX code prediction and available test data from the United Technologies tunnel by about 10%.

The SSC-A09 airfoil exceeded the SC1095 airfoil maximum lift coefficient by 2% and each transonic airfoil tested showed "gentler" stall characteristics. Low lift, low Mach number drag levels ranged from .0067 to .0088. The transonic airfoils had lower drag levels than the baseline airfoils.

The transonic airfoils produced significant performance improvements at higher Mach numbers. The maximum lift of the SSC-A09 exceeded that of the other airfoils tested at Mach numbers between 0.50 and 0.74. Above a Mach number of 0.74 the SSC-A07 had superior maximum lift capability (see Figure 43). Figure 44 shows the zero lift drag for the tested airfoils. The type of leading edge camber used for the SC1094 R8 results in an early drag rise

and a drag divergence Mach number that is significantly lower than the other airfoils. The transonic airfoils maintain low drag characteristics to Mach numbers above 0.833. The drag divergence Mach number occurs at lower drag levels for the improved airfoils, providing more drag reduction than indicated by changes in drag divergence Mach number. The lift-drag ratios for the airfoils designed using modern design methods are superior to earlier rotorcraft airfoils. The airfoils in the SSC-AXX family have better maximum L/D values than the other tested airfoils (Figure 45).

High-Lift Airfoils

Several third generation high lift airfoils for rotary wing applications have been designed at Sikorsky Aircraft and Experimentally verified in the Ohio State University 6 x 22 inch transonic test facility (OSU).

The design of these airfoils was spurred when a recent investigation into possible improvements for a high speed rotor revealed potential benefits of redesigning the existing mid span airfoil, the SC1094 R8. A significant gain in rotor lift to drag ratio could be realized if the SC1094 R8 drag divergence characteristics were improved: specifically a reduction in drag creep typical of this airfoil plus an increase in the zero lift drag divergence Mach number. An examination of the SC1094 R8 for this new rotor revealed the present maximum lift coefficient for all operating Mach numbers to be adequate, but any significant reduction in its value could compromise the rotor's performance. The present third generation rotor tip airfoil, the SSCA09, has the superior drag divergence characteristics necessary, but its maximum lift levels are inadequate for the mid span region of the rotor. For these reasons an effort was initiated to design a new (third generation) mid span airfoil with maximum lift levels comparable to the SC1094 R8 values and drag characteristics approaching those of the SSCA09. Special attention was given to reducing the SC1094 R8 drag creep.

The design effort was conventional in approach in that modifications to existing airfoil designs were made and performance predicted by numerical methods, specifically GRUMFOIL for drag divergence estimates and EPPLER for maximum lift estimates.

Two ten percent thick airfoils, the SC2110 and SC2210, are the end result of the design study and were selected for testing at OSU over Mach number and angle of attack ranges capable of providing maximum lift coefficient and zero lift drag divergence values.

Figure 46 presents lift and drag experimental results for the baseline and two new designs. These results indicate that the two new airfoils maximum lift level is higher than that of the baseline airfoil for the critical Mach number of 0.4, one of the primary design goals. This is also the case for all Mach numbers greater than 0.4, however the SC1094 R8 retains its lead in maximum C_L at 0.3 Mach number. Although absolute values of maximum lift are underpredicted by EPPLER, the relative performance of the three airfoils compares well with the numerical predictions. The improvements in zero lift drag for the two new airfoils predicted by GRUMFOIL are verified by the experimental results. Large improvements in drag characteristics are obtained for both the new airfoils with drag creep reduction showing the most significant gain. Once again, absolute values of predicted drag differ from the experimental results while relative changes between airfoils are adequately predicted.

Examination of the experimental results reveals the SC2110 to be the better performer of the two new designs and is the airfoil of choice for future Sikorsky rotor applications.

Figure 47 illustrates the performance improvements obtained by the third generation airfoils. This plots maximum lift coefficient for the critical Mach number of 0.4 against zero lift drag divergence Mach number for second and third generation root and tip airfoils, plus several competitors' airfoils. The performance gains made since the first generation rotary wing airfoil, the NACA 0012, are significant and the third generation of Sikorsky airfoils has pushed the attainable rotor operating envelope to levels comparable with other present state-of-the-art airfoils. It must be noted that Figure 47 contains data obtained in facilities other than the OSU facility and are shown as flagged symbols. For this reason Figure 47 is used only as means of illustrating the performance gains produced by the design effort.



Figure 1. SHADOW Aircraft

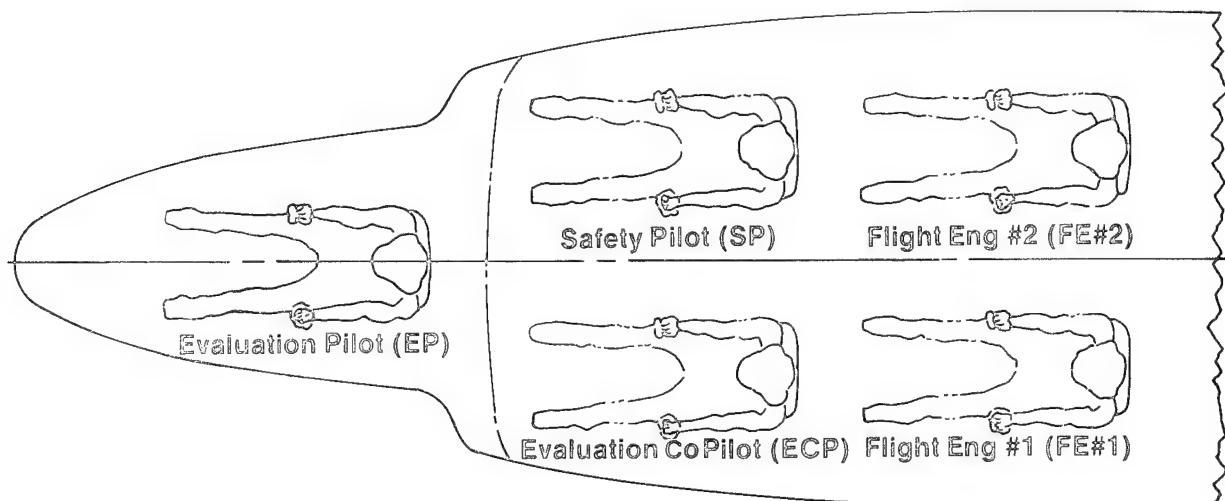


Figure 2. Crew Layout

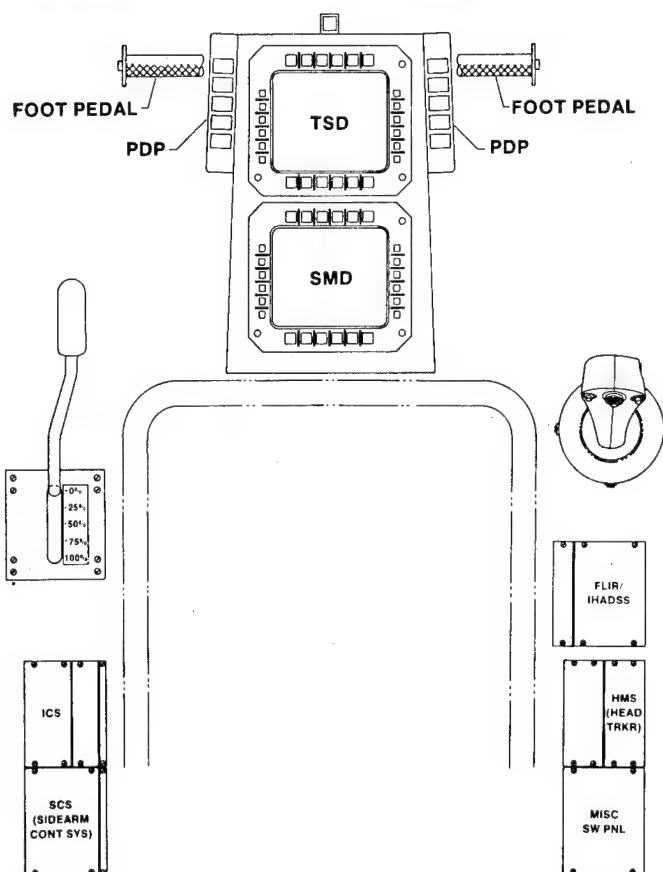
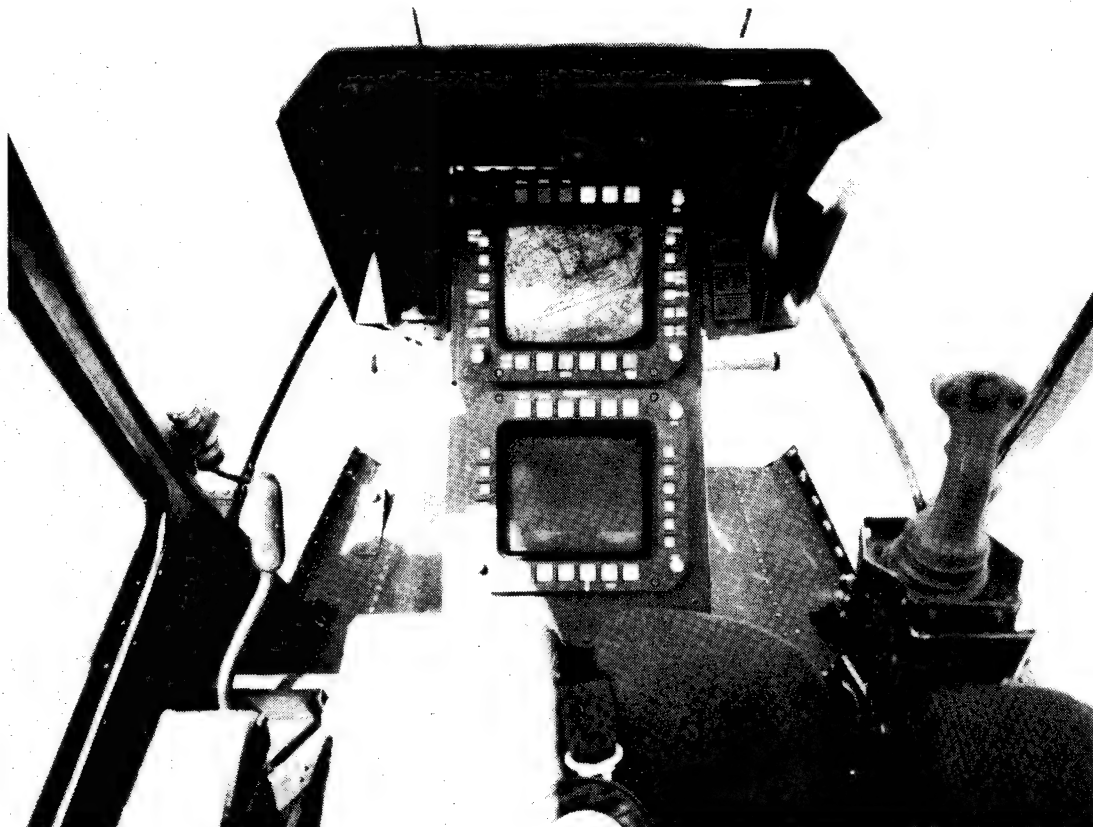


Figure 3. SHADOW Evaluation Pilot Cockpit Layout

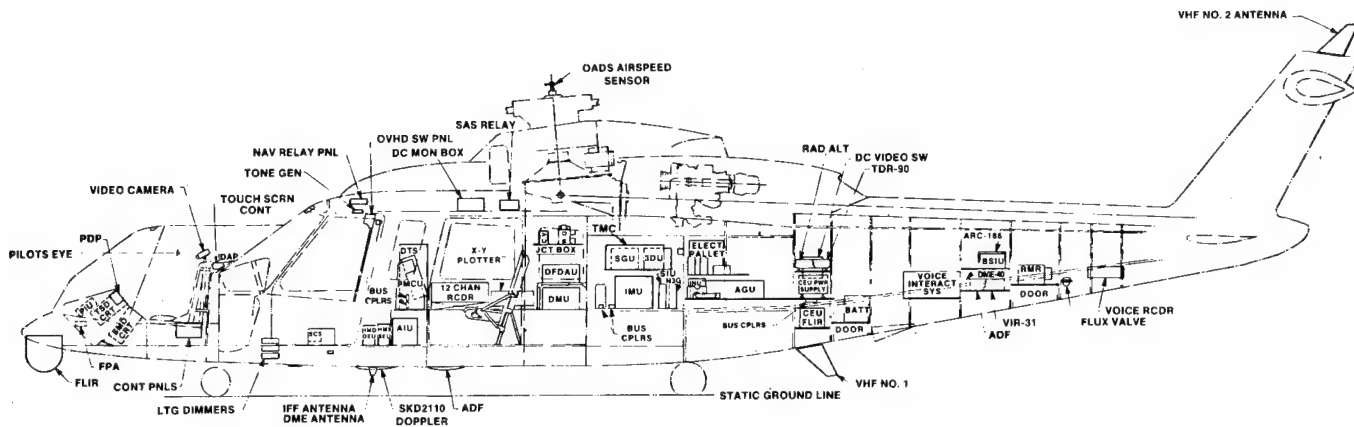


Figure 4. Avionic Layout

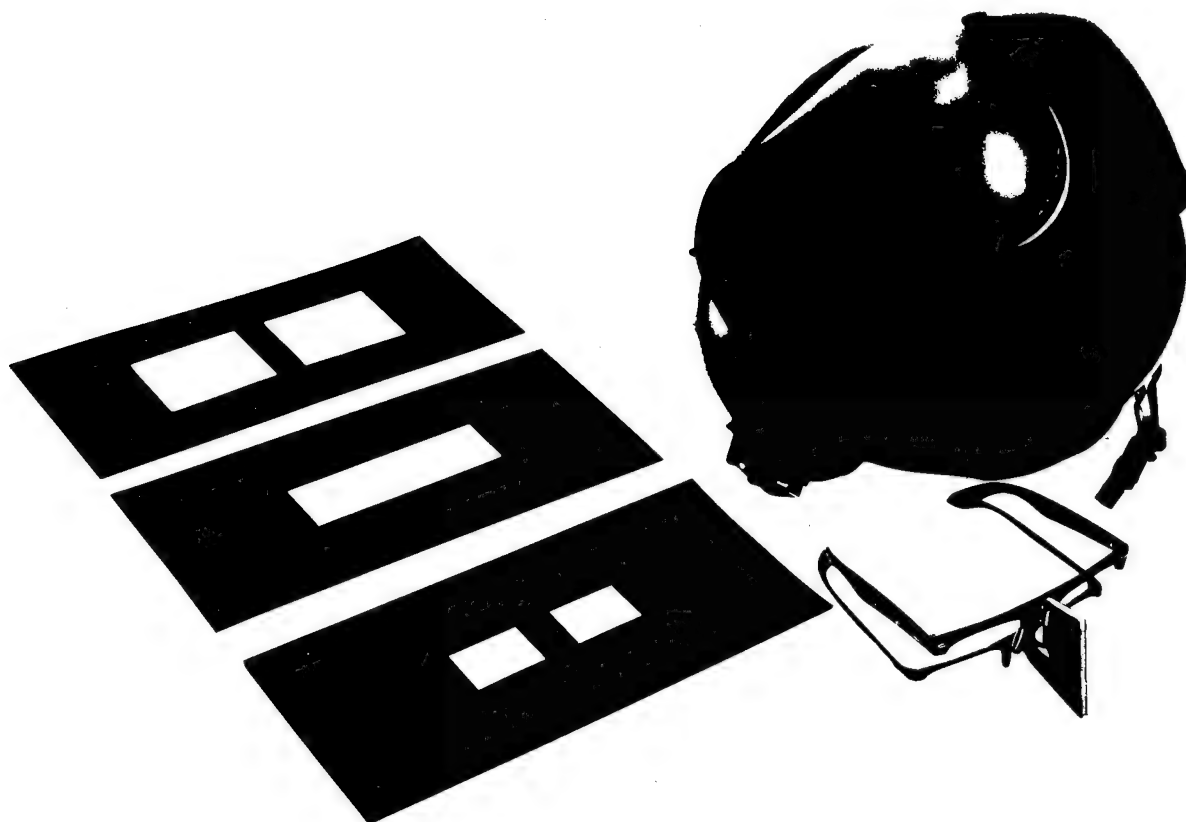


Figure 5. Photo of Three Masks, Septum and Layout

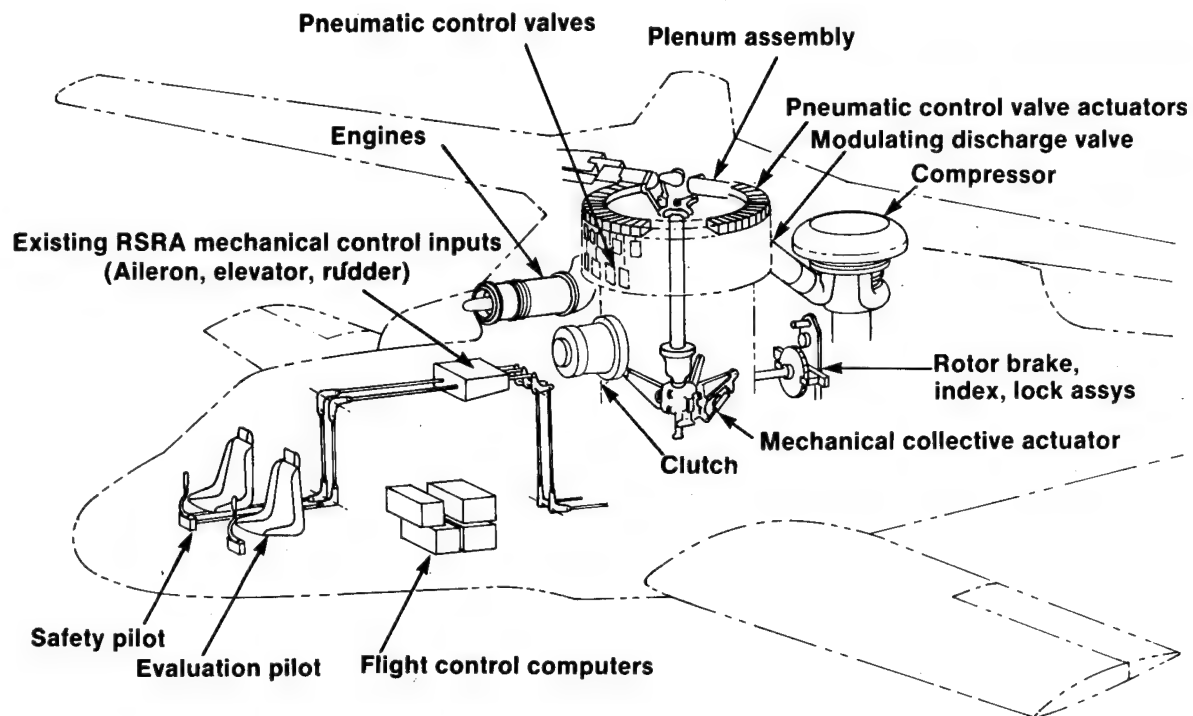


Figure 6. RSRA/X-Wing Vehicle Management System Installation

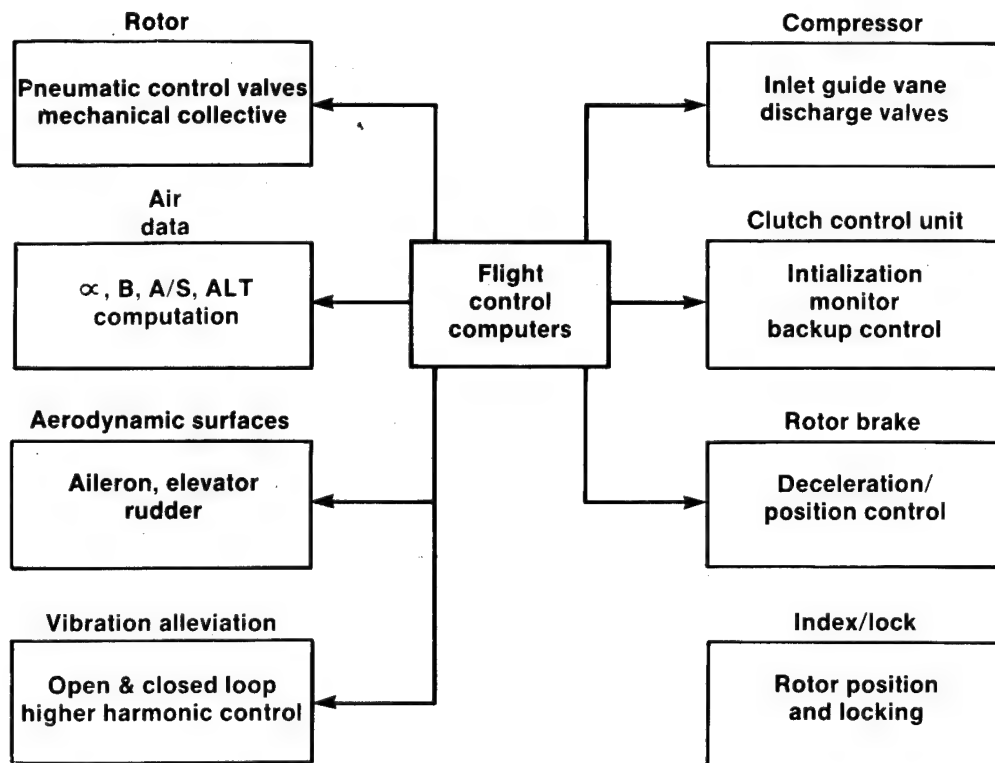
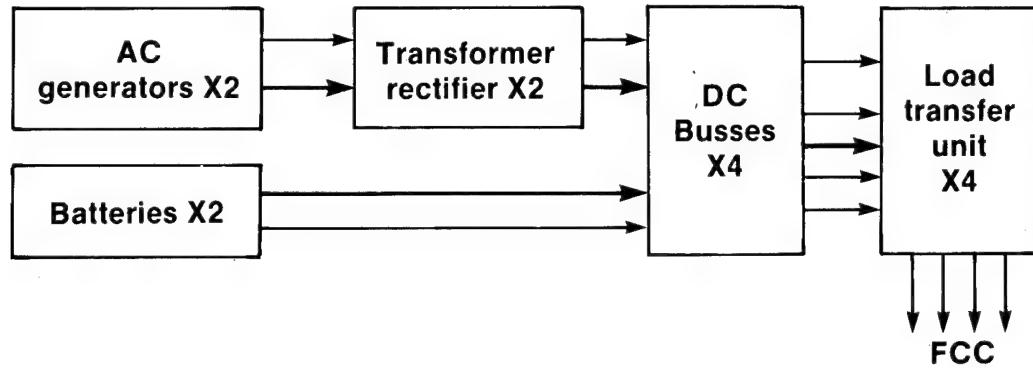


Figure 7. Vehicle Management System Functions

Electrical



Hydraulic

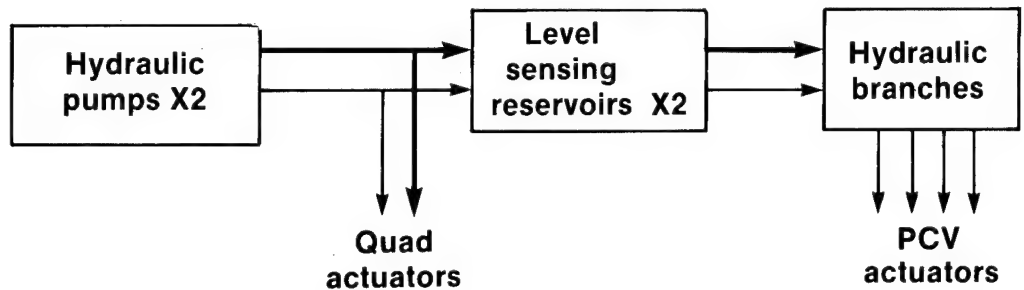


Figure 8. Power Redundancy

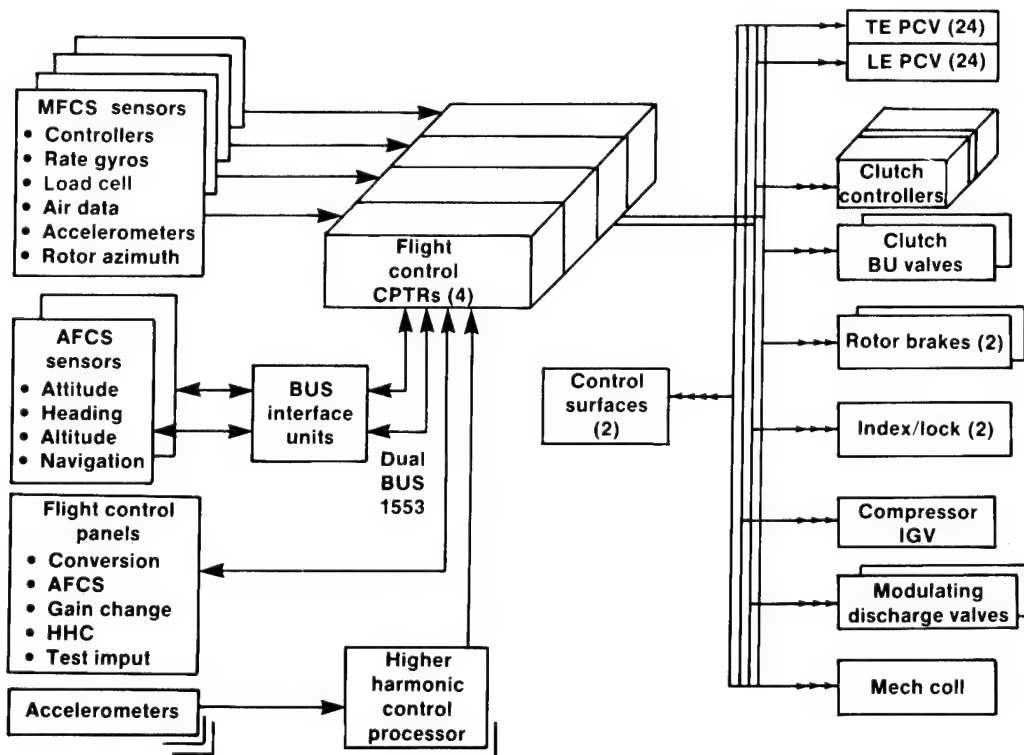
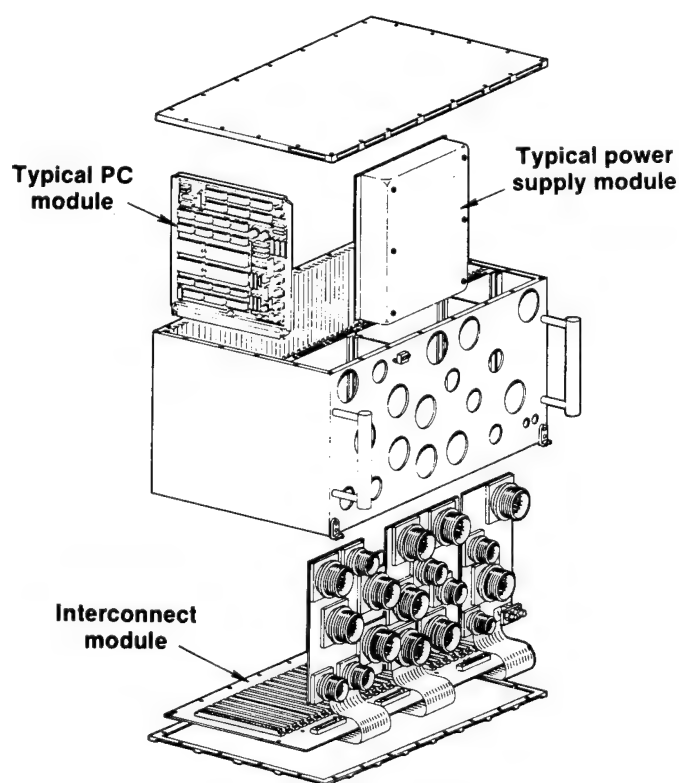


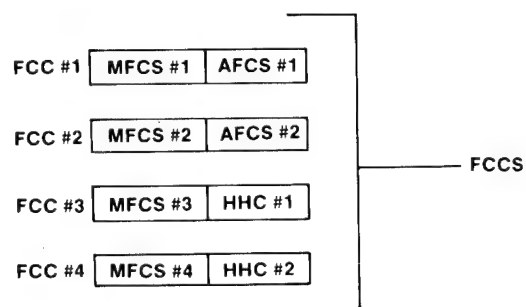
Figure 9. System Architecture

	MFCS	Direct link	Plenum dump	BUCS	Blade jettison
Full-up control laws	X		X		
• RW SAS					
• HMF					
Full redundancy	X	X	X	X	
HHC	X	X			
CCR "Blowing"	X	X			
Mechanical collective	X	X	X	X	
RSRA fixed wing controls	X	X	X	X	X

Figure 10. Control System Features Several Backup Modes



RSRA/X-WING FCC ARCHITECTURE



MFCS PROCESSOR CONFIGURATION

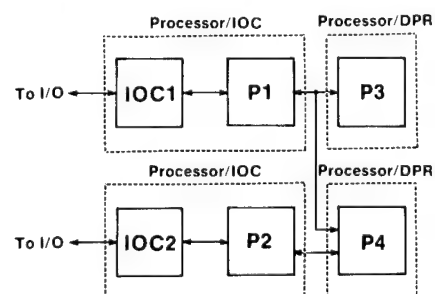


Figure 11. X-Wing FCC

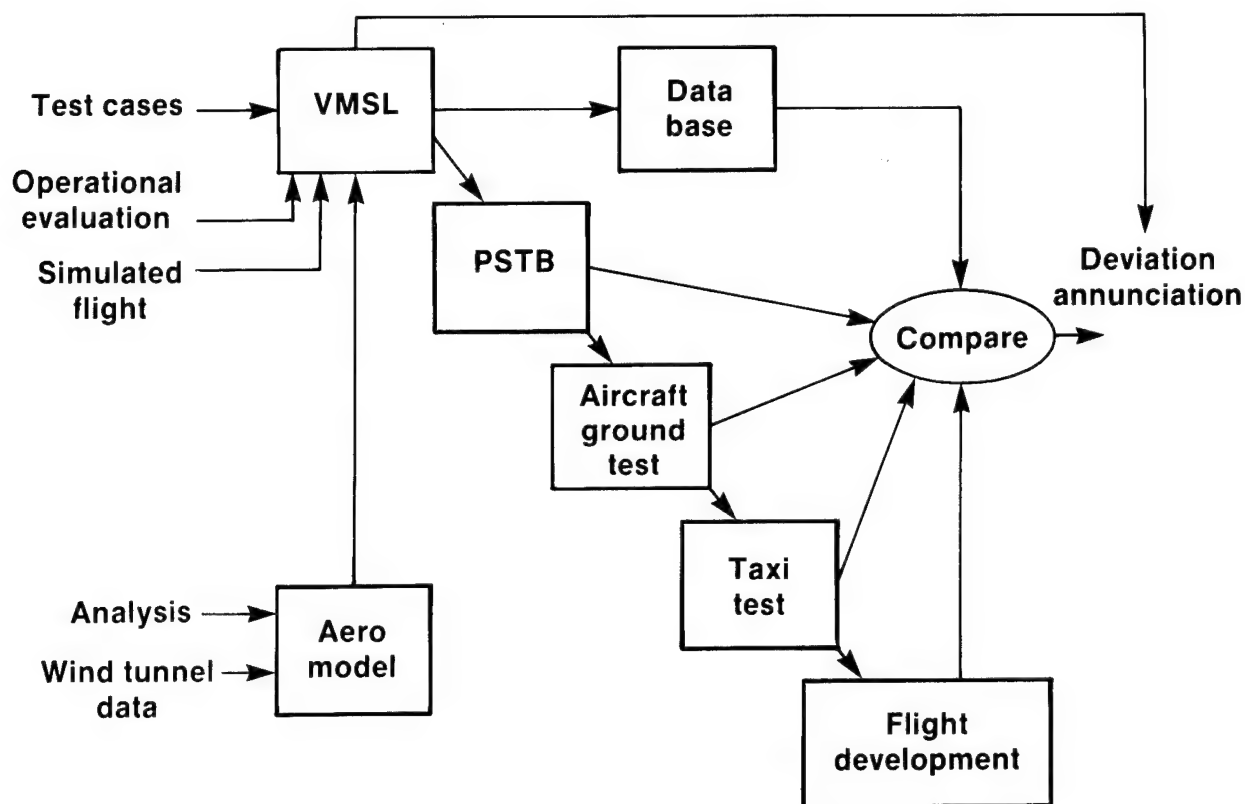


Figure 12. FCS Validation

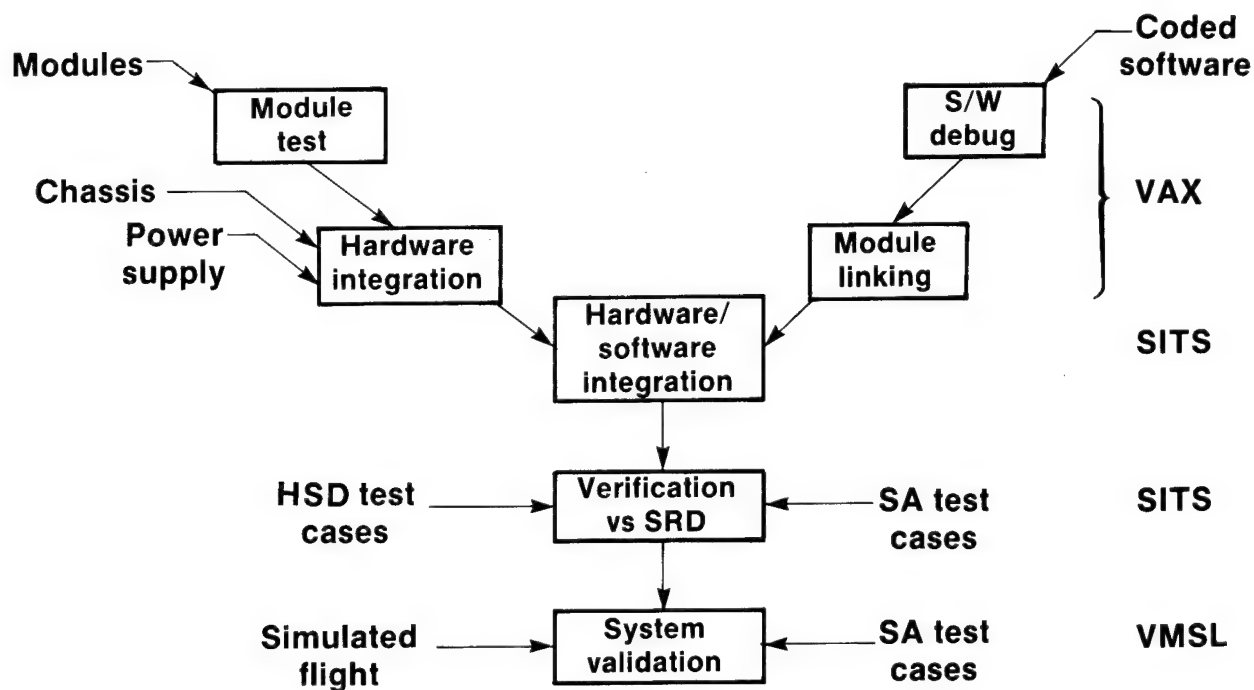


Figure 13. Flight Control System Development and Verification

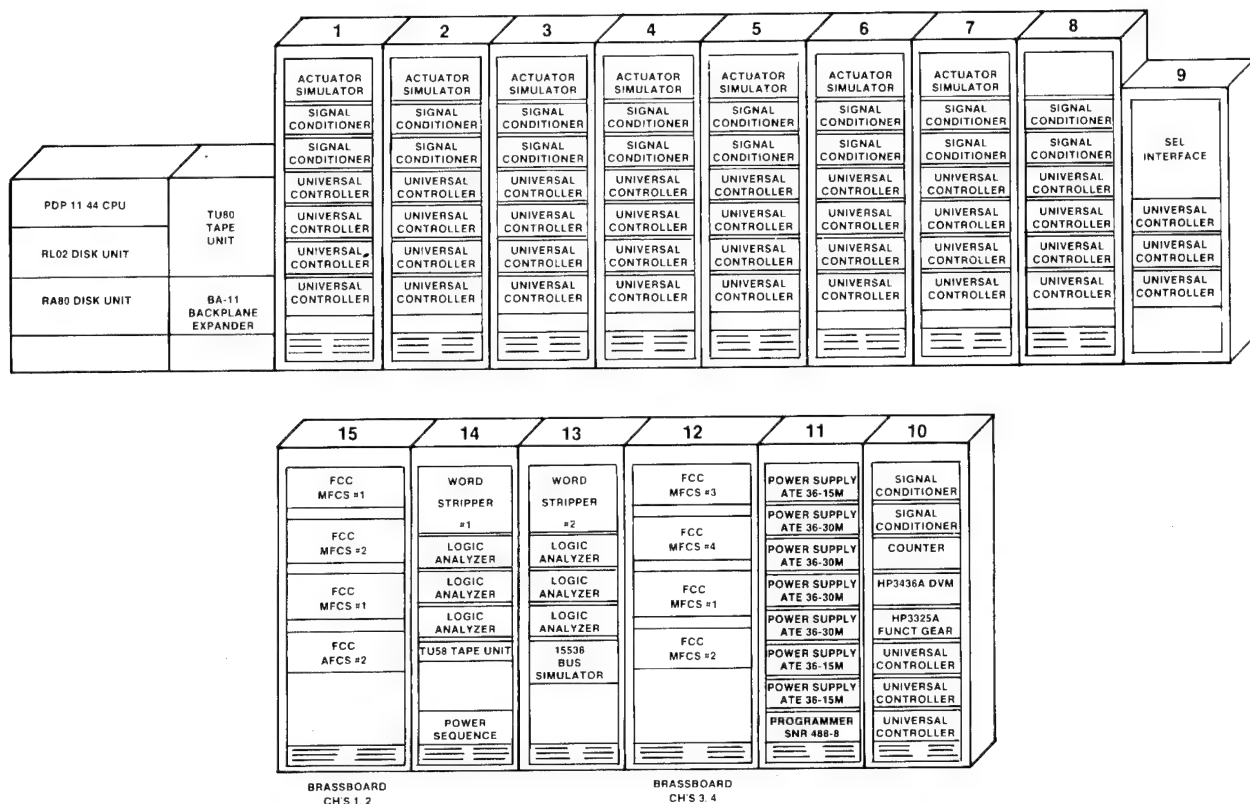


Figure 14. RSRA/X-Wing Systems Integration and Test Stand

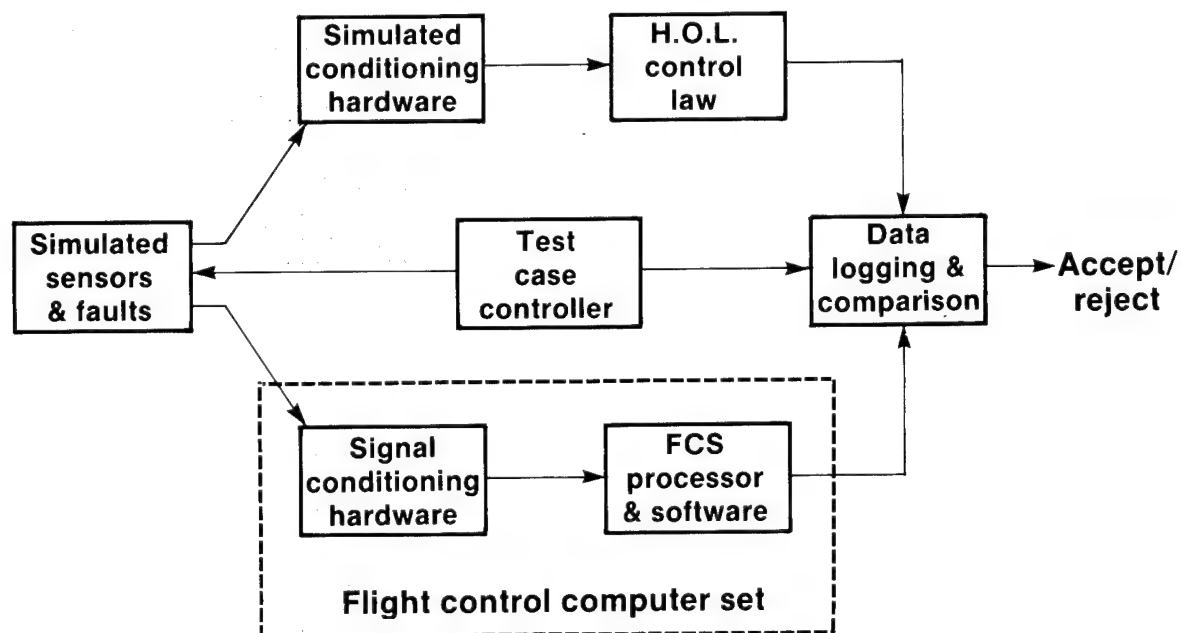


Figure 15. Automated Software Verification

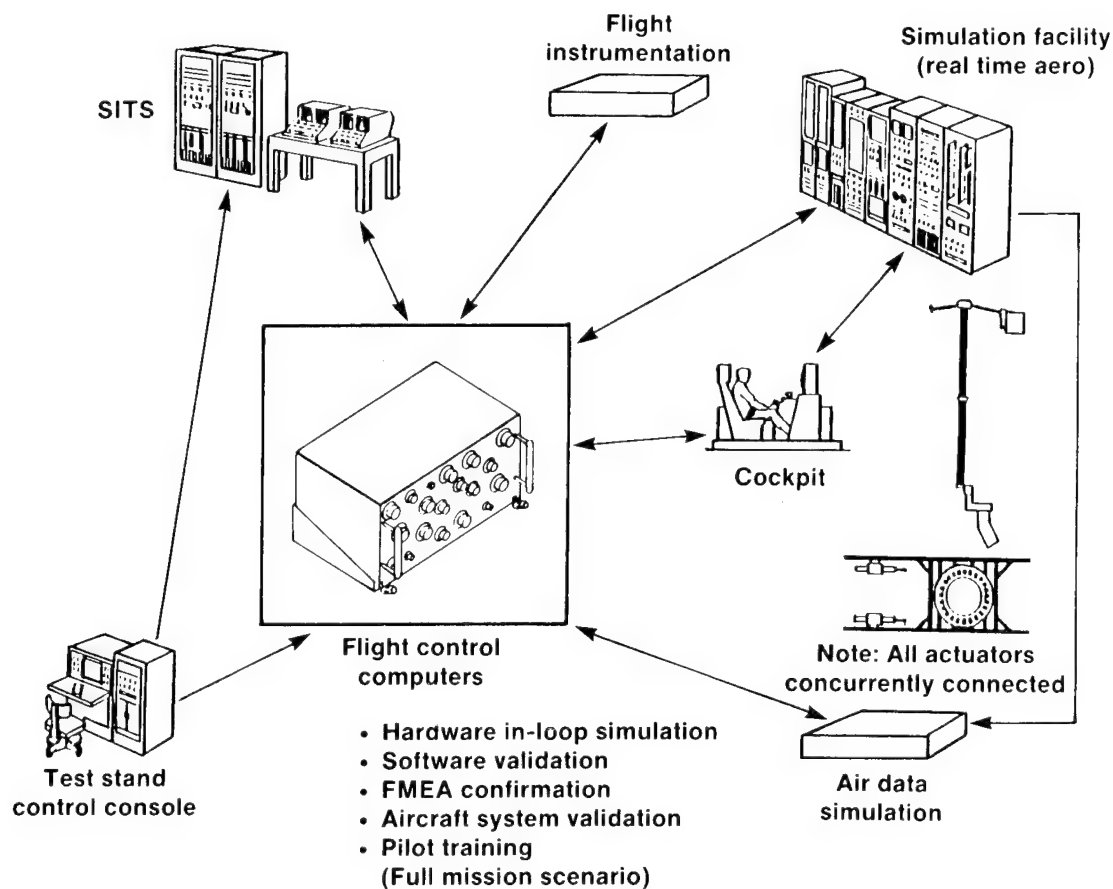


Figure 16. Vehicle Management System Lab

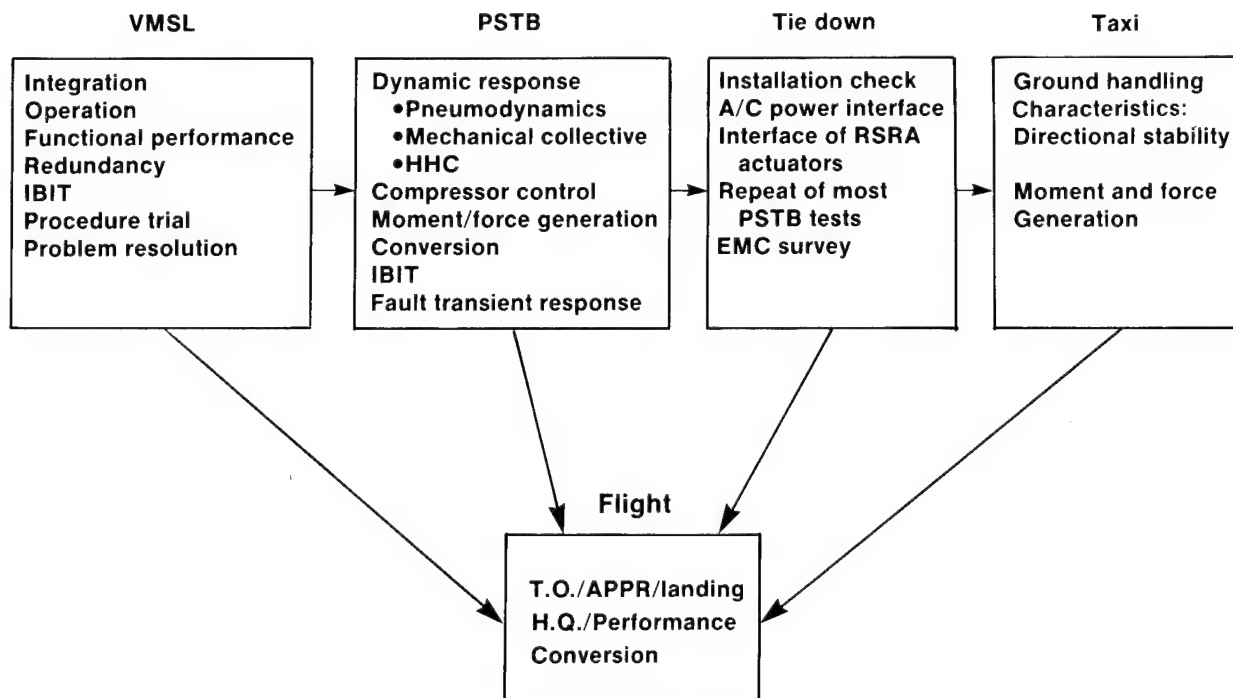


Figure 17. Validation Elements

	Rotor off	No blowing stopped	Blowing stopped	Rotary mode	Conversion
Direct Link	No FCC	* No FCC	✓	✓	✓
Unified Control Laws	↓	↓		✓	✓
BUCS			✓	✓	✓
HHC				✓	✓
AFCs			Partial	✓	✓

* Blade feathering locked in place

Figure 18. RSRA/X-Wing Code Usage During Flight

- Reprogrammable memory
- Alternate gains
- Test input panel
- HHC optimization panel
- Realtime and stored data acquisition
- PMCU

Figure 19. System Flight Development Features



Figure 20. The Sikorsky S-76 in Flight

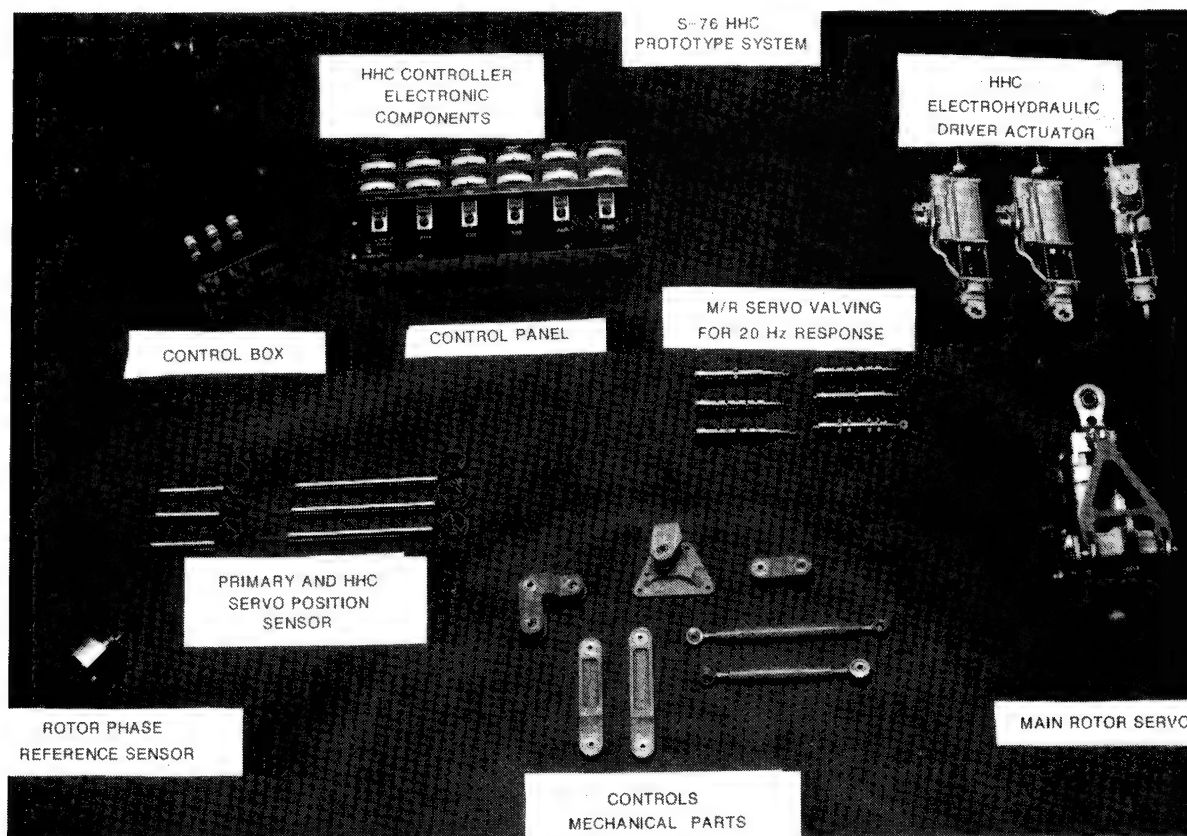


Figure 21. Mechanical and Electrical Elements of the HCC System

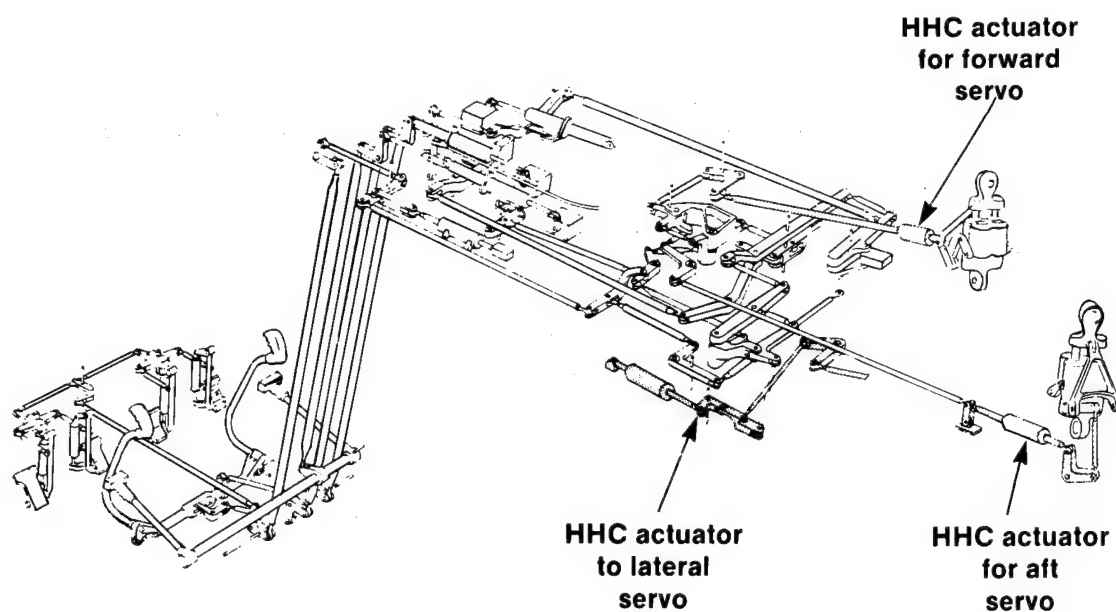


Figure 22. Schematic of HHC Modifications to the S-76 Control System

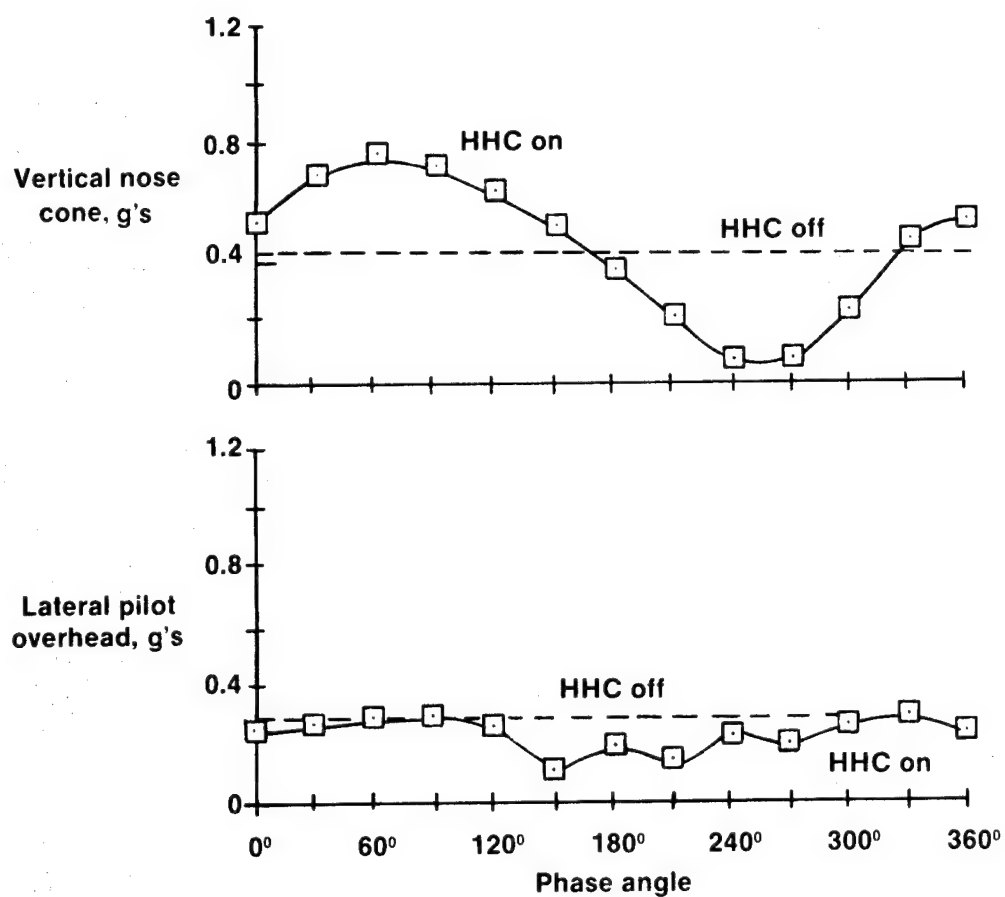


Figure 23. Effect of HHC Longitudinal Cyclic Mode on Cockpit Vibration, Level Flight, 80 Knots, 100% NR

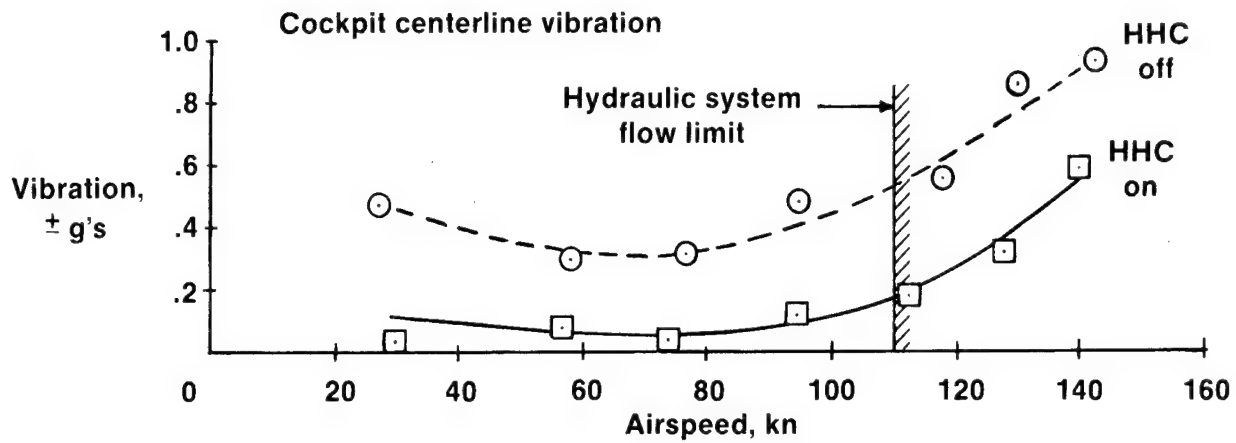


Figure 24. Reduction in Cockpit Centerline Vertical Vibration, 100% NR

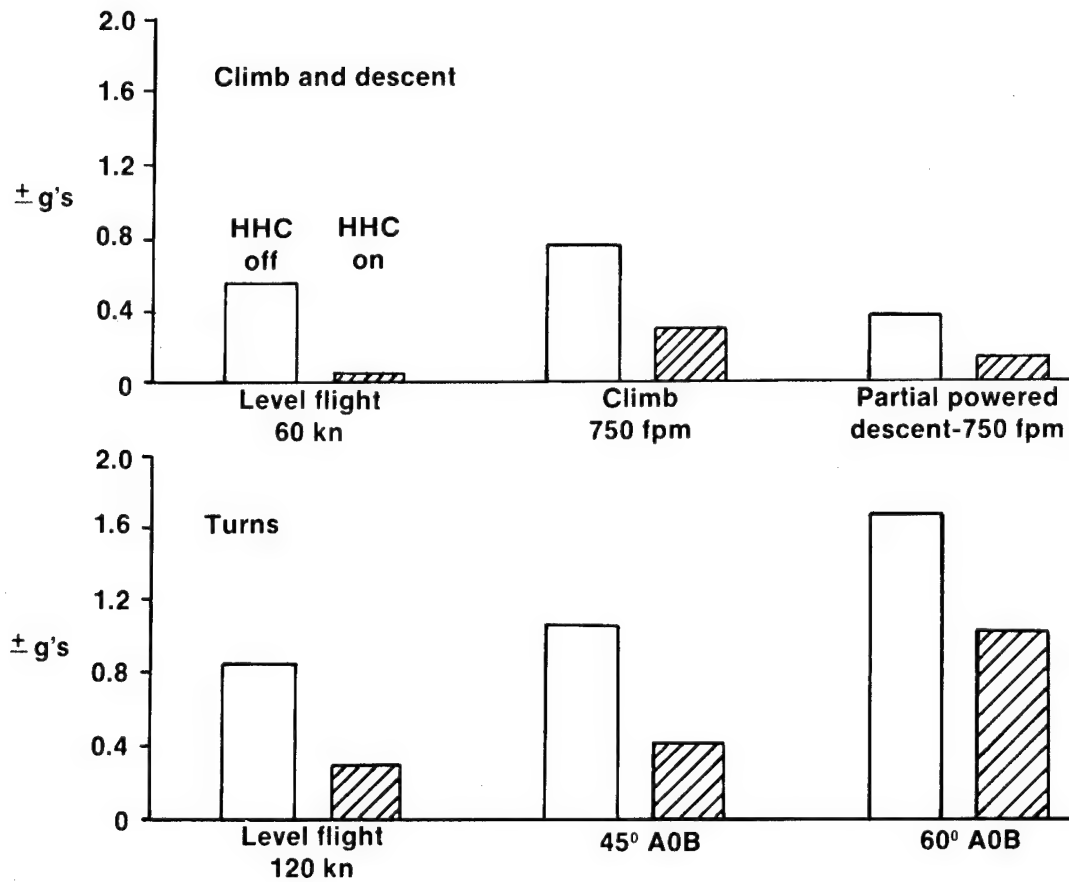


Figure 25. Reduction in Nose Vertical Vibration During Maneuvers

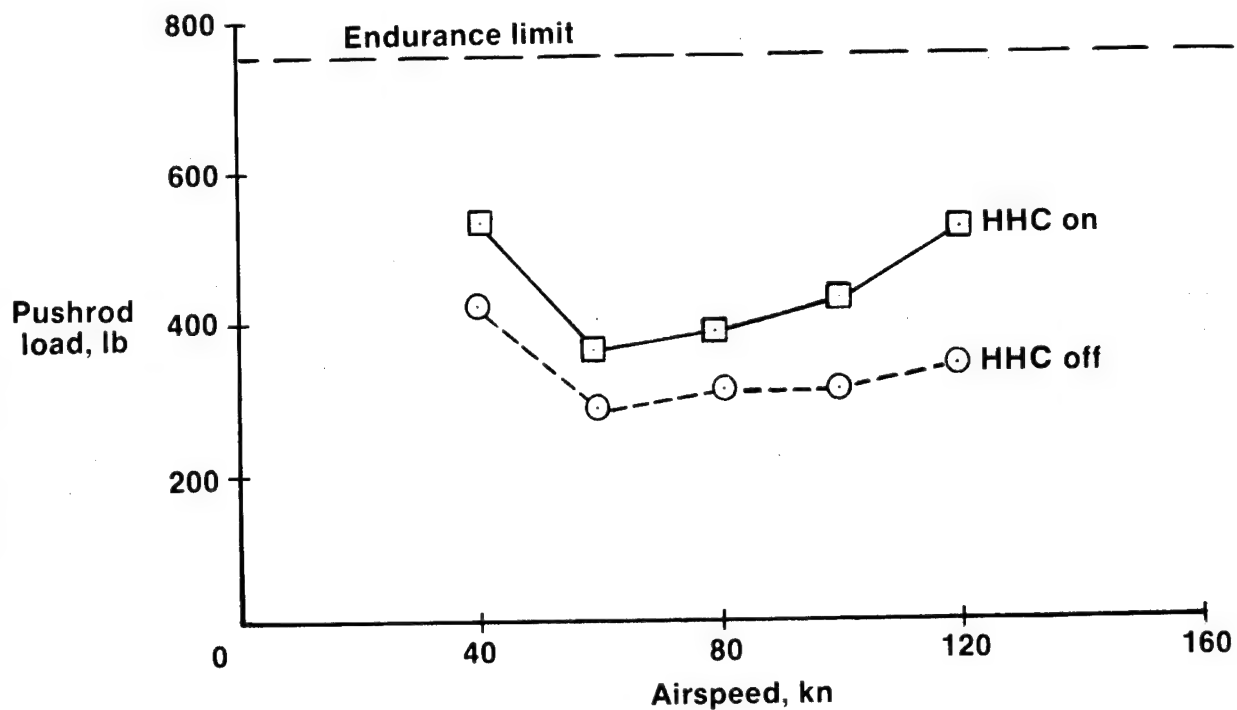


Figure 26. Effect of HHC Longitudinal Mode Input on Pushrod Vibratory Load

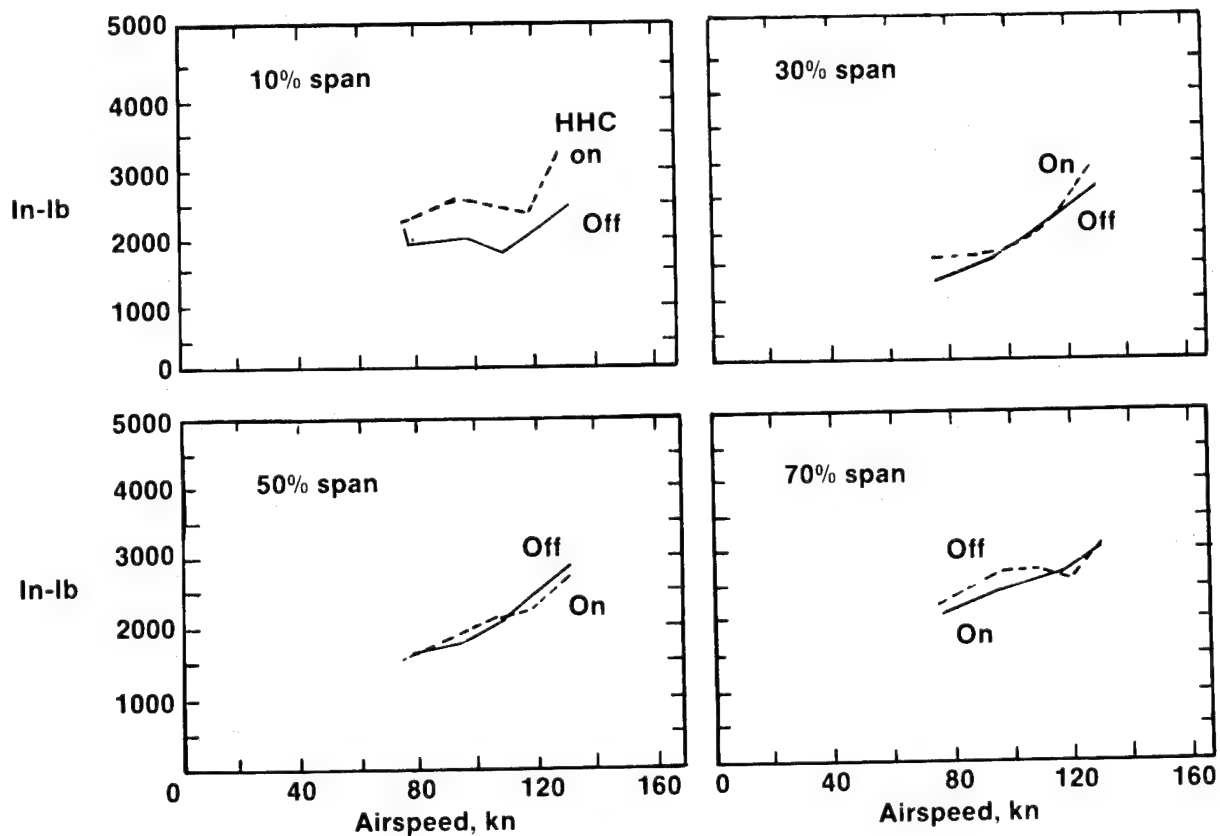


Figure 27. Effect of HHC on Blade Flatwise Vibrator Bending Moment

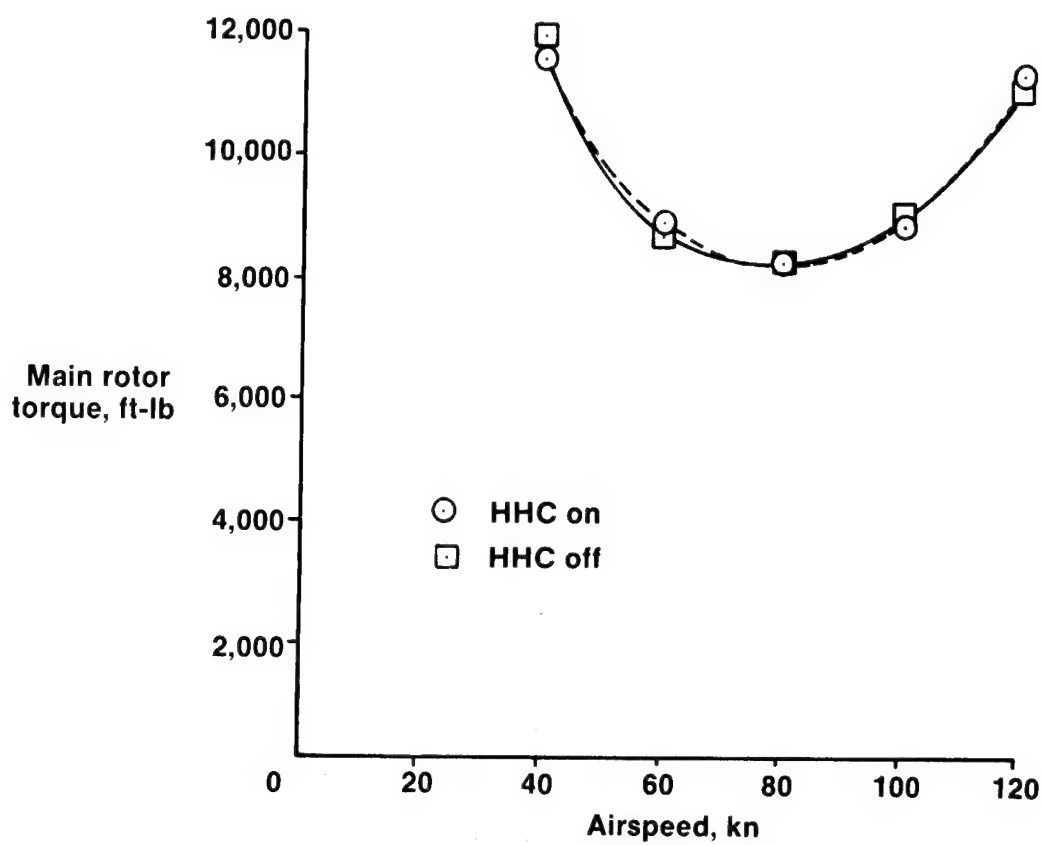


Figure 28. Level Flight Performance, Effect of HHC Longitudinal Mode, 107% NR

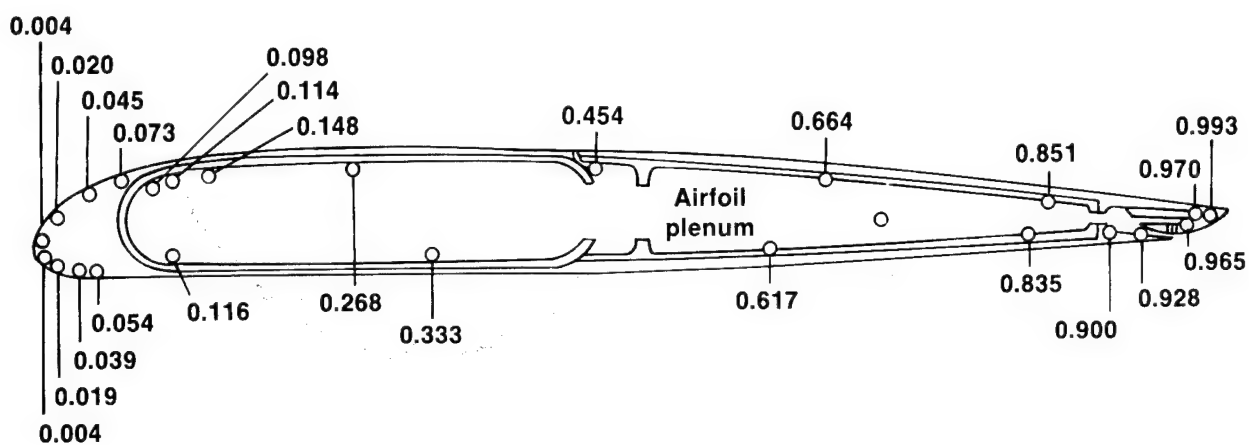


Figure 29. Airfoil Section and Transducer Locations

$M = 0.4$, $\alpha = 3.8^\circ$, $F = 15 \text{ Hz}$, $P = 15 \text{ psi}$

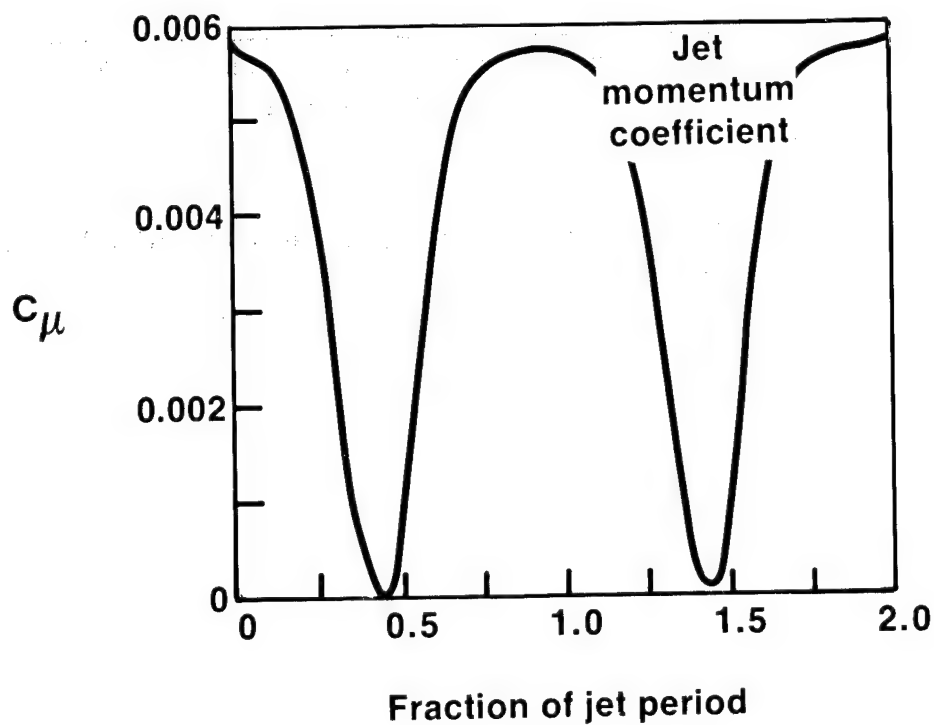


Figure 30. Time Histories for Jet

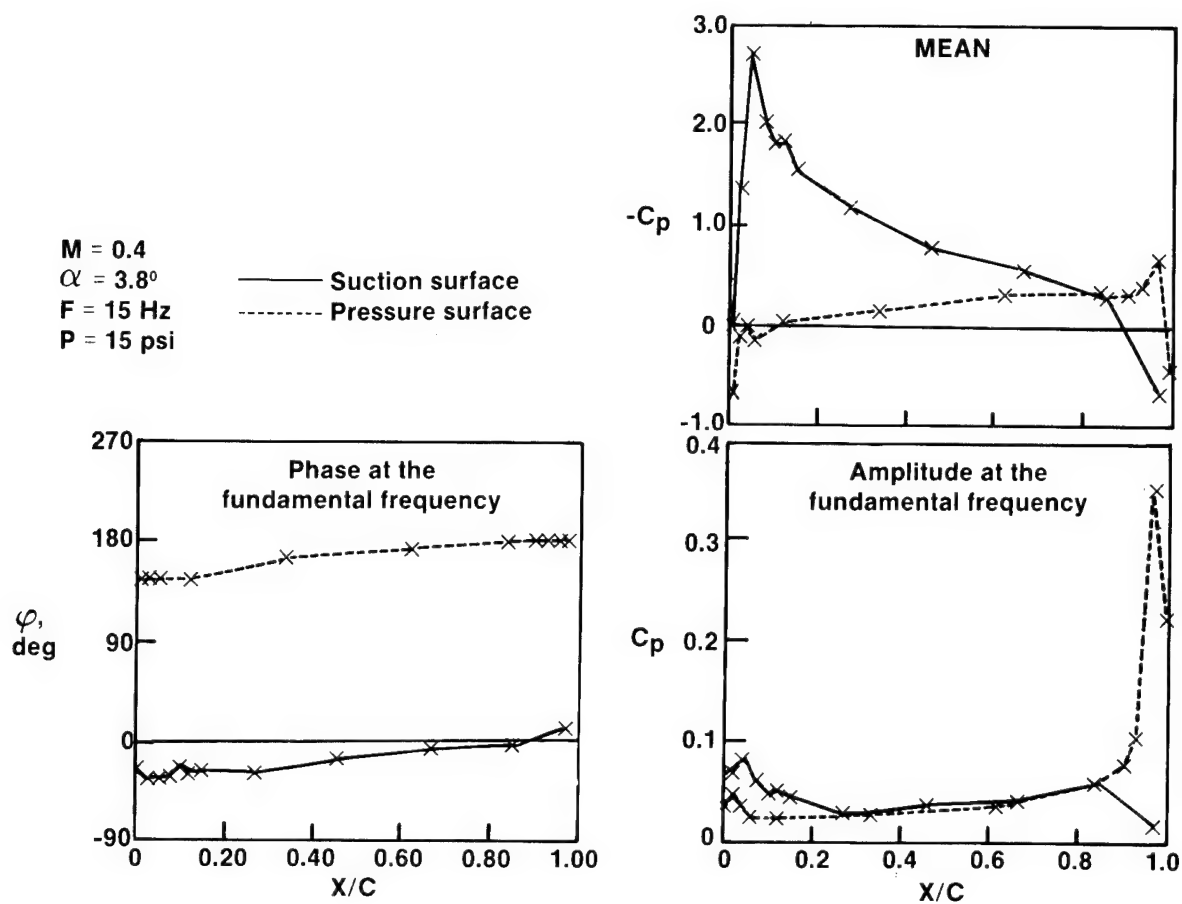


Figure 31. Surface Pressure Distributions

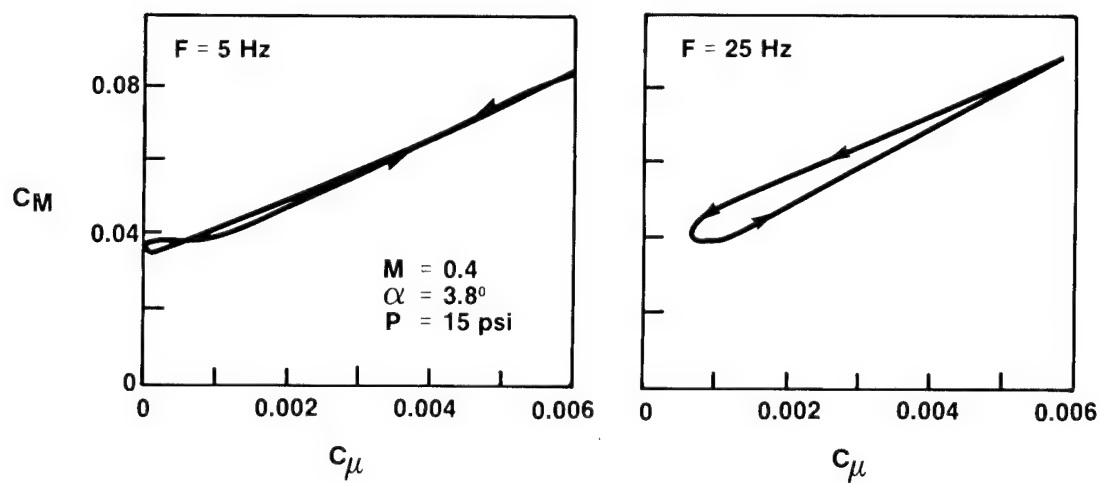


Figure 32. Loops of C_M vs. C_u

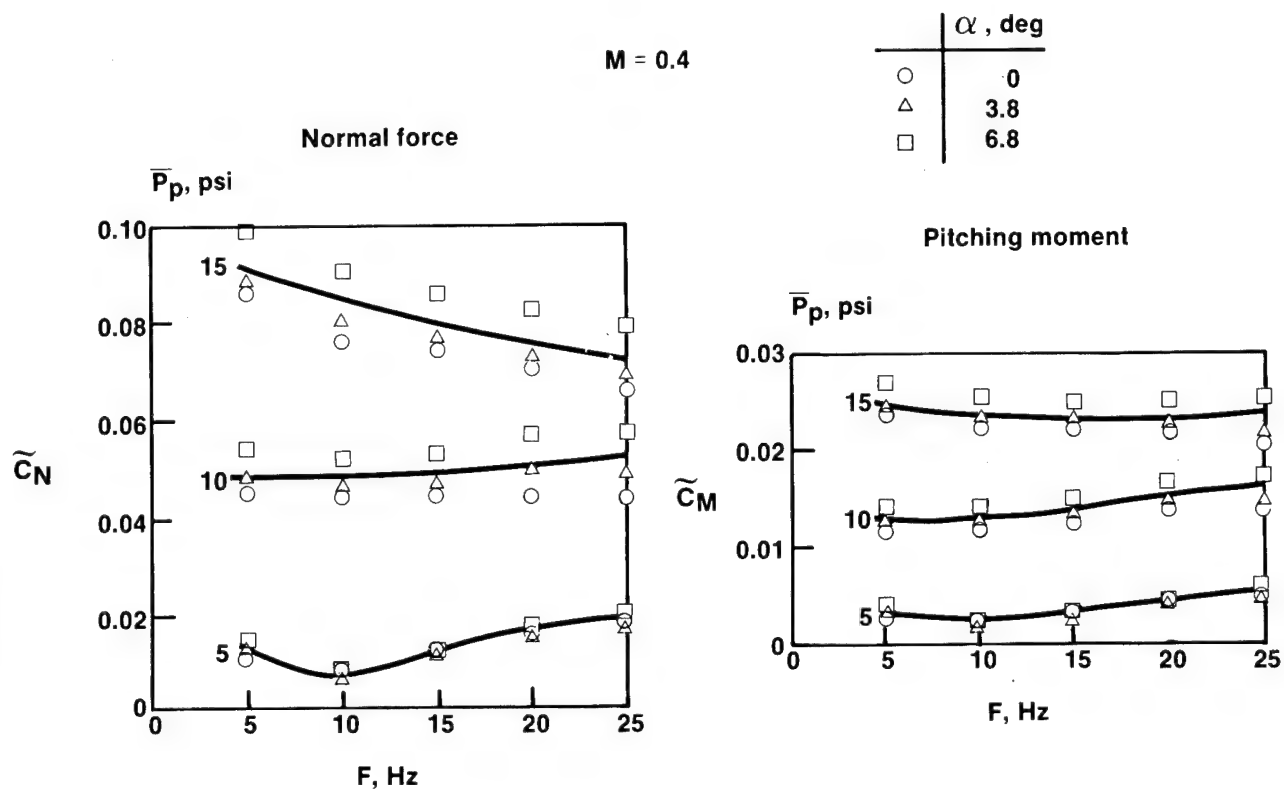


Figure 33. Fundamental Amplitudes vs. Frequency

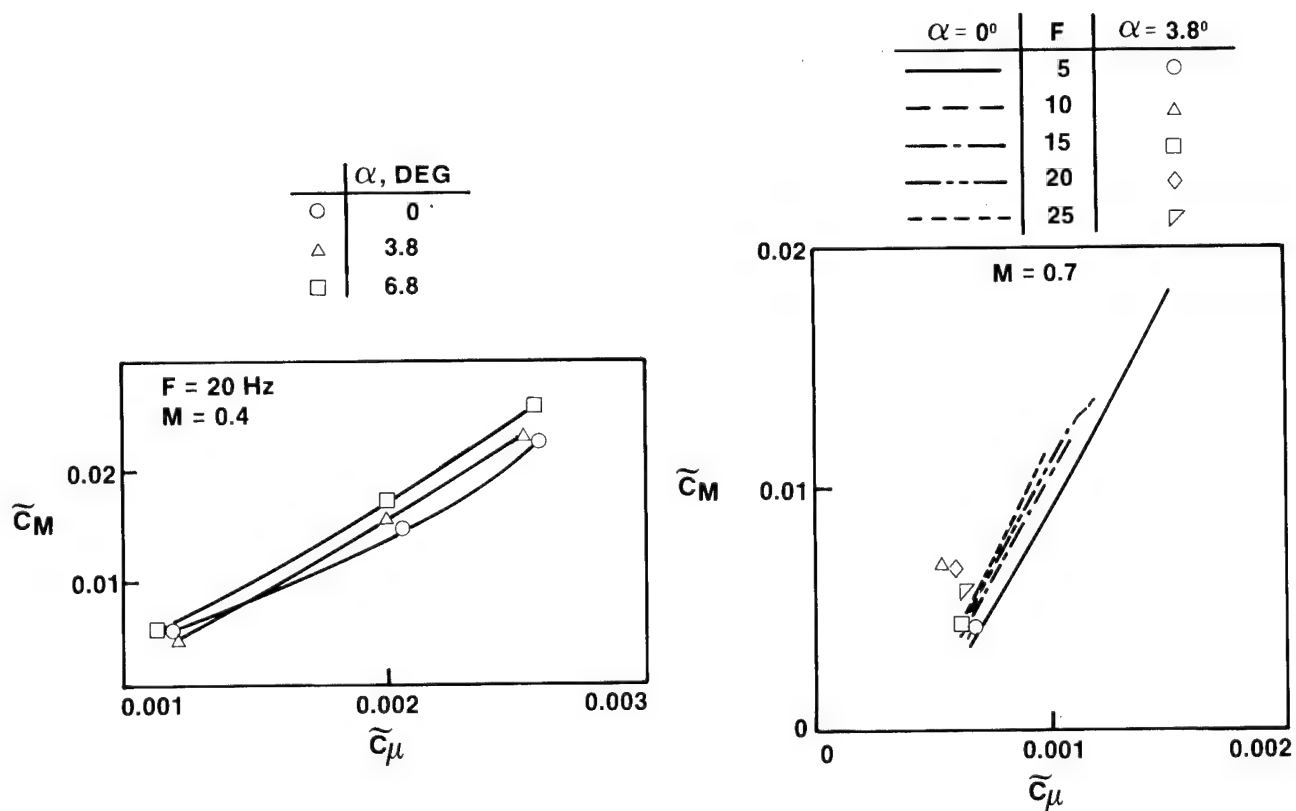


Figure 34. Fundamental Amplitude vs. Jet Momentum

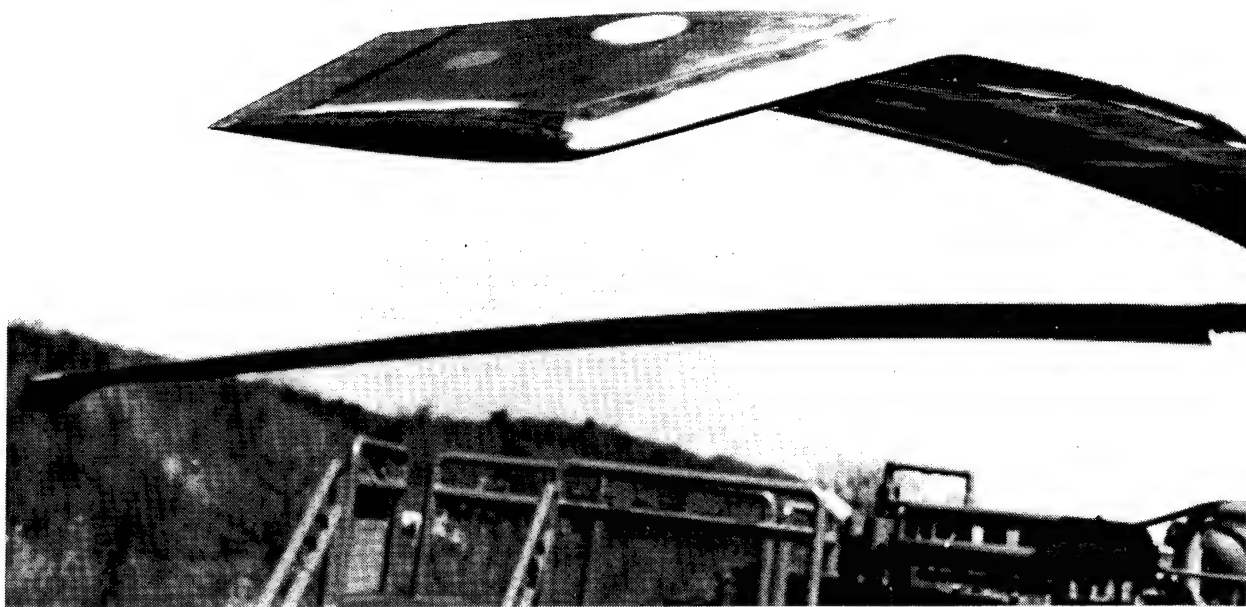


Figure 35. UH-60A Main Blade with Anhedral Tip Installed

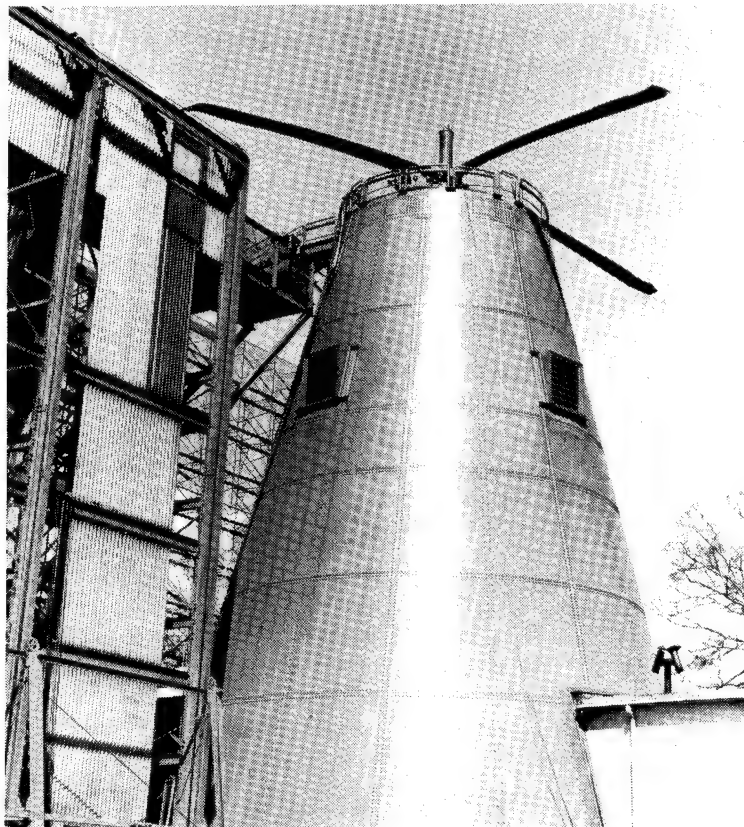


Figure 36. 10,000 Horsepower Main Rotor Stand with UH-60A Rotor System Installed with Anhedral Tip Caps

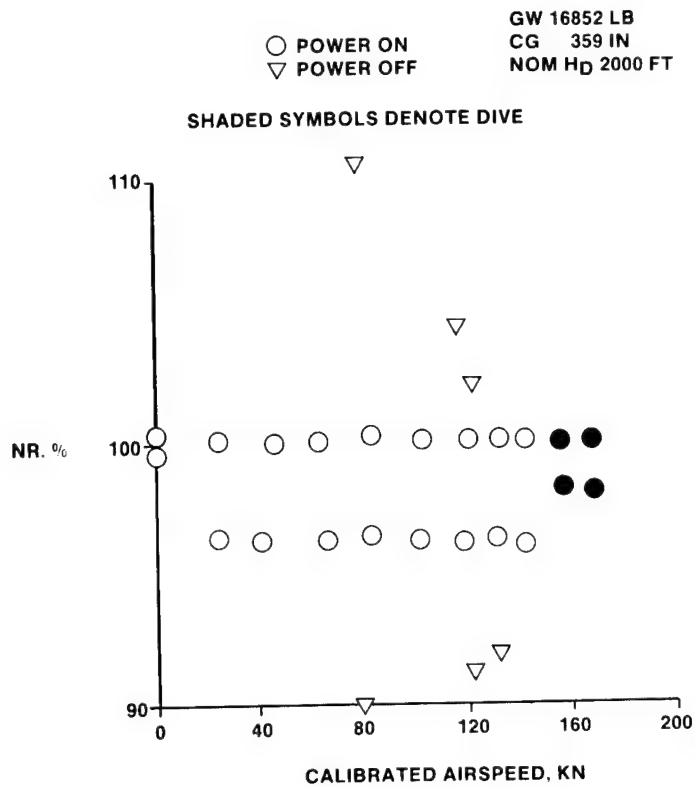


Figure 37. Main Rotor Speed Envelope for UH-60A Rotor with Anhedral Tip Caps

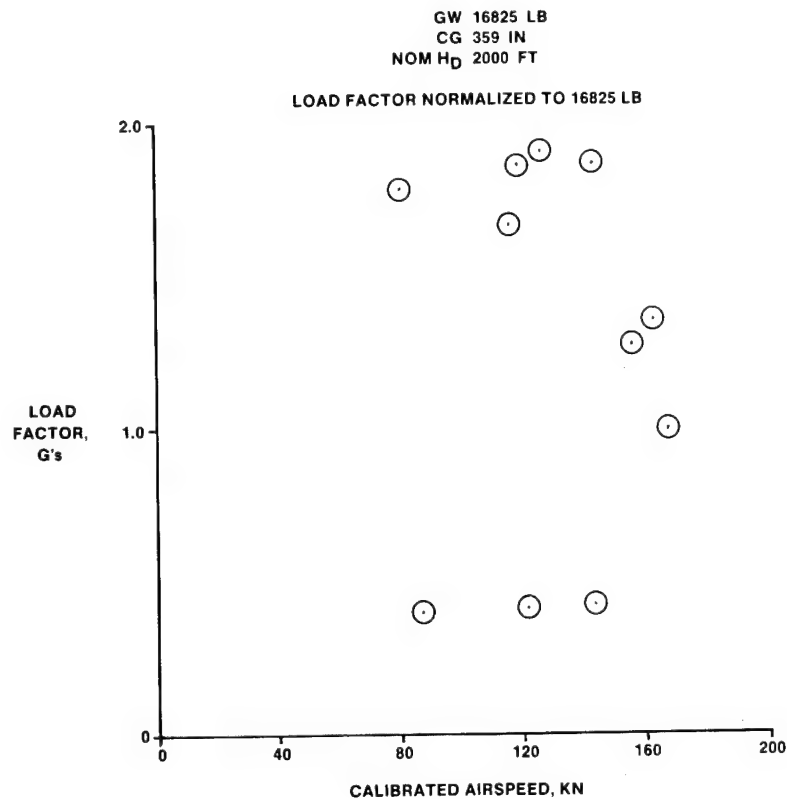


Figure 38. Load Factor Envelope for UH-60A Rotor with Anhedral Tip Caps

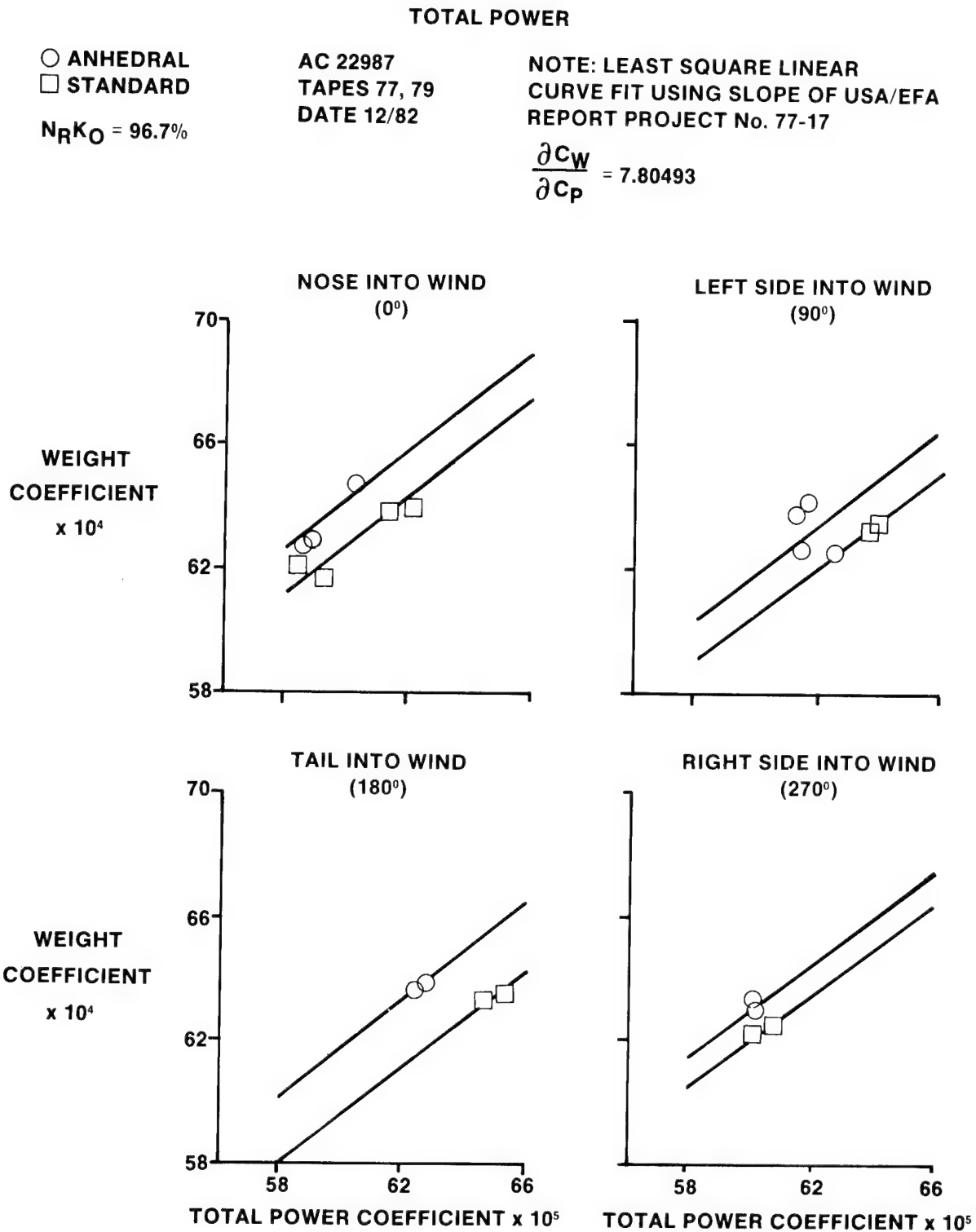


Figure 39. Nondimensional Hover Total Power vs. Wind Azimuth

MAIN ROTOR POWER

—○ ANHEDRAL WINDS 1-4 KN TAPES 77, 79
 - - - □ STANDARD WINDS 2 KN DATE 12/82

NOTE: LEAST SQUARE CURVE FIT WITH INTERCEPT EQUAL TO HOVER POWER AT $C_W = .0064$

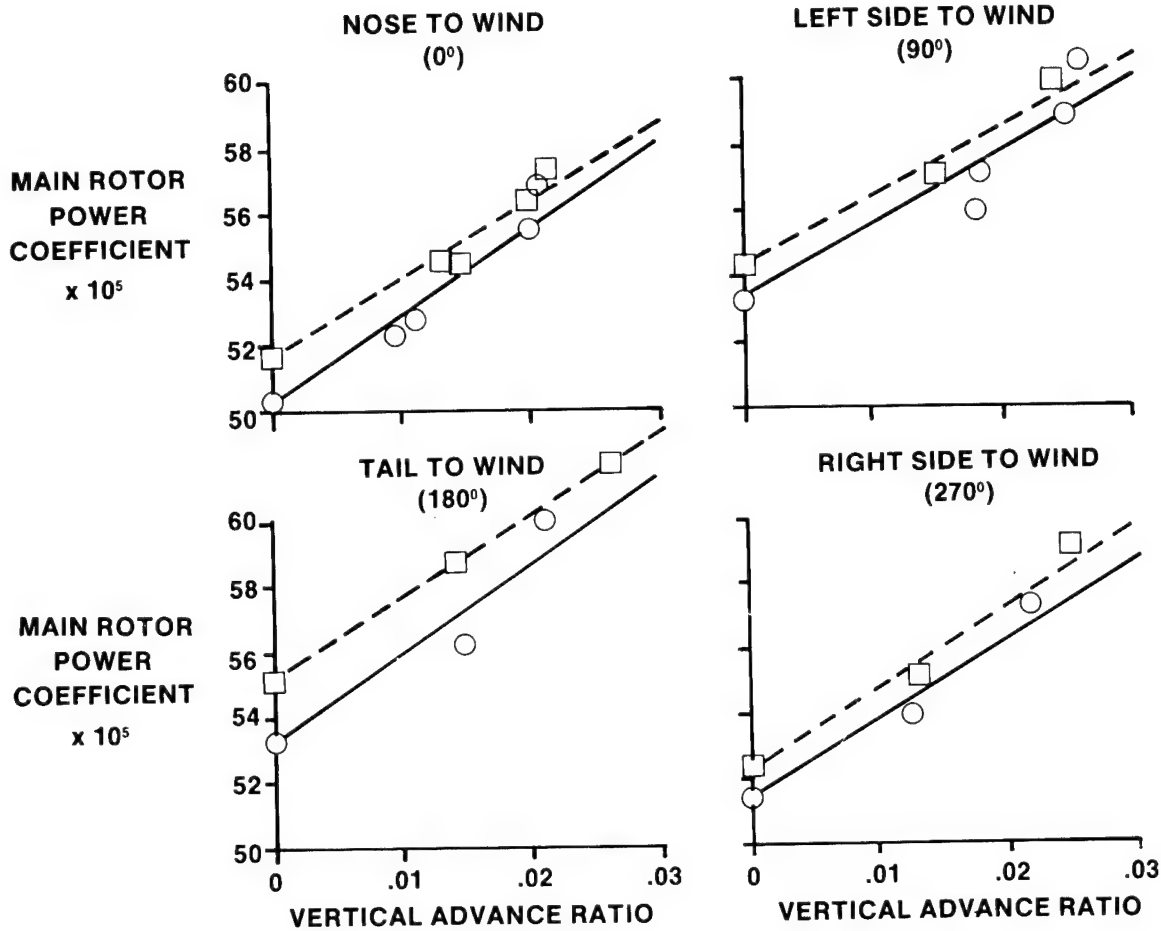


Figure 40. Nondimensional Level Flight Power Required

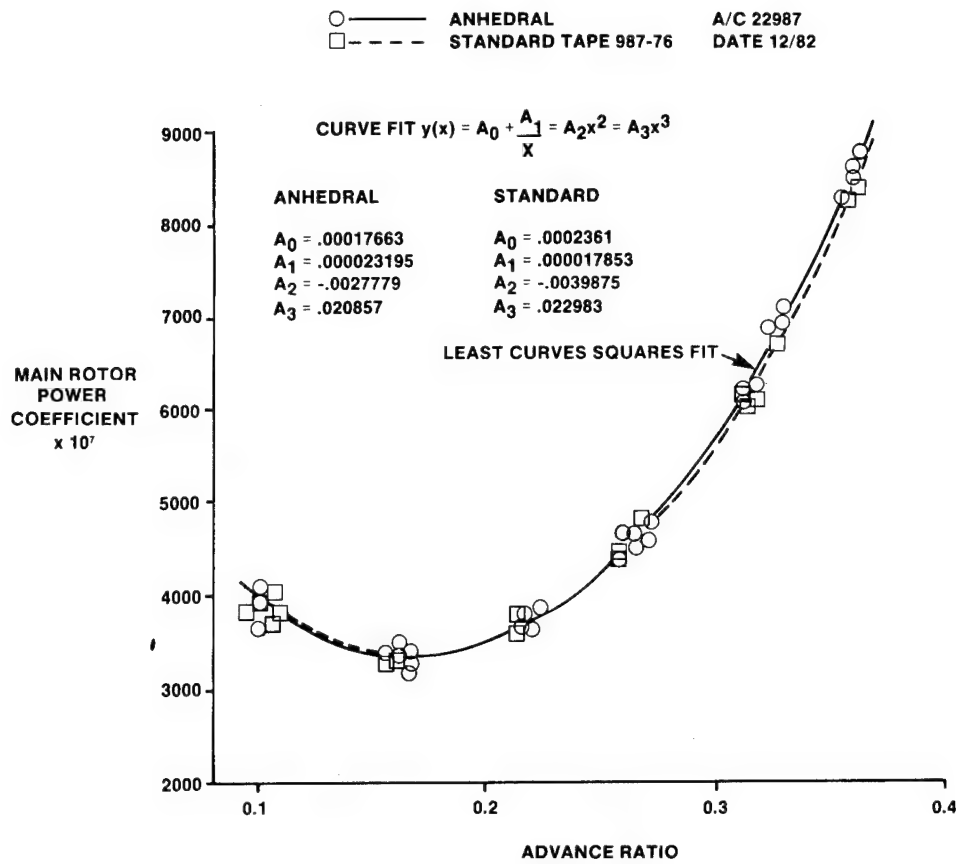


Figure 41. Nondimensional Level Flight Power Required

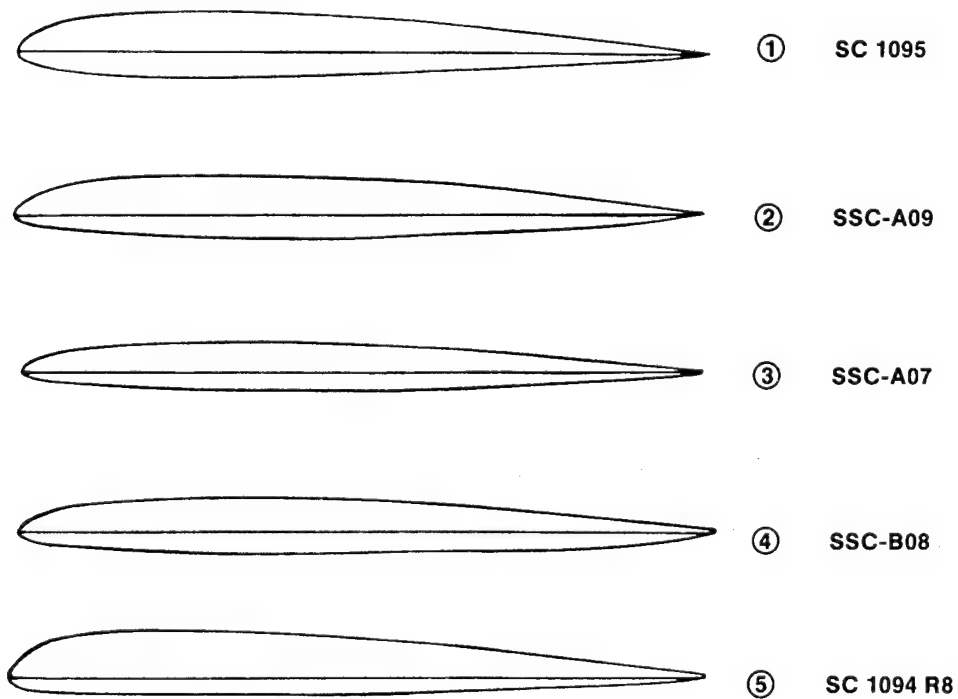


Figure 42. Airfoil Section Profiles

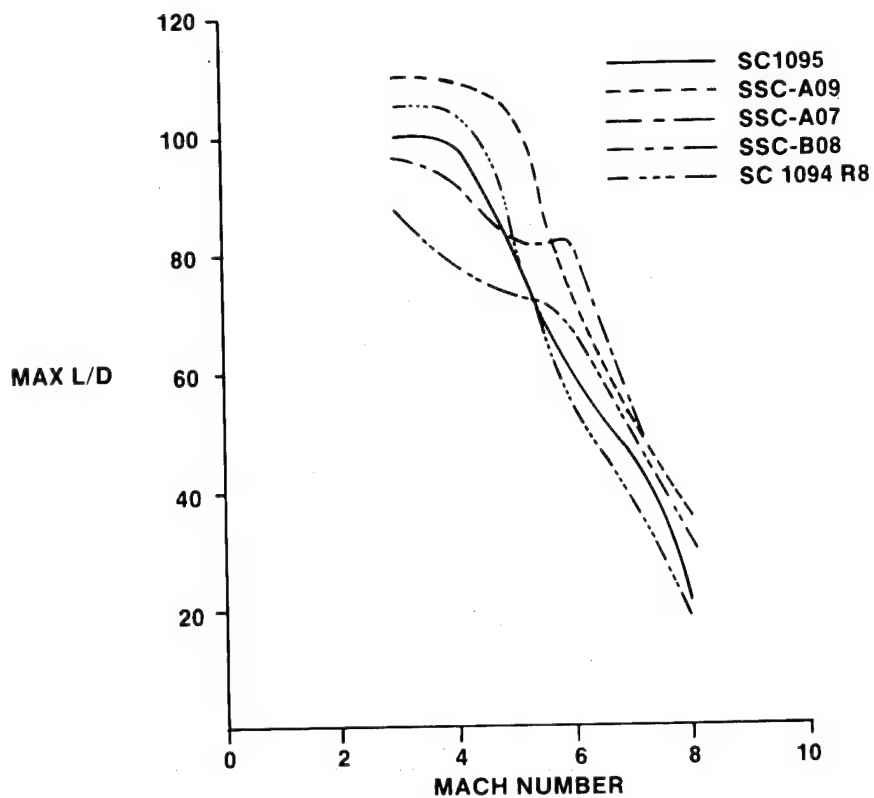


Figure 43. Maximum L/D vs. Mach Number

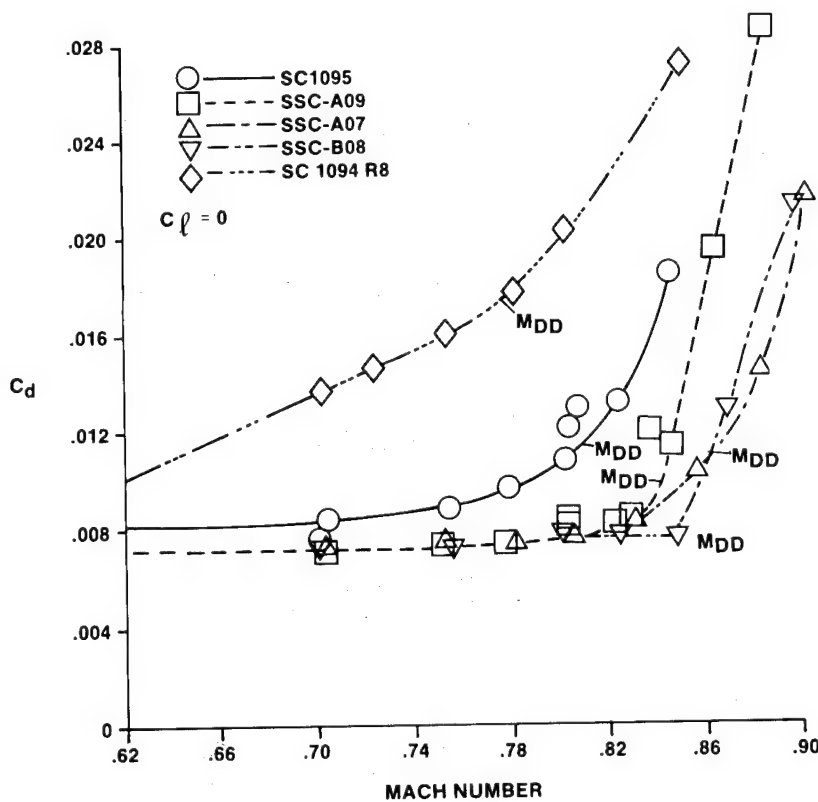


Figure 44. Variation in Drag Coefficient at Zero Lift vs. Mach Number

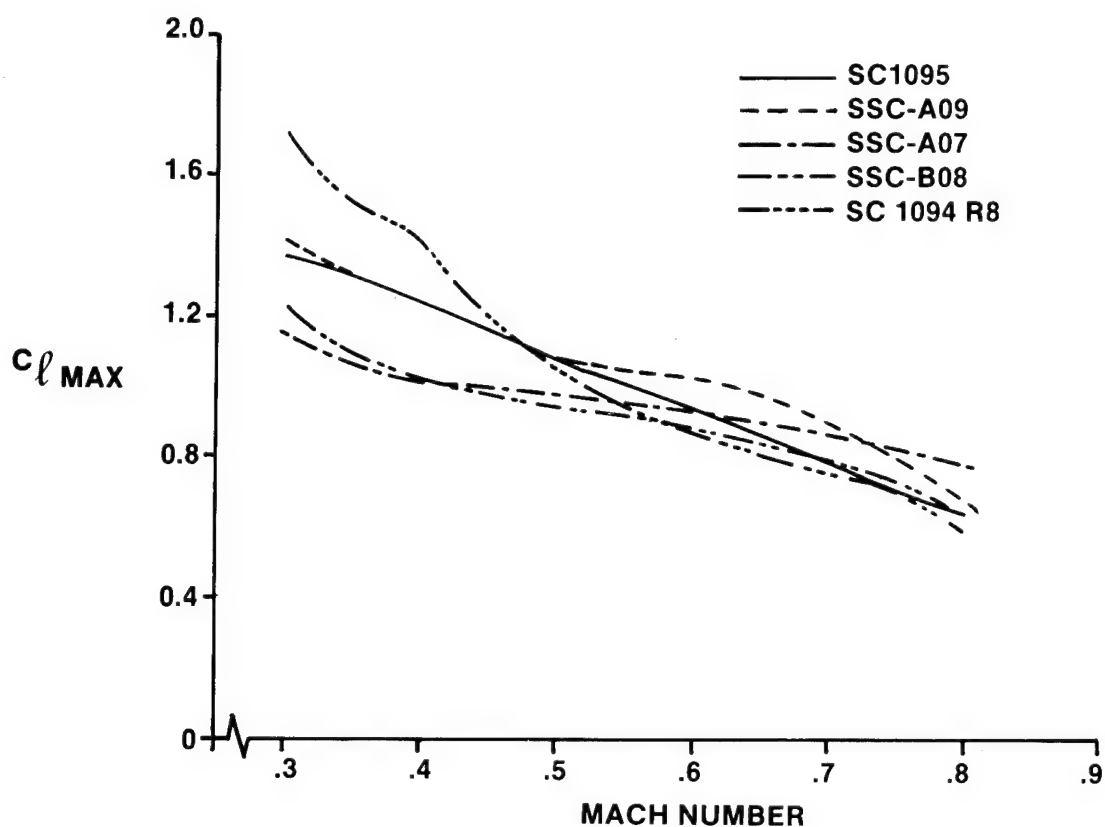


Figure 45. Variation in Maximum Lift Coefficient vs. Mach Number

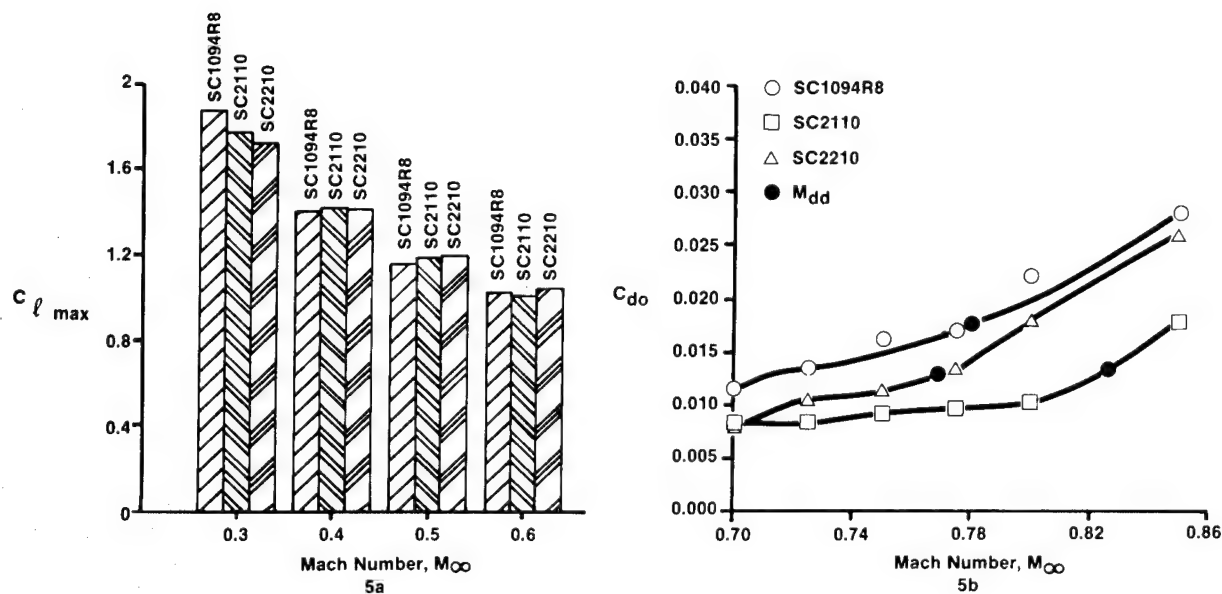


Figure 46. OSU Experimental Results for Maximum Lift and Zero Lift Drag, Baseline and Comparison Airfoils

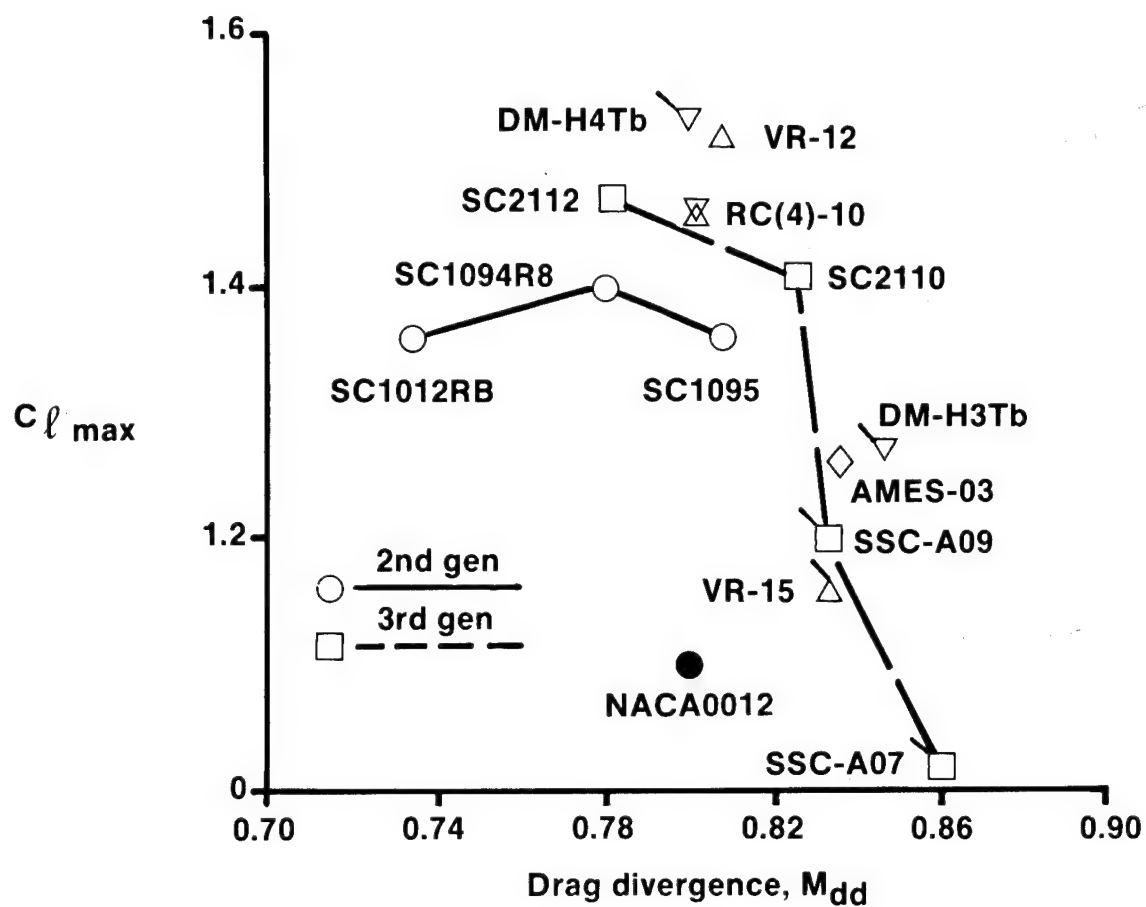


Figure 47. Third Generation Performance Improvements

MCDONNELL DOUGLAS HELICOPTER COMPANY
INDEPENDENT RESEARCH AND DEVELOPMENT - PREPARING FOR THE FUTURE
BY A. C. HAGGERTY
EXECUTIVE VICE PRESIDENT/ENGINEERING AND OPERATIONS
MCDONNELL DOUGLAS HELICOPTER COMPANY

ABSTRACT

Over the course of the 1970's and 1980's, there was a broad industrial investment in research and facilities to update rotary wing technology. Hand-in-hand with the industry's Independent Research and Development (IRAD) investment, went a similar government investment in Contracted Research and Development (CRAD). These two initiatives have converged to produce the technology present in the 80's that we see in aircraft such as the LHX and future models. This paper discusses the technology that is reaching maturity and moving into the application stage of future programs. Technology is discussed in six major thrust areas: Advanced Concepts, Analysis Techniques, Structures, Systems, Simulation, and Research and Development facilities. The partnership of McDonnell Douglas Helicopter Company and the government in developing these technologies is illustrated in several programs.

INTRODUCTION

Over the course of the last 10 to 15 years, rotary wing technology has advanced on a broad front (Figure 1). This technology advancement has included not only the small individual projects and their interaction, but also the use of these projects as building blocks to be combined and integrated into current and future operational aircraft. At McDonnell Douglas Helicopter Company (MDHC), these programs have included a wide range of technology demonstrators including infrared suppression, advanced rotors and hubs, advanced directional control devices, simulation and analysis development. These technology programs were then integrated into the current operational aircraft at McDonnell Douglas to provide wind tunnel test beds to further flight development. Unique to McDonnell Douglas Helicopter Company was the application of these technologies into our Ordnance programs to develop integrated weapons platforms.

There's a strong interaction between McDonnell Douglas Helicopter's main aircraft products: the MD 500 series, AH-64A, and Advanced Concepts (LHX). The light MD 500 series aircraft is used to validate and demonstrate that technology in a cost efficient, rapid method and then the concepts are transferred into the AH-64 where they are developed and matured to the point for application to the LHX, a program scheduled for a 1988 initiation. All of these programs have interactive cross fertilization as part of their development. Concepts developed and validated on the MD 500 influence the Apache developments which then influence the LHX development. Conversely, concepts seen in LHX and projected for LHX are being tested and integrated into the AH-64 and down into the MD 500 series and its derivatives.

These technology developments were in the truest sense a partnership between McDonnell Douglas Helicopter and government contracting agencies. McDonnell Douglas Helicopter Company through its IRAD funded programs would advance a technology to a certain stage, at which time Contracted Research and Development (CRAD) support was provided to move the technology to the next higher integration level. The results would then develop into joint programs so that the technology development we're talking about today is truly the result of a partnership between government and industry.

The partnership and the technology that it has produced can be grouped in six major thrusts: Advanced Concepts, Analysis Techniques, Structures, Systems, Simulation, and Research and Development Facilities as shown in Figure 2. A review of these major thrusts will illustrate the level of technology available and the development process.

ADVANCED CONCEPTS

The research work in Advanced Concepts produced designs that improved the current generation helicopters along the lines of noise, safety, vibration control, speed enhancements and signature. Typical of the Advanced Concepts is the No Tail Rotor (NOTAR)[™] concept which replaces the conventional tail rotor with a combination of a circulation control tailboom and direct jet thruster. In the NOTAR concept (Figure 3), the tailboom now generates force using circulation control principles. A thin stream of air emitted out of one side of the tailboom influences the main rotor downwash to flow around the tailboom to produce an anti-torque force in much the same manner as the circulation control airfoils on the X-wing. In hover, under high downwash conditions, the circulation control tailboom generates the majority of the trim anti-torque force. For the additional trim anti-torque force and for maneuvering, or when the circulation control tailboom is ineffective, a direct jet thruster at the aft end of the aircraft provides the required force. The direct jet thruster is a cone within a cone. The inner cone has fixed exit areas, right and left. The outer cone rotates about the inner cone to modulate the amount and direction of the thruster force. The air for both the circulation control tailboom and the direct jet thruster is provided by a variable pitch fan mounted at the forward end of the aircraft. The pressures and flow velocities within the NOTAR concept are relatively low for circulation control, being about a half a pound per square inch, producing slot and thruster velocities on the order of 250 feet per second.

The thruster and the pitch of the variable pitch fan are controlled from the pilot's directional control inputs in the same manner as it is in conventional helicopters (Figure 4). For a pedals-neutral type position, there is a moderate blade pitch, a flow of air from the slot and the thruster is open to the left (the primary turn direction). To initiate a pedal turn either right or left, blade pitch is increased, the thruster is rotated to provide force to initiate the turn in the desired direction. In this illustration, pedals are used but a side-arm controller could also be used.

The history of NOTAR and how it grew from a small company-funded technology evaluation program through a government-contracted concept evaluation and then into a government-supported demonstrator aircraft, is an excellent example of the partnership of IRAD and CRAD (Figure 5). The NOTAR concept was initially a company-funded program to evaluate the ability of circulation control to produce anti-torque force. This concept was demonstrated on a bench set up at the whirl tower at our Culver City facilities. Once the base data was acquired, the power efficiency of the circulation control tailboom and its potential for integration into a total directional control device became apparent.

That circulation control tailboom concept was then carried into flight evaluation sponsored by AATD. From the results of that program, NOTAR grew into a DARPA and AATD supported demonstrator aircraft that integrated the circulation control tailboom, direct jet thruster and the variable pitch fan. The integrated aircraft was then flown to demonstrate response and handling qualities and validate the total concept. The results were very encouraging, however, more technology development was indicated. McDonnell Douglas Helicopter Company carried on the NOTAR concept using IRAD funding to evaluate the technology questions that grew out of the demonstrator aircraft, to mature the NOTAR technology and to make it ready for the next generation of rotorcraft.

An example of the application of company funds was the effort initiated to understand the flow around the circulation control tailboom. The objective was to eliminate the fences that were added during previous flight tests. After several attempts at an analytical solution, McDonnell Douglas Helicopter Company embarked on an experimental program. A scale model NOTAR configuration was built and tested at the McDonnell Douglas Research Laboratory water tank hover test facility in St. Louis (Figure 6). The flow conditions seen in the base aircraft were evaluated and configurations developed. The water tank testing provided flow visualization data using laser doppler experimentation to improve the aerodynamic characteristics of the NOTAR aircraft (Figure 7). With the excellent visualization techniques, we were able to define the flow attachment around the boom and its interaction with other sections of the aircraft. In the water tank, we successfully duplicated the adverse flow condition found in flight; duplicated the effects of the flow fences we had developed in flight; and then using that validated technique, developed an alternate configuration without aerodynamic fences that provided the proper flow characteristics around the boom (Figure 8). The final solution turned out to be the addition of a second slot upstream of the initial circulation control slot. Based on that laboratory result, the flight aircraft was modified in early 1986 under company funds and successfully flown as shown in Figure 9, "completing the loop" of laboratory tests and flight test validation.

The improved NOTAR successfully flew over the entire flight envelope demonstrating dramatic expansions of the base aircraft envelope. This aircraft has continued to fly to provide the data base necessary to support this application in future rotorcraft.

Another example of the cooperation between industry and government in Rotorcraft Technology Development is the cooperative Army/NASA/McDonnell Douglas Helicopter Company research program in Higher Harmonic Control (HHC). HHC is an active closed loop vibration suppression system. The need for HHC grew out of work done through the 1970's that indicated that the vibration level of rotorcraft had reached a plateau and to achieve the reduced vibration levels desired would require an active system as shown in Figure 10. The Higher Harmonic Control system (Figure 11) has vibration sensing accelerometers located within the aircraft at desired locations to monitor vibration level. The vibration level is then fed to a computer that decides how to modulate main rotor pitch to reduce vibration. The pitch modulation is then fed into high frequency actuators in the main rotor system to change the pitch on the main rotor blades. For this particular test aircraft with four blades, the primary frequencies driven are the three, four and five per revolution. To date, the test aircraft has demonstrated a 10:1 reduction in vibration levels as compared to the baseline aircraft. To the maximum speed envelope of the OH-6A test aircraft, vibration levels on the order of 0.02G's have been demonstrated. Refinement of this work has continued in order to be prepared for the application to our future rotor wing designs.

The Higher Harmonic Control concept grew out of the NASA and Army Laboratories in the early 1970's where model wind tunnel testing indicated the potential for an active system to reduce vibration. Based on the results of the wind tunnel tests, the concept was taken to the flight phase under a NASA/Army contracted program with McDonnell Douglas Helicopter Company (then Hughes Helicopters). Concurrent with that contract, McDonnell Douglas Helicopter Company provided IRAD funding to develop and advance the state of the controller technology to support open-loop flight testing.

Subsequent to the completion of the flight testing phase, further algorithm developments were funded by McDonnell Douglas Helicopter Company to improve the HHC effect and further expand the flight test envelope.

Another example of an advanced concept growing out of our company-funded program into the flight vehicles of today is a unique Infra-Red (IR) suppression device (Figure 12). This engine exhaust IR suppression device (called BHO) is found in two configurations. One is an externally cooled fin system and the other is an internally cooled fin. In both concepts, the exhaust gases are used as ejectors to draw in cool ambient air to dilute the plume and cool the metal thickness. The present design of the BHO is found on the AH-64A. The second generation (self-contained) IR suppression system has been shown and demonstrated for the Bell H1 series of aircraft as well as for the Sikorsky CH53E. This technology was originally developed and demonstrated on a small Bell OH-58 aircraft; it then evolved through our own MD 500 series aircraft into the H1 series, the AH-64 Apache, and then it was demonstrated on the ground on the CH53E (Figure 13). In all cases, the suppressor has shown outstanding performance. It is currently being incorporated as part of the next aircraft generation.

ANALYSIS TECHNIQUES

Rotary wing analysis development is a complex, inter-related challenge. In addition to the traditional rotor and fuselage aerodynamic/dynamic issues, there are rotor-body, body-rotor, and rotor-rotor interactions. The main rotor sees the complete flight spectrum from retreating blade stall to high advancing blade tip Mach numbers and the resulting transonic issues. These phenomena must be integrated into a single analysis technique to provide for vibration reduction and prediction of rotor blade loads, aerodynamic performance and acoustic signature.

McDonnell Douglas Helicopter Company has been active in attacking this analysis issue in all fronts through its internally funded efforts that are summarized in Figure 14. In addition to programs on fuselage aerodynamics such as VSAERO and X3D (full Euler code), there are programs in retreating blade dynamic stall, hub dynamics and rotor fuselage coupling. The high speed advancing tip, three dimensional flow field is being integrated as part of our aeroacoustic effort to be fed into the definition of external noise. These analysis efforts are largely company-funded and aimed at supporting our own rotorcraft design efforts. However, the NASA and Army Laboratories have supplied us with their computer programs to complement our efforts. This is truly a cooperative, cost effective effort.

An example of a McDonnell Douglas Helicopter company-funded analytical program development is Rotor Airframe Comprehensive Aerolastic Program (RACAP). RACAP models the complete elastic response of the main rotor system as well as the elastic coupling between the main rotor and the fuselage. It is aimed at providing rotor blade loads of advanced bearingless rotors to be used in performance and vibration analysis. RACAP was developed in-house and is now being moved forward and integrated into the NASA sponsored DAMVIBS effort. An example of RACAP's correlation with flight test data is shown in Figure 15 which shows RACAP's predictions using two wake models. In both cases the correlation is shown to be very good.

The impact of using a coupled rotor fuselage approach as opposed to an isolated rotor is shown in Figure 16. Here we can see a dramatic improvement in flap bending moment prediction versus azimuth with the incorporation of the elastic coupling between the rotor and the fuselage. All of these RACAP capabilities are exploited when RACAP is combined with a finite element NASTRAN analysis of the fuselage. On Figure 17, we can see the predicted impact on AH-1G fuselage flight test vibrations of the elastic rotor fuselage attachment. There is a dramatic improvement in the correlation with flight test data moving from a fixed hub model to a flexible hub fuselage coupling.

The advent of multi-disciplinary optimization codes have also provided a powerful analysis tool to rapidly analyze new designs. McDonnell Douglas Helicopter Company has been active in integrating optimization codes into its design process. These efforts have been funded internally but supported in a very active and important way with the research work being done in the Army and NASA laboratories. McDonnell Douglas Helicopter Company's plan was to

initially develop the optimizing approach and optimizer techniques using a well-bound design problem. The aerodynamic performance of the rotor was selected for analysis development. Having once achieved capability in this area, these techniques would then be extended to more complex mathematical efforts such as structural optimization. In this effort, we were supported by the NASA/Army labs in providing optimization codes that they had evaluated and were under development in their own research organization. These codes hold great promise in that they allow simultaneous variation of many design parameters to achieve an optimum design (Figure 18). By expressing this optimization procedure mathematically and being able to automate the design approach, an optimum design can be obtained in a fraction of the time needed for more traditional parametric studies. McDonnell Douglas Helicopter Company's approach to the optimization effort is shown on Figure 19. Here we start with mission requirement definitions, move to a global level of optimization where the base configuration and base parameters are defined and then into a component level of optimization where the particular aircraft components are subject to indepth optimization techniques. As part of company-funded programs, we currently have efforts underway that look at the component level of optimization for airfoils performance, aeroelastic analysis, and structural analysis.

With the support and guidance of the Army/NASA researchers, McDonnell Douglas Helicopter Company evaluated several optimization codes and have used two primarily. One is CONMIN and the other is ADS, with ADS rapidly becoming our preferred optimization approach. The ADS code has been coupled with our own in-house analysis techniques for rotor loads (RACAP), structural response (NASTRAN), and performance analysis (BTRIM).

An example of this application is the development of a light helicopter rotor that was optimized for both forward flight at 140K and hover at 13,000-foot altitude. In this exercise, optimum twist, plan form, airfoil section, and airfoil distribution were selected by the ADS optimizer to satisfy the two design points of hover and forward flight as shown on Figure 20. The use of the ADS optimizer shows that rotor design can be achieved in 1/6 the time of more traditional parametric variation approaches. Since this initial exercise in rotor optimization, the optimizer techniques have been extended to the structural optimization of composite flexbeams.

STRUCTURES

The development of Advanced Structures has been driven primarily by the application of new materials and processes. The all metallic structure is rapidly being augmented with composite materials structures which promise reductions in weight and cost with attendant increases in fatigue life and strength. Both McDonnell Douglas Helicopter Company and the NASA/Army agencies have been active in defining material properties for composite materials and exploring their application on rotorcraft. Two examples of these are the Helicopter Advanced Rotor Program (HARP) and the Composite Fuselage work currently being done at McDonnell Douglas Helicopter Company.

The HARP rotor is an all composite rotor system that replaces all the bearings and joints of the conventional single rotor with a composite material flexure. Figure 21 shows the HARP rotor with its composite flat strap cruciform flexbeam, composite pitch case, and composite rotor blade. An elastomeric snubber damper is provided on the inboard end to provide in-plane damping as well as eliminate pitch flap coupling. The materials used in this experimental hub include Kevlar, fiberglass and graphite. The program concept behind HARP was to initially design the rotor system for the Apache helicopter (Figure 22). Further, once that rotor concept had been designed, it was scaled down so it could be flight tested on our Model 500 series aircraft. The rotor would then be flight tested through the entire envelope in order to create a data base that would support both the LHX development and Advanced Apache configurations. The initiation and execution of the HARP program is an example of the power of research initiatives within the Army/NASA laboratories. As a result of the Integrated Technology Rotor (ITR) efforts sponsored by the Army and NASA laboratories, McDonnell Douglas Helicopter Company launched the HARP program supported by company funds. This funding has moved the HARP from an initial design through laboratory and component testing, fabrication of flight worthy hardware, and through a complete flight program (Figure 23). The HARP has been demonstrated over the complete Model 500E envelope of speeds and load factors, demonstrating exceptional performance and structural integrity (Figure 24). Concurrent with the flight program the HARP model was scaled down and tested in the McDonnell Douglas Aircraft Company wind tunnel in St. Louis, Missouri over the same flight regime (Figure 25). This dynamically scaled model provides a flexible and important tool to extend the bearingless composite flexbeam rotor concept into other flight regimes. The data base from both flight test and scale model testing were used to design an advance composite hub for the AH-64 aircraft under contract from AATD (Figure 26). Again, we see an example of the partnership between industrial and government research efforts.

Another major thrust within McDonnell Douglas Helicopter Company as well as industry, has been the application of composite materials to helicopter fuselage structures. With the impetus of the government funded Advanced Composite Airframe Program (ACAP), a multi-phased, internally funded program at McDonnell Douglas Helicopter Company was initiated (Figure 27). The phases of the program flowed from initial coupon material characterizations, into concept development, through large scale component tests, and finally major airframe structure design. These phases were all aimed at developing a technology demonstrator that supports the upcoming programs in LHX, product improvement programs for Apache components and advanced commercial helicopters. The initial step in the composite fuselage program was to develop the component concepts to form a data base to support the total overall design. Typical of the type of design challenges were the stiffener shapes and intersections used in various designs. Through an intensive preliminary design effort, concepts were presented, fabricated and then taken forward into the laboratory test phase where they could be evaluated for their strength and energy absorption characteristics. Figure 28 shows several typical bulkhead tunnel beams of different design approaches under laboratory crush tests to evaluate their strength and energy absorption characteristics.

Once through that cycle, with the data base having been developed, full scale fuselage components were designed and tested to evaluate a total integrated design using our MD 500 series aircraft as the technology demonstrator (Figure 29). Concurrent with those totally integrated designs, larger components were then extracted from the lower fuselage to be fabricated and tested. A large section of the belly of the MD 500 series was extracted and used as a subject for a manufacturing and design study to improve the tooling and producibility effects (Figure 30). A series of tests and evaluations were conducted to validate both the design and the manufacturing approach. A unique crash impact test facility was developed to evaluate the energy absorption characteristics of the composite floor sections (Figure 31). In this test fixture, sections as well as the complete fuselage floor were crushed under controlled conditions to measure the strength and energy absorption capabilities. These tests were carried out in a sequential "building-block" approach and proved to be highly successful. The tests demonstrated a composite floor section capable of safely absorbing its energy share in a MIL-STD-1290 impact situation.

SYSTEMS

Advanced Avionics Systems have had a major impact on helicopter design; the pace of electronic improvement will guarantee this impact will accelerate in the future. An example of the impact of Advanced Avionics is crew station design. McDonnell Douglas Helicopter Company is currently pursuing the systems architecture technology required to provide a one-pilot operational capability. To support this effort, the front seat of the Apache helicopter has been transfigured into a one-pilot operable aircraft using advanced digital flight control technology (Figure 32). In this design, advanced digital flight control computers are integrated with multi-function displays and a full-authority side-arm controller to provide the single-pilot operability. The full authority digital flight control system commands all flight control elements within the aircraft to eliminate cross axis coupling. Automatic flight moding and artificial stabilization and flight control are also included in the full authority digital flight control system. This aircraft is now undergoing extensive flight testing to validate the flight control laws developed in the simulation.

As further support to the flight controls and systems development, the MD 500 series of aircraft has been used extensively to develop cockpit integration and sensor development techniques that flow technology through to the larger AH-64A aircraft (Figure 33). The MD 500 series aircraft has been used to develop FLIR, low light-level TV sensors, and multi-function display cockpit integration techniques such as demonstrated on the MD 530 MG and the MD 530 Night Fox. These systems have been flight tested and demonstrated to validate their value in expanding helicopter operational capability.

Both the Model 500 series systems demonstration efforts and the Apache AV05 flight controls experiments are all building a technology base to support an integrated cockpit for the advanced versions of the Apache. The current AH-64A pilot crew station (Figure 34) was designed during the mid-70's and represents a 1970's era level of system integration. The step beyond the AH-64A would be the AH-64B pilot crew station. Here extensive uses of flat

panel, multi-function displays, integrated crew stations, side-arm controllers, computer keyboard entry, touch screen technology and a full authority digital flight control system all dramatically improve the use of the cockpit real estate. In addition, these technologies supply to the pilot a greatly enhanced capability to perform the mission by dramatically reducing pilot workload.

An integral part of the crew station development will be the use of Artificial Intelligence (AI) techniques to augment the pilot. McDonnell Douglas Helicopter Company has been active over the last several years in developing the AI technology in its applications to some of the operational analysis efforts. Under recent AATD funding, McDonnell Douglas Helicopter Company has taken these AI techniques and applied them to maintenance diagnostics on the AH-64A helicopter (Figure 35). Under that program, McDonnell Douglas Helicopter Company developed an Intelligent Fault Locator (IFL) for four subsystems on board the Apache: the fuel system, communication/navigation avionics system, mechanical flight controls, and auxiliary propulsion unit (APU) systems. The knowledge base was created, the AI techniques developed, and all were integrated into a portable computer to be fielded with the maintenance personnel. The IFL is now on field evaluation with the Army at Ft. Rucker, Alabama and Ft. Hood, Texas. To date, it has a 100 percent success rate for fault location for fielded Apache aircraft. Also under contract to AATD, a flight data recorder effort has been initiated to monitor and record the aircraft health parameters. This flight data recorder data coupled with the AI maintenance diagnostic rules, will now allow onboard health monitoring as well as maintenance action.

Another application of AI techniques which has proved quite beneficial in developing aircraft system concepts is the development of the intelligent adversary for use in air-to-air combat (Figure 36). Using AI techniques, an intelligent adversary can be developed for each aircraft and allow these aircraft to fly against one another in a simulated air-to-air engagement. In this manner, real time evaluation of system capability and system improvements can be presented. To date, this intelligent adversary has been correlated with the data acquired by McDonnell Douglas Helicopter Company in the Army's Air Combat Test phase 3 at Patuxent River test station. During that test phase, an MD 530 aircraft was flown in a series of air-to-air engagements against adversary aircraft and engagement rules were developed. Again, this was a demonstration of a joint MDHC/Army program to evaluate the important airframe parameters influencing air-to-air combat success. This program is now being carried forward by the Army and McDonnell Douglas Helicopter Company into ACT IV with the involvement of the AH-64 in an air-to-air evaluation.

This jointly funded AATD/MDHC effort, is aimed at evaluating the impact of off-axis firing and sophisticated fire control systems in air-to-air combat success.

SIMULATION

As revolutionary as the impact of avionics on helicopter systems, the use of man-in-the-loop simulation to design the current generation of helicopters has undertaken a major role. McDonnell Douglas Helicopter Company has built a modern rotorcraft simulation facility within its current Mesa, Arizona plant (Figure 37). This simulation facility is integrated in with the laboratory and flight test environment and adjacent to a major DoD range and field training resource. This total integration of simulation, flight test and training provides an optimum use of the simulation results. As part of the simulation facility, three 20-foot diameter domes are being installed to provide cockpit and systems development capability. General Electric CompuScene IV digital visual displays have been installed in these domes. This simulation capability has been used to support the full range of engineering services (Figure 38). Crew station arrangements, avionics system developments, and advanced side-arm controllers (coupled with visionics and sensors) have been integrated and evaluated in the simulation capability. This simulation capability has also been used in support of flight test in diagnosing aircraft performance problems.

RESEARCH AND DEVELOPMENT FACILITIES

All of these major thrusts are dependent upon an increase in the research and development facilities currently used by the helicopter industry (Figure 39). McDonnell Douglas Helicopter Company has made a commitment to those advance facilities in the development of its current Advanced Development Center (ADC) in Mesa, Arizona. The 345,000 square feet ADC houses the most modern laboratories (Figure 40) including the flight simulation laboratories, materials and process laboratories, mission equipment development laboratories, structures laboratories, composite material fabrication laboratories as well as the prototype development area. Also as a part of the Advanced Development Center is a model rotor whirl tower and a propulsion integration test cell. A small laboratory wind tunnel to be used in the development of preliminary designs and concepts is also part of the laboratory capability. The ADC has over seven acres under one roof to provide the integrated experimental facilities needed to develop the next generation of rotorcraft.

SUMMARY

All of these major thrusts come together to support the next generation of helicopter programs extending beyond the capability of the current AH-64, the most modern helicopter in the Army inventory (Figure 41). We see these thrusts coming to maturity on the LHX program and Advanced Apaches. The LHX with its requirement for low weight and high performance, drives the industry into the area of advanced structures, improved rotor concepts and advanced cockpit designs. The technology programs of the 1970's and 1980's coupled with the continuing partnership of industry and government that we have highlighted will ensure the success of these future programs.

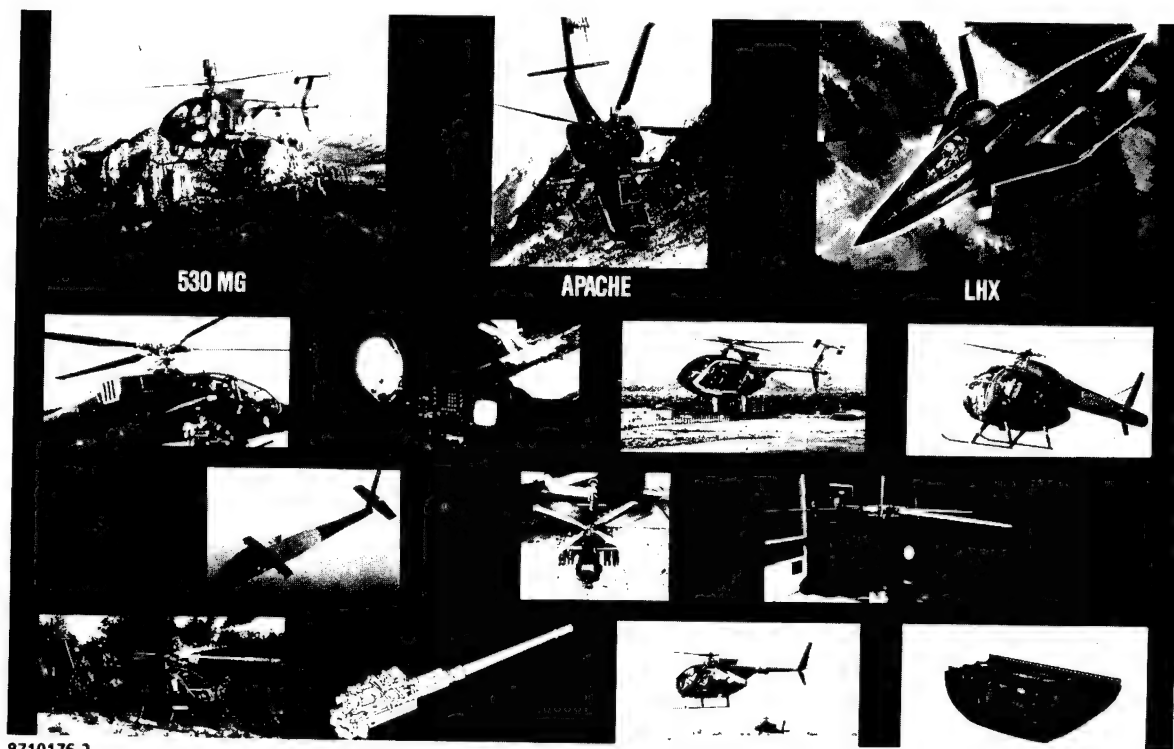
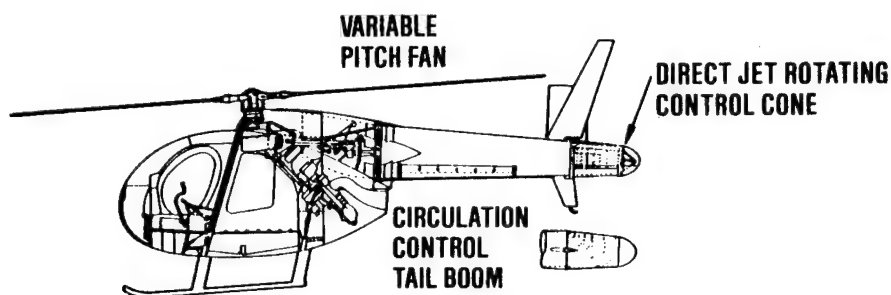
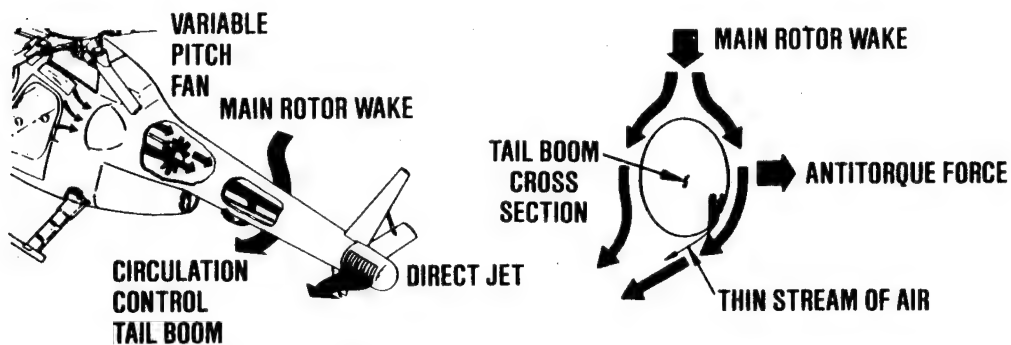


Figure 1. Technology Advances on a Broad Front

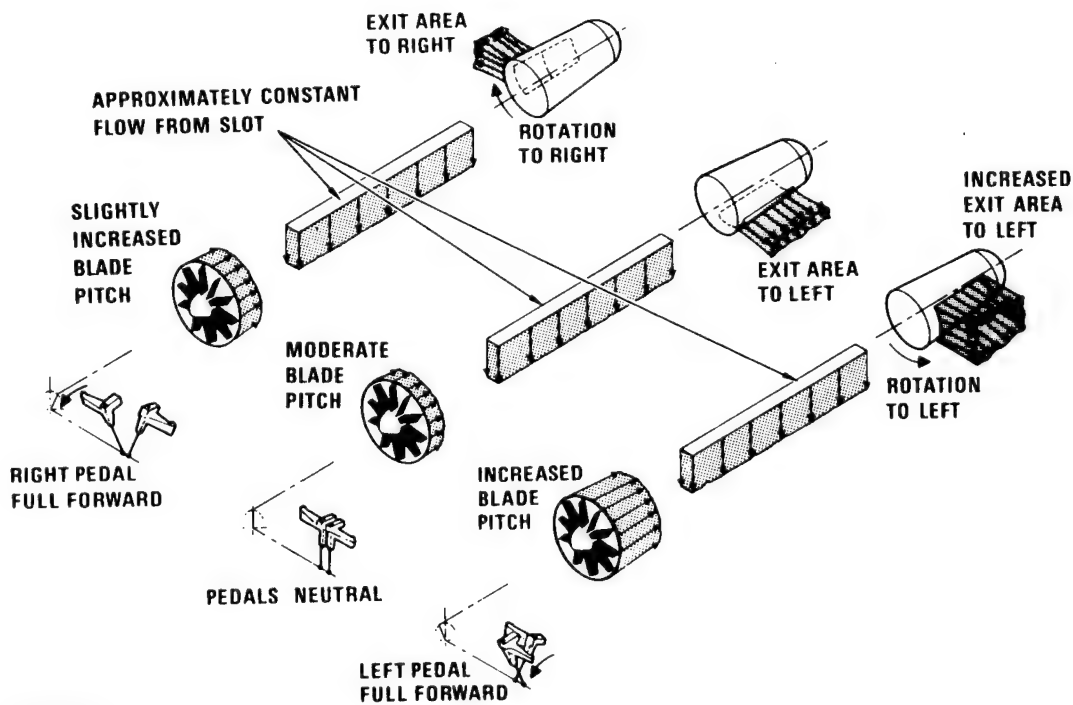
- ADVANCED CONCEPTS
 - ANALYSIS TECHNIQUES
 - STRUCTURES
 - SYSTEMS
 - SIMULATION
 - R&D FACILITIES

Figure 2. Major Technology Thrusts



8710176-5

Figure 3. NOTAR (No Tail Rotor) Concept



8710176-6

Figure 4. NOTAR System Function

AUG 1976 — BASIC DATA GENERATION — MDHC WHIRL TOWER

DEC 1977 — FIRST CONCEPTUAL FLIGHT

APR 1980 — NOTAR PATENT ISSUED

SEP 1981 — GROUND TESTS — FAN/THRUSTER/THRUSTER TRANSIENT RESPONSE

DEC 1981 — FIRST TOTAL SYSTEM FLIGHT, OH-6A

SEP 1982 — SIMULATION — FLIGHT SIMULATION ON FLIGHT SIMULATOR FOR ADVANCED AIRCRAFT AT AMES

MAY 1983 — GOVERNMENT PILOT EVALUATION

MAY 1983 — USAAVRADCOM TECHNICAL REPORT

DEC 1983 — AERODYNAMIC PANEL MODELS

FEB 1984 — TIEDOWN TESTS — AIRCRAFT ON TOWER TO SIMULATE OUT OF GROUND EFFECT HOVER

AUG 1984 — NEW FAN DESIGNED, INLET MODS

SEP 1985 — FAN/STATOR GROUND TESTS

OCT 1985 — WATER TANK TESTING

OCT 1985 — WIND TUNNEL TESTS

DEC 1985 — GROUND TEST WITH NEW FAN/INLET AND MORE POWERFUL ENGINE

MAR 1986 — SECOND SLOT FLIGHT TEST

8710176-7

Figure 5. NOTAR Test/Analyses History

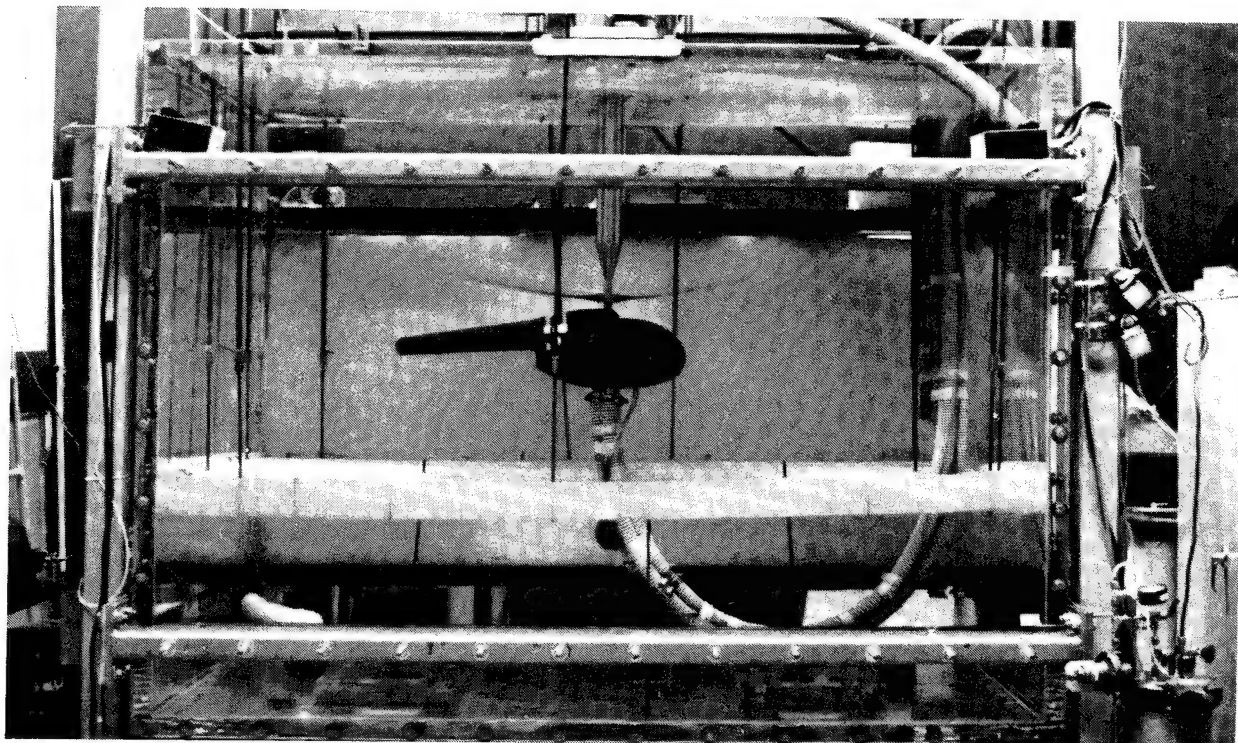
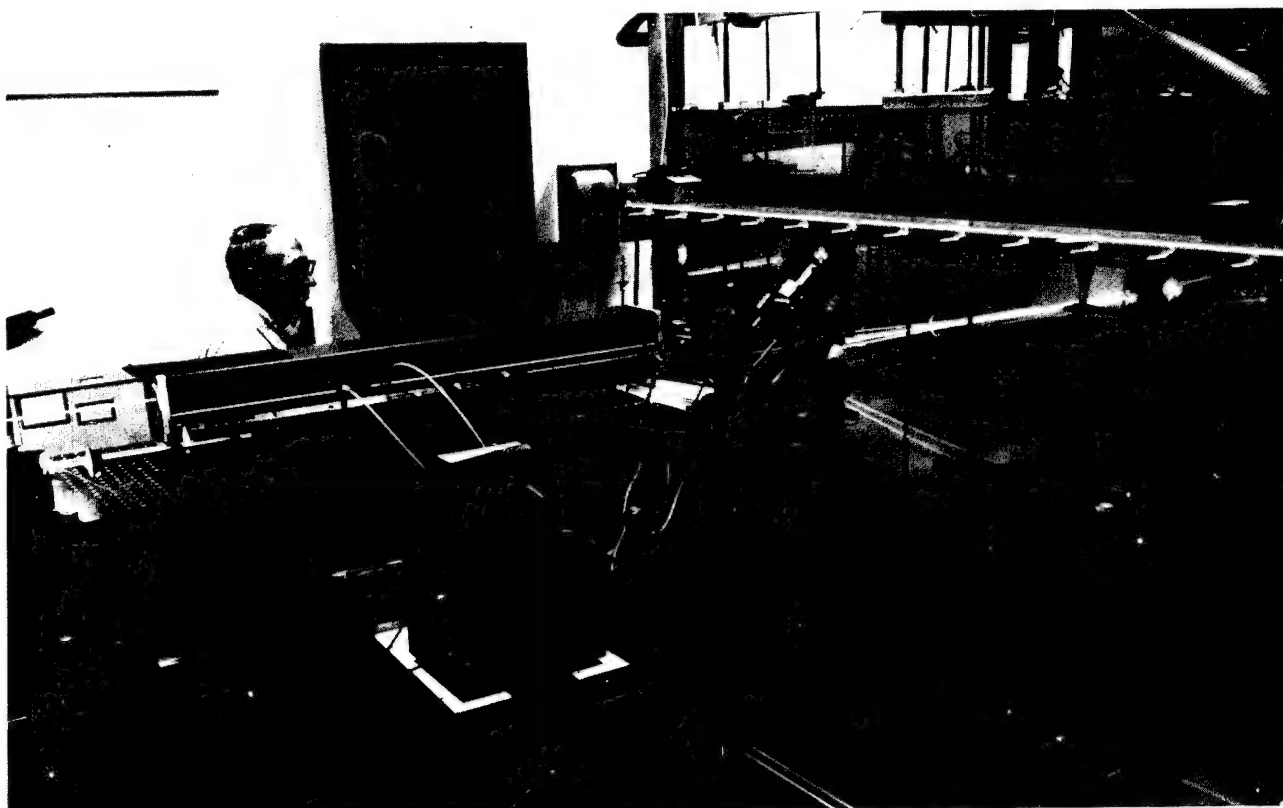
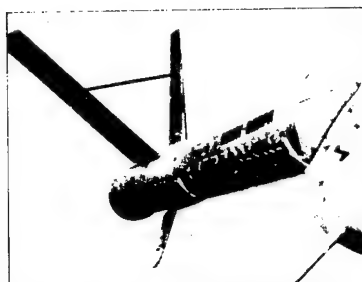


Figure 6. MDRL Hover Test Facility



8710176-9

Figure 7. Laser Doppler Velocimeter Measurements in Hover Test Facility

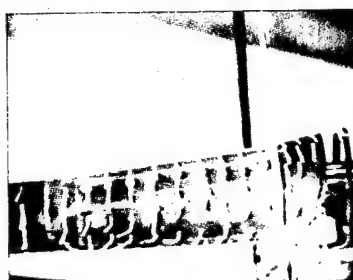


ADVERSE TAILBOOM FLOW

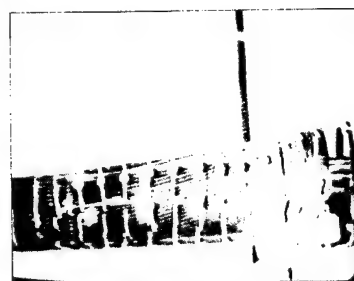


EFFECT OF FLOW FENCES

FLIGHT TEST



SIMILAR MODEL FLOW



EFFECT OF SECOND SLOT

HOVER MODEL TEST

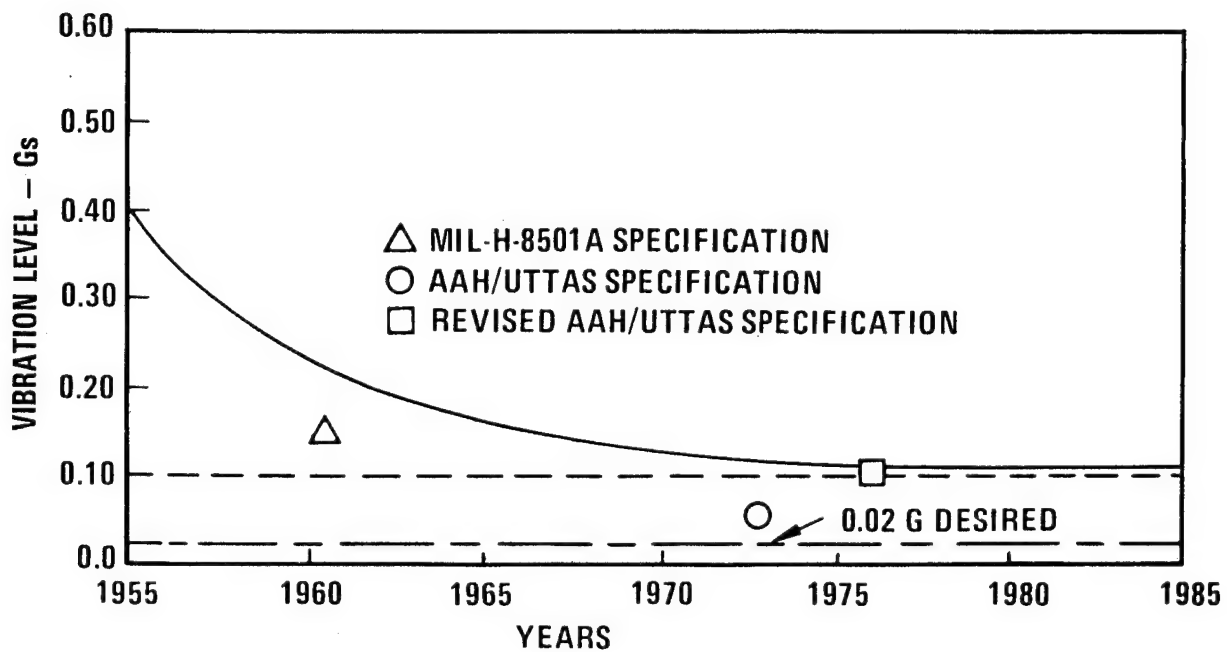
8710176-10

Figure 8. NOTAR Tests



8710176-11

Figure 9. First Flight of Improved NOTAR



8710176-12

Figure 10. Why Higher Harmonic Control?

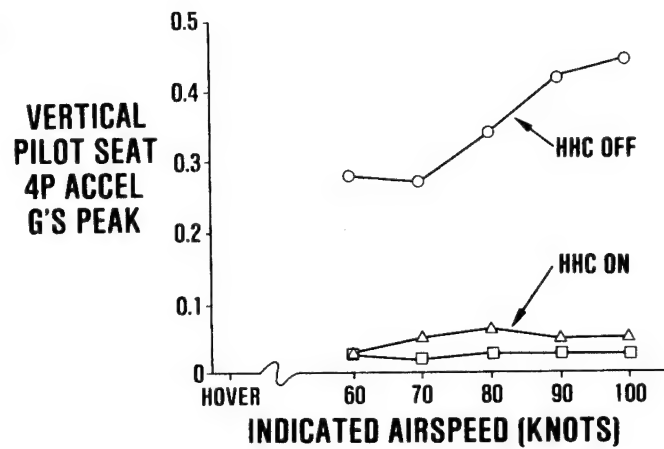
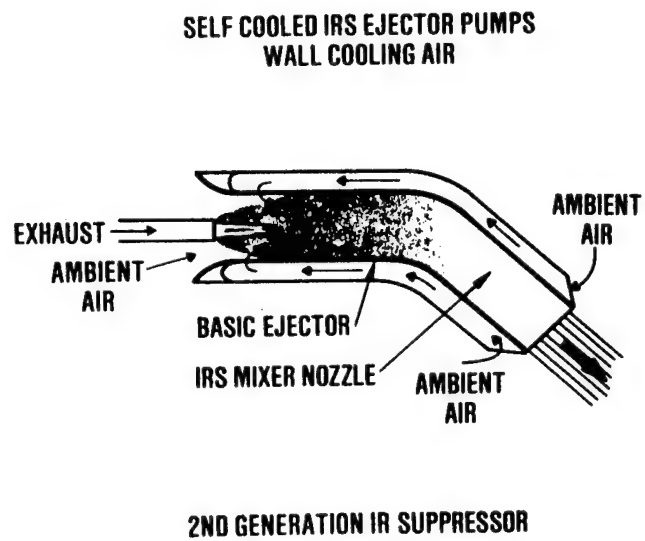
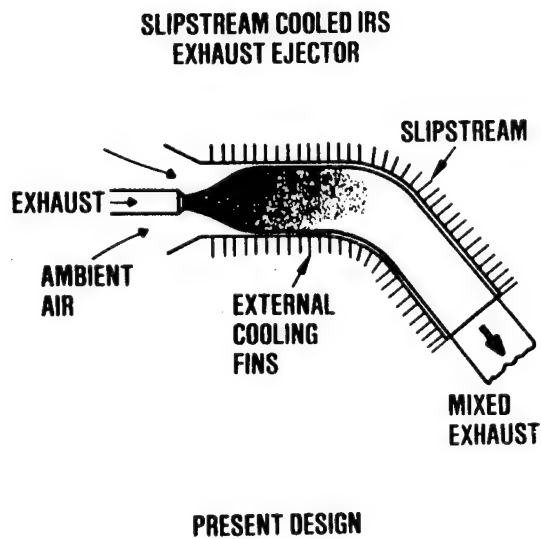


Figure 11. Higher Harmonic Control



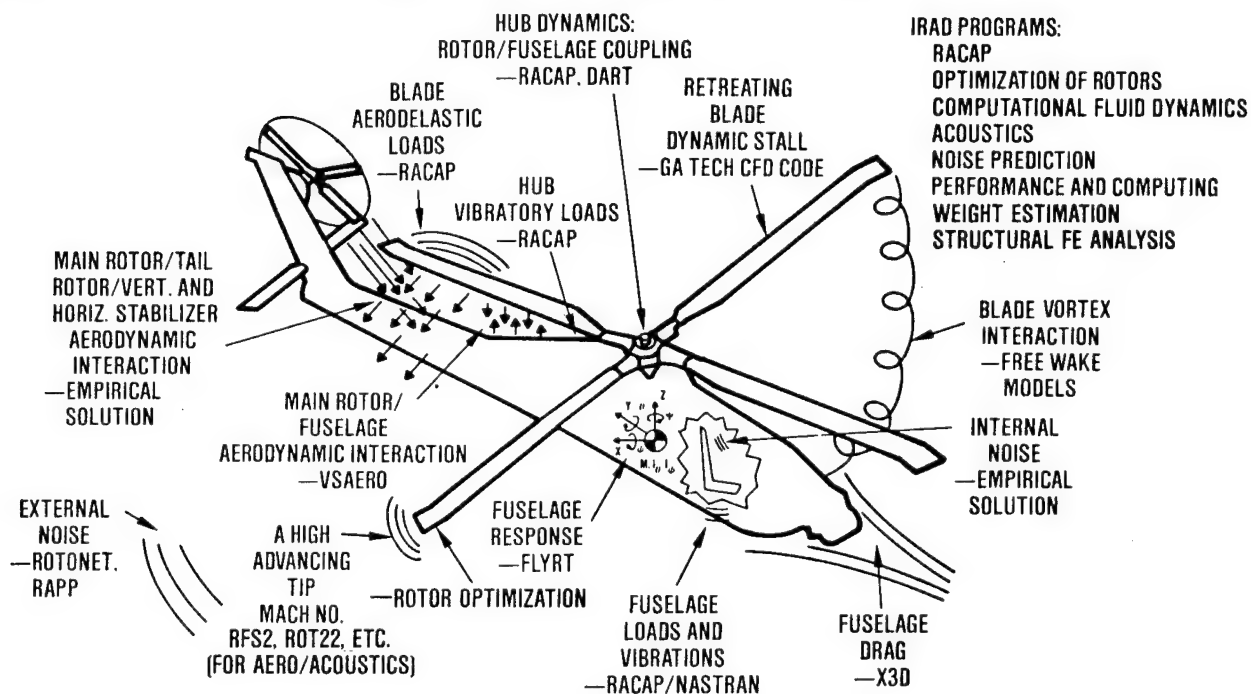
8710176-14

Figure 12. Engine Exhaust IR Suppressor



8710176-15

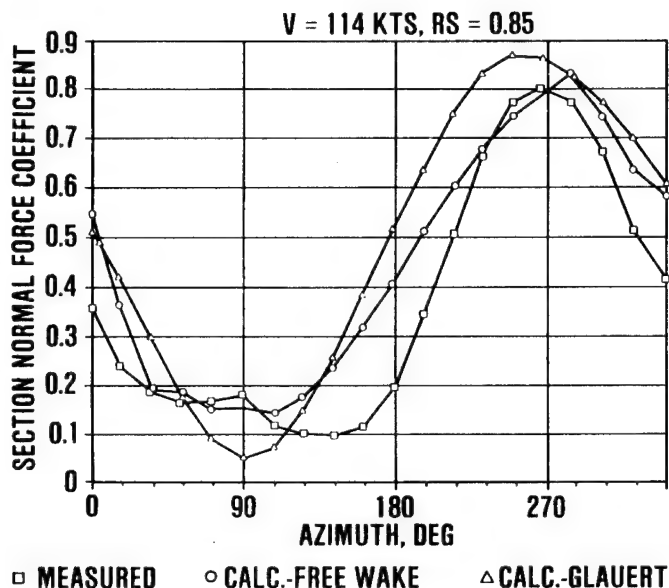
Figure 13. IR Suppressor History



8710176-17

Figure 14. Analysis Techniques

NORMAL FORCE CO-EFFICIENT (C_N) COMPARISON BETWEEN FLIGHT TEST AND ANALYTICAL PREDICTIONS



8710176-18

Figure 15. Analysis Techniques - Rotor Airframe
Comprehensive Aeroelastic Program (RACAP)

AH-1G AT 114 KTS FLAP BENDING MOMENT VS AZIMUTH

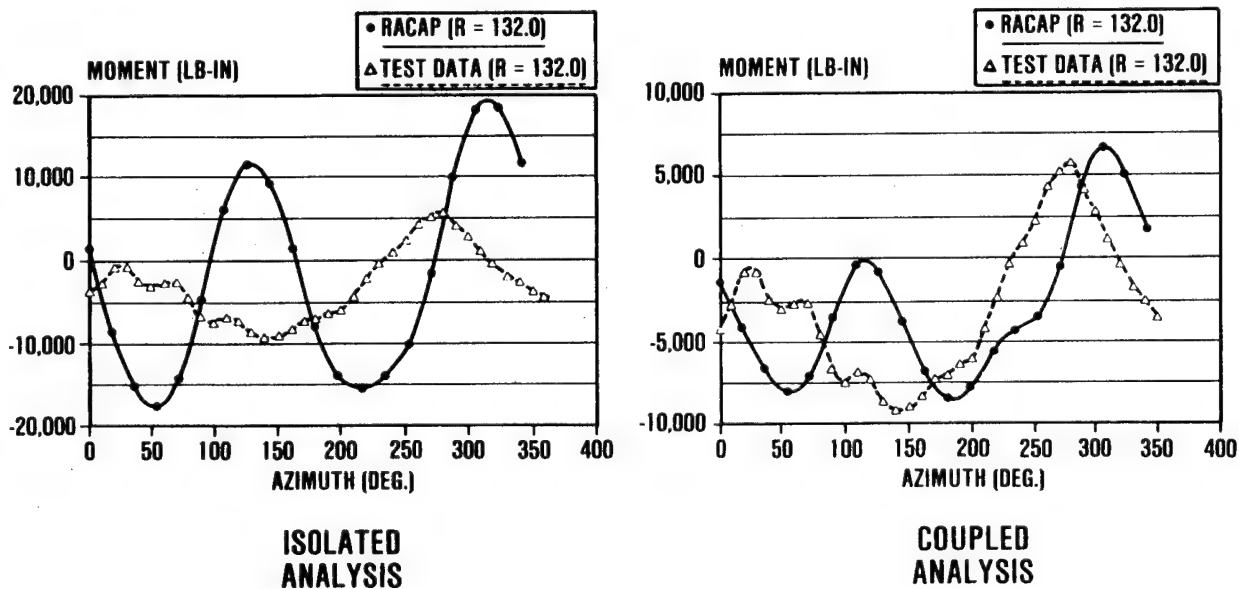
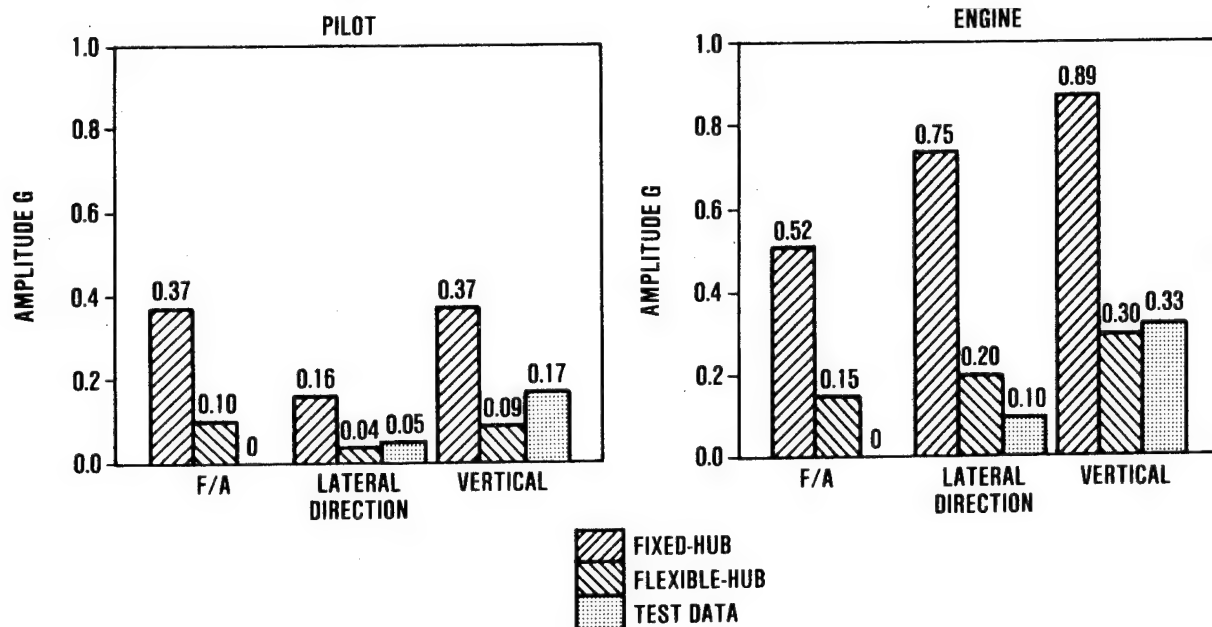


Figure 16. Analysis Techniques - Rotor Airframe
Comprehensive Aeroelastic Program (RACAP)

AH-1G 2P FUSELAGE VIBRATION LEVELS FLT 35A COUNTER 614 SPEED = 114 (KTS)



8710176-20

Figure 17. Analysis Techniques - Rotor Airframe
Comprehensive Aeroelastic Program (RACAP)

PURPOSE: SIMULTANEOUSLY VARY DESIGN PARAMETERS TO ACHIEVE
AN "OPTIMUM" DESIGN

APPROACH: MATHEMATICAL PROGRAMMING APPROACH

MINIMIZE $J(\bar{D})$

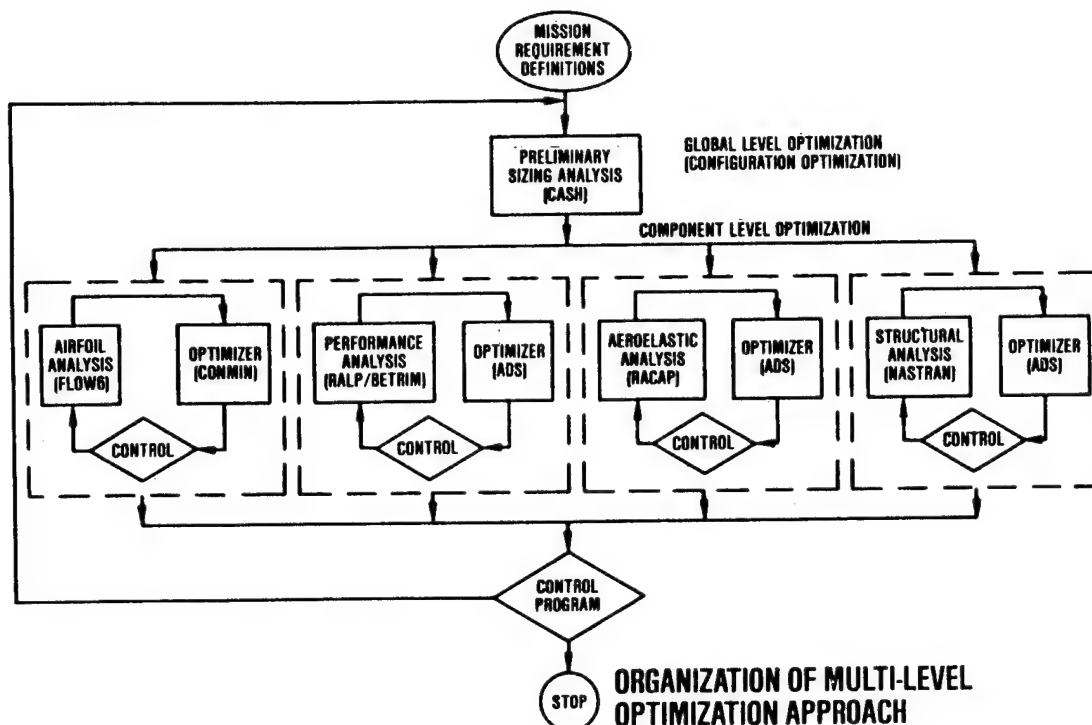
SUBJECT TO $g_q(\bar{D}) \leq 0, \quad q = 1, 2, \dots, Q$
 $D_i^L \leq D_i \leq D_i^{(u)}, \quad i = 1, 2, \dots, N_D$

ADVANTAGE: ACHIEVE "OPTIMUM" PERFORMANCE

OBTAIN DESIGN IN A FRACTION OF THE TIME NEEDED FOR
PARAMETRIC STUDIES

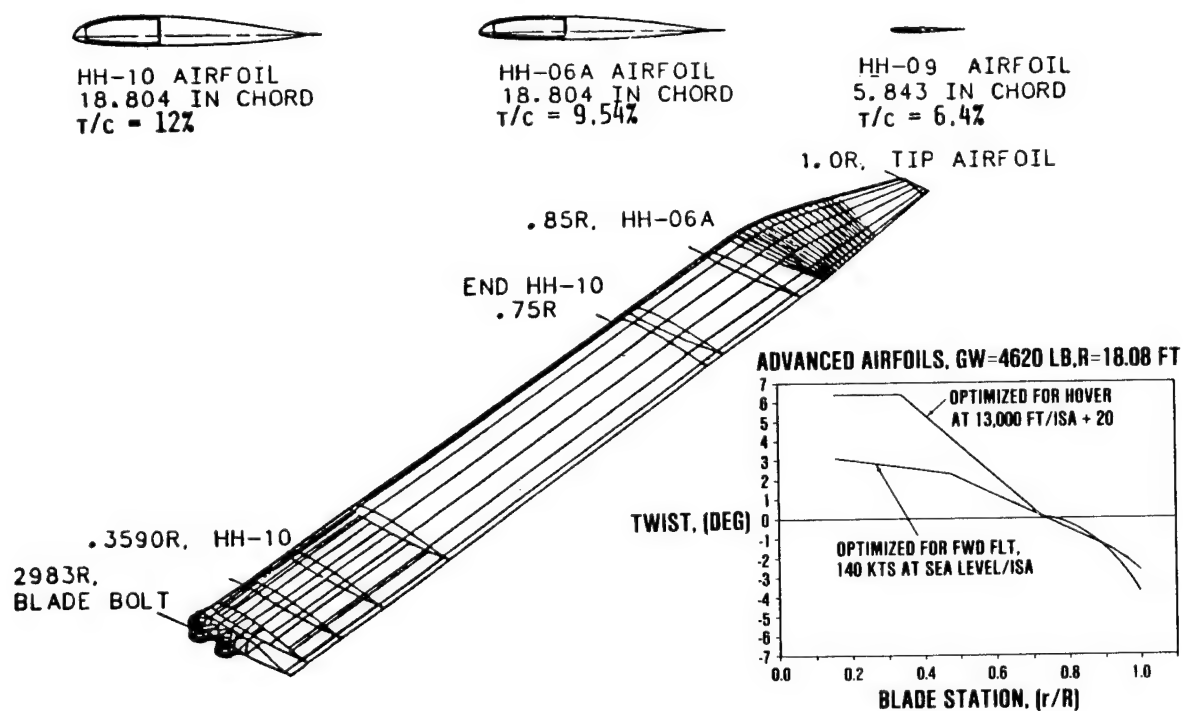
8710176-21

Figure 18. Optimization Analysis



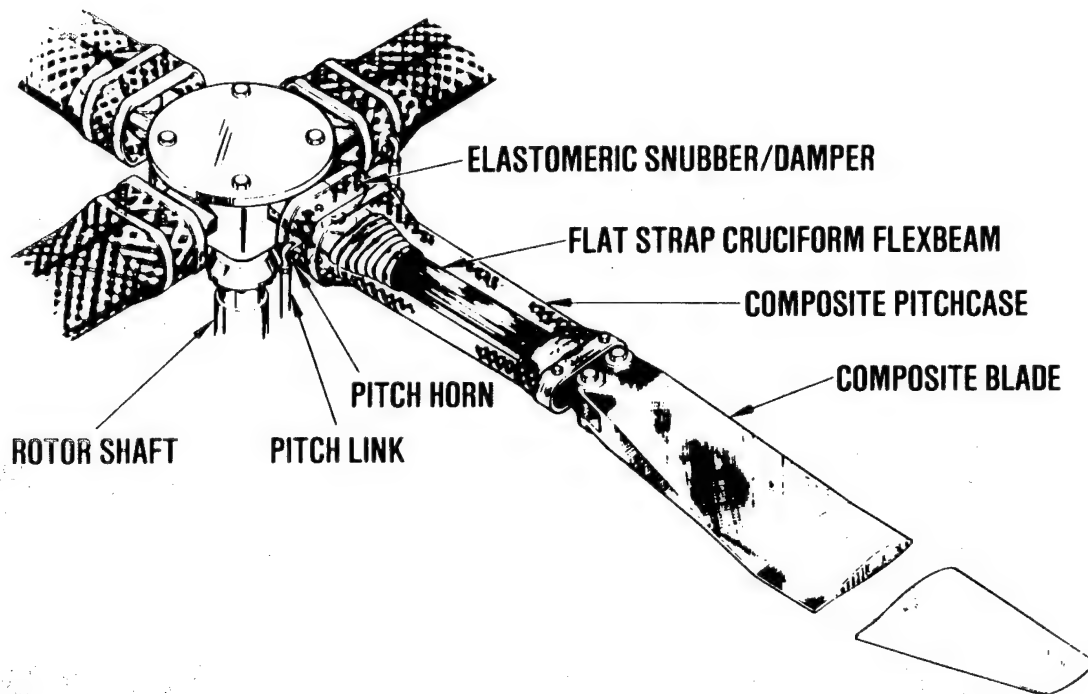
8710176-22

Figure 19. Optimization Analysis Approach



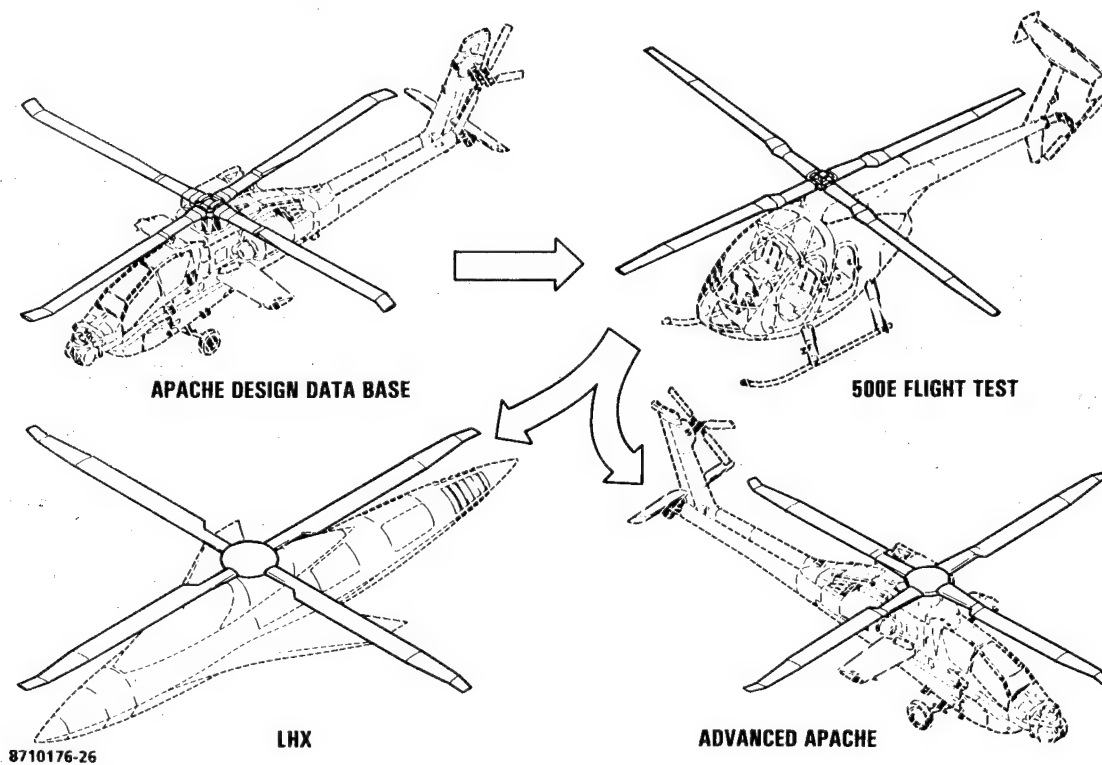
8710176-23

Figure 20. Optimized Blade Section



8710176-25

Figure 21. MDHC Advanced Rotor (HARP)



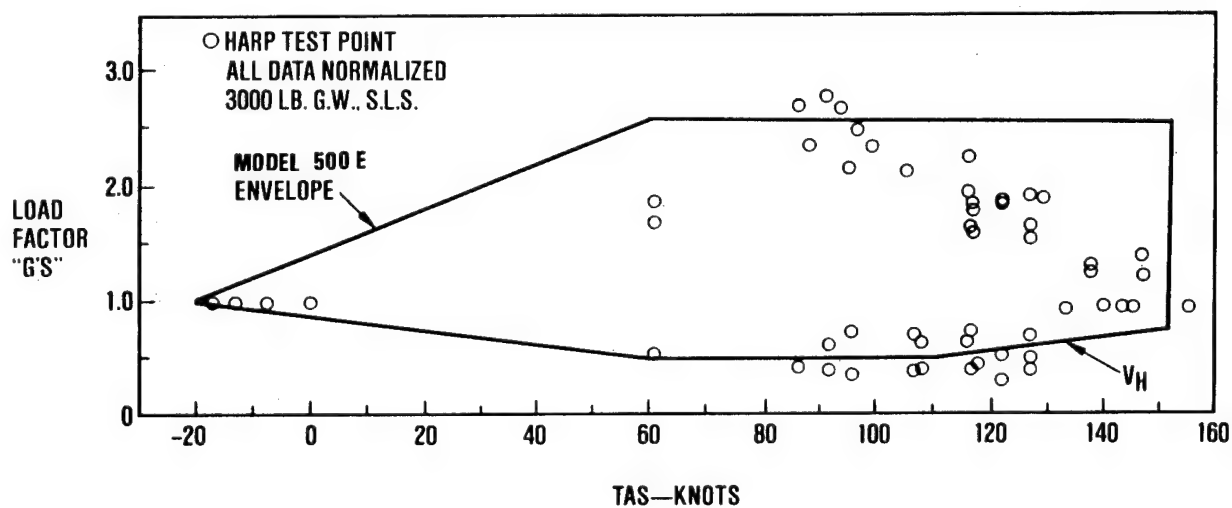
8710176-26

Figure 22. HARP Program Concept



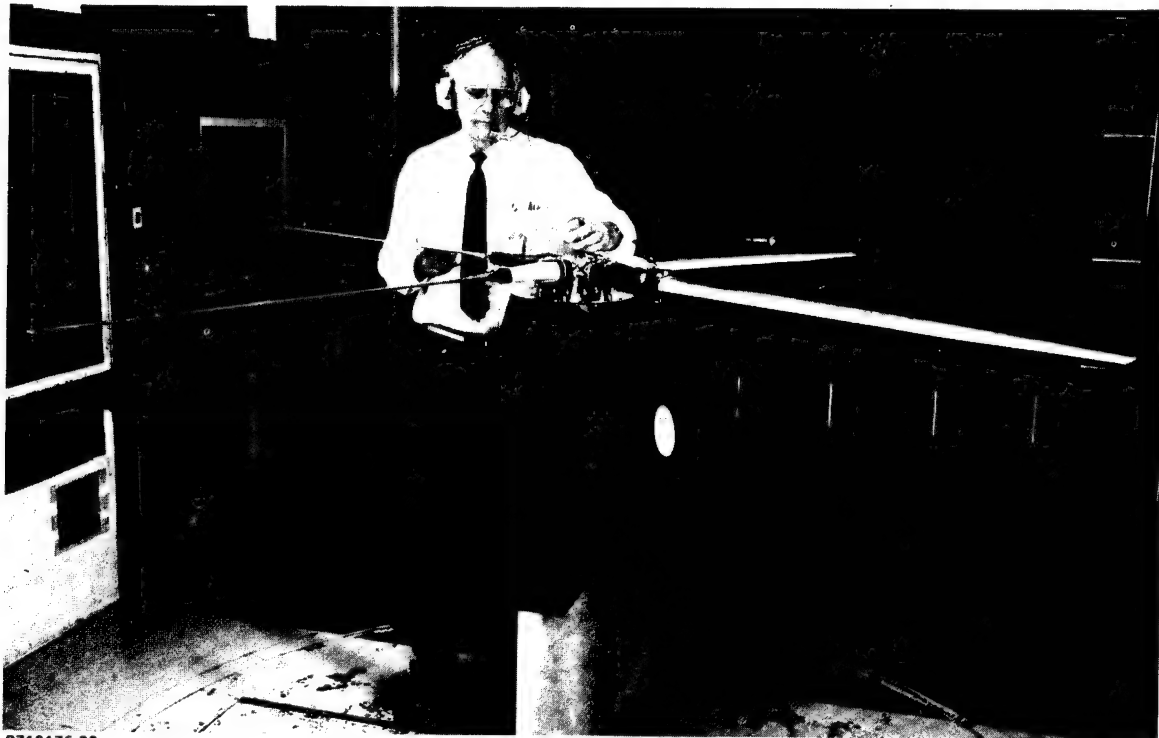
8710176-27

Figure 23. HARP First Flight



8710176-28

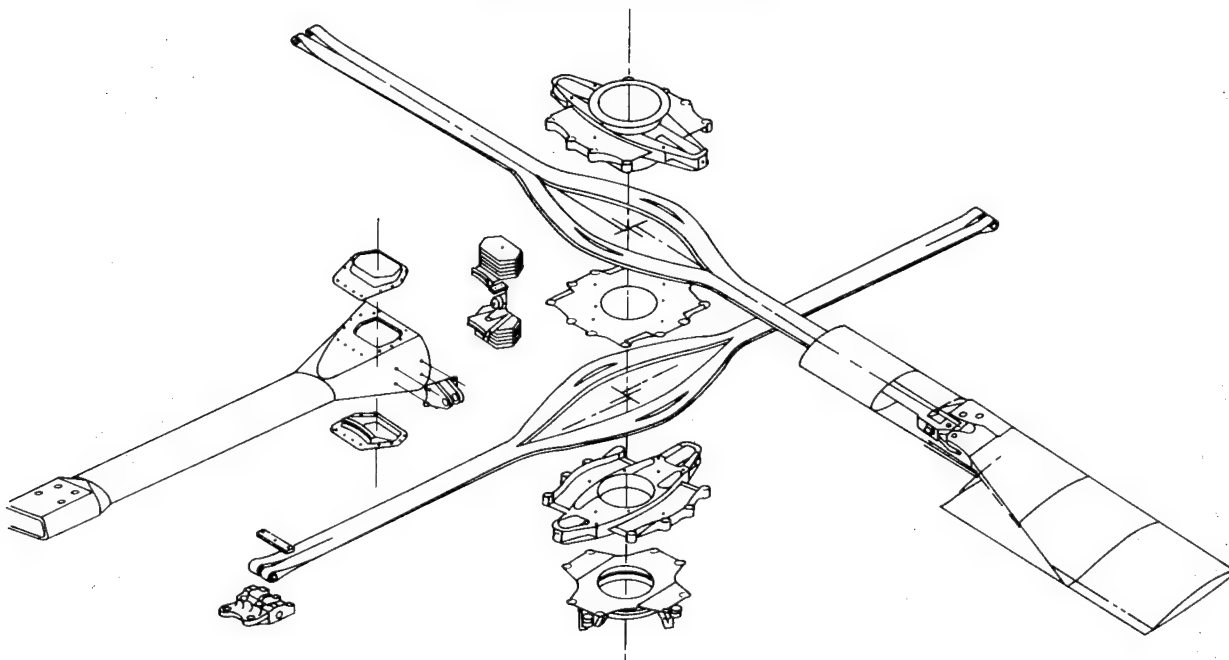
Figure 24. HARP Demonstrated V-N Envelope



8710176-29

Figure 25. Model Rotor in McAir Wind Tunnel

CONTRACT NO. DAAJ02-85-C-0037



8710176-30

Figure 26. AH-64 Advanced Composite Hub (ACH Prototype Hub)

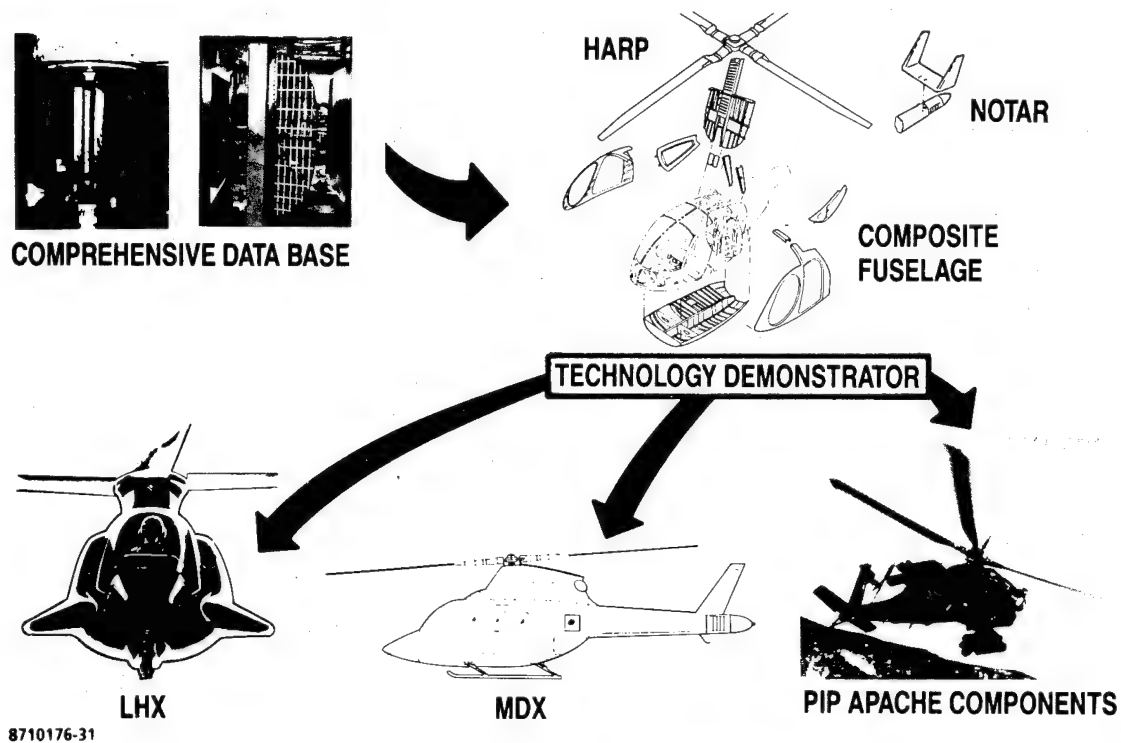


Figure 27. Flightworthy Composite Fuselage Program Concept

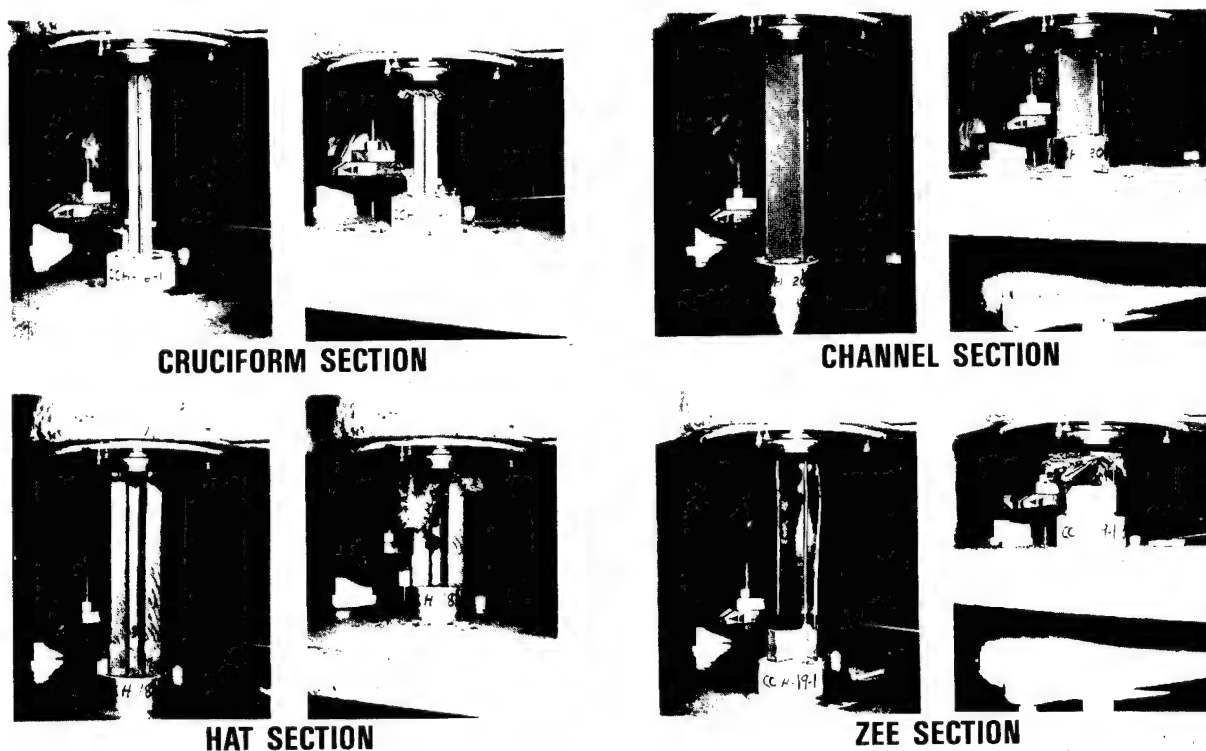


Figure 28. Bulkhead Tunnel Beams

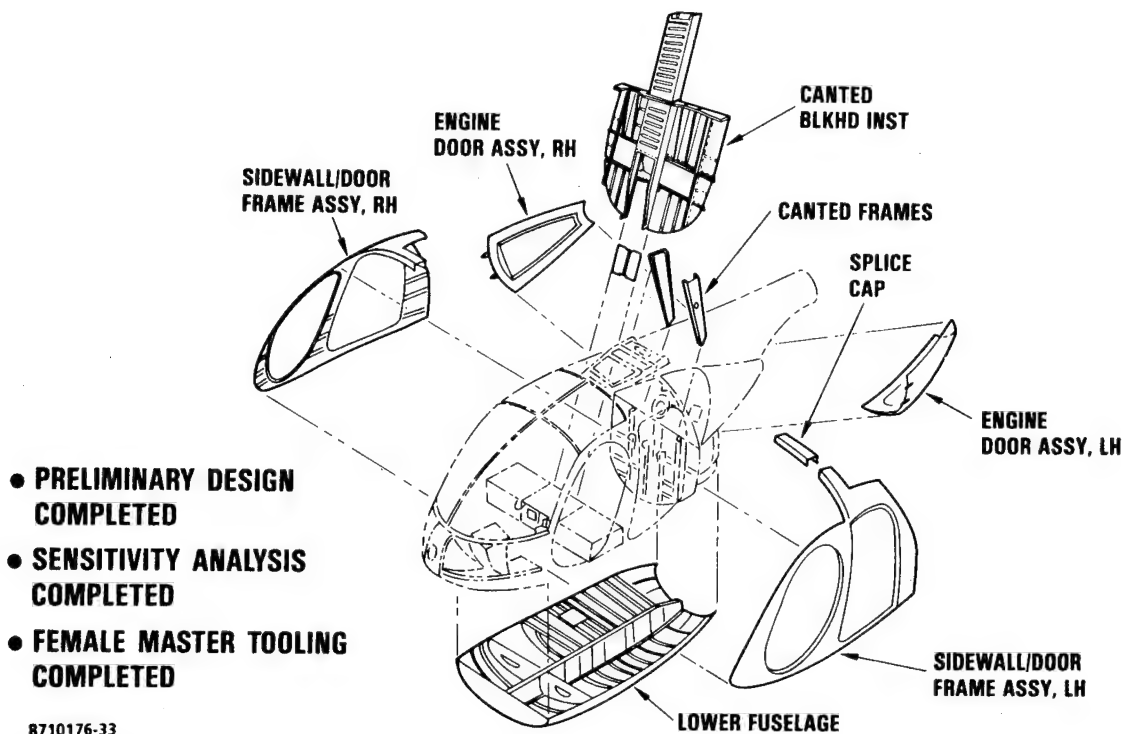


Figure 29. Full Fuselage

- PARTS COUNT REDUCED FROM 33 TO 13
- LABOR HOURS REDUCED 30%

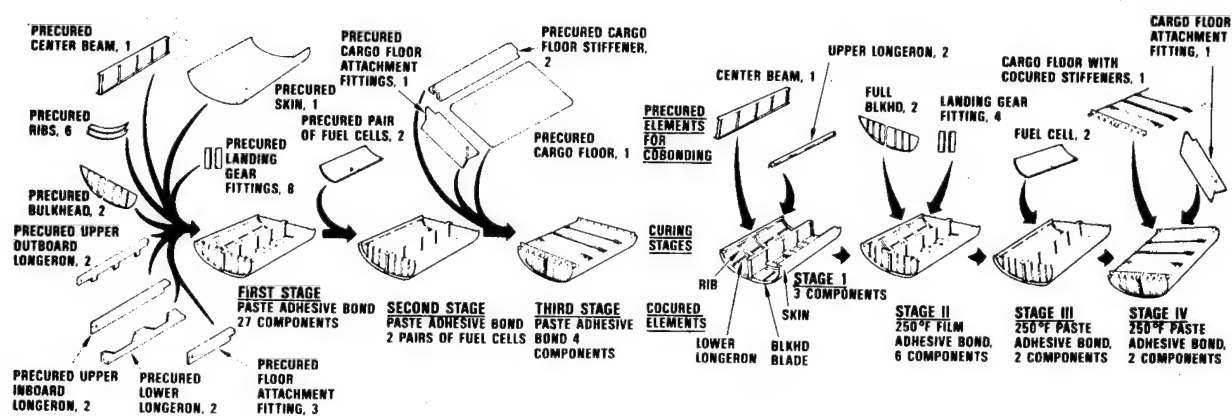


Figure 30. Improved Tooling Approach



8710176-35

Figure 31. Third 25-Inch Subassembly Impact Test Set-Up

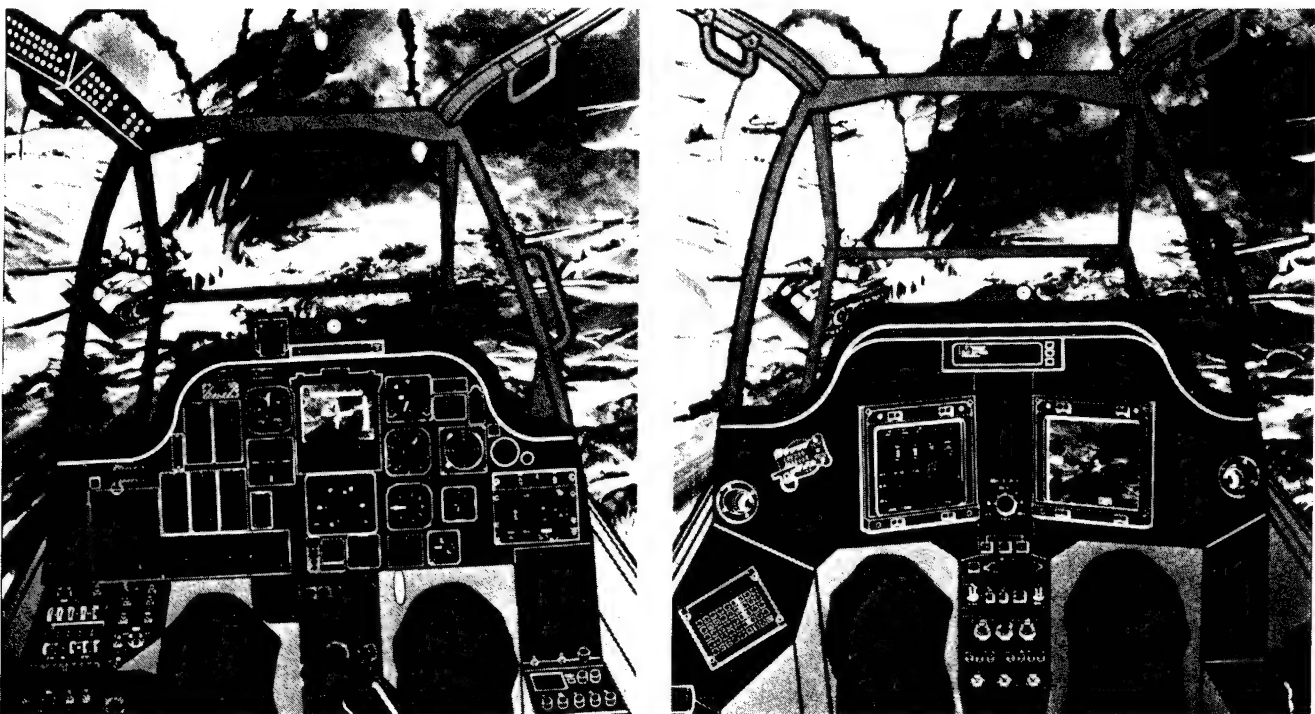


8710176-37

Figure 32. Advanced Digital Flight Control System
AV05 First Flight



Figure 33. Light Helicopter Systems Integration



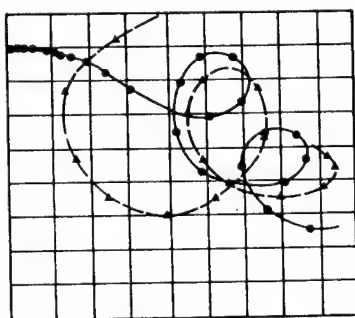
8710176-39

Figure 34. AH-64A Pilot Crewstation

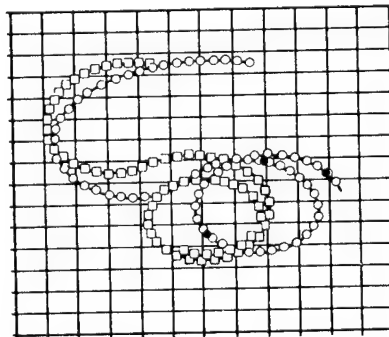


8710176-40

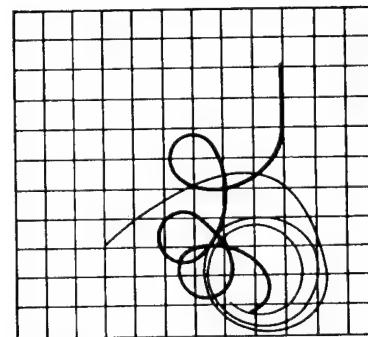
Figure 35. Intelligent Fault Locator Using Artificial Intelligence



AACT III



ALES

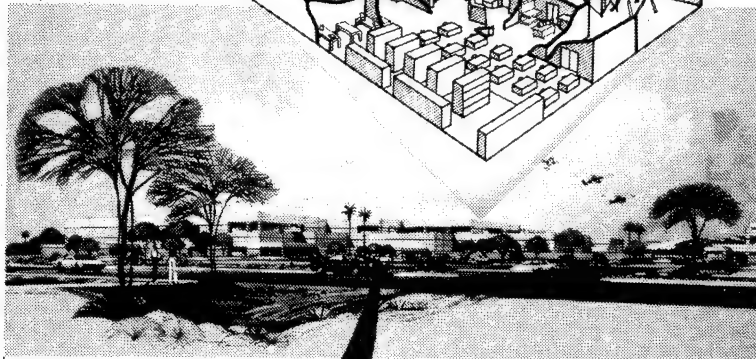
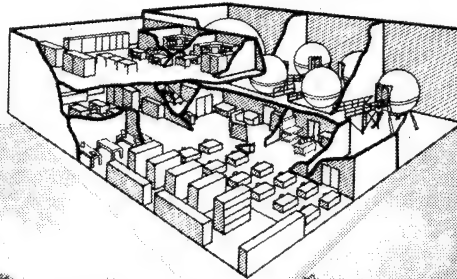


ALES AND A/I

Figure 36. Mission Analysis, Air-To-Air
Ground Traces Of A Maneuver

ROTORCRAFT TECHNOLOGY SIMULATION FACILITY...

Three high bays
Tempest secure environment



New 1.3 million-square-foot addition to McDonnell Douglas Helicopter Company's facility in Mesa, Arizona. The master plan includes areas for engineering, administration, and support activities.

**...WITHIN A MODERN
LABORATORY AND FLIGHT TEST
ENVIRONMENT**



**...ADJACENT TO MAJOR DOD
RANGE AND FIELD TRAINING
RESOURCES.**

Figure 37. Simulation

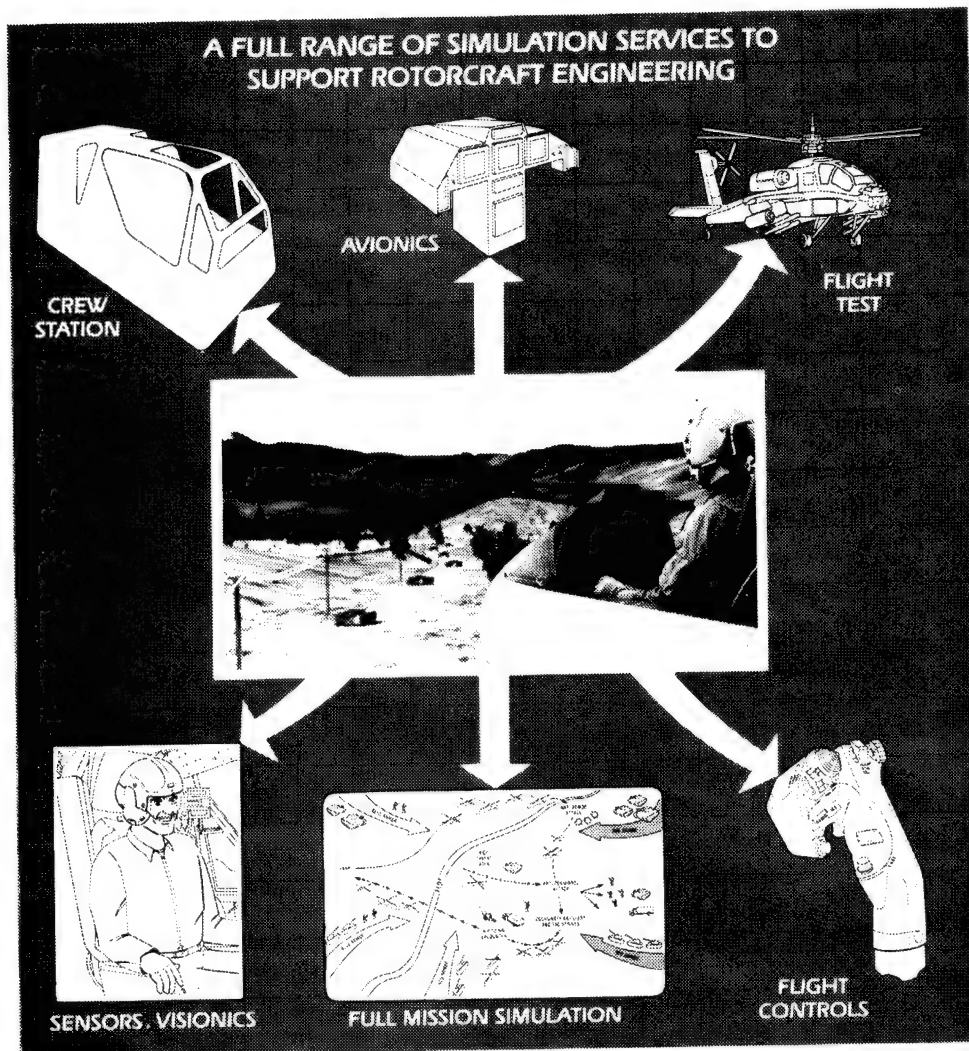


Figure 38. Simulation



Figure 39. Mesa Facilities Overview

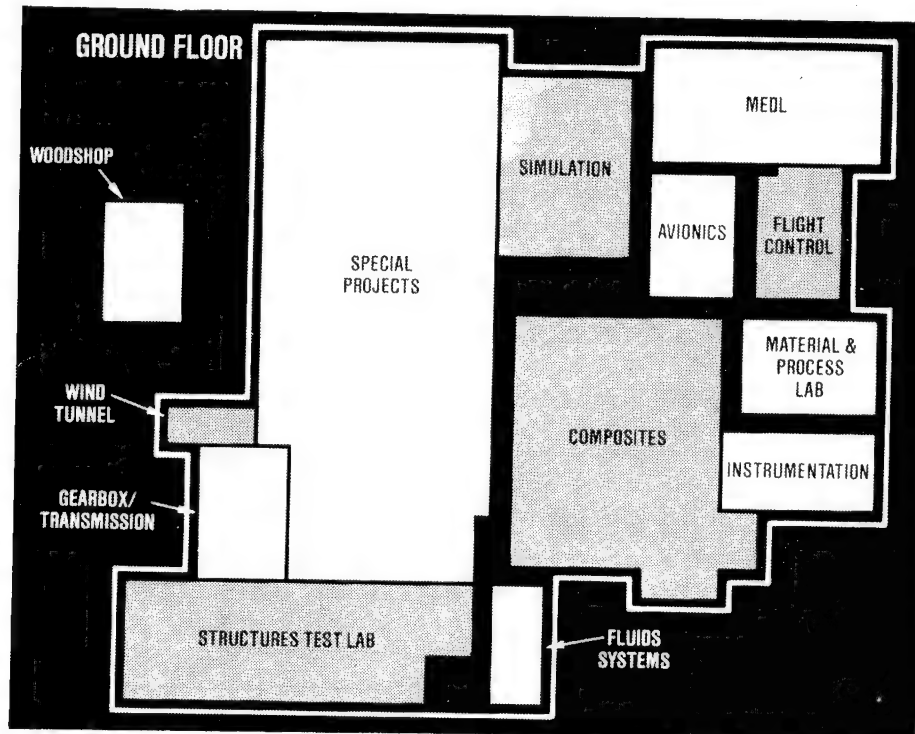


Figure 40. Advanced Development Center

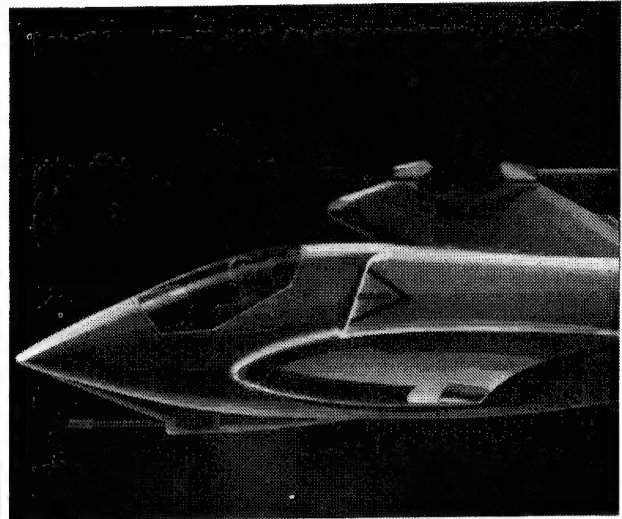


Figure 41. Beyond Apache

CONFERENCE ATTENDEES

ACREE, CECIL W
NASA/Ames
MS 237-5
Moffett Field, CA 94035

ACURIO, JOHN
Army/ARTA
21000 Brookpark Road
Cleveland, OH 44135

ADAMS, BOBBY R
Army Materiel Cmd
5001 Eisenhower Avenue
Alexandria, VA 22335

ALBERS, JAMES A
NASA/Ames
MS 200-3
Moffett Field, CA 94035

ALMOJUELA, THOMAS N
Army/ARTA
MS 207-5
Moffett Field, CA 94035

ALTON, LARRY R
NASA/Ames
MS 237-11
Moffett Field, CA 94035

ANDRE, WILLIAM L
Army/ARTA
Ames Research Center
Moffett Field, CA 94035

ANISMAN, GEORGE F
Dowty Aerospace Corp
1640 Fifth St, Suite 223
Santa Monica, CA 90401

ARTIS, DON
Army/ODCSRDA
Pentagon/Attn: DAM-AR
Washington, DC 20310

AUSTIN, EDWARD E
Army/ARTA-AVSCOM
Attn: SAVRT-TY-ATA
Fort Eustis, VA 23604

BALL, CALVIN L
NASA/Lewis
21000 Brookpark Road
Cleveland, OH 44135

BALLARD, RICHARD L
Army/DAMA WSA
Washington, DC 20310

BANDO, SHUNICHI
Kawasaki Heavy Ind
Helicopter/Aircraft Div.
Nagoya, JAPAN

BANERJEE, DEV
McDonnell Douglas
5000 E McDowell Road
Meza, AZ 85205

BARNABY, KEN
External Affairs
125 Sussex Drive
Ottawa, Ontario, CANADA K1A0G2

BARNES, CLEM S
Flight Research Div.
Royal Aircraft Est.
Bedford, ENGLAND

BARTLETT, F D
Army/ARTA-AVSCOM
NASA Langley Research Ctr
Hampton, VA 23665

BAUCHSPIES, JAMES S
ORI, Inc
8201 Corporate Drive #350
Landover, MD 20785

1987 NASA/Army
Rotorcraft Technology Conference

BELLAVITA, PAOLO
Agusta S.P.A
20153 Milano, ITALY

BELMAN, HARRIS J
IBM Corporation
Federal Systems Division
Owego, NY 13850

BENSHOOF, STEVE
McDonnell Douglas
5000 E McDowell Road
Mesa, AZ 85205

BIGGERS, JAMES C
Navy/DTRDC
Bethesda, MD 20084

BILL, ROBERT C
US Army Propulsion
21000 Brookpark Road
Cleveland, OH 44135

BILLMAN, BARRY
FAA Technical Center
Atlantic City Airport
Atlantic City, NJ 08405

BLAHA, JOHN T
USA Test Activity
Edwards AFB
Edwards, CA 93523

BLANKEN, CHRIS
Army/ARTA
MS 210-7
Moffett Field, CA 94035

BOBULA, GEORGE A.
Army/ARTA-AVSCOM
21000 Brookpark Road
Cleveland, OH 44135

BORGMAN, DEAN
McDonnell Douglas
5000 E McDowell Road
Mesa, AZ 85205

BOUSMAN, WILLIAM G
Army/AFD
MS 215-1
Moffett Field, CA 94015

BOWES, MICHAEL A
Kaman Aerospace Corp
PO Box 2, Old Windsor Rd
Bloomfield, CT 06002

BROOKS, ARNOLD
General Electric
1000 Western Avenue
Lynn, MA 01910

BROWN, WILLIAM P
McDonnell Douglas
5000 E McDowell Road
Mesa, AZ 85205

BRYANT, WILLIAM R
ORI, Inc
8201 Corporate Drive #350
Landover, MD 20785

BURKS, JOHN S
NASA
2302 Riviera Drive
Vienna, VA 22180

BURROWBRIDGE, WILLIAM R
Army/FSTC
220 7th St NW
Charlottesville, VA 22901

CARADONNA, FRANK
Army/AFDD
Ames Research Center
Moffett Field, CA 94035

**1987 NASA/Army
Rotorcraft Technology Conference**

CARLSON, RICHARD
Army/ARTA
MS 207-5
Moffett Field, CA 94035

CARTA, FRANKLIN O
United Technologies
Silver Lane
E Hartford, CT 06108

CHEN, ROBERT T
NASA/Ames
MS 211-2
Moffett Field, CA 94035

CHILDRESS, OTIS S
NASA/Langley
Research Center
Hampton, VA 23665

CHOPRA, P I
Univ. of Maryland
Dept. of Aerospace Eng
College Park, MD 20742

CIFFONE, DONALD L
Army/ARTA
Ames Research Center
Moffett Field, CA 95035

CLINE, JOHN H
NASA/Langley
98 Brown's Neck Road
Poquoson, VA 23662

CLINGINGSMIT, TOM W
LTV A&D
PO Box 655907
Dallas, TX 75265

CONDON, GREGORY W
NASA/Ames
MS 243-1
Moffett Field, CA 94035

COY, JOHN J
NASA/Lewis
21000 Brookpark Road
Cleveland, OH 44135

CRAWFORD, CHARLES C JR
Army/AVSCOM
4300 Goodfellow Blvd
St Louis, MO 63120

CURTISS, HOWARD JR
Princeton University
Engineering
Princeton, NJ

CZELUSNIAK, DANIEL P
Naval Air System Cmd
PMA-266
Washington, DC 20361

DADONE, LEO
Boeing Vertol Co
PO Box 16858
Philadelphia, PA 19142

DECKERT, WALLACE H
NASA/Ames
Moffett Field, CA 94035

DEXTER, H. BENSON
NASA/Langley
MS 1888
Hampton, VA 23665

DIAMOND, JACK
Boeing Vertol Co
PO Box 16858
Philadelphia, PA 19142

DIGIACOMO, FRANK S
Army/FSTC
220 7th St, NW
Charlottesville, VA 22901

**1987 NASA/Army
Rotorcraft Technology Conference**

DOMANOVSKY, PAUL
Aerospatiale Helicop
2701 Forum Drive
Grand Prairie, TX 75053

DULL, ANDREW
US Military Academy
West Point, NY 10996

DYKSTRA, JOSEPH
Western Gear Corp
14724 E Proctor Avenue
City of Industry, CA 91744

ECKERT, WILLIAM
Army/AFD
MS TA-19
Moffett Field, CA 94035

EDENBOROUGH, KIPLING
NASA/Ames
MS 247-3
Moffett Field, CA 94035

ELBER, WOLF
Army/ARTA-AVSCOM
Langley Research Center
Hampton, VA 23665

ESCULIER, JACQUES
STPA/HE
4 Ave. de la Porte D'issy
75996 Paris Armees, FRANCE

EVERETT, RICHARD A
NASA/Langley
MS 188E
Hampton, VA 23665

FARLEY, GARY L
Army/ARTA-AVSCOM
Langley Rsch Center
Hampton, VA 23665

FEASTER, LEWIS L
HQ AVSCOM
4300 Goodfellow Blvd
St Louis, MO 63120

FEIK, ROBERT
Aeronautical Res Lab
PO Box 4331
Melbourne, Vic, AUSTRALIA 3001

FELKER, FORT
Army/AFD
MS: TR32
Moffett Field, CA 94035

FERGUSON, SAMUEL W
Systems Tech Inc
2672 Bayshore Pkway, #505
Mountain View, CA 94043

FEW, DAVE D
NASA/Ames
MS 237-2
Moffett Field, CA 94035

FLANARY,, THOMAS N II
Bell Helicopter
2101 Executive Drive, T65
Hampton, VA 23666

FLETCHER, JAY W
NASA/Ames
Moffett Field, CA 94035

FUJII, SHOICHI
Nat'l Aerospace Lab
7-44-1 Jindaijigashi-Mach
Chofu-Shi, Tokyo JAPAN 182

GESSOW, ALFRED
Univ. of Maryland
College Park, MD 20742

1987 NASA/Army
Rotorcraft Technology Conference

GMELIN, BERND
DFVLR
Flughafen-Braunschweig
WEST GERMANY, D3300

GODFREY, JEFFREY H
Army/Ames
Moffett Field, CA 95008

GOOD, DANNY E
Army/AATD
SAVRT-TY-ATS
Ft Eustis, VA 23604

GOSSETT, TERRY D
Army AVSCOM-AFDD
Moffett Field, CA 94035

HAGGERTY, ALLEN C
McDonnell Douglas
5000 E McDowell Road
Mesa, AZ 85205

HAM, NORMAN D
MIT
128 Clinton Road
Brookline, MA 02146

HAMEL, PETER G DR
DFVLR
Flughafen-Braunschweig
WEST GERMANY, D3300

HARSE, JAMES H
Bell Helicopter
5721 Rockhill Road
Fort Worth, TX 76112

HART, SANDY
NASA/Ames
MS 239-3
Moffett Field, CA 94035

HARTZELL, EARL J
NASA/Ames
MS 239-21
Moffett Field, CA 94035

HAYDEN, JAMES S
Air Force/AEFA
Savte-CT
Edwards AFB, CA 93523

HEFFLEY, ROBERT K
Robert Heffley Eng.
349 First Street
Los Altos, CA 94022

HENDERSON, ED W
Aerospatiale Helicop
2701 Forum Drive
Grand Prairie, TX 75053

HENDRICKSON, JOHN F
HQ AMC-LABCOM
2800 Powdermill Road
Adelphi, MD 20783

HOOVER, W. EUAN
Boeing Vertol Co
PO Box 16858
Philadelphia, PA 19142

HOPKINS, ARTHUR S
Army/AFDD
Moffett Field, CA 94035

HORNBLOWER, CHRIS
Rolls-Royce
1201 PA Ave., NW #230
Washington, DC 20004

HOUSE, THOMAS L
Army/AATD
Ft. Eustis, VA 23062

1987 NASA/Army
Rotorcraft Technology Conference

HUBER, HELMUT
MBB
PO Box 801109
8000 Munich, WEST GERMANY

HUNTHAUSEN, ROGER J
Army/AATD
Ft. Eustis, VA 23604

HUSH, WILLIAM P
Singer Link Flight
Binghamton, NY 13902

JAMES, HARRY A.
Teledyne Ryan
2701 Harbor Drive
San Diego, CA 92138

JENNEY, DAVID S
Sikorsky Aircraft
6900 Main Street
Stratford, CT 06601

JOHNSON, WAYNE
Johnson Aeronautics
505 Hamilton Ave, #309A
Palo Alto, CA 94301

KAMBROD, MATTHEW R.
U.S. Army
Pentagon, Room 2E673
Washington, DC 20310

KELLY, PATRICK
Martin Marietta
PO Box 5837
Orlando, FL 32855

KENNEDY, JOHN P
Navy/DTNSRDC
Bethesda, MD 20084

KERR, ANDREW
Army/AFD
MS 215-1
Moffett Field, CA 94035

KEY, DAVID L
NASA/Ames
MS 210-7
Moffett Field, CA 94035

KITABAYASHI, SHUZO
Fuji Heavy Industry
Aircraft Engineering Div
Tokyo, JAPAN

KITAPLIOGLU, CAHIT
NASA/Ames
MS TR-32
Moffett Field, CA 94035

KUNDE, COL. GERALD R
Chief, Aviation Sys
Army/DAMA-WSA
Washington, DC 20310

KURKOWSKI, RICHARD L
NASA/Ames
MS 237-11
Moffett Field, CA 94035

KVATERNIK, RAYMOND G
NASA/Langley
Hampton, VA 23665

LANDGREBE, ANTON J
United Tech Rsch Ctr
Silver Lane
E Hartford, CT 06108

LANE, JAMES W
NASA/Ames
201 Flynn Ave., #3
Mountainview, CA 94043

1987 NASA/Army
Rotorcraft Technology Conference

LEBACQZ, J. VICTOR
NASA/Ames
MS 211-2
Moffett Field, CA 94035

LEWIS, MICHAEL S
NASA/Ames
Aeroflightdynamics
Moffett Field, CA 94036

LOGAN, A. H
McDonnell Douglas
5000 E McDowell Road
Mesa, AZ 85205

MACRINO, JOHN A
Army/ARTA-AVSCOM
Ft. Eustis, VA 23604

MALONEY, PAUL F
Kaman Aerospace Corp
Old Windsor Road
Bloomfield, CT 06002

MARCHINSKI, LEONARD J
Leonard Assoc., Inc
6 E. Avenue
Mt. Carmel, PA 17851

MASSOGLIA, PETER L
FAA
800 Independence Ave, SW
Washington, DC 20591

MCCLURE, WILLIAM E
Sikorsky Aircraft
North Main Street
Stratford, CT 06601

MCHUGH, F J
Boeing Vertol
PO Box 16858
Philadelphia, PA 19142

LEMNIOS, ANDREW Z
Kaman Aerospace Corp
Old Windsor Rd, PO Box 2
Bloomfield, CT 06002

LOEWY, ROBERT G
Rensselaer Poly. Ins
110 Eighth Street
Troy, NY 12181

LUEDERS, HOWARD G
Allison Gas Turbine
PO Box 420, SC T13
Indianapolis, IN 46206

MAISEL, MARTIN
NASA/Ames
MS 237-5
Moffett Field, CA 94035

MANTAY, WAYNE R
Army/ARTA-AVSCOM
Langley Research Center
Hampton, VA 23665

MARSHALL, ROY
NASA HQ
600 Independence Ave., SW
Washington, DC 20546

MCALISTER, KEN W
Army/AFDD
MS 215-1
Moffett Field, CA 94035

MCCROSKEY, WILLIAM J
Army/AFD
MS 258-1
Moffett Field, CA 94035

MCKEITHAN, CLIFFORD
NASA/Ames
MS 237-11
Moffett Field, CA 94035

**1987 NASA/Army
Rotorcraft Technology Conference**

MCNULTY, MICHAEL J
Army/AFD
MS 215-1
Moffett Field, CA 94035

MCQUINN, WARREN
Pratt & Whitney/GPD
PO Box 2691
W Palm Beach, FL 33402

MEIER, JOHN G
Avco Lycoming
550 S Main Street
Stratford, CT 06497

MICHAUD, NORMAN H.
NASA/Ames
MS 247-1
Moffett Field, CA 94035

MIHALOEW, JAMES R
NASA/Lewis
21000 Brookpark Road
Cleveland, OH 44136

MILSTEAD, LAURENCE C
Army/Aviation Center
111 Shulsen Drive
Ozark, AL 36360

MONDO, JAMES A
Dupont Composites
Chestnut Run, Bldg 705
Wilmington, DE 19898

MORGAN, HOMER G
NASA/Langley
MS 462
Hampton, VA 23665

MORSE, ANDREW H
U.S. Army
Moffett Field, CA 94035

MRAZ, CHARLES L.
McDonnell Douglas
5301 Bolsa Avenue
Huntington Beach, CA 92647

MULVILLE, DANIEL R.
NASA HQ
Code RM
Washington, DC 20546

NAGEL, DAVID
NASA/Ames
MS 239-1
Moffett Field, CA 94035

NAOKI, IWAMURA
Mitsubishi
OF Minato-KU
Nagoya, JAPAN

NEUGEBAUER, ALAN K
McDonnell Douglas
5000 E McDowell Road
Mesa, AZ 85205

NIEDZWIECKI, RICHARD
NASA/Lewis
21000 Brookpark Road
Cleveland, OH 44135

NYE, JAMES L
General Electric
1000 Western Avenue
Lynn, MA 01910

NYGREN, KIP P
US Military Academy
Dept. of Mechanics
West Point, NY 10996

O'BRIEN, T. KEVIN
Army/RTA
MS 188E
Hampton, VA 23665

1987 NASA/Army
Rotorcraft Technology Conference

OLSON, ROBERT
United Technologies
Silver Lane
E Hartford, CT 06108

OSDER, STEPHEN S
McDonnell Douglas
5000 E McDowell Road
Mesa, AZ 85205

PAHL, KURT P.
Chandler Evans
Charter Oak Blvd
W Hartford, CT 06101

PAY, GRAHAM D.
British Embassy
3100 Mass. Ave., NW
Washington, DC 20008

PETERS, DAVID A
Georgia Tech
4971 Oak Trail Drive
Dunwoody, GA 30332

PIASECKI, FRANK N
Piasecki Aircraft
W Terminus of 2nd Street
Essington, PA 19029

POWELL, ROBERT D
Kaman Aerospace Corp
110 Yorkview Road
Yorktown, VA 23692

PURCELL, TIMOTHY W
Army/AFDD
MS 215-1
Moffett Field, CA 94035

REAL, JACK G
McDonnell Douglas
Centinelaeteale Streets
Culver City, CA 90230

ORMISTON, ROBERT
Army/AFD
MS 215-1
Moffett Field, CA 94035

OSSI, RONALD
AVCO Lycoming
550 S Main Street
Stratford, CT 06497

PARKINSON, C. HARRY
Dynamic Engineering
703 Middle Ground Blvd
Newport News, VA 23606

PECK, ROBERT S
Rockwell Int'l.
865 E Sepulveda Blvd
Carson, CA 90745

PHILIPPE, JEAN J
ONERA
29 Avenue de la Division
Chatillon, FRANCE 92320

PINARD, ROLAND
Embassy of France
4101 Reservoir Rd, NW
Washington, DC 20007

PROPEN, MICHAEL
AVCO Lycoming
550 South Main Street
Stratford, CT 06497

PURSEL, ROBERT
FAA
Atlantic City Airport
Atlantic City, NJ 08405

REICHERT, GUENTHER
Univ. Braunschweig
3300 Braunschweig
WEST GERMANY

1987 NASA/Army
Rotorcraft Technology Conference

RENIRIE, L T
NLR
PO Box 90502
Amsterdam, NETHERLAND

ROHM, BARRY N
GM/Allison
2001 S Tibbs Plt8 822A
Indianapolis, IN 46206

ROSEN, KEN
Sikorsky Aircraft
North Main Street
Stratford, CT 06601

RUTKOWSKI, MICHAEL J
Army/AFDD
Moffett Field, CA 94035

SATTERWHITE, JAMES J
Sikorski Aircraft
6900 Main Street
Stratford, CT 06601

SCHLEICHER, RAY A
Naval Air System Cmd
Washington, DC 20361

SCHMITZ, FREDERIC
NASA/Ames
MS 247-3
Moffett Field, CA 94035

SCHRAGE, DANIEL P
Georgia Tech
Aerospace Engineering
Atlanta, GA 30332

SCHROERS, LAUREL G
NASA/Ames
MS 237-5
Moffett Field, CA 94035

SCHUCK, JACK W
Honeywell
1625 Zarthan Avenue
St Louis Park, MN 55416

SCHWARZ, RUDY A
Rolls-Royce
1201 PA Ave., NW #230
Washington, DC 20004

SCIPIONI, LOUIS
GM/Allison
1911 N Ft Myer Dr, #800
Arlington, VA 22209

SCOTT, WILLIAM B
Aviation Week
42940 Chicory Avenue
Lancaster, CA 93534

SETO, EDWARD I
NASA/Ames
Mountainview, CA 94035

SHAPLEY, JOHN J
FAA
PO Box 1689
Fort Worth, TX 76101

SHARPE, DAVID L
U.S. Army
Moffett Field, CA 94086

SHAW, JOHN
Boeing Vertol Co
PO Box 16858
Philadelphia, PA 19142

SHAW, ROBERT J.
NASA/Lewis
21000 Brookpark Road
Cleveland, OH 44125

1987 NASA/Army
Rotorcraft Technology Conference

SHEEHY, HUGH F
NASA/Ames
MS TR032, NAS Moffett
Sunnyvale, CA

SHIVELY, R J
Army/AFDD
MS 239-3
Moffett Field, CA 94035

SHOWMAN, ROBERT D
NASA
10176 Carol Lee Drive
Cupertino, CA 95014

SIMMS, GORDON
Pratt & Whitney CANA
PO Box 10
Longueuil, CANADA

SMITH, EDMUND H
Naval Air System Cmd
Jefferson Plaza #2
Washington, DC 20361

SMITH, CHARLES
NASA/Ames
MS TR32
Moffett Field, CA 94035

SMITH, ROBERT D.
FAA
800 Independence Ave., SW
Washington, DC 20591

SNYDER, THOMAS
NASA/Ames
MS 200-3
Moffett Field, CA 94035

SNYDER, LYNN E.
Allison Gas Turbine
PO Box 420, MS T-23
Indianapolis, IN 46206

SNYDER, WILLIAM J
NASA/Ames
MS 237-5
Moffett Field, CA 94035

SOHNER, THOMAS M
Rockwell Int'l.
400 Collins Rd., NE
Cedar Rapids, IA 52498

SOLLART, GEORGE
Simmons Precision
197 Ridgedale Avenue
Cedar Knolls, NJ 07927

SRADERS, GUNTIS
Dept. of Defense
Pentagon, Room 3E1049
Washington, DC 20301

STEPHENS, WENDELL B
Army/ARTA
Ames Research Center
Moffett Field, CA 94035

STETSON, HAROLD D
Pratt & Whitney GVT
PO Box 109600
W Palm Beach, FL 33410

STURGIS, BARRY K
Naval Air System Cmd
AIR-5302H2
Washington, DC 20361

SUMMERS, MICHAEL H
Pratt & Whitney
1825 Eye St, # 700, NW
Washington, DC 20006

SUNDSRUD, GERALD J
3M Structural Prods
3M Cntr., 230-1F-02
St Paul, MN 55144

1987 NASA/Army
Rotorcraft Technology Conference

TALBOT, PETER D
NASA/Ames
Moffett Field, CA 94035

TAYLOR, RODNEY S
Bell Helicopter
3709 Hillwood Way
Bedford, TX 76021

TEARE, PAUL A
Boeing Vertol Co
PO Box 16858
Philadelphia, PA 19142

TOLER, DONALD L
Rotor & Wing Intl
PO Box 1790 News Plaza
Peoria, IL 61656

TORRES, MANUEL
Aerospatiale
13725 Marignane
FRANCE,

TUCK, DENNIS A
SFENA Corporation
2617 Aviation Parkway
Grand Prairie, TX 75051

TUNG, CHEE
U.S. Army/AFDD
MS 215-1
Moffett Field, CA 94035

UNGER, GEORGE
NASA HQ
Code RF
Washington, DC 20546

VARNER, CHARLES E
Army/ARTA
Moffett Field, CA 94035

WAGNER, SIEGFRIED N
Univ. Bundeswehr
Werner-Heisenberg-Weg 39
Neubiberg, WEST GERMANY 8014

WALKER, BOB E
Bell Helicopter
PO Box 482
Ft Worth, TX 76101

WARD, JOHN F
Consultant
5 Federal St., Suite 210
Easton, MD 21601

WARMBRODT, WILLIAM
NASA/Ames
MS TR-32
Moffett Field, CA 94039

WATTS, MICHAEL E
NASA/Ames
MS 237-5
Moffett Field, CA 94035

WEDEN, GILBERT J
Army/Propulsion Dir
15638 Indianhead Lane
Strongsville, OH 44136

WHALLEY, MATTHEW S
NASA/Ames
Aeroflight
Moffett Field, CA 94035

WHITE, JOHN W
Army/AATD
Ft. Eustis, VA 23604

WHITNEY, WELLS
Raychem Corporation
300 Constitution Drive
Menlo Park, CA 94025

1987 NASA/Army
Rotorcraft Technology Conference

WIESNER, ROBERT
Boeing Vertol Co
PO Box 16858
Philadelphia, PA 19142

WILLIAMS, JAMES R
U.S. Army NASA LARC
MS 268
Hampton, VA 23665

WILLIS, EDWARD A
NASA/Lewis
21000 Brookpark Road
Cleveland, OH 44135

WILLS, DONALD
Chandler Evans Colt
Charter Oak Blvd, #10651
W Hartford, CT 06101

WILSON, JOHN
Army/AFD
MS 286
Hampton, VA 23665

WINTER, J. S.
British Embassy
3100 Massachusetts Ave, NW
Washington, DC 20008

WINTUCKY, WILLIAM T
NASA/Lewis
21000 Brookpark Road
Cleveland, OH 44135

WONG, JIM
Army/ARTA
Ames Research Center
Moffett Field, CA 94035

YEN, JING G
Bell Helicopter
1812 Lakemont Court
Arlington, TX 76013

YOUNG, WARREN
Bell Helicopter
Dept 81 PO Box 482
Fort Worth, TX

YU, JAMES C.
NASA HQ
Code Rm
Washington, DC 20546

YU, YUNG
Army/ARTA
MS 214-1
Moffett Field, CA 94035

ZINNER, RUSSELL A
NASA/Ames
MS 215-1
Moffett Field, CA 94035

ZUCKERMANN, KARL H
Dornier GMBH
PO Box 1420
Friedrichsha, W.Ger,

ZUGSCHWERT, JOHN F
American Helic. Soc
217 N Washington Street
Alexandria, VA 22314

ZUK, JOHN
NASA/Ames
MS 237-11
Moffett Field, CA 94035



Report Documentation Page

1. Report No. NASA CP-2495	2. Government Accession No.	3. Recipient's Catalog No.	
4. Title and Subtitle NASA/Army Rotorcraft Technology Volume III - Systems Integration, Research Aircraft, and Industry		5. Report Date February 1988	
		6. Performing Organization Code RJ	
7. Author(s)		8. Performing Organization Report No.	
		10. Work Unit No.	
9. Performing Organization Name and Address Office of Aeronautics and Space Technology National Aeronautics and Space Administration		11. Contract or Grant No.	
		13. Type of Report and Period Covered Conference Publication	
12. Sponsoring Agency Name and Address National Aeronautics and Space Administration Washington, DC 20546		14. Sponsoring Agency Code	
15. Supplementary Notes The conference was jointly sponsored by the National Aeronautics and Space Administration and the Department of the Army, with the participation of industry coordinated by the American Helicopter Society, Inc.			
16. Abstract The 1987 NASA/Army Rotorcraft Technology Conference was held at Ames Research Center, Moffett Field, California, March 17-19, 1987. The Conference Proceedings is a compilation of over 30 technical papers presented at this milestone event which reported on the advances in rotorcraft technical knowledge resulting from NASA, Army, and industry rotorcraft research programs over the last 5 to 10 years. The Conference brought together over 230 government, industry, and allied nation conferees to exchange technical information and hear invited technical papers by prominent NASA, Army, and industry researchers covering technology topics including aerodynamics, dynamics, and aeroelasticity, propulsion and drive systems, flight dynamics and control, acoustics, systems integration, and research aircraft.			
17. Key Words (Suggested by Author(s)) helicopter flight dynamics and rotor aerodynamics control rotor dynamics propulsion acoustics		18. Distribution Statement Unclassified - Unlimited Subject Category 01	
19. Security Classif. (of this report) Unclassified	20. Security Classif. (of this page) Unclassified	21. No. of pages 382	22. Price A17